Composite Materials in Concrete Construction

Proceedings of the International Seminar
held at the University of Dundee, Scotland, UK
on 5-6 September 2002

Edited by

Ravindra K. Dhir
Director, Concrete Technology Unit
University of Dundee

Kevin A. Paine
Research/Teaching Fellow, Concrete Technology Unit
University of Dundee

and

Moray D. Newlands
CPD/Consultancy Manager, Concrete Technology Unit
University of Dundee

Thomas Telford

Published by Thomas Telford Publishing, Thomas Telford Ltd, 1 Heron Quay, London E14 4JD.
www.thomastelford.com

Distributors for Thomas Telford books are
USA: ASCE Press, 1801 Alexander Bell Drive, Reston, VA 20191-4400, USA
Japan: Maruzen Co. Ltd, Book Department, 3–10 Nihonbashi 2-chome, Chuo-ku, Tokyo 103
Australia: DA Books and Journals, 648 Whitehorse Road, Mitcham 3132, Victoria

First published 2002

The full list of titles from the 2002 International Congress 'Challenges of Concrete Construction' and available from Thomas Telford is as follows

- Innovations and developments in concrete materials and construction
- Sustainable concrete construction
- Concrete for extreme conditions
- Composite materials in concrete construction
- Concrete floors and slabs
- Repair, rejuvenation and enhancement of concrete

A catalogue record for this book is available from the British Library

ISBN: 0 7277 3174 2

Printed and bound in Great Britain by MPG Books, Bodmin, Cornwall

PREFACE

Concrete is a global material that underwrites commercial well-being and social development. Notwithstanding concrete's uniqueness, it faces challenges from new materials, environmental concerns and economic factors, as well as ever more demanding design requirements. Indeed, the pressure for change and improvement of performance is relentless and necessary.

The Concrete Technology Unit (CTU) of the University of Dundee organised this Congress to address these issues, continuing its established series of events, namely, Creating with Concrete in 1999, Concrete in the Service of Mankind in 1996, Economic and Durable Concrete Construction Through Excellence in 1993 and Protection of Concrete in 1990.

The event was organised in collaboration with three of the world's most recognised institutions: the Institution of Civil Engineers, the American Concrete Institute and the Japan Society of Civil Engineers. Under the theme of Challenges of Concrete Construction, the Congress consisted of three Seminars: (i) Composite Materials in Concrete Construction, (ii) Concrete Floors and Slabs, (iii) Repair, Rejuvenation and Enhancement of Concrete, and three Conferences: (i) Innovations and Developments in Concrete Materials and Construction, (ii) Sustainable Concrete Construction, (iii) Concrete for Extreme Conditions. In all, a total of 350 papers were presented from 58 countries.

The Opening Addresses were given by Mr Jack McConnell MSP, First Minister of the Scottish Executive, Sir Alan Langlands, Principal and Vice-Chancellor of the University of Dundee, Mr John Letford, Lord Provost, City of Dundee, Professor Adrian Long, Senior Vice-President of the Institution of Civil Engineers, Dr Taketo Uomoto, Director of the Japan Society of Civil Engineers and Dr Terence Holland, President of the American Concrete Institute. The Congress had six Opening and six Closing Papers dealing with the main themes of the Seminars and Conferences. Opening Papers were presented by Professor Gerard Van Erp, University of Southern Queensland, Australia Dr Peter Seidler, Astradur Industrieboden, Germany and Professor Kyosti Tuttii, Skanska Teknik AB, Sweden, Professor Surendra Shah, Northwestern University, USA, Dr Philip Nixon, Building Research Establishment, UK and Mr Hans de Vries, Ministry of Transport, the Netherlands. Closing Papers were presented by Dr Gier Horrigmoe, NORUT Technology Ltd, Norway, Professor Andrew Beeby, University of Leeds, UK, Professor Peter Robery, FaberMaunsell, UK, Professor Heiki Kukko, VTT Building and Transport, Finland, Dr Mette Glavind, Danish Technological Institute, Denmark and Professor Yoshihiro Masuda, Utsunomiya University, Japan. The Congress was closed by Professor Peter Hewlett, Chief Executive of the British Board of Agrément, UK.

The support of 23 International Professional Institutions and 32 Sponsoring Organisations was a major contribution to the success of the Congress. An extensive Trade Fair formed an integral part of the event. The work of the Congress was an immense undertaking and all of those involved are gratefully acknowledged, in particular, the members of the Organising Committee for managing the event from start to finish; members of the International Advisory and National Technical Committees for advising on the selection and reviewing of papers; the Authors and the Chairmen of Technical Sessions for their invaluable contributions to the proceedings.

All of the proceedings have been prepared directly from the camera-ready manuscripts submitted by the authors and editing has been restricted to minor changes where it was considered absolutely necessary.

Dundee
September 2002

Ravindra K Dhir
Chairman, Congress Organising Committee

INTRODUCTION

The use of concrete in combination with ductile, tension-strong materials is an age-old concept, and traditionally steel bars have had the role of reinforcement. However, over the past decade there has been a growing trend towards two alternative types of composite concrete construction: fibre reinforced plastic (FRP) reinforcement- a direct alternative to steel bars; and fibre reinforced concrete (FRC) - the use of discrete fibres within the concrete matrix.

FRP and FRC have developed independently to emerge as exciting and promising technologies that can be used in new construction, strengthening and rehabilitation. However, given their differences with traditional reinforcement, particularly with regard to stiffness, there has, until recently been a problem in using these materials in combination with structural design codes. It has been necessary, therefore, in most cases to modify and sometimes develop new design approaches for these. This has led to an opportunity for innovative techniques to be addressed and exploited.

As design techniques have evolved there have been simultaneous developments in materials engineering that have led to improvements in fibre geometry and profile, fibre-matrix interfacial bond, strength and ductility. Moreover, new products, including laminate coverings and fabrics have entered the market and extended the range of possibilities. The number of materials employed as fibres has also expanded such that there is now an array of mineral and chemical materials that can be chosen for optimum performance in terms of cost, efficiency and durability for a given application.

Clearly, FRP and FRC have come into their own in aggressive environments, where they are not prone to steel corrosion problems that beset traditional reinforcement. In particular, this has led to the widespread use of FRP as an external strengthening mechanism for concrete bridges, and as the favoured reinforcement solution in marine environments for sea walls, piers and floating oil storage vessels. FRC, meanwhile, has become widely used in elements where it is difficult to fix traditional reinforcement, and is often used in combination with sprayed concrete for strengthening tunnels and water-retaining structures.

The proceedings of this International Seminar; '*Composite Materials in Concrete Construction*' dealt with all of these subject areas and the issues raised, under three clearly defined themes: (i) Structural Design Considerations, (ii) Developments in Reinforcement Materials and (iii) Durability and Maintenance of Composite Construction. Each theme commenced with a Keynote Paper presented by the foremost exponents in their respective fields. There were a total of 32 papers presented during the seminar which are compiled into these proceedings.

Dundee
September 2002

Ravindra K Dhir
Kevin A Paine
Moray D Newlands

ORGANISING COMMITTEE

Concrete Technology Unit

Professor R K Dhir OBE (Chairman)

Dr M D Newlands (Secretary)

Professor P C Hewlett
British Board of Agrément

Professor T A Harrison
Quarry Products Association

Professor V K Rigopoulou
National Technical University of Athens, Greece

Dr S Y N Chan
Hong Kong Polytechnic University

Dr N Y Ho
L & M Structural Systems, Singapore

Dr M R Jones

Dr M J McCarthy

Dr T D Dyer

Dr K A Paine

Dr L J Csetenyi

Dr J E Halliday

Dr L Zheng

Dr S Caliskan

Dr A Iordanidis

Ms P I Hynes (Congress Assistant)

Mr S R Scott (Unit Assistant)

INTERNATIONAL ADVISORY COMMITTEE

Dr C Andrade, *Director of IETCC*
Institute of Construction Sciences Eduardo Torroja, Spain

Professor G Balázs, *Head of Department*
Budapest University of Technology, Hungary

Professor Y Ballim, *Associate Professor*
University of the Witwatersrand, South Africa

Professor A Bentur, *Head Division of Building Materials*
Technion Israel Institute of Technology, Israel

Professor J M J M Bijen, *Professor*
Delft University of Technology, Netherlands

Professor A Brandt, *Head of Department*
Insistute of Fundamental Tech Research, Poland

Professor K-J Byun, *Dean/Professor in Concrete Engineering*
Yonsei University, Korea

Dr J-M Chandelle, *Chief Executive*
CEMBUREAU, Belgium

Professor T-P Chang, *Professor*
National Taiwan University of Science & Technology, Taiwan

Professor M Collepardi, *Professor*
Politecnico Di Milano, Italy

Dr J Duncan, *Manager, Building Industry Research*
BRANZ, New Zealand

Professor R I Gilbert, *Head of School*
University of New South Wales, Australia

Professor S Ikeda, *Professor*
Yokohama National University, Japan

Professor B L Jensen,
Danish Technological Institute, Denmark

Dr H Justnes, *Chief Scientist*
SINTEF Civil & Environmental Engineering, Norway

Professor V Kristek, *Head of Department*
Czech Technical University, Czech Republic

Dr A K H Kwan, *Associate Dean of Engineering*
University of Hong Kong, Hong Kong

Professor F de Larrard, *Director MMCER*
LCPC Centre de Nantes, France

INTERNATIONAL ADVISORY COMMITTEE (CONTINUED)

Professor R W Lindberg, *Professor*
Tampere University of Technology, Finland

Dr H-U Litzner, *Senior Chief Executive*
German Concrete Society (DBV), Germany

Mr J E McDonald, *Research Civil Engineer*
US Army Corp of Engineers, USA

Professor S Mirza, *Professor*
McGill University, Canada

Mr J V Paiva, *Head, Building Department*
LNEC, Portugal

Dr T Philippou, *Manager*
Heracles General Cement Company, Greece

Mr S A Reddi, *Deputy Managing Director*
Gammon India Limited, India

Professor F Saje, *Professor of Concrete Structures*
University of Ljubljana, Slovenia

Professor S P Shah, *Director, ACBM*
Northwestern University, USA

Professor H E R Sommer, *Consultant*
Austria

Dr S Tangtermsirikul, *Head of School of Civil Engineering*
Thammasat University, Thailand

Professor K Tuutti, *Director*
Skånska Teknik AB, Sweden

Professor T Uomoto, *Head of Uomoto Concrete Laboratory*
University of Tokyo, Japan

Dr O H Wallevik, *Head of Concrete Division*
Icelandic Buidling Research Institute, Iceland

Professor T H Wee, *Associate Professor*
National University of Singapore, Singapore

Professor M A Yeginobali, *Director, R&D Institute*
Turkish Cement Manufacturers Association, Turkey

Professor H M Z Al-Abideen, *Deputy Minister*
Ministry of Public Works and Housing, Saudi Arabia

NATIONAL TECHNICAL COMMITTEE

Professor S A Austin
Professor of Structural Engineering, Loughborough University

Professor A W Beeby
Professor of Structural Design, The University of Leeds

Professor T Broyd
Research & Innovations Director, W S Atkins

Professor J H Bungey
Head of Department, The University of Liverpool

Mr N Clarke
Publications Manager, The Concrete Society

Mr G Cooper
Development Director, Fosroc International Ltd

Mr S J Crompton
Divisional Manager, RMC Readymix Ltd

Dr S B Desai OBE
Visiting Professor, University of Surrey

Professor R K Dhir OBE (Chairman)
Director, Concrete Technology Unit, University of Dundee

Dr K Elliott
Senior Lecturer, University of Nottingham

Dr S Garvin
Director (Scotland), Building Research Establishment

Professor F P Glasser
Professor, University of Aberdeen

Mr P G Goring
Technical Director, John Doyle Construction

Professor T A Harrison
BRMCA Consultant, Quarry Products Association

Professor P C Hewlett
Chief Executive, British Board of Agrément

Mr A Johnson
Divisional Director and Manager, Mott MacDonald Special Services

Dr M R Jones
Senior Lecturer, Concrete Technology Unit, University of Dundee

Professor R J Kettle
Head of Department, Aston University

Mr P Livesey
National Technical Services Manager, Castle Cement Limited

NATIONAL TECHNICAL COMMITTEE (CONTINUED)

Professor A E Long
Dean of Faculty of Engineering, Queens University Belfast

Mr N Loudon
Senior Technical Adviser, Highways Agency

Mr A C Mack
Operations Director, Bovis Lend Lease (Scotland) Ltd

Professor P S Mangat
Head, Civil Engineering & Construction, Sheffield Hallam University

Mr G G T Masterton
Director, Babtie Group

Professor G C Mays
Deputy Principal, Cranfield University

Professor W J McCarter
Professor, Heriot-Watt University

Dr J Moore
Director, Standards & Technical, British Cement Association

Dr P J Nixon
Director, Centre for Concrete Construction, Building Research Establishment

Mr M Peden
Partner, W.A. Fairhurst & Partners

Dr W F Price
Senior Research Manager, British Cement Assocation

Professor P C Robery
Divisional Director - Midlands, Maunsell Ltd

Mr J M Ross
Chairman, Blyth & Blyth Consulting Engineers

Dr R H Scott
Reader in Engineering, University of Durham

Dr I Sims
Director (Materials), STATS Limited

Professor G Somerville OBE
Independent Consultant

Mr P Titman
Quality and Environment Manager, Edmund Nuttall Ltd

Dr P R Vassie
Research Fellow, Transport Research Laboratory

Professor S Wild
Head, Building Materials Research Unit, University of Glamorgan

COLLABORATING INSTITUTIONS

Institution of Civil Engineers, UK

American Concrete Institute

Japan Society of Civil Engineers

SPONSORING ORGANISATIONS WITH EXHIBITION

Aggregate Industries plc
Babtie Group
British Board of Agrement
British Cement Association
Building Research Establishment
Caledonian Slag Cement
Castle Cement Limited
CEMBUREAU, Belgium
Danish Technological Institute, Denmark
Degussa Construction Chemicals, Italy
Dundee City Council
Elkem Materials Ltd
FaberMaunsell
Fosroc International Ltd
Heidelberg Cement, Germany
Heracles General Cement Company, Greece
Institution of Civil Engineers
John Doyle Construction
Lafarge Cement UK
Makers UK Ltd
MBT Admixtures
Netzsch Instruments, Germany
North East Slag Cement
Palladian Publications
RMC Readymix Ltd
Rugby Cement
ScotAsh Ltd

SPONSORING ORGANISATIONS WITH EXHIBITION (CONTINUED)

Scottish Enterprise Tayside
Thomas Telford Publishing
UK Quality Ash Association
Waste Recycling Action Programme (WRAP)
Wexham Developments
Zwick Testing Machines Ltd

SUPPORTING INSTITUTIONS

American Society of Civil Engineers
Austrian Concrete Society
Belgische Betongroepering, Belgium
Concrete Institute of Australia
Concrete Society of Southern Africa, South Africa
Concrete Society, UK
Concrete Association of Finland
Czech Concrete Society
Entreprises Generales de France, France
European Concrete Societies Network
Fédération de l'Industrie du Béton, France
German Society for Concrete and Construction
Hong Kong Institution of Engineers
Indian Concrete Institute
Institute of Concrete Technology, UK
Instituto Brasileiro Do Concreto, Brazil
Irish Concrete Society
Japan Concrete Institute
Netherlands Concrete Society
New Zealand Concrete Society
Norwegian Concrete Association
Singapore Concrete Institute
Swedish Concrete Association

CONTENTS

THEME 2: DEVELOPMENT IN REINFORCEMENT MATERIALS

THEME 3: DURABILITY/MAINTENANCE OF COMPOSITE CONSTRUCTION

FIBRE COMPOSITES IN CIVIL ENGINEERING: AN OPPORTUNITY FOR A NOVEL APPROACH TO TRADITIONAL REINFORCED CONCRETE CONCEPTS

G Van Erp

C Cattell T Heldt

University of Southern Queensland

Australia

ABSTRACT. This paper presents research findings of an ongoing project into the structural behaviour of a new type of composite bridge beam. The concept combines the high compression capacity of plain concrete with the high strength/low weight characteristics of fibre composites. The basic concept is presented together with a range of static and dynamic test results of small and full-scale beam experiments. The paper finishes with a brief description of the composite bridge design that will be constructed and commissioned in Toowoomba, Australia, in January 2002.

Keywords: Fibre composites, Concrete, Hybrid solutions, Beams, Bridges, Prototype construction, Testing.

G Van Erp is the Executive Director of Fibre Composites Design and Developments (FCDD) and holder of the Composite Institute of Australia research chair in fibre composites. Gerard's career in structural engineering spans 25 years, the last seven in fibre composites R & D. During this time he has been the principal design engineer for a range of large composite structures including Australia's first fibre composite bridge.

C Cattell is a Research Engineer with FCDD specialising in finite element analysis and structural testing.

T Heldt is a Senior Research Engineer with FCDD concentrating on bridge monitoring, strengthening and rehabilitation.

INTRODUCTION

The technological revolution in materials and processes which has occurred over the past 60 years has had a significant impact in almost all sectors of the manufacturing industry. However, the influence of these developments on the construction industry has been significantly less. Due to the disproportionately low research investment in comparison to construction expenditure, the building industry has proceeded on a large scale with only limited innovation. For many decades now steel, concrete and timber have been the dominant construction materials in civil and structural engineering. Even though this situation is likely to continue for quite some time, a number of advanced materials have recently started to make inroads into the construction market. Fibre composites, with greatly improved corrosion resistance and durability, low weight and high strength, ease of transportation, low thermal conductivity, non-magnetic properties and lower energy consumption during manufacture, are about to become an important part of the engineer's response to the construction challenges of the new century.

Many civil engineers are sceptical of these new developments and are yet to be convinced of the potential of fibre composites as structural materials. What most of these engineers do not realise is that reinforced concrete, one of the most successful structural materials available today, is a fibre composite material in its own right. It is based around the use of large steel fibres (re-bar) in a concrete matrix. Fibre composites use the same principle except that the steel fibres are replaced by a large number of synthetic fibres and the concrete matrix by a polymer matrix. In a sense fibre composites are a logical extension of a very successful century old concept.

The introduction of fibre composites, more appropriately referred to as Fibre Reinforced Polymers (FRP), into civil engineering creates the opportunity for a new and innovative approach to structures that have undergone little change for the last one hundred years. This is particularly true for reinforced concrete structures, which despite their success suffer from high self weight and potential corrosion of the steel reinforcement in aggressive environments. Fibre reinforced polymers on the other hand are light weight and have excellent durability with minimal maintenance requirements.

Since reinforced concrete and polymer composites are based on the same basic principle it is worthwhile to investigate if these materials can be combined to create a new superior structure. With this philosophy in mind, the fibre composites research group FCDD at the University of Southern Queensland has developed a new generation composite beam that outperforms traditional reinforced concrete beams in a number of areas. This project started several years ago and following an intensive testing program on individual components, has resulted in the construction of Australia's first full scale (10m span) fibre composite bridge in late 2001.

The basic concept discussed in this paper has been developed independently by a number of other researchers [1,2]. However, the way in which this concept has been translated into a real beam structure is significantly different in the current project. This paper describes the philosophy behind the developments and presents a range of experimental results. The findings confirm the advantages of this new concept such as high load carrying capacity, excellent fatigue behaviour, ability to carry concentrated traffic loads and low cost compared to other polymer composite solutions.

This project has benefited greatly from close collaboration between university researchers, industry and the Australian road authorities. The collaborators in this project are Wagners Composite Fibre Technologies, Huntsman Chemical Company Australia, Queensland Department of Main Roads, Connell Wagner consulting engineers and Roads and Traffic Authority NSW.

Since the majority of the funding for this project was provided by the industry partners, certain design and manufacturing details are not included in this paper for commercial reasons.

BASIC DESIGN APPROACH

Figure 1 shows the basics behind the reinforced concrete beam concept. For slender beams under flexural loading it is assumed that the strains vary linearly over the depth with compressive strains in the top and tensile strains in the bottom part of the beam. The tensile strength of concrete is extremely low and is ignored when determining the ultimate load carrying capacity of the beam. Consequently the main load carrying elements of the beam consist of the concrete compression zone (approximately 20-25% of the cross section) and the steel reinforcement.

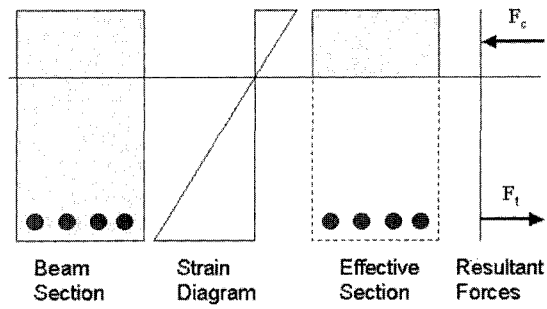

Figure 1 Basic principles of reinforced concrete beams

As indicated previously, the two main disadvantages of reinforced concrete beams are the potential corrosion of the reinforcement and the high self weight. The latter in particular is an important issue given the fact that 75-80% of the material that contributes to the weight does not directly contribute to the overall load carrying capacity. This is not only inefficient but also wasteful from a natural resources perspective. The low cost of concrete is probably the main reason that this has not been a major issue in the past.

The potential corrosion of the reinforcement is a concern in a number of environments. A possible solution to this problem is the replacement of the steel reinforcement by FRP reinforcement, shown schematically in Figure 2. This replacement is relatively straightforward and is currently being investigated at a number of research institutions around the world. Carbon, glass and aramid rebar is available from a number of producers and design guidelines are rapidly becoming available. However, this replacement only addresses the corrosion issue, it does not provide any significant reduction in the self weight.

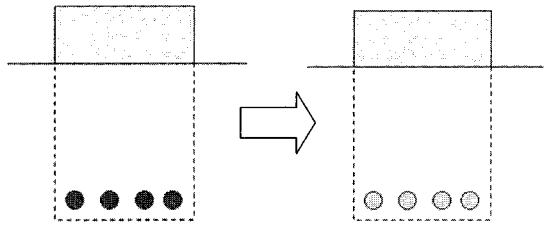

Figure 2 Replacement of steel rebar with FRP rebar

Once the steel reinforcement has been replaced with FRP, the main function of the cracked concrete is to locate the tensile elements relative to the compression zone. Using a large amount of concrete for this purpose is not very efficient. In order to address this issue it is important to realize that locating a number of individual bars is considerably more difficult than locating a single tensile flange. Hence, replacement of the FRP bars with a continuous FRP tensile flange is the logical next step (Figure 3).

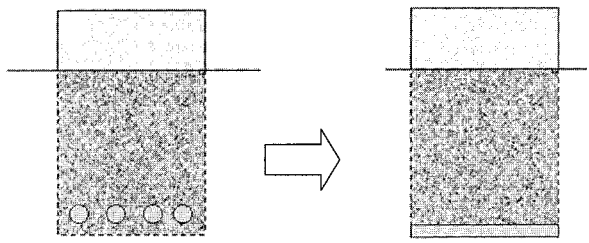

Figure 3 Replacement of FRP bars with a continuous FRP tensile flange

A continuous tensile flange can be easily positioned using a single or double web as is common for steel beam cross sections. Figure 4(b) shows the replacement of the cracked concrete with two FRP web members. By orientating the fibres in the web members at $+45^{o}$ and -45^{o} the webs are ideally suited to carry the shear forces in the beam thereby eliminating the need for any shear stirrups.

By removing the cracked concrete from the cross section an additional problem is created. The cracked concrete not only located the reinforcement relative to the compression zone, it also enabled the compression zone to carry localised loads. In order to reinstate this capability additional FRP reinforcement will have to be applied under the concrete compression flange (Figure 4(c)). Composite action between the concrete and the FRP reinforcement can be achieved through use of a high quality epoxy adhesive. Finally, additional carbon fibre reinforcement can be added to the tensile flange in order to increase the stiffness of the beam (Figure 4(d)).

The final cross section combines both traditional and new high performance materials to create a highly optimised structure. Each component can be tailored to suit specific structural functions, which is economical and resource efficient. Such optimum combination of materials in structural design is becoming increasingly important in a highly competitive society.

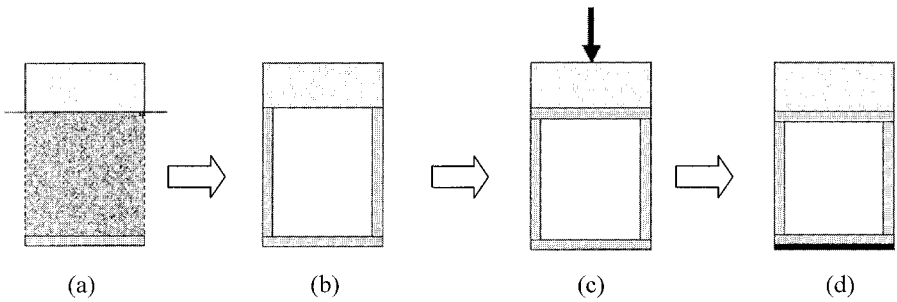

Figure 4 Transition of concrete cross section

STRUCTURAL BEHAVIOUR OF NEW DESIGN CONCEPT

The hybrid concrete-composite cross section can fail in a number of possible ways depending on the final detailing of the concept. Deskovic *et al.* [1] mention that in a well designed hybrid beam the carbon laminate should fail first in order to give warning of collapse. Once the carbon has failed the stresses are redistributed and the section continues to carry load until the concrete fails in compression. According to [1], crushing of the concrete defines flexural collapse of the beam. The arguments used are correct for their specific approach but they are not the only way things can be done. In fact trying to achieve failure of the carbon first results in relatively deep beams, which can be a disadvantage in a number of cases. This can be easily demonstrated by considering the strain distribution in the cross section.

Standard T300 carbon has a failure strain of around 1.0 to1.5% while concrete crushes at approximately 0.3%. Assuming that the neutral axis is located just under the concrete flange, the depth of the FRP part must be around 5 times the depth of the concrete to ensure that the carbon fails first. Consequently, once the thickness of the concrete flange has been determined, the minimum depth of the beam is fixed. For example, the 10m span bridge beam considered in this project requires a concrete flange with a thickness of approximately 100mm to be able to carry a 180kN concentrated wheel load (Australian Bridge Code [3], strength limit state). Based on this depth of concrete, a 600mm deep beam is required to achieve failure in the carbon before crushing of the concrete. This is close to twice the depth of most 10m span prestressed concrete bridges in Australia, which are approximately 350mm deep. Deep beams are generally undesirable in bridges as they result in increased flood loading and costs for the bridge approach works.

The reason that the hybrid beam of Deskovic *et al.* fails when the concrete crushes is that the top flange of the FRP section is given a wall thickness just equal to that required to carry the wet concrete. This thin section has negligible compression capacity and once the concrete crushes there is no compression capacity left in the cross section.

The current beam design differs from the above approach in that the FRP top flange is given sufficient load carrying capacity to help the concrete support the 180kN concentrated wheel load and to provide adequate compression capacity once the concrete has failed. In this approach, the cross section reduces to an FRP box section after crushing of the concrete. By ensuring that the ultimate load carrying capacity of the box section exceeds the crushing load of the concrete flange, a very ductile behaviour is obtained. The stiffness of the FRP box section is significantly lower than that of the hybrid section resulting in very large deflections prior to failure.

In the current project the compression capacity of the FRP top flange has been provided in an innovative way, using minimum additional material. In addition, the 50MPa concrete top flange has been reinforced with strong polypropylene fibres resulting in a post failure strength of the concrete of approximately 10MPa. The combined compression capacity of the FRP top flange and the post failure strength of the crushed concrete provide the cross section with enough compression capacity to continue to carry additional load and eventually fail the carbon and glass reinforcement.

Figure 5 shows the load displacement behaviour of a 3m test beam which was designed using the discussed approach. After failure of the concrete the cross section continued to carry additional load while experiencing large deflections. The final failure load was approximately 20% higher than the crushing load of the concrete. The depth of the beam was 275mm and the ultimate deflection was 108mm. Crushing of the concrete top flange occurred at 38mm deflection (Figure 6).

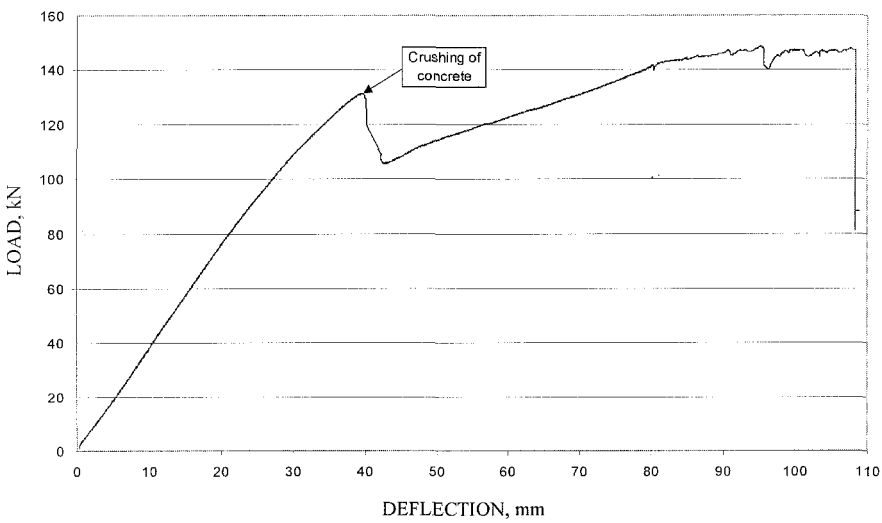

Figure 5 Load – deflection curve for the 3m test beam

In the case of bridge structures, a major advantage of this type of failure behaviour is that crushing of the concrete will show up in the wear surface of the bridge. This is a lot easier to detect than failure in the carbon reinforcement underneath the bridge. Furthermore, localised crushed concrete is relatively easy to repair in comparison to an FRP tensile failure.

Figure 6 Initial failure of 3m test beam.

EXPERIMENTAL PROGRAM

Following the successful findings from the 3m test beam, a 6m and 10m bridge beam were constructed in order to investigate the dynamic/fatigue behaviour of the new concept. The 6m beam was 300mm wide and 325mm deep with a 75mm concrete top flange. The 10m beam measured 350mm x 450mm with a 100mm concrete top flange. The reduced scale 6m beam was included because it is the maximum size beam that can be loaded to failure in FCDD's testing laboratory. At this stage FCDD does not have a loading frame strong enough to break a full scale 10m beam.

Four different types of dynamic tests were undertaken:

1. Dynamic loading of the 6m bridge beam at serviceability loading for 1 million cycles with subsequent loading to failure;
2. Dynamic loading of the 10m bridge beam at serviceability loading for 2 million cycles with periodic overloading;
3. Dynamic loading of a 1m section of the 10m span beam under a concentrated wheel load for 2 million cycles with periodic overloading;
4. Determination of the natural frequency of the 10m span beam.

6m Beam

A 6m scale test beam was constructed to investigate the fatigue performance of the beam, as well as the damage tolerance and end-bearing behaviour. A number of holes of sizes between 25 and 40mm were cut in the sides of the beam to simulate the effect of the holes required for lateral post-tensioning, and potential damage by vandals (Figure 7a). The beam was supported on mortar pads on top of two concrete blocks to simulate in-service conditions (Figure 7b). The beam was loaded, for 1 million cycles at 1Hz, at a level which generated strains equal to those achieved in a full-scale 10m bridge beam under the maximum allowable serviceability deflection. Periodic static tests from zero-load up to the serviceability load were taken to check for stiffness changes, and after 1 million cycles the beam was tested to failure.

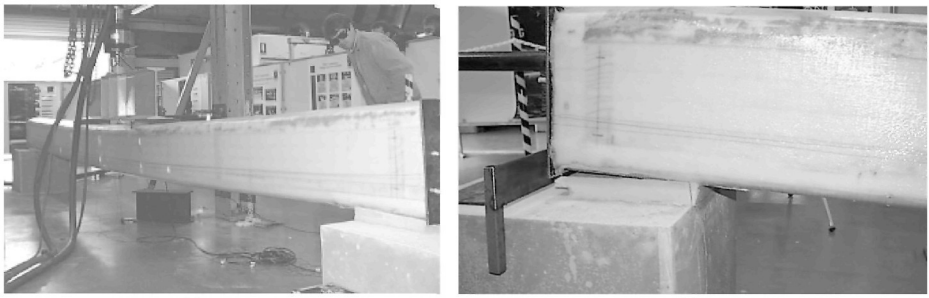

(a) (b)

Figure 7 (a) 6m test beam (note holes in the side) (b) End bearing prior to beam failure

The dynamic testing showed no noticeable impact on the stiffness of the beam, with the load displacement behaviour before and after testing being exactly the same (Figure 8). The end bearing of the beam onto the supports also showed no problems. Even under the line load condition which occurred under the high load, high deflection conditions shown in Figure 7b the beam continued to perform well. The beam failed at the predicted load in a manner similar to that shown in Figure 5.

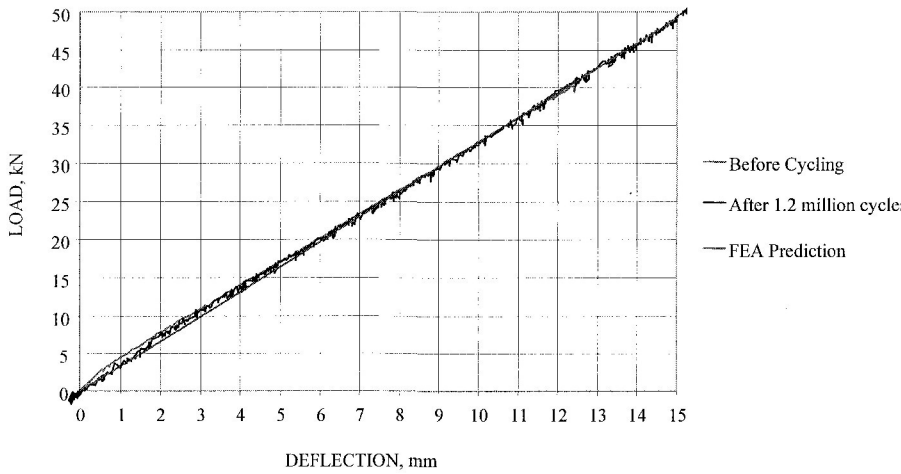

Figure 8 Load deflection behaviour of 6m test beam

10m Beam

The full scale 10m beam was designed to maintain a hog under serviceability conditions through a 30mm pre-camber. The design was governed by the deflection requirement of less than span/500 under serviceability traffic loading. This resulted in considerable excess strength in the beam. The serviceability traffic moment is 65kNm, while the design moment

capacity of the beam at initial failure of the concrete is in excess of 550kNm (at a deflection of 160mm). The residual composite box section left after compression failure of the concrete has an ultimate design moment capacity of almost 700kNm, at a deflection of approximately 550mm.

The beam was initially subjected to an applied load of 30kN at midspan, for 1 million cycles at a rate of 1Hz, to produce the serviceability bending moment of 65kNm in the centre of the beam. This resulted in a midspan deflection of 15mm (L/667). This defection generates a maximum compressive strain in the concrete of 0.018% (180με) and a tensile strain in the glass reinforcement of 0.055% (550με). Given that the failure strain of the unidirectional E-glass laminate is approximately 1.6%, this serviceability strain level represents less than 3.5% of the ultimate strain capacity. At such small strain levels fatigue is not likely to be a problem. This was confirmed in the testing with no indications of deterioration or damage either visually, or in the deflection and strain readings.

As pointed out by the Australian road authorities, trucks in excess of three times the legal limit have been detected on roads in remote parts of Australia. This represents a gross vehicle mass of approximately 120 tonne. These extreme loads can initiate cracks or cause damage in a bridge structure, which may propagate under subsequent dynamic loading, resulting in a significantly decreased life span. To replicate the effects of these extreme loads on the test beam, a periodic overload was applied to the beam every 100,000 cycles. Each periodic overload consisted of two static tests to a specific level of overload, the first at a loading rate of approximately 50mm per minute, immediately followed by a second overload at a rate of approximately 400mm per minute.

During the initial 1 million cycles applied to the beam, a periodic overload of 100kN (about three times serviceability) was applied to the beam every 100,000 cycles. There were no indications of damage. The load spike was then increased to 150kN, 5 times serviceability, every 100,000 cycles for the next 500,000 cycles. As there were still no indications of damage, the periodic overload was increased to 220kN, approximately seven times serviceability. This overload was applied every 100,000 cycles for another 500,000 cycles. This level of overload is 2.5 times the ultimate design load and generated a deflection of 100mm in the beam (Figure 9). Once again there were no indications of deterioration or damage either visually, or in the deflection and strain readings.

Figure 10 shows that the load-displacement behaviour of the beam continued to be linear and consistent even at high levels of overload. At seven times overload, the concrete had a maximum compressive strain of 0.14% (1400με) and the laminate had a maximum strain of 0.3%.

In total the 10m beam underwent 2 million cycles (4 times the requirement of the Australian Bridge Design Code) at the serviceability traffic load, as well as being loaded 16 times to 100kN, 10 times to 150kN, and 12 times to 220kN.

There is currently no testing frame in FCDD's testing facilities that is strong enough to fail a 10m beam, however it is planned to take this beam to another research facility in Australia that has the capacity to test the beam to failure early in 2002.

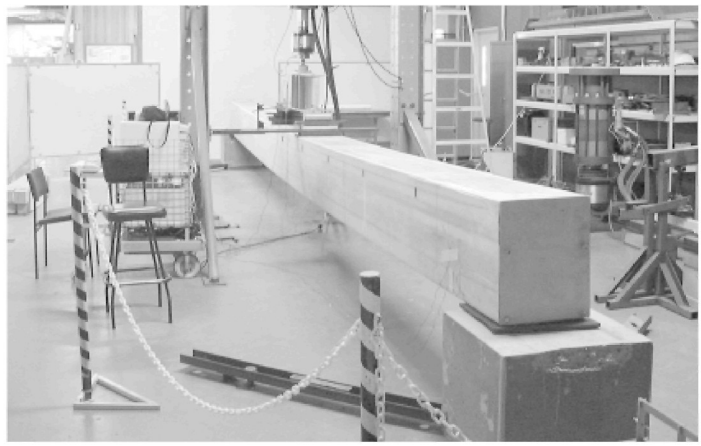

Figure 9 10m test beam under seven times serviceability load

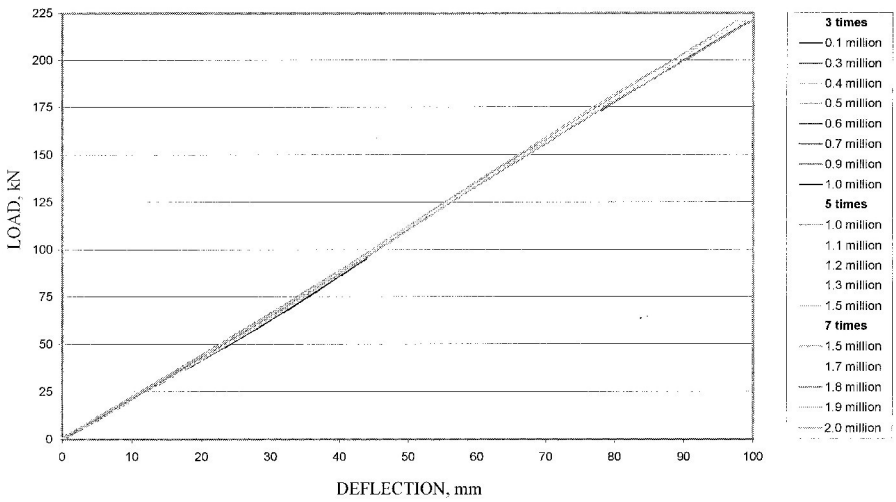

Figure 10 10m test beam - periodic overload graphs

Concentrated Wheel Load

Due to the relatively low Modulus of Elasticity of fibre composites, most FRP bridge beams and decks suffer from buckling and delamination under high localised wheel loads. In the current solution the concrete flange essentially insulates the composites from localised pressures, which eliminates most associated buckling and delamination problems. In order to test the behaviour of the present concept under a high localised load, a 1m long section of the 10m span bridge beam was constructed. The bottom flange of the section was fully supported and a localised load was applied to a 300mm x 150mm loading plate (Figure 11).

Fatigue testing under a serviceability load of 100kN was undertaken for 2 million cycles at 3Herz. To simulate periodic overloading, the load on the section was increased twice daily to 200kN as part of the standard 2 million cycles testing program (200kN is 10% higher than the Ultimate Strength Limit State loading). No visual or aural evidence of damage was noticed during this testing program. However, the reading of one of the strain gages located under the concrete changed slightly after the first overload which could be the result of some micro cracking in the concrete. The reading did not change with further cycling. An error in the loading during one of the load spikes took the load to 260kN almost instantaneously. Some change in the strain gauge reading was noticed but once again there was no further change during the remainder of the dynamic testing.

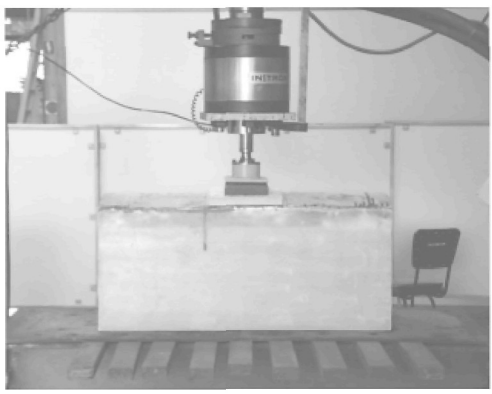

Figure 11 1m beam section under localised load

After 2 million cycles the load on the cross section was increased to 500kN (the limit of the hydraulic actuator). The section carried this load without any noise or noticeable deflection.

This concentrated load test is more severe than any loading condition that is likely to occur in a real bridge. In most cases there will be a 50-100mm asphalt concrete wear surface on the bridge which will spread the concentrated wheel load over a significantly larger area than that used in the test. Since the 500kN actuator is the largest available in FCDD's testing laboratory, the section will be taken to a research facility with a 1000kN actuator early in 2002 in order to try and determine the ultimate load carrying capacity of the cross section.

Natural Frequency

The natural frequency of the beam was determined by attaching an accelerometer to the beam and impacting it with a rubber mallet. This method yielded a natural frequency for the beam of approximately 9Hz, which is in close agreement with the finite element analysis value of 8.5Hz.

BRIDGE DESIGN CONCEPT

Initially, the bridge design was based on the traditional plank bridge concept, in which a number of individual beams or planks are laterally post tensioned to create a bridge. The advantages of this concept include:

- No joints between deck and girders (the girders are the deck);
- Excellent resistance against flood loading and side impact;
- Significant redundancy in the structure due to large number of beams;
- The concept is well understood by bridge engineers;
- Significant understanding of the bridge behaviour can be obtained through testing of individual beams.

Given the fact that the FRP part of the hybrid beam is significantly more flexible than concrete, questions were raised regarding the effectiveness of the transverse stressing. In order to investigate this issue in more detail a half scale model of the bridge (5m span, 3m wide) was constructed. This half scale model also created an opportunity for the civil engineering contractor to become familiar with the manufacture of this new type of fibre composite bridge. Figure 12 shows a picture of the 5m bridge being lifted into place.

Figure 12 5m test bridge being lifted into place

It was found that there was a significant loss of pre-stress due to the flexibility of the fibre composites. The bars had to be re-tensioned a number of times before the structure finally settled down and the pre-stress stayed relatively constant. Even though the system seemed to work in the end, the project participants did not feel comfortable with the findings and it was decided to replace the transverse stressing with a composite laminate in transverse direction along the bottom of the beams (Figure 13).

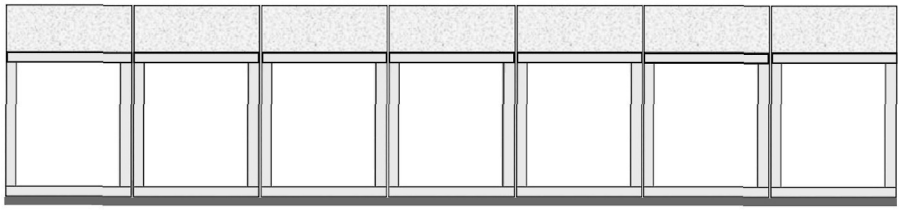

Figure 13 Cross section of 2.5m bridge section

A full-scale bridge (10m span, 5m wide) is currently under construction and is expected to carry traffic loading by the end of January 2002. The bridge will be constructed as two 2.5m wide sections that will be jointed on site. The overall bridge weighs approximately 20,000kg (excluding the bitumen wear surface) and the installed cost is very similar to that of comparable pre-stressed concrete bridges.

The bridge will be constructed in a quarry road approximately 10 km west of Toowoomba. This site has been selected for the following reasons:

1. It is a road with restricted access to the public and as such eliminates many liability issues associated with the testing;
2. A large number of heavily loaded vehicles (more than 150 per day) will cross the bridge prior to their entry to the public road network;
3. The site is immediately adjacent to a weighbridge, meaning that load effects can be accurately determined;
4. The site is secure, offering increased protection for expensive testing and long term monitoring equipment.

FIELD TESTING

Extensive field testing will be conducted to investigate the in-service performance of the bridge structure. The objectives of field testing are:

1. Investigate the performance of the bridge under typical heavy vehicle loading;
2. Investigate the dynamic response of the bridge structure, and the bridge – vehicle interaction.

This testing requires two different sites in the quarry. One of the sites will be in a straight road which allows the trucks to get up to 100km/h safely and the other site will be close to the loading area of the quarry trucks in order to get a steady stream of heavy traffic over the bridge for six months. Due to the lay out of the quarry there is not one site that can handle both types of testing in one location. Due to the light weight of the bridge, it will be moved from the first site to the second using a standard wide body truck.

Approximately 100 transducers will be installed on the bridge. A HMX bridge health monitoring system will be used to monitor the transducers, although not all transducers will be monitored simultaneously. The monitoring programme is quite comprehensive and consists of four phases as follows:

Phase 1

This involves the systematic testing of the instrumentation system. This will facilitate an understanding of the response of the bridge to diurnal cycling, and verify that the various strain gauge locations are responding in a predictable manner. In addition, some moderate magnitude static loads will be passed over the bridge prior to installation of the wear surface, kerbs and guardrails. This allows for the effect of these components on bridge performance to be investigated.

Phase 2 and 3

Phase 2 will investigate the response of the structure to a steel suspended body truck. Generally, tests will run with the truck travelling along the centre of the bridge. The effect of vehicle mass, travel direction, and vehicle speed will be investigated. While the vehicle is at maximum mass, crawl tests will be completed on either side of the bridge from both directions to investigate the transverse behaviour and load distribution of the bridge. Again at full mass, and varying speeds, the effect of placing a full width bump immediately before the bridge will be studied. Similarly a half width bump will be placed on the bridge to investigate the effect of asymmetry on bridge response. Phase 3 will be a repeat of phase 2, but with an air suspended vehicle.

Phase 4

The bridge will be health monitored for approximately 6 months in a site adjacent to the weighbridge. Health monitoring allows for the response of the bridge, subject to known heavy vehicle traffic, to be investigated for a more prolonged period.

Phases 2 and 3 combined allow quantification of the following factors on bridge response:

- Vehicle suspension type;
- Vehicle mass;
- Vehicle speed;
- Irregular approach surface.

In addition, natural frequency and damping will also be determined from these results. By comparing the results from Phase 1 with Phases 2 and 3, the effect of the asphalt concrete wear surface, kerbs and guardrails will become apparent.

CONCLUSIONS

The experimental results of this project have demonstrated that advanced fibre composites and concrete can be combined in a very efficient way to produce a new type of composite beam that outperforms traditional reinforced concrete beams in a number of areas. The advantages of the new concept include high load carrying capacity, excellent fatigue behaviour, outstanding durability, ability to carry high concentrated loads and low cost compared to other polymer composite solutions. The failure behaviour of this new type of beam is very predictable and provides ample redundancy and warning of failure. Analytical and numerical predictions of the behaviour agree well with experimental results.

ACKNOWLEDGEMENTS

The authors gratefully acknowledge the financial and technical support provided by Wagners Composite Fibre Technologies, Huntsman Chemical Company Australia, Queensland Department of Main Roads, Connell Wagner Consulting Engineers, Roads and Traffic Authority New South Wales, Zoltek and the Composites Institute of Australia.

REFERENCES

1. DESKOVIC, N., TRIANTAFILLOU T AND MEIER U (1995), Innovative Design of FRP Combined with Concrete: Short-Term Behaviour, Journal of Structural Engineering, Vol 121, No.7, July 1995, pp 1069-1078.

2. CANNING L, HOLLAWAY, L AND THORN, A M, (1999), Manufacture, testing and numerical analysis of an innovative polymer/concrete structural unit, Proc. Inst.Civ Engrs. Structures and Bridges, Vol. 134, pp 231-241.

3. AUSTROADS (1992), Australian Bridge Design Code, Section2 - Design Loads. AUSTROADS Publication No. AP-15.2

THEME ONE:
STRUCTURAL DESIGN CONSIDERATIONS

Keynote Paper

COMPOSITE MATERIALS IN CONCRETE CONSTRUCTION

P Lowe
University of Auckland
New Zealand

ABSTRACT. In this paper questions are asked about the future prospects for the traditional bar reinforced concrete composite material. The paper is not a general survey of the entire field of concrete composites. Steel is the only reinforcing material considered but this reinforcement may not necessarily be employed in bar form. The main content in the paper is a list of criteria in the nature of ' ideal' properties for a construction material. These criteria are not of equal importance, and only some appear to have present day appeal for the Industry. No new experimental data are presented. Instead, more philosophical aspects of our subject will be discussed. It is argued that innovation in new construction technologies should be welcomed, and studied to ensure the long-term health of the entire sector. In the concluding sections, one possible practical material for achieving many of these supposed (ideal) properties, so called Externally Reinforced Concrete, is reviewed.

Keywords: Innovation, Invention, Appropriate technology, Efficiency of construction, Standards, Environmental sustainability, Ideal construction materials, Mechanisation of the construction process, Waste reduction in construction.

Peter G Lowe is Emeritus Professor of Civil Engineering in the University of Auckland, New Zealand. His most recent interests have included researching new construction technology, use of waste materials in construction and engineering heritage.

INTRODUCTION

All indigenous construction industries are of immense strategic importance and capital value to their respective countries. In world terms construction is one of the most universal of all industries. Portland cement concrete is a key component in construction materials and is used in almost all construction. The ramifications for the use of Portland cement concrete are the core interest for these Dundee Seminars and Conferences.

As the new millennium unfolds, new challenges emerge for the engineering profession, the construction industry and the public, to wrestle with and find solutions to. On the 26th January 2001, in mid-morning, the Gujarat Earthquake, magnitude 7.9, occurred and left a fearsome toll of death and destruction on that whole surrounding area in India. This stricken region experienced what is all too common: communities almost instantaneously wiped out in a natural disaster. Among other outcomes, there was massive destruction of concrete buildings. A common element in many such sorry sagas is that they point to the need for *more effective use of the concrete materials*. The typical scenario is that a technology appropriate to a developed country, in this case conventional bar reinforced concrete material technology, is probably being applied in an economic and social environment where the technology is not built to adequate inspection and safety standards. The result is often suspect buildings and construction, which the earthquake unerringly exposes, with all the attendant human and economic consequences when damage occurs.

It is evident from the number of papers being presented at these Seminars and Conferences that even in the developed countries, this now mature technology is not fully understood. The destruction reported in high profile and very damaging events such as earthquakes, almost always includes widespread damage and collapse of reinforced concrete buildings. Many of these collapsed structures would not have collapsed had they been built to the relevant Western Standard. We must ask the question: are there basic deficiencies in the current technology and/or its application? Because this is a situation that is repeated over and over again, worldwide and all too frequently, an interim, answer to the question must be, Yes, there are basic deficiencies.

The technologies employed in the construction industry are largely divided into those that use concrete as the basic material and those that use steel. There is uncomfortably little dialogue between these two dominant technologies. Although it was no doubt not in the organisers mind when deciding upon inviting speakers to talk to particular topics, my choice here is to broaden my scope to include steel as a stand alone construction material and as a possible choice in the present study.

Now since we are considering steel/concrete composites, any proportion of either material is therefore potentially a choice, from pure concrete at one limit, through composites of various proportions of each material to pure steel at the other limit. At a 'concrete' conference this may seem an odd decision. The object is to allow a wide-ranging review of the (ideal) material property requirements. No one particular composite of concrete and steel is being preferred at this stage.

The review then leads to the conclusion that there are some reasonably specific combinations of the two materials that best incorporate the major (ideal) features for a building material, and that indeed the steel-only option is not the best choice.

As engineers we cannot be in the least complacent. Huge effort and expense have been applied to the better understanding of reinforced concrete construction over tens of decades: this series of Conferences is some current testimony to this massive effort. Additionally, many thousands of engineers have spent whole careers studying the material and the technology applied in earthquake situations, now for generations. But since the 'Gujirat' situation keeps arising there obviously is still a long way to go before the possible future beneficial possibilities have been exhausted. We must almost take as an axiom that improvements are possible using the materials at hand.

APPROPRIATE TECHNOLOGY

One proposition to be debated must be the wisdom of applying developed country technology in less developed countries, where it may not be appropriate! Given the massive expenditure over the years that has been made in studying construction and building technology in the developed countries, not to forget the code writing and certification regimes which have grown up, there are paradoxical aspects to this statement. The paradoxical aspects relate to the obvious inability for the typical less developed country to generate its own building technology. If unable to generate its own then it is more likely to adopt technology from elsewhere, and most likely from the developed world. The history of building technology is usually one of slow adoption in the country of origin. As an extension of this it should not be surprising if transplanted technology often does not succeed in the transplant environment!

If there are better ways to employ the concrete materials then these other ways must command our attention. On the other hand, if there are *not* better ways to employ these materials then there can be no proper justification for the holding of Seminars such as the present series. Which is the case? Our premise in this paper is the optimistic view that there are indeed better ways to employ the materials. Then the onus on all the parties is to identify what these improved methods might be, and to study them with vigour.

In many respects, of all the industries worldwide, the construction industry is one of the most *conservative*. This conservatism has both positive and negative aspects. First there is the positive aspect of *continuity* that conservatism implies. For example there are certain broad features of construction and building that have remained largely unchanged for long periods. The Roman engineer, Vitruvius, writing in about 20 BC and whose work is the only written record of construction which has survived from ancient times, can be read today in modern translation [1]. There is a good educational case for us all to read this work at intervals during our working careers.

Much of the content of the 'Ten books of architecture' describes buildings and structures that are not greatly different from some of the structures being built for similar purposes today. But in at least one very important respect the Roman buildings are different, namely they were very largely constructed from masonry (also brick and timber) where today a cement-based material and/or steel would be used, not forgetting the concrete dome of the Pantheon. And of course there is a vast amount of additional knowledge, materials and equipment that can now be applied to construction, which was not available in those earlier times.

The rival material, steel, as a material available to satisfy the demands of the construction industry, has been produced in bulk for about 150 years. This is about the same length of time that modern cements have been manufactured in bulk. During most of that time there have

been innovators producing inventions. They have sought to use the steel as a premier construction material.[1] All-steel construction is a competitor for reinforced concrete, and the two industries and technologies have always coexisted, with minimal contact or technical cooperation, even though bar steel reinforcement is the almost universally used tensile component in composite with concrete. But is steel bar the most suitable or desirable reinforcing material? Steel bar has been used as the reinforcement in concrete in largely an unchanged form for more than one hundred years. What does the future hold for the continued use of this form of steel in association with concrete? This is one of the key questions that we consider in this paper.

Reinforced concrete using bar reinforcement has been in use for more than one hundred years, and has been used very successfully. Why should there be any suggestion that other alternatives should be considered? Evidently there is still a need for (large) seminars and conferences, such as the present series, where essentially this bar-reinforced material is at the centre of the discussion.

In this paper the proposition we follow is that there are many possible radical, new developments in reinforced concrete, based on a composite with steel. It is the primary function of this paper to work away at the notion that some of these new composites do indeed offer prospects for a superior material to the current norm. And it is here where the question of *conservatism* in the industry plays such a vital role. If conservatism prevails, then radical new composite materials will not be examined and will certainly not be adopted. The challenge, it is suggested, is to create the environment in the engineering profession, the construction industry and the consuming public for major new technology to be seriously considered and then, if the prospects are sufficiently attractive, to be adopted and further developed. This must be the way forward!

Of course any new technology must offer advantages over the existing alternatives. It is one function of Seminars and Conferences, such as the present series, to provide the forum for reviewing the technical backup where many of these questions can be discussed.

In this paper we seek to identify a series of features which our ideal composite technology should incorporate. This is the core of the paper. As an illustration of some of these features we then discuss one possible new composite as an example of what could emerge in the future as a new generation of building material for use in concrete composite construction.

FEATURES OF AN 'IDEAL' CONSTRUCTION MATERIAL

As has already been stated, here we are primarily considering steel/concrete composites. Conventional reinforced concrete is the current standard material. Some would say that the present material satisfies all the reasonable needs, and that there is no usefulness in seeking to change it or research alternatives. The premise here is that there *is* a need for change, or at least there is a need to consider what could possibly be achieved by change.

---

[1] Here the nouns innovation and invention are being used almost as synomyms. Hewlett [2] makes a distinction, and suggests that innovations are to be preferred to inventions in the construction context. This paper of Hewlett's , which occupied a similar position in the 1999 (fourth) Dundee Conference series to the present paper in the 2002 (fifth) Dundee Conference series, should be regarded as preliminary reading for the present paper.

At this stage we do not know the configuration of any new product that might emerge. It could look very similar to the current material, reinforced concrete. On the other hand it could be substantially different. As few constraints are possible are being placed on the product, at least during this early investigative stage.

First we seek to identify the features that the ideal steel/concrete composite material should possess. Then we consider whether a material displaying some or all of these features can be made for regular application and use. The more important items will be expanded upon later in the paper.

The list of IDEAL FEATURES for a construction material (and an associated method of construction) should include the scope to achieve some or all of the following. There may not be general agreement on one or more of the statements, and the relative importance of each is not at present being discussed.

A. An over-riding aim in all aspects of the construction process, from the choice of materials to the finished structure, should the aspect of *simplicity* of the operations. Associated aspects are that the materials should be simple to produce in industrial terms, with as little waste and pollution production as possible. Using a temporary formwork for concrete could be justified on cost grounds but would lead to waste when the formwork is discarded. Such a choice would not fit with our present criteria. Permanent formwork is one possible, acceptable alternative. Courses of instruction in most Universities tend to emphasise safety for the adequacy of a design before simplicity of construction, and this is a reasonable starting point. At some point in the professional life of the designer the scope to emphasise simplicity, based on experience, hopefully progresses to the point that it can take precedence over safety decisions, which of course would continue to be met.

B. Structures all contain junctions or joints between members and frequently many are one-offs in construction. An ideal is that the actions, the forces and moments at the joint position, should be transmitted through continuous structural material and not through added, load bearing weld material or material specifically required by the jointing function. This feature is particularly relates to all-steel construction. Expressed another way, jointing methods frequently produce solutions that have all the major actions transmitted from member to member through systems of bolts or welds which are serving only jointing functions. These are locally the weakest sections in both strength and stiffness terms in the construction. Recent earthquakes, such as the 1994 Northridge Earthquake in California, have shown in dramatic fashion how long accepted jointing systems for steelwork were very poor performers in such (moderate) events, and has lead to major reconsideration. Lapping of the reinforcing bars in traditional reinforced concrete is a widespread practice and is a potential local weakness in the member. The preferred choice of composite discussed below has produced jointing systems that can avoid all of these localised effects of traditional jointing systems.

C. Many components require welds to complete the fabrication. There should be an avoidance of welds that are circumferential, and hence load bearing, in a normal use situation in beams in bending, for example. Longitudinal welds on the other hand are, in general, not transmitting major actions, and are more acceptable.

D. Simplification of the fabrication and assembly processes should be a constant aim. There are many levels of simplification. What is being signalled here is that simplification in the fabrication and assembly operations is most likely to be associated with use of machines to replace manual operations. However, these machines should not be overly sophisticated or expensive since these features would restrict the adoption of the technology in less affluent societies and environments.

E. The fabrication/handling operations, which would involve both the steel and concrete materials, should be achieved by use of the lightest tools and appliances. A corollary is that there should be scope to use a relatively wide range of equipment. Cost is also important. The choices should include lightweight, and 'low tech', equipment

F. There should be the capability of full mechanisation of the processes when used in the more sophisticated economies and industrial environments.

G. The technology employed should not require heavy site lifts. Precasting, tilt-slab and some other construction methods place greater emphasis on lifting capacity than do in-situ methods. Additionally there are 'awkwardness', size and site danger factors introduced when manoeuvring precast elements into position.

H. In-situ concrete should be the norm rather than the exception, with a view to single age concrete in a structure. Concretes of different ages are essentially different materials. They can at most be in contact and, inherently, are not continuous.

I. All concrete should be maintained in an environment where it does not dry out, and hence does not stop hydrating. This is simply stated but difficult to achieve. The surface material is the first to dry, and as will be emphasised in later discussion, is the most important but least protected material in the structure – the cover concrete.

J. Related to drying out is the scope to retain as much mix water as possible to assist in hydration and fire protection. This item has particular relevance for the final composite that emerges as the preferred option – see later.

K. If there is scope available to create tubular members this represents a best case scenario given their inherently better torsion properties as compared with open sections. A related desirable feature is scope to create hollow members. 'Hollowness' provides a means to achieve several other features as a by-product, including secure housing of services.

L. A primary requirement is that the material should respond in a ductile manner, in all circumstances. Much progress has been made in providing a degree of ductility to bar reinforced concrete. This is however only a limited and imperfect ductility and is not easily further enhanced. The position will be reached later where a much closer approach to ideal ductility can be achieved if the bar reinforcement is exchanged for reinforcement based on sheet.

M. Associated with the ductility requirement is the supplementary desire to achieve a material that rarely, perhaps never, shows shear weakness or similar undesirable behaviour. Strictly speaking, excluding such behaviour is part of the overall ductility requirement. Given the amount of effort and expense which has been incurred over the years in understanding and designing for ever present shear weakness potential in

conventional reinforced concrete, specific mention should be made of this feature. In the case of bar reinforced concrete, questions of the adequacy of the bond between the bar and the concrete must also be achieved. The associated feature of bar lapping is dealt with below. Bond between the bar and the concrete is an important property. It is also a property that other composites of steel and concrete may not require.

N. The practice of lapping bar reinforcement should be systematically phased out, particularly so in environments where there is even the slightest risk of earthquake damage. The 7.2 magnitude Great Hanshin, also known as the Hyogoken-Nambu or Kobe, Earthquake of 17th January 1995 [3] should be required study for us all. Kobe, a modern city in one of the most technically sophisticated economies in the world, was largely torn apart by the earthquake. The age of the buildings and structures was not a significant parameter. New building and infrastructure suffered along with the not-so-new. First came loss of cover concrete, causing lap jointed steel to be exposed. This quickly lead to joint breakdown and frequently subsequent total collapse. These were the features of some of the most spectacular collapses of major structures in Kobe. This one event should be enough to convince us of the need to improve current technology in two very important respects. First, the need to protect cover concrete. Secondly, the need to bring to an end the very crude practice of lapping of bars in concrete structures.

O. Inspection and checking procedures for all stages of the construction process should be adequate, reliable and easily performed. When the important component, the reinforcement, is partly or wholly hidden from view as it is with bar reinforcement, checking is at best difficult. In countries or communities where inspection integrity may be suspect, for what ever reason, failure to comply may go undetected, and the long term consequences can be dire.

P. Unnecessary weight in the finished construction should be avoided. The concrete industry, worldwide, has been slow to produce lighter weight concrete materials that are price competitive. The result is that some of the concrete used is unnecessarily heavy and unnecessarily strong. An ideal would be to devise a cement-based lightweight material that uses waste material, [4]. The strength of such a material could be quite low, around 1 MPa , and still be a very useful choice in building operations.

Q. All the usual features of cost, strength, durability, stability, appearance, fire-safety, scope to repair, environmental aspects etc. for any new material, must at least meet best present practice.

R. If bar reinforcement is to be the continued choice into the future, then methods must be devised for affording protection to the cover concrete. At present no specific protection is provided for this vital part of the material. In the earthquake or similar situation, loss of the cover material is often widespread. This is a prelude to loss of integrity of lapped bars, to be followed thereafter by a general breakdown of the material structure. Loss of this material also presents a difficult repair operation.

As has been said, these (ideal) features are not of equal importance or scope to be achieved. Several of them appear to be of little current interest to the Industry. Let us consider some of them in more detail.

PRIORITIES FOR CHANGE?

Of great importance in any construction, in whatever material, is the degree to which simplicity of the processes can be achieved. If the processes can be made simple then there will be greatest scope for costs to be controlled and quality assured. Simplicity is also compatible with eventual mechanisation of processes. Many of the features included in the list in the previous section can make a contribution to simplicity.

The aim is to control cost without an impact on quality. Certainly the cost should be kept to an affordable level, but minimum cost may be in conflict with other requirements. Best value will require several factors to be considered, of which cost is one component.

A central and costly feature of all current reinforced concrete construction has always been the handling and placement of the reinforcement. Another is the provision of formwork, whether single use, multi-use or permanent. There has been little progress in automating the bar handling processes apart from machine pre-bending of the shapes. Despite much ingenuity on the part of operators and equipment makers, there has been little progress towards automating the bar placing and fixing operations. Any improved future concrete composite technology must make improvements in this part of the construction.

If automation of the bar handling operations is not possible this means that there is limited scope to achieve many of the desired goals in the future. These operations also are a rather grey area in relation to construction tolerances. The specific technology discussed later is capable of being fully automated and of achieving construction tolerances that compare favourably with the best available in the entire construction industry.

Intimately connected with the use of bar reinforcement in our concrete composite are questions about inspection and quality of the product. Even with the best-practice applied in the most rigorous manner, there are practical difficulties to consistently achieving all the bars to be within tolerance for shape and placed all within tolerance in the desired positions in our constructions. If the operator skills are not of the highest order and inspection is in the least suspect, then quality of the product is bound to fall below the ideal and may be lowered to danger levels. Certainly, some recent collapses, even in the most sophisticated countries in a technical sense, can be traced to deficiencies in the bar number and placement.

Connected with these questions of shaping and placing of bar reinforcement are all the associated questions of how the work practices in countries with less sophisticated industries can be expected to cope. There is considerable scope to cheat and for error in this department of the construction. The 'best' codes and the most competent operators can probably achieve a satisfactory product in most countries, but left to local expertise the best codes, even assuming good intentions, are an inadequate safeguard to achieve end product quality. To compound the problem, old reinforced concrete construction cannot easily be assessed for bar numbers or their position. On the other hand, as will be seen later, the composite reviewed later does have this capability, for easy assessment of reinforcement amount and positioning.

The capability of varying the section properties along the length of a member may be difficult to achieve and is seldom exploited. For some steel/concrete composites, such as the example discussed below, it can be achieved both easily and effectively.

ENVIRONMENTAL ASPECTS AND WASTE MINIMISATION

Concrete products are incorporated into a myriad of end products. Much though not all concrete is reinforced, to produce the current composite. Construction waste has become a serious environmental problem [3,5], arising either from new construction waste or demolition. Separating reinforcing bar from a concrete matrix during demolition is an expensive and crude operation. Often there is no attempt at separating the components when a structure is demolished. The materials recovered are of a degraded quality compared with their original condition.

We need to give much thought as to how to curb this build up of construction 'Entropy', by analogy with thermodynamic and information disorder. Unlike the presently used reinforced concrete where orderly recovery is difficult, easy recovery of the steel component in the composite is a feature of the example material discussed below.

In the historical context there is both the greater scale of demolition now as compared with previous ages, as well as the shorter life span of many of the buildings that have been and are being built. What can we expect of the stock of buildings and infrastructure built in a current generation? How many of these constructions will survive for 400, or 2000 years? The trend seems to be towards ever shorter average life span.

DUCTILITY, LIFE-SAFETY AND DAMAGE CONTROL

These topics are most often discussed in situations were, in particular, earthquakes are prevalent, but they can become headline issues when unexpected collapses occur, such as the recent reports of a crowded building space collapsing in Israel. We know that many forms of concrete construction are inherently brittle. Brittleness can be minimised but frequently is not.

Ductility is only partially achieved in the currently used concrete composite. At the limit concrete crushing occurs and strength and stiffness loss results. The ductile response is more easily achieved with steel, but may be curtailed because the member buckles before it yields if the slenderness of the member is high enough. An improved material would offer the prospect of full ductility without attendant buckling and this can be achieved if the composite is made in the manner described below.

Life-safety has for long been a primary goal for earthquake engineers. Much has been achieved to reduce the likelihood of building collapse. In future the additional requirement of also achieving damage control in the structures experiencing e/q effects will add to the design requirements.

Traditional concrete composites are not easily protected to mitigate damage since it is inherent features such as the vulnerability of cover concrete and the bar laps that provide the greatest potential for damage. At present there is essentially no protection afforded to cover concrete, even in the most technically sophisticated countries. But other sorts of composites, in particular the example discussed below, can offer considerable scope to limit damage to the structure.

TECHNOLOGY TRANSFER?

Methods of construction that are fashionable, economic and employed in a developed economy may be quite inappropriate if used in a less developed economy. Tilt-slab and large-scale precasting are methods that are widely employed in New Zealand. These are methods that are less suited to use in less developed economies. Also, according to the 'ideals' listed above, neither method employs in-situ concrete, and the resulting structures will contain concretes of widely different ages in contact with one another. Such different age concretes are at best in intimate contact, but they are not bonded in any sense.

For many reasons building technologies may not transfer successfully. Superficially all the requirements for a successful transfer may be met, but unless all aspects, including inspection and tolerances can be successfully and consistently achieved then the transplant has only limited scope of success.

EXTERNALLY REINFORCED CONCRETE – AN OPTION

We come now to the discussion of a specific composite material that will be reviewed in the light of the various (suggested) ideal criteria for a (concrete composite) constructional material. The selected composite, termed Externally Reinforced Concrete, is what has previously been described at two earlier Dundee Congresses [6,7].

The point of departure from the current composite is the abandonment of bar reinforcement in favour of sheet (steel) reinforcement. If this choice of sheet steel is followed through logically then a large number of the features that have been identified as desirable in the list of 'ideal' features can be quite easily realised in the new composite material. The most obvious of these are, first that the reinforcement is dual purpose – it is both reinforcement and a permanent formwork for the concrete. The material is far more ductile than any bar reinforced equivalent. There is no cover concrete to be damaged. The need to lap reinforcement is removed. All the fabrication operations can be readily automated, and there are many other subsidiary benefits.

Equally important for the quality of the structural product is the manner in which the concrete is handled. In ERC all the concrete is placed, hardens and cures in a near perfect environment of enclosure with the inherent ability to retain all mix water. Drying out of outer surfaces, an ever-present feature of conventional concrete, is eliminated. A whole range of other benefits flow from this feature.

There may of course be possible down-sides, such as corrosion resistance, fire protection and other aspects. These have been studied but the space afforded in this paper does not allow these points to be given adequate treatment.

To recap, the ERC concept is that all members, beams, columns, panels, cladding etc are constructed as hollow steel tubes, folded up from thin coiled steel sheet material and welded longitudinally to complete the tubular shape. Sheet of 2 or 3 mm thickness is a preferred choice for a wide range of member sizes. Such material can be handled, shaped and fabricated essentially as sheet metal rather than as (thicker) steel plate which requires far more heavy duty equipment and work related practices.

Consider first a simple beam in flexure. As illustrated in [6], most beam sections are best constructed as an outer and a smaller inner casing, with the inner case positioned in the tension zone. The annular space between the pair of cases is then filled with in-situ concrete. In a practical situation this would be an operation carried out on site when the beam had been placed in its permanent position.

Such a member proves to be extremely ductile, stiff and strong. No special bond provision is made or needed at the interface steel/concrete, and there is only a minor tendency for the concrete to be forced out of the open end of the case. In many practical situations, the member ends would be closed and in contact with surrounding structure. The bar reinforced material depends critically on effective bond between the bar and the concrete. The ERC material does not depend upon conventional bond. The composite action between the steel (case) and the concrete is generated not by bond but by the containment of the concrete within the casing.

The experimental observation is that members made in this way are very ductile and reach a fully plastic condition if a sufficiently large moment is applied. Since the member is tubular, the torsional properties are excellent. Slenderness is not an issue, despite the use of very thin steel as one of the materials, because the steel is always supported by the adjacent concrete. A simple mechanical model can then be used to explain the observed behaviour. These general features are described in greater detail in the two papers, [6,7], and in the other references included in those papers.

Viewed in terms of the list of 'ideal' properties, such a typical ERC beam can be seen to incorporate the most important of these ideal features as being essentially inherent features of the material. Such a material is probably best categorised as a radial new material. Experience, now over many years, has shown that Industry in the developed economies is inherently not receptive to such classes of product. There are too many new variables introduced into an already multi-variable equation. For these and other reasons, some observers have consistently commented that this type of radically different technology may first find application in less developed parts of the world, where the inertia in the whole system is less, though the practical difficulties may be greater.

The earlier two papers [6,7] describe a range of other features, such as assembly of beams and columns into frames, fire resistance, prestressing etc.. A finished structure is also described. Considerable progress can be made with all of these aspects, and in quite natural ways. In particular, simple and strong jointing systems have been achieved which entirely avoid weak sections at beam/column interfaces- see Item B in the 'Ideal' list.

When considering bi-material combinations, steel/concrete combinations in the present study, various parameters can be defined to describe the ratios used. The ratio of the two material areas in a typical cross-section, r, is one. Another is the material unit weight ratio, m, and a third the material strength ratio, s. There could be others. The product of all such ratios when set equal to unity gives a crude measure of how the materials combine in some useful choices. For the present study of steel and concrete, the primary unknown is r. The value of m is around 78/24 and of s about 350/40 say, being the densities and typical MPa strengths, tensile for steel and compressive for concrete. Typically then r is in the range of $1/(m.s) = 24.40/(78.350)$. This gives a value for r of 0.035. In the typical experimentation reported in [6] and [7] this 3.5% of steel compared with the concrete area is about typical of the experiments described.

Since 1999 the new studies made at Auckland relating to ERC-type technology have focussed on the use of external reinforcement as a means to repair damaged conventional structures. Some of these results may be presented in a paper included in this conference series.

To conclude, we return to the 'Gujurat' earthquake, to questions of appropriate technology, and all the issues that contribute to building quality. The traditional bar reinforced composite is of course what is extensively used world-wide. The relevant codes are written in the wealthier countries and are processed through International Bodies such as the International Standards Organisation. One of many major advantages that an ERC type material has over conventional reinforced concrete is the ability to check the position, amount and type of reinforcement from external observation. The ease of making such checks is important, especially in situations where building quality and site supervision may be suspect. This is a matter of public safety.

If any substantially different building technology is to enter the market place there are many long and expensive avenues to be travelled before acceptance is achieved in the world of international standards. This situation could be reason enough for new building technologies to be trialed in countries where the pressures to build are great, and the requirement to build to ISO or equivalent standards is not appropriate.

Herein lies a paradox since standards are, in principle, designed to protect the public and yet, due to the inertia and cost involved, new technology may effectively be excluded from being employed if there is no relevant standard. There is also a trend over the years for standards to acquire more and more detail, making them less and less relevant for use in the less developed world. Standards are, by their nature, conservative documents. Conservatism in building and construction generally is one of the factors which impinges on new technology at an early stage. New technology we must have, if not today, then tomorrow or the next day! Concrete in all its various forms as used in construction is an essential material and has had a huge contribution to civilisation in the past one hundred and fifty years. Significant technological and social questions remain open as to the future use, scope and nature of concrete construction. There is always a need to review priorities. This paper is intended as a contribution toward a current review.

REFERENCES

1. VITRUVIUS., Ten books of architecture, a new translation by I. D. Rowland, with commentary and illustrations by T. N. Howe, and assisted by M. J. Dewar, Cambridge University Press, 1999.

2. HEWLETT, P. C., Interfacing innovation with best practice, a paper in *Innovation in Concrete Structures: design and construction*, being the content of Conference Three, Proceedings of the International Conference held at The University of Dundee, Scotland, U. K., September 1999, p. 1 – 13, Thomas Telford, London, 1999.

3. PRELIMINARY REPORT on The Great Hanshin Earthquake, Japan Society of Civil Engineers, (Tokyo), 1995, p.346.

4. LOWE, P. G., A lightweight cement-bonded building material, Mechanics of Structures and Materials, Eds. Bradford, Bridge and Foster, Balkema, Rotterdam, 1999, pp 361 - 366.

5. GUTHRIE, P.M., and WOOLVERIDGE, C., 'Minimising waste in Construction' Proceedings IPENZ Annual Conference, Auckland, 1998, p. 27 – 31.

6. LOWE, P.G., Externally reinforced concrete: a re-think of steel/concrete composites, Concrete 2000, Eds. R.K. Dhir and M.R. Jones, E. & F. N. Spon, 1993, pp 1717 – 1726.

7. LOWE, P.G., Steel/Concrete composites – an up-date on the externally reinforced option, in Innovation in Concrete Structures: design and construction, Eds. R. K. Dhir and M. R. Jones, Telford, 1999, pp 353 – 363.

CONCRETE-FILLED PVC TUBES AS COMPRESSION MEMBERS

M Marzouck
Suez-Canal University
Egypt
K Sennah
Ryerson University
Canada

ABSTRACT. Poly Vinyl Chloride is a polymer used in the construction industry. Vinyl is the plastic matter not completely from petroleum. This provides some main attributes that make it useful in the construction of certain structures exposed to corrosive environments. This paper evaluates the utilization of the commercially available PVC tubes as compression members filled with concrete. An experimental study is conducted on which four concrete filled PVC columns are tested up-to-failure. All specimens are of 100 mm diameter and of different heights. Two reference plain concrete specimens are tested to provide the contribution of the PVC tube in the confinement of concrete. All specimens are tested vertically and are subjected to monotonically increasing axial load until compression failure occurred. Axial load-displacement relationships are recorded for each specimen. This paper provides a scope for further research on conducting experiments on concrete filled PVC tube with different slenderness ratios and different concrete properties to further identify the behavior and then, propose a design approach of using such composite columns in light construction.

Keywords: Confined concrete, Lateral pressure, PVC tubes, Compressive strength, Ductility, Failure, load-displacement relationships.

M Marzouck is a lecturer in the Department of Civil Engineering at Suez-Canal University, Port-Said, Egypt. His research focuses mainly in the behavior of reinforced concrete structures and bridges and rehabilitation of structures using advanced composite materials.

K Sennah is an assistant professor of Structural Engineering in the Department of Civil Engineering at Ryerson University, Toronto, Canada. His research focuses in the behavior of composite concrete-steel structures and bridges, advanced composite materials, and safety issues in vehicle and transportation infrastructures.

INTRODUCTION

Plastics have exceptional properties, which make these materials attractive for different structural applications. Some of these properties include high resistance to severe environmental attacks, electromagnetic transparency, and high strength to weight ratios. Due to these properties, there is a great demand for structures such as piling, poles, highway overhead signs and bridge substructures to be made of materials that are more durable in comparison to traditional materials and systems.

Composite Columns, made of structural steel tubing filled with concrete, have been used in building construction with great efficiency for many years. Many authors have dealt with theoretical and experimental investigations on the behavior as well as the ultimate compressive strength of concrete-filled steel columns (among them: Uy, B., 2000 [1], Faruqi et al., 2000 [2], O'Shea et al., 2000 [3] and Campione et al., 2000 [4]). Rapid deterioration of infrastructures increased the demand on rehabilitating and retrofitting existing concrete columns in building and bridge substructures. Advances in the field of advanced composite materials have resulted in development of fiber reinforced polymer sheets to confine existing concrete columns, resulting in enhancing the compressive strength and ductility and improving the durability over conventional methods. Few authors (among them: Saafi et al., 1999 [5], Toutanji, H., 1999 [6]) tested to-collapse concrete columns wrapped using carbon and glass fiber sheets.

Saafi et al. [5] proved that the increase in axial stress over the confined specimen ranged from 51 to 137 percent for the concrete-filled glass tubes and 57 to 177 percent for the concrete-filled carbon tubes. However, with the high cost of the advanced composite materials, the use of this material in composite columns in light construction is not recommended. Another alternative to the advanced composite materials tubing is the commercially available PVC sewers pipes. The use of PVC tubes in composite columns and piles in light construction will eliminate the reinforcing steel and the formwork. So, the objective of this paper is to examine the compressive strength and overall behavior of concrete-filled PVC tubes subjected to increasing axial forces.

Poly Vinyl Chlorides, PVC, are polymers used vastly in the construction industry. Vinyl is a plastic material not completely originated from petroleum. This provides some main attributes that make it useful in the construction of certain structures exposed to corrosive environments. PVC tubes are characterized by having lightweight, which permits easy handling. They are impermeable to gases and fluids and durable (their life cycle in civil construction goes beyond 50 years). Very few authors have dealt with the ultimate strength of plastic columns with concrete core (Daniali, S., 1992 [7]; Kurt, C. E., 1978 [8]). However, a comprehensive experimental study is required to provide database for the experimental compressive strength of concrete-filled PVC tubes. This database would include different tube sizes, slenderness ratio and concrete properties.

EXPERIMENTAL PROGRAM

The experimental program included testing to-collapse six concrete columns under increasing axial load. The plastic tubes used *were PVC Sewers/EGOUT pipes, SDR 35 CSA certified.* All the specimens except the fourth and the sixth ones were concrete-filled PVC tubes of lengths 758, 562, 416 and 270 mm, respectively.

The diameter of the concrete core was 100 mm, while the thickness of the PVC tubes was 3 mm. Specimens No. 4 and No. 6 were plain concrete columns of heights similar to those of specimens No. 3 and No. 5, respectively. These two specimens were intended to assess the contribution of the PVC tubes on the compressive strength. Table 1 summarizes specimen properties and strength. After pouring of concrete, each specimen was saw-cut to provide flat ends normal to its longitudinal axis to avoid eccentricity of loading. Each specimen was tested under increasing monotonic axial loading using a 4500 kN MTS Compression Tester at the Structural Laboratory at Ryerson University. A spherical bearing block at the upper end of the machine provided a uniform distribution of applied stress in the test specimen and ensured the pin-ended restraint of the specimens. While flat-ended conditions were considered at the lower end of the specimens. The axial load was applied in increments (1000 N per second). The axial displacement between the two heads of the tester was monitored using a built-in LVDT. Figure 1 shows the test setup with specimen No. 3 after failure.

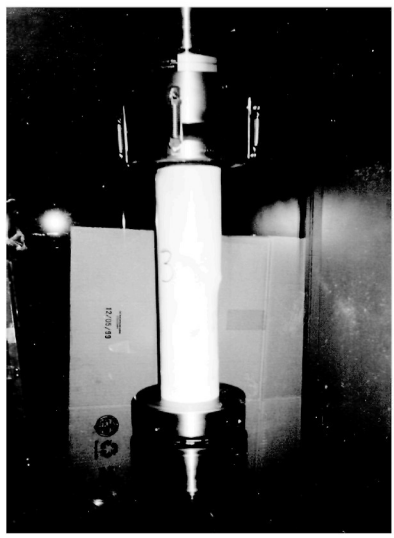

Figure 1 Test setup

Table 1 Specimen properties and strength

SPECIMEN NUMBER	PIPE THICKNESS (mm)	CONCRETE CORE DIAMETER (mm)	HEIGHT (mm)	COMPRESSIVE AXIAL RESISTANCE (kN)
1	3	100	758	287
2	3	100	562	291
3	3	100	416	311
4	N/A	100	416	265
5	3	100	270	318
6	N/A	100	270	287

RESULTS

Concrete-filled PVC tubes tested herein exhibited strength, ductility and energy absorption capacity superior to those of unconfined concrete. Table 1 summarizes the ultimate axial compressive force carried by each specimen. It can be observed that concrete confinement produced by the PVC tube of 3 mm thick increased the ultimate compressive strength of specimen No. 3 by 17% and that of specimen No. 5 by 11%. Figure 2 shows the load-axial displacement relationship for specimen No. 3 of concrete-filled PVC tube and No. 4 of concrete only. It can be observed that the ultimate load for each specimen reached at approximately the same axial displacement. However, the presence of the lateral confinement provided by the PVC tube significantly increased the axial plastic strain before collapse. This would provide warning to progressive failure rather that brittle failure of plain concrete specimens.

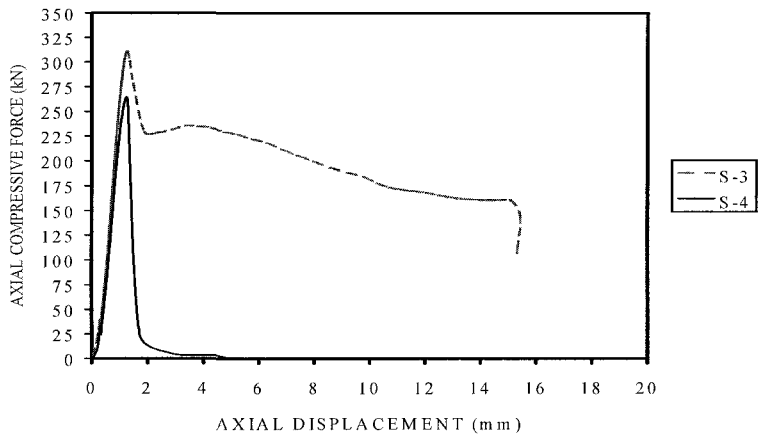

Figure 2 Load-displacement relationship for specimens No. 3 and 4

Similar behavior is observed in Figure 3 for specimen No. 5 of concrete-filled PVC tube and No. 6 of concrete only. Figure 4 shows the axial load-displacement relationship of the concrete-filled PVC tubes of different heights. The representative specimens No. 1, 2, 3 and 5 have slenderness ratios of 30, 22, 17 and 11, respectively. The ultimate compressive load values are listed in Table 1. It can be observed that ultimate compressive load decreases with increase in slenderness ratio.

The mode of failure of the concrete-only specimen was traditional shear mode failure, splitting of concrete laterally with an angle of shear failure approximately 45°. Similar shear mode failure in the concrete core was observed in all the concrete-filled PVC tubes. However, the slippage of concrete at approximately 45° was contained by the PVC tube since it can withstand large lateral deformation without rupture of the tube material. Figure 5 shows view of the failure mode for each specimen. It can be observed that the shown PVC specimens exhibit large and noticeable lateral deformation after collapse.

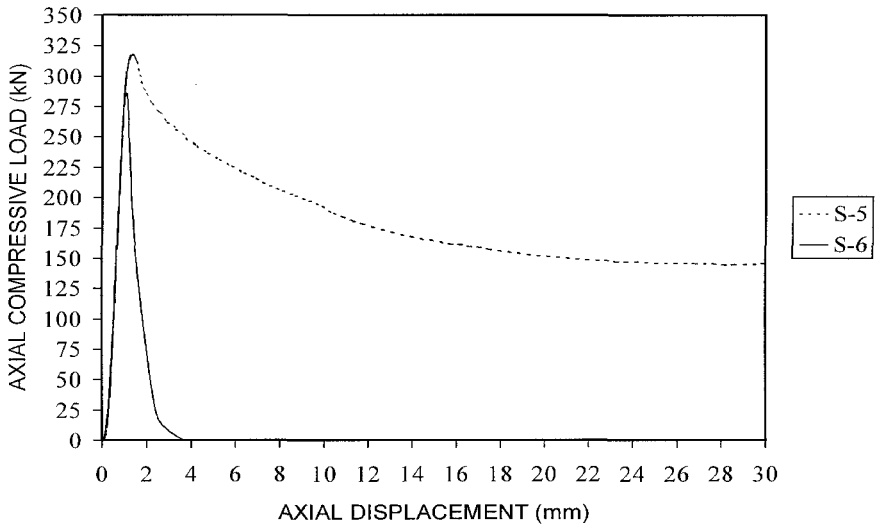

Figure 3 Load-displacement relationship for specimens No. 5 and 6

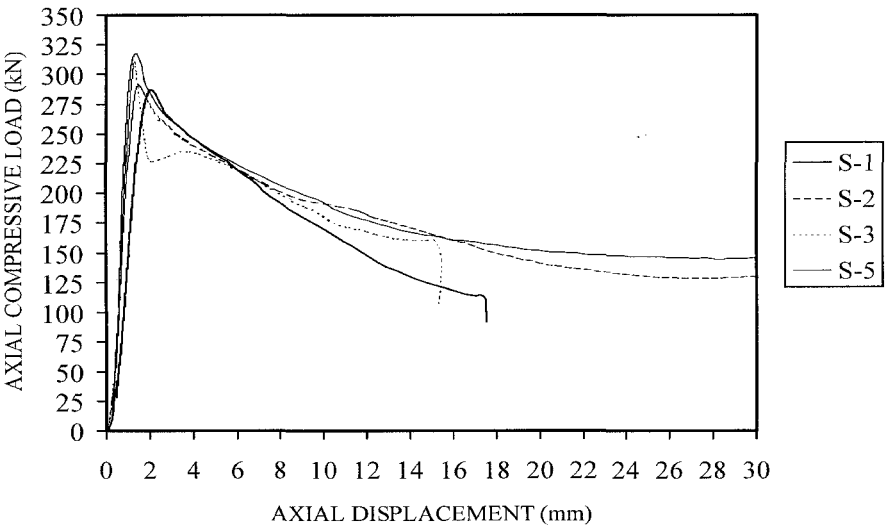

Figure 4 Load-displacement relationship for concrete-filled tubes

Figure 5 View of the specimens after failure

CONCLUSIONS AND RECOMMENDATIONS

This paper presents preliminary results on the behavior as well as the ultimate compressive strength of concrete-filled PVC tubes. The following conclusions and recommendations are drawn:

1. The use of PVC tube provides considerable lateral confinement to the concrete columns and hence, increases the ultimate compressive strength of such columns.

2. Concrete-filled PVC tubes possess a great level of ductility as observed from the axial load-displacement relationship. The tube acts as containment to the failed concrete core and exhibits large lateral deformation before failure.

3. As the slenderness ratio increases, the compressive strength of the concrete-filled PVC tubes decreases.

4. Further research is required to evaluate the compressive strength of concrete-filled PVC tubes with wide range of slenderness ratios and tube sizes, and different concrete properties.

ACKNOWLEDGEMENTS

This research was supported partially by the Egyptian Scientific mission Department. The authors are grateful to Mr. Dan Peneff of Ryerson University for laboratory support.

REFERENCES

1. UY, B. Strength of concrete filled steel box columns incorporating local buckling, ASCE Journal of Structural Engineering, Vol. 126, No. 3, 2000, pp 341-352.

2. FARUQI, M. A., PLEIMANN, L. G., LEELANI, P. A mathematical evaluation of compressive behavior of steel tubular structures filled with composite materials, Construction and Building Materials, ELSEVIER, 14, 2000, pp 1-5.

3. O'SHEA, M. D., BRIDGE, R. Q. Design of circular thin walled concrete filled steel tubes, ASCE Journal of Structural Engineering, Vol. 126, No. 11, 2000, pp 1295-1303.

4. CAMPIONE, G., MINDESS, S., SCIBILIA, N., ZINGONE, G. Strength of hollow circular steel sections filled with fiber-reinforced concrete, Canadian Journal of Civil Engineering, Vol. 27, No. 2, 2000, pp.364-372.

5. SAAFI, M., TOUTANJI, H. A., LI, Z. Behavior of concrete columns confined with fiber reinforced polymer tubes, ACI Materials Journal, Vol. 96, No. 4, 1999, pp 500-509.

6. TOUTANJI, H. A. Stress-strain characteristics of concrete columns externally confined with advanced fiber composite sheets, ACI Materials Journal, Vol. 96, No. 3, 1999, pp 397-404.

7. DANIALI, S. Investigation of the behavior of reinforced plastic columns with concrete core, Materials Performance and Prevention of Deficiencies and Failures, American Society of Civil Engineers, August 1992, pp 666-676.

8. KURT, C. E. Concrete filled structural plastic columns, American Society of Civil Engineers Journal of the Structural Division, Vol. 104, No. ST1, 1978, pp 55-63.

CONSTITUTIVE MODEL FOR THE STRESS-STRAIN RESPONSE OF FIBRE REINFORCED CONCRETE IN COMPRESSION

P Manita

University of Patras

S J Pantazopoulou

Demokritus University of Thrace

Greece

ABSTRACT. Using an extensive database of test results a constitutive model of the compressive stress-strain response of fibre-reinforced concrete is developed. The experimental databank includes test specimens with a variety of fibre type and volumetric content. The model relates mechanical resistance at any level of axial deformation to damage buildup. Expansion in the microstructure due to crack initiation and propagation is used in the model as a measure of damage. Initiation of a post-peak descending branch in the stress-strain response is associated with the occurrence of instability in the specimen structure; in this modelling framework, fibres provide kinematic restraint to dilation in a manner analogous to conventional passive confinement. The role of fibres is evaluated through indices of mechanical behaviour such as the deformation capacity of the material, whereas the model is expressed mathematically through the mechanical properties of the fibres, the volumetric fraction of fibres and the intrinsic properties of the mortar/concrete matrix.

Keywords: Fibre reinforced concrete, Constitutive relations, Stress-strain models, Deformation, Triaxial stress, Fibres, Bond.

P Manita, is a PhD candidate in the Department of Civil Engineering at the University of Patras, Greece. Her research interests include microstructure of mortar and concrete, durability of mortar and concrete, with an emphasis on characteristics of historic mortars and properties and composition of repair mortars.

S J Pantazopoulou, is Professor of Civil Engineering at Demokritus University of Thrace, Greece. She holds MS and PhD degrees from the University of California at Berkeley, and an Engineering Diploma from the National Technical University of Athens, Greece. Prior to her current appointment she was tenured Associate Professor at the University of Toronto, Canada. She is member of several International Technical Committees in the field of Structural Concrete and earthquake engineering. Her research interests include the mechanics of concrete and concrete structures.

INTRODUCTION

A familiar attribute of concrete's behaviour is significant compressive strength in the presence of confinement and insignificant resistance accompanied with brittle response under tension. When unconfined, concrete demonstrates brittle behaviour even in compression, as tensile fracture occurs parallel to the load due to the so-called Poisson's effect. Lateral expansion of unrestrained concrete is so significant that after attainment of peak strength, failure is characterised by uncontrolled volumetric expansion. In this regard, any kinematic restraint to dilation favours the mechanical properties of concrete, by increasing its deformation capacity and, depending upon the manner of its application, it may even lead to substantial improvement of mechanical strength.

In this work, mass reinforcement such as fibres in fibre reinforced concrete (FRC) is treated as a device of kinematic restraint to volumetric expansion. Using this concept, a constitutive model of the compressive stress-strain response of this type of concrete is developed, using as a point of reference the observed response of FRC based on an extensive database of test results. The experimental databank includes test specimens with a variety of fibre type and volumetric content. The model relates mechanical resistance at any level of axial deformation to damage buildup. Expansion in the microstructure due to crack initiation and propagation is used in the model as a measure of damage.

Initiation of a post-peak descending branch in the stress-strain response is associated with the occurrence of instability in the specimen structure. In this modelling framework, fibres provide kinematic restraint to dilation in a manner analogous to conventional passive confinement. The role of fibres is evaluated through indices of mechanical behaviour such as the deformation capacity of the material, whereas the model is expressed mathematically through the mechanical properties of the fibres, the volumetric fraction of fibres and the intrinsic properties of the mortar/concrete matrix.

BEHAVIOUR OF PLAIN CONCRETE UNDER COMPRESSION

In Figure 1, ε_3 represents the strain in the axial direction of the compressed specimen, σ_3 represents the average imposed axial compressive stress and ε_v represents the volumetric strain. The latter quantity results from the sum of the three principal strains of concrete, $\varepsilon_1+\varepsilon_2+\varepsilon_3$, where the axis 1 and 2 are perpendicular to the axis 3, that coincides with the

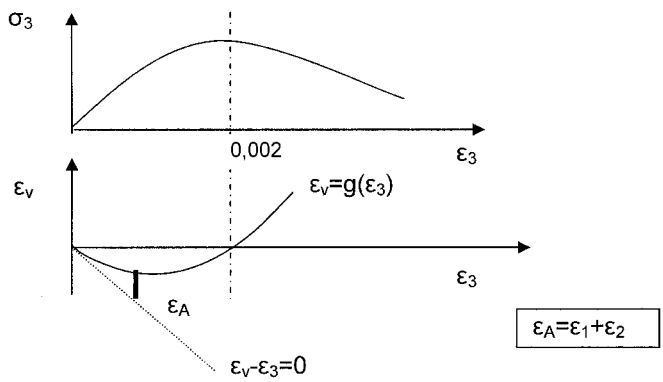

Figure 1 Axial stress-strain diagram of conventional concrete under uniaxial compression

direction of applied load. From the above, it follows that the sum $\varepsilon_1+\varepsilon_2 = \varepsilon_V-\varepsilon_3$ describes the dilation of the cross section (area strain, ε_A). The schematic representation of the relation $\varepsilon_V - \varepsilon_3$ in a diagram shows that ε_A, i.e. the area strain of the cross section supporting the load at an axial strain of ε_3, is the coordinate bound between the ε_V-ε_3 curve and a 45 degree line in the contractive quadrant. Note that sign convention for volumetric strains is positive for tension (expansion) and negative for compression (contraction).

Recent experimental data have illustrated that nominal failure (i.e. the initiation of descending branch of the stress-strain curve) is associated with prevailing net volumetric growth of concrete due to damage buildup, i.e. $\varepsilon_V > 0$. Consequently, the point of alteration of concrete's stable behaviour to instability is defined from the requirement that $\varepsilon_V = g(\varepsilon_3) = 0$. According to the definition of area strain ε_A, at the onset of the post-peak branch, ε_A is equal in magnitude to the imposed axial strain ε_3. The value of $|\varepsilon_3|$ that satisfies the above kinematic condition is defined as the strain at maximum stress, since it separates the region of volume contraction to volume expansion, and also defines the strain limit beyond which the strength of concrete deteriorates from its peak value [1]. This characteristic strain magnitude is referred to in the remainder of this paper as ε_3^{co} for plain unconfined concrete, ε_3^{cc} for confined concrete and ε_3^{cf} for fibre reinforced unconfined concrete.

$$\varepsilon_3^{co} < \varepsilon_3^{cc} \quad ; \quad \varepsilon_A^{co}(\varepsilon_3) > \varepsilon_A^{cc}(\varepsilon_3) \quad \& \quad \varepsilon_3^{co} < \varepsilon_3^{cf} \quad ; \quad \varepsilon_A^{co}(\varepsilon_3) > \varepsilon_A^{cf}(\varepsilon_3) \qquad (1)$$

The above observations have also been confirmed experimentally for fibre-reinforced concrete, regardless of imposed lateral confining stress or the method of applied lateral restraint [2,3]. In the presence of kinematic restraint (as provided by a confining jacket or by means of added fibre content), the accumulation of area growth ε_A in the cross section supporting the compressive strut is slowed down as compared to the area growth observed in tests of plain unconfined concrete. For this reason an increase of axial strain capacity prior to failure and a slower rate of decay in the descending branch have been reported in these cases (Equation 1). A similar improvement of compressive strength, although not as marked as the increase of deformation capacity, is observed only in the case of actively confined concrete. It is noteworthy that the strength increment due to confinement is usually quantified over the strength of plain concrete having the same mix design and without fibre reinforcement.

PHYSICAL MODEL OF FIBRE REINFORCED CONCRETE

As already explained, passive confinement does not directly counteract the imposed pressure but resists the imposed expansion of the encased concrete. Through this mechanism of resistance, confinement counteracts propagation of macrocraks, delays the onset of softening and generally causes a less brittle pattern of failure. A mechanical analogue of the function of external kinematic restraint as provided by means of passive confinement (as in the case of a jacket) is modelled in Figure 2a. The mechanism providing the confining action imposes stiffness K per unit of lateral area of the material mass, so the confining pressure σ_{lat} is given by

$$F_{lat} = K\delta \le F_{lat}^{y} \qquad (2)$$

where F_{lat}^{y} is the nominal strength at the yield point of the spring-system per unit surface area of the cylinder and δ is the lateral translation due to expansion of the cylinder boundary

(compression of the springs, equal to the dilation $\varepsilon_l * D/2$ of concrete, where D is the diameter of the element). From the free-body diagram of Figure 2b, it is easy to derive that the magnitude of lateral pressure applied on concrete is $\sigma_{lat} = F_{lat} = K\delta$. The same model is used in Figure 3a in order to explain the restraining role of fibres in fibre reinforced concrete. In this case, it is considered that springs are acting internally in the mass of the concrete element and although the general form of the Equation (2) is still valid, the significance of the terms used, such as the stiffness K, is different. Stiffness K is given by

$$K = k_f \rho_f \tag{3}$$

where k_f is the stiffness of an anchored fibre and ρ_f is the total area ratio of fibres in an arbitrary section of the element. According to [4] the number of fibres per unit area of concrete is $N_l = 0.605 V_f / A_f$ (S. I. system of units) derived from experiments with steel fibres having 50 mm length (2 inch), where V_f, the volumetric percentage of fibres and A_f, the area of a single fibre. Note that when using the more common 25-30 mm long fibres (approximately 1 inch), the above relation is modified to $N_l = 0.605 \times (50/25) \times V_f/A_f = 1.21 V_f/A_f$ and $\rho_f = N_l A_f = 1.21 V_f$.

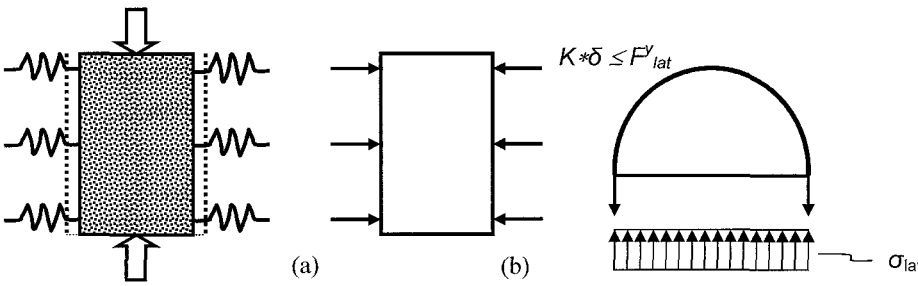

Figure 2 Mechanistic analogue of passive confinement action on the lateral surface of concrete cylinder (a) spring-model (b) free-body diagram at an arbitrary section

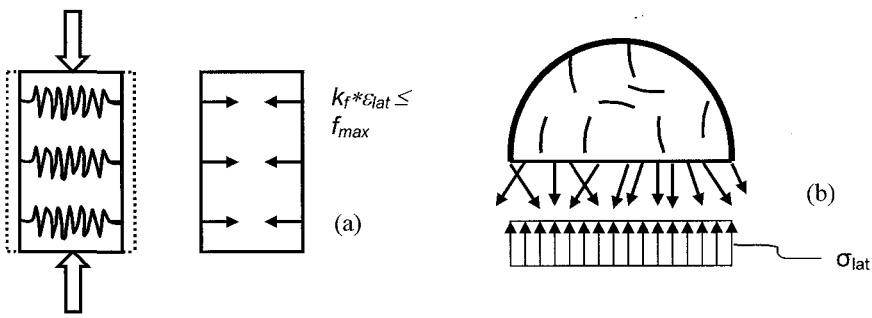

Figure 3 (a) Model of fibre function on a concrete specimen
(b) Estimation of lateral confining pressure of fibre-reinforced concrete

Failure of the kinematic restraint provided by the fibre, when it occurs, depends on the anchorage capacity, f_{max} of the fibre in concrete. After the formation of a crack in concrete, stress is supported entirely by fibres bridging the two sides of the crack.. If the load resisted by the fibre is less than either the pullout strength or the fibre yield/fracture capacity, the fibre remains elastic during elongation and transmits the load to the surrounding concrete [5]. The

load transmission due to the bond mechanism of the fibre to concrete continues until the occurrence of localised deformation in the fibre, either due to fibre slip through pullout from the anchorage length or due to exceedance of fibre tensile strength, whichever occurs first. Thus, three alternative cases of fibre failure can be identified. For fibre pullout from the anchorage, necessarily accompanied with partial failure of the fibre-concrete interface, the force developed in the fibre is limited by the anchorage strength, F_e. Force F_e depends upon the fibre characteristics and the concrete properties at the fibre-concrete interface. If fibre fracture prevails prior to pullout, then the fibre strength is developed, F_r. Particularly when using ductile steel fibres, yielding at a force F_y limits the strength. Strengths F_r and F_y of the two latter cases are independent of concrete properties, and are characteristic of fibre type and material. Consequently, the maximum confining pressure that fibres may provide to concrete is limited by fibre/interface failure as described in the preceding.

From the free body diagram shown in Figure 3b it is evident that a lateral compressive stress σ_{lat} develops in concrete so as to counteract fibre tension, as required to maintain equilibrium. σ_{lat} is obtained as follows:

$$f_f k_e \rho_f + \sigma_{lat} = 0 \quad ; \quad \sigma_{lat} = -f_f k_e \rho_f \tag{4}$$

where k_e the coefficient of fibre effectiveness (which accounts for the fact that fibres are not generally perpendicular to the arbitrary section considered; for random fibre distribution it can be shown that k_e=0.5, by considering a Gaussian distribution for the fibre orientation-angle θ_f. Note that θ_f is measured between the fibre axis and the horizontal, and ranges from 0 to 180 degrees. Therefore, k_e is calculated from $\int_0^{\pi} \sin\theta_f d\theta_f$). Parameter f_f represents the average stress in the fibres intersected by the arbitrary section.

$$f_f = k_f \varepsilon_{lat} \le f_{\max} = \min \begin{cases} 2u_b \dfrac{l_f}{d_f} \\ f_y, f_r \end{cases} \tag{5}$$

In Equation (5) the limit value $2u_b l_f/d_f$ is derived with reference to Figure 4 (fibre pullout), where u_b is the average bond stress along the fibre during pullout (assuming constant bond stress distribution), l_f is the length and d_f is the diameter of the fibre and, f_y and f_f represent

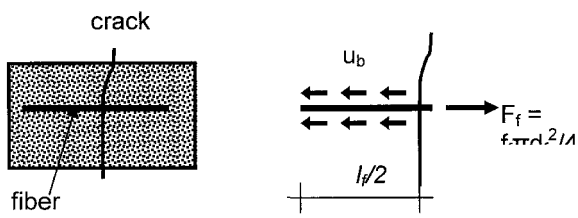

Figure 4 Calculation of the strength along fibre anchorage

fibre strength (at yield or fracture depending on the type of fibre – ductile or not). According to experimental results from studies on fibre-reinforced concrete ([6], [7], [8]), the residual frictional bond resistance (past the point of slip initiation and after the initial adhesion strength has been exceeded) is about equal to tensile strength of concrete. Thus, u_b= $0.5(f_{ck})^{1/2}$ MPa and if l_f/d_f = 30, f_{max} is determined from the bonding mechanism (90~180 MPa < 220 ~ 400 MPa). Thus, in long fibres (l_f/d_f = 60) pullout is expected only in case of medium to low strength concrete (3×60=180 MPa, F_{max}=35 N (d_f= 0.5mm)), whereas yield or

fracture of fibres is expected in the case of high strength concrete. In the case of non-metallic fibres (i.e. polypropylene fibre) characterised by low modulus of elasticity, the magnitude of localised strain that can be developed (width of crack) before fibre slip may begin is excessively high and f_{max} is estimated from the fracture value of the fibre (f_r < 180 MPa). Referring to Figure 5b, note that the above values concerning bond strength correspond to the initiation of the descending branch in the bond-slip characteristic diagram (pullout mechanism). Significantly higher values have been reported in the literature for the peak bond strength, $u_{b,max}$ (2~3 fold increase over the frictional limit).

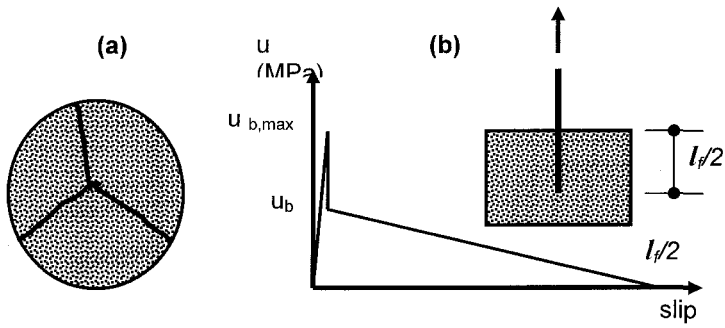

Figure 5 (a) Axisymmetric failure is considered,
(b) Assumed bond stress – fibre slip variation

CONSTITUTIVE MODEL OF FIBRE-REINFORCED CONCRETE UNDER COMPRESSIVE STRESS

Addition of fibres to a mixture of plain concrete increases significantly the post-peak deformation capacity and tensile strength, reduces the rate of post-peak strength degradation and decreases the development of macrocracks in the matrix, but may have marginal or even negative effect on compressive strength. The improvement of concrete's ability to absorb energy during deformation is quantified by the area enclosed between the stress-strain curve and the horizontal axis. It is observed that this area is much larger than the corresponding value for conventional concrete.

To formulate the equation of the energy, plain and fibre-reinforced concretes of the same mix design and porosity need be related. It is noteworthy that adding fibres to concrete leads to an increase of the matrix porosity because of air entrainement and a decrease in volumetric fraction of cement paste (V_p) equal to the volumetric fraction of the added fibre (V_p–V_f). The latter remarks highlight that differences in response characteristics are likely to exist between the plain mixture and the one referred in the literature as the reference mixture (without fibre reinforcement). The index "corr", when used, in terms of the above equation, underlines this difference between the characteristics of plain concrete mixture (of same porosity) and the reference mixture. Based on the expansion-strain model [1], the modified magnitude of the strain at peak stress, $\varepsilon_A{}^o = \varepsilon_{3u}$, may be calculated from the reduced volume fraction of paste when accounting for air-entrainement and fibre volume. Similarly the reduction in the magnitude of the initial modulus of elasticity E_o, owing to the same reasons was computed using the models by [9] and [1].

Neglecting second order terms, the equation of the energy is equivalent as follows

$$\frac{\varepsilon_{3u}}{\varepsilon_{3u}^{o,corr}} = \left(1 + 0.75 \frac{\sigma_{lat}}{\sigma_{3u}^{o,corr}} \frac{\varepsilon_{lat}}{\varepsilon_{3u}^{o,corr}}\right) \cdot \frac{\sigma_{3u}^{o,corr}}{\sigma_{3u}^{c}} \qquad (6)$$

where:

$$\varepsilon_{lat} = -0.5\varepsilon_{3u} + \frac{\sigma_{lat}}{2E^{c}_{\sec}} \quad ; \qquad (7)$$

Previous experimental findings ([2], [3]) have been used in deriving Equations (6) and (7). According to this, the lateral strain of concrete at the onset of the descending branch is approximately equal to half the value of the corresponding axial strain (i.e., the active Poisson's ratio ν is taken as 0.5 at peak stress). The secant stiffness of concrete at that point is taken as $E^{c}_{sec}=\sigma_{3u}{}^{c}/\varepsilon_{3u}$ (using a Hognestad-type parabola for the ascending branch of the stress-strain diagram). Note that at low confining pressures, the second term in Equation (7) is negligible. To compute the strength increase due to confining pressure σ_{lat}, the classical form was used as follows [10]:

Using again the energy balance approach, it is also possible to obtain a closed form expression for strain $\varepsilon_{3,50}$, i.e. the post-peak axial strain corresponding to 50% loss of

$$\sigma^{c}_{3u} = \sigma^{o,corr}_{3u} + 4{,}1\sigma_{lat} \qquad (8)$$

strength. The same definition is used both for plain and for fibre-reinforced concrete. Here it is assumed that three symmetric planes of fracture occur in the cylindrical specimen (Figure 5a) whereas bond stress is taken to decay linearly from maximum load to zero capacity at complete fibre pullout (Figure 5b). Based on these assumptions it may be easily shown that

$$\varepsilon_{3,50} = \varepsilon_{3u} + \frac{\ell_f^2 d_f}{8D} \lambda \frac{u_b}{\sigma^{c}_{3u}} N_1 = \varepsilon_{3u} + \frac{\lambda}{2\pi} \frac{d_f}{D} \left(\frac{\ell_f}{d_f}\right)^2 0.605 V_f \frac{u_b}{\sigma^{c}_{3u}} \qquad (9)$$

where $\lambda = 1.5$ for the case depicted in Figure 5a.

Equations (6) – (9) describe the constitutive behaviour of fibre-reinforced concrete associated with the mechanical properties of the basic concrete mixture and the properties of the fibre used. Note that the maximum strain resulting from Equation (9) is derived with reference to size effect.

COMPARISON WITH THE EXPERIMENTAL EVIDENCE

Only few experiments report on the critical model parameters in published experimental literature (such as the water-cement ratio, aggregate type and volumetric ratio, and air-entrainement percentage) in addition to the mechanical characteristics of the fibres used. An additional drawback is that axial strain is not always measured within an acceptable gauge length (sometimes authors report relative displacement of loading platens during the compression test, thereby including spurious sources of strain such as, for example, the

compressive strain of the caps). For this reason only few tests can be used reliably for correlation of the model, and hence its effectiveness in reproducing observed behaviour of FRC, is for now, mainly qualitative. Table 1 summarises the fibre content of concrete (volumetric percentage), the fibre type (l_f/d_f), the compressive strength of the cylinder, the correspondent axial strain ε_{3u} and the strain $\varepsilon_{3,50}$ for two relevant sets of experiments [11], [7].

Table 1 Experimental results from the literature

#	V_f (%)	FIBRE TYPE	f_{3u} (MPa)	ε_{3u}	$\varepsilon_{3,50}$	REFERENCE
(1)	0% [3]	-	81.4	0.0030	0.0040	[11]
(2)	0.5%	l_f/d_f=60[1]	82.1	0.0036	0.0058	
(3)	1%		82.1	0.0038	0.0077	
(4)	0% [4]	-	38.0	0.0016	0.0036	[7]
(5)	0.4%	l_f=60[1,2]	39.5	0.0020	0.0080	
(6)	0.8%		39.0	0.0024	0.0160	
(7)	0%[5]	-	72.5	0.0022	0.0028	[7]
(8)	0.75%	l_f=30[1,2]	74.0	0.0025	0.0074	
(9)	1.1%		80.0	0.0033	0.0095	

In assembling Table 1, it was assumed that an air-entrainement of 5% occurred for addition of fibre content by ≈1% per volume. Linear interpolation was used for the remaining values (V_f=0-1%). It was assumed that: [1]f_y=400 MPa; [2]d_f=0.8mm and *0.5* mm respectively; [3]it was specified that *w/c*=0.28; [4]it was assumed that *w/c*=0.5; [5]it was assumed that *w/c*=0.4.

Table 2 Calculated results from the model (applied to cases with $V_f \neq 0$)

#	V_f(%)	ρ_f (%)	σ_{lat} (MPa)	$\sigma_{3u}{}^{c}$ (MPa)	$v_{cpl}{}^{corr}/v_{cpl}{}^{o}$	$\varepsilon_{3u}{}^{o,corr}$	ε_{3u}	$\varepsilon_{3,50}$
(2)	0.5%	0.302%	0.60	81.1	1.139	0.0034	0.0034	0.0039
(3)	1%	0.605%	1.20	80.7	1.260	0.0037	0.0038	0.0047
(5)	0.4%	0.242%	0.48	38.6	1.045	0.0017	0.0017	0.0031
(6)	0.8%	0.484%	0.97	39.3	1.090	0.0018	0.0018	0.0046
(7)	0.75%	0.907%	1.81	76.3	1.083	0.0024	0.0025	0.0041
(8)	1.1%	1.330%	2.65	78.0	1.145	0.0025	0.0026	0.0048

CONCLUSIONS

An analytical model was developed to simulated the behaviour of fibre-reinforced concrete under compression. Model formulation was based on experimental observation and records from an extensive triaxial test programme that was conducted on cylindrical specimens of fibre-reinforced concretes containing various volume fractions and types of fibre. In the model, fibre action was interpreted as a kinematic restraint against concrete lateral expansion, which is perpetrated by damage accumulation due to cracking. Using this model it was possible to estimate an effective passive confining pressure which develops internally in concrete as fibres become mobilised in tension. This effective confining pressure is manifest by consequent enhancement of deformation capacity of fibre-concrete over the corresponding plain concrete of the same basic composition. It was shown through the analysis that compressive strength is influenced to a lesser degree by the addition of fibre, first because fibre addition increases the inherent porosity of the mix due to entrainement of air, but also because the function of the fibre as a confining mechanism becomes mobilised only once sufficient dilation due to cracking has taken place in the material microstructure (near peak stress). The deformability of fibre-reinforced concrete under compression was computed using energy methods at the critical point of the maximum load and at nominal failure.

REFERENCES

1. PANTAZOPOULOU S. J., MILLS R., "Microstructural Aspects of the Mechanical Response of Plain Concrete", ACI Materials Journal, 1995, V 92, No 6, pp.605-616.

2. IMRAN I., PANTAZOPOULOU S., "Experimental Study of Plain Concrete under Triaxial Stress", ACI Materials Journal, 1996, V 93, No 6, pp.589 – 601.

3. PANTAZOPOULOU S. J., ZANGANEH M.R, "Triaxial Behavior of Fibre – Reinforced Concrete", submitted for publication, 2000, 30 pp.

4. SOROUSHIAN P., LEE C.D., "Distribution and Orientation of Fibres in Steel Fibre Reinforced Concrete", ACI Materials Journal, 1990, V 87, No 5, pp.433-439.

5. TRIANTAFILLOU T.C., "Building Materials", personal edition, 3rd ed., Patras, Greece, 1997, 421pp.

6. FANELLA D. A., NAAMAN A. E., "Stress-Strain Properties of Fibre Reinforced Mortar in Compression", ACI Materials Journal, 1985, V 82, No 4, pp.475-483.

7. BALAGURU P. N., SHAH S. P., "Fibre-Reinforced Cement Composites", McGraw-Hill Intnl., 1992, 530 pp.

8. DANIEL J., SHAH S. P., "Fibre Reinforced Concrete – Developments and Innovations", ACI SP-142, American Concrete Institute, Detroit, 1994, 318 pp.

9. FAGERLUND G., "Elastic Moduli of Concrete", Proceedings of the International Conference on Pore Structure and Properties of Materials, RILEM/IUPAC, Prague, Czechoslovakia, 1973, V. II, pp. D129-D141.

10. RICHART F. E., BRANDZAEG A., BROWN R. L., "A Study of the Failure of Concrete Under Combined Compressive Stresses", Bulletin No. 185, Engineering Experimental Station, University of Illinois, Urbana, Ill, 1928.

11. HSU L. S., HSU C. T., "Stress-Strain Behavior of Steel-Fibre High-Strength Concrete Under Compression", ACI Structural Journal, 1994, V 91, No 4, pp.448-457.

PROPERTIES OF CONCRETE INCORPORATING HIGH VOLUMES OF CLASS-F FLY ASH AND STEEL FIBRES

R Siddique
University of Wisconsin-Milwaukee
United States of America

ABSTRACT. The results of an experimental investigation to study the effects of replacement of cement (by mass) with three percentages of high fly ash content, and the effect of addition of steel fibres on the slump, Vebe time, compressive strength, split tensile strength, flexural strength and impact strength of high fly ash concrete are presented. A control mix of proportions 1:1.4:2.6 with water cement ratio 0.46 and superplasticizer-cementitious ratio of 0.015 was designed. Cement has been replaced by mass with 35, 45, and 55% of fly ash content. Three percentages of steel fibres (0.30, 0.60 and 0.90%) of aspect ratio 80 have been used in the investigation. The test results indicate that replacement of cement with fly ash increases the workability (slump and Vebe time), decreases compressive strength, split tensile strength, flexural strength, and have no significant effect on the impact strength of plain concrete. Addition of steel fibres reduces the workability, does not significantly affect the compressive strength, and increases the split tensile strength and flexural strength, and tremendously enhances the impact strength of high fly ash concrete with an increase in percentages of fibres.

Keywords: Compressive strength, Flexural strength, High volume fly ash concrete, Impact strength, Steel fibres, Slump, Split tensile strength, Vebe time.

Rafat Siddique is presently working at Center for By-Products Utilization, University of Wisconsin-Milwaukee, USA. He is Senior Assistant Professor of Civil Engineering at Thapar Institute of Engineering & Technology (Deemed University), Patiala, India. His research interests are fibre reinforced concrete, high volume fly ash concrete, high performance concrete and structural engineering. He has published more than 40 research papers and has authored two books.

INTRODUCTION

Cement is the most cost and energy intensive component of concrete. The unit cost of concrete can be reduced by partial replacement of cement with fly ash. Accordingly, the replacement of cement with fly ash reduces the unit cost of the concrete, and conserve energy. In concrete, the replacement of cement with fly ash has its beneficial effects of lower water demand for similar workability, reduced bleeding, and lower evolution of heat. It has been used particularly in mass concrete applications and large volume placement to control expansion due to heat of hydration and also helps in reducing cracking at early ages.

Recently, high fly ash concrete has emerged as a construction material in its own right. These concretes normally contain more than 35 to 40% fly ash by mass of total cementitious materials. Many researchers have reported their findings on the various aspects of high volume fly ash concrete[1-6].

The use of fly ash in concrete is found to affect strength characteristics adversely. A loss in the strength of concrete can be retrieved to a large extent by incorporating steel fibres, which have proved their worth in enhancing the strength characteristics of concrete. Extensive work have been reported on the steel fibre reinforced concrete [7-11]. In this paper, an effort has been made to study the effects of steel fibres on the properties of high fly ash concrete. The effects of steel fibres on the slump, Vebe time, compressive strength, split tensile strength, flexural strength and impact strength of the high fly ash concrete have been reported in this paper.

EXPERIMENTAL PROGRAMME

Materials used in this experimental programme include: (1) Portland cement having a density of 3140 kg/m^3; (2) locally available sand as a fine aggregate with a density of 2610 kg/m^3 and a fineness modulus of 2.65; (3) coarse aggregate having a maximum size of 19 mm with density of 2620 kg/m^3 and a fineness modulus of 6.86; (4) Class F type fly ash, whose physical and chemical properties, as per ASTM C 618, are given in Table 1. In this investigation, cement was replaced with three percentages of fly ash (35, 45, 55) by mass of cement; (5) Straight steel fibres with an aspect ratio of 80 (length 32.8 mm, diameter 0.41 mm, tensile strength 850 N/mm^2) and three percentages by volume of concrete (0.30, 0.60 and 0.90%) were used; (6) Superplasticizer Centriplast FF90, based on melamine formaldehyde; (7) tap water; (8) Concrete mix ratio of 1:1.4:2.6 with a water-cement ratio of 0.46 and a superplasticizer- cementious material ratio of 0.015.

Following the mixing, slump and Vebe time tests were performed for plain concrete, high fly ash concrete and fibre reinforced high fly ash concretes. Standard 150- mm cubes were used for compressive strength, cylinders of 153 mm in diameter and 305 mm in length were used for determining split tensile strength, 101.6 x 101.6 x 508 mm beams for flexural strength and concrete slabs of size 500 x 500 x 30 mm were used for impact strength. The specimens were covered immediately for complete moisture retention. The specimens were demoulded after 24 hours of casting, and were then placed in a water tank at 26° C. The specimens were tested after 28 days of curing. The plain concrete specimens were designated as PC. Fly ash concrete specimens were designated as FC35 (Concrete containing 35 percent fly ash). Results of slump test, Vebe time test, compressive strength, split tensile strength and flexural strength of plain and fly ash concrete are tabulated in Table 2.

Table 1 Physical and chemical properties of fly ash

PHYSICAL PROPERTIES	VALUE
Colour	Whitish grey to grey with slight black
Bulk Density	2200 to 2400 Kg/m^3
Density	2.146 to 2.429 g/cm^3
Chemical Properties	
Constituents	**Mass, percent**
Silica (SiO_2)	57.3
Alumina (Al_2O_3)	27.1
Ferric Oxide (Fe_2O_3)	5.4
Calcium Oxide (CaO)	6.1
Magnesia (MgO)	2.0
Ignition Loss	1.8

Table 2 Test results of plain and high fly ash concrete

MIX TYPE	SLUMP, mm	VEBE TIME, Sec	COMPRESSIVE STRENGTH, MPa	SPLIT TENSILE STRENGTH, MPa	FLEXURAL STRENGTH, MPa
PC	43	31	37.0	4.00	5.30
FC35	60	25	28.5	3.10	3.30
FC45	66	22	24.7	2.60	2.80
FC55	73	17	22.1	2.12	2.25

RESULTS AND DISCUSSION

Workability

The results of the effect of replacement of cement with three percentages of fly ash on slump and Vebe time are given in Table 2. It is evident from Table 2 that with an increase in the percentage of fly ash content, workability (slump and Vebe time) increases. This increase in the workability of concrete is due to the "ball bearing" action of the spherical particles. The effects of steel fibres on the slump and Vebe time of high fly ash concrete are shown in Figures 1 and 2. The slump is found to decrease with an increase in the percentage of steel fibres for all the three percentages of fly ash. Similarly, the steel fibres have their adverse effect on the Vebe time of high fly ash concrete. Vebe time of high fly ash concrete increases with an increase in the percentage of steel fibres for all the three fly ash contents.

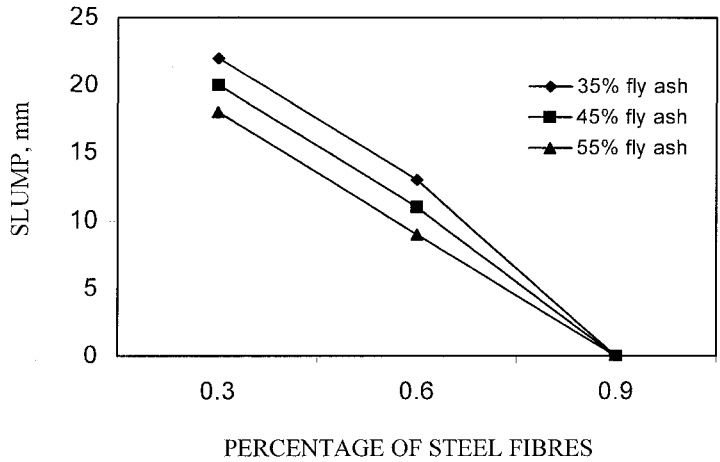

Figure 1 Effect of steel fibres on slump of high fly ash concrete

Compressive Strength

The effect of replacement of cement (by mass) with three percentages of fly ash on the compressive strength of concrete are shown in Table 2. It is clear from Table 2 that the replacement of cement with 35, 45 and 55% of fly ash content reduces the compressive strengths of concrete by 22.8, 33.2 and 40.2 percent, respectively. The results of the addition of steel fibres on the compressive strength of high fly ash concrete are shown in Figure 3.

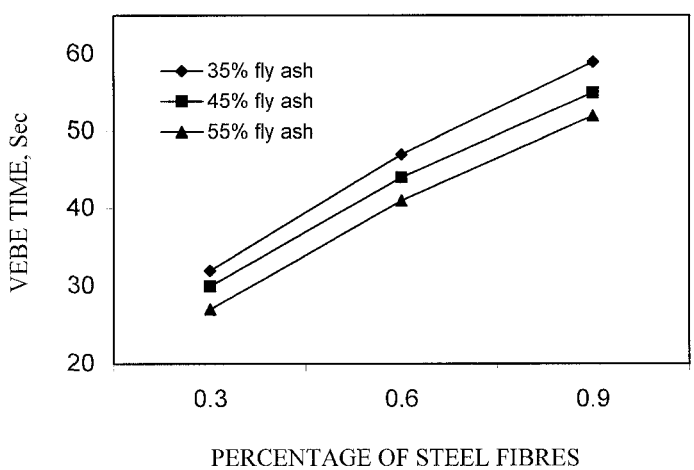

Figure 2 Effect of steel fibres on vebe time of high fly ash concrete

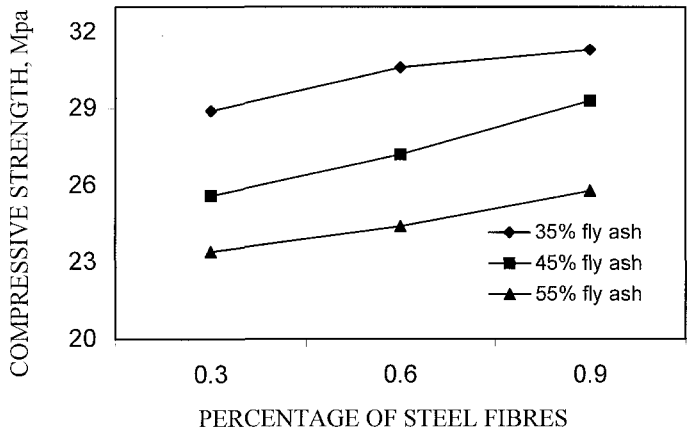

Figure 3 Percentage of steel fibres on compressive strength of high fly ash concrete

It is clear from Figure 3 that for a particular percentage of fly ash content, there is an increase in the compressive strength of high fly ash concrete as the percentage of steel fibres is increased from 0.30 to 0.90%. This increase in the compressive strength is in the order of 8.6 to 18.2% in case of 35 percent fly ash content, 3.8 to 19.4% with 45 percent fly ash content and 1.8 to 12.2% with 55 percent fly ash content.

Split Tensile Strength

The test results of the replacement of cement with three percentages of fly ash on the split tensile strength of concrete are tabulated in Table 2. It is clear from Table 2 that replacement of cement by 35, 45 and 55% of fly ash by mass of cement reduces the split tensile strength of concrete by 22.5, 35.0, and 47.0 percent, respectively. The results of the addition of steel fibres on the split tensile strength of high fly ash concrete are shown in Figure 4. Figure 4 shows that for a particular percentage of fly ash content, there is an increase in the split tensile strength of high fly ash concrete as the percentage of steel fibres is increased from 0.30 to 0.90%.

The increase in the split tensile strength is in the order of 23 to 46% in case of 35 percent fly ash content, 21 to 37 % with 45 percent fly ash and 20 to 38% with 55 percent fly ash content.

Flexural Strength

The effect of replacement of cement with three percentage of fly ash on the flexural strength of concrete is shown in Table 2. It is clear from Table 2 that replacement of cement by 35, 45 and 55% of fly ash by mass of cement reduces the flexural strength of concrete by 37.7, 47.16, and 57.5 percent, respectively.

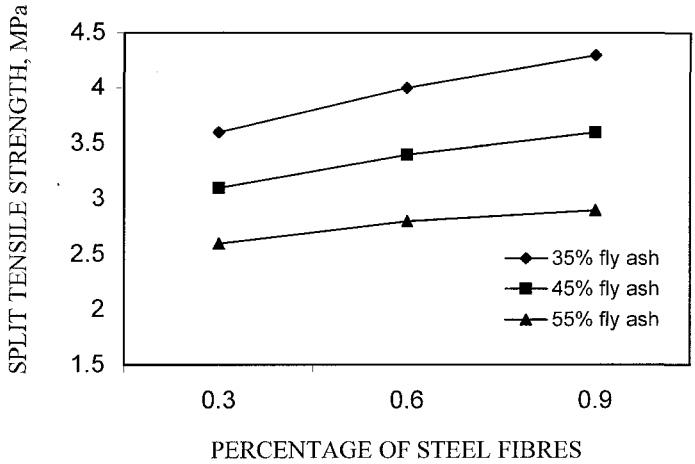

Figure 4 Effect of steel fibres on split tensile strength of high fly ash concrete

The results of addition of steel fibres on the flexural strength of high fly ash concrete is shown in Figure 5. Figure.5 shows that for a particular percentage of fly ash content, there is an increase in the flexural strength of high fly ash concrete as the percentage of fibres is increased from 0.30 to 0.90%. An increase in the flexural strength is of the order of 10.4 to 21.2% in case of 35 percent fly ash content, 9 to 19% with 45 percent fly ash, and it is 7 to 15% with 55 percent fly ash content.

Impact Strength

The test results of impact strength of steel fibre reinforced high fly ash concrete at ultimate failure are shown in Figure 6. Impact strength test was carried out by a falling weight method. In this test a cylindrical metallic piece of weight 40 N was dropped from a constant height (1000 mm).

The number of blows required to fail the specimens gives the impact strength of the slabs. Since damage inflicted by the blows of impact load stays during the subsequent blows, it was assumed that impact energy imparted by the drop of load is absorbed by the slabs. The cumulative energy imparted to the slab in N-m to cause failure is expressed as mgh x average number of blows.

From the Figure 6 it is clear that for all three fly ash contents, addition of steel fibres enhances the impact strength with the increase in percentage of fibres. With 35% fly ash content, the improvement in strength is 4 to 11 times with the increase in percentage of fibres, whereas it is 4 to 9 times, and 4 to 6 times with 45 and 55% fly ash content respectively.

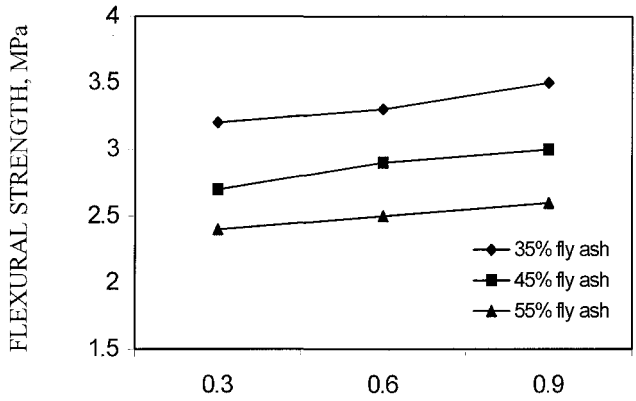

Figure 5 Effect of steel fibres on flexural strength of high fly ash concrete

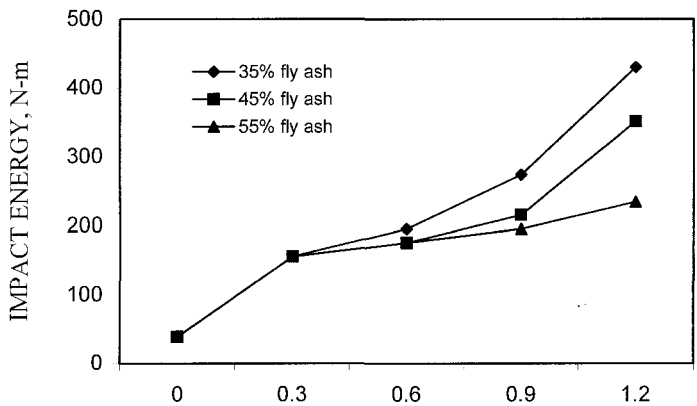

Figure 6 Effect of steel fibres on impact strength of high fly ash concrete

CONCLUSIONS

The following conclusions are drawn from the present study:

1. The replacement of cement (by mass) with three percentages of fly ash (35, 45 and 55%) increases the workability (both slump and Vebe time) of concrete with an increase in fly ash percentages. This is due to the "ball bearing" action of the spherical particles of fly ash. The slump of high fly ash concrete is found to decrease with an increase in the percentage of steel fibres for all the three percentages of fly ash content. Steel fibres have adverse affect on the Vebe time of high fly ash concrete. Vebe time of high fly ash concrete increases with an increase in the percentage of fly ash for all the three contents of fly ash.

2. The replacement of cement with three percentages of fly ash content reduces the compressive strength of concrete by 22.78, 33.24, and 40.2 percent, respectively. However, addition of steel fibres marginally enhances the compressive strength of high fly ash concrete.

3. The split tensile strength of concrete decreases by 22.5, 35.0, and 47.0 percent with the replacement of cement by 35, 45 and 55% of fly ash content. Addition of steel fibres significantly increases the split tensile strength of high fly ash concrete as the percentage of fibres is increased from 0.30 to 0.90%.

4. Replacement of cement with the three percentages of fly ash reduces the flexural strength by 37.7, 47.16 and 57.5 percent, respectively. However, addition of steel fibres marginally increases the flexural strength of high fly ash concrete as the percentage of fibres is increased from 0.30 to 0.90%.

5. For all three fly ash contents, addition of steel fibres substantially enhances the strength with the increase in percentage of fibres. With 35% fly ash content, the improvement in strength is 4 to 11 times with the increase in percentage of fibres, whereas it is 4 to 9 times, and 4 to 6 times with 45 and 55% fly ash content respectively.

REFERENCES

1. HAQUE, M N, High fly ash concrete, ACI Materials Journal, Vol 81, No 1, Jan-Feb 1984, pp 54-60.

2. SWAMY, R N, Mineral admixtures for high strength concrete, Indian Concrete Journal, Vol 65, No 6, Jun 1991, pp 265-271.

3. BISAILLON, A, MICHEL, R, and MALHOTRA, V M, Performance of high-volume fly ash concrete in large experimental monoliths, ACI Materials Journal, Vol 91, No 2, Mar-Apr 1994, pp 178-187.

4. SYED, E H AND RASHEEDUZZAFAR, Corrosion resistance performance of fly ash blended cement concrete, ACI Materials Journal, Vol 91, No 3, May-June 1994, pp 264-272.

5. CHITHARANJAN, N, Feasibility study of using fly ash concrete for reinforced flexural members, Indian Concrete Journal, Vol 70, No 9, Sept 1996, pp 503-508.

6. ALHOZAIMY, A, SOROUSHIAN, P, and MIRZA, F, Effects of curing conditions and age on chloride permeability of fly ash mortar, ACI Materials Journal, Vol 93, No 1, Jan-Feb 1996, pp 87-95.

7. ROMUALDI, J P, and BATSON, G B, Mechanics of cracks arrest in concrete, Journal of Engg Mechanics Division, ASCE, Vol 89, June 1963, pp 147-160.

8. ROMUALDI, J P, and BATSON, G B, Behaviour of reinforced concrete beams with closely spaced reinforcement, Journal of the American Concrete Institute, Proceedings, Vol 60, No 3, June 1963, pp 775-789.

9. SNYDER, M J, and LANKARD, D R, Factors affecting the flexural strength of steel fibrous concrete, Journal of the American Concrete Institute, Proceedings Vol 69, No 2, Feb 1972, pp 96-100.

10. SWAMY, R N, and MANGAT, P S, Flexural strength of steel fibre reinforced concrete, Institution of Civil Engineers, Proceedings Part 2, Research and Theory, Vol 57, Dec 1974, pp 701-707.

11. HUGHES, B P, and FATTUHI, N I, The workability of steel fibre reinforced concrete, Magazine of Concrete Research, Vol 28, No 96, Sept 1976, pp 157-161.

EXPANDED WIRE FABRIC PERMANENT FORMWORK FOR IMPROVING FLEXURAL BEHAVIOUR OF REINFORCED CONCRETE BEAMS

I G Shaaban

Zagazig University

Egypt

ABSTRACT. A new technique for using expanded wire fabric (EWF) as additional reinforcement and permanent formwork for reinforced concrete beams is proposed. Five beam specimens were experimentally tested, namely, an under reinforced control beam containing only conventional reinforcement and other four beams additionally reinforced with EWF for shear and flexure. The studied parameters included the orientation of EWF, the amount of longitudinal and transverse EWF, and the method of application of EWF. The results showed that the use of EWF led to an improvement in deflection and ductility of test beams. In addition, beams reinforced with EWF showed better crack control in comparison with the control beam having only conventional reinforcement. The orientation and method of application of EWF have a great effect on flexural behaviour of beams. The beam reinforced with U shape EWF jacket and additional layer of EWF flexural reinforcement showed better properties compared with the other beams. Its load capacity was increased by 20%, strain reached the maximum of (0.014) and the crack widths were reduced by approximately 35% compared to the control beam with conventional reinforcement. A proposed formula was developed for predicting the effect of EWF on crack control. The results obtained by this formula were in good agreement with the experimental results.

Keywords: Expanded wire fabric, Crack control, Deflection, Ductility, Reinforcement orientation, Flexural behaviour, Ferrocement.

I G Shaaban is an associate professor for the analysis and design of RC structures in Civil Engineering Department at Zagazig University (Banha Branch), Cairo, Egypt. He obtained his MSc from Ain Shams University, Cairo, Egypt, in 1988 and his PhD from University of Dundee, Scotland, U.K, in 1993. His research interests include the structural behaviour of RC and high strength concrete structures (HSC), nonlinear static and dynamic analysis of such structures, repair and strengthening of RC structures, concrete durability and its relation to the design of reinforced concrete structures.

INTRODUCTION

The rapid increase in the cost of construction has forced engineers to look for economical and better methods for building and/or repair of distressed structures. Among the materials used for construction and repair, ferrocement is comparatively a promising approach. Ferrocement is constructed of hydraulic cement mortar reinforced with closely spaced layers of small wire diameter mesh, or wire fabric, made of metallic or any other suitable material [1]. Ferrocement possesses a high degree of toughness, ductility, durability, strength and crack resistance within a relatively small thickness (approximately 25 mm), [2]. Combining these advantages with the fact that steel stresses of more than 550 MPa can be tolerated without excessive cracking, indicates a material which is ideally suitable for rehabilitation and/or new construction [2]. Hussin and Zakaria [3] and Nedwell and Swamy [4] reported that by proper choice of reinforcement and method of production, ferrocement pools, houses and boats were more economical than reinforced concrete ones. In Egypt, it is believed that the use of ferrocement in the construction can be a competitive modern building material because of its low cost in comparison with conventional concrete. Therefore, it can be considered one of the ideal solutions for the housing problem [5].

Recently, extensive research work has been carried out into ferrocement properties and applications [6 and 7]. Abdul Kadir et al [8] tested the flexural behaviour of sixteen simply supported RC beams with ferrocement permanent formwork. The test results showed that such beams failed by flexure. The composite beam with shear connectors carried about 12% higher load and 10% reserved flexural strength and showed lower deflection when subjected to the same loads as compared to reinforced concrete beams without shear connectors. Lin and Perng [9] investigated the flexural behaviour of beams with welded wire fabric (WWF) as shear reinforcement. The parameters studied in their research included concrete strength, shear span to depth ratio, amount of fly ash, amount of longitudinal reinforcement and amount of transverse reinforcement. It was found that beams with WWF shear reinforcement exhibit higher strength, better ductility and crack control than those with conventional shear reinforcement due to better confinement. In 1988, ACI Committee 549 [10] updated both of the guides for the design, construction and repair of ferrocement, and State-of-the-Art Report on Ferrocement. The main objective was to provide owners with a reference document to check the acceptability of a ferrocement alternative in a given application. However, since 1988 no update was issued to these documents [11].

The objective of this research is to study the use of expanded wire fabric (EWF) as a multipurpose material, as a formwork instead of the traditional wood formwork and as an additional reinforcement for reinforced concrete (RC) beams to improve flexural and shear behaviours of such beams. The results reported in this investigation are part of a wider research program study the potential application of EWF in RC beams. The studied parameters were the orientation of EWF, amount of longitudinal and transverse EWF, and the method of application of EWF. The behaviour of the test beams was monitored by measuring deflections, crack widths, horizontal and shear strains for different load stages.

EXPERIMENTAL PROGRAM

Five beam specimens were cast in this study. The control beam was designed according to EC 2000 [12]. The reinforcement was chosen to approach the lower limit of an under-reinforced beam. This allowed the Expanded Wire Fabric (EWF) to be added to the other test beams without over-reinforcing such beams, which would lead to premature brittle failure of concrete in compression.

The dimensions, reinforcement of the control beam and the combination of conventional and EWF reinforcement used in the other test beams are shown in Figures 1 and 2. The control beam was cast in the usual manner. A formwork of EWF of diameter 1 mm and diamond shape was used as additional shear and flexural reinforcement for the other four test specimens as shown in Table 1 and Figure 2. Then the fresh concrete was poured in the middle of the beams until mortar started to pass through the EWF openings. After that the external surfaces of the EWF were plastered using semi-dry mortar until the EWF was fully coated with mortar. The parameters investigated were amount of EWF for flexure and shear, EWF orientation and method of application.

All the specimens were tested under monotonic loading. A 50 ton Shimadzu universal testing machine with a computer controlled hydraulic servo system was adopted to apply loads. The load was spread into two point loads on the beams at a 1 mm/min rate of loading. Demec studs were glued to the sides of the test beams. Three groups were fixed on one side of each beam for the measurement of concrete surface strains and principal strains at various locations on the top compression and bottom tension surfaces of the beams. The measurements were carried out using a 100 mm demountable digital demec gauge. The deflections were measured using dial gauges (0.01 mm divisions) fixed on the bottom surfaces of the test beams. Crack widths were also observed and measured before yield. The load-deflection curve was plotted during test. Figure 3 shows a schematic diagram for a simply supported typical test beam with load position and demecs fixed at its side. It can be seen from Figure 3 that shear span/depth ratio of studied beams was kept constant (0.4/0.3).

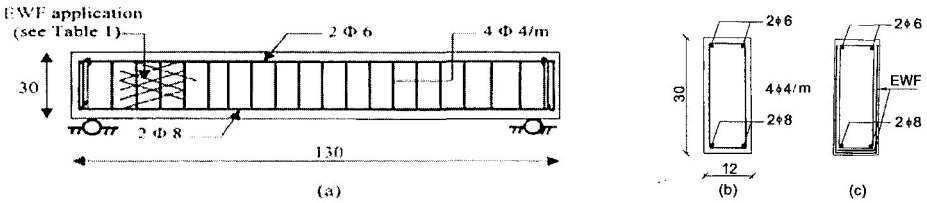

Figure 1[+] A typical studied beam specimen; (a) Sectional elevation for reinforcement details; (b) Cross section of control beam; (c) Cross section of Beams reinforced with EWF.
[+](Dimensions are in cm, 1cm = 10 mm)

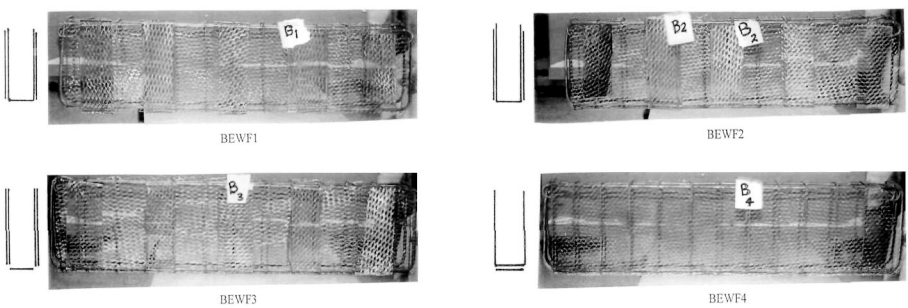

Figure 2 Photographs for using EWF as reinforcement and formwork for different beams.

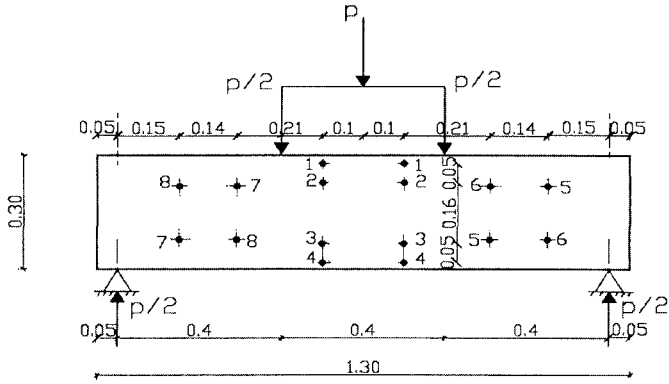

Figure 3 Loading arrangement and demec points for a typical test beam.

Table 1[+] Details of beams reinforced with Expanded Wire Fabric (EWF)

Specimen	TYPE AND ORIENTATION OF EWF REINFOREEMENT (SEE FIGURES 1 ADN 2)		
BEWF1	One Jacket of EWF (U shape, *Orientation = 30°). 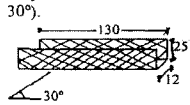	Wings of EWF (U shape) each of width equals 5 cm and spaced at 20 cm (*Orientation = 60°). 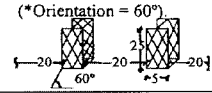	----------
BEWF2	One Jacket of EWF (U shape, *Orientation = 30°). 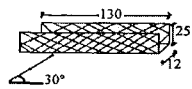	Wings of EWF (U shape) each of width equals 5 cm and spaced at 20 cm (*Orientation = 45°). 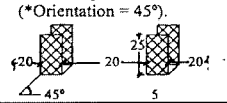	----------
BEWF3	Two side strips of EWF for shear reinforcement, 25 x 130 cm each, *Orientation = 30°. 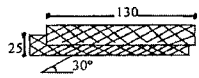	One horizontal strip of EWF for flexure reinforcement at bottom of the beam, 12 x 130 cm, *Orientation = 30°. 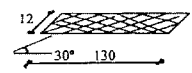	Vertical strips of EWF for shear reinforcement each of width equals 5 cm, 25 cm height and spaced at 20 cm (*Orientation = 45°). 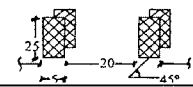
BEWF4	One Jacket of EWF (U shape, *Orientation = 45°). 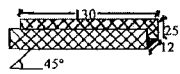	One horizontal strip of EWF for flexure reinforcement at bottom of the beam, 12 x 130 cm, *Orientation = 30°. 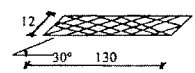	----------

*Orientation angle is measured from the horizontal direction

[+](Dimensions are in cm, 1cm = 10 mm)

RESULTS AND DISCUSSION

General Behaviour and Crack Pattern

The observed crack patterns till brittle shear failure for a typical test beam reinforced with EWF (BEWF1) are shown in Figure 4. The crack patterns developed similarly for all the beams reinforced with EWF. First cracking usually occurred at a higher load than in the control beam (see Figure 5). Initially, the cracks were vertical, as would be expected for flexural cracks, but later they would bend over in the shear regions. Crack widths of the beam specimens reinforced by EWF were generally smaller than that of beams reinforced by conventional reinforcement. After the control beam specimen reached its peak load, the concrete cover started to spall. Concrete cores of the beam specimens with EWF reinforcement remained more intact than those of specimens with conventional reinforcement after spalling of concrete cover due to the fact that the spaces of EWF were smaller and they provided better confinement.

Load-Deflection Relations

The load deflection relationships for the control beam B0 and the other beams reinforced with EWF are shown in Figure 5. Before yielding of the flexural reinforcement, the load-deflection curves were quite linear. It can be seen from the figure that the use of EWF as a formwork and additional reinforcement led to an increase in beam's capacity by approximately 5-20% without the use of wooden formwork. It is worth mentioning that the increase in beam's capacity to 20% was achieved by using one layer only of EWF for reinforcement.

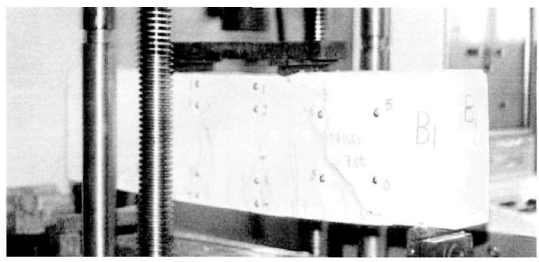

Figure 4 A typical test beam reinforced with EWF during testing.

Such enhancement may be attributed to the better confining effect from transverse (vertical) reinforcement as compared to ACI nominal strengths. Although, the amount of EWF used for Specimen BEWF3 was higher than that used for Specimen BEWF4, as mentioned earlier in Table 1 and shown in Figure 2, the capacity of the latter was higher than that for the former (see Figure 5). It can be argued that the horizontal strip used in BEWF4 improved its flexural strength and the U shape jacket used in the same beam contributed to both the shear strength and confinement. Moreover, the orientation of EWF for Specimen BEWF4, shown in Figure 2 and reported in Table 1, had a more pronounced effect on its behaviour compared to the orientation applied to the other specimens. This can be attributed to the use of an orientation angle for vertical wings of the U shape jacket of 45°, which is ideal for shear resistance, and that for horizontal part of the U shape jacket, used for flexure, was 30° giving maximum contribution for flexural reinforcement.

Crack Width

Widths of flexural cracks were measured during the tests and crack widths of the different beam specimens were compared. Typical load versus crack width curves is shown in Figure 6. It can be seen that beams with EWF reinforcement showed better crack control over the control beam B0.

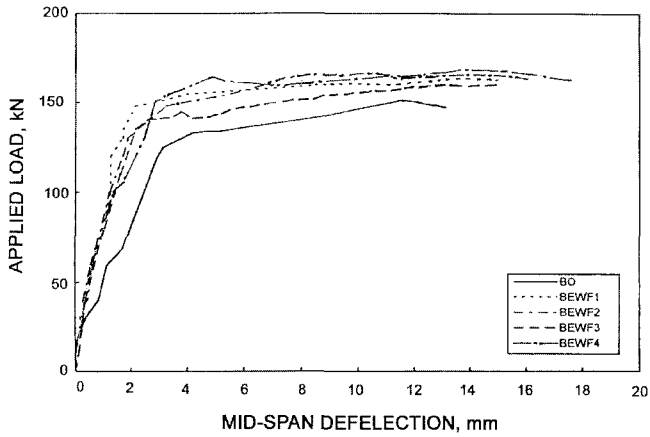

Figure 5 Load deflection relationships for different studied beams.

The loads at allowable crack width proposed by ACI code, which is about 0.3mm, can be also used for comparison [9]. Loads on the beams reinforced with EWF were generally higher than those on the control beam B0. It can be seen from Figure 6 that the beam BEWF4 had the minimum crack widths compared with the other beams reinforced with EWF. This may be attributed to the fact that this beam has a combination of good confinement, as a result of using U shape EWF jacket, and closely spaced wires, as a result of using two layers of EWF in flexural reinforcement.

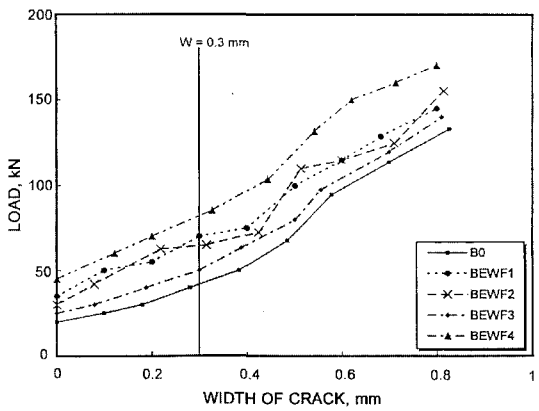

Figure 6 Crack width for different studied beam specimens.

Strains

(a) Horizontal strains

The measurement of the horizontal strain distribution across the depth of the test beams for different load steps were recorded and plotted in Figure 7. It can be seen from the figure that the tensile strains were much higher than the compressive strains and the strain distribution was almost linear across the beam depth except for beam BEWF1. This finding reflected the ductile behaviour of the beams as the tensile reinforcement reached its yield strength. The horizontal strain results measured at the demec points (1-4) on the sides of beams (see Figure 3) were highly affected by the formation of cracks. It can be seen from Figure 7 that the strains in the tension zone increased slowly for different beams to different load levels before the formation of cracks. After the formation of cracks, the contribution of reinforcement led to a rapid and significant increase in strains until failure occurred. The contribution of EWF enhanced the ultimate capacity of the studied beams to different degrees. Figure 7 shows also that the horizontal strains at maximum ultimate loads of the studied beams ranged between 0.006 to 0.014. The beam BEWF4 had the maximum strain (0.014) at a maximum ultimate load (160 kN) which indicates the high ductility of this beam compared with the control beam and the other beams reinforced with EWF. This is in good agreement with the findings observed earlier for the load-deflection relationships and crack widths.

(b) Principal tensile strains

The relationship between applied loads and principal tensile strains is shown in Figure 8. It can be seen from the figure that reinforcing beams with EWF improves both of the beams' capacity and ductility. As observed earlier for the horizontal strains, all the beams show slow increase in principal tensile strains before cracking. After cracking, only the EWF and steel reinforcement provide tensile resistance, and hence, principal tensile strains increases much more rapidly. Figure 8 shows that the beam BEWF4 sustained a higher load at low strain compared to that of the other studied beams. The other beams sustained almost equal loads at low strains till cracking, after cracking the beams reinforced by EWF showed higher resistance compared to the control beam B0. It is interesting to note that the order of improvement in the behaviour of beams reinforced with EWF in principal tensile strains was not the same as that in horizontal strains. For example, despite that Specimen BEWF4 showed excellent ductility till failure, at a maximum load for horizontal strains compared with the other beams (see Figure 7), Specimen BEWF3 sustained ultimate principal tensile strains higher than that of BEWF4 by 65% (0.068 mm/mm) at almost equal loads (see Figure 8). This may be attributed to the fact that the amount of EWF for shear reinforcement of Beam BEWF3 was higher than those for Beam BEWF4 (see Table 1 and Figure 2).

THEORETICAL PREDICTION OF CRACK WIDTHS

The maximum crack width for square mesh reinforcement in flexural members was predicted earlier [1] as follows:

$$W_{max} = \frac{f_s}{E_r} S\beta \qquad (1)$$

Where

f_s = stress in the outermost layer of steel.
S = spacing of transverse wires.
β = ratio of distances to the neutral axis from the extreme tensile fibre and from the outer most layer of steel.
Er = effective modulus of the reinforcing system.

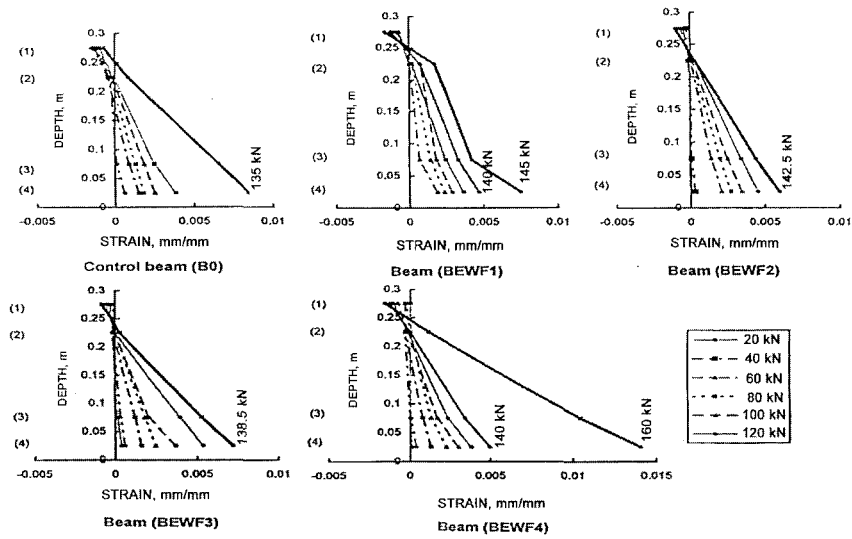

Figure 7 Strain distribution for studied beams.

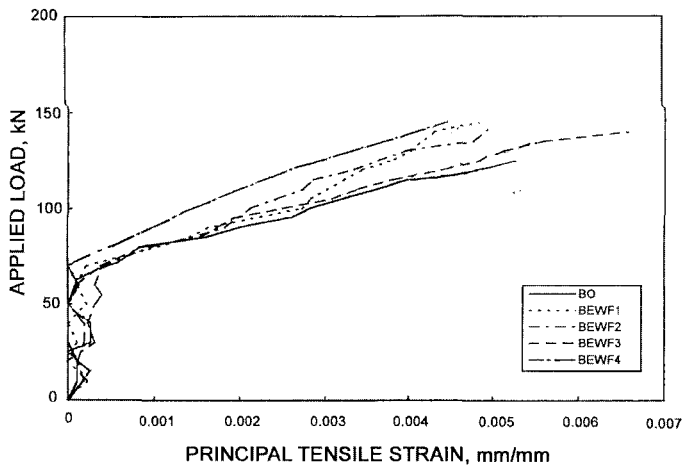

Figure 8 Load-principal tensile strain relationship for different studied beams

Equation (1) is based on the observation that the average crack spacing in flexure is approximately equal to the spacing of transverse wires and was found to represent an upper bound in observed data on average crack width. An overall linear regression equation for predicting the maximum crack width in flexure was developed [1] based on experimental data on cracking of ferrocement specimens reinforced with different amounts of square meshes with wire spacing of 12 mm and 6 mm.

$$W_{max} = (1.194\, f_s - 111)\ \frac{15.85}{E_r} \qquad (2)$$

Where W_{max} is in mm, f_s and E_r are in MPa (N/mm^2).

The following conservative procedure [12] can be followed, assuming the stress in the steel is less than the yield strength and in any case less than 414 MPa, to predict maximum crack width in tensile ferrocement members:

For $f_s \leq 345\ S_{r\ell}$

$$W_{max} = \frac{35000}{E_r} \qquad (3)$$

Where

fs is in MPa, W_{max} in mm and E_r in (N/mm^2).
$S_{r\ell}$ is the specific surface of reinforcement in loaded direction is cm^{-1} and is defined as the total bonded area of reinforcement (interface area or area of the steel that comes in contact with the mortar) divided by the volume of composite.

For a ferrocement section of width b and depth h, the specific surface of reinforcement can be computed from

$$S_r = \frac{\Sigma_0}{bh} \qquad (4)$$

In which Σ_0 is the total surface area of bonded reinforcement per unit length (the perimeter of flexural reinforcement bars and EWF are considered in full contact with concrete).

For $f_s > 345\ S_{r\ell}$ (applicable for the studied beams in this investigation)

$$W_{max} = \frac{20}{E_r}\ [175 + 3.69\,(f_s - 345\ S_{r\ell})] \qquad (5)$$

The above equation is modified herein for the application to RC beams reinforced with EWF used in this study, as follows:

$$W_{max} = \frac{20}{E_r}\ [175 + 3.69\,(f_s - 345\ \{\sum_{1}^{\ell}\ \alpha\ S_{r\ell}\cos\theta + S_{rb}\})] \qquad (6)$$

Where

S_r is divided into two terms, the contribution of longitudinal reinforcement bars (traditional reinforcement) "S_{rb}" and summation of specific surface of reinforcement for EWF layers, ℓ "$S_{r\ell}$" which includes strips, jackets, and wings. Since the predicted crack widths are the flexural ones, the calculated S_r is for flexural reinforcement only.

θ is the orientation angle of EWF with the horizontal direction.

α is a confinement factor and is estimated as 16 for EWF wings or jackets, 8 if jackets and wings are acting together and 1 for EWF strips.

$f_s = 140$ MPa (N/mm^2).

E_r in the longitudinal and transverse directions for EWF were reported in [10] as follows:

$E_{r\,(long)} = 138 \times 10^3$ (N/mm^2). & $E_{r\,(trans)} = 69 \times 10^3$ (N/mm^2).

The prediction of crack widths is normally carried out during service loads. However, the predicted crack widths obtained by the above equations are not functions in applied loads. Therefore, experimental values of crack widths, which are related to applied loads as shown in Figure 6, can not be compared with those predicted by Equation (6). It is more practical to compare the effect of EWF reinforcement on the crack widths obtained experimentally with that predicted theoretically. This effect can be estimated by;

$$\frac{\text{Crack width of a beam reinforced with EWF, } W_{EWF}}{\text{Crack width of the control beam, } W_o} \qquad (7)$$

The experimental effect of EWF is obtained on two steps. Firstly, by extracting crack widths for studied beams from Figure 6 at a load level less than the service loads, which are assumed to be half of the maximum test loads. Secondly, by applying Equation (7) to the experimental results. Predicted values of crack widths can be obtained by applying Equation (6) to each studied beam while the effect of EWF on predicted crack width is obtained by applying Equation (7). Table 2 shows a comparison between the experimental and predicted effect of reinforcing beams with EWF. The good agreement between the experimental and theoretical results shown in Table 2 indicates the sensitivity of Equation (6) to the studied parameters such as orientation of EWF, quantity of EWF reinforcement (number of reinforcement layers) and type of reinforcement (strips, jackets, wings and traditional reinforcement).

Table 2 Experimental and theoretical evaluation of EWF effect on crack width

BEAM SPECIMEN	CRACK WIDTH RATIO, W_{EWF}/W_o	
	Experimental Ratio	Predicted Ratio
BEWF1	0.5	0.52
BEWF2	0.48	0.5
BEWF3	0.9	0.9
BEWF4	0.3	0.28

CONCLUSIONS

Based on the experimental results reported herein and theoretical prediction presented in this investigation regarding the effectiveness of using permanent EWF formwork as additional reinforcement, the following conclusions can be drawn:

- Using EWF as additional reinforcement results in a reduction of deflection, increasing loads at first cracking, and enhancing section ductility. In addition the close spacing between wires in the EWF can reduce crack widths.

- The beams reinforced with a U-shaped EWF layer around the beam cross-section and additional layer at the tension face showed excellent response compared with other beams reinforced with EWF. Its load capacity was increased by 20%, strain reached the maximum of (0.014) and the crack widths were reduced by approximately 35% compared to the control beam with conventional reinforcement.

- Using EWF as a permanent formwork is a promising technique since it can achieve two goals, firstly it can replace the traditional temporary timber formwork which, in turn, lead to a reduction of the overall cost and avoid problems of placing concrete. Secondly, it can be used as additional reinforcement for improving shear and flexure behaviour. However, further research is needed to study the potential application of this technique widely for beams of large spans.

- A proposed formula was developed for predicting the effect of EWF on crack widths. The prediction was in a good agreement with the experimental results.

REFERENCES

1. ACI Committee 546, "State-of-the-Art Report on Ferrocement," (ACI 549 R-88), ACI, Detroit, 1988, 24pp.

2. AHMED H.I, ROBLES –AUSTRIACO L, "State-of-the-Art Report on Rehabilitation and Restrengthening of Structures Using Ferrocement," Journal of Ferrocement, Vol. 21, No. 3, July 1991, pp. 243-258.

3. HUSSIN M.W, ZAKARIA F.H (Editors), "Ferrocement-Current Research, Applications and Developments", Proceedings of the Second National Seminar on Ferrocement, Johr Bahru, Malaysia, August 1993, pp. 129.

4. NEDWELL P.J, SWAMY R.N (Editors) "Ferrocement, proceedings of the Fifth international Symposium on Ferrecement", 1994, E@FN Spons, London, pp. 507.

5. PRAWEL S.P, REINHORN A, "A Competitive Modern Building Material," Concrete International, Vol. 5, No. 11, November, 1983, pp. 17-21.

6. MANSUR M.A, TAN K.L., NAAMAN A.E., PARMASIVAM, P. ,"Bolt Bearing Strength of Thin-walled Ferrocement", ACI Structural Journal, Vol. 98, No. 4, July 2001.

7. AL-KUBAISY M.A., JUMAAT M.Z., "Strengthening of Reinforced Concrete Beams Using Ferrocement Laminate", Concrete International, Vol. 22, No. 10, October, 2000, pp. 37-43.

8. ABDUL KADIR M.R, ABDUL SAMAD A, MUDA Z.C, ALI A.A, "Flexural Behaviour of Composite Beam with Ferrocement Permanent Formwork," Journal of Ferrocement, Vol. 27, No. 3, July 1997, pp. 209-214.

9. LIN C.H, PERNG S.M, "Flexural Behaviour of Concrete Beams with Welded Wire Fabric as Shear Reinforcement," ACI Structural Journal, Vol. 95, No. 5, September-October 1998, pp. 540-546.

10. ACI committee 549, "Guide for the Design, Construction, and Repair of Ferrocement," (ACI 549. 1R-88), ACI Structural Journal, May-June 1988, pp. 325-351.

11. PARAMASIVAM P., LIM C.T.E., ONG K.C.G, "Ferrocement in Structural Upgrading and Rehabilitation-An Overview", ACI SP.193-22, Vol. 193, August 2000.

12. E.C 2000, "Egyptian Code for the design and Construction of Reinforced Concrete Structures", Cairo, 2000.

13. NAAMAN A.E., "Design Predictions of Crack Widths in Ferrocement", Ferrocement – Materials and Applications, SP-61, American Concrete Institute, Detroit, 1979, pp. 25-42.

BASIS OF OPTIMISING STRENGTH THEORY OF REINFORCED CONCRETE BAR ELEMENTS AND CONSTRUCTIONS

V P Mitrofanov

Poltava State Technical University

Ukraine

ABSTRACT. The general Optimizing Strength Theory of Concrete Elements (OSTCE) of the normal and inclined sections (cracks) under co-action of the bending moments M, shear Q and longitudinal N forces is suggested. The OSTCE uses, generalizes and develops the known principles of the strength designs of the RC elements: design on the failure stage, entire use of reinforcement strength and connected with this the plastic failure, ultimate equilibrium method for the redundant structures. So, the OSTCE guarantees the plastic failure not only of normal sections but inclined ones under shear forces action. The OSTCE overcomes the important disadvantages of the known strength design methods, in particular, absence of system unity of all known elements strength designs and non-deriveness of the partial design cases from the general ones that testified about of principle imperfection of these designs and about corresponding non-optimality of structures projected by such designs. The great role of extreme strength criteria in the OSTCE caused its name "Optimizing". The central place of the OSTCE is occupied by the general strength design case of the inclined section under co-action M, Q, N forces from which there are derived the partial strength design cases of the inclined and normal sections under co-action of M and Q and also designs of the normal section under co-action M and N and one M or N. In the OSTCE the improved design of the normal section is worked out for two levels of accuracy and simplicity which are stipulated by the assumed stress distribution on the height of compressed concrete zone: 1) uniform; 2) curve according to the entire compression diagram of concrete. The mastering of the OSTCE signifies the acquisition of knowledge of at once all the most meeting in practice the strength designs of the RC elements.

Keywords: Concrete elements strength, Forces co-action, Dangerous normal and inclined cracks, Non-overreinforcing, Plastic failure.

PhD Prof V P Mitrofanov, is Founder and Head of the Research Group FARCON: Fundamental and Applied Researches of Concrete Construction, Poltava State Technical University, Ukraine. He specializes in design methods of concrete and prestressed structures and their elements under complex static and dynamic loading. His interests include the behavior of the concrete under multiaxial non-uniform stress-strain states, the use of the Theory Plasticity and Fracture Mechanics to design of concrete structures and Statistical Thermodynamics of Irreversive Processes in Concrete.

INTRODUCTION

The development of theory and design methods of the Reinforced Concrete (RC) structures is one of the most important factors stipulating the progress in practice of concrete construction. The history of science and technique shows the trend development of knowledge from the lower empirical level to the highest level - scientific theory distinguishing by the system's, generality and profundity of explanation of phenomena essence that is necessary for creation of the perfect complex technical systems.

The present ample quantity of experimental data about strength of RC structures and their elements are still not systematized, not generalized and not developed to the level of enough wide scientific theory but one testifies about approach of such stage. At present the level of strength designs development may be estimated as largely empirical one the essential demerits of which are often not realized: 1) errors of the determining factors selection; 2) errors of the analytic relationship selection; 3) limited possibilities of structures optimization owing to the noted errors; 4) great expenditures of various resources for the experiments. The negative features of the empiricism, not high level of theoretical analysis and generalization of the test facts, insufficient use of the fundamental sciences are sources of the known strength design methods disadvantages among of which two ones are especially considerable.

Inexact understanding of the essence of the entire concrete compression diagram σ_b - ε_b as curve restricted on the descending part by the point of the sudden failure with so called "ultimate strain ε_{bu}" being assumed as deforming failure criterion of concrete compressed zone element

$$\varepsilon_b = \varepsilon_{bu} \approx 3{,}0 \ldots 3{,}5‰ , \tag{1}$$

where ε_b is strain of compressed element side in dangerous normal section. The actual entire diagram σ_b - ε_b includes the critical descending part that is *stable* boundary between sudden and gradual failure of concrete and one is obtained by the known rigid loading regime leading to the state of *residual strength* $\sigma_{br} << R_b$ with strain $\varepsilon_{br} > \varepsilon_b$. It may show [1] that the entire diagram σ_b - ε_b excludes the necessity of the inexact deforming criterion (1) because the entire real σ_b - ε_b diagram leads in strength control problem to the *force extreme failure criterion* of the concrete compressed zone and whole normal section of element

$$F(\varepsilon_{bm}) = \max, \tag{2}$$

where F is the load parameter of section (M or N) and the ultimate strain ε_{bm} *is found from (2) in the design process* as one of unknown quantities. For the problem of tensile A_s and compressed A_s' area reinforcement selection as *double-dealing* to the strength control problem (2) the following extreme criterion must be used instead

$$V_s = A_s + A_s' = V_s(\varepsilon_{bm}) = \min. \tag{3}$$

Non-deriveness of the strength design of normal section under moment M action from the more general strength design of the inclined section under co-action M and Q owing to empirical character of latter as for example in accord with SNIP2.03.01-84*, ACI318-89,

BS8110-1, DIN1045-1(2.97) and others. This demerit especially clearly shows the non-systemness and non- generality of the known strength designs of RC elements and corresponding non-optimality of structures projected on the base of the above-mentioned designs.

BASIC ASSUMPTIONS

Design state of elements and structures is considered as failure stage. Moment of failure is assumed as destruction state of *concrete* in the most deformed and most stressed zone.

Classification of RC elements is conducted depending on quantity of longitudinal and shear reinforcement, completeness of its strength use, type of destruction. Four main (principal) elements groups A,B,C,D are distinguished (Figure1):

- **Group A:** elements are overreinforced by longitudinal reinforcement and non-overreinforced by shear one; longitudinal reinforcement (usually without breaks and bents) does not reach the ultimate stress; shear reinforcement reaches one; group A elements are destroyed brittlly on the *dangerous inclined crack* (DIC) or on the normal crack;

- **Group B:** elements are overreinforced by longitudinal and shear reinforcement; the stresses do not reach the ultimate values in longitudinal and shear reinforcement; group B elements are destroyed brittlly by crushing of concrete struts between a number of inclined cracks or on the normal crack;

- **Group C:** elements are non-overreinforced by longitudinal and shear reinforcement; longitudinal reinforcement (with breaks or bents) and shear one reach the ultimate stresses; group C elements are destroyed plastically on the DIC or on the normal crack;

- **Group D:** elements are non-overreinforced by longitudinal reinforcement and overreinforced by shear one; the stress reaches the ultimate value in longitudinal reinforcement and it does not reach in shear one; group D elements are destroyed plastically on the normal crack which may be located in action zone of shear forces.

Besides the main elements groups there are 5 intermediate (boundary) elements groups which have intermediate properties between corresponding main groups.

The classification distinguishes expedient for practice the group C of elements which are remarkable for the most economical steel expenditure, plastic failure and comparatively simple design. That is why the OSTCE mainly concerns the group C of elements.

Definition of concrete structure element is assumed as structure part on the length l of which the moments M, forces Q and N have constant signs. The above-mentioned element definition leads to unified design scheme of its dangerous cracks, reinforcement and forces (Figure 2). The end points A and B of the DIC are considered as theoretical points of break or bent of longitudinal reinforcement.

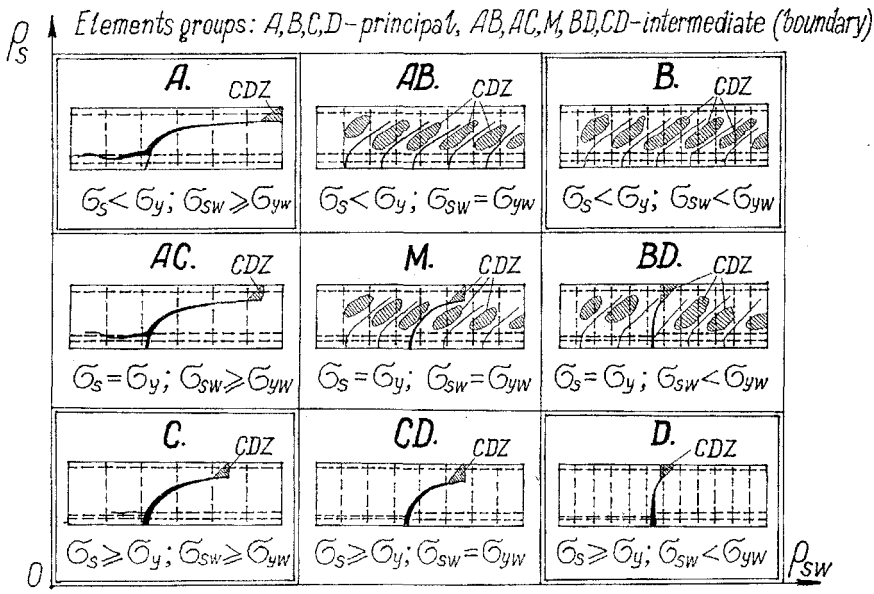

Figure 1 RC elements classification depending on quantity of longitudinal (ρ_s) and shear (ρ_{sw}) reinforcement and element destruction type. CDZ – concrete destruction zone

Ultimate forces of the concrete destruction zone of element (shear Q_b and longitudinal compressive N_b) were found with taking into account all stress components σ_x, σ_y, τ_{xy} of the plastic plane stressed state of the truncated wedge with angle α_w as model of concrete region above the DIC [2]. It was discovered the possibility of 3 failure cases depending on the ratio Q_b / N_b (Figure 3). For being considered here non-short elements the failure cases 1 and 2 have primary meaning. Approximate linear relationship as strength criterion for concrete failure zone was received

$$Q_b = AR_b bx + a_N N_b, \tag{4}$$

where b, x are width and height of the concrete failure zone,
for the wedge failure case 1

$$A = - a_N = tg\gamma, \tag{5}$$

for the wedge failure case 2

$$A = tg\gamma / (1 + tg\gamma\, tg\alpha_w),\ a_N = tg(\alpha_w - \gamma), \tag{6}$$

$$tg\gamma = 2(R_{br}/R_b)^{1/2}. \tag{7}$$

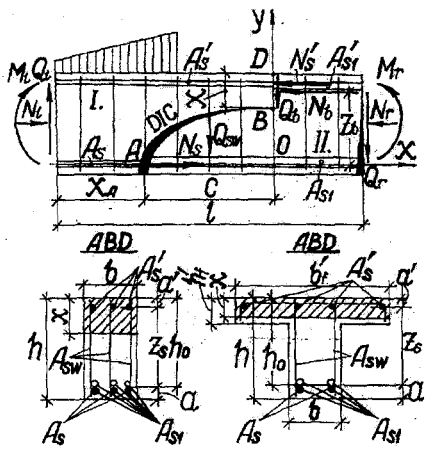

Figure 2 Design element scheme

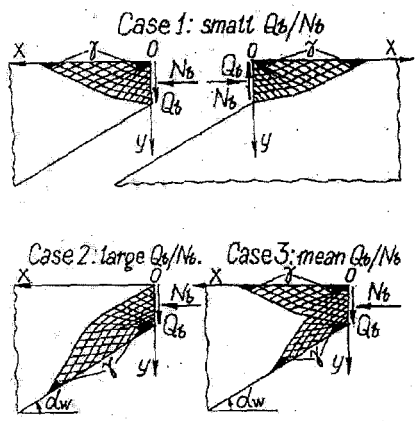

Figure 3 Destruction cases of concrete truncated wedge depending on ratio Q_b/N_b

Interlock forces in the DIC and dowel action of longitudinal reinforcement are neglected because in mutual movement of divided by the DIC parts 1 and 2 of group C elements (Figure 2) the rotation and corresponding DIC opening predominate and shear slip of no important takes place in the DIC, so that, accordingly to the criterion of existence of roughness interlock at adjacent rupture surface of concrete [3], the interlock in the DIC is really absent. Dowel action decreases also owing to the breaks and bents diminishing the longitudinal reinforcement cross area.

Definitions of the large and little eccentricities cases of the eccentrically compressed elements are defined more precisely and unlike SNIP2.03.01-84* clearly separate the influence of reinforcement quantity (completeness of strength use) and influence of strictly eccentricity value.

Loading regime of structures and their elements is considered as proportional. The load parameter F is chosen and forces in dangerous cracks (sections) are expressed by means of F

$$M = F f_M, \qquad Q = F f_Q, \qquad N = F f_N, \tag{8}$$

where f_M, f_Q, f_N are load functions which depend on the DIC parameters X_A, C (Figure 2).

Distribution of the normal stress σ_b along the concrete failure zone height of inclined crack (section) is assumed uniform. Strength designs on the normal sections (cracks) are worked out for two exactness levels depending on used distribution of σ_b:

1) uniform,
2) 2) curve in accordance with the entire concrete compression diagram.

BASIC RELATIONSHIPS

If the bent bars are absent the equilibrium equations for the element part 1 on the design scheme (Figure 2) with taking into account (8) are

$$\Sigma X = 0;\ F f_N - \sigma_s A_s - \sigma_s' A_s' - N_b = 0; \tag{9}$$

$$\Sigma Y = 0;\ F f_Q - (\sigma_{sw} A_{sw} C) / S - Q_b = 0; \tag{10}$$

$$\Sigma M_0 = 0;\quad F f_M - (\sigma_{xw} A_{sw} C^2) /2S - \sigma_s' A_s' Z_s - N_b (h_0 - x/2) = 0; \tag{11}$$

where σ_s, σ_s', σ_{sw} are stresses in longitudinal tensile, compressed and shear reinforcement accordingly, S - stirrup distance, Z_s, h_0 - see (Figure 2). Eliminating the Q_b, N_b, X from (4) and (9) - (11) the resulting relationship is derived

$$P^2 f_N(f_Q - f_N a_N)/2A + P[f_M/h_0 + \omega f_Q - f_N(1 + m_{sw}\xi_{sw} C/2Ah_0 - \eta)] - (m_{sw}\xi_{sw}/2)(C^2/h_0^2 + 2\omega C/h_0) - B = 0, \tag{12}$$

where $P = F/R_b b h_0$, $\quad \omega = \eta/2A$, $\quad \eta = m_s\xi_s - m_s'\xi_s'$, \tag{13}

$$B = \eta(1 - \eta/2) + m_s'\xi_s' Z_s / h_0, \tag{14}$$

$$\xi_s = R_s A_s / R_b b h_0,\quad \xi_s' = R_{sc} A_s' / R_b b h_0,\quad \xi_{sw} = R_{sw} A_{sw} / R_b b h_0, \tag{15}$$

$$m_s = \sigma_s / R_s,\quad m_s' = \sigma_s' / R_{sc},\quad m_{sw} = \sigma_{sw} / R_{sw}, \tag{16}$$

R_s, R_{sc}, R_{sw}, m_s, m_s', m_{sw}, - rated strength and efficiency coefficients of resistance use of corresponding reinforcement.

The volume coefficient of reinforcing of the element is

$$V_s = R_b\xi_s X_A / R_s l + R_b\xi_s' (X_A + C)/R_{sc} l + R_b\xi_{sw}/R_{sw} + R_b\xi_{s1}(1 - X_A/l)/R_s + R_b\xi_{s1}'[1 - (X_A + C)/l]/R_{sc}, \tag{17}$$

where $\xi_{s1} = R_s A_{s1} / R_b b h_0$, $\quad \xi_{s1}' = R_{sc} A_{s1}' / R_b b h_0$, \tag{18}

A_{s1}, $\quad A_{s1}'$ - see Figure 2.

FORMULATION AND SOLUTION OF THE BASIC PROBLEMS

It is mainly considered the strength design on the inclined crack (section) from which the design on the normal crack (section) is obtained as particular case when $C = 0$, $\xi_{sw} = 0$, $\xi_s = \xi_{s1}$, $\xi_s' = \xi_{s1}'$, $X_A = l$.

By such way the 1-st mentioned accuracy design level of normal section is received. The more high 2-nd accuracy level is necessary for design elements with steel having proof stress $\sigma_{0.2}$, for more exact determination of the overreinforcing boundary and for increase of the

strength design reliability of normal sections especially in the eccentrically compressed elements with the little eccentricity. Problem of the strength sections element verification is formulated and solved as optimization problem with aim function (12) for load parameter F that satisfies for inclined section to criterion following from the kinematic theorem of the ultimate equilibrium

$$F(C) = \min \tag{19}$$

and to criterion (2) for normal section on the curve distribution of the stress σ_b.
The additional conditions of this problem are

$$m_s = m_s' = m_{sw} = 1, \tag{20}$$

corresponding to the group C elements.

The control of non-overreinforcedness of the inclined sections is conducted in accord with condition

$$A_s \le A_s^{opt},\ A_s' \ge A_s'^{opt},\quad A_{sw} \le A_{sw}^{opt}, \tag{21}$$

in which the optimal values of corresponding reinforcement area A_s^{opt}, $A_s'^{opt}$, A_{sw}^{opt} are found from the solution of problem of the requisite reinforcement selection.

Problem of the requisite longitudinal and shear reinforcement selection is formulated and solved as optimization problem with aim function (17) that satisfies to criterion (3) receiving for inclined section the form

$$V_s = V_s(A_s, A_s', A_{sw}, C, X_A, m_s, m_s', m_{sw}) = \min. \tag{22}$$

The additional conditions are (12), natural restrictions for values m_s, m_s', m_{sw}

$$m_s \le 1,\ m_s' \le 1,\ m_{sw} \le 1 \tag{23}$$

and restriction for the location of the DIC

$$X_A + C \le l. \tag{24}$$

System of the Kuhn-Tucker conditions for the above formulated problem is compatible and leads to the optimal solution (20) showing that optimal reinforcement coincides with the complete use of all reinforcement strength in the section (crack) of element.

IMPROVEMENT OF THE ULTIMATE EQUILIBRIUM METHOD

The plastic failure of the inclined non-overreinforced sections of the group C elements allows to take into account in the redundant RC structures the forming of plastic hinges not only in normal sections as one is made at present but at inclined sections. As a result the number of possible kinematic failure schemes of structure is considerably increases at the expense of plastic hinges in the inclined sections and combinations of them with plastic hinges in the

normal sections (Figure 4). The use of the OSTCE to the redundant structures includes two additional problems, the formulation and solution of which have certain peculiarities connected with overcoming of structures redundancy. In the strength verification problem the redundancy of each failure scheme is opened by additional equations which means the equality of the ultimate load parameters corresponding to all plastic hinges. As real ultimate load parameter is selected that is minimum among ones for the full totality of the failure structure schemes. The non-over reinforcedness control of redundant structures is carried out on base (21) where optimal reinforcement areas must be known.

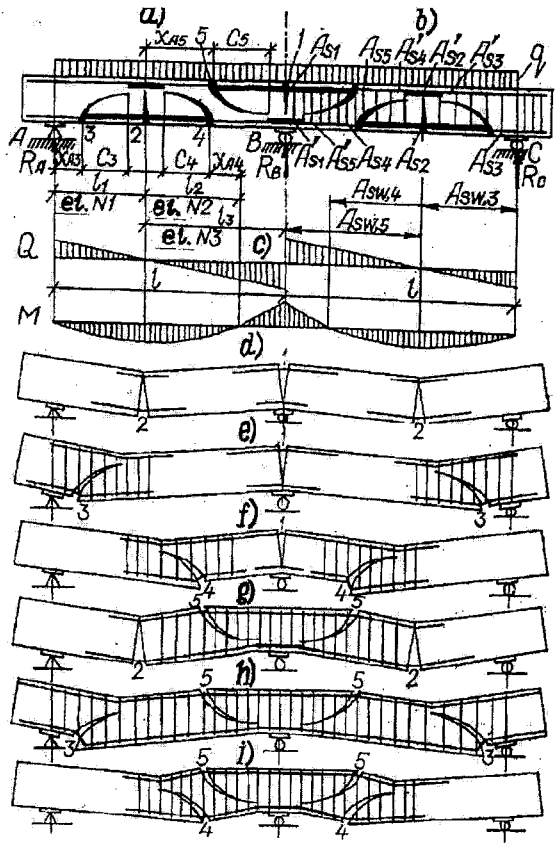

Figure 4 Continuous beam with its dangerous normal 1, 2 and inclined 3, 4, 5 cracks, divisionon elements №№ 1, 2, 3 (a), reinforcement in cracks (b), forces (c), failure schemes with normal (d) normal and inclined (e, f, ,g) and inclined (h, I) cracks

In the reinforcement selection problem the redundant structure is considered as equally-strength on all normal and inclined sections. Then this problem may be reduced on basis of the OSTCE to search of the minimum of total expenditure of reinforcement steel for the whole structure in the n- dimensional space of the superfluous brace reactions (n-redundancy degree). Herewith the suitable calculate algorithm may be the Monte Carlo method.

EXPERIMENTAL VERIFICATION OF THE OSTCE

The many-sided experimental control of the OSTCE was carried out. The strength criterion (4) was thoroughly verified by the experiments on the wedge specimens of heavy [2] and lightweight [5] concrete, as well as on the beams with artificial DIC which allowed to eliminate the DIC sides interlock and to determine reliably the experimental Q_b and N_b values. Control of the relationship (4) was also conducted on a great number of real group A beams in which forces carried across the DIC and dowel force of the longitudinal reinforcement were found on the models worked out by author [3]. The mentioned many-sided tests [2,3,5] corroborated the reality of the theoretical failure cases of concrete wedges and reliability of the relationship (4). It is necessary to emphasize that researches of RC and prestressed elements strength under shear forces action were being conducted in many countries of world almost solely on the elements of groups A and B. Such researches leaded to the inexact notion about only brittle failure of RC elements under shear force action. In 1970 the plastic failure on the inclined crack was received in author's experiments. Then the systematic researches of the group C elements began in PSTU. The carried out to present researches includes tests of the RC [3,6] and prestressed [6] simple beams, the two-span continuous beams (Figure 5), simple beams with inclined compressed upper side, the RC beams being failured on the normal section under moment with considerable shear force influence [7], the columns under joint action of the M, N, Q [8].

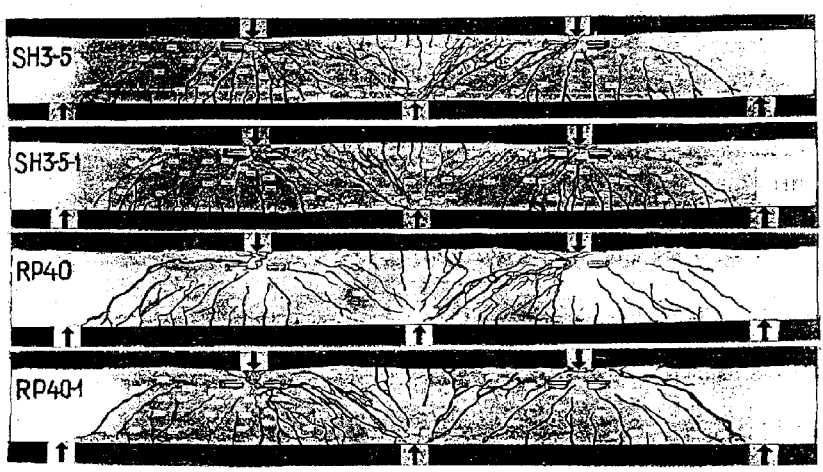

Figure 5 Reinforced in accordance with OSTCE two-span symmetrical redundant beams in failure state

All test beams and columns were reinforced in accordance with optimizing design on the given load. The tests corroborated the plastic behavior in the shear forces action zone of structures with group C elements. In tested continuous beams the equally-strength on the planned dangerous sections (cracks) was reached and state of the ultimate equilibrium beams had clearly plastic character (Figure 5). The test data of 126 beams and columns showed the mean ratio F^{test}/F^{calc} of experimental ultimate load parameter F^{test} to theoretical one F^{calc} averaged 1.073 herewith coefficient of variation 9.525%.

CONCLUSIONS

The main features of the OSTCE characterizes its practical importance:

1) considerable systemness level and generality: taking into account of joint action of forces M, Q, N, strength design of inclined and normal sections on base of the common conceptions and deriveness of particular latter from more general former;

2) mathematical strictness and explanatory ability increasing the possibilities of deliberate control by the parameters of the RC structures;

3) optimal reinforcement steel expenditure owing to complete use of steel strength of all reinforcement (longitudinal and shear) and close corresponding of reinforcement change to internal forces change along axis elements and structure;

4) plastic failure of structures on the normal and inclined sections (cracks);nearness of theoretical strength to experimental one;

5) constructive, technological and service peculiarities of structures: breaks and bents of longitudinal reinforcement, limited or partial prestressing.

OSTCE more than known strength design methods corresponds to ideology of future code which ought to include the general theories of designs, general principles and criteria of projecting of concrete and reinforced concrete structures and their elements.

REFERENCES

1. MITROFANOV. V., ARTSEV S., Ultimate compressibility of concrete of normal sections of RC elements. Problems of theory and practice of RC. Poltava: PSTU, 1997. pp 333-337.

2. MITROFANOV. V., Investigation of destruction zone resistance of HSC of beams under shear forces action. Proceedings of 5-th International Symposium on HS/HP concrete, Sandefjord, Norway, 1999. Vol. 1, pp 461-468.

3. MITROFANOV. V., Stress-strain state, strength and cracking of RC elements under cross bending. Moscow: VZISI, 1982.

4. MITROFANOV. V., ARTSEV S., Reinforced concrete bar systems with optimal steel expenditure. Proceedings of International Conference INDIS'97, Novi Sad, Yugoslavia, 1997. Vol. 1, pp 257-265.

5. POGREBNOY. V., Strength of concrete and RC elements under shear. Poltava: PSTU, 2001.

6. MIKITENKO. S., Strength under bending of RC and prestressed elements with complete resistance use of shear and highly-strength longitudinal reinforcement. Poltava: PSTU, 1995.

7. MITROFANOV. V., VOSKOBOINIK P., Shear forces influence on strength of normal sections of bent elements. Concrete and reinforced concrete, N9, 1982. pp 41-43.

8. KOTLYAROV. V., Strength of reinforced concrete elements under joint action of bending moments, axial compressing and shear forces. Poltava: PEBI, 1992.

BENDING CAPACITY OF STEEL FIBRE REINFORCED CONCRETE (SFRC) BEAMS

D Dupont

L Vandewalle

Catholic University of Leuven

Belgium

ABSTRACT. This paper describes a study of the flexural capacity of Steel Fibre Reinforced Concrete (SFRC) beams. The study includes an experimental program of 28 full-scale beams, tested in four point bending at the Department of Civil Engineering of the K.U.Leuven. The different tested parameters are the fibre content, the concrete grade, the span to depth ratio and the reinforcement ratio. For each combination of parameters two identical beams were tested in order to control the scatter. The experimental load deflection curves are compared with theoretical load deflection curves, calculated by using the stress strain relation as proposed by Rilem TC162-TDF [1]. The results show that the influence of the fibres on the flexural capacity is rather small. The stress strain diagram as proposed by Rilem gives in most cases a small overestimation of the flexural capacity. Also there seems to be a significant scatter in the flexural capacity for the beams without conventional reinforcement.

Keywords: Steel fibre, Concrete, Beams, Bending, SFRC, Fibre reinforcement, Flexural capacity, Stress strain relation.

D Dupont is a research assistant in the Civil Eng. Dept., Catholic University of Leuven, Belgium. Currently he is working on a Brite Euram project about steel fibre concrete. The aim of the project is to evaluate and produce recommendations for a new European standard with regard to the testing and design of SFRC. Besides he is also working on a Ph.D. about the stress strain relation of SFRC and the cracking behavior of SFRC structures.

L Vandewalle is an associate professor in the Civil Eng. Dept., Catholic University of Leuven, Belgium. She received her engineering degree in 1981 and Ph.D. in 1988. Her field of interest mainly concerns fibre concrete, high strength concrete and prestressed concrete. She is chairlady of RILEM TC162-TDF "Test and design methods for steel fibre reinforced concrete" and convenor of FIB TG 8.3 "Fibre Concrete". She is member of ACI Committee 544 "Fibre Reinforced Concrete".

INTRODUCTION

Steel fibres have been used in concrete structures for several years now. They are known to give the concrete a better ductility and improve the cracking behavior and the shear capacity of concrete structures. Applications in Steel Fibre Reinforced Concrete (SFRC) are still very limited due to the lack of generally accepted design guidelines. The existing design guidelines are mostly empirical, do not show much transparency and seem to be arbitrarily chosen. This situation does not create much confidence and as a result the use of SFRC remains limited, despite of some of its very good material properties. To overcome the existing problems, more fundamental research is needed to obtain a basic understanding of the material SFRC.

During the last decades, a lot of research has been done with regard to the basic constitutive relation of SFRC. This has resulted in two methods. The first method is the stress-crack width approach. This fracture mechanics based approach was introduced by Hillerborg [1] and later on further developed by Li, Krenchel and Stang [2]. The second method is a stress strain approach. Both approaches are still under development and a stress strain diagram is proposed by Rilem [3]. This stress strain approach has been used in this paper to calculate the load deflection curve of SFRC beams.

Since the advantage of SFRC is situated mainly in the post-cracking zone, also the material testing needs to be done in the post-cracking zone. This makes the testing of SFRC complicated and rather expensive. One of the more simple tests is a bending test on a beam. Although it is generally recognized that steel fibres are much less efficient in flexure than conventional reinforcement, a beam test on a SFRC beam can give valuable information about the stress strain relation of the material.

TESTING PROGRAMME

At the Department of Civil Engineering of the Catholic University of Leuven, Belgium, 28 full-scale beams have been cast and tested under four point bending in the framework of the Brite Euram project BRPR-CT98-0813 [4]. The details of the dimensions are given in Table 1. All reinforcement bars have a concrete cover of 15 mm.

The beams were all subjected to a four-point load as shown in Figure 1. The distance between the two loads was always equal to 200mm. The distance between the supports was either 1000 mm or 2000 mm, as specified in Table 1. All the beams were tested in steps. For each next step the deflection was incremented with a small amount. At each deflection increment the deflection and the load were measured.

Together with the beams also cubes (150 mm x 150 mm x 150 mm) were cast to measure the cube compressive strength and prisms (150 mm x 150 mm x 600 mm) to determine the flexural tensile strength $f_{ct,fl}$ and the equivalent flexural tensile strengths $f_{eq,2}$ and $f_{eq,3}$ according to the bending test proposed by Rilem TC162-TDF (Test and design methods for steel fibre reinforced concrete) [5]. The cylinder compressive strength is taken as 0.79 times the cube compressive strength. The flexural tensile strength $f_{ct,fl}$ is recalculated for a beam with a depth of 200mm by using the formula:

$$f_{ct,fl,200} = \frac{f_{ct,fl} \times (1600-200)}{(1600-125)} \quad (1)$$

In the calculations $f_{ct,fl,200}$ will be used instead of $f_{ct,fl}$. The results of the control specimens are shown in Table 2. The steel reinforcement is assumed ideally elasto-plastic with an average yielding strength f_{ym} as mentioned in Table 1.

Table 1 Dimensions of the test beams

	SPAN	DEPTH	WIDTH	FIBRE DOSAGE	REINFORCEMENT	f_{ym}
	mm	mm	mm	kg/m^3	# x mm	N/mm^2
Beam 1+2	1000	200	200	25	-	-
Beam 3+4	1000	200	200	50	-	-
Beam 5+6	1000	200	200	60	-	-
Beam 7+8	2000	200	200	25	-	-
Beam 9+10	2000	200	200	50	-	-
Beam 11+12	2000	200	200	60	-	-
Beam 13+14	1000	200	200	25	2 x ϕ 8	623
Beam 15+16	1000	200	200	50	2 x ϕ 12	639
Beam 17+18	1000	200	200	60	2 x ϕ 16	652
Beam 19+20	2000	200	200	25	2 x ϕ 8	623
Beam 21+22	2000	200	200	50	2 x ϕ 12	639
Beam 23+24	2000	200	200	60	2 x ϕ 16	652
Beam 25	1000	200	200	50	2 x ϕ 8	623
Beam 26	1000	200	200	25	2 x ϕ 12	639
Beam 27	2000	200	200	50	2 x ϕ 8	623
Beam 28	2000	200	200	25	2 x ϕ 12	639

Figure 1 Test setup of a short beam (span = 1m)

Table 2 Material Properties of all beams

BEAMS	$f_{cm,cub}$ N/mm^2	$f_{cm,cyl}$ N/mm^2	$f_{ct,fl}$ N/mm^2	$f_{ct,fl,200}$ N/mm^2	$f_{eq,2}$ N/mm^2	$f_{eq,3}$ N/mm^2	FIBRE DOSAGE kg/m^3
1, 2, 7, 8	47.1	37.2	3.7	3.5	2.6	2.6	25
3, 4, 9, 10	41.6	32.9	4.4	4.1	4.9	4.7	50
5, 6, 11, 12	82.6	65.3	6.5	6.1	7.3	9.3	60
13, 14, 19, 20	41.3	32.6	3.4	3.2	3.1	3.0	25
15, 16, 21, 22	40.7	32.2	4.0	3.8	4.4	4.0	50
17, 18, 23, 24	86.5	68.3	6.6	6.3	8.7	10.1	60
25, 27	47.5	37.5	4.4	4.2	5.2	5.0	50
26, 28	47.4	39.0	3.9	3.7	2.1	2.1	25

DESIGN METHOD

The material properties of Table 2 have been used to predict the load deflection curves of the beams. The procedure in which this is done is schematically explained in Figures 3 and 4. The tensile behavior of the SFRC is characterized by the stress strain diagram as proposed by Rilem [3]. Firstly a table is calculated in which for a series of tensile strains ε_t the corresponding compression strains ε_c (Figure 2) are plotted together with the bending moments causing such strain distributions (see Figure 3). Figure 3 can be run for a number of tensile strains ε_t, so that a complete table with a moment strain relation is created. This moment-strain table is used to determine a Load deflection relation. For each "bending moment M" the corresponding "bending load P" is calculated:

$$\frac{P}{2} = \frac{M}{a} \qquad \text{Where, a = shear span} \qquad (2)$$

To determine the corresponding deflection at mid span, only one half of the beam is considered (symmetry!). The beam is divided into a number of small parts (1 to n) of equal length l_{div} as demonstrated in Figure 5. The boundary points of these divisions (0 to n) are further called integration points (in total n + 1 integration points). At each of the integration points, both the bending moment M_i and corresponding curvature ($1/\rho$) are calculated for a certain bending load P. The calculation procedure for $1/\rho$ is explained in Figure 4.

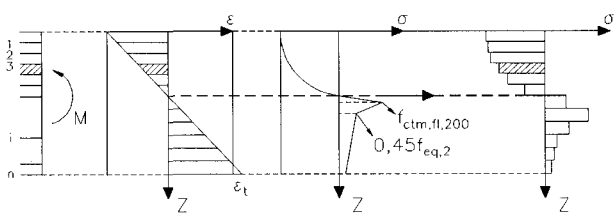

Figure 2 The used stress strain diagram

$$N = \sum_{i=1}^{n} \sigma_i \cdot h_i \cdot b = 0 \tag{3}$$

$$M = \sum_{i=1}^{n} z_i \cdot \sigma_i \cdot h_i \cdot b \tag{4}$$

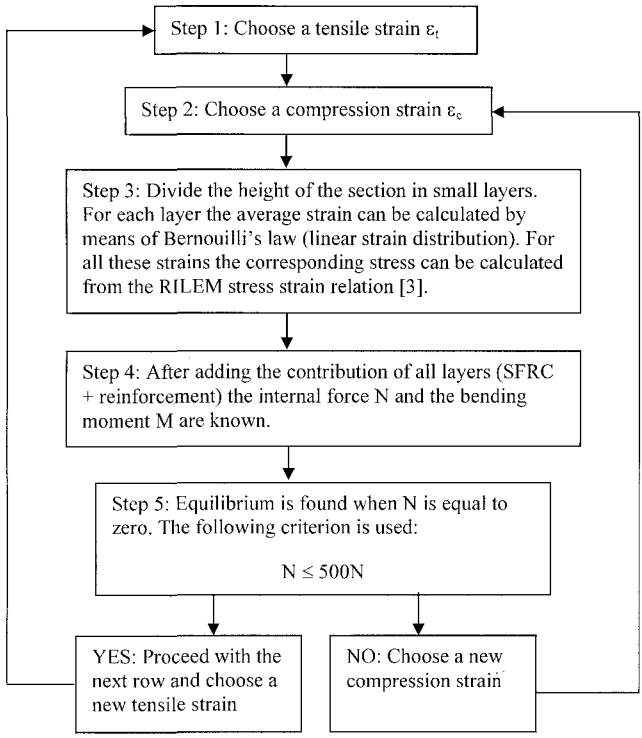

Figure 3 Calculation of a moment strain table

The next step is to integrate the curvatures over the length of the beam, using the proper boundary conditions (See Figure 5). These are: The slope is equal to 0 at mid span and the deflection is equal to zero at the supports. In a first step the average slope of the division between the integration points i and i-1 is calculated with the following formula:

$$\left(\frac{dv}{dx}\right)_{i-1} = \left(\frac{dv}{dx}\right)_i + \frac{1}{2}\left[\left(\frac{d^2v}{dx^2}\right)_i + \left(\frac{d^2v}{dx^2}\right)_{i-1}\right] \times l_{div} \tag{5}$$

The boundary condition for this integration step is:

$$\left(\frac{dv}{dx}\right)_n = 0 \tag{6}$$

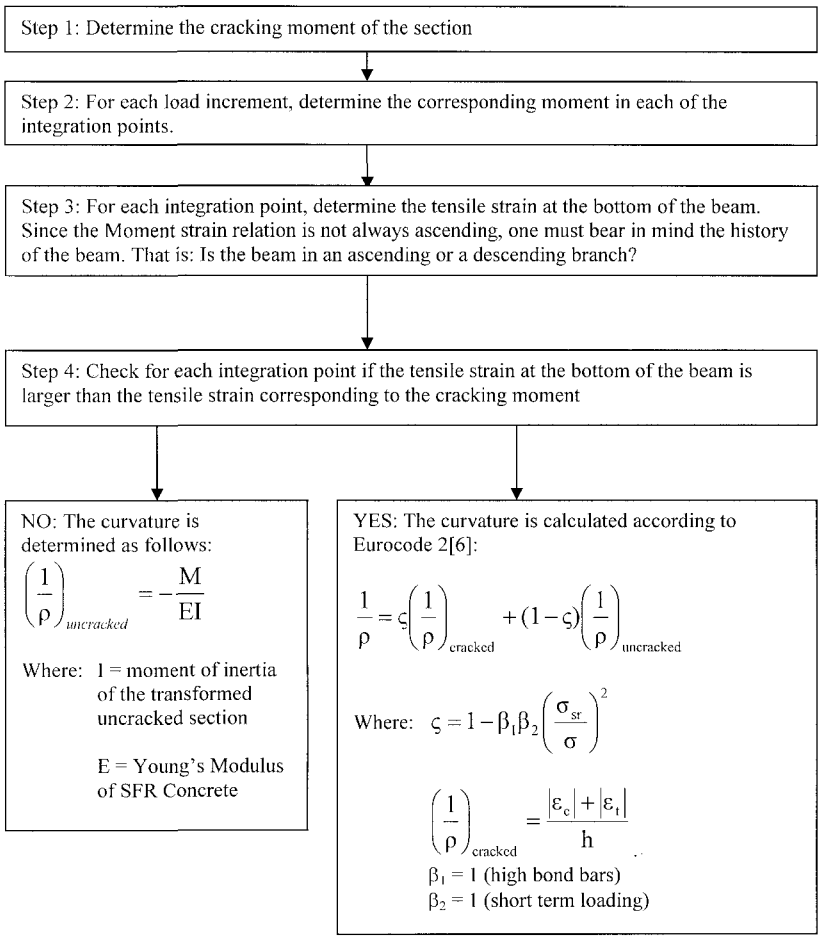

Figure 4 Calculation of the curvature in the integration points

The next integration procedure is as follows:

$$v_i = v_{i-1} + \left(\frac{dv}{dx}\right)_{i-1} \times l_{div} \tag{7}$$

Where: v_i = Deflection of the beam at integration point i. The boundary condition for this integration step is $v_0 = 0$. This calculated deflection only takes into account the contribution of a bending moment on the deflection. In reality also shear stresses contribute to the deflection, but taking into consideration the large shear span to depth ratios of the test program, this is neglected here.

The length l_{div} is quite important for the beams without reinforcement. This length is assumed equal to 100 mm for the beams without steel bars. For the beams with reinforcement the length is equal to 25 mm or smaller. For these elements this parameter is not so important, since the strain is not as local as for the beams without reinforcement.

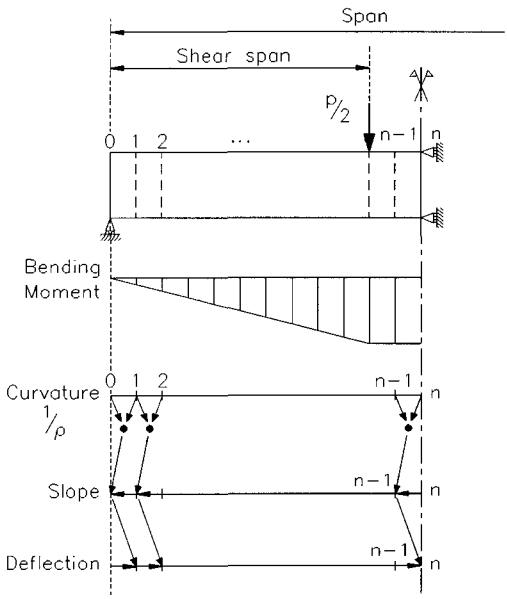

Figure 5 Integration scheme for the determination of the deflection of the beam

COMPARISON BETWEEN THEORETICAL AND EXPERIMENTAL RESULTS

The measured and calculated load deflection curves are shown in Figures 4 to 19. The measured curves have a full line, while the calculated curves have a dotted line.

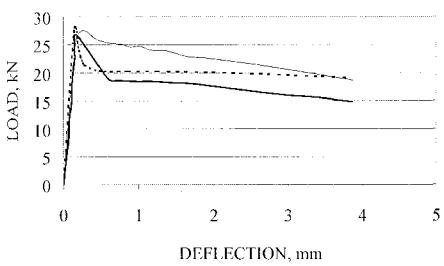

Figure 6 Beam 1 + 2

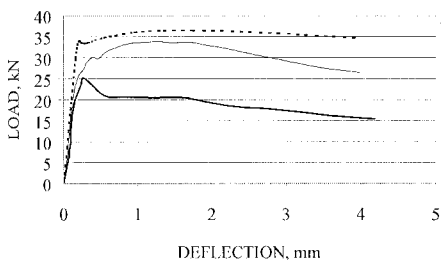

Figure 7 Beam 3+4

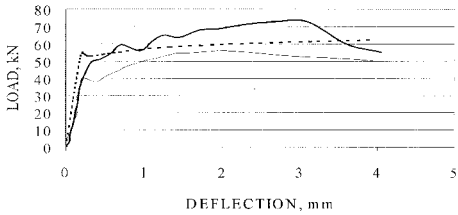

Figure 8 Beam 5 + 6

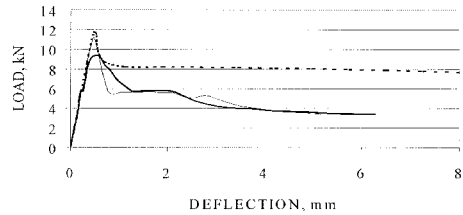

Figure 9 Beam 7+8

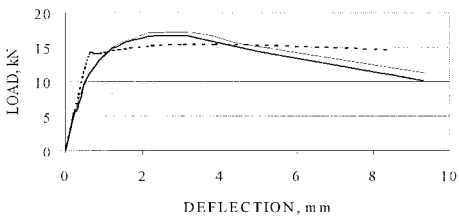

Figure 10 Beam 9 + 10

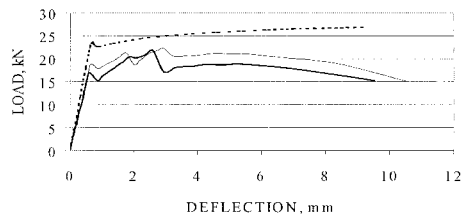

Figure 11 Beam 11+12

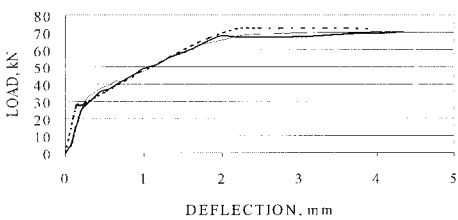

Figure 12 Beam 13 + 14

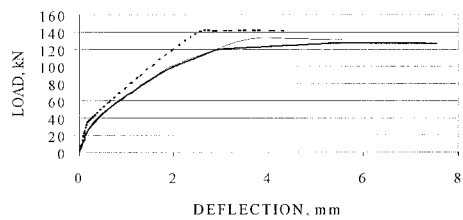

Figure 13 Beam 15+16

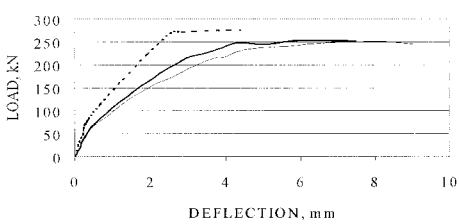

Figure 14 Beam 17 + 18

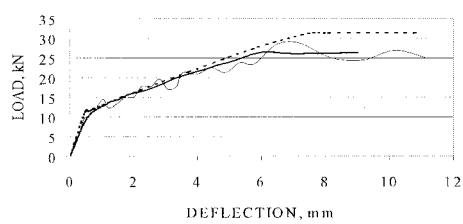

Figure 15 Beam 19+20

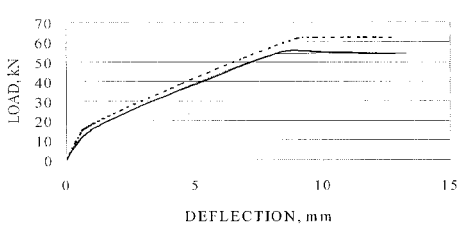

Figure 16 Beam 21 + 22

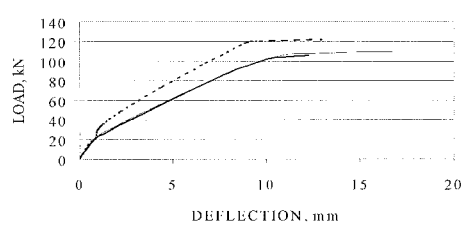

Figure 17 Beam 23+24

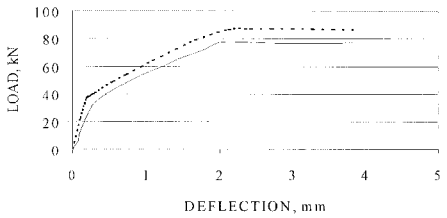

Figure 18 Beam 25

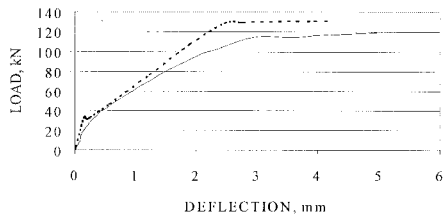

Figure 19 Beam 26

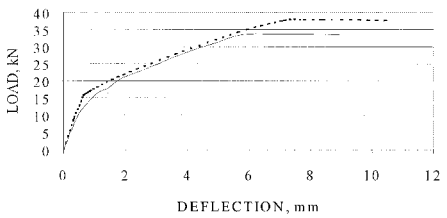

Figure 20 Beam 27

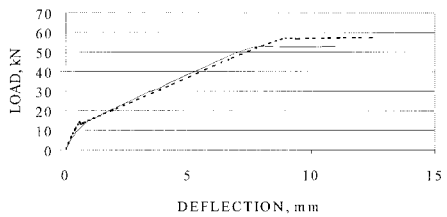

Figure 21 Beam 28

It can be seen from the first 6 graphs (Figures 6 –11) , which are the test results of the beams without conventional reinforcement, that there is a big difference between the two tested beams. This scatter is mainly due to the variability of the steel fibre concrete. In the other graphs the variability of the steel fibre concrete is also present, but the impact is smaller, since the reinforcement bars take most of the load. For the beams with reinforcement bars (beams 13 – 28) it can be seen that after cracking there is an ascending branch until a plateau is reached where the reinforcement bars start to yield. This is typically what one would expect from a bending test.

In most cases there seems to be a fairly good match between the calculation and the test results. It can be seen that the calculated curve has the same shape as the experimental curve. This shows that the used calculation method models quite well the behavior of the beam. Unfortunately the calculations are mostly on the unsafe side of the test results. The reason for this must be found in an incorrect input of the material properties. More in particular the authors think that the used stress strain diagram for SFRC, proposed by Rilem TC162-TDF [3], needs some corrections.

The correlation between the calculated curves and the test results does not seem to be much influenced by the different investigated parameters (span, fibre dosage, reinforcement ratio and concrete class). This shows that the used calculation model takes these parameters in a proper way into account. Further research could therefore be focussed on other parameters like the width and the depth of the cross section to take into account possible size effects.

CONCLUSIONS

In this paper the results are presented of a testing program of 28 full-scale beams, tested in four point bending. The investigated parameters are the span of the beams, the fibre dosage, the reinforcement ratio and the concrete strength.

A calculation method has been explained in detail and the load deflection curves resulting from the calculations are compared with the experimental curves. The conclusions of this comparison are that the investigated parameters seem to be well incorporated by the calculation model. The calculated curves in general are a little bit optimistic regarding the load carrying capacity of the beams. It is felt that the main reason for this overestimation must be found in the input of the material properties of the SFRC: the stress strain relation proposed by Rilem TC162-TDF [3].

ACKNOWLEDGMENTS

This study is part of the Brite Euram project "Test and Design Methods for Steel Fibre Reinforced Concrete", contract n° BRPR-CT98-0813. The partners in the project are: N.V. Bekaert S.A. (Belgium, coordinator), Centre Scientifique et Technique de la Construction (Belgium), Katholieke Universiteit Leuven (Belgium), Technical University of Denmark (Denmark), Balfour Beatty Rail Ltd. (Great Britain), University of Wales Cardiff (Great Britain), Fertig-Decken-Union GmbH (Germany), Ruhr-University-Bochum (Germany), Technical University of Braunschweig (Germany), FCC Construccion S.A. (Spain), Universitat Polytécnica de Catalunya (Spain).

REFERENCES

1. HILLERBORG A, Analysis of fracture by means of the fictitious crack model, particularly for fibre reinforced concrete, The International Journal of Cement Composites, 1980, Vol. 2(4), 177-184.
2. LI V, STANG H, KRENCHEL H, Micromechanics of crack bridging in fibre reinforced concrete, Materials and Structures, 1993, Vol. 26(162), p486-494.
3. RILEM TC162-TDF, Test and design methods for steel fibre reinforced concrete: σ–ε design method, Materials and structures, 2000, Vol. 33, March, p75-81.
4. BRITE-EURAM BRPR-CT98-0813, Test and design methods for steel fibre reinforced concrete (Design of SFRC), Final report of subtask 4.1: Trial beams in bending and bending + compression, August 2001.
5. RILEM TC162-TDF, Test and design methods for steel fibre reinforced concrete: Bending test, Materials and structures, 2000, Vol. 33, January-February, p3-5.
6. ENV 1992-1-1: 1991.1991. Eurocode 2: Design of concrete structures - Part 1: General Rules and rules for buildings.

EXPERIMENTAL INVESTIGATION ON TENSION STIFFENING EFFECTS OF FRP REINFORCED CONCRETE MEMBERS

M A Aiello

M Leone

L Ombres

University of Lecce

Italy

ABSTRACT. The paper describes results of an experimental investigation on tension stiffening effects of Fibre Reinforced Polymer (FRP) concrete members. The analysis was performed on cylindrical concrete tension specimens reinforced with Carbon FRP rebars. Tensile tests were carried out by a testing machine under displacement control. The influence of different size of specimen, that is the ratio concrete cover-to-rebar diameter (c/d) was analysed. Obtained results in terms of cracking and deformation of specimens are presented and discussed.

Keywords: Tension stiffening, Carbon fibre reinforced polymer, Concrete, Cover, Cracking, Deformation.

M A Aiello is a Researcher in Structural Engineering in the Department of Engineering Innovation at the University of Lecce, Italy. Her main research interests include the structural analysis of the Fibre Reinforced Polymer reinforced concrete members, the adhesion systems between polymers and concrete and the analysis of composite laminated structures.

M Leone is currently undertaking research into the bond behaviour of FRP reinforced concrete elements in the Department of Engineering Innovation at the University of Lecce, Italy.

L Ombres is Associate Professor in Structural Engineering in the Department of Engineering Innovation at the University of Lecce, Italy. His main research interests include the analysis of structural behaviour of concrete elements (High Strength Concretes, Fibre Reinforced Concretes, Fibre Reinforced Polymer reinforced concrete) and the analysis of sandwich laminated composite structures.

INTRODUCTION

The tension stiffening, that is the ability of cracked concrete to reduce strain in reinforcement due to tensile stresses in the concrete between cracks, is the most important phenomenon governing the structural behaviour of reinforced concrete structures.

The bond between the concrete and the reinforcement is fundamental to evaluate tension stiffening effects since it controls the ability of the reinforcement to transfer tensile stress to the concrete. Consequently, main parameters influencing the tension stiffening are the shape of reinforcement, such as the bar size an the outer surface treatment, the concrete strength and the concrete cover thickness [1].

For traditional steel reinforced concrete structures, tension stiffening effects are well-defined and usually considered in the structural analysis by using Code relationships [2], [3]. On the contrary, for concrete structures reinforced with Fibre Reinforced Polymers (FRP), tension stiffening effects are not completely defined; many researches, both theoretical and experimental, are still in progress.

The use of FRPs as reinforcement, however, involves high deformability of concrete structures; as a consequence the design of such structures is mainly governed by the deformability check instead of the ultimate strength [4]. For this reason an accurate analysis of cracking and deformations is needed taking into account the contribution of tension stiffening; investigations on this topic are, thus, essential [5].

The present paper describes first results of an ongoing investigation devoted to study the tension stiffening of FRP reinforced concrete members; at this aim the behaviour of tensile concrete members reinforced with Carbon FRP (CFRP) rods, commercially available, has been analysed in order to evaluate, in a simplest way, problems, as cracking and deformability, that more generally are fundamental for flexural concrete elements.

An experimental investigation on cylindrical concrete tension specimens reinforced with CFRP rods was performed; the effects of different concrete cover thickness values on the cracking and deformability of specimens, were investigated. Obtained results are presented and discussed.

EXPERIMENTAL INVESTIGATION

An experimental investigation has been planned in order to analyse the contribution of the tension stiffening on cracking and deformability of FRP reinforced concrete members. FRP reinforced concrete members subjected to uni-axial tension have been tested, as obtained results could be extended to flexural reinforced concrete elements. The experimental plane, still in progress, aims to check the influence of some key parameters on the stiffness of reinforced concrete members; in particular, the mechanical properties of concrete, considering both ordinary concrete (OC) and high performance concrete (HPC), the mechanical properties of FRP rebars and the amount of concrete confinement will be analyzed. First obtained results, reported in this paper, refer to tension members made with ordinary concrete and reinforced with CFRP (Carbon Fibre Reinforced Polymer) rebars; tested elements present different confining action, given from the thickness of the concrete embedding the FRP reinforcement.

Materials

The compressive strength of concrete was determined by standard compressive tests on cubes 150 mm high; the mean value was f_c=46.5 N/mm^2. The average tensile strength, determined by splitting test on cylinders with diameter of 150 mm and height of 300 mm, was f_{ct}=4.35 N/mm^2.

The utilized CFRP rebars, produced from the Sireg Co, Italy, have a diameter of 8 mm and are externally sanded and spiral wounded with carbon fibers. The constitutive law has been experimentally determined, the mean values of strength and Young modulus resulting σ_R=2401 N/mm^2 and E=110 kN/mm^2, respectively.

Specimens and Test Set-up

Cylindrical concrete specimens were made with a CFRP rebar embedded in the concrete block. A tensile force was applied by means a testing machine, under displacement control. Electrical strain gauges have been glued to the FRP rebar, before the casting, to measure the strain of the reinforcement during the test.

To record the strain evolution within the concrete, electrical strain gauges were put on the concrete, at the same positions of those glued to the rebar, and on both side of the block in order to evidence any load eccentricity. In addition, two LVDT were utilized to measure the elongation of the rebar embedded within the concrete block and that of the concrete.

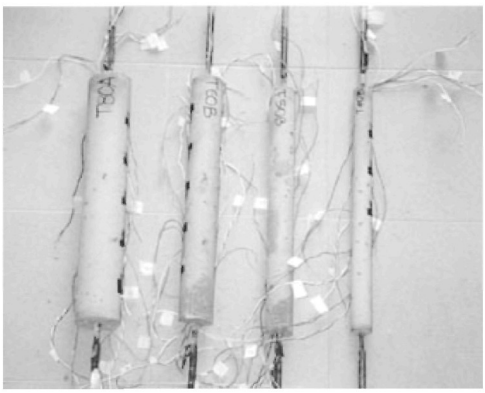

Figure 1 Tested specimens

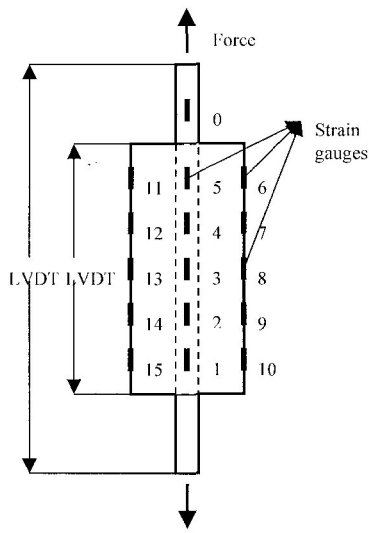

Figure 2 Test Set-up

Geometrical details of tested specimens are reported in Table 1, while in the Figures 1-2 the tested specimens and the test set-up are drawn respectively.

Table 1 Dimension of specimens

NUMBERS OF SPECIMENS		HEIGHT (mm)	DIAMETER (mm)
2	T40A, T40B	450	40
2	T50A, T50B	450	50
2	T60A, T60B	450	60
2	T80A, T80B	450	80

RESULTS AND DISCUSSION

In the Figures 3-6 curves F-ε are reported for all tested specimens, being F the tensile applied force and ε the mean strain of the member response. In the same Figures the curve F-ε, obtained for the CFRP rebars is drawn, in this case ε is the local strain in the naked bar.

Analysing the Figures it clearly appears that the rebar embedded in the concrete presents a higher stiffness, at all stress levels, than the non-embedded bar. The difference between the two curves, for each specimen and at any load level, gives a measure of the tension stiffening contribution. The decrease of the reinforcement strain is due to the bond stresses that allow the load transfer between reinforcement and surrounding concrete.

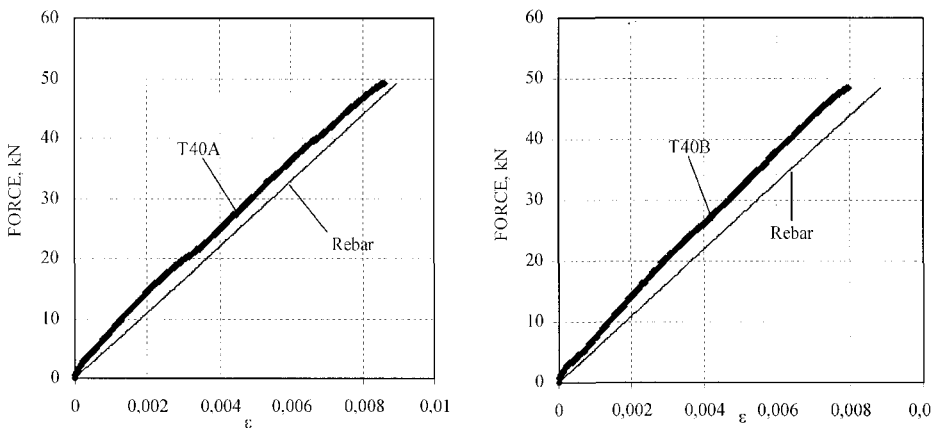

Figures 3 F-ε curves for T40A and T 40 B specimens

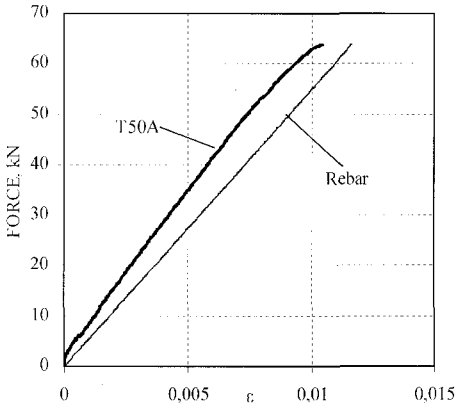

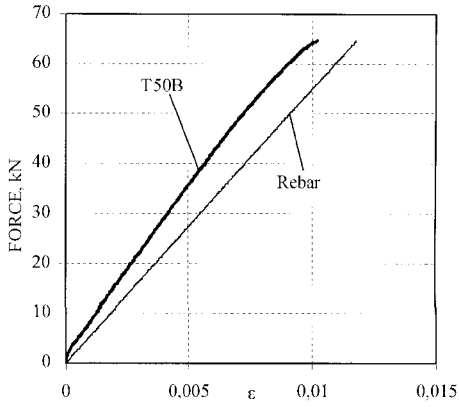

Figures 4 F-ε curves for T50A and T 50 B specimens

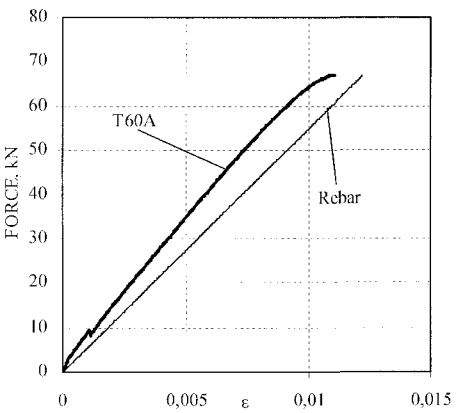

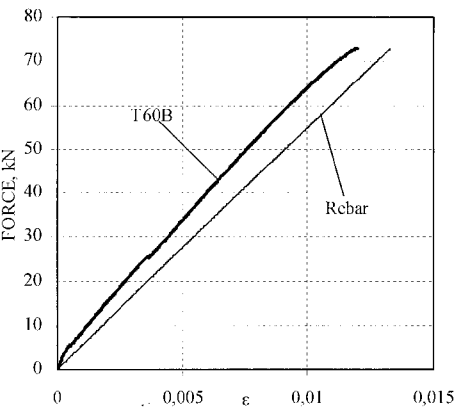

Figures 5 F-ε curves for T60A and T 60 B specimens

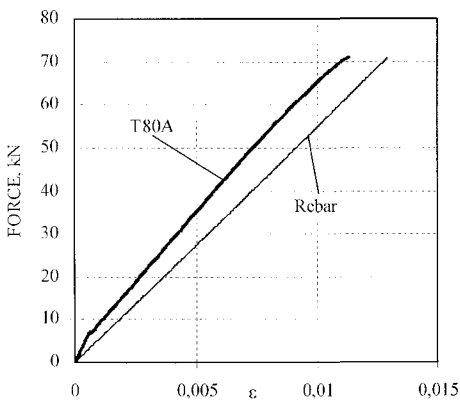

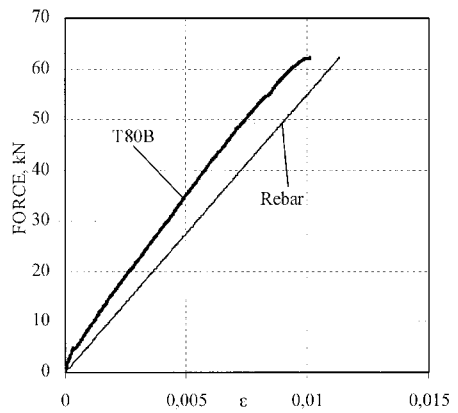

Figures 6 F-ε curves for T80A and T 80 B specimens

In Figure 7 curves F-ε are compared for specimens of the group A. The tension stiffening contribution increases when the diameter of the surrounding concrete increases as well. However the Figure 7 shows that the scatter between curves reduces above a certain amount of confinement; in fact a relevant difference has been recorded between strain of the T40 A and T50 specimens while small scatters can be evidenced between T50A, T60A and T80A specimens.

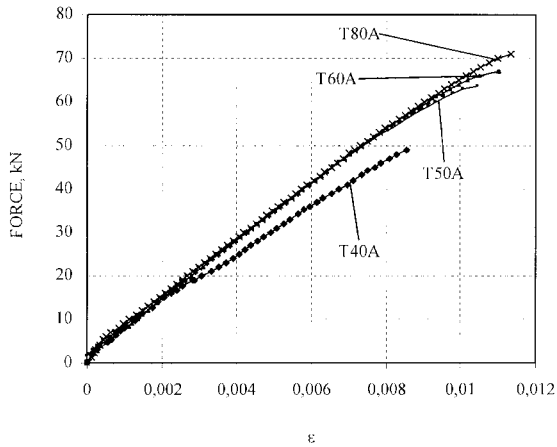

Figure 7 F-ε curves for specimens of the A group

In the Figures 8-9 the curves F-ε of T40B and T50B specimens are reported for low load levels in order to better evidence the behaviour of the tension reinforced concrete elements. As one can see, once the cracking phenomenon takes place, the deformability of members increases even if embedded rebars present higher stiffness with respect to the non-embedded bar. The formation of new cracks, indicated from the arrows in the figures, involves a further increase of deformability and, therefore, a reduction of the tension stiffening contribution.

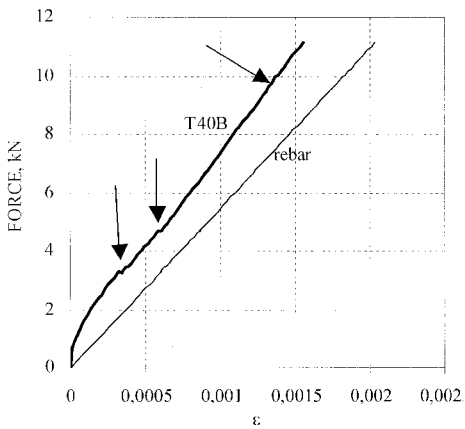

Figure 8 F-ε curves for T40B specimen at low load level

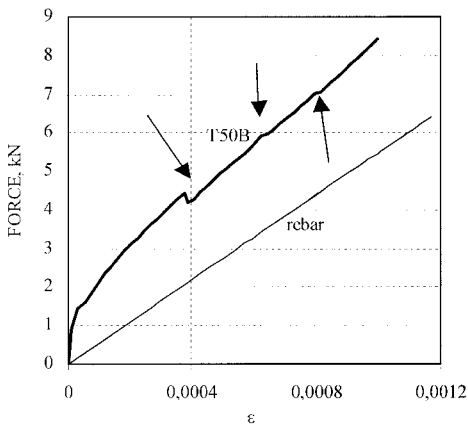

Figure 9 F-ε curves for T50B specimen at low load level

The evolution of the cracking phenomenon has been also recorded for all tested specimens. In Figure 10 the number of cracks versus the diameter of the concrete specimen is reported while in Figure 11 the mean cracks width versus the diameter of the concrete block is reported in correspondence of the ultimate load and up to 50% of the ultimate load respectively. Figures show as increasing the concrete dimension the number of cracks drastically drops and the mean width of cracks increases, such an occurrence involves a reduction of the member ductility.

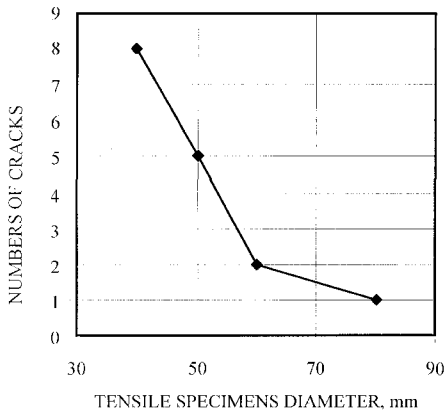

Figure 10 Number of cracks versus diameter of the tension member

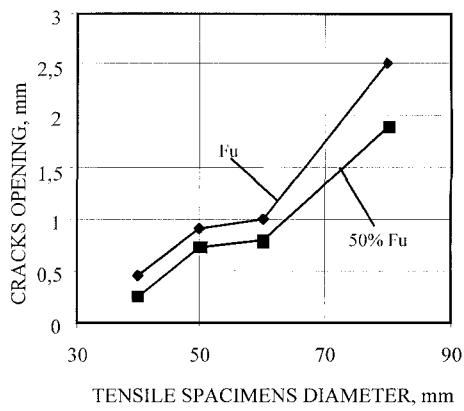

Figure 11 Mean cracks width versus diameter of the tension member

CONCLUSIONS

The analysis of the experimental results show the following aspects:

1. Tension stiffening effects are influenced by the ratio concrete cover-to-rebar diameter. The tension stiffening contribution, in fact, increases when the diameter of the surrounding concrete increases as well.

2. For a given rebar diameter it is possible to determine an optimal value of the concrete cover–to-rebar diameter that corresponds to a maximum tension stiffening contribution. For cases examined in this study this ratio is equal to 3 (specimen T50A).

3. Increasing the size of concrete specimens the number of cracks drastically drops while the crack width increases.

Further investigation considering the influence of other parameters, such as the rebar diameter, the outer surface treatment of FRP rebars, the type of FRP rebars, the strength of the concrete, are needed in order to evaluate completely the tension stiffening contributions that, as evidenced in the first phase of the research seem to be very influential and effective in reducing the strain of the reinforcing bars.

On the order hand a theoretical analysis is suggested, that taking into account all parameters involved, would aim to furnish useful design indications regarding the tension stiffening contribution.

REFERENCES

1. CEB. CEB-FIP Model Code 1990. Bulletin d'information no 203-205,1991.

2. COMMISSION OF THE EUROPEAN COMMUNITIES. Eurocode No 2-Design of Concrete Structures, 1994.

3. ACI COMMITTEE. Control of cracking in concrete structures. Concrete International, 2, No 10, 1980.

4 NANNI, A. Fiber-Reinforced Plastics (FRP) reinforcement for concrete structures; properties and applications. Elsevier Ed, 1993.

5. AIELLO, M A and OMBRES, L. Load deflection analysis of FRP reinforced concrete flexural members, Journal of Composites for Constructions, No 4, 2000, pp 164-171.

A NEW METHOD FOR CONTROLLING SECONDARY FLEXURE DURING UNIAXIAL TENSION TEST OF CONCRETE

H Akita

D Sohn

H Koide M Ojima

Tohoku Institute of Technology

Japan

ABSTRACT. The authors have already established a test procedure for uniaxial tension test of concrete, eliminating secondary flexure, multiple cracks and overlapping cracks. In this paper, another approach for controlling secondary flexure is presented. It gives an artificial flexure to a specimen by non-equal-depth-notches and by maintaining deformation difference of opposite faces at a low constant level. The flexure control makes the whole cross section of the specimen softened, and provides an accurate tensile strength. Tension softening curves obtained are more monotonous and continuous under this condition than in the case of complete elimination of the flexure. Thus, this new control method of secondary flexure is evaluated to be superior than complete elimination of the flexure.

Keywords: Uniaxial tension, Tension softening, Test method, Secondary flexure, Notch, Concrete.

H Akita is a Professor in the Department of Civil Engineering at Tohoku Institute of Technology. His research interest relates to the fracture mechanics of concrete.

D Sohn is a post doctoral fellow in High Technology Center at Tohoku Institute of Technology. His research interest relates to the utilization of cementitious materials and recycling of concrete.

H Koide is an Associate Professor in the Department of Civil Engineering at Tohoku Institute of Technology. His research interest relates to the fracture mechanics of concrete and the reliability analysis of concrete structures.

M Ojima is a Research Associate in the Department of Civil Engineering at Tohoku Institute of Technology. His research interest relates to the fracture mechanics of concrete.

INTRODUCTION

Knowledge of the tension softening process of concrete is essential to understand fracture mechanism, to analyze fracture behavior, and further to evaluate properties of concrete. The best way to investigate the tension softening behavior is applying uniaxial tension force directly on a concrete specimen, because it provides more reliable information than any other alternative methods. In this method, both tensile strength and tension softening curve of concrete are measured directly from identical specimen.

However, no standard tests have been established to provide a direct measurement of tension softening curve of concrete. The problems of investigating tension softening behavior under the uniaxial tension load are unstable fracture, secondary flexure, multiple cracks, and overlapping cracks.

The first problem of unstable fracture can be solved by the suitable choice of measuring length and the adoption of a closed-loop loading machine controlled by the deformation of the specimen. If the measuring length of a specimen is chosen smaller than the characteristic length of concrete, a stable fracture will be easily produced and maintained [1].

The second problem, secondary flexure is denoted as the induced flexure (or lateral flexing) caused by the heterogeneity of concrete specimen, even though there is no eccentricity in load. It is usually induced by local softening at the weakest zone of a specimen or non-symmetrical crack arrest by aggregates. The secondary flexure produces strain gradient, being half of the section softened and the other half section relatively contracted at peak load. The cohesive stress in the softening zone slightly reduces from tensile strength, and the opposite side stress reduces considerably because of bending compression.

Consequently, the reduction of the observed peak load or tensile strength would sometimes exceed 20 % of their true values due to the flexure as obtained by the authors. Therefore, it is necessary to prevent completely or to minimize the secondary flexure for obtaining reliable results. Despite the significance to avoid the flexure, many researchers have ignored it [2], [3] or failed to avoid it [4], [5]. In order to eliminate the secondary flexure, a specifically designed adjusting gear systems was developed by the authors [6].

Even though the problem of the secondary flexure is solved, the success in the observation of the tension softening behavior is still unknown. Heilmann et al's results imply that the test would fail when multiple cracks, as shown in Figure 1, were generated in spite of preventing secondary flexure within long measuring length [7].

Since the generation of multiple cracks produces a couple of secondary flexures, these cracks should be avoided. By employing a notched specimen, the occurrence of multiple cracks can be easily prevented.

Commonly, it is thought that strong stress concentrations due to notches may mislead the observation of the tensile strength of concrete. However, simulation approaches reported by Zhou show that the influence of notches on the tensile strength is insignificant [8].

The authors confirmed Zhou's results by performing an independent simulation with a prismatic specimen of 100 x 100 x 400 mm. Details are presented elsewhere [9].

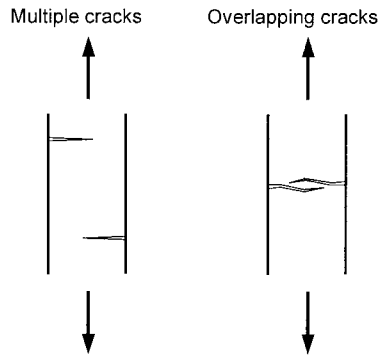

Figure 1 Multiple cracks and overlapping cracks

The last serious problem is the generation of overlapping cracks during testing (See Figure 1). Since overlapping cracks increase the observed fracture energy above acceptable rates, they should also be avoided. The overlapping crack generation is prevented by applying guide notches to a specimen. Figure 2a shows the position of both primary and guide notches in a prismatic specimen of 100 x 100 mm cross section. The primary notches are applied on the side (not on the cast face nor the bottom face) in order to avoid influence of strength variations in casting direction. The 5 mm depth guide notches on other laterals are employed as usual. Though the previous test method of controlling the secondary flexure gives good results, a better method is presented in this paper.

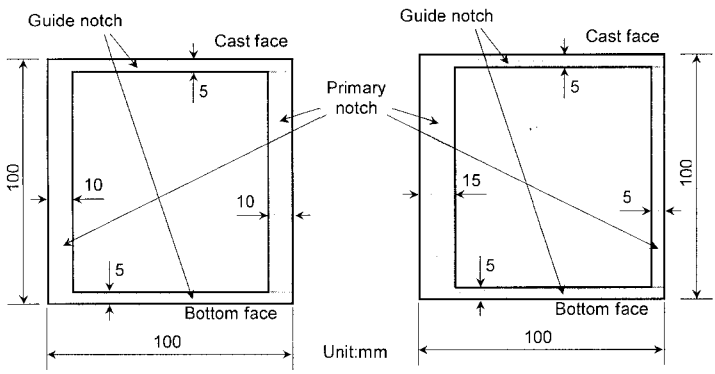

Figure 2 Position of notches for a) complete elimination method and b) constant difference method

THE CONCEPT OF NEW CONTROL METHOD

Since secondary flexure produces a considerable error on the observed tensile strength, the complete elimination of the flexure is a normal solution. However, another possibility is to maintain the secondary flexure within a low constant level.

This new control method stands between the complete elimination of the flexure and leaving the flexure as it is. The reason why tensile strength can be obtained accurately by the new method is explained by the following comparison of stress distributions along notched sections with respect to both control methods.

Figure 3a shows the stress distributions along the notched section predicted by simulations for complete elimination of the secondary flexure with respect to three levels of subjected load. Because of the symmetry, the stress distributions are presented only along a half of the section. Each stress distribution was expressed in terms of each tensile stress σ versus tensile strength f_t. P_{true} means the true peak load which is realized when the entire ligament is subjected uniformly by tensile stress equal to tensile strength. Because of a high stress concentration caused by notches, stress level near the notch tip reaches tensile strength, even at low loading, such as when $P/P_{true} = 0.35$. As the load increases, a fictitious crack, which models the softening zone, develops and expands from the notch tip toward the center. The size of crack opening displacement within the fictitious crack is so small that each cohesive stress within the zone is almost same as tensile strength. When P/P_{true} becomes 0.79, the stress distribution consists of an expanded plateau and a concave. When the crack tip reaches the specimen center, P/P_{true} becomes 0.99 and a single plateau across the whole cross section is created, resulting in softening of the entire cross section. The peak load was only reduced a little, compared with the true peak load in spite of existing notches.

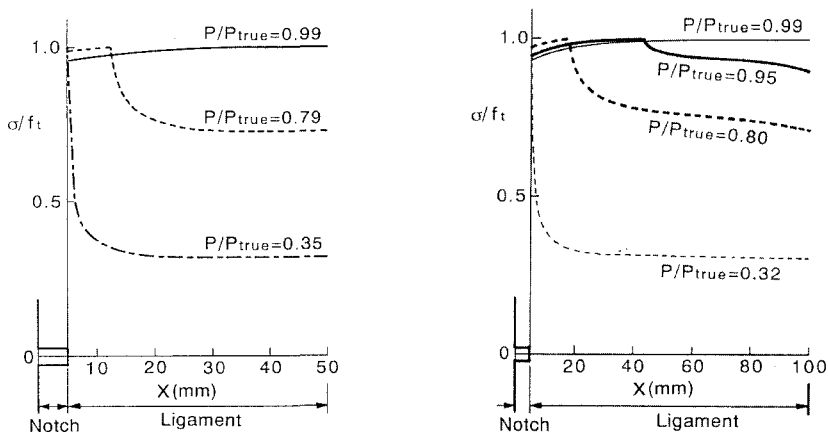

Figure 3 Stress distributions of notched section for a) complete elimination method and b) constant difference method

Figure 3b shows the same stress distributions for the method maintaining the flexure within a low constant level. The stress distributions are quite similar to the former, for example, when $P/P_{true} = 0.32$, 0.80 and 0.99 in Figure 3b corresponds to when $P/P_{true} = 0.35$, 0.79 and 0.99 in Figure 3a, respectively. This surprising similarity comes from the fact that deformation difference exists even in the complete elimination method between notched face and the center of the specimen, though there is no difference between both faces. It means that two cracks propagate from both faces to the center in the elimination method, whereas one crack propagates from larger deformation side to smaller deformation side in the new method.

Thus, it implies that the peak load reduction or tensile strength reduction will be the same level, if the deformation difference of both sides in the new method is the same level as that between side face and the center in the elimination method. In fact, the reduction of the peak load is estimated to be only 1.3 % of P_{true} by simulation in the case of maintaining a 2-μm deformation difference in the new method.

Since some flexures are indispensable in the constant difference method, they are produced artificially in the present procedure. In order to produce an artificial flexure, two mutually different notch depths are employed for primary notches as shown in Figure 2b. Contrary to primary notches, guide notches are equal to each other, and the secondary flexure is completely eliminated in this direction.

It implies that all the cracks are restricted to develop perpendicular to cast direction in the present procedure. However, if it is necessary, such a crack can also be produced that develops from bottom face to cast face. The produced crack correlates to bending crack which initiates at bottom face in the concrete beam cast horizontally.

There is a dilemma in determining an appropriate value of a deformation difference. The less difference in deformation, the less reduction in the peak load. However, too small difference will sometimes cause reverse directional crack propagation due to the arrest of initial crack propagation by aggregates. When such crack inversion is occurred, it is impossible to maintain the artificial flexure at the objective constant level. This bifurcation was predicted by Rots et al. [10] in simulation and observed experimentally by the authors.

TESTING PROCEDURE

Ordinary strength concrete was cast on three different dates with the same mix proportion as shown in Table 1. Cylindrical specimens (ϕ=100 mm and H=200 mm) were employed for compression test and splitting tension test. Prismatic specimens (100 x 100 x 400 mm), as shown in Figure 4a, were employed for uniaxial tension test. After making notches by diamond saw, the prismatic specimens were covered with wet clothes in order to avoid unnecessary drying except at the end faces. A steel frame with aluminum plate (See Figure 5) was glued to a specimen end by epoxy resin and connected to a universal joint by a pin. Deformations of four sides were measured separately by extensometers of 70 mm measuring length as shown in Figure 4b.

Table 1 Mix proportion of concrete

WATER CEMENT RATIO W/C	UNIT CONTENT (Kg/m^3)			CHEMICAL ADMIXTURE %
	CEMENT	AGGREGATE		
		0 – 5 mm	5 – 20 mm	
50	330	660	1245	0.019

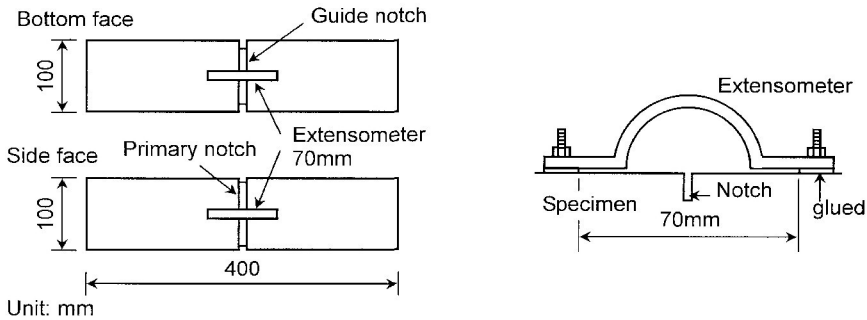

Figure 4 Shapes of a) specimen and b) extensometer

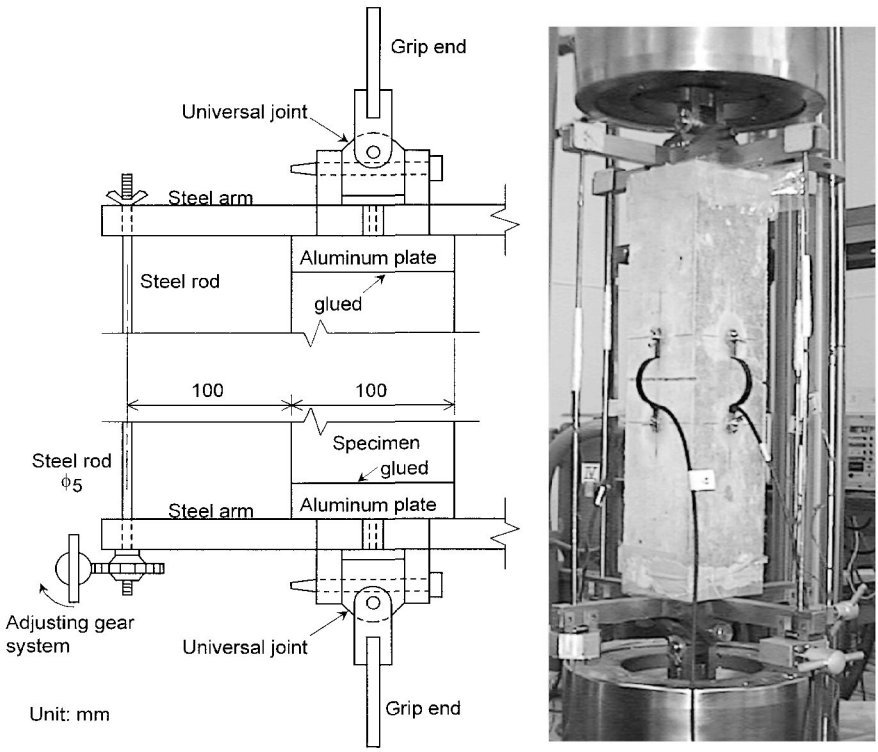

Figure 5 Adjusting gear system and experimental set up

The adjusting gear systems, as shown in Figure 5, are operated manually as following. When one side of a specimen is more elongated than the opposite side, the side elongated longer should be contracted by the adjusting gear on that side until reaching a proper balance in elongation (zero difference for complete elimination method or finite difference for constant difference method). For the operation, it is necessary to observe deformation (or elongation) of all sides of a specimen. Continuous care should be paid to watch four side deformations in order to operate for reducing the deformation difference without a delay. As steel rods give compressive forces to the specimen, applied load is corrected by subtraction of these forces from machine load. Load control for uniaxial tension test is performed through four stages as shown in Table 2. The average of the four side deformations were used as feedback signal for load control in deformation control or strain control stages. These stages were determined from two demands. One was to adopt a low strain rate near the peak load and the other was to reduce total loading time. By these controls, the total loading time was about 2 hours.

Table 2 Control stages of machine load

STAGE	CONTROL METHOD	DURATION	RATE	DEFORMATION RATE
1	Load control	~ 15 kN	50 N/s	14×10^{-6} mm/s
2	Strain control	$+ 200 \times 10^{-6}$	0.1×10^{-6}/s	7×10^{-6} mm/s
3	Strain control	$+ 400 \times 10^{-6}$	0.2×10^{-6}/s	14×10^{-6} mm/s
4	Strain control	~ Last	0.4×10^{-6}/s	28×10^{-6} mm/s

TEST RESULTS AND DISCUSSION

Figure 6 shows load-deformation curves (P-δ curves) obtained from the complete elimination method, relating to each individual deformation of the mutually opposite face ch-2 or ch-4 in 6a, and to the average deformation in 6b.

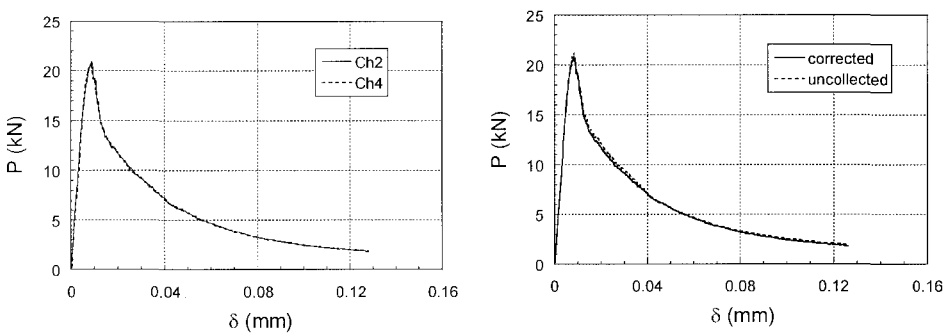

Figure 6 Load-deformation curves by complete elimination method
a) individual deformation and b) average deformation

Figure 6a shows that the two curves almost coincide, indicating that all the unexpected flexures are well eliminated. It can be seen that the curve for average deformation (solid line in 6b) coincides to those for both individual deformation (6a) in the case of complete elimination method. In Figure 6b, "uncorrected" means just the machine load and "corrected" means applied load to the specimen, correcting machine load by the subtraction of all the adjusting forces. The correction is small enough relating to the adjusting forces.

Figure 7 also shows load-deformation curves obtained from the constant difference method, relating to each individual deformation ch-2 or ch-4 in 7a and to the average deformation in 7b. 7a shows that two curves initially coincide, then gradually separated and maintained a constant difference afterward. It indicates that all the unexpected flexures in the direction of ch-2 and ch-4 are well controlled to maintain a small constant deformation difference. In Figure 7b, the correction of load is also very small, and average load-deformation curve is almost coincide to both individual curves in 7a.

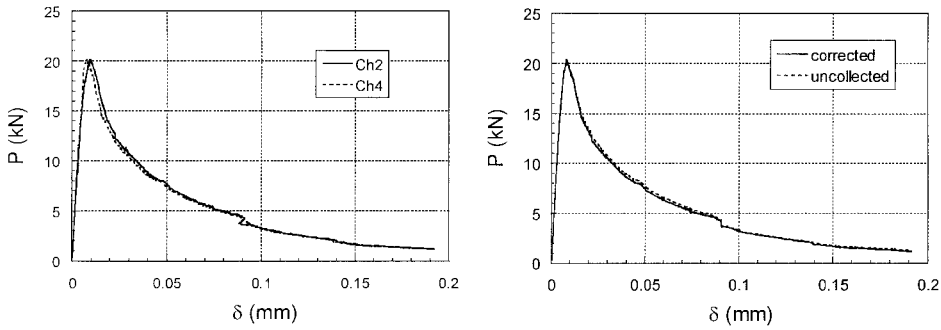

Figure 7 Load-deformation curves by constant difference method
a) individual deformation and b) average deformation

The tension softening curves (σ-w curves) of four specimens by the complete elimination method are shown in Figure 8a. It shows the reliability of the test procedure that these four curves are not significantly different from each other. However, some of the curves in the figure show sudden decrease and sequent recover or slight flutter.

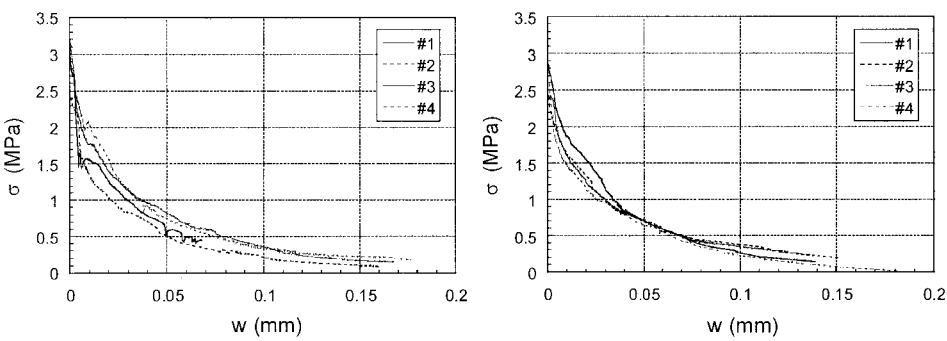

Figure 8 Tension softening curves by a) complete elimination method and
b) constant difference method

Figure 8b shows the four tension softening curves obtained by the constant difference method. Compared to 8a, 8b shows less scattering and smoother variation of curves. These are the superiorities of the new method to the elimination method despite the existence of difficulties to perform the test.

Figure 9a shows tensile strength values obtained by the two uniaxial tension tests and by the splitting tension test. Each age in the Figure means the age of specimens for the splitting test. The uniaxial tension tests were performed a few days before or after the indicated age. A, B and C indicate respective concretes cast in different dates. Tensile strengths obtained by the tree methods are not significantly different from each other reflecting their scatters. It means that both control methods have almost the same accuracy in tensile strength.

By extrapolating with a tangential line at each end of tension softening curves, the values of fracture energy were calculated. Figure 9b shows the results of fracture energy for the uniaxial tension test. There is no significant difference in fracture energy between the complete elimination method and constant difference method. So far fracture energy, there is no superiority or inferiority between both control methods.

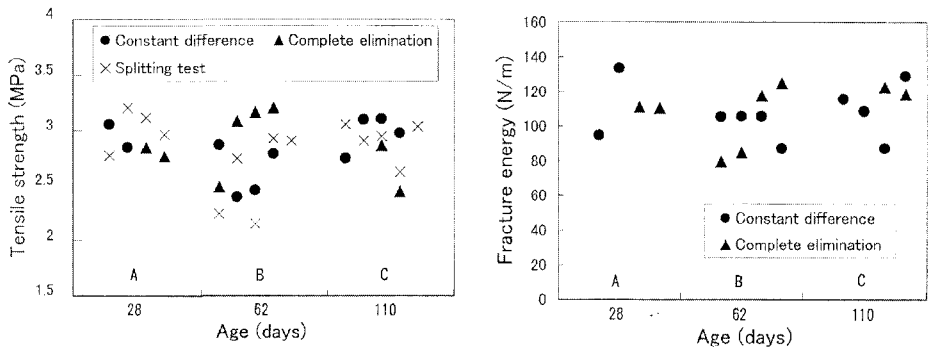

Figure 9 a) Tensile strength and b) fracture energy

CONCLUSIONS

In uniaxial tension test of concrete, the new control method of a secondary flexure by maintaining deformation difference within low constant level was evaluated superior to the complete elimination method of the flexure. The new control method gave smoother tension softening curves without reducing the accuracy of tensile strength and fracture energy.

REFERENCES

1. PETERSSON, P. E., Crack growth and development of fracture zones in plain concrete and similar materials, Technical Report TVBM 1006 (Lund Institute of Technology), 1981.

2. LI, Z., KULKARNI, S. M. and SHAH, S. P., New test method for obtaining softening response of unnotched concrete specimen under uniaxial tension, Experimental Mechanics, Vol.33, No.3, 1993, pp181-188.

3. LI, Q. and ANSARI, F., High-Strength concrete in uniaxial tension, ACI Materials Journal, Vol.97, No.1, 2000, pp 49-57.

4. VAN MIER, J. G. M., SCHLANGEN, E. and VERVUUT, A., Tensile cracking in concrete and sandstone: Part 2 - Effect of boundary rotations, Materials and Structures, No.29, 1996, pp 87-96.

5. HORDIJK, D. A., REINHARDT, H. W. and CORNELISSEN, H. A. W., Fracture mechanics parameters of concrete from uniaxial tensile tests as influenced by specimen length, Fracture of Concrete and Rock, Soc. Exp. Mech., Bethel, 1987, pp138-149.

6. AKITA, H., KOIDE, H., TOMON, M. and SOHN, D. A practical method for uniaxial tension test of concrete, Concrete Science Engineering, (in submitting).

7. HORDIJK, D. A., Deformation-controlled uniaxial tensile test on concrete, Technical Report 25.5-89-15/VFA, Delft University of Technology, 1989.

8. ZHOU, F. P., Influences of notch size, eccentricity and rotational stiffness on fracture properties determined in tensile tests, Fracture Mechanics of Concrete Structures AEDIFICATIO Publishers, Freiburg, 1995, 65-74.

9. AKITA, H., SOHN, D. and OJIMA, M., Computer simulation of tension softening behavior under various conditions of secondary flexure, Concrete Science Engineering, (in submitting).

10. ROTS, J. G. and DE BORST, R., Analysis of concrete fracture in direct tension, Journal of Solids and Structures, Vol.25, No.12, 1989, pp1381-1394.

THEME TWO:

DEVELOPMENTS IN REINFORCEMENT MATERIALS

Keynote Paper

INORGANIC POLYMER COMPOSITES IN CONCRETE CONSTRUCTION: PROPERTIES, OPPORTUNITIES AND CHALLENGES

P N Balaguru

Rutgers, State University of New Jersey

United States of America

ABSTRACT. Use of high-strength composites in concrete construction is gaining worldwide acceptance. The major application areas are repair and retrofit to improve the performance or correct deficiencies. These composites have very high specific strength and do not corrode. The major disadvantages are the weakness of the resin under high temperature and UV radiation. Recent advances led to the development of high temperature matrices. The results reported in this paper deal with composites made with inorganic polymer that is not only high temperature resistant but also environmental friendly. The water-based system is completely nontoxic. The performance of this adhesive is compared to an organic adhesive for strengthening plain and reinforced concrete beams using carbon fibre sheets. The comparison is made using the experimental results of plain and reinforced concrete beams strengthened with bonded carbon fibre sheets and tested to failure under flexural loading. Strength, failure pattern, and cracking of beams strengthened with the two systems are compared. The results indicate that the inorganic adhesive is as effective in increasing the strength and stiffness of reinforced concrete beams as the organic adhesive. For plain concrete, the behaviours of the two systems are comparable for equivalent fibre volume fraction. The inorganic matrix has a tensile strain capacity of only 0.07%, whereas the organic matrix has a strain capacity of about 4.8%. The brittleness of the inorganic matrix results in crack formation in the composite and a minimum build-up of strain along the interface of the composite and concrete. This phenomenon leads to failure of the composite by rupture of the carbon sheets instead of delamination, which occurs in most of the organic matrix repaired beams. Based on the results available so far, the inorganic matrix composite can be used in standard repairs of reinforced and prestressed concrete structures. The challenge is to create field workable system that can compete with the inorganic systems.

Keywords: Concrete, Carbon, Fibre, Inorganic, Strength, Durability.

P N Balaguru is Professor of the Department of Civil and Environmental Engineering, at Rutgers, the State University of New Jersey. Currently he is serving as Program Manager at National Science Foundation, USA. His research interests include fatigue of reinforced concrete, behaviour of reinforced concrete and ferrocement, corrosion of reinforced concrete, use of inorganic polymers for composites, development of innovative construction materials.

INTRODUCTION

The worldwide need for major repair and rehabilitation of infrastructures is stimulating research to develop repair and strengthening techniques that are durable, economical and easy to implement. Externally bonded steel plates had been used successfully in the 1960's. The development of high strength aramid, carbon, and glass fibres provided a lightweight alternative for steel plates (1). These systems, called fibre-reinforced polymers (FRP) have some major advantages including: low weight, corrosion resistance, and ease of application. The low weight reduces the duration and cost of construction because heavy equipment is not needed. The composites can be applied layer by later or as a thin plate.

A major disadvantage of composites is their lack of fire resistance. Some compositions are also vulnerable to degradation under ultraviolet light, leading to long-term durability problems. Since carbon and glass fabrics can withstand normal fire exposure and are durable under ultraviolet light, the organic polymers used to attach these fabrics to concrete become the weak link. Results reported in this paper deal with the use of an inorganic matrix, which is an alumino-silicate that can sustain up to 1000° C and does not degrade under ultraviolet light. In addition, the water-based matrix is non-toxic so that cleaning and disposal of excess materials is not a problem. The matrix also provides a hard surface that cannot be easily vandalized. This aspect becomes important for structures located in urban areas.

The inorganic matrix in combination with carbon sheets was used to strengthen plain and reinforced concrete beams. Background information on the inorganic matrix composites, review of the behaviour of reinforced concrete beams strengthened with organic polymers, performance of plain and reinforced concrete beams strengthened with carbon sheets and inorganic matrix, and the comparative behaviour of organic and inorganic matrix in terms of strength, stiffness, failure pattern, and cracking are presented in the following sections. In addition the opportunities and challenges for this new system are discussed briefly.

PROPERTIES OF THE INORGANIC MATRIX - FIBRE COMPOSITES

Mechanical properties of composite plates made with the inorganic polymer in combination with carbon, glass, and steel fabrics and sheets have been reported in the following references (2-6). The durability of the composites and the durability of concrete prisms coated with discrete and continuous fibre reinforced matrix have also been studied. The following are the major conclusions.

- The system is very easy to work with and all the techniques used for organic polymers can be used for the inorganic matrix.
- The matrix is compatible with carbon and glass fabrics. The carbon composite can sustain about 650 MPa, 550 MPa, and 30 MPa in tension, flexure and shear respectively.
- The matrix adheres well to wood, concrete, and steel. The shear strength obtained using glued steel plates was 15 MPa.
- The fatigue performance of carbon composites is comparable to the fatigue performance of organic polymer-carbon composite.

The results obtained so far indicate that the inorganic matrix has excellent potential for use in concrete structures as a durable coating material or a strengthening system.

REVIEW OF REINFORCED CONCRETE BEAMS STRENGTHENED WITH CARBON SHEETS AND ORGANIC POLYMERS

Strengthening reinforced concrete beams with FRP plates or sheets has been studied extensively by a number of researchers worldwide. Beams have been strengthened both with prefabricated FRP plates (7-10) as well as with flexible sheets or fabrics (11-13). In all of these experimental studies, a two-part epoxy was used as the adhesive. The major conclusions from these studies were as follows:

- Significant increases in flexural strength are achieved by bonding composite plates. The greatest gains occur in beams with low steel reinforcement ratios.
- The number of cracks is increased and the average crack width is decreased.
- Failures that occur due to delamination or shearing off of the concrete cover at the rebar level require further experimental and analytical study. The failure criteria for these failure modes must be established for accurate prediction of ultimate capacity.

The authors of other papers also came to similar conclusions. The common feature of all the results is that failure rarely occurs by fracturing of the composite.

REVIEW OF PLAIN CONCRETE STRENGTHENED WITH ORGANIC POLYMERS

The primary application of this system is in the area of strengthening unreinforced walls. These walls, constructed using concrete or brick masonry or plain concrete, are very weak in the lateral direction. Carbon and glass fabrics can be very effectively used for strengthening these walls, Ehsani and Saadatmanesh (14). A number of studies have been conducted to evaluate beams made with clay bricks, concrete hollow core blocks, and carbon fabrics (15, 16). Walls reinforced with fabrics have also been tested, (17, 18). All of these studies indicate that high strength composites have excellent potential for this application. They are easy to apply and occupy very little space and hence can be applied even in locations with very little clearance.

RESEARCH PROGRAMME

Various aspects of the inorganic matrix in conjunction with concrete and timber structures are being evaluated at Rutgers University, USA. The focus of the research program reported in this paper is to compare the behaviour of an inorganic matrix that is brittle to a ductile organic matrix when used to bond carbon fibre sheets to plain and reinforced concrete beams. The primary comparisons to be made between the two are:

- Differences in failure mode
- Magnitude of strength increase over their respective controls, and
- Crack patterns

The second part of the paper deals with the durability aspects of the composite. In this program concrete strengthened or coated with composite were evaluated under wetting and drying and scaling conditions.

EXPERIMENTAL INVESTIGATION: STRENGTH TESTS

The experimental program for reinforced concrete was designed to simulate the research conducted by M'Bazaa et al (11), in which a total of eight reinforced concrete beams were constructed and load tested in four-point flexure over a span of 3000 mm with loads at one-third points. The primary variables were carbon length, end anchorage, and the amount of strengthening reinforcement. The beam with 3 layers of unidirectional carbon tow sheet, 166.7 mm wide and 2900 mm long bonded to the tension face of the beam, is of particular interest to the current investigation because the areas of carbon are comparable. The carbon area was 0.8258 cm^2.

The beams constructed for the current study were of identical span, width and depth (3000 x 200 x 300 mm) and effective cover. Strengthening was done using 2, 3, and 5 layers of unidirectional carbon sheets, providing 0.2845 cm^2, 0.4265 cm^2, and 0.7220 cm^2 of carbon fibre area respectively.

The beams for both the current and previous studies were significantly over designed for shear. The No. 10 M stirrups at 100-mm spacing used in the Sherbrooke study had a shear capacity of 281 kN and #3 stirrups at 95-mm spacing used in the current study had a shear capacity of 226 kN. The maximum shear encountered in a test was 55.0 kN and hence, shear performance was not a parameter. The details of steel reinforcement and carbon sheets are summarized in Table 1.

For plain concrete the parent concrete prisms were cast using the following mix proportions. The cement, fine and coarse aggregate contents were: 401, 860, and 720 kg per cubic meter of concrete. The water to cement ratio was 0.5. The 50 x 50 x 330 mm prisms were cast using steel molds and table vibrators and cured at 100% relative humidity for at least 28 days.

Table 1 Test beam summary

BEAM DESIGNATION	FLEXURAL STEEL	CARBON AREA, cm^2	MATRIX TYPE
OC	2 #10M bars	None	None
IC	2 #4M bars	None	None
OS	2 #10M bars	0.826	Organic (epoxy)
IS1	2 #4M bars	0.285	Inorganic
IS2	2 #4M bars	0.427	Inorganic
IS3	2 #4M bars	0.711	Inorganic

Note: All beams tested over 3,000 mm span, loads (P/2) at one-third points, and all beams significantly over-designed for shear

STRENGTHENING PROCEDURE

Prior to applying the carbon fabric, the beams were ground with an abrasive wheel to remove the laitance and expose part of the coarse aggregate. Subsequently, the ground surface was sand blasted, washed with hot water and allowed to dry. The roughened surface was primed with inorganic resin and allowed to air dry until tacky (approximately 1 hour). Meanwhile, the fabrics were saturated with resin and allowed to air dry until tacky. A bonding layer of resin was placed on the primed surface, followed immediately by the pre-saturated fabric. The fabric was rolled firmly to remove excess resin. Subsequent layers of fabric were placed similarly. After placing the final layer of carbon, the repaired area was vacuum bagged to remove vapor and promote resin flow. The repaired area was covered with a Teflon release film, followed by a breather fabric, followed by a Nylon bagging film. The bagging was sealed and a vacuum pump was used to draw a vacuum of about 740 mm Hg around the carbon repair. Finally, the beams were heated to 80° C for 24 hours for curing.

For plain concrete, the same procedure was followed for inorganic matrix. For the organic matrix, the manufacturer's recommendations were followed. The cleaned surface was coated with primer and cured for three days. The matrix and the carbon were placed on the primed surface and bonded using rollers. After applying the top coat, the samples were left at room temperature for at least seven days before testing.

RESULTS AND DISCUSSION: REINFORCED CONCRETE

The results discussed in the following sections focus on failure modes, crack patterns, load-deflection behaviour, strength increase, and strains. Table 2 provides a summary of the results. It is very important to note the difference in carbon sheet properties used in the investigations. For tests conducted using the organic system, carbon sheets were specially developed for the strengthening of structural components. The fibres were properly aligned and kept in place by sizing and a special back-up paper. The organic matrices were also specially formulated to provide the maximum efficiency in terms of penetrating carbon sheets and bonding to concrete. The system was developed over a number of years to achieve aligned fibres, attaining the highest possible carbon strength.

Table 2 Summary of experimental results

BEAM (1)	LOADS, kN		DEFLECTION, mm			MAXIMUM STRAIN, mm/mm		FAILURE MODE (9)
	Steel yield (2)	Ultimate (3)	At yield (4)	At ultimate (5)	Ductility Δ_y, col (5)/col(4) (6)	Concrete (7)	Carbon (8)	
OC	45.06	63.61	10.77	88.90	8.25	0.00145	-	UR[1]
IC	57.83	74.51	11.00	93.98	8.55	0.00182	-	UR[1]
OS	67.30	99.64	12.27	28.19	2.30	0.00129	0.00693	DE[2]
IS1	73.40	80.51	12.95	20.14	1.55	0.00075	0.00553	CR[3]
IS2	75.62	91.90	12.90	23.32	1.81	0.00131	0.00581	CR[3]
IS3	84.52	110.09	13.97	24.05	1.72	0.00142	0.00641	CR[3]

[1] Under-reinforced, [2] Delamination. [3] Carbon rupture

For the inorganic system, commercially available carbon sheets were used. Unlike the organic system that used backing paper to keep the fibres aligned, the carbon used in this system was woven with cross-directional glass fibres to keep it in place. This carbon system does not provide very good fibre alignment because the amount of sizing used is limited and because the fibre tows are undulated by the weaving process. When these thin sheets were placed on beams, they also tend to undulate to fit the prepared concrete surface. To the best of the author's knowledge, this is the first time an inorganic carbon fibre system was used. Further refinement in terms of special preparation of fabrics will definitely enhance the performance.

LOAD-DEFLECTION BEHAVIOUR

The load-deflection curves for beams strengthened with the inorganic matrix are presented in Figure 1. As expected, increase in carbon area resulted in increased post-crack stiffness, post-yield stiffness, and ultimate load. The load-deflection behaviour of beams strengthened with inorganic matrix is similar to the beam strengthened with organic matrix.

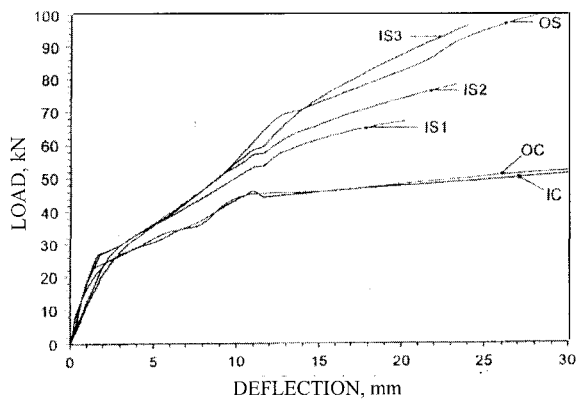

Figure 1 Load vs deflection curves for all beams

COMPARISON OF STRENGTH INCREASE

Strength increase is quantified as the difference between the maximum moments of the respective control and the strengthened beams. To account for differences in carbon area, increases were computed for unit carbon area using the equation:

$$\text{Moment increase per unit carbon area} = \frac{\Delta M}{A_{car}} \quad (1)$$

Where:
ΔM = moment increase with respect to the control (kN-m)
A_{car} = carbon area (m^2)

A comparison of strength increase is presented in Table 3. A careful review of these results leads to the following observations.

- The inorganic and epoxy systems provided comparable strength increase. The moment increase for unit carbon area for Beam IS2 was very close to that of OS, while IS3 was higher than OS and IS1 was lower than OS.

- For beams strengthened with inorganic matrix, the moment increase for unit carbon area seems to increase with the area of carbon, suggesting greater efficiency with larger carbon plates. This trend has not been observed previously, in part because the effect of increasing area has not been studied systematically.

COMPARISON OF STRESSES AND STRAINS

The peak carbon strains recorded during tests for the OS, IS1, IS2, IS3 beams were 0.00693, 0.005534, 0.005807, 0.006413 mm/mm respectively. Assuming the tensile modulus of 240 GPa (20) for the OS composite and 200 GPa (2) for the IS composite, the peak carbon stresses are computed and presented in Table 4. Here, the OS carbon delaminated when the carbon stress was approximately 1663 MPa, whereas the IS carbon ruptured when the average carbon stress was 1184 MPa. Note that in the inorganic system, the critical stresses occur in carbon fibres where the matrix is cracked whereas in the organic system the carbon plate acts as a composite plate since the strain capacity of epoxy is much higher than the carbon fibre strain capacity.

Table 3 Comparison of strength increase

BEAM	ULTIMATE MOMENT (kN-m)	MOMENT INCREASE (kN-m)	MOMENT INCREASE PER UNIT CARBON AREA (MN)
OC	31.805	-	-
IC	37.255	-	-
OS	49.820	18.015	218.2
IS1	40.255	3.000	105.4
IS2	45.950	8.695	203.9
IS3	55.045	17.790	250.2

Table 4 Maximum carbon and interface stresses

BEAM	CARBON STRESS AT ULTIMATE (MPa)	PROPORTION OF COUPON STRENGTH (%)	CARBON LOAD AT ULTIMATE (kN)	AVERAGE SHEAR STRESS AT ULTIMATE (kPa)
OS	1663	39	137.33	867.2
IS1	1107	79	31.49	217.5
IS2	1161	83	49.52	342.0
IS3	1283	92	91.22	630.1

Table 4 includes the average shear stress at the interface of carbon and the concrete at ultimate loading. This stress was computed by dividing the maximum carbon force by the bond area outside of the constant moment region. Based on this calculation, the limiting average shear stress is 867 kPa for the OS. This strain compares well with the results of Ritchie et al who estimated the limiting average shear stress to be between 758 kPa and 827 kPa. Because the IS beams did not delaminate, the limiting average shear stress could not be estimated. However, the maximum average shear stress sustained was 630 kPa for beams with five layers of carbon fabric. Hence, the limiting shear stress is more than or equal to 630 kPa. The fact that the shear strength of the adhesive is sufficient to fracture the carbon fibres is more significant than the numerical value.

TEST RESULTS AND DISCUSSION: PLAIN CONCRETE

For plain concrete, the primary response variables were: strength and stiffness increase, non-linearity produced by the composite strengthening system, and failure pattern. These parameters are discussed in the following sections.

FAILURE PATTERN

As expected, the control beams behaved linearly elastic up to peak load, followed by brittle failure. The post-peak curve could be obtained if special loading methods such as crack mouth-opening displacement controls were used. Since the focus of the current research is on strength increase, special test methods were not used to capture the post-peak response. All of the strengthened beams had post-peak strength.

Each of the strengthened beams carried considerable load after the development of the crack at the mid span. Only one crack developed which widened until failure of the specimen. The crack width at failure increased with an increase in reinforcement area. An increase in deflection at failure was also experienced as the crack width increased.

In the case of the organic matrix, the crack at midspan extended at the interface towards the supports. In each case, failure occurred because of debonding of the reinforcement. After the tests were completed, the debonded tows and fabrics could easily be peeled away from the sample. It can be hypothesized that a thin layer of concrete near the interface was weakened by the shear produced by the carbon fibres.

In the case of the inorganic matrix, the failure was always caused by fracture of the carbon fibres. It should be noted that the inorganic matrix is much more brittle than the organic matrix and hence microcracks occur within the composite plate. Therefore, the fibres act individually rather than as a single plate reducing the possibility of delamination. The reinforcement was not easily peeled away from the prisms after failure as in the case of the organic matrix.

The absence of effective load transfer between the fibres within the composite reduces the shear stress at the interface. The positive effect is the absence of debonding failure. The negative effect is the inefficient use of carbon fibres. The carbon fibres at the microcracks experience higher stresses, resulting in fibre failure at lower average strains as compared to organic matrices. This aspect of the failure pattern is further discussed in a later section.

LOAD-DEFLECTION BEHAVIOUR

The load-deflection behaviour of beams strengthened with inorganic and organic matrices is presented in Figures 2 and 3, respectively. In Figure 2, the behaviour of beams strengthened with 1, 2, and 3 tows, 1 and 2 layers of fabric, and control beams are presented. In Figure 3, an additional curve for the unidirectional carbon sheet is also presented. A careful review of these curves leads to the following observations.

- The load-deflection behaviour of these plain concrete beams is different from the curves corresponding to the strengthened reinforced concrete beams. The major difference could be due to the single crack that occurs in plain concrete beams. This difference in behaviour should be considered when high strength composites are used to strengthen non reinforced concrete and masonry. The test results also provide an opportunity to understand the mechanism of load transfer near the crack.

- As expected, the beams strengthened with the organic matrix had larger deflections before failure. As mentioned earlier, the inorganic matrix cracks at strains of about 0.007 mm/mm. In addition, the silicate matrix bonds with the concrete chemically by transfer of CaOH and KOH between parent concrete and the adhesive, resulting in the absence of a well defined interlaminar layer. Therefore, when the concrete cracks, the cracks will go through the repair layer, transferring the forces to the carbon fibres. As a result, the debonding of the repair plate at the crack is much less in the inorganic matrix and the average strain in the plate at failure is also lower.

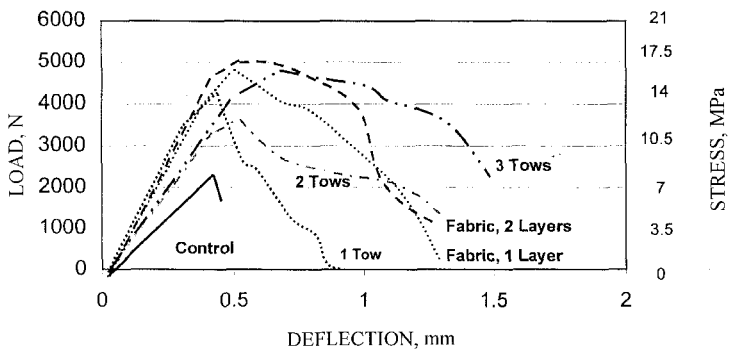

Figure 2 Load vs deflection, inorganic matrix

INCREASE IN FAILURE LOADS

Increase in failure loads is compared in Figure 4. The increases are presented as a factor of control strength for easy comparison. In beams reinforced with carbon tows, the strength increase for the inorganic and organic matrices is not significantly different. In the case of the inorganic matrix, the beam reinforced with only one tow had a greater strength increase than the beam reinforced with two tows. Initially, this was assumed to be an experimental error. Additional tests confirmed that the increase was not an experimental error. Strength analysis and close observation of the failed specimens lead to the following hypothesis.

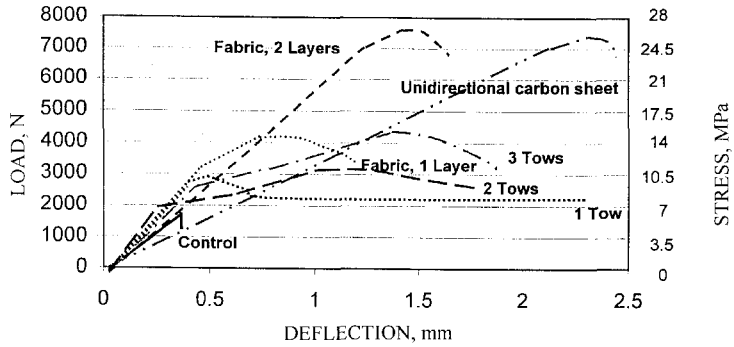

Figure 3 Load vs deflection, organic matrix

When inorganic matrix is used for repair, the amount of fibres and their distribution plays an important role near the crack and load transfer. In the case of one tow, the fibres are well spread out and are very close to the bonded surface. As soon as the crack forms in the parent concrete, it penetrates the repair matrix. The author believes that this penetration occurs when the crack width is only a fraction of a millimeter. This process enables the contribution of the carbon fibres at very low crack width and hence the tension force contribution of the concrete is not lost. Strength calculations confirm that, on the onset of cracking, both carbon and tension zone concrete contributes to strength capacity. The disadvantage in this load transfer mechanism is the reduction in ductility of the specimen. When more fibres are added, the load transfer becomes much less localized and an increased crack width opening occurs before failure. This results in an increased ductility but less utilization of tension zone concrete. The average stress and strain of carbon at failure reduces as the amount of fibres is increased. Ductility can also be improved by adding short fibres to the matrix. The stress and strain failures also decrease with an increase in fibre content in organic matrices. But the decrease in failure strains is more gradual as discussed in a later section.

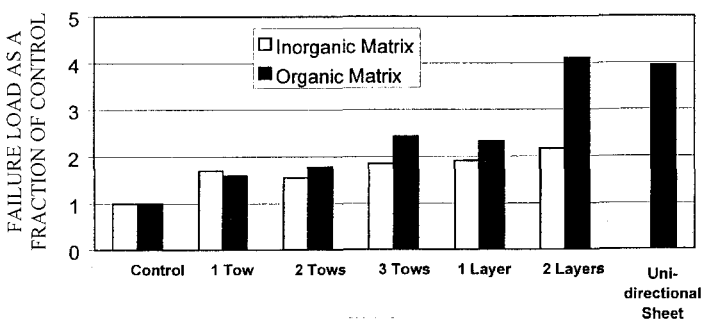

Figure 4 Increase in failure loads

EXPERIMENTAL PROGRAM: DURABILITY TESTS

The effectiveness of a strengthening system consisting of an inorganic matrix used in conjunction with several commercially available forms of carbon was studied. The matrices were applied to high strength concrete specimens and subjected to wet-dry and scaling conditions. The effectiveness of the matrix was studied using the results of flexure tests obtained before and after exposure to wet-dry and scaling conditions.

Details of Specimens

The specimens consisted of:

- High strength plain concrete
- High strength prisms reinforced with discrete carbon fibres, carbon tows and fabrics.

Preparation of Samples

The dimensions of the prisms were 50 x 50 x 300 mm. The cement: fine aggregate: coarse aggregate ratio was 1: 2.14: 1.79. The maximum size of the coarse aggregate was 9.5 mm. The water/cement ratio was *0.5*. The prisms were cast using 50 x 50 x 300 mm. steel molds, covered with polyethylene sheet and kept for 24 hours at room temperature and humidity. At the end of 24 hours, the samples were removed from the molds and cured for 28 days in a room maintained at 100% relative humidity.

Strengthening Procedure

The preparation of the samples involved sand blasting and cleaning with a wire brush. Sand blasting was performed using silica quartz sand at a pressure of 80 psi. Once the surface was cleaned, a thin layer of the inorganic matrix was applied to fill the small air voids and to create a smooth surface. Pre-cut carbon tows and sheets were impregnated with the matrix and placed on the prepared concrete surface and bonded using grooved rollers. A second layer of the matrix was applied as a protective coating. The samples were cured for at 24 hours at room temperature followed by 24 hours at 80^0C. The elevated temperature was used to ensure adequate curing in a two-day period. One day curing at 80^0C is equivalent to about one week curing at room temperature.

Wet-Dry Machine

A special set-up was built for exposing the samples to wetting and drying. A 1350 x 685 x 152 mm stainless steel basin containing the specimens was elevated to a height of 1.2 m. A reservoir containing 75 liters of a 3% saline solution was installed beneath the basin. A heater and a temperature gage were attached to the salt water reservoir to ensure that the water remained at a constant temperature of 50^0 C. Elevated temperature was used to further accelerate the deterioration process. The salt water was transported from the reservoir to the basin containing the samples by a pump. A timing valve attached to the drain of the basin controlled the flow of the water back into the reservoir. A 450mm fan was installed 600 mm above the basin to help circulate air during dry cycles.

After the test specimens were placed in the stainless steel basin, the timers were set to allow for a three-hour wet and three hour dry cycle. At the beginning of each wet cycle, the pump filled the basin to a level that totally submerged the samples with salt water from the reservoir. After three hours, the basin's drain valve opened allowing water from the basin to drain back into the reservoir and the fan began to circulate air above the basin. At the conclusion of the three-hour dry cycle, the wet portion of the next cycle began. Visual inspection confirmed the complete drying of the samples.

Scaling Test Set-Up

A special set-up was built for exposing the test samples to scaling conditions. Rectangular plastic dams were built to fit atop the coated surface of the specimens. The height of the dams was 25 mm. The dams were attached to the coated surface of the samples with a bead of waterproof caulk. The dams were filled with three percent saline solution to a depth of 6 mm.

The scaling test described in ASTM C672 was designed to allow the completion of one scaling cycle in a 24-hour period. The samples with the dams containing the saline solution were placed in a freezing chamber. They were kept at -5^0C for sixteen hours. At the end of this freezing cycle, the samples were removed from the freezing chamber and kept at room conditions. After eight hours in this environment, the thaw cycle was completed and a new scaling cycle began as the samples were returned to the freezing chamber.

Flexure Testing

Samples strengthened with carbon reinforcement were tested in flexure using three-point bending test. The load was applied using an MTS testing machine with a 45kN capacity. The mid-span deflection was measured using an LVDT. Both load and deflection were recorded by a computer.

The samples with the strengthening systems were exposed to a full series of either 50 or 100 wet-dry cycles before they were removed from the wet-dry machine. When scaling tests were conducted, the samples were exposed to 50 scaling cycles. These samples were tested in flexure.

TEST RESULTS AND DISCUSSION: WET-DRY EXPOSURE

The test samples consisted of the following:

- Two control samples
- Two samples strengthened with both two and four percent discrete carbon fibres
- Two samples strengthened with one, two, and three carbon tows
- Two samples strengthened with one and two layers of carbon

For each variable, two specimens were tested at 0, 50, and 100 cycles of exposure. The objective was to determine whether discrete fibres would add strength and toughness to plain concrete and whether it is possible to add continuous reinforcement to plain concrete. In both cases, the wet dry cycling provided the information on durability. Note that carbon fibres do not corrode and therefore the failure can occur because of the deterioration of the matrix or the interface.

The second type of reinforcement that was studied utilized carbon tows. The load-displacement relationship of these samples is shown in Figure 5. As in the control samples, behaviour was linearly elastic prior to cracking of the concrete. The addition of the carbon tows, however, greatly improved the ability of the sample to sustain load after cracking. Increased carbon area provided increase in the sustained load. Additionally, load was sustained through a greater displacement as the number of carbon tows was increased. In each case, the peak load of the samples exposed to 100 cycles of wet-dry was greater than the unexposed samples. Comparable values were observed in the toughness of the exposed and unexposed samples.

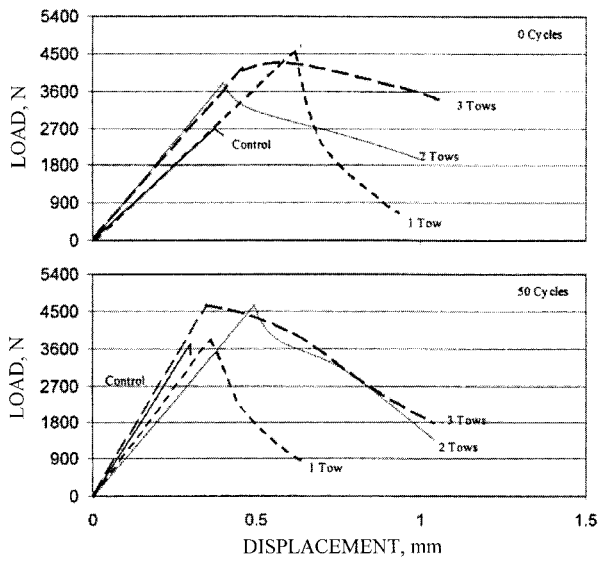

Figure 5 Comparison of load-deflection response; Control, 1, 2 and 3 carbon tows, wet-dry exposure

Samples were also strengthened with unidirectional carbon sheets and exposed to wet-dry conditions. Either a single or double layer of carbon was bonded to the tension face of the samples before exposure to wet-dry conditions. The load-displacement behaviour was identical to the behaviour of samples strengthened with carbon tows. Comparable peak load values and increases in toughness were observed after wet-dry exposure.

TEST RESULTS AND DISCUSSION: SCALING EXPOSURE

The samples exposed to scaling conditions were strengthened with the same forms and areas of carbon that were discussed in the wet-dry section. Peak load, flexural stiffness, and toughness were used to evaluate samples subjected to 50 cycles of scaling.

In samples strengthened with two and four percent discrete carbon fibre, the load-displacement relationship was linearly elastic until the peak load for both virgin samples and samples exposed to scaling.

The strength increases were less than ten percent when two or four percent carbon was used. An insignificant drop in the toughness was observed for each of the samples after exposure to scaling conditions. The flexural stiffness of each of the samples increased by at least 50 percent after fifty scaling cycles.

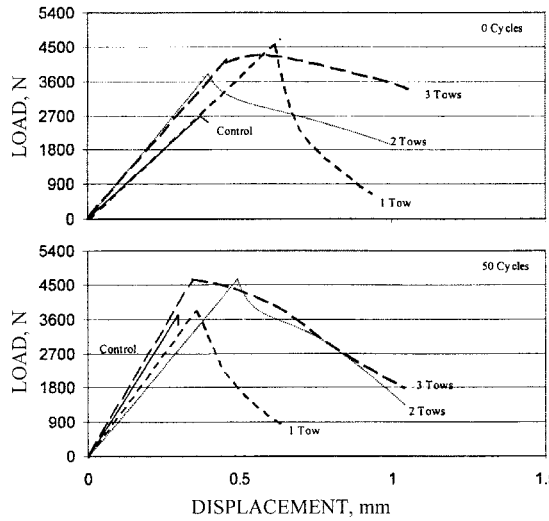

Figure 6 Comparison of load-deflection response; Control, 1, 2 and 3 carbon tows, scaling exposure

As in the wet-dry experiment, carbon tows were used to strengthen the samples. The tows were externally bonded to the tension face of the samples with the inorganic matrix. The load-displacement relationship of these samples is shown in Figure 6. The response was linearly elastic prior to cracking of the concrete. The ability of the samples to sustain load after cracking, however, was greatly improved by the carbon tows. As the area of the carbon was increased, a larger percentage of the cracking load was sustained by the sample. Exposure to scaling conditions had minimal effect on the strength capacity of these samples. When a single tow was used, weakening occurred but samples with two or three tows had higher strength after exposure. In each case, the variation was less than ten percent. An inverse relationship was noted between the toughness and flexural stiffness of the samples. When an increase in toughness was observed, the flexural stiffness of the sample decreased.

The next set of samples was strengthened using unidirectional carbon sheets. Either a single or a double layer of the carbon was bonded to the tension face of the specimens. The behaviour was identical to that of the samples strengthened with carbon tows. Insignificant changes in the flexural strength of the samples were noted after exposure to the scaling conditions. Exposed samples maintained at least 97 percent of their flexural strength. Any changes in the toughness or flexural stiffness of the samples were consistent with the slight decrease in failure load and do not indicate significant weakening of the samples.

OPPORTUNITIES AND CHALLENGES

Based on the results of the investigation at Rutgers University, a number of demonstration applications have been carried out in New Jersey and Rhode Island. These projects were for surface protection. For strengthening applications, more experimental results are needed to convince the users. Currently two investigations: one at the University of Alabama at Huntsville and the other at Perth University in Western Australia are being conducted. The results from these investigations are expected to reinforce the results of Rutgers study. Once credibility of the system is established, the matrix could replace organic matrices for all civil engineering infrastructure applications.

The major challenge is developing a marketing system. Since the system is field applied all the problems that are encountered in concrete construction are also applicable to this system. The cost of carbon fabrics is another challenge. The cost is slowly reducing to about $25 US dollars per kilogram.

CONCLUSIONS

Based on the experimental results presented in this paper and comparisons with other experimental results reported in the literature, the following conclusions can be drawn:

- The inorganic and organic systems provide comparable performance with respect to the increase in strength of reinforced concrete beams. For non reinforced concrete, organic polymers provide larger strength increase.
- For inorganic systems, the strength increase for unit carbon area seems to increase with the number of carbon layers for reinforced concrete beams.
- For plain concrete, which develops a single crack, this aspect seems to reverse itself. Larger carbon areas provide small increase per unit area. However the differences are not significant.
- For reinforced concrete beams, the inorganic system and the epoxy system improved post-crack stiffness equally well. It was found that each strengthening system provided approximately the same post-crack stiffness increase for unit carbon area.
- The inorganic system increased the post-yield stiffness more than the epoxy system. It was found that the inorganic adhesive system provided higher post-yield stiffness increase for unit carbon area.
- All the beams strengthened with the inorganic adhesive system failed in carbon rupture. In contrast, the beam strengthened with the epoxy adhesive system failed in delamination. This difference can be explained by differences in the load transfer mechanism between composite and parent concrete.
- The author believes that the inorganic system adhesive's bond behaviour is similar to that of rebar in concrete. The bond fails adjacent to cracks, facilitating local bond slip in the carbon while bond is maintained intermittently. This mechanism reduces the tensile strain on the concrete at the interface. Complete delamination does not occur because the interface is strong in shear when it is not highly strained. This concept deserves further investigation because of its importance for eliminating brittle bond failure of strengthened beams.

- Both the matrix and the interface are durable under wetting and drying and scaling conditions. There is no decrease in the maximum load capacity after 100 cycles of wetting and drying or 50 cycles of scaling
- There is an insignificant decrease in toughness (area under the load-deflection curve) after scaling exposure.

ACKNOWLEDGEMENTS

The author gratefully acknowledges the support provided by the New England Transportation Consortium. The project was also partially supported by the National Science Foundation. The author would also like to thank Christos Papakonstantinou for his contribution in the preparation of the paper

REFERENCES

1. ACI COMMITTEE 440, (1996), State-of-the-Art Report on Fiber Reinforced Plastic (FRP) Reinforcement for Concrete Structures, ACI 440-R-57, American Concrete Institute, Detroit.

2. FODEN, A.J., (1999), Mechanical Properties and Material Characterization of Polysialate Structural Composites, Ph.D. Dissertation, Rutgers, The State University of NJ, New Brunswick, NJ.

3. HAMMELL, J.A., LYON, R.E., AND BALAGURU, P., (1998), Influence of Reinforcement Types on the flexural properties of geopolymer composites, SAMPE International Symposium, 43, pp. 1200-1210.

4. FODEN, A., LYON, R., BALAGURU, P., DAVIDOVITZ, J. (1996) High Temperature Inorganic Resin for Use in Fiber Reinforced Composites, Proc., 1st Int. Conf. on Compos. in Infrastruct. ICCI'96, Dept. of Civ. Engg. and Engg. Mech., Univ. of Arizona, Tucson, AZ, 166-177.

5. LYON, R.E. (1997), Fire Resistant Aluminosilicate Composites, Fire and Materials, John Wiley & Sons, Vol. 21, pp. 67-73.

6. DAVIDOVITZ, J. (1991), Process for Obtaining a Geopolymeric Alumino Silicate and Products thus Obtained, International Patent Application PCT/FR91/00177 WO 91/13830.

7. SAADATMANESH, H., EHSANI, M.R. (1991a), RC Beams Strengthened with GFRP Plates, I: Experimental Study, Jo. of Struct. Engg., ASCE, 117(11), 3417-3433.

8. RITCHIE, P.A., THOMAS, D.A., LU, L.-W., AND CONNELLY, G.M. (1991), External Reinforcement of Concrete Beams Using Fiber Reinforced Plastics, ACI Struct. Jo., 88(4), 490-499.

9. SHARIF, A., AL-SULAIMANI, G.J., BASUNBUL, I.A., BALUCH, M.H., AND GHALEB, B.N. (1994), Strengthening of Initially Loaded Reinforced Concrete Beams Using FRP Plates," ACI Struct. Jo., 91(2), 160-168.

10. ROSS, C.A., JEROME, D.M., TEDESCO, J.W. AND HUGHES, M.L., (1999), Strengthening of Reinforced Concrete Beams with Externally Bonded Composite Laminates, ACI Struct. Jo., 96(2), 212-220.

11. M'BAZAA, I.M., MISSIHOUN, M., AND LABOSSIERE, P., (1996), Strengthening of Reinforced Concrete Beams with CFRP Sheets, Proc., 1st Int. Conf. on Compos. in Infrastruct., ICCI 96, Dept. of Civ. Engg. and Engg. Mech., Univ. of Arizona, Tucson, AZ, 746-759.

12. NAKAMURA, M., SAKAI, H., YAGI, K., AND TANAKA, T. (1996), Experimental Studies on the Flexural Reinforcing Effect of Carbon Fiber Sheet Bonded to Reinforced Concrete Beam, Proc., 1st Int. Conf. on Compos. in Infrastruct., ICCI'96, Dept. of Civ. Engg. and Engg. Mech., Univ. of Arizona, Tucson, AZ, 760-773.

13. ARDUINI, M., AND NANNI, A. (1997), Behaviour of Precracked RC Beams Strengthened with Carbon FRP Sheets" J. Comp. Const., ASCE, 1(2), 63-70.

14. EHSANI, M.R., AND SAADATMANESH, H., (1996) Seismic Retrofit of URM Walls with Fiber Composites, TMS Journal, The Masonry Society, V. 14, No. 2.

15. ROKO, K., BOOITHBY, J.E., BAKIS, C.E., (1999), Failure Modes of Sheet Bonded Fiber Reinforced Polymer Applied to Brick Masonry, Americna Concrete Institute SP, 188-28, pp.305-312.

16. MARSHALL, O.S., SWEENEY, S.C., AND TROVILLION, J.C., (1999) Seismic Rehabilitation of Unreinforced Masonry Walls, American Concrete Institute SP. 188-26, pp. 287-29.

17. HAMILTON III, H.R., HOLBERG, A., CASPERSEN, J., AND DOLAN, E. W., (1999), "Strengthening Concrete Masonry with Fiber Reinforced Polymers," American Concrete Institute SP, 199-92, pp. 1103-1111.

18. EHSANI, M.R., SAADATMANESH, H., AL-SAIDY, A., (1997), Shear Behaviour of URM Retrofitted with FRP Overlays, Journal of Composites of Construction, Vol. 1, pp. 17-25.

19. TONEN CORPORATION (1996), Forca Tow Sheet Technical Notes

20. HUANG, G. G., (1995), An Inorganic Polymer for Use in Fiber Composites, Project Report, Rutgers, The State University of New Jersey, USA., pp. 73.

21. TOUTANJI, H., AND GOMEZ, W. (1997), Durability Characteristics of Concrete Beams Externally Bonded with FRP Composite Sheets, Cement and Concrete Composites, 19, pp. 351-358.

NEW APPROACH TO MULTI-SPAN CFRP CONTINUOUS PRESTRESSED CONCRETE BRIDGES

N F Grace
Lawrence Technological University

B M Tang
Federal Highway Administration
United States of America

G Abdel-Sayed
University of Windsor
Canada

ABSTRACT. This investigation addresses the response of a newly developed two-span continuous double-T (DT) bridge system, internally and externally prestressed using carbon fibre reinforced polymer (CFRP) Leadline tendons. The effect of pre-tensioning and post-tensioning on the overall strain distribution was examined. The bridge was subjected to an ultimate load test after it had been subjected to 15 million cycles of two repeated loads of constant amplitudes equivalent to the service load at Midspan 1 and twice the service load at Midspan 2. It was concluded that the presence of continuous externally draped CFRP tendons (in the positive and negative moment region), CFRP grids, and the adjusted (increased) level of external prestressing forces results in a ductile CFRP continuous bridge system. Also, the measured ductility index was observed to increase by 48 percent, while maximum midspan deflection was reduced by 75 percent in comparison to corresponding values of a simply supported bridge using the same construction components.

Keywords: Continuous bridge, Prestressing systems, Carbon fibre reinforced polymer, Post-tensioning, External prestressing, Ductility

Nabil F Grace is a professor and chairman of the Civil Engineering Department at Lawrence Technological University, Southfield, Michigan. He is also the director of the Structural Testing Center. His research projects are currently funded by the National Science Foundation, Federal Highway Administration, and several DOTs.

Benjamin M Tang is an engineer in the Office of Bridge Technology, US Department of Transportation, Federal Highway Administration, Washington, D.C., USA

George Abdel-Sayed is a professor emeritus, Department of Civil Engineering, University of Windsor, Windsor, Ontario, Canada.

INTRODUCTION

Early research investigations [1-3] indicate that internally bonded tendons in combination with externally unbonded tendons can be used to design a reasonably ductile simply supported bridge (system). However, an extensive literature review has revealed little work on continuous prestressed concrete bridge systems using CFRP tendons.

In the present investigation, the feasibility of draping and post-tensioning of CFRP tendons from the sagging moment region (midspan, i.e., positive moment) to the hogging moment zone (intermediate support, i.e., negative moment) and back to the sagging moment region in a multi-span continuous bridge is examined.

The main emphasis of this paper is to examine the behavior of a two-span continuous double-T (DT) bridge model during an ultimate loading test after it has been subjected to 15 million cycles of two repeated loads of constant amplitude equivalent to service load (at Midspan 1) and twice the service load (at Midspan 2). Two bridge models were constructed and tested. The first one (CDT1) used CFRP Leadline tendons funded by Mitsubishi Chemical Corporation Japan, whereas the second one (CDT2) used CFCC (carbon fibre composite cables) strands provided by Tokyo Ropes Manufacturing Company, Japan. This paper addresses only bridge model CDT1.

BRIDGE SYSTEM AND CONSTRUCTION DETAILS

The two-span continuous CFRP prestressed concrete bridge studied in this investigation consists of the following:

1. Precast modified double-T (DT) girders [to be used as simply supported girders] prestressed with straight and internally draped bonded Leadline tendons.
2. Transverse (unbonded) CFRP tendons post-tensioned through tendon deviators and crossbeams.
3. CFRP reinforced concrete deck slab.
4. CFRP three-dimensional NEFMAC grids, which project beyond the top flanges of the DT girders, crossbeams and tendon deviators.
5. Continuous externally draped CFRP Leadline tendons.

In this bridge system, CFRP three-dimensional grids (see Figure 1) replaced conventional steel reinforcements. Hold-up and hold-down devices used to develop the desired draped profile of CFRP tendons were made of stainless steel to avoid corrosion problems. Continuous externally draped tendons were used to provide continuous prestressing in the positive and negative moment regions.

Other construction details are given elsewhere [4, 5]. Four double-T (DT) girders, designated as CDT1-1, CDT1-2, CDT1-3, and CDT1-4, were fabricated and prestressed with CFRP tendons. In this notation, CDT stands for continuous double-T bridge system; the first digit refers to the type of strand used, and the last digit refers to the DT girder number.

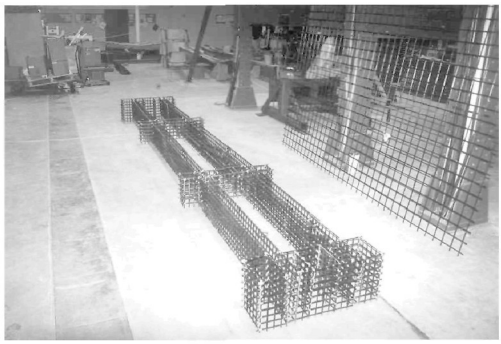

Figure 1 Three dimensional CFRP grid reinforcements

POST-TENSIONING OF BRIDGE MODEL CDT1

Details of the complete construction of bridge model CDT1 can be found elsewhere [5]. The total width of the bridge model was 2030 mm and each span measured 5890 mm. The full prestressing force of 78 kN per prestressing externally draped tendon and 45 kN per transverse tendon was applied after the placement and curing of deck slab. Note that the initial post-tensioning forces were re-adjusted (increased) during the testing stage of the bridge model, after the bridge had been subjected to 7.5 million cycles of repeated loads. The adjustment in the post-tensioning forces was made to determine whether increasing the post-tensioning forces at a particular age of the bridge could increase the life span of the developed bridge system. Repeated loads from 0 to 7.5 million cycles were applied and then, the post-tensioning forces in the externally draped tendons were increased (adjusted) by about 31.5 percent. It was thought that, this adjustment would restore any loss in parametric values such as deflection and strain. Then, an additional 7.5 million cycles of repeated loads were applied to the bridge model, subjecting the bridge model to a total of 15 million cycles of repeated loads before the ultimate load test. Details of the post-tensioning forces (initial and adjusted) along with stresses and elongation in each pair of prestressing tendons (designated as X1-a, X1-b, X2-a, X2-b, X3-a, X4-a, and X4-b) are presented in Table 1.

Table 1 Post-tensioning forces of externally draped CFRP tendons

DESIGNATION	INITIAL POST-TENSIONING @ 0 CYCLES			ADJUSTED (INCREASED) POST-TENSIONING FORCE @ 7.5 MILLION CYCLES		
	Post-tensioning Force, kN	Stress, MPa	Elongation, mm	Post-tensioning Force, kN	Stress, MPa	Elongation, mm
X-1a	77.0	835.0	76	102.7	1117	99
X-1b	77.8	844.6	79	102.3	1110	102
X-2a	77.4	839.8	66	102.7	1117	89
X-2b	79.2	859.1	84	101.9	1103	109
X-3a	79.2	859.1	66	101.9	1103	104
X-3b	77.4	839.8	64	101.9	1103	86
X-4a	77.8	844.6	71	104.1	1131	91
X-4b	77.4	839.8	71	102.7	1117	104

INSTRUMENTATION, LOADING SET-UP, AND DATA ACQUISITION

The loads were applied using load controlled MTS actuators placed at the middle of each span, using a four-point loading system resembling the front and rear axles of a truck. A lightweight truck of 84.6 kN in Span 1 and a heavy truck of 178 kN in Span 2 were simulated. Repeated cyclic loads ranging from 8.9 to 93.5 kN on Span 1 and 22.3 to 200.3 kN on Span 2 were applied. Note that the 84.6 kN load simulates the service load, while the 178 kN load simulates about twice the service load. These two repeated loads were selected to evaluate the performance of the developed bridge in order to examine the effect of a service load and an overload for 15 million cycles and to suggest ways to regain the strength of an overloaded bridge if any adverse effect on the strength of the bridge system was observed.

RESULTS AND DISCUSSION

Post-tensioning forces in the continuous externally draped tendons and transverse prestressing tendons were monitored by load cells attached at their dead ends. The deflections were measured using linear motion transducers (LMT) located along the lengths of both spans and along their widths at midspan, while strain measurements were made by electrical resistance strain gages. Figure 2 shows the strain distribution at the top of flanges and at the bottom of the webs for the intermediate support and Midspan 2 sections at three typical stages of construction: pre-tensioning of the internal CFRP tendons, placement of the deck slab, and post-tensioning of the external tendons. Noted that the strains shown (after the addition of the deck slab) at the top of the deck slab refer to those strains at the top of the flanges of the girders. The strains in the concrete throughout the depth of the girders are compressive before and after the placement of the deck slab. However, post-tensioning of the externally draped tendons causes a further increase in the compressive strains at the bottom of the girders, as well as a small tensile strain at the top of the deck slab at midspan. The opposite strain distribution occurs at the intermediate support. Thus, the strains developed at the top and bottom of the bridge after the post-tensioning of the externally draped tendons are opposite in sign to those strains which will be caused due to the superposition of live loads. This is the desired effect, since the sections are maintained in pure compression even with the added tensile strains caused by live loads. Thus, no tensile cracks develop under service loads.

The variation of load and deflection with time for Midspan 2 during the ultimate load test is shown in Figure 3. The load varies linearly until crushing of the concrete begins at the top of the deck slab at midspans and at bottom of the webs at the intermediate support. The reason for showing the variation of response for Midspan 2 is that the span was subjected to a heavier repeated load and failed earlier than span 1. Figure 3 also shows that the variation of load occurs in a zigzag pattern during crushing of the concrete. However, the absolute variation in load from the instant crushing begins to the ultimate bridge failure was 19 percent of the ultimate failure load. Crushing of concrete began in the deck slab at midspans and at the bottom of the webs at the intermediate support. Wider cracks at the bottom of midspans followed.

As shown in Figure 3, CFRP tendons failed by progressive rupture (staggered failure) leading to a complete loss of strength and stiffness of the bridge, as indicated by a negligible load and very large deflections. This occurred 22 minutes after the beginning of the test.

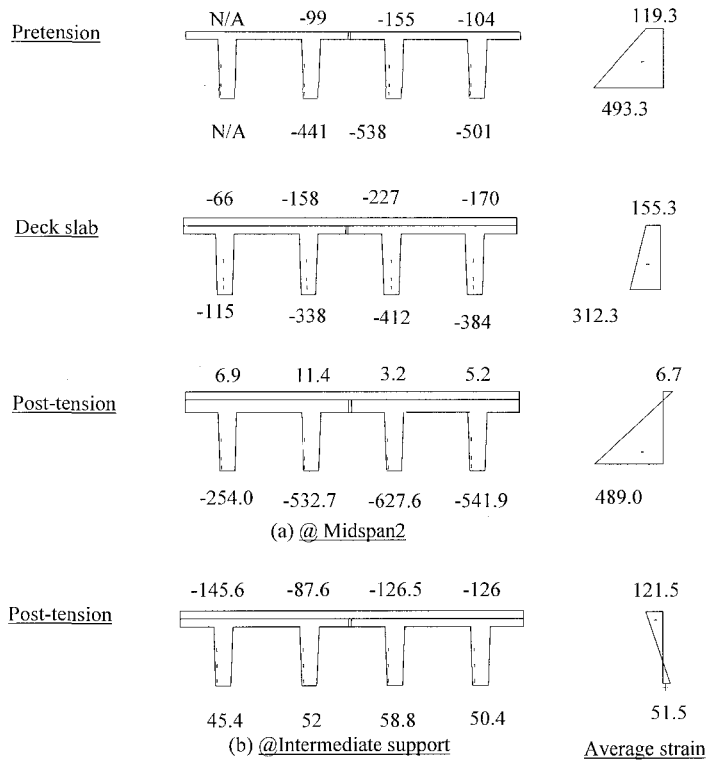

Figure 2 Strain distribution of bridge model CDT1

The deflection of the bridge varied linearly with time, and the time rate of variation became almost constant during crushing of the concrete. However, after the ultimate load of the bridge was reached, deflection increased rapidly (but not suddenly) after the failure of the first CFRP tendon.

The complete failure of bridge model CDT1 is shown in Figure 4. The load corresponding to the collapse of Span 2 was 721 kN, while the load corresponding to the collapse of Span 1 was 734 kN. The failure sequence started with crushing of concrete and then followed the rupture of NEFMAC grids and internal CFRP tendons at midspan. The other critical failure sections of the bridge were the locations of hold-down arrangements of the internally draped tendons.

In order to examine the ductility of the bridge system, several loading and unloading tests were carried out so that the inelastic energy absorbed in the system could be separated from the total energy of the system (see Figures 5 and 6). This inelastic energy absorbed in the system was used to determine the ductility of the system. Here, ductility is defined as the ratio of total inelastic energy absorbed to the total energy of the system.

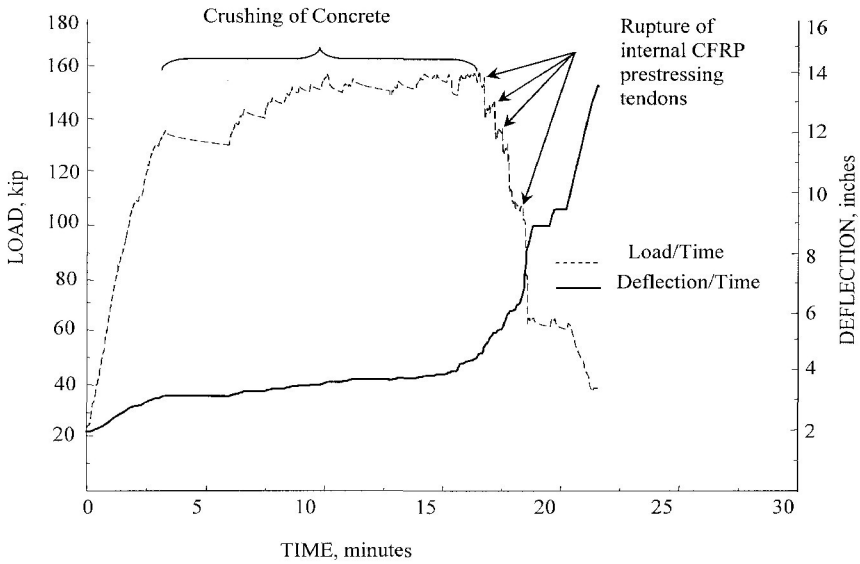

Figure 3 Variation of load and deflection with time for Midspan 2 of bridge model CDT1 under ultimate load test

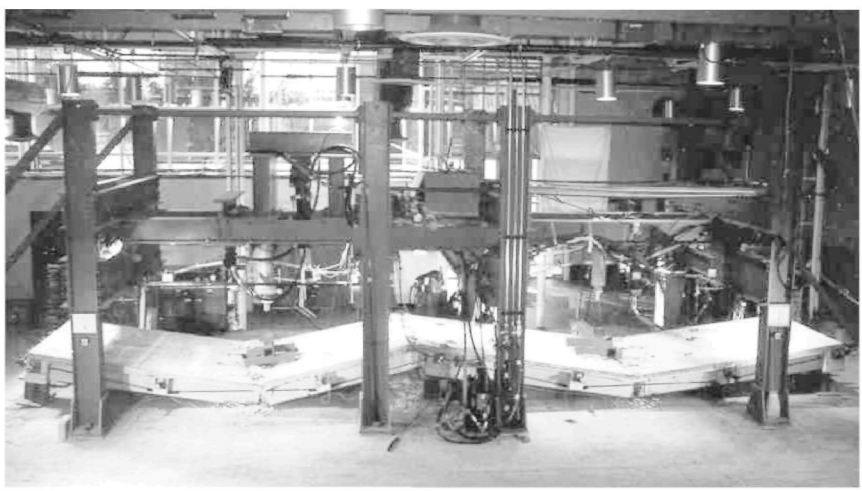

Figure 4 Bridge model CDT1 under ultimate load test

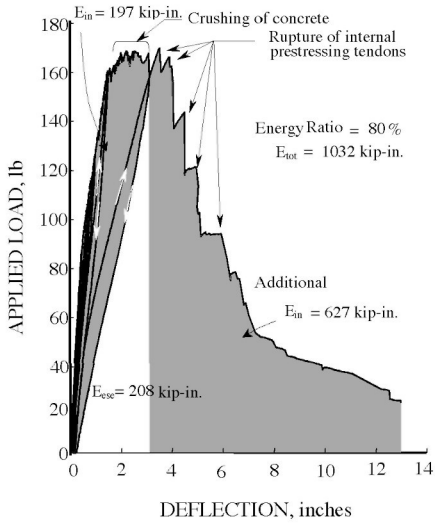

Figure 5 Energy ratio for Midspan 1

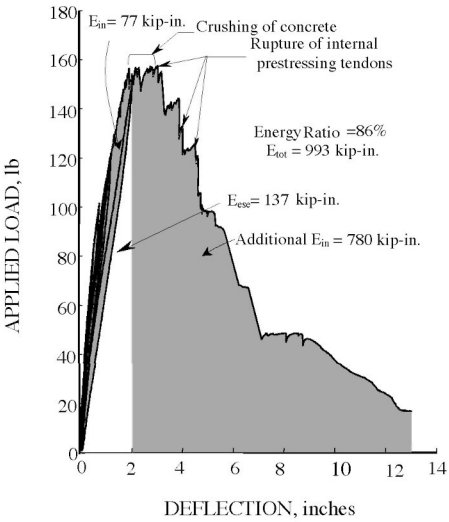

Figure 6 Energy ratio for Midspan 2

In these loading/unloading cycles, the load was increased from 0 to a maximum value [267, 401, 445, 490, 534, 623, 712 kN, respectively, which followed in sequence] and then unloaded to zero load. Each loading/unloading cycle followed the same procedure and was continued until the failure load [721 kN (162 kips)] was reached.

Figures 5 and 6 show that the measured energy ratios for Midspan 1 and Midspan 2 are 80 percent and 86 percent, respectively. These energy ratios clearly indicate that the failure of the bridge was not brittle. These ratios are similar to the energy ratios that may be experienced by prestressed concrete structures using conventional reinforcements [3].

Comparing the response of this bridge system with that of a simply supported bridge of the same construction components [3] suggests the following:

- The deflection of the continuous bridge at its ultimate load is much smaller than that of simply supported bridge at its ultimate load (about 75 percent smaller).

- The ductility of the continuous bridge is greater than the ductility of the simply supported bridge, as indicated by higher value (48 percent on average) of the energy ratio for the continuous bridge.

- The increase in ductility and the decrease in deflection of the continuous bridge are attributed to the continuity of the external tendons and the deck slab, as well as the presence of flexural and shear reinforcements in the form of the CFRP cage in the webs, deck slab, and flange.

- The increase in post-tensioning forces due to the application of static load to failure in the continuous bridge is not as significant as in the simply supported bridge of the same construction. There is only an approximate 40 percent increase in the post-tensioning forces observed in the continuous bridge, whereas in the simply supported bridge [3], the post-tensioning forces increased to about twice the initial prestressing value.

CONCLUSIONS

1. The presence of continuous externally draped CFRP tendons and the continuity of the deck slab resulted in a ductile CFRP continuous bridge system.

2. The measured energy ratio for the continuous bridge model was increased by 48 percent while the maximum midspan deflection at failure was reduced by 75 percent in comparison to corresponding values of a simply supported bridge using the same construction components. The ultimate load carrying capacity is equal to about eight times the service load.

3. The variation of load and deflection during crushing of the concrete is not appreciable, however, a significant loss in strength and stiffness of the bridge occurs after the ultimate load of the bridge is reached, due to the progressive failure of the internal CFRP tendons.

REFERENCES

1. GRACE, N. F., ABDEL-SAYED, G., "Behavior of externally/internally prestressed concrete composite bridge system," Proceedings of the Third International Symposium on Non-Metallic (FRP) Reinforcement for Concrete Structures (FRPRC), Sapporo, Japan, Vol. 2, 1997, pp 671-678.

2. GRACE, N. F., ABDEL-SAYED, G., "Ductility of prestressed concrete bridges using CFRP strands," Concrete International, Vol. 20, No. 6, 1998, pp 25-30.

3. GRACE, N. F., ABDEL-SAYED, G., "Behavior of externally draped CFRP tendons in prestressed concrete bridges," PCI Journal, Vol. 43, No. 5, 1998, pp 88-101.

4. GRACE, N. F., "Transfer length of CFRP/CFCC strands for double-T girders," PCI Journal, Vol. 45, No. 5, 2000, pp 110-126.

5. GRACE, N. F., "Response of continuous CFRP prestressed concrete bridges under static and repeated loading," PCI Journal, Vol. 45, No. 6, 2000, pp 84-102.

EXPERIENCES AND DESIGN CONSIDERATIONS OF CONCRETE MEMBERS REINFORCED BY FRP

A Borosnyói

G L Balázs

Budapest University of Technology and Economics

Hungary

ABSTRACT. Present paper intends to review experiences on characteristics of firbre reinforced polymers (FRP) for civil engineering applications and to discuss design considerations by applying FRP bars or tendons embedded in concrete as prestressed or non-prestressed reinforcement. Test results on FRP indicate high tensile strength, high fatigue strength as well as low relaxation and creep, however, due to lower transverse strength special anchoring devices can be needed. On the other hand, special attention has to be taken against brittle failure due to the linear elastic behaviour of FRP. Design of FRP reinforced or prestressed members can be based on the conventional way of design of reinforced concrete members, however, special considerations are needed to bond, cracking, deflection, minimum cover, minimum reinforcement, thermal effect, ductility and failure mode.

Keywords: Reinforcement, Prestressing tendon, FRP bars, Creep, Relaxation, Bond, Fatigue, Minimum reinforcement, Minimum cover, Deflection, Crack width, Thermal expansion.

Adorján Borosnyói MSc (CE), PhD candidate at Budapest University of Technology and Economics. Main fields of interest: serviceability and durability of reinforced concrete and prestressed concrete structures, applicability of non-metallic (FRP) reinforcements in reinforced or prestressed concrete, bond in concrete, strengthening with advanced composites. In his PhD work he deals with deflection and cracking phenomenon of CFRP prestressed concrete members. Member of the *fib* TG 4.1 "Serviceability Models" and the Hungarian Group of *fib*.

György L Balázs PhD, Dr Habil, Professor in structural engineering, Head of department of Construction Materials and Engineering Geology at the Budapest University of Technology and Economics. His main fields of activities are: experimental and analytical investigations as well as modelling of reinforced and prestressed concrete members, fibre reinforced concrete (FRC), fibre reinforced polymers (FRP), high performance concrete (HPC), bond and cracking in concrete and durability. He is convenor of fib Task Groups on "Serviceability Models" and "fib seminar". In addition to he is a member of several *fib*, ACI, and RILEM Task Groups or Commissions. He is president of the Hungarian Group of *fib*.

INTRODUCTION

Corrosion of steel reinforcement and prestressing tendons exposed to de-icing salts is increasingly becoming a significant issue. Deterioration often resulting in reduced serviceability and requiring extra costs for maintenance and rehabilitation. Non-corrosive Fibre Reinforced Polymer (FRP) reinforcements tend to be a promising alternative to overcome corrosion of steel reinforcement. Their advantages are superior resistance to corrosion, as well as acidic or alkaline solutions, high tensile strength, low self-weight, electromagnetic neutrality, high fatigue strength, low relaxation and good long term characteristics. Though, these materials have been present in special fields of civil engineering for more than 15 years some misunderstanding and mistrust still exist in practitioners that can be originated from the lack of standards in this field and basic human fear from unknown issues.

OBSERVED BEHAVIOUR

In the last decade several experimental investigations were carried out worldwide on various fields of the use of FRP reinforcements for concrete structures. To examine applicability of FRP materials some engineering structures have been built already, both experimentally and full scale. More than fifty bridges exist all over the world in which non-metallic reinforcement was applied instead of steel. Important details are summarized in the following.

Mechanical Characteristics

Corrosion resistant non-metallic reinforcements are made of Fibre Reinforced Polymers (FRP). These reinforcements consist of thousands of high strength fibres of diameter 8 to 10 μm embedded into a resin matrix. The load carrying fibres can be made of glass, aramid or carbon. The matrix is usually epoxy resin. FRPs have tensile strengths of 700 to 3500 N/mm^2, modulus of elasticity of 38000 to 300000 N/mm^2, failure strain of 0.8 to 4.0%. FRPs show no yielding, behave linearly elastic up to failure with brittle rupture. Qualitative stress-strain diagrams are indicated in Figure 1. Mechanical characteristics in longitudinal direction depend on the type of fibre, in transverse direction the matrix also has a considerable effect. Mechanical properties in transverse direction are minor to those of longitudinal direction.

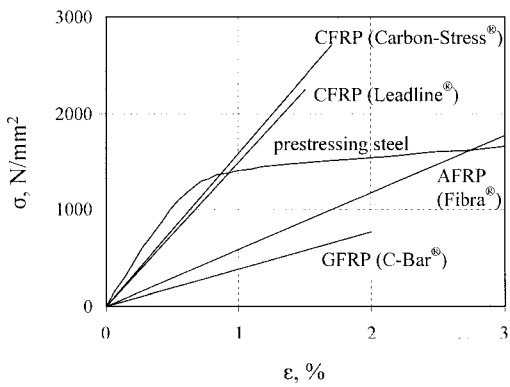

Figure 1 Qualitative stress-strain diagrams of FRPs

Long Term Properties

Short-term characteristics of FRPs can be more or less easily determined, however, long-term properties may require specific considerations. Long-term characteristics of FRP reinforcements can be different from that of ordinary steel reinforcements due to not only the different materials but also the composite behaviour: time dependent phenomena can take place within the material phases (fibre, matrix) and on the interface (bond, delamination). Generally FRPs show better creep, relaxation and fatigue behaviour than steel prestressing tendons [1-9]. However, influence of environmental effects on the long-term properties needs further experimental investigations. Available data on long term properties of FRPs are given in Table 1.

Table 1 Long term properties of FRPs

	GFRP	AFRP	CFRP	PRESTRESSING STEEL
Creep $\Delta\varepsilon$ [‰] ($\sigma = 0{,}8f_{fu}$; t = 1000 h)	3 – 10	1,5 – 10	< 0,1 (!)	2,5 – 6,0
Relaxation ρ_{1000} [%] ($\sigma = 0{,}8f_{fu}$)	1,8 – 2,0	5,0 – 10,0	0,5 – 1,0	2,0 – 12,0
Long term tensile strength (estimated for 100 years)	$0{,}4f_{fu} - 0{,}7f_{fu}$	$0{,}5f_{fu} - 0{,}7f_{fu}$	$> 0{,}9f_{fu}$	–

Bond

FRP reinforcements are usually produced by pultrusion process. Rods with almost smooth surface are not suitable for concrete structures due to the lack of adequate bond. Therefore, surface treatments (such as spiral fibre winding, indentations, periodic ribs, stranded or braided shapes, or sanded surfaces) are needed to improve bond characteristics. These treatments can increase bond strength of FRP reinforcements even more than that of steel tendons. Qualitative bond-slip diagrams are indicated in Figure 2. During pull-out bond failure the outer layers of FRP reinforcements can be damaged which never occurs in the case of steel tendons or reinforcing bars. This difference may influence structural behaviour.

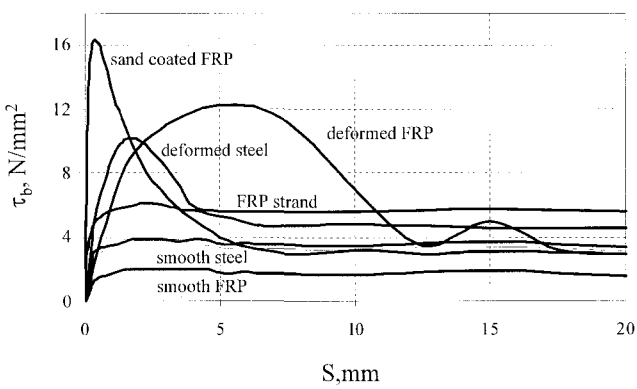

Figure 2 Qualitative bond-slip diagrams of FRPs

Structural Behaviour of Beams

FRP reinforced concrete beams in flexure show almost negligible plastic deformation that is attributed only by the crushing of concrete in the compressed zone at load levels close to failure. Figure 3 indicates a typical example for the load vs deflection behaviour of a GFRP reinforced beam [10].

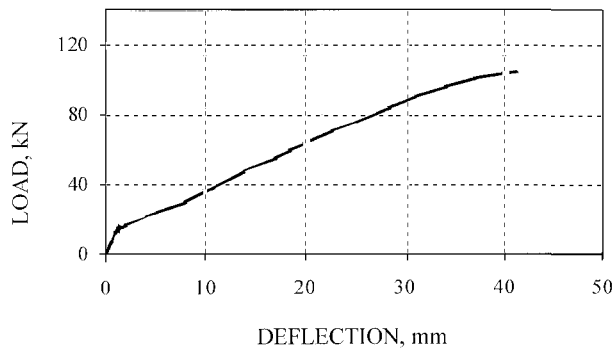

Figure 3 Load-deflection response for GFRP reinforced beam [10]

In the case of FRP prestressed members usually bilinear load-deflection responses can be observed [11 - 18]. Figure 4 indicates typical examples of load vs. deflection behaviours of a CFRP prestressed beam in comparison to a steel prestressed beam [19].

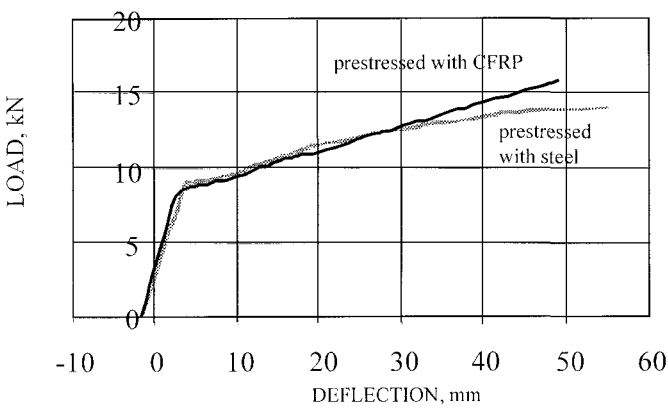

Figure 4 Load-deflection responses for CFRP or steel prestressed beam [19]

Special Applications

FRP materials for civil engineering purposes are basically developed for embedded reinforcement (prestressed or non-prestressed) in concrete elements or as externally bonded reinforcement for strengthening.

However, the possible use of these non-corrosive reinforcements is as wide as the use of ordinary reinforcements. Several applications can be found in the following fields:

1. Prestressed bridges: cantilever bridge [7], stress ribbon bridge [20], bulb-T pretensioned bridge girders [21] [22], monolithic superstructure [23], internal and external post-tensioned cables [24], draped prestressing tendons [25] etc.
2. Non-prestressed bridge superstructure: continuous deck slab [26], steel free deck slab [27].
3. Stay cables for cable stayed bridges [28] [29].
4. Ground anchors [7] [30].
5. Reinforcement for shotcrete [31].
6. Mesh reinforcement for brickwork and concrete [32].
7. FRP dowel bars [30].
8. Prestressed floor system [7].
9. Prestressed poles for power transmission lines [23].
10. Prestressed wood structures [7].
11. Marine applications (anchoring cable for platforms) [23].
12. "Smart reinforcements" (FRP reinforcements with integrated fibre optic sensing system) [33], etc.

DESIGN CONSIDERATIONS

Ultimate Limit State

As FRPs show linear elastic behaviour and brittle failure they have considerable release of elastic energy. Almost all of the stored energy during loading is elastic, which releases suddenly by failure. Therefore, special attention has to be taken against brittle failure.

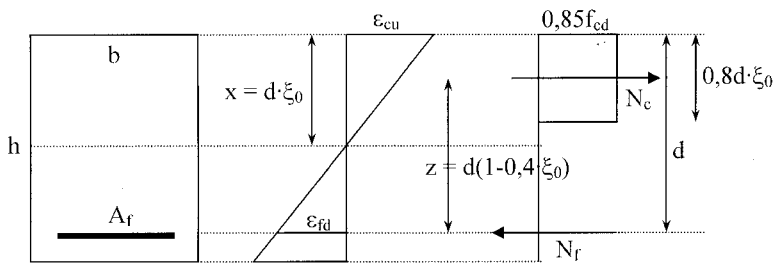

$$\rho_0 = \xi_0 \frac{\alpha f_{cd}}{f_{fd}}$$

$$N_c = b \cdot 0{,}8\xi_0 d \cdot 0{,}85 f_{cd}$$

$$N_f = A_f E_f \varepsilon_{cu} \frac{1-\xi_0}{\xi_0}$$

$$M = 0{,}68 b d^2 f_{cd} \xi_0 (1 - 0{,}4\xi_0)$$

Figure 5 Internal forces for balanced condition

Bending moment capacity of FRP reinforced cross sections can be determined using the conventional theory of composite cross sections, ie analysis of internal forces taking into account that plane cross sections remain plain during loading.

Failure has to occur with crushing of compressed concrete zone – rupture of reinforcement has to be avoided due to its sudden energy release. Concrete crushing is always reached if the reinforcement ratio is more than the so-called balanced reinforcement ratio (ρ_0) (whenever reinforcement yielding and concrete crushing occurs simultaneously: $\varepsilon_c = \varepsilon_{cu}$ and ε_s ε_{yd}) (Figure 5).

Minimum reinforcement ratio for FRP reinforced concrete cross sections can be: $\rho_{min} = 1.3 \times \rho_0$. Change of $E_f \times \rho_{min}$ in the function of the Young's modulus (E_f) of FRP reinforcement is indicated in Figure 6.

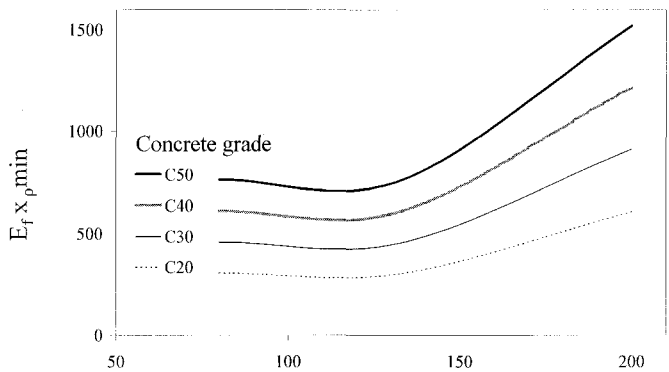

Figure 6 Change of $E_f \times \rho_{min}$ in the function of the Young's modulus (E_f) of FRP reinforcement

Typical moment-curvature diagrams are indicated in Figure 7 for CFRP prestressed concrete cross section (f_{fu} = 1333 N/mm^2, ε_{fu} = 10 ‰; concrete grade: C40).

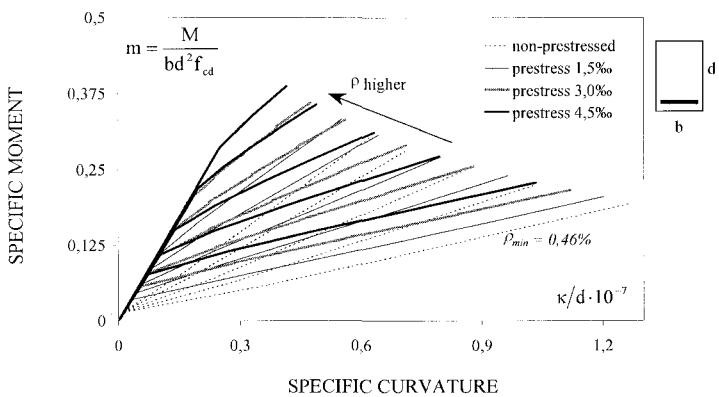

Figure 7 Moment-curvature responses for CFRP prestressed cross section

Serviceability Limit State

Young's modulus of FRP reinforcements is usually lower than that of steel reinforcing bars, therefore, the moment of inertia of a FRP prestressed or reinforced member in the cracked elastic state is lower than that of steel prestressed or reinforced ones. The lower the Young's modulus of the tendon, the lower the moment of inertia in the cracked elastic state. In cracked elastic state deflections of FRP prestressed or reinforced members will be greater than that of steel prestressed or reinforced members. Due to the lower Young's modulus, the strain of CFRP reinforcements in the cracked section would be greater. It may influence both crack widths and tension stiffening. Ratio of moment of inertia in uncracked and cracked elastic states (I_1/I_2) in the function of the Young's modulus of FRP (E_f) reinforcement is indicated in Figure 8.

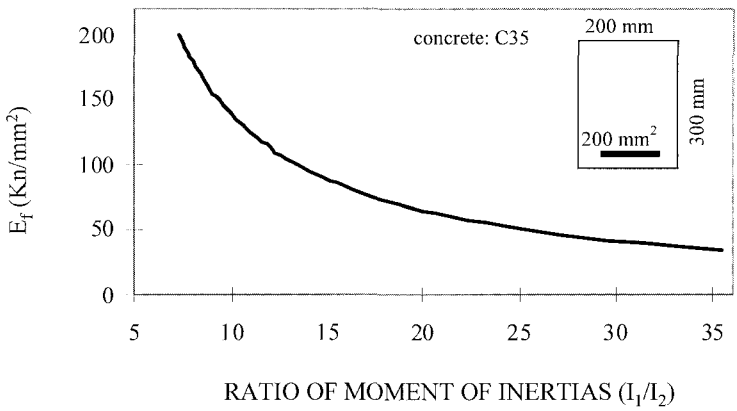

Figure 8 Ratio of moment of inertia in uncracked and cracked elastic states (I_1/I_2) in the function of the Young's modulus of FRP (E_f) reinforcement

For the calculation of deflection of FRP reinforced flexural members conventional methods can be used, however empirical parameters have to be determined from experiments to take into account bond characteristics and Young's modulus for each type of FRP reinforcement. Parameters of flexural crack pattern (crack spacing and crack width) are influenced mostly by the bond characteristics of reinforcement. Therefore, ordinary methods can be used for the calculation of crack widths introducing always empirical parameters that are determined from experiments to take into account bond characteristics of FRPs.

Prestressing

Because of low relaxation and creep as well as lower Young's modulus of FRP tendons, majority of losses of prestressing force are lower than that of steel prestressed members. However, due to the lower Young's modulus of FRP tendons, greater travel length of the prestressing jack is needed to develop an adequate prestressing force. On the other hand, FRPs have much lower strength in transverse direction than in longitudinal direction, thus prestressing of FRP tendons can not be carried out by using conventional anchoring devices. There were several anchoring systems developed for non-metallic prestressing tendons, but they have a restricted use.

FUTURE WORK

Besides the above mentioned issues further questions are still open. Most important of them are discussed herewith.

Minimum concrete cover

Minimum concrete cover in reinforced concrete members is required mainly for durability of reinforcement. In the case of FRPs this requirement can be neglected (non-corrosive reinforcement), however, other important parameters have to be taken into account such as fire protection (resin matrix is deteriorated at max. 200°C), cover against splitting in anchorage zone (due to high bond forces) or different coefficients of thermal expansion. For these purposes concrete cover of FRP reinforced members can not be reduced too much. It is advised to keep concrete cover requirements of ordinary steel reinforced members before detailed studies are available.

Allowable deflection and crack width

Deflection control under service loads is important for aesthetical reasons or connection of structural elements, thus these requirements can not be changed for FRP reinforced members. However, calculation of deflections is essential according to the lower Young's modulus of FRP reinforcements.

Crack control in the case of FRP reinforcement is needed only for aesthetical reasons (no durability problem) therefore, strict requirements for allowed crack widths can be relaxed in certain cases.

Thermal effects

Thermal actions can influence both mechanical characteristics and bond behaviour of FRPs. As indicated in Table 2 coefficient of thermal expansion (CTE) of fibres, resins, FRPs and concrete are differing from each other.

Table 2 Coefficients of thermal expansion of fibers, resins, FRPs and concrete

MATERIAL	COEFFICIENT OF THERMAL EXPANSION, $\times 10^{-6}$ 1/K	
	longitudinal	transverse
Carbon fiber	–0.9...+0.7	8...18
Aramid fiber	–6.0...–2.0	55...60
Glass fiber	5...15	5...15
Resins	60...140	
CFRP	–0.5...1.0	20...40
AFRP	–2.0...–1.0	60...80
GFRP	7...12	9...20
Concrete	6...13	

In the longitudinal direction FRPs have lower or nearly identical CTEs than that of concrete, however, in the transverse direction – governed mostly by the resin – have 5 to 8-times higher values. In specific cases, when high temperature variation takes place the large difference between CTEs can lead to high radial pressure on the surface of the reinforcement that can cause longitudinal splitting of concrete cover. It reflects on the importance of sufficient concrete cover especially if AFRP reinforcement is applied. Critical concrete cover (whenever splitting occurs) of AFRP tendons with sand coated surface was found to have $2.8\times\varnothing$ [34]. Authors found sufficient concrete cover of $2.5\times\varnothing$ to CFRP tendons with sand coated surface for pretensioned application with ten hours heat curing of maximum temperature of 75°C [35]. Thermal effects can also have influence on aging of resins, in this way the residual strength of FRP reinforcements. Experimental data on change of long-term residual strength of FRPs due to thermal cycles are not available.

Ductility

Definition of ductile behaviour requires plastic behaviour of structural materials. As FRPs are linearly elastic brittle materials ordinary definitions of ductility and ductility indexes can not be applied. However, due to the lower Young's moduli of FRPs deformability of these structures is considerable, warning can take place. To redefine ductility indexes still no generally accepted proposal exist.

Durability

Environmental effects can considerably influence long-term characteristics of FRPs. Liquids (water, alkali and salt solutions) can diffuse into resins of FRPs that can cause decrease in mechanical characteristics. Least diffusion can be found in vinyl ester resins. Glass fibres tend to deteriorate by alkali and chloride ions resulted in corrosion-induced failure. Aramid fibres can absorb water that cause reversible loss in strength, however, can cause bond splitting by swelling. Aramid fibres also suffer deterioration in alkaline environment. Carbon fibres are resistant to any kind of harsh environment. Limited experimental data are available in this field [5] [6] [36] [37] [38].

Future work is encouraged in these fields.

CONCLUSIONS

1. Fibre reinforced polymers (FRP) are increasingly used for civil engineering applications as prestressed or non-prestressed reinforcement.
2. Principle reasons for the application of FRPs their corrosion insensitivity, high strength, high axial fatigue strength and low relaxation. High material costs, low transverse strength and alkali sensitivity (for glass fibres) are the drawbacks.
3. Our design considerations indicate that:
   - conventional sectional analysis for reinforced members seem to be applicable, however
   - bond of FRP bars,
   - allowable crack width and deflection,
   - minimum concrete cover,
   - influence of elevated temperature,

- ductility of member,
- durability of member and
- anchoring of post-tensioned tendon

require special attention as well as future work.

ACKNOWLEDGEMENTS

Authors are grateful for the financial support of the Hungarian National Highway Administration (ÁKMI) Grant 3810.3.3/2001.

REFERENCES

1. ANDO, N, MATSUKAWA, H, HATTORI, A, MASHIMA, M (1997) Experimental Studies on the Long-Term Tensile Properties of FRP Tendons, *Proc.* 3rd Int. Symp. FRPRCS-3, JCI, 1997, Vol 2, pp 203-210.

2. MACHIDA, A (1993) State-of-the-Art Report on Continuous Fibre Reinforcing Materials, JSCE, Tokyo, 1993.

3. MACHIDA, A (1997) Recommendation for Design and Construction of Concrete Structures Using Continuous Fibre Reinforcing Materials, JSCE, Tokyo, 1997.

4. ROSTÁSY, F, (1996) State-of-the-Art Report on FRP Materials, *FIP Report, Draft*, 1996 (unpublished).

5. SAADATMANESH, H, TANNOUS, F E, (1999) Relaxation, Creep, and Fatigue Behavior of Carbon Fibre Reinforced Plastic Tendons, *ACI Materials Journal*, V 96, No 2, March-April 1999, pp 143-153.

6. SAADATMANESH, H, TANNOUS, F E (1999) Long-Term Behavior of Aramid Fibre Reinforced Plastic (AFRP) Tendons, *ACI Materials Journal*, V 96, No 3, May-June 1999, pp 297-305.

7. TOKYO ROPE (1993), Technical Data on CFCC®, Tokyo Rope Mfg. Co, Ltd. *Manual*, Tokyo, October 1993.

8. UOMOTO, T, NISHIMURA, T, OHGA, H, (1995) Static and Fatigue Strength of FRP Rods for Concrete Reinforcement, *Proc* 2nd Int. Symp FRPRCS-2, E & FN Spon, London, 1995, pp 100-107.

9. WOLFF, R, MIESSELER, H-J, (1993) Glass-fibre prestressing system, *Alternative Materials for the Reinforcement and Prestressing of Concrete,* Ed Clarke, Chapman & Hall, London, 1993, pp 127-152.

10. ZHAO, W, PILAKOUTAS, K, WALDRON, P, (1997) FRP Reinforced Concrete: Calculations for Deflections, *Proceedings* of the Third International Symposium (FRPRCS-3), Vol 2, Sapporo 1997, Japan Concrete Institute pp 511-518.

11. ABDELRAHMAN, A A, RIZKALLA, S H (1997) Serviceability of Concrete Beams Prestressed by Carbon-Fibre-Reinforced-Plastic Bars *ACI Structural Journal*, July-August 1997, pp 447-457.

12. AROCKIASAMY, M, ZHUANG, M, SANDEPUDI, K, (1995) Durability Studies on Prestressed Concrete Beams with CFRP Tendons, *Proceedings of the Second International RILEM Symposium (FRPRCS-2)*, Ghent 1995, L Taerwe, Editor, E & FN Spon, London. pp 456-462.

13. BAKIS, C E, BHAT, B B, SCHOKKER, A J, BOOTHBY, T E, (2001) Flexure of Concrete Beams Prestressed with FRP Tendons, *Proc.* 5th Int. Symp. FRPRCS-5, pp 689-697.

14. BRAIMAH, A, GREEN, M F, SOUDKI, K A, CLAPP, F (1999) Long-Term Behaviour of Concrete Beams Prestressed with Carbon Fibre Tendons, *Proc.* 4th Int Symp FRPRCS-4, ACI SP-188, American Concrete Institute, 1999, pp 547-557.

15. FAM, A Z, ABDELRAHMAN, A A, RIZKALLA, S H, SALTZBERG, W, (1995) FRP Flexural and Shear Reinforcements for Highway Bridges in Manitoba, Canada, *Proceedings of the Second International RILEM Symposium (FRPRCS-2)*, Ghent 1995, L Taerwe, Editor, E & FN Spon, London, pp 395-402.

16. MOSS, R M, ARORA, S K, (1996) The Flexural Behaviour of Simply Supported Beams with Different Types of Fibre Reinforced Plastic Reinforcement, *BRE Note, N122/96*, Building Research Establishment, August 1996.

17. NAAMAN, A E- JEONG, S M, (1995) Structural Ductility of Concrete Beams Prestressed with FRP Tendons, *Proceedings of the Second International RILEM Symposium (FRPRCS-2)*, Ghent 1995. , L.Taerwe, Editor, E & FN Spon, London. pp 379-386.

18. ZOU, X W, GOWRIPALAN, N, GILBERT, R I, (1997) Short Term Behaviour of Concrete Beams Prestressed with CFRP Tendons, *Proceedings* of the Third International Symposium (FRPRCS-3), Vol 2, Sapporo 1997, Japan Concrete Institute pp 743-750.

19. BALÁZS, G L, BOROSNYÓI, A, (1999) Flexural Behaviour of Concrete Beams Prestressed with CFRP Tendons, *Werkstoffe im Bauwesen – Theorie und Praxis (Construction materials – Theory and applications)*, Hans-Wolf Reinhardt zum 60. Geburtstag (Editor: R Eligehausen), *ibidem*-Verlag, Stuttgart, November 1999, pp 429-438.

20. HATA, K, (1998) Single-Span Prestressed Concrete Stress-Ribbon Bridge – Yumetsuri Bridge, *Prestressed Concrete in Japan*, Japan Prestressed Concrete Engineering Association, National Report of XIII. FIP Congress, Amsterdam, 1998, pp 95-98.

21. RIZKALLA, S H, TADROS, G, (1994), A Smart Highway Bridge in Canada, *Concrete International*, Vol 16, No 6, June 1994, pp 42-44.

22. RIZKALLA, S H, SHEHATA, E, ABDELRAHMAN, A A, TADROS, G, (1998): The New Generation – Design and construction of a highway bridge with CFRP. *Concrete International*, June 1998, pp 35-38.

23. FRP International – *Quarterly Technical Paper*, Editor S H Rizkalla (*ACI, ASCE, CSCE, Composite Institute, JCI, ACMBS Network of Canada, ISIS Canada*).

24. KARBHARI, V M, (1998) Sone Viaduct – External Cable Anchor Block, *Use of Composite Materials in Civil Infrastructure in Japan*, WTEC Monograph, International Technology Research Institute, World Technology (WTEC) Division, Loyola College, Maryland, October 1998.

25. GRACE, N F, ABDEL-SAYED, G (1998) Behavior of Externally Draped CFRP Tendons in Prestressed Concrete Bridges, *PCI Journal*, September-October 1998, pp 88-101.

26. THIPPESWAMY, H K et al. (1998), FRP Reinforcement in Bridge Deck, *Concrete International*, Vol 20, No. 6, June 1998, pp 47-50.

27. BAKHT, B, MUFTI, A, (1998) Five Steel-Free Bridge Deck Slabs in Canada, *Structural Engineering International*, Journal of the IABSE, SEI Volume 8, Number 3, 1998, pp 196-200.

28. MEIER, U, MEIER, H, (1996) CFRP finds use in cable support for bridge, *Modern Plastics*, April 1996, pp 87-91.

29. TAERWE, L, MATTHYS, S, (1999) FRP for Concrete Construction: Activities in Europe, *Concrete International*, October 1999, pp 33-36.

30. ISIS Canada (2000) Homepage: http://www.isiscanada.com

31. FUKUYAMA, H, (1999) FRP Composites in Japan, *Concrete International*, October 1999, pp 29-32.

32. AKZO (1992) Aragrid®: Non Corrosive Mesh Reinforcement for Brickwork and Concrete, *Technical Data*, 1992.

33. LIU, S C, (editor) (2000) Smart Structures and Materials 2000 – Smart Systems for Bridges, Structures and Highways, *Proceedings of SPIE*, Vol 3988, 2000.

34. TAERWE, L, PALLEMANS, I, (1995) Force Transfer of AFRP Bars in Concrete Prisms, *Proc.* 2nd Int Symp FRPRCS-2, E & FN Spon, London, 1995, pp 154-163.

35. BALÁZS, G L, BOROSNYÓI, A, (2001) Prestressing with CFRP Tendons, *Proceedings* of the UEF International Conference on High Performance Materials in Bridges and Buildings, July 29 – August 3, 2001, Kona, Hawaii.

36. GERRITSE, A. (1993) "Aramid-based prestressing tendons", *Alternative Materials for the Reinforcement and Prestressing of Concrete,* Ed. Clarke, Chapman & Hall, London, 1993, pp. 172-199.

37. ROSTÁSY, F, (1997) On Durability of FRP in Aggressive Environment, *Proc.* 3rd Int Symp FRPRCS-3, JCI, 1997, Vol 2, pp 107-114.

38. UOMOTO, T, NISHIMURA, T, (1999) Deterioration of Aramid, Glass and Carbon Fibers Due to Alkali, Acid and Water in Different Temperatures, *Proc* 4th Int Symp FRPRCS-4, ACI SP-188, American Concrete Institute, 1999, pp 515-522.

BEHAVIOUR OF CONCRETE SHEAR WALLS REINFORCED WITH PERFORATED STEEL PLATES

A Khaloo

M N Shokoufi

Sharif University of Technology

Iran

ABSTRACT. A new method of concrete reinforcement is proposed in this experimental study. The behaviour of three shear wall specimens that were reinforced with steel perforated plates was investigated under cyclic semi-dynamic loads. The main parameter was the volumetric ratio of reinforcing steel. The other parameters were similar in all of the walls. Bending strength was calculated using the concrete beam bending theory according to ACI code and was compared with experimental results. The Experiment shows 30 percent increase in ultimate bending strength. Hysteresis diagram of the specimens indicates considerable energy absorption capacity of the walls reinforced with perforated plates. Also, the walls were capable of carrying loads to high deflections. This system of reinforcing shear walls provided good performance based on strength and ductility.

Keywords: Reinforced concrete, Shear wall, Perforated plate, Cyclic loading.

Professor A R Khaloo, is a Professor of Civil Engineering at Sharif University of Technology, Tehran. He is the President of Iran chapter of ACI. His research interests include reinforced concrete structures and concrete composite materials.

Dr M N Shokoufi, obtained his MS in Structural Engineering from Sharif University of Technology. His main research interest is related to RC shear walls

INTRODUCTION

Concrete shear walls are often used in multi story buildings to resist lateral wind and earthquake loads. In each story, wall panel is simultaneously subjected to gravitational and lateral forces and thus contains normal and shear forces and bending moment.

Numerous studies have been conducted to improve wall behaviour by concentrating on reinforcement detailing and type of concrete [1-8], however; little attention is paid to improve the reinforcement system.

Perforated plates have been previously used as ties in columns [9], longitudinal reinforcement in beams [10] and reinforcing mesh in slabs [11]. Considerable improvement has been in performance of these structural elements. Increase in strength, energy absorption and ductility are advantages of this type of reinforcement compared to conventional reinforcement.

These advantages are due to the confining effect of perforations on the concrete that is within the holes and better monolithic behaviour of elements as a result of reinforcement continuity and better stress distribution.

The aim of this investigation was to conduct an experimental study on the behaviour of shear walls reinforced with perforated plate. In this study, Hysteresis diagram of load-displacement of the walls has been obtained. The test results have been compared against those by ACI building code [12] equations for the behaviour of conventionally reinforced walls.

EXPERIMENTAL PROGRAM

In this study, the behaviour of shear wall was studied as an isolated member. The specimens were free of axial force and only a lateral force was applied on them. The lateral force was applied in a cyclic manner and continued until the plates tore or a large displacement was achieved.

Test Specimens and Fabrication

Three wall specimens, consequently labelled SWPP-1, SWPP-2 and SWPP-3 were built. The specimens were of the same shape and size. They were consisted of three parts: (a) Head beam (b) Main body of the wall and (c) Wall foundation. Specimens' reinforcements were the same in the Head beam and wall foundation. Head beam and foundation were reinforced using conventional steel bars. Dimension and reinforcement of the head beam and wall foundation were designed so that the failure would occur in the main body of the wall. Figure 1 shows the wall specimens dimensions and reinforcements.

Computer analysis indicated that the head beam in addition to transferring the applied load to the body of the wall avoids the local failure at loading point and provides a better shear force distribution on the wall [13]. Main body of the wall was reinforced by reinforcing steel perforated plates. Reinforcing perforated plate was the same for all specimens except the thickness of the plate.

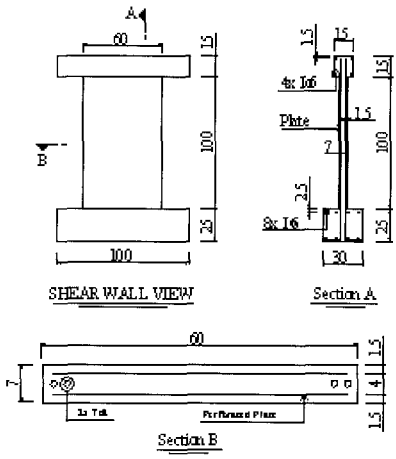

Figure 1 Wall specimens dimensions and reinforcements

Plates with thickness 1,1.25 and 1.5 mm were chosen as wall reinforcement. Plates were perforated by holes of 70mm diameter with a centre to centre spacing of 90mm. The holes were drilled to minimize microscopic cracks and warping on the plates that might be produced by punching holes. Table 1 shows the details of the reinforcing plates for each specimen. Figure 2 shows the shape of the plates.

Table 1 Details of the reinforcing plates

SPECIMEN	THICKNESS (mm)	VOLUMETRIC RATIO	SECTIONAL RATIO
SWPP-1	1	0.00646	0.00634
SWPP-2	1.25	0.0808	0.00793
SWPP-3	1.5	0.00969	0.00951

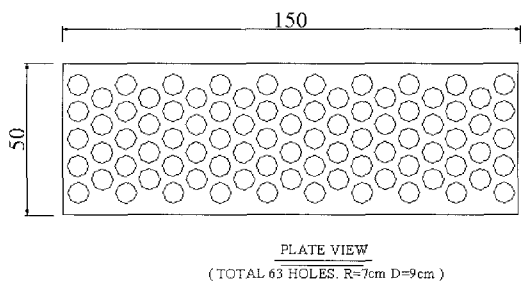

Figure 2 Shape of the perforated plate

To prevent buckling of the plates, special detailing was used. Two plates were used in each specimen at a distance of 40 mm. The plates were attached to each other by steel screws of 6mm diameter and steel pipes of 9mm diameter. This detailing showed to be effective against buckling of each single plate.

The maximum size of aggregates was limited to 10 mm. Type 2 Portland cement was used. Strength and workability of the concrete is given in Table 2.

Table 2 Strength and workability of the concrete

SPECIMEN	f'c (N/mm²)	SLUMP (mm)
SWPP-1	42.8	105
SWPP-2	34.0	120
SWPP-3	37.0	85

Test Setup

A steel frame was built to support the loading device and to load the walls horizontally. The frame consisted of two supported columns of section Double IPE240 shape with supports of double section IPE240. The frame was attached to the strong floor of SUT Structure Lab. A system of hydraulic pump and jacks was used for loading. This system could provide a 24 tons force within the 15 cm displacement of the head of the jack.

Specimens were attached to the ground using 12 M20 bolts. Rotation and displacement was measured to be very little at the base of specimen, a picture of test setup is shown in Figure 3.

Test setup was changed for specimen SWPP-1 so to evaluate the shear strength of the wall. A support was applied to the head beam and the specimen was loaded in the middle height of the wall.

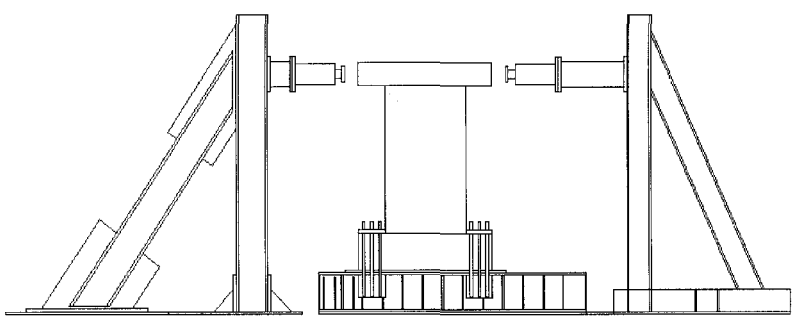

Figure 3 Test setup

Loading Pattern

The specimen SWPP-2 was loaded in two steps: first in force-controlled cycles and then deflection-controlled. In the force-controlled cycles, there were two cycles of loading to 10 kN and then one cycle of loading to 20 kN. After that came a cycle of loading to 40 kN and then a cycle to 50 kN was carried out. As large deflections were observed during this last cycle, next cycles were deflection-controlled. The steps in the force-controlled cycles were 5 kN. In the deflection-controlled cycles the steps were chosen to be 10 mm. The deflection-controlled cycles were continued up to the failure of the specimen.

The loading of specimen SWPP-3 was more ordered: first a loading cycle to 10 kN and then succeeding cycles to 20, 30, 40 and 50 kN. Loading steps were 5 kN except for the 50 kN cycle that was loaded in 2 kN steps to get a more detailed load-deflection diagram were the specimen shows plastic behaviour. After these cycles, loading was continued by the deflection-controlled method. Deflection steps were 10 mm. Unloading was force-controlled and the unloading steps were 5 kN.

Specimen SWPP-1 was loaded directly to 134 kN. No cyclic loading was applied to this wall.

EXPERIMENTAL RESULTS

Specimen SWPP-1

Test setup for this specimen was planned to lead it through shear cracking. No cracks were observed in the first 80 kN of load and then a very small crack was opened under the load. At the load of 110 kN a shear crack appeared under the loading point and was continued an angle of 45-degree to a length of about 80 mm. An increase the load to 134 kN resulted in no further cracks. A large local crack under the point load caused local failure of the specimen.

Specimen SWPP-2

During the loading of specimen SWPP-2 merely no plastic deflection was observed during the first two cycles of loading. Neither there was any large crack that could be viewed. First cracks appeared at load of 20 kN; these cracks had a small width and were re-closed in the reversal loading. The first large cracks were observed at the load of 40 kN. Most noticeable cracks were the flexural crack in the bottom portion of the wall body. The appeared cracks were re-closed in the reversal loading and same cracks occurred on the other side of the wall. In 50 kN loading cycle, large flexural cracks appeared on the wall, mostly on the 1/6 bottom portion of the wall. No shear cracks were observed. In this cycle, the perforated plate in the compression part of the wall buckled at load of 20 kN. The buckling was caused by inadequate support of one of the screws connecting two plates. This buckling had a noticeable effect on the behaviour of the wall and decreased the stiffness to great extents.

Deflection of the head beam was 135 mm at failure. This is equal to 13% of wall height. The plate yielded in every direction at the time of failure, showing good interaction between perforated steel plates and concrete. Cracking pattern of this specimen is showed in Figure 4. Load-deflection diagram for specimen SWPP-2 is given in Figure 5.

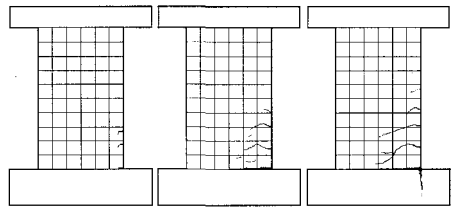

Figure 4 Cracking pattern of specimen SWPP-2

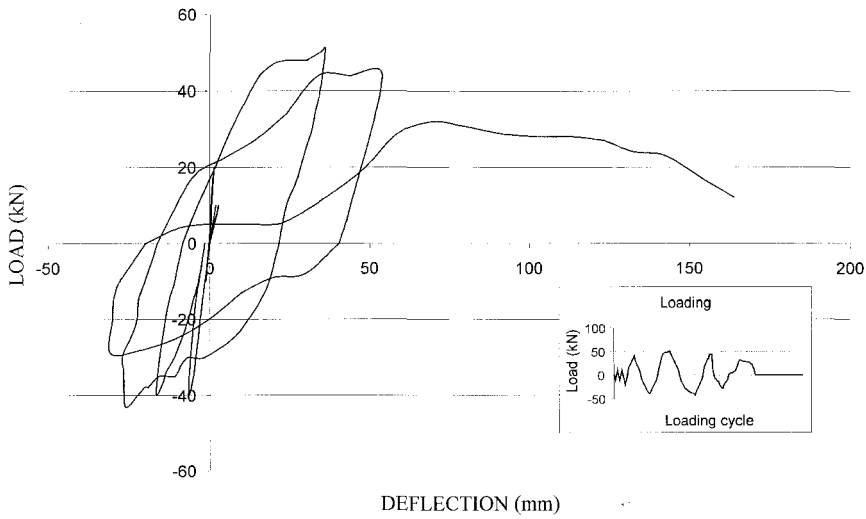

Figure 5 Load-deflection diagram for specimen SWPP-2

Specimen SWPP-3

Overall behaviour of the specimen SWPP-3 was very similar to that of SWPP-2. Although the thicker plates were used, there was little difference between cracking pattern and strength of the specimens SWPP-2 and SWPP-3.

The buckling of plate in compression occurred at the load of 49 kN instead on 20 kN, indicating the considerable effect of the connecting bolts on preventing the buckling of steel plates.

Load-deflection behaviour of this specimen is shown in Figure 6.

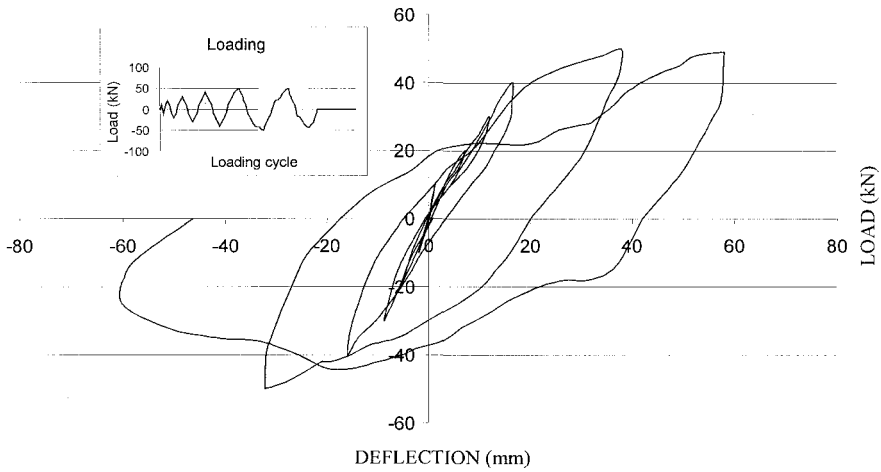

Figure 6 Load-deflection diagram for specimen SWPP-3

ANALYTICAL PERFORMANCE OF SHEAR WALLS

Flexural Strength

Common beam theory is used for the flexural analysis of the wall. As the steel is distributed in total depth of the section, a trial and error process was used to determine the place of the neutral axis and the ultimate flexural strength of the wall specimens. Table 3 presents the calculated flexural strength of the walls. The experimental results of the shear walls reinforced with the perforated plate provide in average 30 percent higher flexural strength than calculated according to ACI code (Table 3).

Table 3 Ultimate moment capacity of the specimens

SPECIMEN	PLATE THICKNESS (mm)	VOLUMETRIC RATIO	SECTIONAL RATIO	ULTIMATE MOMENT (ACI) (kN-m)	ULTIMATE MOMENT (Exp.) (kN-m)
SWPP-2	1.25	0.00808	0.00793	34.9	51.5
SWPP-3	1.5	0.00969	0.00951	42.4	53.5

Ductility

Ductility is important in seismic behaviour of the structure. It shows the reserved safety of the structure and its energy absorption capacity.

The yield occurs when the slope commences to decrease. The ultimate displacement was chosen as the point where the wall's flexural strength decreases to 85 percent of its maximum value.

The displacement ductility is defined as the ratio of yield to ultimate displacement. The displacement ductility for the specimen SWPP-2 is 5.88 and for the specimen SWPP-3 this value is 5.77. These values are higher than those of conventional shear walls that are about 3.5 [8].

Shear

Deep-beam equations were used to determine the theoretical behaviour of the wall. The effect of the longitudinal reinforcement was considered using compression field theory. ACI Code equations were used.

As the specimen SWPP-1 failed because of a local cracking under the load point, the ultimate shear strength of the wall was not achieved and the only data was the shear cracking strength of the specimen. The results are given in Table 4. It is seen that a 90 percent increase in shear cracking strength is gained.

Table 4 Cracking shear of the specimen SWPP-1

SPECIMEN	PLATE THICKNESS (mm)	VOLUMETRIC RATIO	SECTIONAL RATIO	ULTIMATE MOMENT (ACI) (kN)	ULTIMATE MOMENT (Exp.) (kN)
SWPP-1	1	00646	0.00634	38.52	74.00

CONCLUSIONS

A new method for wall reinforcement was proposed and was tested in this study. Two perforated steel plates were used instead of the conventional bar reinforcement.

Three wall specimens were built and tested to failure to observe the flexural and shear behaviour of walls. It was seen that the ultimate flexural strength of the walls is approximately 30 percent higher than that according to analysis for conventionally reinforced walls. Shear cracking strength was about 90 percent higher than ordinary reinforced walls. Considerable ductility was achieved in walls reinforced with perforated steel plates. Load-deflection hysteresis diagram of the specimens showed significant energy absorption capacity and load carrying capacity at high deflections.

ACKNOWLEDGEMENT

The support of Sharif University of Technology in conducting this research study is gratefully appreciated. The help of structural lab technicians, Cheraghali, Ghanbari, Bakhtiari and Gamalipour was instrumental in carrying out the tests.

REFERENCES

1. PARK, R., PAULAY, T., Reinforced concrete structures, John Wiley & Sons Inc, New York, 1975.

2. BACHMANN, H., LINDE, P., Dynamic ductility demand and capacity design of earthquake-resistant reinforced concrete walls, Proceedings of Thomas Paulay Symposium, California, 1993, p 117-142.

3. CORLEY, W. G., Ductility of columns, walls and beams – How much is enough?, Proceedings of Thomas Paulay Symposium, California, 1993, p 331-350.

4. SALONIKIOS, T. N., KAPPOS, A. J., TEGOS, I. A., PENELIS, G. G., Cyclic load behaviour of low-slenderness reinforced concrete walls: Design basics and test results, ACI Structural Journal, Vol 96, No 4, July-August 1999, p 649-660.

5. SALONIKIOS, T. N., KAPPOS, A. J., TEGOS, I. A., PENELIS, G. G., Cyclic load behaviour of low-slenderness reinforced concrete walls: Failure modes, strength and deformation analysis, and design implications, ACI Structural Journal, Vol 97, No 1, January-February 2000, p 132-141.

6. GUPTA, A., RANGAN, B. V., High-strength concrete (HSC) structural walls, ACI Structural Journal, Vol 95, No 2, March-April 1998, p 194-203.

7. MICKLEBOROUGH, N. C., NING, F., CHAN, C-M., Prediction of stiffness of reinforced concrete shear walls under service loads, ACI Structural Journal, Vol 96, No 6, November-December 1999, p 1018-1027.

8. OSTERLE, R. G., ARISTIZABAL-OCHOA, J. D., FIORATO, A. E., et al, Earthquake resistant structural walls- test of isolated walls – Phase II, Final Report, Portland Cement Association, Skokie Illinois, October 1979.

9. KHALOO, A. R., Compressive behaviour of concrete confined with high stiffness perforated steel plates, ACI Structural Journal (under review).

10. KHALOO, A. R., Response of concrete beams and splitting tension cylinders reinforced with perforated steel plates, ACI Structural Journal (submitted).

11. KHALOO, A. R., Behaviour of concrete two way slabs reinforced with perforated steel plates (manuscript in process).

12. ACI COMMITTEE 318, Building code requirements for structural concrete (ACI 318-99) and commentary (318R-99), American Concrete Institute, Farmington Hills, Mich., 1999.

13. SHOKOUFI, M. N., Shear walls reinforced with perforated steel plates, MS Thesis, Department of Civil Engineering, Sharif University of Technology, October 2000.

THE EFFECT OF THERMAL LOAD ON HYGROTHERMAL PROPERTIES OF GLASS FIBRE REINFORCED CEMENT COMPOSITES

J Toman J Drchalová

M Totová J Poděbradská R Černý

Czech Technical University

Czech Republic

ABSTRACT. The effect of thermal load on the basic thermal and hygric properties of three types of glass fibre reinforced cement composites (GFRCC) is analyzed in the paper. Thermal conductivity, specific heat and moisture diffusivity are determined after high temperature exposure to 600 and 800^0C. The linear thermal expansion coefficient and the thermal diffusivity are determined in the high temperature range up to 1000^0C. A decrease of thermal conductivity as high as 50% and an increase of moisture diffusivity in the range of one to two orders of magnitude are observed for all types of materials after heating to 800^0C. On the other hand, specific heat and density in the same situation decrease by only about 10%. An application of wollastonite and vermiculite is found to have a positive effect on the high temperature properties of the studied GFRCC compared to the usual sand aggregates. The thermal conductivity is decreased in a significant way, and the high temperature linear thermal expansion coefficient decreases when using wollastonite and vermiculite instead of sand.

Keywords: Glass fibre reinforced cement composites, Thermal conductivity, Specific heat, Moisture diffusivity, Linear thermal expansion coefficient, Thermal diffusivity, Thermal load.

Professor J Toman is Professor of Physics at the Department of Physics, FCE CTU Prague. His main research interest is in measuring thermal properties of building materials under nonstandard conditions.

Dr J Drchalová is an Assistant Professor at the Department of Physics, FCE CTU Prague. She specializes in measuring hygric properties of building materials.

M Totová is a PhD student at the Department of Structural Mechanics, FCE CTU Prague. Her research interest is in measuring thermal and hygric properties of building materials.

J Poděbradská is a PhD student at the Department of Structural Mechanics, FCE CTU Prague. She specializes in measuring thermal properties of building materials at high temperatures.

Professor R Černý is a Professor at the Department of Structural Mechanics, FCE CTU Prague. He works in the field of mathematical modeling and experimental monitoring of heat, moisture and salt transport processes in building materials.

INTRODUCTION

Fibre reinforced cement composites are often employed in severe conditions. These might be exposed for instance to high temperatures and/or high mechanical loads. However, their thermal and hygric properties are mostly measured in laboratory conditions only, so that designers cannot take into account the changes in their material parameters after loading. In this paper, basic hygric and thermal properties of selected glass fibre reinforced cement composites are determined as functions of thermal load.

METHODS FOR MEASURING THERMAL AND HYGRIC PARAMETERS

Thermal Conductivity and Specific Heat

The measurements were performed at room temperature using the microprocessor controlled portable device ISOMET 104 (Applied Precision). This device enables the thermal conductivity λ, thermal diffusivity a, specific heat C and temperature T to be directly obtained. The measurement is based on an analysis of the temperature response of the analyzed material to heat flow impulses. The heat flow is excited by electrical heating of resistive heater mounted into the probe having direct thermal contact with the samples. The temperature is sampled and as a function of time is on-line evaluated by means of polynomial regression. The coefficients of the evaluated regression polynomials are then used to calculate the measured quantities.

Thermal Diffusivity

The measurements were done in the high temperature range up to 1000^0C using the double integration method [1]. We will introduce the basic ideas of the method in what follows, for the convenience of the reader.

We have the one-dimensional heat conduction Equation in the form

$$\frac{\partial T}{\partial t} = \frac{\partial}{\partial x}(a\frac{\partial T}{\partial x}), \tag{1}$$

where a is the thermal diffusivity. We suppose $T(t)$ and $T(x)$ to be monotonous functions and choose a constant value of temperature, $\tau = T(x,t)$. Then, there must exist one-to-one parametrizations $x = x_o(\tau, t)$, $t = t_o(\tau, x)$, where x_o and t_o are monotonous functions. Considering this fact, an integration of heat conduction Equation (1) by x and t can be done,

$$\int_{t_1}^{t_2}\int_{0}^{x_0(\tau,t)} \frac{\partial T}{\partial t}(x,t)dxdt = a(\tau)\int_{t1}^{t2}\frac{\partial T}{\partial x}(x_0(\tau,t),t)dt + \int_{t_1}^{t_2}\frac{q(0,t)}{\rho(\tau)c(\tau)}dt\,. \tag{2}$$

After some algebraic modifications (see [1] for details), we arrive at the relation for calculating the thermal diffusivity $a(\tau)$ in the form:

$$a(\tau)=\frac{1}{\int_{t_1}^{t_2}\frac{\partial T}{\partial x}(x_0(\tau,t))dt}\Big(\int_0^{x_0(\tau,t_2)}T(x,t_2)dx-\int_0^{x_0(\tau,t_1)}T(x,t_1)dx-$$

$$-\tau[x_0(\tau,t_2)-x_0(\tau,t_1)]-\int_0^l[T(x,t_2)-T(x,t_1)]dx\Big). \qquad (3)$$

The thermal diffusivity is then determined using the results of experimental measurements of temperature fields in the sample at one-sided heating in the solution of the inverse heat conduction problem (3).

The Linear Thermal Expansion

The measuring device for determining the linear thermal expansion of porous materials in the high temperature range (see [2]) is based on the application of a comparative technique. Therefore, the measurement is performed at the same time on the sample of a standard material (such as special steels where the $\alpha(T)$ function is known) and the studied material. The length change of the measured sample is calculated from the following formula:

$$\Delta l(T_i)=\Delta l_m(T_i)-\Delta l_s(T_i)+l_{o,s}\int_{T_0}^{T_i}\alpha_s(T)\cdot dT, \qquad (4)$$

where Δl_m, Δl_s are the final readings of total length changes of the studied material and of the standard including the length changes of the ceramic rods (part of measuring device), respectively, $l_{o,s}$ is the initial length of the standard, and α_s is the known linear thermal expansion coefficient of the standard. The corresponding value of relative elongation can be expressed in the form:

$$\varepsilon(T_i)=\frac{\Delta l(T_i)}{l_{o,m}}, \qquad (5)$$

where $l_{o,m}$ is the initial length of the measured sample. The measurements are then repeated with other chosen values of furnace temperatures T_i, and the calculation of the α(T) function of the measured material is performed.

Moisture Diffusivity

Moisture diffusivity κ can be considered as one of the basic parameters for characterizing moisture transport in capillary porous materials. In this paper, we employed for determination of moisture diffusivity a simple method based on the assumption that κ can be considered as piecewise constant with respect to the moisture content u (PCK method in what follows).

Contrary to the most frequently used methods for κ determination, the PCK method is very fast even for materials with low κ, and in addition it exhibits a reasonable precision [3]. Therefore, its application for concrete is very suitable.

The experimental setup of the PCK method is identical with that of a common water sorption experiment. As a result of the measurement, the amount of water in the specimen as a function of time is determined. Assuming κ to be constant in certain (not very wide) range of moisture content, we can employ analytical solution of the moisture transport Equation to the identification of κ which is the only unknown parameter.

Knowing the total mass of water which penetrated to the sample during time interval *(0, τ)*,

$$m_m(\tau) = S\rho_s \int_0^l dx\left(u(x,\tau) - u_2\right), \tag{6}$$

we can formulate a transcendent Equation for moisture diffusivity in the form (see [3], for details):

$$\frac{m_m(\tau)}{S\rho_s} - (u_1 - u_2)\frac{l}{2} + \frac{2l}{\pi^2}(u_1 - u_2)\sum_{n=1}^{\infty}\frac{1}{n^2}\left(1 - \cos(n\pi)\right)\exp\left(-\frac{\kappa\, n^2\pi^2 t}{l^2}\right) = 0, \tag{7}$$

where ρ_S is the initial moisture density (i.e., the mass of liquid moisture per unit volume) in the sample, S is the cross section of the sample in the direction perpendicular to the moisture transfer, u_2 is the equilibrium moisture content (equals to the initial conditions and to the boundary condition on the end of sample not exposed to water penetration) and $u_1 \equiv u_{\max}$ the boundary condition on the wet end of the sample, u_{max} is the saturated moisture content of the sample.

The Equation (7) can be solved by some of the iterative methods. Moisture diffusivity value, calculated using (7) is then attributed to the value of the moisture content u_c.

$$u_c = \frac{m_m(\tau)}{2Sl\rho_s} + \frac{u_{\max} + u_2}{2}. \tag{8}$$

In the measurements throughout this paper, the value of u_c corresponded to about 60-80% of the moisture saturation value.

MATERIAL SAMPLES

Measurement were conducted on three types of glass fibre reinforced cement composites, denoted as SC I, II, III in what follows. The samples of all types of glass fibre reinforced cement composites were plate materials with Portland cement matrix, which was reinforced by alkali-proof glass fibres, the materials SC II and III contained vermiculite and wollastonite. The basic composition of SC I, II, III is shown in Table 1 (the percentage is calculated among the dry substances only, water corresponding to the water to cement ratio of about 0.3 is to be added to the mixture).

Table 1 Composition of glass fibre reinforced cement composites in %

	CEMENT	SAND	PLASTICIZER	ALKALI-PROOF FIBRE	WOLLA-STONITE	VERMI-CULITE	MICRO-SILICA
SC I	47.99	47.99	0.62	3.40	-	-	-
SC II	47.60	-	0.45	3.84	38.50	9.61	-
SC III	56.88	-	0.92	7.66	8.68	21.51	4.35

The samples for the determination of thermal conductivity, specific heat and moisture diffusivity were exposed to the thermal load prior to the measurements. The chosen temperatures were 600 and 800^{0}C. For the sake of comparison, also the measurements with unloaded samples were done. The samples had prismatic shape, for SC I 60 x 70 x 10 mm, for SC II and SC III 60 x 60 x 13 mm. The specimens were water and vapor-proof insulated on four edges by two-component epoxy resin Chs.Epoxy 1200. The samples for measuring high temperature thermal expansion had the dimensions 100 x 40 x 40 mm, those for measuring the high temperature thermal diffusivity were cubic, 71 x 71 x 71 mm.

EXPERIMENTAL RESULTS

The measurements of room temperature values of thermal conductivity λ, specific heat C and moisture diffusivity κ after thermal load are summarized in Tables 2-4. Both thermal conductivity and specific heat are found to decrease with increasing the loading temperature, and the decrease of thermal conductivity is very remarkable, almost 50% compared to the room temperature data. The moisture diffusivity exhibits an opposite behavior, a two order of magnitude increase for SC-I and one order of magnitude increase for SC-II and SC-III are observed comparing the room temperature data with the data for high temperature exposure to 800^{0}C. It should be noted that the changes of thermal and hygric parameters are more remarkable between 25^{0}C and 600^{0}C than between 600^{0}C and 800^{0}C.

The high temperature data of linear thermal expansion and thermal diffusivity are shown in Figures 1,2. Apparently, the SC-I specimens (see Figure 1) exhibit a similar high temperature behavior as cement mortar and concrete, the linear thermal expansion coefficient α remains almost constant to about 400^{0}C, then is increases to about 600^{0}C, and finally decreases even under the room temperature value at approximately 800^{0}C. On the other hand, the linear thermal expansion coefficients of SC-II and SC-III specimens decrease in the whole temperature range from 20^{0}C to 800^{0}C, which is a positive feature for a material designed as fire protection because it results in lower thermal strains.

The thermal diffusivity (see Figure 2) was determined on the SC-III samples only because of the limited availability of SC-I and SC-II specimens. Apparently, the thermal diffusivity increases with temperature in the whole temperature range studied, which is not a usual behavior for cement composites in general.

Table 2 Thermal and hygric parameters of SC I

TEMPERATURE EXPOSURE [°C]	ρ_s [kg m^{-3}]	C [J kg^{-1} K^{-1}]	λ [W m^{-1} K^{-1}]	u_{max} [%]	κ [m^2 s^{-1}]
25	1960	920	1.124	10.6	$1.28.10^{-9}$
600	1865	920	0.706	15.6	$9.57.10^{-8}$
800	1820	900	0.666	16.2	$1.79.10^{-7}$

Table 3 Thermal and hygric parameters of SC II

TEMPERATURE EXPOSURE [°C]	ρ_s [kg m^{-3}]	C [J kg^{-1} K^{-1}]	λ [W m^{-1} K^{-1}]	u_{max} [%]	κ [m^2 s^{-1}]
25	1090	1090	0.275	47.5	$2.52.10^{-8}$
600	1030	1050	0.198	56.8	$1.27.10^{-7}$
800	990	960	0.160	56.8	$3.18.10^{-7}$

Table 4 Thermal and hygric parameters of SC III

TEMPERATURE EXPOSURE [°C]	ρ_s [kg m^{-3}]	C [J kg^{-1} K^{-1}]	λ [W m^{-1} K^{-1}]	u_{max} [%]	κ [m^2 s^{-1}]
25	970	1285	0.274	58.1	$3.36.10^{-8}$
600	900	947	0.198	68.4	$1.92.10^{-7}$
800	900	837	0.159	68.4	$3.36.10^{-7}$

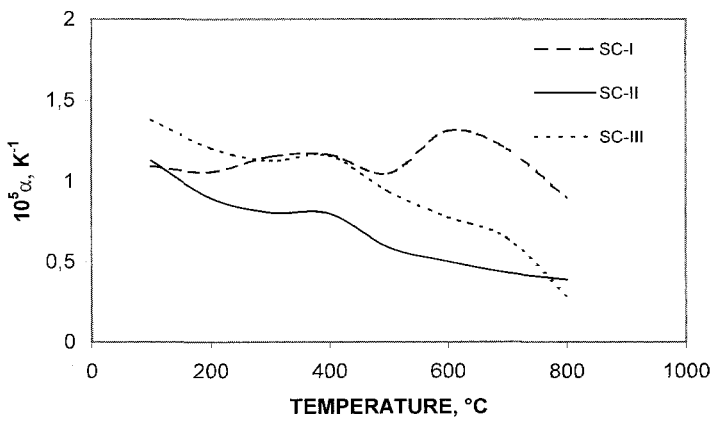

Figure 1 Linear thermal expansion of glass fibre reinforced cement composites SC-I, SC-II, SC-III

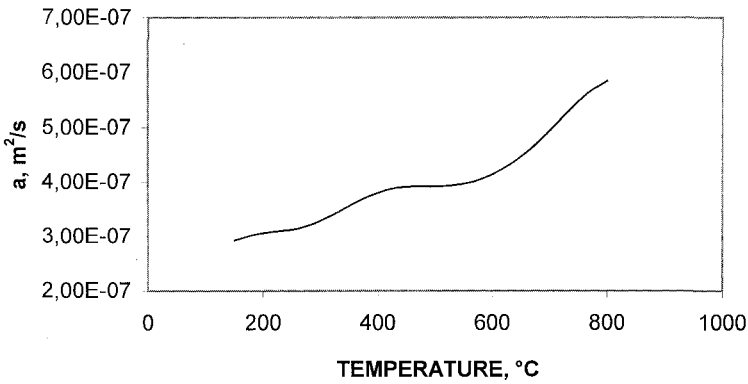

Figure 2 Thermal diffusivity a of glass fibre reinforced cement composite SC-III

DISCUSSION

Room temperature properties of the three analyzed types of glass fibre reinforced cement composites (GFRCC) are affected by the type of aggregates in the most significant way. Application of wollastonite and vermiculite instead of usual sand aggregates leads to a remarkable decrease of thermal conductivity. On the other hand, moisture diffusivity of GFRCC with wollastonite and vermiculite is higher compared to the sand aggregates, which is a clear consequence of a decrease of density to about one half. These are the logical consequences particularly of the character of vermiculite which has remarkably lower density compared to the sand.

On the other hand, the behavior of GFRCC exposed to high temperatures is affected by the properties of the cement binder in the most significant way. The very fast increase of moisture diffusivity and a relatively fast decrease of thermal conductivity of all three materials with the heating temperature corresponds to the theoretical predictions of the effects of high temperatures on concrete in general. From the point of view of structural changes in the cement gel, for the temperature range up to 1000^0C two processes are the most important, namely the decomposition of $Ca(OH)_2$ at about 460^0C and decomposition of calcium silicate hydrates at about 700^0C (see e.g. [4]). During these processes, gaseous substances are released, water vapor in the first case, and carbon dioxide in the second. Therefore, the amount of bigger pores increases which makes the liquid water transport easier and faster. In addition, due to the fast generation of a substantial amount of the mentioned gaseous substances, the local overpressure in some parts of the porous system may lead to crack appearance, and consequently to the opening of preferential paths for the pore water flow. The increasing amount of bigger pores then logically leads to a decrease of thermal conductivity because of the increasing amount of the air in the material. The much faster increase in moisture diffusivity of SC-I between 25^0C and 600^0C compared to SC-II and SC-III was most probably a consequence of opening of wider preferential paths after the high temperature exposure because in normal conditions SC-I possesses lower moisture diffusivity than SC-II and SC-III.

A logical reason is the better function of glass fibres in SC-II and SC-III, i.e. their better adhesion to the cement-aggregates matrix. This was also the probable reason of more favorable high temperature data of linear thermal expansion coefficient of SC-II and SC-III compared to SC-I.

CONCLUSIONS

Two main factors were found to affect the properties of the studied GFRCC in the most significant way. For the room temperature parameters, the type of aggregates was found to be dominant, and an application of wollastonite and vermiculite instead of sand aggregates was identified to have a very positive effect. In the case of the high temperature exposure, the decomposition processes in the cement gel can be considered as the most important. The positive effects of using wollastonite and vermiculite can be observed particularly in the values of linear thermal expansion coefficient α, where a significant decrease of α in the high temperature range was found. This leads to lower thermal stress after high temperature exposure, and also to the better fire resistance of the material.

ACKNOWLEDGEMENTS

This research has been supported by the Grant Agency of the Czech Republic, under grants No. 103/00/0021 and 103/97/K003.

REFERENCES

1. ČERNÝ, R., TOMAN, J., Determination of Temperature- and Moisture-Dependent Thermal Conductivity by Solving the Inverse Problem of Heat Conduction. Proc. of International Symposium on Moisture Problems in Building Walls, V.P. de Freitas, V. Abrantes (eds.), pp. 299-308. Univ. of Porto, Porto 1995.

2. TOMAN, J., KOUDELOVÁ, P., ČERNÝ, R., A Measuring Method for the Determination of Linear Thermal Expansion of Porous Materials at High Temperatures. High Temp.-High Press., Vol. 31, 1999, pp. 595-600.

3. DRCHALOVÁ, J, ČERNÝ, R, HAVRDA, J., The Effect of Anisotropy of Building Materials on the Moisture Transfer. Acta Polytechnica, Vol. 40, 2000, pp. 32-35.

4. BAŽANT, Z.P., KAPLAN, M.F., Concrete at High Temperatures: Material Properties and Mathematical Models, Longman, Harlow, 1996.

OPTIMISATION OF STEEL FIBRES REINFORCED CONCRETE MIX DESIGN

T Ayadat

M Beddar

L Belagraa

M'sila University

Algeria

ABSTRACT. Cementitious matrices are the fragile materials that possess a low tensile strength. The addition of fibres randomly distributed in these matrices, improve substantially their cracking strengths. However, the incorporation of fibres into a plain concrete disrupt the granular skeleton and causes very quickly problems of mixing as a result of the loss of mixture workability that will be translated into a difficult concrete casting in site. This study was concerned on the one hand with optimising the fibres reinforced concrete mixes in the fresh state, and on the other hand with assessing the mechanical behaviour of this mixture in the hardened state, in order to establish a compromise between the two states. In the first part of this paper, an experimental study of an optimisation method of fibres reinforced concrete while taking account of some parameters related to the matrix is presented, eg volume of admixture, volume of incorporated fibres and the volume of water and, cement (W, C) in function of workability time. Finally, test specimens of mixture optimised by this method have been tested in compression and tensile by bending. The results have been compared to those of mixture test specimens optimised by Baron – Lesage method.

Key words: Concrete, Fibres, Optimisation, Range, Mixes, Fibre reinforced concrete.

T Ayadat is a Reader in the Civil Engineering Department at M'sila University. He is the President of Scientific Council in the Civil Eng Dept. His research focus is mainly on soil mechanics.

M Beddar is a Senior Lecturer in the Department of Civil engineering at the University of M'sila. Former Head of Civil Eng Institute. His research focuses on concrete materials.

L Belagraa is a senior lecturer in the Civil Engineering Department at M'sila University. Former Research Studies Director. His research focuses on the blending cements and concrete repair materials.

INTRODUCTION

Recently, there are a large variety of composite materials. Most of them are used in the peak technological industries. This one uses composites constituted of carbon fibres, aluminium fibres, and whiskers fibres etc embedded in matrices that are originally organic or metallic. However, today we meet in the building construction field, public works a product, of which its constituents, its manufacturing procedure, properties and the behaviour correlate to those of the composite materials. This product is a fibre reinforced concrete composed of a cementitious matrix in which fibres are embedded.

The mechanism of reinforcement of concrete by fibres consists in distributing short fibres regularly in the concrete matrix. This network of fibres opposes, as much as it is denser, to the widening of the crack and act as crack arrestors by producing a pinching force which tend to make its propagation slower and causes transfer of stress across cracked sections allowing the effected parts of the composite to retain some post-crack strength and to withstand deformations much greater than can be sustained by the matrix alone.

The reinforcement of concrete by fibres permits then to stop the uncontrolled cracks propagation, therefore; what allows this one to acquire some qualities (tenacity, resilience) or to improve some characteristics.

These improvements require, however, that the percent volume of fibres should be sufficient, also the fibre shape offers the advantage of an important report of: lateral surface/volume and the fibre ends are treated to give a good anchorage. These parameters influent also on the main property of fresh concrete as well as its workability. Indeed, the workability, which is the principal characteristic searched in the fibres concrete, poses problem. The addition of fibres in the concrete matrix in a fresh state causes stiffening of the mixture and an accompanying loss of workability; so that mixing difficulties in mixing, placing and finishing procedure will be arise.

The incorporation of fibres in the concrete disorganizes the granular skeleton and leads to loss of mixture workability that results in a difficult concrete placement. Gains brought by fibres are only obtained after an optimisation of the mixture. Within the scope, several methods of composition optimisation of fibres concrete have been propped (SEMA-ROS, (1984); DEHOUSE (1975); EDINGTON (1973); BARON-LESAGE (1982). Although these methods are very useful in the field performance of fibres reinforced concrete, mainly the one of Baron-Lesage, but research and development another methods of optimisation permitting to have more economy and more security prove to be necessary.

The aim of this experimental study is to verify the possibility to propose a new method of optimisation of steel fibres reinforced concrete mix design while keeping constant the dosage of granular skeleton compounds proposed for the plain concretes.

TEST PROCEDURES

The objective consists therefore to obtain good fibres reinforced concrete workability with a good mechanical strength. For this raison, we have suggested to study the possibility to establish a referential standard range that gives the percentage of fibres as well as the percentage of admixtures corresponding.

The purpose of this research study presented here is as follows:

1. To record the time of out flow, of the LCL workabilimeter of a fresh concrete according to the percentage of admixture and dosage in fibres.

2. Establish a range giving the optimal quantities of admixtures and fibres permitting to obtain an optimal mix design having the best workability.

3. To compare the characteristics of fibre reinforced concrete prepared from the range obtained and the one of fibre reinforced concrete formulated by Baron-Lesage method (the same dosage of fibres will be used).

4. To verify the validity of the method for high dosages of fibres.

MATERIALS AND EQUIPMENT

Sand

The sand used in this study was a clean, siliceous and fine sand of fraction 0/5 taken from Bousaâda region. Its different characteristics are regrouped in Table 1. Its grading curve is shown in Figure1.

Gravel

Gravel is obtained by crushing of the limestone rock from the quarry of COSIDER situated in EL-ECH region (Bordj-Bou Arreridj). The gravel has two fraction 3/8 and 8/15 (see Table 1 and Figure 1).

Table 1 Some characteristics of the sand and gravel used in the tests

MATERIALS	DENSITY	POROUS/ DENSE	COMPACTNESS	POROSITY	SAND EQUIVALENT
Sand	2.56	1.64 / 1.83	36.42 / 70.76	36.58/29.24	75.4 / 77.2
Gravel (3/8)	2.68	1.28	47. 46	52.24	
Gravel (8/15))	2.68	1.32	49. 25	50.75	

Cement

The cement used was type CPJ 45. This cement was chosen because of its wide availability and largely used in the concrete construction sector in Algeria.

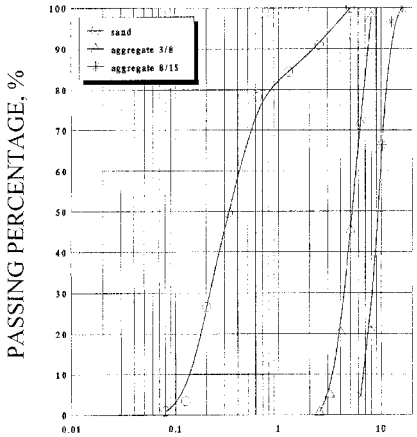

Figure 1 Grain size distribution of the sand and the aggregates used

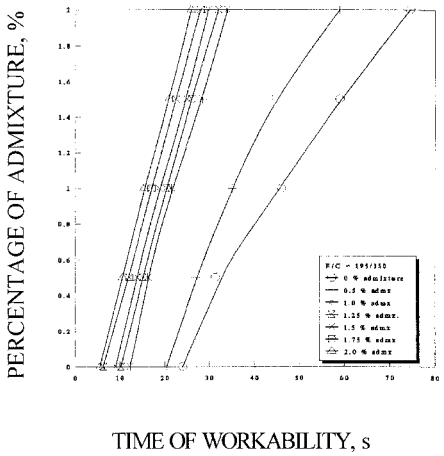

Figure 2 Variation of time of workability in function of percentages of fibre for the different percentages of admixture

Admixture

The admixture product used in our research is a super-plasticizer manufactured by the Granitex Society situated in O. SMAR (Algiers). This super-plasticizer, named "Medafluid SFA," has a density of 1.2; a content of dry matter of 36.16% and a PH of the order of 7.

Fibres

The fibres used in this study were steel fibres having 1.2 mm diameter, 30÷50 mm length, where $\sigma_n = 2.12$ KN/mm^2.

Concrete mix

The concrete mix proportion used (class 350 daN/ cm^2) has been determined by absolute volume method " SCRAMTAIEV METHOD," Komar, A (1982).

Cement: 350 kg / m^3

Sand: 758 kg / m^3

Gravel: 1073 kg /m^3

Total Water: 215 l /m^3

(This quantity takes into account the degree of aggregates absorption).

TESTING

Workability

Methods used to assess the workability of plain concrete are not always adapted to fibres reinforced concretes. The method of measure adopted in this case was the LCL Workabilimeter. It consists in measuring the time of out-flow of a fresh concrete between the stage of its setting up in the device and the stage of its out-flow under the action of stationary feature vibration. The workabilimeter was constructed by Lesage in the Laboratoire Central des Ponts et chaussées (LCPC) in Paris toward 1958 to permit to assess the ability of concrete to be casted. This device, that is normalized (NF.P18.425). Two models are available, one for the testing of concrete and the other for the mortars.

Compressive strength

Compression tests were carried out at the age of 28 days, on cubic specimens (100 × 100 × 100 mm). Tests were done using a hydraulic press model, type "STRASSENTEST (FHF)." The specimens were centred on the tray of the press then a continuous load was applied on the specimen. The compression ultimate load for each concrete and fibres reinforced concrete specimen was recorded.

Flexural strength

Flexural strength Tests at the age of 28 days were performed on plain and steel fibre reinforced concrete prisms ($70 \times 70 \times 280$ mm^3); with the same machine that used in the compressive tests. The loading was done in an automatic manner with a constant and continuous speed. The flexural strength of different mixes had been evaluated by the classic formula.

ANALYSIS OF RESULTS

Presentation of results

Initially, concrete mixes in one cubic metre has been chosen (according the method of absolute volumes), and then its equivalent in 10 litres of concrete had been prepared in order to facilitate reading on the workabilimeter.

The following fibres percentages: 0; 0,5; 1; 1,5 and 2 % were chosen for corresponding percentages of admixture values: 0; 0,5; 1; 1,25; 1,5; 1,75 and 2 %. Therefore five values of fibres concentration for seven different values of admixtures. The test programme contains therefore 35 mixes. For every mixture, flow time has been assessed using the workabilimeter. Results obtained permit to draw seven different curves (Figure 2).

Knowing that a good workability (using LCL) must have a flow time contained within the limits of 10 and 15 seconds, then we have to take two straight parallel lines (Δ_1) correspondent to t_1=10 seconds and ($\Delta 2$) correspondent to t_2 = 15 seconds. These two straight lines cross the 7 curves of the figure.2 in five points in each line. The five points of (Δ_1) give the lower limit and the other five points (those of $\Delta 2$) give the upper limit of our range (Figure 3).

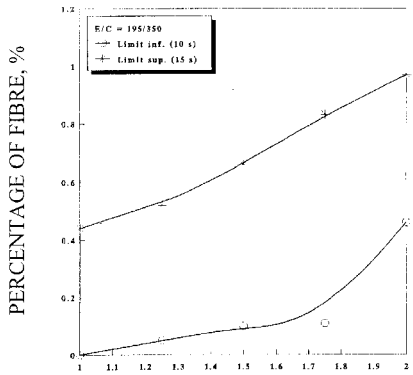

Figure 3 Optimisation of mix-composition of fibre concrete

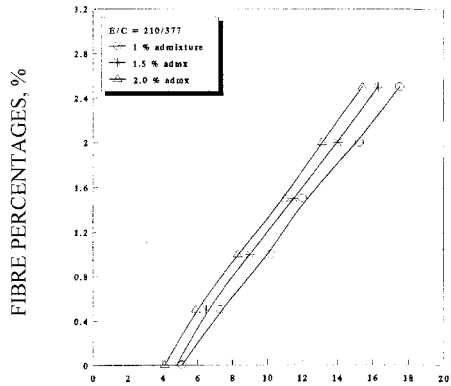

Figure 4 Variation of time workability in function of fibre percentages for the different percentages of admixture

To verify the reliability of our range, we have proposed to prepare concrete test specimens with quantities of fibres and admixture taken within the limits of this range. We have taken therefore some intermediate points to Δ_1 and $\Delta 2$ (Average values of the lower and super limits). Percentages of fibres selected are noted f_1, f_2, f_3, f_4 and f_5.

Every percentage of fibres chosen had permitted to cast three cubic test specimens (100 × 100 × 100 mm), which have tested to the compression, and three other prismatic test specimens (7 × 7 × 28 cm) for the flexural tests where the age of the testing was twenty-eight days.

It has been noted that the obtained range only covers the lower percentages of fibres that are less than 1%. To resolve this problem, it has been suggested to lead this second stage of this study, which consists on the investigation of volume increase influence (W and C), keeping the ratio $\left(\frac{w}{c}\right)$ constant in the translation range limits. It has been found that the percentage of 7 % could be sufficient to displace and enlarge our range to cover the high fibres percentages (Figure 4). The aim of the third part of this research was to compare mechanical characteristics of fibres reinforced concretes prepared from the obtained range and those of fibres reinforced concretes formulated by Baron-Lesage method with the same dosage of fibre that have been used in the first stage (to know f_1, f_2, f_3, f_4 and f_5).

Let's recall that in the method of Baron-Lesage :

- At the beginning, we fix a percentage of superplasticizer in compliance with the manufacture's recommendations (1.5 % of the cement weight).

- We fix, at every time, the percentage of fibres (f_1, f_2, f_3, f_4 and f_5) and we studied the influence of the variation of the S/G ratio on the flow time of fresh concrete.

After several operations (for every quantity of fibres), we obtained the optimal ratio of S/G that gives the biggest workability (the shortest flow time of workability).

For every optimal ratio (S/G), we have prepared some cubic tests specimens (10 × 10 × 10 cm) that has been tested to the compression and prismatic tests specimens tested to evaluate flexural strength at the age of 28 days.

RESULTS AND DISCUSSION

Influence of fibres content and the admixture percentage on the workability

Observing the curves shown in Figure 2, we notice that if the percentage of admixtures is less than 1% then workability is poor (the flow time is long). It is recommended therefore not to use (with fibres) dosage of admixture less than 1%.

An optimal workability range (function of the fibres concentration less than 1% and the dosage of admixture) has been established. Curves of lower and higher limits tendency, forming the range, follow an increasing monotonous law of polynomial type of equation:

$$Y = a X^2 + b X + c$$

With:

Y : percentage of fibres
X: percentage of admixture,
a, b, c: are constants that depend on quantities of W and C and the type, shape and fibres dimensions.

We have also noted that for a fixed admixture dosage, the flow time is proportional to the percentage of fibres. However, if we fix the fibres percentages, the flow time will be in inverse proportionality to the admixture dosage. The existence of such a relation permits us, for a fixed flow time, to determine or to choose, first time, for all fibre reinforced concretes, the percentage of admixtures and the fibres percentage corresponding. The range established in this investigation is a confirmation what has just been cited above.

The improvement of the range to cover high fibre contents consists on giving greater values for the upper and lower limits. We estimate that the rate fibres must be accompanied with an increase of the $\left(\frac{w}{c}\right)$ ratio. In general, the higher the $\left(\frac{w}{c}\right)$ the higher the workability (with or without fibres). Only, following the fibres nature, the best workable mixture is not always the most homogeneous. The presence of an abundant quantity of water leads to the segregation phenomenon. In addition, the augmentation of water quantity increases the porosity of the mixture that has an effect to decrease the mechanical performances and to reduce partially the beneficial effect of fibres in the matrix. For our study, we have preferred to keep the ratio w/c constant and undertake slight variation on W and C quantities (water, cement) in such manner not to effect the mechanical performances of the matrix. This consideration has to permit us to obtain a new range covering the slightly elevated fibres percentages (more than 2%). Curves representing the lower and higher limits of the range (Figure 4) follow the same polynomial law governs by the previous equation.

Mechanical strengths study

The efficiency and the reliability of our range appear in the comparison between values of mechanical strength obtained while considering our optimisation method and those determined by Baron-Lesage method.

Compressive strength

According to the Figure 5, the compressive strengths determined by our method are, generally, superior compared to those obtained by Baron-Lesage method and all the percentages of fibres used. Two ranges were only noticed. In the interval [0,05 – 0.23 %], values of Baron-Lesage method are superior to those determined by our method. This can confirm that the method of Baron-Lesage is better for plain concrete; as it was developed for this type of concrete. In the interval [0.23 – 0.73], it is clear that our method of optimisation is the most efficient.

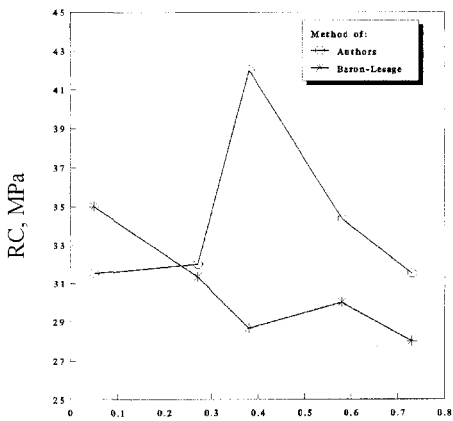

Figure 5 Variation of compressible stress (RC) in function of fibre percentages

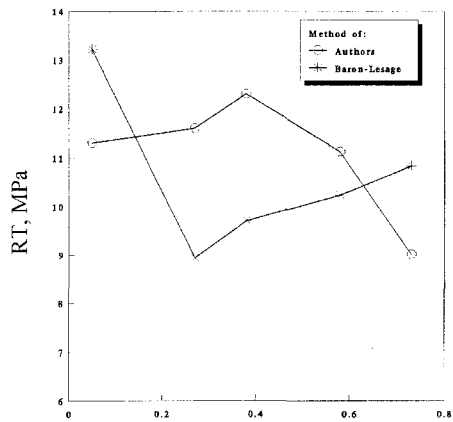

Figure 6 Variation of tensile stress (RT) in function of fibre percentages

Flexural strength

Flexural strength in bending test specimen showed nearly by bending the similar path as the compressive strength. To the exception at the 28 days age, the values of R_t determined using our method from the range, are generally, superior to those determined by the Baron Lesage method (Figure 6).

CONCLUSIONS

Regarding the results obtained in this study, the following conclusions can be made:

1. Admixture percentages less than 1% give the poor workability of fibres reinforced concretes.

2. Proposing of an optimisation method of fibres reinforced concrete mix design based only on the variation of the admixture contents and the quantities of W and C keeping (W/C constant).

3. Proved the possibility of the establishment, basically; for a given fibres reinforced concrete, a range of optimisation that depends on the type of fibres used, their dimensions, the quantities of water (W) and cement (C). The lower and upper limits of the range follow a law governed by a polynomial equation of the second degree.

4. An improvement of mechanical properties of fibre reinforced concrete results using this method showed an advantage compared to those of Barron-Lesage.

REFERENCES

1. LE BETON DE FIBRES METALLIQUE: état actuel de connaissance. Annales de l'ITBTP, N° 515, béton 302, Juillet-out 1993.

2. BETON DE FIBRES: synthèse des études et recherches réalisées au CEBTP. Annales de l'ITBTP, N° 520, béton 305, Janvier 1994.

3. CARACTERISATION ET CONTROLE DES BETONS RENFORCES DE FIBRES. Annales de l'ITBTP, N° 494, Béton 280, Juin 1991.

4. MEDDAH, M S. Etude d'un béton renforcée de fibres issues de déchets industriels, thèse de magistère, C U de Lagouat, Juin 2000.

5. KOMAR, A. Matériaux et éléments de constructions, Edition Mir , Moscou , 1982.

FLEXURAL BEHAVIOUR OF CONCRETE BEAMS REINFORCED WITH NEW CARBON-FIBRES SYSTEM

T Ohta

R Djamaluddin

A Ohta

Kyushu University

Japan

ABSTRACT. This paper presents the results of an experimental study that was carried out to examine the flexural behaviour of concrete beams reinforced with new carbon-fibres system. The system is named Unresin Carbon-fibre Assembly System (UCAS). By UCAS, a set of cables made of unresin continuous carbon fibres (UCCF) is applied to concrete structure as the reinforcement. The merits of UCAS method include economic advantage, lightweight, uncorrosive, high strength, and adaptability to IT era, etc. By this method, cables made of UCCF with a tensile strength of more than 1.4 GPa may be achieved. In addition, a grid system is considered herein to obtain the role of mechanical bonding like on the usual steel reinforcement. In order to verify the capability of this method, three types of concrete beam have been tested under flexural failure test. The results indicated that the concrete beam reinforced with UCAS showed good statically mechanical behaviour and could be a good alternative for reinforcement of concrete structure members.

Keywords: Flexural behaviour, Carbon fibres, Concrete beam, IT, Grid, Tensile reinforcement, Ultimate moment, Bond capacity.

Toshiaki Ohta is Professor of Civil Engineering at the Kyushu University, Fukuoka, Japan. His research interests include the application of advanced composite materials in civil engineering structures, rehabilitation and strengthening of structures. Recently, his research focuses mainly on the application of unresin continuous carbon fibres as reinforcement for non-prestressed concrete as well as for prestressed concrete.

Rudy Djamaluddin obtained his Master degree in civil engineering at Kyushu University. He is currently pursuing his Ph.D at Kyushu University. His research interests include the application of unresin continuous carbon fibre materials in civil engineering.

Aya Ohta is a contracted research associate of civil engineering at Kyushu University. She obtained her Doctor degree in Civil Engineering at Kyoto University. Her research focuses mainly on the conceptual design as well as aesthetic design of structures.

INTRODUCTION

Reinforced concrete is probably the most widely used building material in the world. For more than a century it has been playing a key role in the building of modern architecture and social infrastructure, since the reinforcement work method was first applied by Monier, a Frenchman, to bridge structure in 1873 [1]. In reinforced concrete, the concrete is strong in compression, but it has a very limited tensile strength. Usually, steel is used to overcome this shortcoming. Unfortunately, for structures in extremely aggressive environments, corrosion of the steel can be a significant problem [2-4]. Furthermore, in modern times when structures are being built densely in larger numbers, the construction of good-quality reinforced concrete structures is becoming difficult especially in Japan where the use of sea sand is inevitable and skilled workers have been decreasing [1]. Many approaches are being tried to inhibit the corrosion mechanism in aggressive environments. One alternative approach being developed worldwide at an increasing pace is the replacement of the steel by man-made fibres, such as carbon, glass or aramid. Generally, the fibres are encased in a resin to form a FRP composite [5-6].

Furthermore, in 21st century society also known as the IT era, the information technology (IT) has been rapidly changing worldwide social and economic systems. In Japan, IT has been influencing every political and economic field and demanding structural changes [1]. By looking into the recent problems and demands of the 21st century then the keywords representing 21st century construction include digitalization, weight reduction, automation, size reduction, fast distribution, labor saving, corrosion resistance, recycling, and mechanical properties may be taken out. Materials compatible with those keywords include carbon fibres, aramid fibres and polyethylene fibres. Carbon fibres are considered most suitable in view of the strength, tensile modulus, resistance to corrosion, lightweight, creeping characteristics and fire resistance [1].

For the purposes of this study programme, an automatic reinforcement arrangement robot (Figure 1) has been developed under the cooperation of researchers from robotic engineering at Kyushu University to assemble a reinforcement system as designed. This assembling system is named UCAS (Unresin Carbon-fibres Assembly System). The merits of this method include economic advantage, lightweight, uncorrosive, high strength, and adaptability to IT era, etc.

This paper reports the result of a research programme that investigates the behaviour and capability of concrete beams reinforced by UCAS. For the investigation purposes, three types of concrete beam have been tested under flexural test.

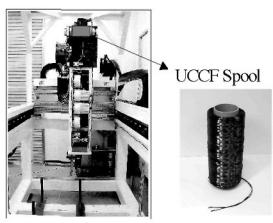

Figure 1 Assembler robot and UCCF spool

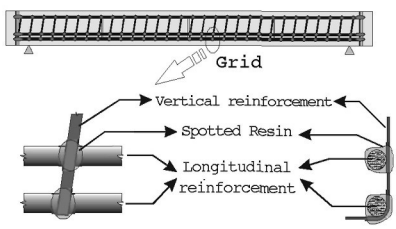

Figure 2 Detail of grid system

Because the robot is still under development, then, in this experimental research programme, some of the reinforcement construction process is still done by hand. In this method, cables made from unresin continuous carbon fibres (UCCF) are constructed and applied to the concrete beam as tensile reinforcement. These cables have a tensile strength of 35% of the nominal tensile strength provided by maker [7]. These cables have much higher strength than the tensile strength of usual steel reinforcement and enough for applying as reinforcement material. As tensile reinforcement, it is necessary that the reinforcement bond to the concrete for an effective reinforcing action [4], except in the special case of an un-bonded tensile reinforcement system. Accordingly, a grid-system (Figure 2) has been developed on UCAS to create a mechanically bonding effect between longitudinal reinforcement and concrete.

TEST PROGRAMME

Test Specimens and Assembling Process

Three types of concrete beam, as listed in Table 1, with spans of 1400 mm were tested under flexural test. The specimen details are presented on Figure 3. Types A, B and C have nominal reinforcement ratios of 0.78%, 0.61%, and 0.49%, respectively. All specimens were reinforced by four cables as tensile reinforcement. Two cables were also placed in compression section for vertical reinforcement turning purposes. The UCCF cables were assembled by assembler robot. The cables were made by turning UCCF string between two end-anchors as designed. The specimen types A, B and C respectively consisted of 22, 17, and 14 turns for each cable. And then, the assembled cables were installed on the special steel mould that facilitates the strengthening of the cables under 0.8 kN of tensile forces, as shown on Figure 4a. Vertical reinforcement was constructed by turning the UCCF string helically covering the longitudinal reinforcements (Figure 4b). The grids were constructed by connecting the intersection points of a pair of longitudinal reinforcement and vertical reinforcement with epoxy resin (Figure 4c). The resin was allowed to harden before the concreting process. The beam specimens were remolded a day after concreting and cured in the curing room for 14 days. Material properties of UCCF string, resin and concrete are shown in Table 2.

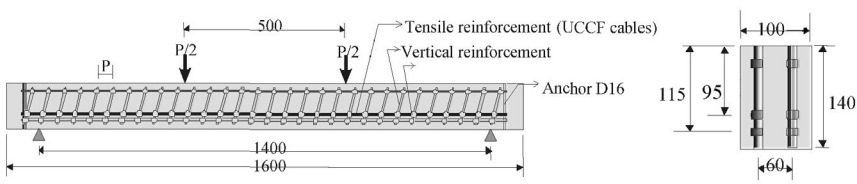

Figure 3 Detail of specimen

Test Setup

Each specimen was subjected to two equal static loads at the center of its span (Figure 5). The beams were instrumented with three linear variable differential transformers (LVDTs) at mid-span and at the two loading points to monitor deflection. Also, strain gauges were bonded to the concrete surfaces, as well as on the reinforcement to measure deformations. The beams, spanning 1400 mm, were subjected to four-point flexural bending testing (pure bending) with

a loading point distance of 500 mm. An automatic data acquisition system connected to a computer was used to monitor loading, as well as the deflection and deformations in the concrete and reinforcement. The load was applied to the beam, step by step at a rate of 1 kN per step, by means of a hydraulic jack and was measured with a load cell. At the end of each step, cracks were sketched and measurements of deflection and strain gauges reading were recorded for later processing. The test was stopped when deflection at mid-span reached 30 mm.

Table 1 Specimen Types

TYPE	SPECIMEN NAME		REINFORC-EMENT TYPE [1]	REINFORCEMENT					EXPECTED FAILURE MODE [4]
				Longitudinal			Vertical		
				No. of turning [2]	n x A, mm^2 [3]	Ratio, %	(strings)	Pitch, mm	
A	A-60	1 2 3	UCCF 12K	22	4 x 20.2	0.78	5	60	Compression
	A-40	1 2 3	UCCF 12K	22	4 x 20.2	0.78	3	40	Compression
B	B-60	1 2	UCCF 12K	17	4 x 16.5	0.61	5	60	Comp-Tens
	B-40	1 2	UCCF 12K	17	4 x 15.6	0.61	3	40	Comp-Tens
C	C-60	1 2	UCCF 12K	14	4 x 12.9	0.49	5	60	Tensile

Notes: (1) 12K = 12000 of filament in one string (2) per one cable
(3) n = number of cables for tensile reinforcement (4) see also Table 3

PRESENTATION AND DISCUSSION OF TEST RESULTS

Load-Deflection Response

Figures 6 and 7 show the load-deflection curves for the beams tested. Initially, the beams were un-cracked and stiff, like usual reinforced concrete beams. With further loading, cracking occurred at mid-span when the applied moment exceeds the cracking moment *Mcr*, causing a reduction in stiffness, which is greater for the specimens with lower reinforcement ratio. This can be attributed to the fact that crack openings are wider and crack spacing narrower in specimens with lower reinforcement ratio. From here, the load was still increasing followed by crack widening and the appearance of new cracks. The over opening of one crack can be avoided because of the existence of grids. The load-deflection curve for this step was almost linear until the concrete compressive zone started to deteriorate. The crushing of concrete at compression side led to a sudden decrease in load capacity with almost no change in deflection, prominently on specimens A-60 and A-40. From here, the beams enter into the next condition where deflection increases with little change in load. On the specimens B-60, B-40, and C-60, grid failure had been observed before the concrete

crushed. This caused the crack to open fast and go upwards which reduce the compressive zone and was followed by the crushing of concrete. From here, the load did not drop significantly as for the specimen type A, but the deflection increased with little change in load and showed pseudo-ductile behaviour. The test was stopped when deflection at mid span reached 30 mm.

Table 2 Material Properties

MATERIAL NAME		STRENGTH, N/mm2			YOUNGS MODULUS, kN/mm^2	MASS DENSITY kg/m^3	AREA, mm^2
		Tensile	Compe	Shear			
UCCF 12K String [1]		4800	-	-	230	1820	0.46
Resin		29.4	68.6	9.8	-	-	-
Concrete	A-60 A-40	2.95	40.0	-	29.6	2400	-
	B-60, B-40, C-60	3.24	46.5	-	35.5	2400	-

Notes: (1) Provided by maker (nominal properties of Torayca-T700S) [9]

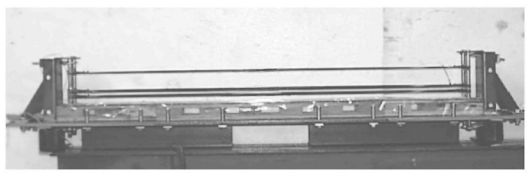

(a) strengthened cables on special formwork

(b) Vertical reinforcement

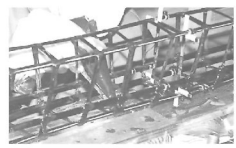

(c) Jointing of intersection

Figure 4 Assembling of reinforcement

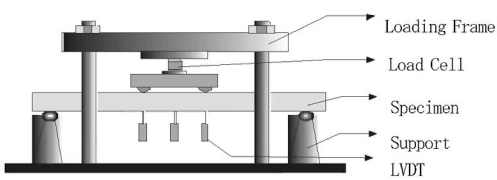

(a) Loading system

(b) Specimen under testing

Figure 5 Test set-up

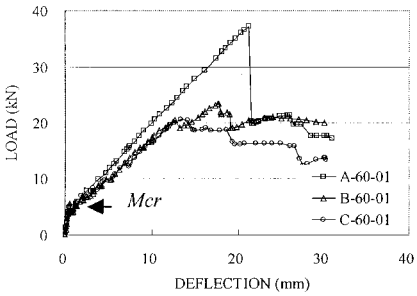

Figure 6 Load-deflection curves for A-60, B-60 and C-60

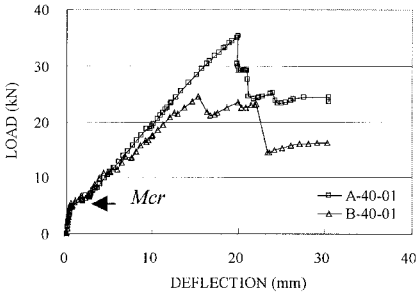

Figure 7 Load-deflection curves for A-40 and B-40

From this investigation, the load-deflection relationship of a concrete beam reinforced by UCAS may be divided into three steps, which are, the uncracked step; from zero to first crack, the crack propagating step; from first crack to maximum capacity and the pseudo-ductile behaviour which is indicated by rather horizontal load-deflection relationship.

Load Carrying Capacity

Table 3 presents the balanced reinforcement ratio ρ_b calculated based on the rectangular stress block assumed for concrete as well as the nominal reinforcement ratio ρ_n according to the section area factor *Sa* value. The nominal reinforcement ratio was calculated by multiplying the ρ_b with *Sa* as expressed by Equation (1).

$$\rho_n = \frac{0.85\beta_1 f_c'}{f_{fm}}\left(\frac{\varepsilon_{cu}}{\varepsilon_{cu}+\varepsilon_{fm}}\right)S_a = \rho_b S_a \tag{1}$$

Here, β_1 is equal to 0.8 for $f'c$ up to 50 MPa, and equal to 0.72 for $f'c$ higher than 50 MPa [10]. The section area factor *Sa* represents the fact that it is impossible to consider that all carbon fibre filaments can work uniformly when the cables sustain tension forces. A balanced beam failure was assumed when concrete reached its ultimate compressive strain (ε_{cu}=0.0035) and UCCF cables reached their design tensile strain (ε_{fm}=0.0073 at 35% of nominal tensile strength), simultaneously. On Table 4, the experimental moment at first crack *Mcr*, and the maximum moment *Mmax* of specimens are presented. The theoretical *Mcr* was calculated by Eq.(2), where f_{ct} = tensile strength of concrete, I_g= the moment of inertia of the gross section and y_t=the distance from centroid to extreme tension zone.

$$M_{cr} = \frac{f_{ct} I_g}{y_t} \tag{2}$$

The *Mmax* seems to agree with the predicted balanced moment capacity by using *Sa*=1.5, while it is approximately 40% and 60% smaller in specimen types B and C, respectively. So, by using *Sa*=1.5, the actual ultimate moment Mu_a^o may be predicted using Eq.(3), where *An*=nominal section area of reinforcement, *Sa*=Section area factor=1.5, f_{fm}= maximum tensile strength of cable, *d*= effective depth of section, *a*=depth of rectangular compression stress block assumed for concrete.

$$Mu_a^o = \left(\frac{A_n}{S_a}\right) f_{fm} \left(d - \frac{a}{2}\right) \quad (3)$$

Although the specimen type C was designed to fail under cable tension failure it can be observed, through Table 4, that all beams failed in compression. Furthermore, Table 4 also shows that Eq.3 with *Sa*=1.5 agrees for specimen type A but still overestimates (about 20% higher than the experimental ultimate moment) for beam types B and C. These differences may be attributed to the variability of the tensile strength of the UCCF cables, effect of cement paste on cables and bond capacity of grids. As discussed previously, the grid failure for specimen types B and C has been observed and this caused the reduction of maximum capacity of the beams. So, maximum load of specimen types B and C tends to be controlled by the bond capacity of the grid rather than by concrete strength or cable strength.

Table 3 Reinforcement Ratio

TYPE	SECTION AREA FACTOR, S_a	BALANCED REINFORCEMENT RATIO, %		SECTION AREA, mm^2		NO. OF TURNING PER CABLES, Nn *	COMMENTS
		ρb	$\rho_n = \rho_b x S_a$	A_b	$A_n = A_b x S_a$		
A	1.5	0.52	0.78	54.6	81.9	22	Over reinforced
B	1.0	0.61	0.61	64.1	64.1	17	Balanced
C	0.8	0.61	0.49	64.1	51.2	14	Under reinforced

* Four cables as tensile reinforcement for each beam

Table 4 Load Carrying Capacity

TYPE	SPECIMEN NAME		THEORETICAL			EXPERIME-NTAL			RATIO			MODE
			M°cr kNm	S_a	Balanced M°ub	Actual M°ua	Mcr kNm	Mmax kNm	Mcr/ M°cr	Mmax / M°ub	Mmax/ M°ub	
A	A-60	1	0.96	1.5	8.47	8.47	0.88	8.39	0.92	0.99	0.99	Comp
		2	0.96		8.47	8.47	0.82	8.61	0.85	1.02	1.02	Comp
		3	0.96		8.47	8.47	0.88	8.34	0.92	0.99	0.99	Comp
	A-40	1	0.96		8.47	8.47	1.10	7.95	1.15	0.94	0.91	Comp
		2	0.96		8.47	8.47	1.10	7.73	1.15	0.91	0.94	Comp
		3	0.96		8.47	8.47	0.88	7.28	0.92	0.86	0.86	Comp
B	B-60	1	1.06	1.0	9.79	6.88	1.33	5.08	1.25	0.52	0.74	Comp
		2	1.06		9.79	6.88	1.33	5.28	1.25	0.54	0.77	Comp
	B-40	1	1.06		9.79	6.88	1.33	6.67	1.25	0.68	0.97	Comp**
		2	1.06		9.79	6.88	1.22	5.21	1.15	0.53	0.76	Comp
C	C-60	1	1.06	0.8	9.79	5.60	1.10	4.30	1.04	0.44	0.77	Comp
		2	1.06		9.79	5.60	1.33	4.48	1.25	0.46	0.80	Comp

* Calculated with Sa=1.5, ** Compression-shear failure

Crack Pattern and Failure Mode

Typical crack pattern and failure mode photographs of the specimen types A, B and C are shown in Figure 8. The existence of grids caused most of the flexural crack to widen and extend slowly upward to the compression face. Crack spacing in the specimen with higher reinforcement ratio was observed to be smaller than other ones. The grid failure on the beam types B and C occurred early and this caused the crack to widen and extend fast toward the compression face. All beam specimens failed under compressive failure of concrete except for one of the beams type B-40 which seemed to fail under shear-compression failure. The grid pitch did not significantly affect the crack spacing.

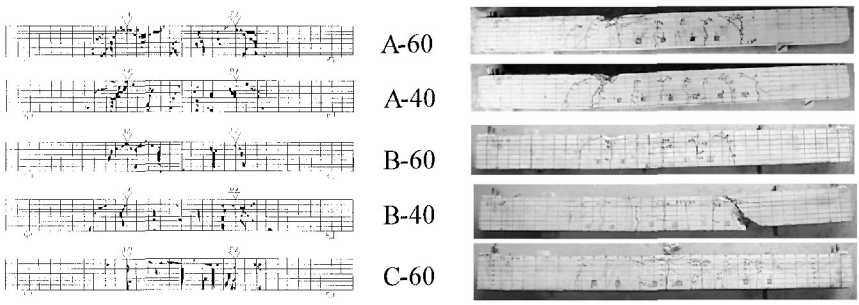

Figure 8 Typical crack pattern and failure mode photos

Strain Distribution

Typical strain distribution, both along half of the longitudinal reinforcement and along the height of the beams cross section at center span for A-60 and B-60 are presented in Figure 9. Strain distribution results were similarly distributed. The strain was distributed from approximately zero on F1b to approximately 7000×10^{-6} in strain on F3b and F4b. This strain distribution pattern indicated that the grid-system worked effectively as mechanical bonding between longitudinal reinforcement and concrete. After the grid failed (post peak), the strain decreased. About the strain distribution along the height of cross section at center span, the strain distribution pattern was also similar. The dot represents strain measurement on the reinforcement cables at maximum load. The measured strains at maximum load can be considered linear from concrete compression strain to tensile reinforcement strain. This agrees with the basic assumption of flexural theory, that the strain in reinforcement is equal to the strain in the concrete at the same level [11].

Limit Moment (LM)

As discussed previously, grid failure followed by the crushing of concrete occurred on specimens B and C. Although this phenomenon could not be identified visually on specimen type A, the grid failure may also occur. This phenomenon caused the maximum capacity of the beam to be controlled by the grid bond capacity. Figure 10 shows the grid bond surface details.

(a)

(b)

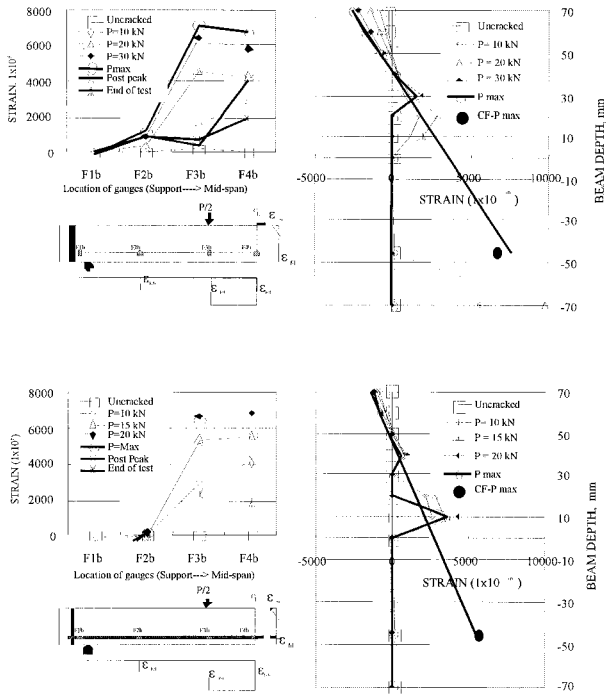

Figure 9 Strain distribution along cable and centre-span cross-section (a) A-60, (b) B-60

To avoid confusion, the maximum capacity controlled by the grid is called the Limit Moment LM and the maximum capacity controlled by concrete or reinforcement is called the ultimate moment. When the grid controls the maximum capacity of the beam, the beam capacity will be lower than the ultimate capacity. If w (mm) is taken as 5 times of the nominal diameter of stirrups then the bonding surface of the grid on the first layer and the second layers of reinforcement may be expressed, respectively as follows: $A_{b1} = 1.8D_n(0.75+0.25\pi)(w+10)$ and $A_{b2} = 1.8D_n(w+10)$, where D_n is the nominal diameter of cables calculated based on the section area of fibre filament. So, the bond capacity may be calculated from Eq.(4) and Eq.(5), where τ_e is the shear bond strength of resin.

$$P_{b1} = \tau_e . A_{b1} \tag{4}$$

$$P_{b2} = \tau_e . A_{b2} \tag{5}$$

Table 5 presents the bond capacity of each specimen type. This bond capacity is an important variable in order to develop a good interaction between reinforcement and concrete. This significantly influences the maximum capacity of beam. When the LM is smaller than the ultimate moment of the beam, then the maximum capacity of the beam will be controlled by grid bond capacity. In contrary, if LM is higher than the ultimate capacity, then the maximum capacity is controlled by the concrete and tensile reinforcement capacity. The LM may be defined as the moment that can be carried by the beam until the grid fails. So, the relationship between applied moment and force that works on grid needs to be determined. Figure 11 shows the diagram of strain distribution along tensile reinforcement when full bonding condition is assumed. By assuming that grid develops full bond mechanism, the forces which occur due to applied load on grid may be defined as deviation of strain between two grids and can be mathematically expressed as:

$$F_g = \frac{A_n}{S_a N_g} \Delta\varepsilon E_{cf} \tag{6}$$

where A_n is nominal section area of tensile reinforcement, N_g is the number of grids on that section and E_{cf} is young modulus of carbon fibres. This F_g must be distributed to the intersection point on first and second layers of cables. If F_g exceeds the P_{b1} (Eq.4) or P_{b2} (Eq.5), then the grid breaks. The LM may be predicted based on the relationship between grid force F_g and applied load as shown in Figure 12. That curve is determined by calculating the F_g at first crack Fg_{cr}, service load Fg_s and ultimate load Fg_u. To simplify, this curve is approximated with a linear relationship that can be expressed by Eq.7, where P_{LM} is applied load when grid forces equal to F_g, and C and m are curve constants. Then, the load P_{LM} when grid force is equal to F_g can be easily converted to the moment that represents the LM.

$$P_{LM} = 1/m\,(F_g - C) \tag{7}$$

Table 5 presents the predicted bond capacity of each beam (P_{b1} and P_{b2}) and Table 6 presents the grid forces F_g and LM. It can be observed that all beams have smaller LM than ultimate capacity (calculated by Eq.(3)). This result indicates that the maximum moment of beam will be controlled by grid bond capacity. This is also observed when testing. This predicted capacity is in accordance with the experimental results except for specimen A-60 that seems to have higher grid bond capacity than predicted. When the beam has a LM point small enough, then its behaviour will be a pseudo-ductile.

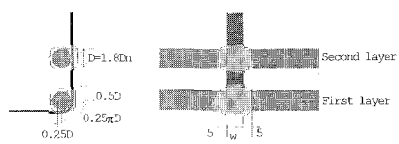

Figure 10 Bond surface of grid (unit: *mm*)

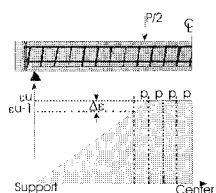

Figure 11 Strain distribution model

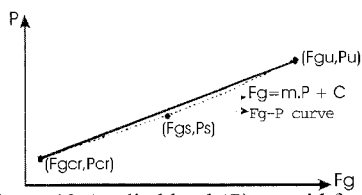

Figure 12 Applied load (P) vs grid force (Fg)

Table 5 Bond capacity of grid

TYPE AND NUMBER		REINFORC-EMENT POSITION	TURNING PER CABLES	Dn, mm	D, mm	w, mm	BOND LENGTH mm	BOND WIDTH mm	P_b, kN
A	A-60	Second layer	22	5.08	9.14	8.56	9.14	18.56	1.66
		First layer		5.08	9.14	8.56	14.04	18.56	2.55
	A-40	Second layer	22	5.08	9.14	6.63	9.14	16.63	1.49
		First layer		5.08	9.14	6.63	14.04	16.63	2.29
B	B-60	Second layer	17	4.46	8.03	8.56	8.03	18.56	1.46
		First layer		4.46	8.03	8.56	12.32	18.56	2.24
	B-40	Second layer	17	4.46	8.03	6.63	8.03	16.63	1.31
		First layer		4.46	8.03	6.63	12.32	16.63	2.01
C	C-60	Second layer	14	4.05	7.29	8.56	7.29	18.56	1.33
		First layer		4.05	7.29	8.56	11.19	18.56	2.04

P_b = bond capacity

Table 6 Limit moment (LM)

TYPE AND NUMBER		REINFORC-EMENT POSITION	$\Delta\varepsilon$ $x10^{-6}$	Fg, kN	Pb, kN	P_{LM}, kN	LM, kNm	M°u, kNm	Mmax kNm	LM/ Mmax	LM/ M°u
A	A-60-1	Second layer	836.7	2.65	1.66	24.34	5.48	8.47	8.39	0.65	0.65
		First layer	1111.1	3.52	2.55	27.46	6.18			0.74	0.73
	A-60-2	Second layer	836.7	2.65	1.66	2.4.34	5.48	8.47	8.61	0.64	0.65
		First layer	1111.1	3.52	2.55	27.46	6.18			0.72	0.73
	A-60-3	Second layer	836.7	2.65	1.66	24.34	5.48	8.47	8.34	0.66	0.65
		First layer	1111.1	3.52	2.55	27.46	6.18			0.74	0.73
	A-40-1	Second layer	557.8	1.77	1.49	31.24	7.03	8.47	7.95	0.88	0.83
		First layer	740.7	2.35	2.29	35.47	7.98			1.00	0.94
	A-40-2	Second layer	557.8	1.77	1.49	31.24	7.03	8.47	7.73	0.91	0.83
		First layer	740.7	2.35	2.29	35.47	7.98			1.03	0.94
	A-40-3	Second layer	557.8	1.77	1.49	31.24	7.03	8.47	7.28	0.97	0.83
		First layer	740.7	2.35	2.29	35.47	7.98			1.10	0.94
B	B-60-1	Second layer	836.7	3.07	1.46	22.61	5.09	6.88	5.08	1.00	0.74
		First layer	1111.1	4.07	2.24	25.38	5.71			1.12	0.83
	B-60-2	Second layer	836.7	3.07	1.46	22.61	5.09	6.88	5.28	0.96	0.74
		First layer	1111.1	4.07	2.24	25.38	5.71			1.08	0.83
	B-40-1	Second layer	557.8	2.04	1.31	28.75	6.47	6.88	6.67	0.97	0.94
		First layer	740.7	2.72	2.01	32.52	7.32			1.10	1.06
	B-40-2	Second layer	557.8	2.04	1.31	28.75	6.47	6.88	5.21	1.24	0.94
		First layer	740.7	2.72	2.01	32.52	7.32			1.40	1.06
C	C-60-1	Second layer	836.7	3.07	1.33	20.53	4.62	5.60	4.30	1.07	0.82
		First layer	1111.1	4.07	2.04	22.97	5.17			1.20	0.92
	C-60-2	Second layer	836.7	3.07	1.33	20.53	4.62	5.60	4.48	1.03	0.82
		First layer	1111.1	4.07	2.04	22.97	5.17			1.15	0.92

CONCLUSIONS

1. Test results have shown that the flexural behaviour of UCAS-concrete beam that failed under grid failure (Type B and Type C) is good behaviour according to safety considerations because the flexural behaviour shows that after peak load, the beam capacity does not fail rapidly but the beam shows a mechanism where the deflection propagates with almost no significant change in load.

2. The maximum capacity of concrete beam may be controlled by the bond capacity of the grid. When the LM is smaller than ultimate capacity of beam, then the capacity of beam tends to be controlled by the grid bond capacity. On the contrary, if LM is higher than ultimate capacity, then the beam capacity will be controlled by concrete strength or by reinforcement strength.

3. UCAS-beam fail under bond-failure shows a pseudo-ductile performance. It should be noted here that although the grid fails, the existing of end anchors causes the tensile reinforcement to still sustain the tensile load.

4. The predicted maximum capacity shows close agreement to the experimental results except the experimental result for specimens A-60 that seems to have a higher grid bond capacity than predicted.

ACKNOWLEDGMENT

The authors gratefully acknowledge the generosity of TORAY industries of Japan, for supplying the carbon fibres for this study. The authors would also like to thank the research members of robotic engineering at Kyushu University for their cooperation in the making of UCAS cables.

REFERENCES

1. OHTA, T. New concept of concrete structure in IT era and its life cycle assessment, JSCE, Vol.86.No.3, March 2001, pp.46-49 (in Japanese).

2. RUDY, D., KOBAYASHI, Y, NAGAHAMA, T., OHTA, T. Application of Unresin Continuous Carbon Fibers as Flexural Reinforcement in Concrete Structure, JCI, V-22, No.3, 2000, pp.283-288. 3.

3. BENMOKRANE, B, ,CHAALLAL, O., .MASMOUDI, R. Flexural Response of Concrete Beam Reinforced with FRP Reinforcing Bars, ACI Mat. J., V-91, No.2. May-June 1995, pp.46-55.4.

4. MASMOUDI, R., BENMOKRANE, B., CHAALLAL, O. Cracking behavior of concrete beams reinforced with fiber reinforced plastic rebars, Can.J.Eng.23, 1996, pp.1172-1179.5.

5. KAY, M., ERKI, M A. Flexural behavior of concrete beams pretensioned with aramid fibre reinforced tendons, Can. J. Civ. Eng. 20, 1993, pp.688-695.6.

6. NANNI, A. Fiber-Reinforced-Plastic (FRP) Reinforcement for concrete structures: Properties and Application, Elsevier, 1993, 450pp.7.

7. OHTA, T. YAMAGUCHI, K., HARADA, K., SAMIZO, K. Fundamental Studies on Mechanical Properties of UCCF cables for UCAS method, submitted for 26th conference on Our World in Concrete & Structure, Singapore, August 2001, pp.521-526.8.

8. NANNI, A. Flexural behavior and design of RC members using FRP reinforcement, Journal of structural Engineering, Vol.119, No.11, November 1993, pp.3344-3359.9.

9. PEEBLES, L.H. Carbon fibers: Formation, Structures, and Properties, CRC Press, 1995.10.

10. JAPAN HIGHWAY BRIDGE ASSOCIATION, Specification for Highway bridge Part III: Concrete Bridge Design, 1996, 175pp.11.

11. McGREGOR, J.G. Reinforced Concrete: Mechanics and Design, Prentice Hall, A Division of Simon & Schuster, Englewood Cliffs, New Jersey, 1988, 799pp.

A REVIEW OF THE USE OF FIBRE REINFORCED COMPOSITES BY THE UK HIGHWAYS AGENCY

N Loudon
Highways Agency
United Kingdom

ABSTRACT. The paper discusses the current and potential uses of fibre reinforced composites by the UK Highways Agency to strengthen concrete highway structures, and for more fundamental structural applications. It will provide background to research that has been carried out by the Agency, but also identify needs for future work. The advantages of fibre reinforced composites are well known, and have been established in the aerospace and marine industries. However there are still reservations about the use of composites such as glass, aramid, and carbon fibre in construction. They are light and easily handled materials and not subject to corrosion, and are therefore a low maintenance and durable option for bridge decking and strengthening of structures. There are however some potential disadvantages using composites, and areas of uncertainty such as longer term durability. The Highways Agency has undertaken a number of projects to use composites to strengthen existing structures. There have been two main applications – column and deck strengthening, primarily for impact loading and bending. The paper highlights several case studies and the development of design guidance and specifications, and the need for quality control systems and procedures for management of composites.

Keywords: Highways Agency, UK, Composites, Design, Management.

Neil Loudon graduated from Aston University in 1974 with a first class honours degree, and has worked for the Highways Agency, and its predecessors since 1970. He was formerly Regional Bridge Engineer managing 2500 structures. Currently he is a Senior Technical Advisor, responsible for concrete, concrete repair materials and techniques, including the use of innovative technology such as fibre reinforced composites, and post-tensioning systems and materials. He sits on a number of national committees including the Concrete Society committee responsible for TR47 'Durable Bonded Post-tensioned Concrete Bridges', and was also a member of the Expert Group set up by the DETR investigating the thaumasite form of sulfate attack. He chaired two Concrete Society Working Groups producing guidance on composites.

INTRODUCTION

The UK Highways Agency are undertaking increasing numbers of projects using fibre reinforced composites mainly to strengthen existing structures, but also for more fundamental structural applications. There is currently a lot of activity and interest in the construction industry regarding advanced composites, and therefore it is opportune to summarise and review the current position regarding their use, and outline future activities, to embrace these innovative materials, in research and construction work. However the paper does not address the issues concerning the use of non-ferrous reinforcement for reinforced concrete or the use of composites for suspension or post-tensioning cables.

BACKGROUND

FRP composites consist of high strength fibres, and usually are composed of carbon, aramid or glass, embedded in a resin matrix, utilising a number of different production and application techniques. They are not subject to corrosion and are therefore a potential benefit as a low maintenance and durable option for bridge decking and strengthening of structures. An additional advantage is that they can form light structures or components which can be lifted into position with a minimum of disruption to road traffic. However experience in the UK is still relatively limited, although confidence is growing as more applications are completed.

FRP decks have been previously used on the Aberfeldy footbridge and Bonds Mill Road Bridge (not Agency projects). Strengthening schemes are more widespread, and utilise composites bonded to the structure to overcome deficiencies in bending or shear, and to cater for increased loading requirements. Whilst there are many advantages in using these materials there are some potential disadvantages, and areas of uncertainty such as longer term durability. It is essential that design, installation and management information and best practice is published and disseminated based on sound research data, to ensure that the materials are used for suitable applications and that they can be used with confidence. As a corollary, it would be unfortunate if composites were tarnished by inappropriate usage, poor materials or workmanship and by encountering problems in service.

There is much research work currently being carried out both in the UK and abroad into various aspects of composites and new construction techniques. The Highways Agency commissions some of this research itself and keeps in touch with work by other researchers and academic institutions, in order to establish its own more specific design guidance, and detailed materials specification. Also under development is a quality certification scheme, as part of the Highway Authority Product Approval Scheme (HAPAS), which may embrace some of the materials and possibly specialist composite application contractors. The other area of concern is the establishment of regimes for the management of structures using composites – inspection, testing, monitoring, repair and assessment.

HIGHWAYS AGENCY – INTRODUCTION OF COMPOSITES

For some years the Agency has been keeping a watching brief on the developments of advanced composites for use in construction. It became clear that the materials developed and used in the aeronautical and marine industries had potential uses in bridges and other structures. However it was the advent of the 15 year bridge rehabilitation programme in 1987

and the Maunsell investigation on behalf of the Department of Transport and published report 'The performance of concrete bridges' in April 1989 [1], that acted to some extent as the catalyst for the introduction of new materials. Greater emphasis was placed on maintenance of the existing bridgestock. New and innovative solutions were required to strengthen highway structures, to avoid complete rebuilding, and in situations where traffic management and safety constraints, and commitments to road users to minimise delays during maintenance operations were having a significant impact.

Initial ideas involved the use of steel plates bonded to bridge soffits to enhance the bending capacity of bridge decks. To this end the Agency published the Advice Note BA30 'Strengthening of concrete highway structures using externally bonded plates' in 1994 [2], to provide design rules and an outline specification for steel plate and resin adhesive materials. But it soon became clear that the use of steel plates did not provide all the answers – the plates were heavy, and difficult to handle on site, required rigorous site preparation, as well as significant amounts of bolting through to the concrete substrate. Although they did provide a cost-effective solution to strengthening, nevertheless it was apparent that installation operations would still require extensive carriageway possessions. There were also some concerns about the durability of the steel plates, the bond to the concrete substrate, and the ongoing maintenance liability to repaint the steel plates periodically.

In the mid-1990's it also became apparent that some work would be required to upgrade and strengthen bridge supports to withstand greater accidental impact loadings. Early solutions involved the construction of concrete collars and infill between supports, which were cumbersome and inelegant solutions, and required long periods to construct. With this in mind the benefits of using composites were considered.

The Highways Agency looked at the research information that was available elsewhere including Japan and the United States where composites were used to strengthen bridge supports principally as retrofitted anti-seismic measures. It was also important to keep in touch with the main suppliers of the composite materials.

The first practical test of composites was arranged by the Agency and undertaken in 1997 on the A30 Bible Christian Bridge in Cornwall, and was used to assess whether the technique of wrapping bridge columns with composites was viable. It involved the use of glass, carbon and aramid fibre materials applied to three separate bridge columns using wet lay-up techniques. The trial was very successful, and proved that the materials were relatively easy to use, although requiring care and environmental controls during installation. It also demonstrated that composites could be installed in relatively short timescales, and with minimal traffic management. This was clearly an important issue for the Highways Agency where some structures have significant constraints on the duration and type of traffic restrictions imposed.

Further work ensued using the Transport Research Laboratory as a Contractor, and involved static and impact testing of various columns which had been wrapped with an aramid composite. From this evolved a set of generic design rules and graphs, and some guidance on aspects to be considered in a materials specification. This guidance was used in draft form for a couple of years and has now been formally published as BD84 [3] As a result of the issue of the guidance several further column wrapping schemes have now been undertaken, and these operations are becoming relatively commonplace.

Meanwhile other researchers had been looking at the problems associated with deck bending deficiencies. In the UK this was undertaken partly through the ROBUST programme [4], managed by a consortium of interested parties, which did not directly involve the Agency, but also by some pioneering schemes, and by work abroad, particularly in the US, Japan and Switzerland. The first HA scheme was undertaken at M60 Barnes Bridge at Manchester in 1999/2000, and involved using the design approach of BA30 suitably adapted for composites, and a bespoke specification. Several other schemes have also now been completed, and details are provided in Table 1.

Alongside the strengthening applications, the Agency was also looking at interesting developments in the use of composites for more fundamental structural applications. Initially this was for secondary usage such as the adoption of structural steelwork enclosure to ease access for inspection and maintenance and to provide additional protection against the onset of corrosion. This was first used on the A19 Tees Viaduct, in 1988/89 where a pultruded glass reinforced plastic material was adopted, and more recently on the approach spans to the Second Severn Crossing. Later attention turned to bridges themselves, in examining options for alternative designs in locations where access was difficult, or road occupation time was very limited. Such situations occur particularly with the construction or reconstruction of bridges over existing railway lines, or where live traffic is involved. Discussions took place with several of the leading consultants in the composite field and also with research organisations. The Agency has now completed (2001) its first composite decked structure on the A30 in Cornwall, Halgavor Bridge, and details are provided later.

HIGHWAY AGENCY PROJECTS

Strengthening

The M60 Barnes Bridge at Manchester was strengthened in 1999/2000 using carbon fibre plates applied to the soffit of deck. In this instance steel plate strengthening was used on the top of the deck rather than composites - principally due to the concerns about potential damage to the FRP beneath surfacing when subsequent road maintenance operations are undertaken. A further scheme was also completed at M45 Southam Dunchurch Bridge where minor strengthening was undertaken on the edge beam of the deck using carbon fibre plates. In both these cases the design was based on the approach in BA 30 dealing with steel plates, and separate materials specifications were developed for the composite materials.

At Barnes Bridge the existing 4 span continuous reinforced concrete slab bridge has separate 19^0 skewed decks carrying the northbound carriageway of the A34, and the combined southbound carriageway of the A34 plus the lanes of the slip road over the M60 Motorway and slip roads near Cheadle. Three spans are constructed from solid reinforced concrete slabs, the north spans are voided reinforced concrete slabs, and the overall width of the east deck is 23.16m and the west is 11.20m.

Assessment of the bridge found the superstructure had live load deficiencies. As a result interim measures were installed, consisting of removal of the hot rolled asphalt surfacing (replaced with a skid resistant waterproofing membrane) and lane reductions. The permanent strengthening works to the deck involved increasing the moment capacity of the slab at critical sections by plate bonding, and by the insertion of grouted stressed bars inserted through holes in the deck to deal with shear.

Table 1 Fibre reinforced composites register

STRUCTURE	DETAILS/DESIGNER	COMMENTS
A19 Tees Viaduct	1988/89 Maunsell Structural steelwork enclosure using pultruded GRP.	First structural composites application.
A30 Bible Christian Bridge, Cornwall	1998 Cornwall CC Column wrapping using aramid, carbon and glass fibres.	First practical trial.
M60 Barnes Bridge, Manchester	1999 Parkman Carbon fibre plate soffit strengthening, combined with steel plates on top of deck and tie bar shear strengthening.	First Highways Agency use. Generic specification, but restrict to carbon fibre based materials. Composites not used on top of deck.
M45 Southam Dunchurch Bridge, Northants	1999 URS Colquhoun Limited edge beam strengthening using carbon fibre plates.	Similar issues to above.
M40 Loudwater Viaduct, Bucks	2000 UK Highways DBFO Transverse strengthening of top surface of edge of deck	First use of composites under surfacing and waterproofing.
M11 Coopersale Bridge, Essex	2000 PB K&D Column strengthening using wet lay-up aramid.	First column strengthening. Use Interim design, generic specification developed.
A30 Halgavor Bridge, Cornwall	2000/01 Flint and Neill/Balfour Beatty Glass fibre deck suspension foot/cycle/equestrian bridge	Design and build, references to EUROCOMP manual for design.
A38 Western Interchange Bridge	2000/01 Mott MacDonald Shear/bending strengthening of deck, 'L' plates and strengthening of abutments, using carbon fibre plates.	First shear strengthening application. Little research available on which to base decisions. generic specification, and basis for design.
A19 Parkway Interchange, Middleborough	2001 Autolink DBFO Prefabricated glass fibre shells with grouted annulus.	First use of prefabricated materials.
M5 Naas Lane, Clingre Pipe, Michaelwood Service Area Bridges	2001 Atkins Column wrapping	As with M11 Coopersale.
M62 Ashfield Bridge	2001 Parkman Soffit strengthening	As with Barnes Bridge, but new ultra high modulus material used.
A27 Adur Viaduct	2001 Mott MacDonald Strengthening top surface of deck	Concerns about monitoring performance, risk of planer damage and temperature effects.
M6 Piers, Area 17	Lancs Highways Column strengthening	As with M11 Coopersale.

Figure 1 M60 Barnes Bridge - Hammer testing composites

Figure 2 M11 Coopersale Bridge – Column wrapping

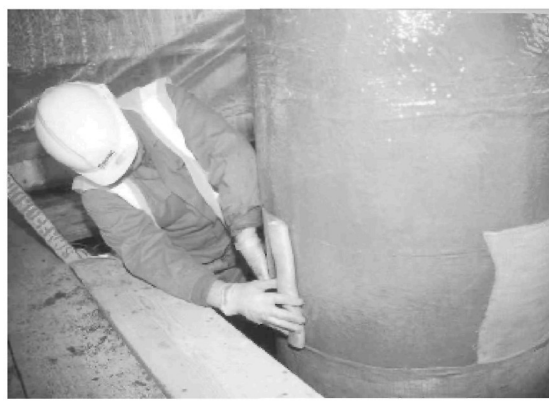

Figure 3 M11 Coopersale Bridge – Column wrapping

Figure 4 A30 Halgavor Bridge – After completion

Figure 5 A30 Halgavor Bridge – In use

The scheme progressed fairly smoothly with few problems, despite stringent lane restrictions and difficult access.

After Barnes Bridge was completed further strengthening schemes emerged where the use of composites was appropriate, and works at M40 Loudwater Viaduct and A27 Adur Viaduct have now been completed. In both cases carbon fibre plates have been bonded to the top surface of the deck, although used as secondary strengthening, to mitigate transverse edge of deck deficiencies. Special consideration was given to the performance, protection, monitoring and inspection of the buried composites, especially their vulnerability to damage and long term durability.

A further scheme at A38 Western Interchange in Cornwall has been undertaken where composites were used to strengthen an abutment, and also the deck of the structure, to mitigate both bending and shear deficiencies. The use of composites to overcome shear

deficiencies is a relatively new area, and comparatively little research has been undertaken - mainly in Switzerland for a particular product manufacturer. In this case preformed 'L' shaped plates were used to strengthen a marginal shear deficiency in the obtuse corner of the skew deck. In order to obtain the necessary anchorage, holes were carefully drilled through the edge of the deck and after the plates were bonded in place the holes were grouted up. Monitoring was installed to assess the effectiveness of the technique.

Column Wrapping

Following on from the successful practical trial in 1998 of composites wrapped round the columns of the A30 Bible Christian Bridge in Cornwall, laboratory work was undertaken at TRL. This has resulted in a draft Interim Advice Note, and subsequently superseded by Standard BD84.

The Interim Advice Note was issued to specific designers to assist with potential column strengthening schemes. The first project completed was the M11 Coopersale Bridge in Essex, and a specification for the composite material was developed based on the Interim Advice Note. This was judged to be highly successful, and resulted in very significant cost savings, and shortened construction period, and in turn reduced the impact of traffic restrictions. Further schemes on the M25 and M5 Motorways have also now been completed, and have mainly adopted aramid as a strengthening composite. It is expected that this technique will find widespread usage.

Another approach that has been adopted for column strengthening, that may be appropriate in certain situations is the use of prefabricated composite shells. This was adopted on the A19 Trunk Road Parkway Interchange on the outskirts of Middlesborough, by road operator Autolink as part of a 30 year design/build/finance/operate contract. Twenty-four tapered columns were strengthened against impact on two bridges. Composites were selected to overcome difficult access problems and the amount of strengthening required, and the need to minimise traffic disruption. There were also benefits from improved aesthetics. The alternative of constructing a conventional reinforced concrete infill wall to tie the columns together was rejected on the grounds of aesthetics, cost, time and access.

There were also advantages in using a factory quality controlled process to produce the shell, but this does require individual moulds to be produced to suit the column geometry, and special fixing arrangements to connect the two half shells together on site. A secondary grouting operation filled the annulus between the shell and the existing column.

Other Applications

The Highways Agency last year completed an innovative contract to construct a grp decked cycle/footbridge/equestrian suspension bridge, over the A30 in Cornwall and known as Halgavor Bridge. The contract was awarded as a Design and Build competition contract, and was won by contractors Balfour Beatty with Flint & Neill as designers. The composite deck fabrication was undertaken by Vosper Thorneycroft, and Maunsell were the independent design checkers. The bridge was one of the last links in the SUSTRANS national cycle network, and the location was adjacent to the National Trust property Llanhydrock House. Design was based on the principles within the EUROCOMP manual [5], and construction and installation were relatively straightforward.

The structural form of the bridge comprised an innovative suspension bridge with a lightweight FRP deck, supported by steel suspension cables, and inclined masts and raked support beams made from stainless steel.

The FRP deck was 47.5m long and consisted of two pultruded FRP edge panels with a sandwich deck panel made from two FRP skins and a 30mm polypropylene core. There were transverse beams of 6mm thick FRP, at each of the parapet post positions along with a central spine beam. The bottom panels were similar in construction to the top deck panels with only a 5mm core. The overall depth of the deck construction was 430mm. All exposed elements were finished with a self-coloured gel coat for maximum resistance to degradation by ultra-violet light. Since the bridge is to be used by equestrians the deck surface of the bridge consisted of special rubber blocks bonded to the grp, which also acted to stiffen the structure.

The bridge deck was constructed at Vospers yard using hand lay techniques, based on specially made moulds, but in a very controlled environment to ensure good quality of finish. It was transported to site in three sections before being bonded together, and lifted into position. A thorough testing regime of materials and components was also arranged.

It is expected that similar bridges will be constructed taking advantage of composite materials, and the Agency is considering opportunities to utilise the advantages of composites in road carrying decks.

MONITORING AND MANAGEMENT

There is little publicly available information on the long term durability and performance of composites and adhesives as used in the construction sector, though there is much that can be inferred from the experience of the maritime and aerospace other industries, where similar materials have been used in aggressive environments for many years. The general expectation is that construction composites will have service lives of 30 years, probably longer, with minimal requirements for interim maintenance.

Recent and current HA projects have developed a bespoke approach to in-service monitoring, with initial closely spaced intervals for inspection, until greater confidence in performance is established. Additional 'sacrificial' samples of composites have been bonded on to the structure away from the strengthened areas and on to specimen blocks, which can be subjected to periodic testing. Samples of composites and adhesive specimens have also been retained for future testing.

It is evident that monitoring and testing is an area where there has been comparatively little in the way of research and guidance. Other than unsophisticated 'hammer tapping' and observational methods there are currently no reliable established inspection techniques, though the use of fibre optics, thermography and acoustic emission appear to be promising. Through the links with the composite information networks (referred to below) the Agency is keeping in touch with developments. There is also a need to set performance criteria – what is the significance and acceptability of defects in the bond, or in the component materials themselves?

It is generally accepted that it is fairly easy to repair damaged composites, but there is no authoritative guidance available, particularly where the materials are used in combination with concrete or steel as a means to enhance the strength. Contingency arrangements must be

put in place in Maintenance Manuals and Health and Safety files for schemes under construction. The Agency has been involved in a Concrete Society project to develop guidance to assist clients and designers manage structures that have been strengthened using composites. More information is given later in the paper.

SPECIFICATION AND TECHNICAL APPROVAL

The Highways Agency has a well developed and proven system of technical approval in place to ensure that consistent standards and specifications are adopted for the construction and strengthening of new and strengthened structures. Where no suitable or relevant Agency standards exist, as is generally the case with composites, departure from standard procedures apply. However as standards for column and deck strengthening using composites are published, this will be relaxed.

Generic specifications for composites do not exist at present, though schemes completed or currently underway, have developed documentation that has been subject to departure procedures. The Agency is developing generic specifications based on the experience gained to date, and embracing best practice for manufacture and installation. It is essential to ensure that work is only undertaken by suitably experienced contractors and operatives, and using materials that have been subject to rigorous quality control procedures.

QUALITY AND CERTIFICATION OF MATERIALS

By the varied nature of composite materials, and their means of application there are some inherent problems in setting up a scheme for quality certification. Several years ago in a joint initiative between the County Surveyors Society, British Board of Agrément and the Highways Agency, the HAPAS (Highway Authority Product Approval Scheme) was set up to provide a means for certification of products that were not covered by other schemes. Discussions are ongoing to see if a scheme can be developed for composites, and in parallel a specialist applicators scheme is also under consideration. However such schemes can only work if there is support from all sectors of the industry, and particularly material suppliers, and also that certification requirements are called up in Client specifications.

HIGHWAY AGENCY RESEARCH

The Agency has completed research on strengthening bridge supports using composites, and that has resulted in a draft Interim Advice Note and subsequently BD84 [3] available to designers. Further work is in hand to develop design guidance on strengthening bridge decks against bending deficiencies, and will be published formally in due course as BD85 [6].

HA is currently investigating the use of FRP as modular bridge decking panels and undertaking fatigue testing at TRL, with a view to producing generic design requirements and guidance in due course. There is also a project looking at the safety of composites, which will consider bond strength, the application of FRP in complex geometric shapes, the effects of voids and debonding and shear strengthening.

OTHER RESEARCH

In addition to HA's own dedicated research programme it is evident that a great deal of research has already been undertaken into composites. Mention has already been made of the EUROCOMP[5] design manual produced by Dr John Clarke (now of Concrete Society) as lead author, the ROBUST[4] project completed some 4 years ago, with Mouchel as a lead partner and EPSRC funded academic research which is being undertaken. Maunsell have also developed some pioneering work with deck plank systems. There is also a lot of information available from abroad, primarily Switzerland, Japan and the USA.

Highways Agency (in the person of the author) chaired a Concrete Society Steering Group, which prepared design guidance for strengthening all types of concrete structures using composites and published as TR 55 'Design guidance for strengthening concrete structures using fibre composite materials' [7]. This group consisted of major clients, Railtrack, London Underground in addition to HA, many of the leading designers with specialist knowledge of composites, contractors and most importantly, most of the specialist suppliers of composites. This was the first time in the UK that this information was collated, in a usable form and relied heavily on the experience of the various collaborating members and research data. It was intended to promote the use of composites for strengthening, but particularly to ensure that these materials were being used appropriately. The report provides an overview of the available materials and application techniques, gives structural design guidance for strengthening against flexural and shear deficiencies, and column wrapping, as well as explaining some of the detailing, workmanship and installation issues.

One of the issues that emerged from this Concrete Society project was the need to develop guidance to assist clients and consultants manage structures strengthened with composites. Although some research and case study information was available there is very little practical guidance for clients and consultants to assist with the establishment of regimes of inspection, monitoring, testing and repair, to ensure that structures continue to be safe and durable. As a result, a further project was set up with cross industry support, under the authorship of Dr. Allan Hutchison of Oxford Brookes University, with Dr John Clarke of the Concrete Society. This work was scheduled for publication by the Concrete Society earlier this year (2002) [8].

One particular application under active consideration is the use of composites to strengthen metallic structures, however this is outside the scope of the present paper but there are clearly potential advantages. Further work is also being undertaken by CIRIA.

Highways Agency have been keen to work in collaboration and partnership with industry, and were therefore very pleased to be involved with the Network Group for Composites in Construction (NGCC), which was established by BRE with DETR funding. The principal aims have been to facilitate the exchange and dissemination of information, and establish research needs. The author is a member of the Executive Committee. NGCC is run on the basis of specialist sub-groups dealing with i) design information, ii) applications, iii) promotion, education and training and iv) research an development. The research sub-group of the NGCC is linked to a further academic based network set up by the Universities of Surrey and Southampton, with EPSRC funding. It is known by the acronym CoSacNet, and is serving the coordination of research efforts. This is an important function to ensure that any gaps in research knowledge are adequately addressed, and that there is not undue overlap and duplication of research efforts.

THE WAY FORWARD

It is evident that there is a lot of activity concerning composites, both in terms of research and for actual applications. The construction industry has in the past been accused of being somewhat conservative and slow to embrace innovation. With composites there is an excellent opportunity for all parties in the supply chain to work together to ensure that the benefits of these materials are obtained, but there must be technical guidance to ensure that the materials are used appropriately.

The Highways Agency is in a position to be pro-active in the adoption of these innovative materials, and different applicatons. The main areas concern design guidance, specification, quality control systems, the need for research to plug any potential gaps particularly over the long term durability of composites, the establishment of appropriate techniques for managing, monitoring and inspecting and testing of composites in service, and provision of training and guidance to Agency staff likely to be involved with composites in the future.

- Particular aspects for the future:-
- Gradual relaxation of design criteria, building on increased confidence of the performance of composites in service.
- Improved testing and monitoring techniques.
- Better information on durability.
- New applications – structural forms, lighting columns, non-ferrous reinforcement, post-tensioning cables, drainage etc..
- Guidance on assessment and repair of composite structures

REFERENCES

1. DEPARTMENT OF TRANSPORT, The performance of concrete bridges, a study by Maunsell Consultants, HMSO, 1989.
2. HIGHWAYS AGENCY, Advice Note BA30 Strengthening of concrete highway structures using externally bonded plates, HMSO, 1994.
3. HIGHWAYS AGENCY, Standard BD84 Column wrapping using fibre reinforced composites, 2001.
4. HOLLOWAY, L AND LEEMING, M.B. (Eds.), Strengthening of reinforced concrte structures using externally bonded FRP composites in structural and civil engineering, Woodhead publishing, 1999.
5. CLARKE, J.L. (Ed.), Structural design of polymer composites –EUROCOMP design code and handbook, E & F Spon, 1996.
6. HIGHWAYS AGENCY, Standard BD85 Strengthening using fibre reinforced composites, To be published.
7. CONCRETE SOCIETY TR55, Design guidance for strengthening concrete structures using fibre composite materials, Concrete Society, 2000.
8. CONCRETE SOCIETY, TRXX Management of concrete structures strengthened using fibre composite materials, To be published.

FLEXURAL TOUGHNESS AS A MEASURE OF SHEAR STRENGTH AND DUCTILITY OF PRESTRESSED FIBRE REINFORCED CONCRETE BEAMS

K A Paine

University of Dundee

K S Elliott **C H Peaston**

University of Nottingham Arup Research

United Kingdom

ABSTRACT. Research carried out on prestressed fibre reinforced concrete (PFRC) x-beams to measure their shear strength and ductility with and without steel fibres, and relate the results with flexural toughness measurements made on standard prisms is reported. Two types of short steel fibres were used: round hooked end high strength steel fibres, and thin amorphous metal ribbon-like fibres, at volume fractions up to 1.5 %. 18 tests were carried out at two different shear span to effective depth ratios. Flexural toughness parameters were calculated using various European and American test methods. The results showed that whilst shear strength of PFRC beams at first crack was little affected by use of fibres, the ultimate shear strength was closely related to improvements in equivalent flexural strength, which could equally be related to toughness indices. Empirical formulae are given. It is concluded that the behaviour of PFRC beams in shear can be approximated from flexural toughness tests carried out on standard control prisms. Since flexural toughness parameters are widely regarded as being appropriate to structural fibre reinforced concrete design, these results give a clear indication of the further steps required to produce design shear equations for PFRC beams.

Keywords: Flexural toughness, Fibre reinforced concrete, Shear strength, Prestressed concrete, Steel fibres.

Dr Kevin A Paine is a Research/Teaching Fellow in the Concrete Technology Unit, University of Dundee. His research interests are concerned with the use of waste and recycled materials as binder and aggregate components in concrete.

Dr Kim S Elliott is a Senior Lecturer in the School of Civil Engineering, University of Nottingham. He has published more than 70 papers and 3 textbooks on the behaviour of precast and prestressed concrete structures.

Dr Chris H Peaston is a former lecturer at the University of Nottingham where he carried out research into applications of steel fibre reinforced concrete. He currently works for Arup Research.

INTRODUCTION

The extensive amount of research carried out into the use of steel fibres for structural concrete has not led to its widespread use, except perhaps for tunnel segments and in strengthening (e.g. *shotcrete*). This is largely as a consequence of the absence of procedures for using fibre reinforced concrete (FRC) in structural concrete design, resulting from the lack of four interrelated requirements [1]: a relevant measure of FRC properties; accurate models and equations for FRC; formulation of design equations and procedures; and assurance of the reliability of the fibre structural contribution.

The need to find a characteristic material property for FRC that can be used in the design of reinforced fibre reinforced concrete (RFRC) and prestressed fibre reinforced concrete (PFRC) structures has long been recognised. This task has proved difficult since the material property chosen must be consistently defined and well understood, applicable to all fibre types and above all adequately able to distinguish FRC from concrete without fibres. The material property should also be able to reflect the combined effects of many more basic parameters, such as the fibre aspect ratio, fibre-matrix interfacial bond strength, fibre volume, and orientation factors that have often been adopted in empirical design equations.

Flexural toughness is recognised as the property of FRC that most distinguishes it from plain concrete, and furthermore is well understood and requires little adaptation for use in material testing machines. A common form of flexural toughness, ASTM Toughness indices, *I*, are defined in Figure 1. The benefits of using flexural toughness definition for FRC is that it is easy to measure, and the results are directly related to the benefits of fibres in increasing performance. A disadvantage is that the property is not uniquely and consistently defined. Accurate load - deflection curves can only be achieved with closed loop strain controlled testing equipment due to the instabilities after first crack, and any properties calculated within the instability area are machine dependant and effectively useless as design parameters.

However, design guidelines are now using flexural toughness to define the increased ductility and energy absorption of structural members due to fibre addition [2,3]. To make the procedures simple for designers and concrete specifiers, the design equations are generally only slight modifications of those currently used in practice. Despite this, many researchers and designers still oppose use of flexural toughness. Criswell [1] in particular points out that to completely describe toughness both first crack strength f_{fl} and index values *I* are required. As an alternative, a single equivalent post-cracking flexural strength, defined as $f_{fl,eq,300}$ in Figure 2, might overcome this problem.

A programme of experimental work was carried out on prestressed x-section beams, to determine whether *I* values and $f_{fl,eq,300}$ may be adopted for use in the prediction of shear strength of these beams. The work was carried out as part of a much wider study into the use of fibres as secondary reinforcement in prestressed hollow core slabs [4]. This paper examines the possibility of using flexural toughness parameters in the following widely-accepted equation for the ultimate shear capacity V_{co} of a flexurally uncracked prestressed concrete beam:-

$$V_{co} = \frac{Ib}{A\bar{y}}\sqrt{f_{ct}^2 + f_{ct,}\sigma_{cpx}} \qquad (1)$$

where Ay and I = first and second moment of area at the centroid, b = breadth at centroid, f_{ct} = tensile splitting strength, and σ_{cpx} = compressive stress at centroid. (There are no partial factors in Equation. 1, which often appear in codes of practice.)

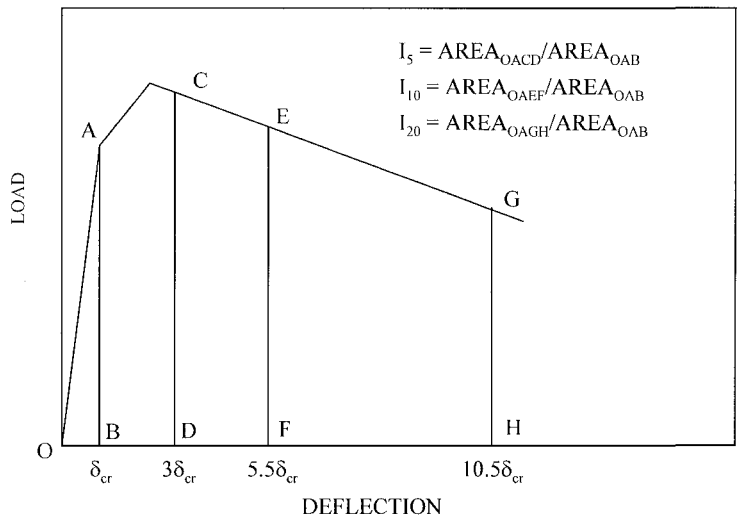

Figure 1 Definition of ASTM toughness indices

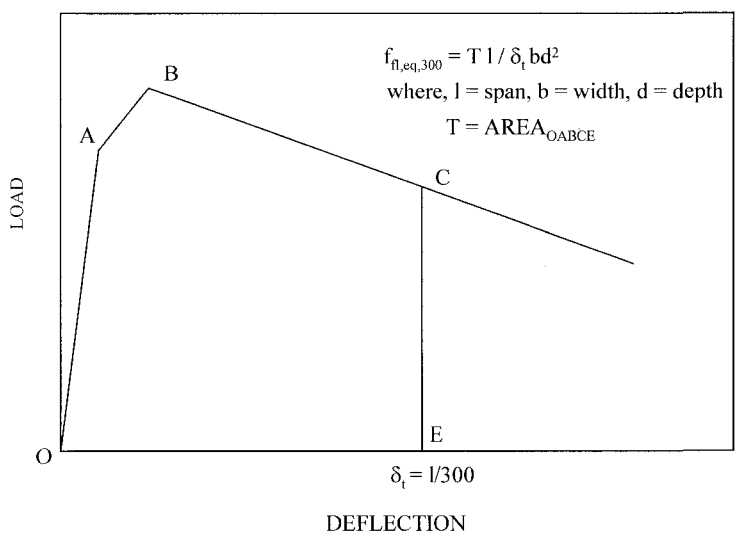

Figure 2 Definition of equivalent flexural strength ($f_{fl,eq,300}$)

TEST PROGRAMME

The aim of the tests was to provide basic knowledge on the use of steel fibres as shear reinforcement in prestressed concrete x-beams, with the later goal of assessing their suitability for use in prestressed hollow core slabs.

A total of 18 test are reported at two a/d ratios: 2.0 and 2.8; see Table 1. Both were expected to give web shear failures, but with the tests over the smaller a/d ratio more affected by compressive strut action. The two failure modes were, therefore, expected to vary slightly. Two types of fibre were investigated: hooked-end steel (HS) fibres and amorphous metal (AM) fibres. The HS fibres, made of drawn wire, were 30 mm long and had a nominal diameter of 0.5 mm. The AM fibres, which were ribbon-shaped and produced by quenching a jet of molten metal on a rotating water-cooled wheel, were 30mm long, 1.6 mm wide and 50 μm thick. HS fibres were tested at fibre volume fractions of 0.5%, 1.0% and 1.5% at both a/d ratios, whilst AM fibres were tested at a/d of 2.8 only; at fibre volume fractions of 0.28% and 0.56%.

Beams were tested approximately 15 days after casting, simply supported over an effective span of 1900 mm with a bearing of 100 mm used on both ends of the beam to imitate typical hollow core slab applications. Linear potentiometers (LP) were placed under the beams to measure deflections at the mid-point, load-point and a position close to support. Test cubes (100 mm), cylinders (150 mm diameter x 300 mm) and prisms (500 x 100 x 100 mm) were match cast in order to provide compressive, tensile splitting and flexural tensile strengths. The prisms also yielded I and $f_{fl,eq,300}$ values given in Table 1.

TENSILE SPLITTING STRENGTH

Splitting tensile strength tests were carried out on cylinders (Brazilian test) made using the same mixes as for the beams. Results are given in Table 1. Linear relationships between the ultimate splitting cylinder strength $f_{ct,sp}$ of FRC and fibre volume fraction V_f were found as follows:- .

For HS fibres:

$$f_{ct,sp} = 0.48 \sqrt{f_{cu}} + 237\, V_f \qquad (N/mm^2) \qquad (2a)$$

and for AM fibres:

$$f_{ct,sp} = 0.48 \sqrt{f_{cu}} + 336\, V_f \qquad (N/mm^2) \qquad (2b)$$

The increase in tensile splitting strength due to the fibres was due to the maximum fibre bridging stress across the tensile crack, which is related to the fibre aspect ratio, cement paste-fibre interfacial bond strength, fibre orientation and fibre volume fraction. Previous research has show that this can be approximated as $0.37 f_{fl,eq,300}$ [5].

Furthermore, the term 0.48 $\sqrt{f_{cu}}$ which relates to the tensile strength of plain concrete, can be approximated as 0.6 f_{fl}, where f_{fl} is the flexural cracking strength of plain concrete [3]. Therefore an approximation to the splitting tensile strength of FRC can be obtained from flexural properties only as (Figure 4):-

$$f_{ct,sp} = 0.6 f_{fl} + 0.37 f_{fl,eq,300} \quad (\text{N/mm}^2) \tag{3}$$

Table 1 Results of compressive and tensile strengths and toughness parameters

BEAM REF	V_f (%)	*a/d*	f_{cu} N/mm^2	$f_{ct,sp}$ N/mm^2	$f_{fl,eq300}$ N/mm^2	I_5	I_{10}	I_{20}	$R_{10,20}$	$R_{1.0\text{-}2.0}$
Reference Beams										
PB1A	0.0	2.0	71.0	4.30	-	-	-	-	-	-
PB1B	0.0	2.0	71.0	4.05	-	2.5	3.2	3.7	4.7	0
PB2A	0.0	2.8	71.0	3.85	-	-	-	-	-	-
PB2B	0.0	2.8	73.0	4.20	-	-	-	-	-	-
HS Fibre Beams										
PB3A	0.5	2.0	73.5	5.20	4.55	4.1	8.1	15.7	76.4	0.56
PB3B	0.5	2.0	69.5	5.15	4.75	4.1	7.5	13.6	61.2	0.37
PB4A	0.5	2.8	77.0	5.25	4.60	4.3	8.2	15.3	63.5	0.40
PB4B	0.5	2.8	75.5	5.50	4.80	4.2	7.7	14.0	72.6	0.57
PB5A	1.0	2.0	75.0	7.05	6.85	4.8	9.9	20.1	101.7	0.66
PB5B	1.0	2.0	77.0	6.65	5.85	4.7	8.5	17.6	91.7	0.74
PB6A	1.0	2.8	79.5	7.45	6.45	4.3	9.1	18.1	91.0	0.45
PB6B	1.0	2.8	75.5	7.05	6.40	5.1	11.0	23.6	125.4	0.58
PB7A	1.5	2.0	82.5	7.85	8.50	5.0	11.4	23.1	116.8	0.79
PB7B	1.5	2.0	82.0	7.45	8.50	4.9	11.3	23.3	120.1	0.74
PB8A	1.5	2.8	67.0	7.40	7.25	4.6	10.2	20.4	102.3	0.70
PB8B	1.5	2.8	68.5	7.15	7.85	5.3	11.0	22.6	116.3	0.79
AM Fibre Beams										
PB9	0.28	2.8	69.5	4.55	2.20	4.1	6.6	9.7	28.4	0.02
PB10	0.56	2.8	71.0	6.20	3.99	4.5	9.3	14.4	51.1	0.09

Figure 5 shows the relationship between equivalent flexural strengths $f_{fl,eq,300}$ and fibre volume. The step between the AM and HS fibres shows the improved efficiency of the hooked end fibres.

It is proposed that f_{ct} in Equation 1 for plain concrete is replaced by $0.6 f_{fl} + 0.37 f_{fl,eq,300}$ for FRC. This proposal was examined experimentally in the shear tests.

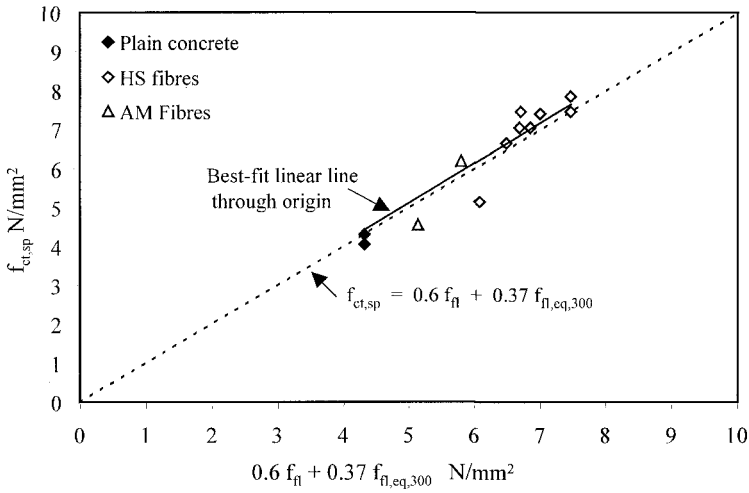

Figure 3 Relationship between splitting tensile strength and flexural strength properties

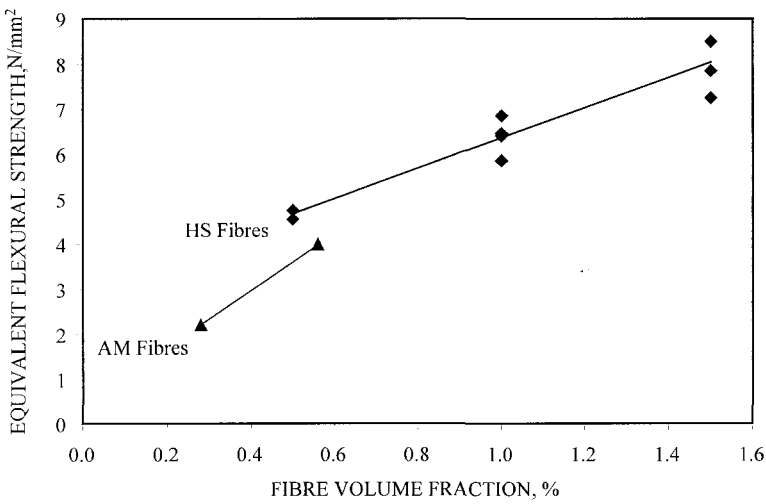

Figure 4 Equivalent flexural strength ($f_{fl,eq,300}$) of HS and AM fibre reinforced concrete

SHEAR STRENGTH

The failure of the beams was by web shear tension in all cases. For beams tested at a/d = 2.0 the critical crack formed at about 100 - 120 mm from the edge of the bearing (*h*/2) in the centre of the web and at its thinnest point. The crack propagated at 40° to 45° to the horizontal towards both the edge of the bearing and the load point. For beams tested at a/d = 2.8 the critical crack occurred at a distance of 150 mm from the edge of the bearing and

propagated at an inclination of about 30° towards the edge of the bearing and load point. After cracking the load carrying capacity of the plain concrete beams reduced considerably leading to an almost instantaneous failure. PFRC beams, however, were able to resist the cracking load due to the ability of fibres to cross the shear crack and resist crack propagation and widening. All PFRC beams ultimately failed due to extreme propagation and widening of the main shear crack due to fibre pull-out and fibre breaking, in addition to some degree of crushing within the compressive zone.

The results of each test are given in Table 2. Two shear capacities have been defined. The first crack shear capacity (V_{cr}) indicates the load at which diagonal cracking first occurred, and the ultimate shear capacity (V_{ult}) refers to the highest value of shear the beam withstood. For each of the plain prestressed beams $V_{cr} = V_{ult}$, with an average shear capacity at a/d = 2.0 of V_{cr} = 43 kN, and at a/d = 2.8 of V_{cr} = 34 kN. The reason for the higher shear capacity at a/d = 2.0, which was also observed for PFRC beams, was because of the increasing effect of compressive strut action closer to the support, and the favourable effect of the support pressure occurring above the 45° line.

Table 2 Results of shear tests and comparison with calculations

BEAM REF	V_f (%)	a/d	σ_{cpx} (N/mm^2)	TEST V_{cr} (kN)	TEST V_{ult} (kN)	CALC. V_{co} (kN)	V_{co} / V_{ult}	V_{250} / V_{cr}
Reference Beams								
PB1A	0.0	2.0	5.7	40.7	40.7	31.6	0.78	-
PB1B	0.0	2.0	5.3	48.5	48.5	31.2	0.64	-
PB2A	0.0	2.8	4.3	31.3	31.3	30.3	0.97	0.38
PB2B	0.0	2.8	5.7	33.5	33.5	31.6	0.94	0.18
HS Fibre Beams								
PB3A	0.5	2.0	5.4	40.5	57.7	31.3	0.54	1.31
PB3B	0.5	2.0	5.4	44.5	56.0	42.1	0.75	1.10
PB4A	0.5	2.8	6.1	34.0	46.3	42.4	0.92	1.14
PB4B	0.5	2.8	4.9	36.0	42.3	41.8	0.99	0.64
PB5A	1.0	2.0	5.1	43.5	55.9	46.6	0.83	1.19
PB5B	1.0	2.0	5.0	42.0	54.5	44.2	0.81	1.10
PB6A	1.0	2.8	5.8	36.0	48.3	46.3	0.96	1.58
PB6B	1.0	2.8	5.0	34.0	43.7	45.5	1.04	0.93
PB7A	1.5	2.0	5.2	44.5	61.9	50.4	0.81	0.79
PB7B	1.5	2.0	5.1	51.0	66.2	50.3	0.76	1.16
PB8A	1.5	2.8	5.0	32.5	44.5	47.4	1.07	1.33
PB8B	1.5	2.8	5.0	34.5	51.7	48.8	0.94	
AM Fibre Beams								
PB9	0.28	2.8	5.4	33.0	38.4	36.3	0.95	0.94
PB10	0.56	2.8	5.4	39.0	43.3	40.4	0.93	0.77

It is clear from Table 2 that fibres do not significantly improve the cracking capacity. This is because such a low volume of fibres have little affect on the direct tensile strength. A V_f of 1% increases the theoretical tensile strength by as little as 5% even when the fibres are perfectly aligned in the direction of the stress.

Fibres do, however, increase the ultimate shear capacity with V_f = 1% (HS fibres) increasing V_{ult} with respect to plain beams by 37% at a/d = 2.0, and 41% at a/d = 2.8. The increase at 0.56% (AM fibres) at a/d = 2.8 was 23%. With both fibre types at a/d = 2.8 there is a tendency for the fibre influence to level off at increasing fibre volume fractions. For the HS fibres the difference between the capacities at a/d = 2.0 and 2.8 at both cracking and ultimate, remains effectively constant at between 25 - 30% independent of V_f. This suggests that the fibre reinforcement mechanism is essentially the same at both a/d ratios and that enhanced shear capacity at lower a/d ratios is independent of fibre addition.

The calculated ultimate shear capacity of FRC beams, V_{co} in Table 2, is obtained from Equation 4, in which flexural properties replace f_{ct} in Equation 1.

$$V_{cu} = \frac{Ib}{A\bar{y}}\sqrt{(0.6f_{fl} + 0.37f_{fl,eq300})^2 + 0.67\,(0.6f_{fl} + 0.37f_{fl,eq300})\sigma_{cpx}} \qquad (4)$$

The results given in Table 2 suggest that if a factor of 0.89 is applied to V_{co} then 90 % of the results are conservative. In using Equation 3, designers should include appropriate factors of safety for f_{fl} and $f_{fl,eq300}$. The 0.67 factor takes care of two things, (a) the reduced value σ_{cpx} of at cracking, and (b) the large influence that the product $(0.6f_{fl} + 0.37f_{fl,eq300})\ \sigma_{cpx}$ has on V_{co}

The calculation model is in good agreement with test results for a/d = 2.8 (less then 7 % differences) but not for a/d = 2.0 (up to 37 % differences). This may be explained by the arching effect due to shear compression for the smaller shear span. However, as most shear failures occur by shear tension the proposed calculation model is suitable for use in design.

FLEXURAL TOUGHNESS

The mean results of the flexural strength and toughness tests for each mix are given in Table 1. The parameters presented are: the ASTM C1018 toughness indices (I_5, I_{10} and I_{20}); ASTM C1018 residual strength factor ($R_{10,20}$) = 20(I_{20}-I_{10}); equivalent flexural strength based on the average strength up to a deflection of span/300 ($f_{fl,eq300}$); and the ratio ($R_{1.0\text{-}2.0}$) of the average load between the deflections of span/300 and span/150 to the first crack load.

Figure 5 shows the relationship between each of the toughness indices (I_5, I_{10} and I_{20}) and the fibre volume fraction. Best fit second-order polynomial lines have been drawn through each index for both matrices, i.e., all mixes. It can be seen that the index I_5 is unable to significantly distinguish between different fibre contents and fibre types. This is because this index is based on the behaviour of the concrete up to a relatively small deflection of approximately 0.1 mm. The other indices are able to show the benefit of fibre addition more effectively.

Figure 6 shows the load based dimensionless index $R_{1.0\text{-}2.0}$ relative to the fibre volume fraction. It can be seen that the AM fibre results are lower than the HS results by as much as an order of ten.

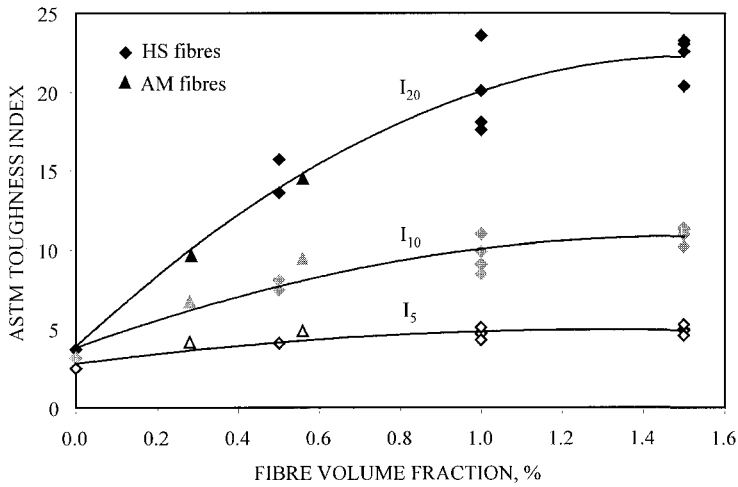

Figure 5 Relationship between fibre volume fraction and ASTM toughness indices

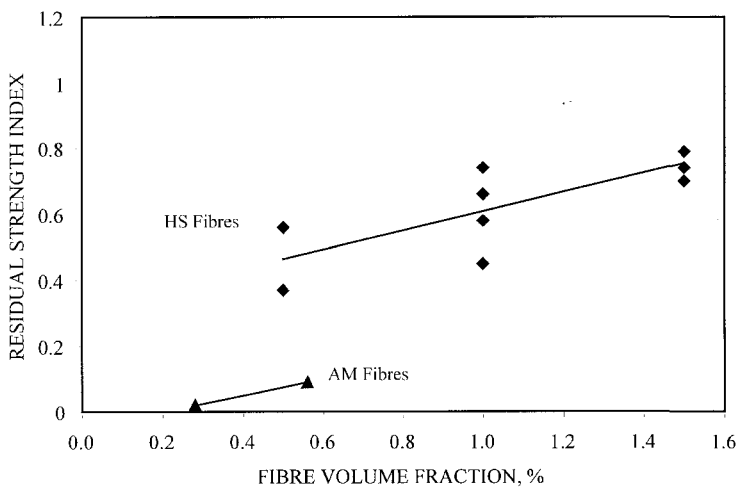

Figure 6 Relationship between fibre volume fraction and strength related index $R_{0.3\text{-}1.0}$

From Figures 4 and 5 it is clear there is synergy between $f_{fl,eq,300}$ and I_{10} or I_{20} values as their basic factors for determination are rather similar (see Figures 1 and 2). Given that the

introduction of $f_{ct,sp} = 0.6 f_{fl} + 0.37 f_{fl,eq,300}$ into the equation for V_{co} has been validated by the shear tests, it is proposed that the expression for $f_{fl,eq,300}$ may be replaced by I values, as shown in Figure 9, as follows;-

$$f_{fl,eq,300} = 1.1\, I_{10} - 4.2 \quad (R^2 = 0.80) \tag{5a}$$

or

$$f_{fl,eq,300} = 0.4\, I_{20} - 1.35 \quad (R^2 = 0.88) \tag{5b}$$

It is therefore proposed that I_{10} or I_{20} values could be introduced into Equation 4 for V_{co}, reflecting the significance of toughness on ultimate shear strength.

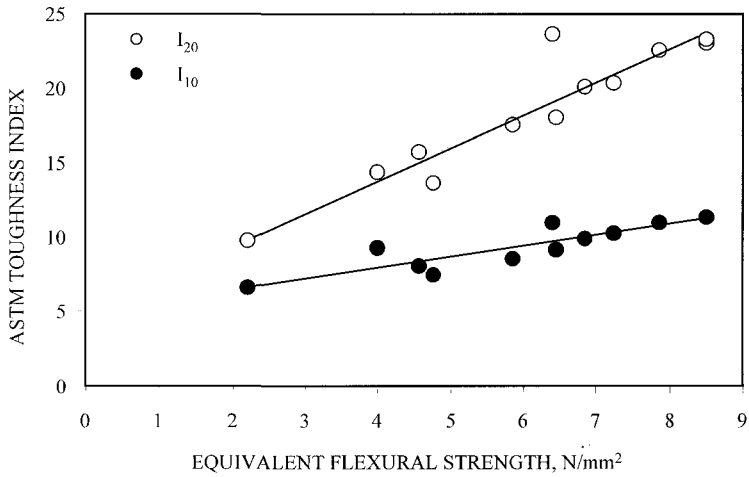

Figure 7 Relationship between toughness indices I_{10} and I_{20} and flexural strength $f_{fl,eq,300}$

DUCTILITY IN SHEAR

In comparing the ductility of the PFRC beams with the plain beams, a relative measure based on load-based dimensionless indices has been used.

The load-based index V_{lim}/V_{cr} is defined as the shear load being sustained at a certain deflection in relation to the first crack shear capacity. The limiting deflections (δ_{lim}) chosen for this study was related to the span (l) as $l/250$ This is of particular interest since it relates to the limiting deflection in BS 8110 before the construction of finishes and partitions.

Figure 8 shows the average value of the index V_{250}/V_{cr} against fibre volume. At a/d = 2.0 it is apparent that as V_f increases the ability of the beams to carry higher loads at equal deformations improves. There is a large improvement in performance between V_f = 0% and 0.5%, where after the improvement in ductility is less noticeable. At a/d = 2.8 there is a large

increase in ductility for the $V_f = 0.5\%$ beams compared with the plain beams, but for $V_f > 0.5\%$ all the PFRC beams appear to have nearly the same level of ductility, *viz* V_{250}/V_{cr} =1.1 to 1.3. The fact that the index V_{lim}/V_{cr} is little different for all fibre volumes shows that the continuing failure of the PFRC beams is essentially by the same mechanism and must be independent of fibres, i.e., fibre pullout at these deflections (which are large) is no longer an issue and failure is due to concrete crushing in the compressive zone and loss of bond around the prestessing wires. Failure is, therefore, substantially different to that in flexural toughness tests.

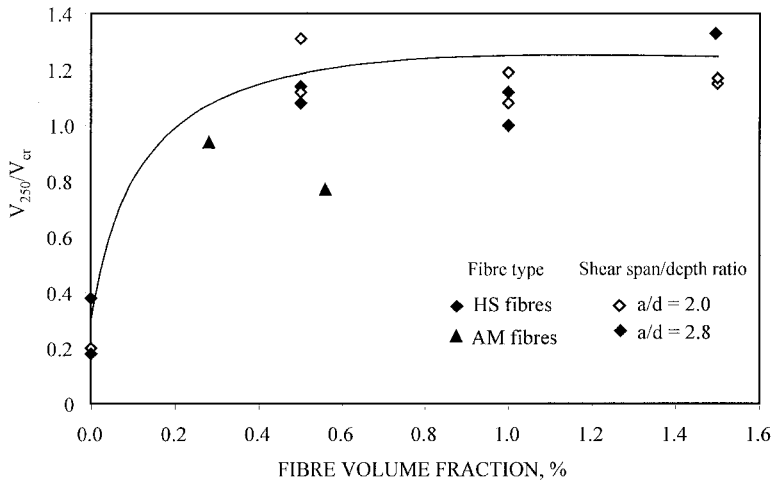

Figure 8 Effect of fibre volume fraction on V_{250}/V_{cr}

CONCLUSIONS

The shear capacity of prestressed fibre reinforced beams uncracked in flexure is given as:-

$$V_{co} = \frac{Ib}{A\bar{y}}\sqrt{f_{ct}^2 + f_{ct,}\,\sigma_{cpx}} \tag{6}$$

For steel fibre reinforced concrete the tensile splitting term (f_{ct}) may be replaced by $0.6\,f_{fl} + 0.37\,f_{fl,eq,300}$. Both these terms can be obtained from a standard 4 point flexural prism test. The agreement in V_{co} with the ultimate shear capacity from 18 full scale shear tests is about 0.89 times test values, and is rightly conservative.

ASTM toughness indices I_{10} and I_{20} were determined from 4 point bend tests, together with other interesting post cracking parameters. The trends in I_{10}, I_{20} and $f_{fl,eq,300}$ with fibre volume were all similar, suggesting that the toughness indices could be used as a sensible replacement for flexural strength in Equation 1. This will forge an empirical link between ultimate shear capacity and toughness of FRC.

The ductility of prestressed beams in shear, as measured at a deflection of span/250, is apparent when $V_f > 0.5\%$. However, improvements found in toughness properties at the higher fibre volumes (1.0% and 1.5%) are not seen in shear ductility, which is fairly constant over this range.

It is concluded that the behaviour of PFRC beams in shear can be determined from flexural toughness tests carried out on standard control prisms. Since flexural toughness parameters are widely regarded as being appropriate to structural fibre reinforced concrete design, these results give a clear indication of the further steps required to produce design shear equations for PFRC beams.

REFERENCES

1. CRISWELL, M E. Reinforced fiber reinforced concrete and issues for its inclusion in structural design codes. Workshop on Fibre Cement and Concrete, University of Sheffield, 28-30 July 1994

2. EFNARC. European specification for sprayed concrete. European Federation of Producers and Applicators of Specialist Products for Structures, 1996, 30pp

3. RILEM TC 162-TDF. Test and design methods for steel fibre reinforced concrete, Materials and Structures, Vol. 33, 2000, pp 75-81

4. PAINE, K A. Steel fibre reinforced concrete for prestressed hollow core slabs. PhD Thesis. University of Nottingham, 1998, 325pp

5. DRAMIX GUIDELINE. Design of concrete structures: Steel wire fibre reinforced concrete structures with or without ordinary reinforcement. Final Draft, 1995

CAPACITY OF REINFORCED CONCRETE STRUCTURAL ELEMENTS RETROFITTED WITH GFRP UNDER CYCLIC LOADING

I G Shaaban
Zagazig University
A M Torkey
Cairo University
Egypt

ABSTRACT. The aim of this study is to evaluate the improvement in seismic behavior of Reinforced Concrete (RC) structural elements as a result of retrofitting such elements using Glass Fiber Reinforced Plastics (GFRP) or enhancing the concrete quality using High Strength Concrete (HSC). A mathematical model was developed for the analysis of RC structures wrapped with FRP and linked to the inelastic damage analysis computer program IDARC3M, developed earlier by the authors for the analysis of HSC structural frames. The results predicted by the developed model were in good agreement with the experimental results obtained in the literature. The predicted results showed that wrapping the studied frame connection with GFRP improved its ductility and increased its capacity over the control connection (before retrofitting) by 82% and 160%, respectively. On the other hand, the analysis of HSC studied column using the computer program showed a large increase in its capacity. However, special precautions should be taken to achieve good confinement in order to obtain acceptable ductility of HSC structural elements.

Keywords: Glass Fiber Reinforced Plastics (GFRP), Retrofitting; High Strength Concrete (HSC), Frame connections, confinement.

I G Shaaban is an associate professor for the analysis and design of RC structures in Civil Engineering Department at Zagazig University (Banha Branch), Cairo, Egypt. He obtained his MSc from Ain Shams University, Cairo, Egypt, in 1988 and his PhD from University of Dundee, Scotland, U.K, in 1993. His research interests include the structural behavior of RC and high strength concrete structures (HSC), nonlinear static and dynamic analysis of such structures, repair and strengthening of RC structures, concrete durability and its relation to the design of reinforced concrete structures.

A M Torkey is an associate professor for the analysis and design of RC structures in Structural Engineering Department at Cairo University, Giza, Egypt. He obtained his MSc from Cairo University in1985 and his PhD from the same University in 1993. His research interests include nonlinear static and dynamic analysis of reinforced concrete structures (normal concrete, high strength concrete and fiber reinforced concrete).

INTRODUCTION

Recent earthquakes in many parts of the world have illustrated the vulnerability of reinforced concrete structures to moderate and strong ground motions. This requires special attention for the analysis and design of building frames such as ductility in frame connections and strong column-weak beam systems [1]. Several investigations studied the use of High Strength Concrete (HSC) in building columns in seismic areas [2]. Experimental results have indicated that the ductility of HSC columns was improved by providing an appropriate confining reinforcement [3]. Existing structures that were designed according to earlier codes may not meet current seismic design standards since many of them are inadequate and pose a severe risk during seismic events. Vulnerable structures may be retrofitted to assure compliance with current design provisions. Among the several methods for retrofitting structural elements, advanced composites, or Fiber Reinforced Plastics (FRP), promise to provide substantially improved load capacity, durability and ductility of such elements [4].

Saadatmanesh et. al. [5] found that both flexural strength and displacement ductility for columns retrofitted by Glass Fiber Reinforced Plastics (GFRP) were higher than those of the original columns. Triantafillou et. al. [6] found that the strengthening of RC beams with FRP plates improved their flexural resistance and decreased the deflection. Chajes et. al. [7] found that beams wrapped with composite reinforcement (GFRP) displayed excellent bond characteristics and an increase in ultimate strength of 60 to 150% was achieved. In addition, it was shown that orientation of the fabrics' fibers influenced the shear strength contribution. Salah-Eldeen et. al. [8] found that Carbon Fiber Reinforced Plastics (CFRP) strips are efficient as a compression reinforcement to avoid concrete crushing failure and to enhance ultimate moment capacity for the repaired beams. Shaheen et. al. [9] found that the use of GFRP sheets for the strengthening of exterior R.C column-to-beam connections improved the ductility of these joints and increased their capacity by approximately 50%. Despite that the improvement of the behavior of structural elements by using GFRP for strengthening them or using HSC for constructing such elements was studied in the literature, as indicated, investigations for comparing the responses of both of them to seismic loading are limited.

The objective of this paper is to evaluate the improvement in the performance of structural elements under simulated seismic loads. Such improvement is achieved either by enhancing the concrete quality using HSC or by retrofitting such elements using advanced composites (GFRP). Ultimate strength results and ductility measures were used to monitor the improvement of structural elements.

MODELLING OF R.C SECTION WRAPPED WITH FRP STRIPS

The stress strain model adopted for concrete sections externally reinforced with fiber composite straps [10] is shown in Figure 1. The model is based on an equation proposed by Popovics [11] in which the longitudinal compressive concrete stress " f_c " is defined as follows:

$$f_c = \frac{f'_{cc} \times r}{r + 1 + x^r} \qquad (1)$$

Where

$$x = \frac{\varepsilon_c}{\varepsilon_{cc}} \tag{2}$$

$$r = \frac{E_i}{E_i - E_{sec}} \tag{3}$$

$$E_{sec} = f'_{cc}/\varepsilon_{cc} \tag{4}$$

$$\varepsilon_{cc} = \varepsilon_{co}\left[1 + 5\left(\frac{f'_{cc}}{f'_{co}} - 1\right)\right] \tag{5}$$

$$f'_{cc} = f'_{co}\left[2.254\sqrt{1 + \frac{7.94\, f_{le}}{f'_{co}}} - \frac{2\, f_{le}}{f'_{co}} - 1.254\right] \tag{6}$$

$$E_i = 51000\ (f'_{co})^{1/3} \tag{7}$$

Where

f'_{co} = the unconfined concrete strength, MPa (N/mm^2).
f'_{cc} = the compressive strength of confined concrete, (N/mm^2).
ε_c = the longitudinal compressive strain of concrete,
ε_{cc} = strain at maximum concrete stress f'_{cc} of confined concrete,
ε_{co} = 0.002 strain at maximum concrete stress f'_c of unconfined concrete,
E_i = initial tangent modulus of elasticity of concrete, (N/mm^2), divided by Poisson's ratio [4],
E_{sec} = secant modulus of elasticity of concrete at peak stress, and
f_{le} = effective lateral confining pressure from transverse reinforcement.

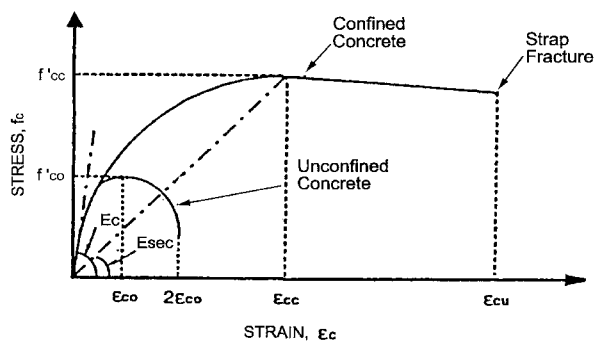

Figure 1 Modeling of stress-strain relationship for unconfined and confined concrete [10].

The effective lateral confining pressure from transverse reinforcement on circular concrete sections as proposed by Mander et. al. [12] is defined as:

$$f_{le} = f_l \, k_e \tag{8}$$

and

$$k_e = A_e / A_{cc} \tag{9}$$

Where

f_l = lateral pressure from transverse reinforcement.
k_e = confinement effectiveness coefficient.
A_e = area of effectively confined concrete core.
A_{cc} = effective area of concrete enclosed by composite strap.

$$A_{cc} = A_c \, (1 - \rho_{cc}) \tag{10}$$

Where

ρ_{cc} = ratio of area of longitudinal reinforcement to gross area of concrete.
A_c = area of concrete enclosed by composite strap.

Sheikh and Uzmeri [13] determined the effective area of confined concrete, A_e, considering that an arching action occurs between straps in the form of a second-degree parabola as shown in Figure 2,

$$A_e = JI/4 \; [\, d_s - S`/2 \,]^2 \tag{11}$$

Where

S` = clear vertical spacing between straps, and
d_s = diameter of column.

Substituting Equations (10) and (11) into Equation (9), the confinement effectiveness coefficient of circular sections can be calculated as:

$$K_e = \left(1 - \frac{S'}{2 d_s} \right)^2 \Big/ \left(1 - \rho_{cc} \right) \tag{12}$$

For rectangular concrete sections, it is necessary to modify the effective lateral confining pressure, fle, by modifying the effective area of confined concrete assuming again the same approach of arching action (in the form of a second-degree parabola), as was shown in Figure 2 for circular columns.

$$A_e = h \, b \, (1 - S`/2h) \, ( 1 - S`/2b) \tag{13}$$

Where

b and h = cross-sectional dimensions.

Substituting Equations (10) and (13) into Equation (9) results in the confinement effectiveness coefficient for rectangular sections given by:

$$K_e = \left(1 - S'/2b\right)\left(1 - S'/2h\right) \Big/ \left(1 - \rho_{cc}\right) \tag{14}$$

The material model for RC sections wrapped with FRP can be easily linked to any nonlinear finite element package. The computer program IDARC3M, developed earlier by the authors for the analysis of HSC structures [14], was modified for the analysis in this study. Linking the material model for RC sections wrapped with FRP was carried out as a further development of the program. The ultimate stresses of confined specimens (at strap fracture) were obtained experimentally [15] in a range of 2% to 4% of the ultimate tensile strength of the FRP sheet. The corresponding maximum strain was approximately 1.5%. Such experimental results are used as input data for the further development of the computer program. The program was verified by comparing its results with experimental results in the literature.

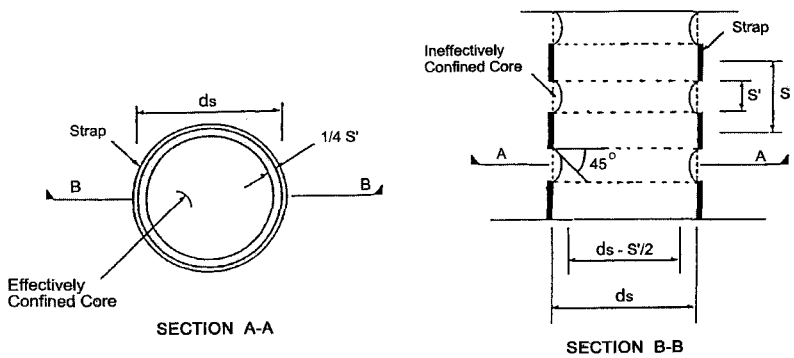

Figure 2 Confinement of FRP straps for circular columns [10]

COMPARISON BETWEEN EXPERIMENTAL AND THEORETICAL RESULTS

Exterior Frame Connections Retrofitted with FRP under Cyclic Loading

Exterior beam-column joint specimens were experimentally tested by Haddad [15]. Two specimens were modeled analytically in this study using the modified computer program IDARC3M, namely, J1 (control specimen) and J6 (specimen strengthened using FRP). The overall dimensions of the test specimens are shown in Figure 3 where the boundary conditions were set to simulate the points of contra-flexure in the beams and columns. Test specimens were cast using Normal Strength Concrete (NSC) where the cube strength after 28 days was 25 MPa (N/mm^2). The specimens reinforcement details are shown in Figure 3. It can be seen from the figure (see Sec. 2-2) that the reinforcement in the beam section is not symmetric around the X-axis. The specimens were detailed to carry gravity loads only without any precautions for seismic loads.

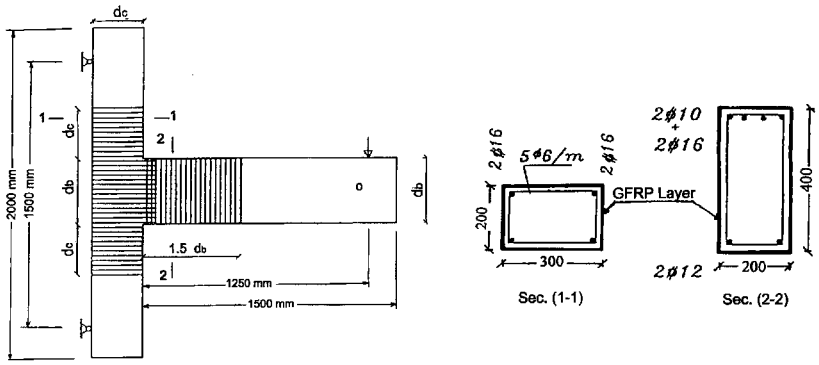

Figure 3 Details of strengthening using GFRP layers [15].

(a) Control specimen "J1"

Specimen J1, the reference specimen, was used to investigate the behavior of the original specimen prior to strengthening using GFRP. The mode of failure of the specimen was a combination of brittle shear failure in the joint region and slippage of the stirrup hanger [15].

Load–displacement relationship

The load-displacement hysteresis loops are shown in Figure 4. It can be seen from the figure that there is a good agreement between the results predicted by the proposed model, linked to the computer program IDARC3M, and the experimental results obtained by Haddad [15]. However, the predicted results are slightly higher than the experimental ones, which indicates the conservative behavior of the proposed model. Figure 4 shows that the behavior of the specimen changed along the two parts of the cycle (negative and positive parts). Such difference in the behavior appeared clearly for the experimental results [15]. This can be attributed to the fact that the specimen reinforcement was not symmetric in the beam part as shown in Figure 3, Sec. 2-2.

Stiffness degradation

The stiffness degradation or the cracked stiffness was calculated at each loading cycle as the ratio of the sum of peak tension and compression loads to the sum of the maximum tension and compression displacement. Both of the experimental and theoretical results for stiffness degradation versus number of cycles are shown in Figure 5. It can be seen from the figure that the experimental results are well predicted by the proposed model. Figure 5 shows that the specimen lost approximately 90% of its initial stiffness after 13 cycles only.

(b) Specimen retrofitted with GFRP "J6"

Specimen J6 was retrofitted with GFRP in order to study the effect of GFRP on the ductility and capacity of the specimen. The method of strengthening of Specimen J6 is reported by Haddad [15]. The critical areas at the beam-column connection were wrapped with GFRP sheet as shown in Figure 3. The fiber direction was parallel to the stirrups in the column and the beam parts in order to achieve good confinement for the column and better shear performance in the beam. The mode of failure of the specimen was a combination of flexure cracks and diagonal tension cracks in the beam part of the connection [15].

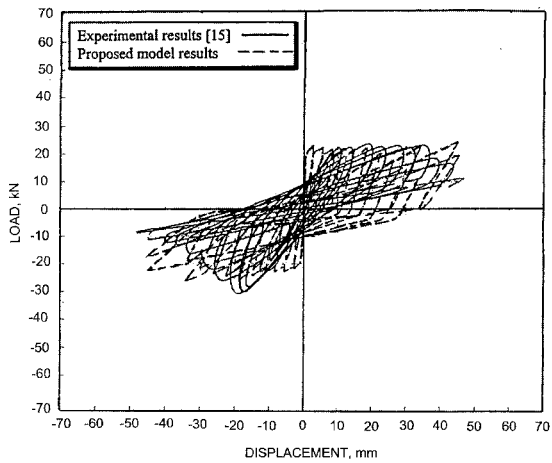

Figure 4 Load-displacement hysteresis loops for Specimen J1

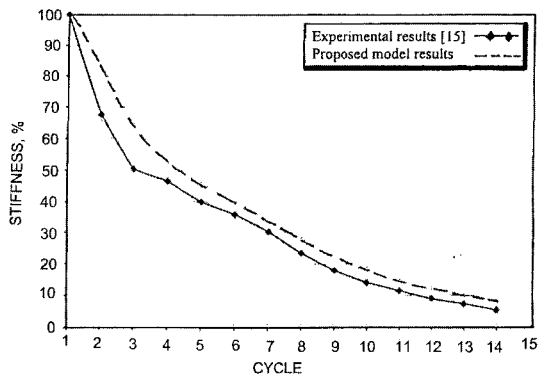

Figure 5 Stiffness degradation for Specimen J1

Load-displacement hysteresis loops

The experimental and predicted results of the load - displacement hysteresis loops are shown in Figure 6. The figure shows good agreement between the experimental results and those predicted by the proposed model. It can be seen from the figure that the theoretical ultimate positive load for Specimen J6 increased gradually up to the peak value (60 kN) which is higher than that of Specimen J1 by 160% (see Figure 4). In addition, the theoretical ultimate positive load for Specimen J6 was higher than the experimental value by approximately 20 %. At the last cycle of loading the theoretical positive load was almost equal to the experimental one. On the other hand, the peak value of the predicted negative load of Specimen J6 was higher than that of Specimen J1 by 114%. It can be seen from Figures 4 and 6 by comparing the behavior of Specimens J1 and J6 that retrofitting of the specimen with GFRP lead to an increase of its capacity and ductility.

It is worth mentioning that the peak value of the predicted negative load of Specimen J6 was almost equals to the experimental one and it took place at a higher value of displacement. It is interesting to notice that the behavior of the specimen along both of the negative and positive parts of the cycle is almost the same. It can be argued that although the steel reinforcement is not symmetric around X-axis as mentioned earlier for Specimen J1 (see Figure 4) but the wrapping with GFRP symmetrically around the beam's X-axis changed the behavior of the specimen.

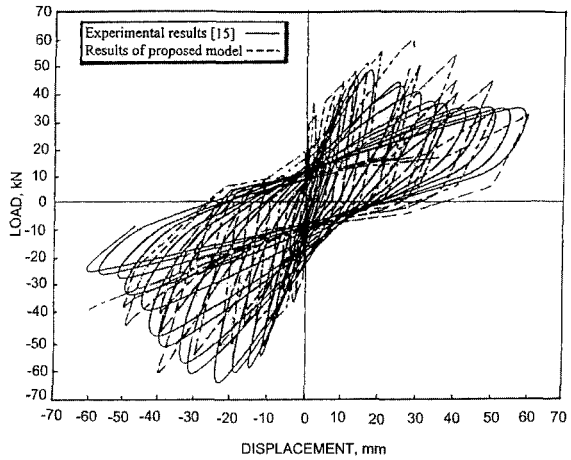

Figure 6 Load-displacement hysteresis loops for Specimen J6.

Energy dissipation

The relationship between the energy dissipation and the cycle number for Specimens J1 and J6 is shown in Figure 7. The figure shows a very close agreement between the experimental and theoretical energy dissipation for Specimen J6 except for the cycles 6 to 11. At this range of cycles, the theoretical values were higher than the experimental ones by approximately 18 %. This may be attributed to the formation of cracks and peeling of GFRP layers through these cycles. Such peeling of GFRP is not included into the proposed model. The theoretical energy dissipation of Specimen J6 was higher than that of J1 up to the last cycle of loading for Specimen J1 (Cycle number 14) by approximately 135 %. In addition, Specimen J6 resisted higher number of loading cycles (17 cycles) till failure compared with Specimen J1, which is an indication of the improvement of capacity and ductility of this specimen.

Ultra High Strength Concrete (UHSC) Columns under Cyclic Loading

Five specimens of 120 MPa (N/mm^2) concrete with (UHS) steel bars were experimentally tested under reversed cyclic loading [16]. All specimens had 225 x 225 mm square section and shear span/depth ratio of 2.0 as shown in Figure 8.

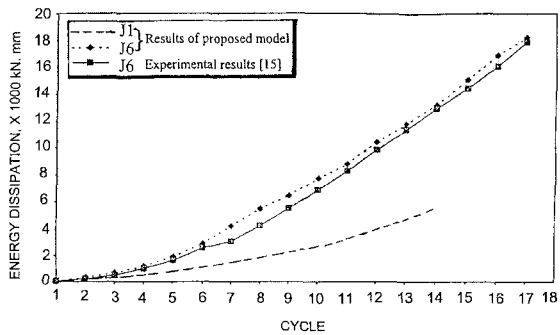

Figure 7 Energy dissipation for Specimen J1 and J6

Ultra high strength deformed bars with yield strength of 1380 MPa were used for both longitudinal and lateral reinforcement. Among the experimentally tested specimens, Specimen "UC15L" was modeled analytically using program IDARC3M [14]. The specimen had twelve longitudinal bars of diameter 10mm and four branches lateral ties of diameter 6.4mm every 35mm and 45mm, respectively. It was subjected to axial stress ratio of 0.36, which is considered low compared with the other test specimens [16]. Reversed cyclic horizontal load under double curvature was applied to each specimen while axial compression was held constant. Loading program consisted of each one cycle at displacement angle of 0.2, 0.33, 0.5 and 0.75% followed by each two cycles at displacement angle of 1.0, 1.5, 2.0, 3.0, 4.0 and 5.0%.

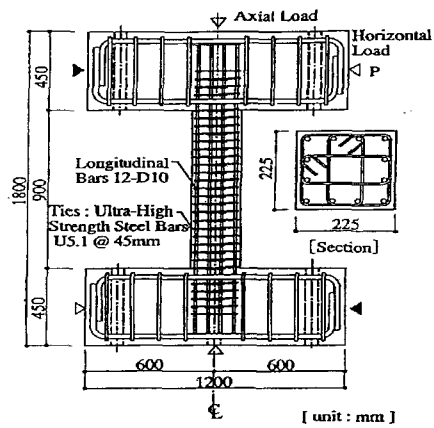

Figure 8 Testing of ultra High Strength Concrete (HSC) columns [16]

Load-displacement hysteresis loops

The load displacement hysteresis loops obtained from both test results and the computer analysis for the analyzed specimen is shown in Figure 9.

It can be seen from the figure that, generally, the predicted results are in good agreement with those obtained experimentally. For example, the maximum load obtained experimentally was 355 kN approximately and the predicted load was higher than this value by 11% only.

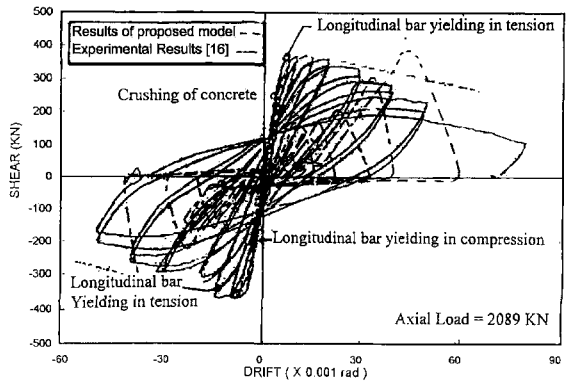

Figure 9 Load displacement loops for Specimen UC15L

COMPARISON BETWEEN THE BEHAVIOR OF NSC STRUCTURAL ELEMENTS RETROFITTED WITH FRP AND HSC STRUCTURAL ELEMENTS

It was difficult to compare the responses of studied structural elements to cyclic loading since these elements are different in shape, dimensions and in the loading scheme. However, the behavior of such elements can be assessed from the predicted load and displacement results obtained from Figures 4, 6 and 9 and tabulated in Table 1. It can be noticed from the table that using GFRP in retrofitting the studied connection raised the peak load from 23 kN to 60 kN (almost 160% increase in the capacity). Table 1 shows that the capacity of the studied HSC element is very high compared to the other specimens. .An attempt to compare the ductility of studied elements was carried out by dividing the ultimate displacement of each of them by the displacement at the peak load (Ductility index). The table shows that the ductility index of the specimen retrofitted with GFRP is the best among the studied elements (higher than that of Specimen J1 by 82%). It is interesting to note that the ductility index of the HSC element is higher than the NSC element before retrofitting with GFRP by 30%. This may be attributed to the fact that the studied HSC structural element is well confined by a large number of high tensile strength stirrups.

Table 1 Predicted Results for Different Structural Elements

TYPE OF STUDIED SPECIMEN	PEAK LOAD (kN)	DISPLACEMENT (0.001 rad)		DUCTILITY INDEX
		At peak	at ultimate	
NSC Specimen "J1"	23	28	30	1.1
NSC Specimen retrofitted with GFRP "J6"	60	20	40	2
HSC Specimen "UC15L"	39.7	42	60	1.43

CONCLUSIONS

The mathematical model developed for the analysis of RC sections wrapped with FRP was successfully linked to the computer program IDARC3M and used in studying the behavior of frame connections under cyclic loading. The results predicted by the developed model were in good agreement with the experimental results obtained in the literature.

The studied connection retrofitted by GFRP showed an improvement in both capacity and ductility over the control connection (before retrofitting) by 160% and 82%, respectively.

The energy dissipation of the connection retrofitted with GFRP was higher than that of the control one by approximately 135 %. Moreover, this studied connection resisted higher number of loading cycles (17 cycles) till failure compared with the control specimen, which is an indication of the improvement of capacity and ductility of this specimen.

Despite the fact that using HSC in structural elements leads to a great increase in the capacity, special precautions should be taken to achieve good confinement in order to obtain acceptable ductility of such elements. On the other hand, using FRP for strengthening structural elements improves the ultimate capacity to acceptable degree and enhances the ductility, which is preferable for seismic design.

REFERENCES

1. MAZZONI S., MOEHLE J. P., "Seismic Response of Beam-Column Joints in Double-Deck Reinforced Concrete Bridge Frames," ACI Structural Journal, Vol. 98, No. 3, May-June 2001, pp. 259-269.

2. AZIZINAMANI A., KUSKA S., BRUNGARDT P., HATFIELD E., "Seismic Behavior of Square High Strength Concrete Columns", ACI Structural Journal, Vol. 91, No. 3, 1994, pp 336-345.

3. NISHIYAMA M., FUKUSHIMA I., WATANABE F., MUGURUMA H., "Axial Loading Tests on High-Strength Concrete Prisms Confined By Ordinary and High-Strength Steel," Proceedings, High-Strength Concrete 1993, Lillehammer Norway, pp. 322-329.

4. TOUTANJI H.A., "Stress-Strain Characteristics of Concrete Columns Externally Confined with Advanced Fiber Composite Sheets", ACI Structural Journal, Vol. 96, No.3, May-June 1999, pp.397-404.

5. SAADATMANESH H, EHSANI M.R, JIN L, "Repair of Earthquake-Damaged RC Columns with FRP Wraps," ACI Structural Journal, Vol. 94, No. 2, March-April, 1997, pp. 206-215.

6. TRIANTAFILLOU T.C, DESKOVIC N, DEURING M, "Strengthening of Concrete Structures with Prestressed Fiber Reinforced Plastic Sheets," ACI Structural Journal, Vol. 89, No. 3, May-June 1992, pp. 235-244.

7. CHAJES M.J, JANUSZKA T.F, MERTZ D.R, THOMSON T.A, FINCH W.W, "Shear Strengthening of Reinforced Concrete Beams using Externally Applied Composite Fabrics," ACI Structural Journal, Vol. 92, No. 3, May-June 1995, pp. 295-303.

8. SALAH-ELDEEN O, KORANY Y., ABDEL-LATIF H., "Application of CFRP Strips in Repairing Reinforced Concrete Beams," Proceedings of the Arab Conference for Repair and Rehabilitation of Structures, Vol. 1, 1998, pp.519-538.

9. SHAHEEN H. H., KHALEEL G. I., HUSSEIN Y. M, "Repair of Exterior Space Beam-Column Joints," The International Workshop on Structural Composites for Infrastructure Applications, Cairo, Egypt, May 2001, pp. 139-152.

10. SAADATMANESH H., EHSANI M.R., LI M.W, "Strength and Ductility of Concrete Columns Externally Reinforced with Fiber Composite Straps", ACI Structural Journal, V91, No.4, July-August 1994, pp.434-447.

11. POPOVICS, S., "Numerical Approach to the Complete Stress-Strain Curves for Concrete, "Cement and Concrete Research, Vol. 3, No. 5, 1973, pp. 583-599.

12. MANDER J. B., PRIESTLEY M. J. N., PARK R., "Theoretical Stress-Strain Model for Confined Concrete," Journal of Structural Engineering, ASCE, Vol. 114, No. 8, Aug. 1988, pp. 1804-1826.

13. SHEIKH S. A., UZUMERI S. M., "Strength and Ductility of Tied Concrete Columns, "Journal of Structural Division, ASCE, Vol. 106, No. 5, 1980, pp. 1079-1102.

14. SHAABAN I. G., TORKEY A. M., "Nonlinear Seismic Analysis of High Strength ConcreteStructures," Journal of the Egyptian Society of Engineers, Vol. 39, No. 2, 2000.

15. HADAD H.S., "Strengthening of the Exterior Beam-Column Connections with GFRP (to resist cyclic loading)", Ph.D Thesis submitted to faculty of engineering, Cairo University, 2000, 217 pp.

16. SUGANO S., "Seismic Behavior of Reinforced Concrete Columns which Used Ultra-High-Strength Concrete", Paper No. 1383, Proceedings of Eleventh World Conference on Earthquake Engineering, Published by Elsevier Science Ltd., 1996.

THEME THREE:

DURABILITY AND MAINTENANCE OF COMPOSITE CONSTRUCTION

Keynote Paper

NON-METALLIC REINFORCEMENTS FOR CONCRETE CONSTRUCTIONS

D Van Gemert

Catholic University of Leuven

K Brosens

Triconsult N.V.

Belgium

ABSTRACT. Non-metallic reinforcements are becoming valuable alternatives for the classical concrete reinforcements. This evolution started in the late eighties of last century. Composite materials of different type were introduced to overcome the inherent disadvantages of concrete: strength, durability, corrosion of steel rods, creep and shrinkage, flexibility and retrofitting aspects. Glass, aramid and carbon are the most popular fibre reinforcements, embedded in a pure polymer or in a polymer modified matrix. Material properties, reinforcement design, analysis and layout became important research topics, but practical applications came immediately after research, and sometimes even preceded research. Some earthquake disasters have strongly stimulated progress in composite reinforcement for concrete.

The paper will deal with important material properties of FRP, on which application and durability as reinforcement is based. Implications on analysis and design are pointed out. Applications in new constructions, in rehabilitation, repair and strengthening are discussed. Information is collected from research and applications in Europe, as well as from communications with the international FRP community, especially in America and Japan, where pioneering work was done on composite reinforcement materials for concrete.

Keywords: FRP, Non metallic reinforcement, CFRP, AFRP, GFRP, Repair, Strengthening.

Professor D Van Gemert, is Professor of Building Materials Science and Renovation at the Department of Civil Engineering, K.U. Leuven, Belgium. He is Head of the Reyntjens Laboratory for Materials Testing. He is actively involved with research and projects on repair and strengthening of constructions, deterioration and protection of building materials and concrete polymer composites.

Dr K Brosens, obtained his is PhD at the Department of Civil Engineering, K.U. Leuven, Belgium in 2001. His research concerns the strengthening and retrofit of concrete structures with externally bonded steel plates and fibre reinforced materials. Especially anchorage phenomena are considered. Nowadays he works as a project engineer for Triconsult N.V., a spin-off company of the K.U. Leuven. Triconsult's major activity is the research, testing and development of materials, and design of components and structures.

INTRODUCTION

FRP materials can be used as tensile reinforcement for new concrete structures as well as for externally bonded reinforcement for strengthening or repairing existing concrete structures. In the first case, the working principle is analogous as for classical steel rebars. Special attention must be made to take into account the brittle behaviour of the FRP materials. A more common application is the use of FRP laminates as externally bonded reinforcement for concrete strengthening.

The strengthening of concrete structures with externally bonded steel reinforcement is already a well-known technique for many years. The basic principle of externally bonded reinforcement is very simple. Additional reinforcement, in most cases for carrying tensile forces, is added to the structure by bonding it onto the structures elements.

Originally only steel plates were used, but with the development of new high grade FRP (fibre reinforced polymers) materials (e.g. in the aerospace industry), new materials became available to be used for structural strengthening purposes. These materials consist of fibres embedded in a resin matrix. Different fibre types can be used, but most commonly carbon, glass or aramid are applied. The corresponding composites are indicated as CFRP, GFRP or AFRP. The good mechanical properties of the FRP materials are only available in the fibre direction.

Externally bonded reinforcement can be used for strengthening, repairing and stiffening and all types of structures can be treated: evidently concrete structures, but also masonry and wooden structures. However, up to now, mainly concrete structures have been dealt with. A lot of scientific research has already been done in that area, combined with practical experience gathered from worldwide applications.

This paper explores the range of reinforcing fibres available for use in reinforced plastics. Details of the fibre properties are presented together with the resulting laminate properties once the fibre reinforcements have been impregnated with a suitable resin. The advantages and disadvantages of the various fibres are discussed together with the properties that are required to successfully reinforce existing structures against a variety of loading cases.

FRP MATERIALS AS STRUCTURAL REINFORCEMENT

Fiber reinforced plastic (FRP) materials have obvious relevance as structural reinforcement for concrete beams and slabs. They are characteristically high in tensile strength, lightweight, and non-corrosive in saline environments. Consideration of these properties suggests improved life cycle performance for reinforced concrete facilities susceptible to reinforcement corrosion.

However, precluding acceptability of FRP as a legitimate structural reinforcement for concrete is the establishment of a design methodology that reflects the inherent elastic-brittle behavior characteristic of the material in uniaxial tension. Intuitively the engineering community is skeptical of endorsing a reinforcement material whose stress-strain response bares little resemblance to that of reinforcement grade steel. Concrete beams reinforced with FRP exhibit no section ductility; consequently, failure is recognized to be unavoidably brittle and catastrophic. As such, quantification of serviceability and safety with respect to plastic straining

in the reinforcement is of no significance where FRP is used instead of steel. Rather, a performance specific design criterion that uniquely reflects the composite behavior of FRP reinforced concrete is required.

Considering the high tensile strength and relatively low elastic modulus characteristic of FRP in uniaxial tension, it is logical to establish ultimate failure in terms of extreme fiber concrete crushing as the performance specific flexural limit-state from which an acceptable criterion for design is derived. Implied therein is awareness that tensile rupture of the FRP would require extremely lightly reinforced sections. For these under reinforced sections, cracking moments would be disproportionably high with respect to ultimate flexural strength. Furthermore, a low cracked section moment of inertia for under reinforced sections leads to the potential violation of deflection criteria.

It is recognized that, in terms of brittle failure, compression crushing of the concrete is a less catastrophic limit-state than is tensile rupture of the FRP. This type of failure is typical for over reinforced concrete sections. In that case only a fraction of the tensile strength in the FRP tensile reinforcement will be reached. This means that the high tensile strength of FRP materials can not be exploited. In many cases, the stress in the tensile reinforcement can easily be taken by classical steel bars meaning that there is no strength requirement to replace the classical steel bars by FRP reinforcements.

EXTERNALLY BONDED REINFORCEMENT: HISTORICAL OVERVIEW

The first initial studies and applications of externally bonded steel plates were done in the late sixties of last century [1]. L'Hermite and Bresson reported on experiences in France [2], Flemming and King on one experiment in South Africa [3]. Also in Belgium, pioneering research work on this topic was done at the Laboratorium Reyntjens starting from the mid seventies. A few years later, the first small scale on site applications were executed in Belgium [4], [5], [6]. One of them consisted of repairing a concrete structure damaged by an explosion followed by a fire.

The first large scale application was the strengthening of three multiple span bridges over the Nete Canal at Lier, Belgium [7]. An extensive test program was carried out. The mechanical behaviour of the strengthening system was tested on rectangular and T-shape test specimen, simulating the real bridge deck behaviour. Also a start of durability measurements was made [6]. Meanwhile, research work concerning externally bonded steel plates was also done in Germany [8] and in Switzerland [9], [10]. In the early nineties of last century, a real explosion of research and applications of externally bonded reinforcement took place. Also the first uses of fibre reinforced plastics appeared.

FRP REINFORCEMENT FOR EXTERNALLY BONDING

Mainly, two types of FRP reinforcement are available on the market: hardened plates and flexible sheets (wet lay up). The end result, the fibres embedded in a resin matrix is often indicated by the term "laminate".

In the early stage, the hardened FRP plates were autoclaved, which limited the available length. Later on, FRP plates produced without autoclaving, came on the market. These plates are available in different thicknesses, widths and stiffnesses and with nearly unlimited length. The application of these hardened FRP plates is analogous to the application of steel plates.

Another type of FRP reinforcement are the UD-sheets, Figure 1, which are very flexible and can easily be cut by means of scissors, Figure 2. At application, the flexible sheets are impregnated with the right ratio of epoxy resin components and the chemical reaction starts. When the first layer has hardened enough, the second layer can be applied in the same manner. The sheets are completely impregnated on the site. These UD-sheets were first developed and produced in Japan. In Belgium the first application of on site hardening CFRP-sheets took place at the beginning of 1996 [14].

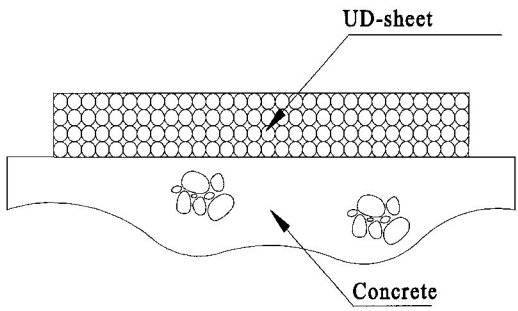

Figure 1 UD-sheet

Both types of FRP, the sheets and the plates, are available on roll, Figure 3, which means that they are available in any length, whereas the steel plate length is limited in practice to 6 meters. The FRP materials consist of continuous fibres embedded within a thermosetting resin system. The resin is required to bond the fibres together and transmit loads between fibres. Some mechanical properties such as in-plane and interlaminar shear are highly resin dependent, whilst others such as longitudinal strength and stiffness are highly fibre dependent.

Figure 2 The flexible CFRP sheets are very suitable to be applied in complex shapes (Securitas, Brussels, 1996)

The most common resins used in FRP are polyester based, which are economical and of low-moderate strength. Numerous grades of polyester resin are available, but the most common consist of either orthophthalic or isophthalic saturated acids. Orthophthalic resins are more economical but exhibit low mechanical properties and chemical resistance and are less likely to be suitable for the reinforcement of concrete structures, where good resistance to alkaline environments may be required.

Vinylester and epoxy based resins offer improved mechanical properties but with increased cost. However, if high performance fibres such as aramid or carbon are being used, the resin will only form a very small portion of the total cost. This is the reason that for structural purposes nearly always an epoxy resin will be used.

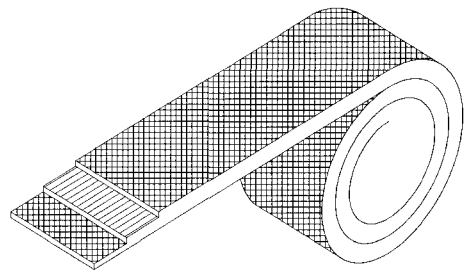

Figure 3 CFRP laminates are delivered on roll

FIBRE TYPES [15]

E-Glass

By far the most common reinforcing fibre is E-Glass, which derives it's name from it's electrical resistance. Individual fibres or filaments are produced with diameters around 10μm and coated with a size or binder that should be compatible with the laminating resin to be used. E-glass is available in a variety of forms such as continuous rovings, woven rovings, stitched fabrics, unidirectional tapes and chopped fibre mats. The fibre is very economical and of moderate strength but low modulus (stiffness). E-glass generally exhibits good chemical resistance, but may require protection against strong acid or alkali environments. Chopped fibre mats are mainly used for non-structural and secondary structure applications and produce laminates with relatively low strength. They are unlikely to be suitable for applications in the strengthening of steel or concrete structures.

Aramid

Aramid or polyaramid fibres, such as Kevlar 49, are man-made organic fibres offering very high tensile strengths and low density. They are used in numerous applications such as bullet-proof vests, vehicle tyres, high speed boat hulls, lightweight high tensile ropes and some aerospace applications. Aramid fabrics are very soft and easy to handle. They can prove difficult to cut with conventional tools due to their very high toughness, but this can be overcome with the use of specialist tools.

Carbon

Carbon fibre is the most expensive of the more common reinforcements but due to it's very high strength and stiffness is the most commonly used fibre in aerospace applications. It is also used extensively in sporting goods such as tennis racquets, golf clubs and fishing rods. They are gaining acceptance in the marine industry for high performance craft and are widely used in the motor racing industry. All carbon fibres are expensive, but high modulus fibres are particularly expensive mainly due to the low volumes produced at the present time. The costs of high strength fibres have gradually reduced with time as volumes have increased and non-aerospace applications have been developed. Several manufacturers of carbon fibres are now concentrating on the non-aerospace markets and it is expected that prices will fall further within the next few years. Carbon fibres are generally classified as either high strength or high modulus, although in reality both the strength and modulus of most carbon fibres are very high. Carbon fibres are produced from precursors of cellulose and polyacrylonitrile (PAN), producing high strength fibres, or a special hydrocarbon pitch producing high modulus fibres. The carbon fibres are produced by heating the precursor to temperatures up to 2600°C for high strength fibres or 3000 °C for high modulus fibres. The fibres are very brittle and can be more difficult than some alternatives to use in contact moulded (hand-laminated) applications.

Polyethylene

Polyethylene (PE) is generally regarded as a cheap, low strength utility plastic, used in numerous applications from washing up bowls to water butts. However, using a process known as Gel Spinning, ultra-high molecular weight polyethylene is drawn into fibres possessing a very high level of macromolecular orientation, dramatically altering the properties of the fibre. This results in high strength fibres, combing other unique properties, for example very low density and high impact strength. It has often been predicted that PE fibres would be developed further and find increasing applications in the composites industry, but in reality they have only been applied in relatively low volumes in niche applications. Unfortunately it can prove difficult to obtain sufficient bond strength between the laminating resin and the fibre and this area needs to be considered carefully if they are to be applied in structural applications.

FIBRE PROPERTIES

Details of the mechanical properties of a range of reinforcing fibres are contained in Table 1.

Table 1 Typical fibre properties

	E-GLASS	S-GLASS	ARAMID (Kevlar 49)	HIGH STRENGTH CARBON	HIGH MODULUS CARBON	POLY-ETHYLENE	STEEL (FE 360)
Tensile strength (N/mm^2)	2400	3100	3600	3300-6370	2600-4700	3000	235 (yield) 360 (ultimate)
Tensile modulus (N/mm^2)	70000	86000	130000	230000-300000	345000-590000	95000	205000
Failure strain (%)	3.5	4.0	2.5	1.5-2.2	0.6-1.4	3.6	20
Density (kg/m^3)	2560	2490	1440	1800	1900	970	7850
Coefficient of thermal expansion ($10^{-6}/°C$)	5.0	5.6	-2 (L) 59 (T)	-1 (L) 17 (T)	-1 (L)	-12 (L)	12

L = longitudinal T = transversal

E-Glass

E-Glass is of lower strength and stiffness than the other fibres being considered, but is also considerably lower in cost. The fibre is denser than the alternatives and resulting structures reinforced with E-Glass will therefore be considerably heavier than those reinforced with higher performance fibres. Typically an E-Glass structure may be over twice the weight of a carbon or aramid reinforced composite structure, although this will still be dramatically lighter than a conventional structure in steel, concrete or even aluminium. For the strengthening of existing concrete structures however, the difference in weight between a glass and high performance fibre solution may not be a significant factor. The fibre is electrically non-conductive and offers good corrosion resistance. It should be noted however, that the fibre can be attacked by strong alkaline solutions and needs to be protected with suitable resins &/or surface tissues in such situations. Laminates produced with unidirectional E-Glass exhibit ultimate strengths in excess of those provided by conventional structural steel, but with much reduced modulus (stiffness).

Aramid

Aramid fibres such as Kevlar 49 offer very high tensile strengths and relatively high elongation to failure. This results in them being very good for absorbing large amounts of energy, for example in structures subject to impact forces. The fibre has very low density and therefore results in extremely lightweight structures. Most FRP materials exhibit slightly lower strengths in compression than tension, but this is particularly true for aramid reinforced FRP and any areas subject to significant compressive stress will require careful consideration. Aramid fibres have a negative coefficient of thermal expansion.

Carbon

Carbon fibres are available in a wide range of grades offering different mechanical properties. All carbon fibres offer relatively high strengths and stiffness, but are brittle and fail at reasonably low strain levels. They have a negative coefficient of thermal expansion. Carbon fibres are the only fibres considered here that are electrically conductive. In many applications this may not be relevant but may be critical in others, for example near railway overhead power lines. It may also be necessary to consider the possibility of electrolytic corrosion in conjunction with other materials. Carbon exhibits a very high electrolytic potential and behaves as a noble material in the galvanic series. While it will not corrode itself, it may cause galvanic corrosion in other materials.

Polyethylene

Polyethylene (PE) fibres exhibit high tensile strengths, but lower modulus than other high performance fibres such as aramid or carbon. They also exhibit very low compressive strengths. They can provide very high levels of impact strength and are being used in applications such as lightweight armour plating. PE fibres have a highly negative coefficient of thermal expansion.

LAMINATE PROPERTIES

The mechanical properties of a FRP laminate are highly dependent on manufacturing techniques, quality, fibre volume fraction, control of fibre direction and straightness etc. The style of reinforcement may also affect the resulting laminate properties. For example a heavy woven

fabric may result in significant crimp in the fibres lowering both strength and modulus values. Typical laminate properties are shown in Table 2, for unidirectional reinforcements with a fibre volume fraction of 40 %. Higher fibre volumes generally result in higher mechanical properties, but thinner laminates, resulting in a similar load carrying capability for a given weight of reinforcement. It should also be noted that hybrid reinforcements can be produced by mixing different types of fibre.

Table 2 Typical laminate properties (gross laminate area)

	E-GLASS	ARAMID (Kevlar 49)	HIGH STRENGTH CARBON	HIGH MODULUS CARBON	STEEL (FE 360)	CONCRETE
Tensile strength (N/mm^2)	650	900	1000-1900	800-1400	235 (yield) 360 (ultimate)	2-5
Compressive strength (N/mm^2)	550	250	~1000	~600	235 (yield) 360 (ultimate)	25-60
Tensile modulus (N/mm^2)	30000	50000	100000-120000	140000-240000	205000	25000-36000
Failure strain (%)	2.3	2.2	1.5-2.2	0.6-1.4	20	0.01
Density (kg/m^3)	1700	1300	1440	1480	7850	2400
Coefficient of thermal expansion ($10^{-6}/°C$)	10	-1	0	0	12	7-12

Unidirectional laminates with fibre volume fraction $V_f = 40$ %. Properties in longitudinal direction. Properties are typical values but are highly dependent on laminate quality, fibre volume fraction, etc.

When reporting laminate properties, it is very important to specify which cross sectional area is involved. A distinction can be made between the gross laminate area and the net fibre area [16].

Gross laminate area: The gross laminate area of a FRP system is calculated using the total cross sectional area of the cured FRP system including all fibres and resin. Gross laminate area is typically used for reporting properties of hardened FRP plates where the cured thickness is constant and the relative proportion of fibre and resin is controlled. The properties mentioned in Table 2 are based on the gross laminate area.

Net fibre area: The net fibre area of a FRP system is calculated using the known area of fibre, neglecting the total thickness of the cured system. Thus resin is excluded. Net fibre area is typically used for reporting properties of flexible sheet systems that use manufactured fibre sheets and on site installed resins. This system leads to a controlled fibre content and a variable resin content.

System properties reported using the gross laminate area have higher relative thickness dimensions and lower relative strength and stiffness values. However, regardless of the basis for the reported values, the load carrying capacity and stiffness of the system remain constant. It is important to notice that properties based on the net fibre area are not the properties of the bare fibres. The properties of a FRP system should be characterised as a composite, recognizing not just the properties of the individual fibres, but also the efficiency of the fibre-resin system and fabric architecture.

FIBRE SELECTION FOR REINFORCING CONCRETE STRUCTURES

There are a number of general characteristics that may influence fibre selection. For example in electrical applications, for example near high voltage power lines it may not be possible to use conductive carbon fibres. For long span structures subject to large temperature variations it may be preferable to use E-Glass as it has coefficients of thermal expansion close to that of steel and concrete. A thermal analysis would be required to determine the effect of using aramid or carbon fibres with negative or very small coefficients of thermal expansion. In structures subjected to high dynamic loads where fatigue is a major consideration, aramid fibres may be selected as these have demonstrated very good fatigue resistance. The labour involved in producing laminates must be carefully evaluated. Existing structures may require reinforcing for a variety of reasons such as:

a) Static Strength — To increase the static load carrying capability, for example upgrading the strength of a bridge deck.
b) Impact Strength — To increase the resistance of a structure to impact loads such as those arising on bridge columns due to vehicle impacts.
c) Seismic Strength — To increase the resistance of a structure to earthquake loads.
d) Blast Resistance — To increase the resistance of a structure blast loads, such as those arising from bombs or explosions for example on an oil refinery.

Static strengthening is usually undertaken to withstand service loading that may occur many times throughout the life of the structure and it is normally expected that the structure should be fully serviceable after the application of such loading. The philosophy for b, c and d above may however be very different. For example, vehicle impact loads occur very infrequently and it may be acceptable to provide sufficient reinforcement to prevent collapse of the structure, but allow some damage and degradation that will require remedial work after such an impact.

Static Strengthening

Concrete structures are commonly designed ignoring any tensile load in the concrete and assuming that tensile loads are carried totally by the steel reinforcement. This philosophy works well with steel reinforcement, as the strain levels in the steel will be low and should not cause excessive cracking in the concrete. However, most FRP materials have lower moduli and fail at much higher strain levels. It may therefore be impossible to generate high loads in the FRP reinforcement, as the strains must be kept sufficiently low to avoid excessive cracking of the concrete. The common used steel rebars reach their yield strength at a strain of only 0.2 %. At such a strain the following stresses would occur in a unidirectional FRP laminate assuming a 40 % fibre volume fraction.

Table 3 Tensile stress for a strain of 0.2 % for FRP laminates

	E-GLASS	ARAMID (Kevlar 49)	HIGH STRENGTH CARBON	HIGH MODULUS CARBON
Tensile stress for a strain of 0.2 % (N/mm^2)	60	100	220	380
Relative values	1	1.7	3.7	6.3

All of the above stresses are well within the laminate strengths and this shows that it is not possible to fully utilise the high tensile strengths provided by unidirectional laminates where such strain limits are necessary. The predicted stresses give an indication of the relative effectiveness of each type of laminate. For example: to provide the same level of strengthening and load carrying it may be necessary to apply 3.7 more glass reinforcement than HS carbon reinforcement. It may initially appear that the most economic option would be to use the cheaper E-Glass reinforcement, but as the HS carbon reinforcement would also save resin and most importantly labour costs, this may prove the more economic total solution. In some situations, it can become very difficult to handle long heavy plates, for example strengthening the underside of a bridge beam. In such a situation it may be more economic to use a single, lightweight, carbon fibre plate than several glass fibre plates, that would be excessively heavy in a single piece. When the total costs are included such as on-site labour, traffic management and possession times, it is often economic to use the more expensive high performance fibres.

It is possible to increase the loads carried by the FRP laminate if it is pre-stressed, for example by stressing a plate prior to bonding or by relieving the structure dead load prior to application, to enable the FRP to carry dead loads in addition to live loads. In such cases it will also be necessary to consider the long-term behaviour of the FRP. All FRP materials are potentially prone to creep under high long term loading, but in the majority of applications considered here the permanent stress in the FRP is likely to be low and within safe limits to avoid creep failure.

Dynamic Strengthening – Seismic, Impact and Blast loads

To strengthen existing structures against exceptional loads such as the above, assuming that some damage, but not collapse may occur, is very different from the static strengthening considered previously. In these cases it may well be acceptable to allow some yielding of the steel reinforcing bars and to allow significant cracking of a concrete structure. This allows the FRP reinforcement to be worked to much higher strain limits and therefore a much greater proportion of it's strength may be utilised. It has also been shown in previous tests that this approach effectively shows a significant increase in ductility and should be superior for absorbing impact energy. Considering only the energy in the FRP laminate, the strain energy or work done may be related to the area under the load-extension curve. Assuming linear behaviour to failure we can calculate the strain energy as follows:

$$\text{Strain Energy} = 0.5\ \sigma^2\ L\ A\ /\ E = 0.5\ P\ e$$

where σ = stress (N/mm^2)
L = length (mm)
A = cross sectional area (mm^2)
E = E-modulus (N/mm^2)
P = load (N)
e = extension (mm)

From the equations above it can be seen that to provide high levels of strain energy, it is advantageous for a material to have high strength, but low modulus and therefore high strain. For typical unidirectional material properties, the following strain energies have been calculated, based on unit volume, Table 4.

Table 4 Strain energy at failure for FRP laminates

	E-GLASS	ARAMID (Kevlar 49)	HIGH STRENGTH CARBON	HIGH MODULUS CARBON
Strain energy at failure (Nmm)	7.5	9.9	7.5-20.9	2.4-9.8
Relative values	1	1.3	1-2.8	0.3-1.3

In reality the situation is much more complex, but this clearly indicates that High Modulus Carbon is less likely to be a suitable material in an impact situation. The higher failure strains of E-Glass and Aramid will also allow greater energy to be absorbed into the steel reinforcement as it yields. The choice between E-Glass, Aramid and HS Carbon is not obvious and may require a detailed study to determine which will give the most economic solution for any particular application. Aramid fibres have been shown to be very successful at withstanding impacts and dynamic loads in other applications and it is expected that they will perform well in areas such as strengthening bridge columns against vehicle impacts. Carbon FRP fails in a very brittle manner and has also been shown in the past to be vulnerable to local impact damage.

CONCLUSIONS

The importance of the use of FRP materials as structural reinforcement as well as for strengthening or repairing purposes is growing very fast. Normal steel reinforcement can easily be replaced by FRP rebars for many applications. Furthermore, the strengthening of concrete structures with externally bonded reinforcement is a very powerful and effective technique. More and more, the classical steel plates are replaced by externally bonded FRP materials. It has been shown that the properties of a FRP laminate can be varied enormously by the selection of different types of fibres. There may be some cases where particular properties such as thermal or electrical properties make particular fibres most appropriate. However, in the majority of cases, it will be a case of whichever fibre produces the most economic solution will be selected. This is not a simple problem to analyse and it is important that the total project cost is calculated including site labour, traffic management etc. In cases where the application of the reinforcement is labour intensive, it is expected that the high performance fibres will provide more economic solutions. For static strengthening in cases where it is necessary to minimise concrete cracking advantages will be found by using HS Carbon fibres or possibly HM Carbon if the cost of the fibres can be justified. In structures subject to dynamic loads such as impacts, seismic and blast loads, where extensive concrete cracking and/or yielding of steel can be tolerated, Aramid fibres will be worthy of further evaluation.

REFERENCES

1. RILEM, Colloque sur les résines de synthèse dans la construction, éd. Eyrolles, Paris, Septembre, 1967.

2. BRESSON, J, Nouvelles recherches et applications concernant l=utilisation des collages dans les structures, Béton plaqué, Annales de l=ITBTP, No 278, 1971, p 22-55.

3. FLEMMING, C J, KING, G E M, The development of structural adhesives for three original uses in South Africa, RILEM International Symposium on Synthetic Resins in Building Construction, Paris, 1997, 1967, p 75-92.

4. VAN GEMERT, D, Versterken en herstellen van betonconstructies met gelijmde wapening, Cement, Vol 31, No 10, 1979, p 437-451.

5. VAN GEMERT, D, Repairing of concrete structures by externally bonded steel plates, ICP/ RILEM/IBK International Symposium 1981, Prague, Czech Republic, Material and Structural Engineering, p 559-570.

6. VAN GEMERT, D, VANDEN BOSCH, M, Durability of epoxy bonded external steel reinforcements, Proceedings of 3rd International Conference on the Durability of Building Materials and Components, 12-15 August, 1984, VTT Symp, Vol 2, Espoo, Finland, p 64-68

7. DE BUCK, J, VAN ESSCHE, T, VAN GEMERT, D, GAMSKI, K, DEGEIMBRE, R, RIGO, J M, WIERTZ, Konceptie, berekening en proefprogramma voor de herstelling van twee bruggen in voorgespannen beton, tijdschrift der openbare werken van België, No 2, 1981.

8. RANISCH, E H, Zur Tragfähigkeit von Verklebungen zwischen Baustahl und Beton - Geklebte Bewehrung, Heft 54, T.U.Braunschweig, 1982.

9. LADNER, M, WEDER, C, Geklebte bewehrung im stahlbetonbau, EMPA, Report 206, Dübendorf, Switzerland, 1981.

10. KAISER, H, Bewehren von Stahlbeton mit kohlenstoffaserverstärkten Epoxidharzen, ETH, Zürich, 1989.

11. VAN GEMERT, D, The plate bonding technique for solving concrete deterioration, International Seminar >Structural Repairs/Strengthening by the plate bonding technique=, 5-7 September, 1990, Sheffield, U.K.

12. AHMED, O, Strengthening of R.C. beams by means of externally bonded CFRP laminates - Improved model for plate end shear, Doctoral thesis, K.U. Leuven, 2000.

13. BROSENS, K, Anchorage of externally bonded steel plates and CFRP laminates for the strengthening of concrete elements, PhD thesis, K.U. Leuven, 2001, p 225.

14. IGNOUL, S, BROSENS, K, VAN GEMERT, D, Strengthening of concrete structures with externally bonded reinforcement - Practical applications in Belgium, International Congress: Challenges of Concrete Structures, Seminar 3: Repair, Rejuvenation and Enhancement of Concrete, Dundee, September 5-11, 2002.

15. KENDALL, D, The selection of reinforcing fibres for strengthening concrete and steel structures using reinforced plastics, Eight International Conference on Structural Faults & Repair - 99, July 13-15, 1999, London.

16. RIZKALLA, S H, SOUDKI, K A, Guide for the design and construction of externally bonded FRP systems for strengthening concrete structures, ACI Committee 440, May, 2000, p 90.

DURABILITY EVALUATION OF GFRP REINFORCED SPECIMENS USING ACOUSTIC EMISSION

R Birgul
University of Muğla
Turkey

G A Sayed
University of Windsor
Canada

H M Atkan
Wayne State University of Detroit
United States of America

ABSTRACT. An experimental investigation was conducted to examine the potential durability gain by replacing steel reinforcement with GFRP bars in buried concrete culverts. Four specimens with steel reinforcement and four specimens with GFRP bars were prepared. Two specimens of each group were subjected to a corrosive and ageing environment to simulate 25 years of accelerated ageing. Specimens were tested before and after ageing. GFRP reinforced specimens failed during the ageing process. Force-deformation data was acquired during testing. Analysis of the experimental data was built on the structural responses of the specimens. The behavior of each specimen was characterized by its response to deflection and crack width at certain level of loads.

Keywords: Durability, Culvert, GFRP, Ageing environment

Recep Birgul is an Assistant Professor in the Department of Civil Engineering at Muğla University of Muğla, Turkey.

George A Sayed is an Emeritus Professor in the Department of Civil engineering at University of Windsor, Canada

Haluk M Aktan is a Professor in the Department of Civil and Environmental Engineering at Wayne State University of Detroit, MI. U.S.A.

INTRODUCTION

One of the major causes of early deterioration of the concrete infrastructure is the corrosion of steel reinforcing bars. Efforts to find a solution to this problem have resulted in costly applications such as epoxy coating of rebars, additives to concrete, cathodic protection, etc. As a cost effective solution non-corrosive composites, namely fibre reinforced polymers (FRP), are increasingly being considered as a potential replacement for steel rebars. The exceptional characteristics of FRP bars suggest that these materials may be a replacement to steel in concrete. These characteristics include high resistance against corrosion, high strength-to-weight ratio and fatigue resistance. The idea is that the durability can be improved by replacing the steel reinforcement with FRP bars or grids in reinforced concrete structures. However, there exists a critical lack of fundamental data and understanding of their behavior in relation to traditional civil engineering materials. Moreover, low elasticity modulus and low ductility are their drawbacks and perhaps the reasons for the limited applications of FRP bars in concrete structures [1]. Although efforts to create a complete design code for FRP reinforced concrete is yet immature [2], research is being performed on the determination of the strength and failure modes [3-5] and on the determination of stiffness properties [6].

When design is governed by deflection of structural members, FRP bars are not desirable due to their low flexural rigidity. However, if the comparison is made on the basis of strength requirements, the cost of the structures with FRP bars (especially glass, GFRP) is close to that of with steel rebars. There is an added advantage of FRP reinforced culverts and similar buried structures. This is because of the behavior of buried structures that is governed by the degree of soil-structure interaction. The bending moment and shear forces are reduced in the walls of the structure due to the reduction of their flexural rigidity with the use of FRP bars.

Durability of RC structures is of prime concern as well as their cost effectiveness. Introduction and use of new materials in the structure has to be validated by its structural integrity over time.

EXPERIMENTS

GFRP and steel reinforced specimens representing culverts were made and tested. The experimental testing program included eight specimens, four specimens with steel reinforcement and four specimens with GFRP bars. Four of the specimens, two with steel reinforcement and two with GFRP bars, were subjected to accelerated ageing to compare the durability of GFRP and steel reinforced culverts. The first stage of tests was designed to evaluate if GFRP was an acceptable replacement for steel.

Experimental Specimens

The moment diagram obtained from the structural analysis of a buried culvert was used to design the shape of the experimental specimen. The specimen represented the portion of the culvert between two inflection points located at quarter points of the circumference. The specimen was loaded by a turnbuckle mounted on a tie rod and placed at the zero moment locations. The specimen was tested with one end hinged and the other one roller support as shown in Figure 1 with the instrumentation.

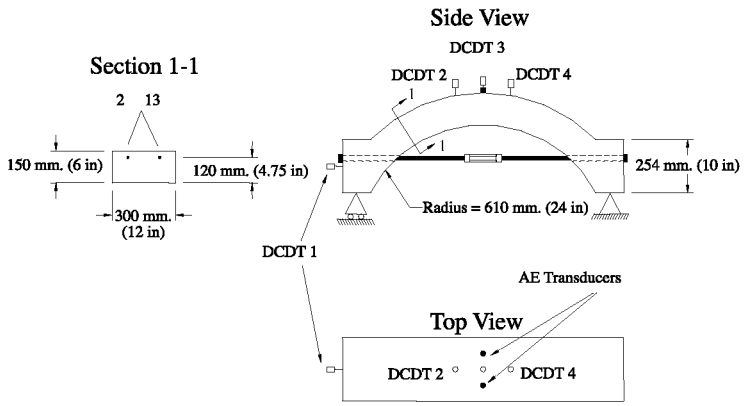

Figure 1 Experimental test specimen

Materials and Material Properties

The proportion of the concrete mix of cement:sand:gravel:water was 1: 2.36 : 2.73 : 0.45, and Type I Portland cement was used. Two sets of plastic concrete tests were made, and the averages showed that the concrete had an entrapped air of 2.1%, a slump of 50 mm (2"), and a unit weight of 2323 kg/m^3 (145 lb/ft^3). The average 28-day compressive strength was 54.6 MPa (7922 psi), the elasticity modulus and Poisson's ratio were: 33.8 GPa (4905 ksi) and 0.245, respectively. Additional cylinder specimens were prepared and kept in the ageing chamber and tested at 90-days. The average 90-day compressive strength of aged cylinders was 58.5 MPa (8,487 psi), the average modulus of elasticity; 36.3 GPa (5,272 ksi); and the Poisson's ratio; 0.241. The control samples were not kept in the ageing chamber, but were kept next to the control culvert specimens. Their average 90-day compressive strength was 60.8 MPa (8,822 psi), the average modulus of elasticity; 38.9 GPa (5,649 ksi), and the Poisson's ratio was 0.220.

The steel bars were tested in the lab. The elasticity modulus was 200 GPa (29,000 ksi), yield strength was 413.7 MPa (60 ksi) and ultimate strength was 620.5 MPa (105 ksi). The GFRP bars were procured from a manufacturer in Houston, TX and used for the specimens reinforced with GFRP. The composition for the type E glass fibre roving was reported to be 75% glass and 25% resin. Ultimate tensile strength and modulus of elasticity values were provided by the supplier as 689.5 MPa (100 ksi) and 49.6 MPa (7,200 ksi), respectively.

Experimental Procedure

All specimens were instrumented to monitor and record deflections and applied load. Direct Current Displacement Transducers (DCDT) were used to record the deflections. Four of the specimens were exposed to an ageing environment. In order to accurately simulate the ageing, it was required to leave the cracks open upon loading to a width of 0.25 mm.

In order to meet this requirement, the applied load must be retained during the ageing process. A turnbuckle instrumented as a load cell was designed both for load application and for load measurement. Four 5/8" turnbuckles (Figure 2) were instrumented using strain gages in full bridge configuration and calibrated.

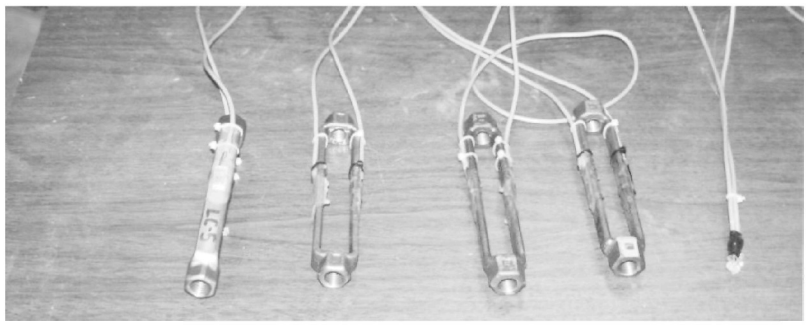

Figure 2 Turnbuckles instrumented for load measurements

During loading, the specimens were placed and secured on the supports. Four DCDTs were used to record the deflections: one at the mid-span, two on both sides of the mid-span and one at the roller support (Figure 1).

The load was applied using the turnbuckle, which also served as the load cell. Load was measured using the calibrated strain gages on the turnbuckle. The ends of the turnbuckle were reverse threaded. A force was created in the bowstring by twisting the turnbuckle.

Accelerated Ageing Procedure

The test specimens were exposed to intermittent wet and dry cycles. Each cycle consisted of 3 days' immersion in water with a 3.5-percent sodium chloride solution at 122 F (50 °C), and 3 days of drying at room temperature. The elevated temperature in water was used to provide the accelerated ageing environment. Litherland et al [7] have shown that one day immersion in water at 50 °C is equivalent to 101 days of natural weathering exposure in England where the mean annual temperature is 10.4 °C. To provide about 25 years of ageing, the time frame for the exposure to the ageing environment was 12 weeks. The ageing chamber is shown in Figure 3. Notice the cylinder samples of concrete that are currently in the off cycle along with the GFRP reinforced specimens in Figure 3.

In order to generate corrosive environment for reinforcing steel the ageing solution contained chloride ions. Corrosion does not occur if chloride concentration from external sources is below 0.60 kg/m^3 to 0.89 kg/m^3 (1.0 to 1.5 lbs/cu ya) of concrete. Obviously, It can take years or decades for this amount of chloride to collect near steel in uncracked concrete from externally applied salts. Thus, the reason for retaining the load on the specimen during the ageing process is to allow the cracks to remain open and speed up the chloride ingress.

Figure 3 General view of ageing environment

RESULTS

In pre-ageing tests on four culvert specimens, load was applied until a maximum allowed crack width of 0.25 mm (0.01 inch) was reached. STEEL01 and STEEL02 designate the specimens reinforced with steel whereas GFRP01 and GFRP02 denote the specimens reinforced with GFRP. The aged specimens were post-designated with an AGED suffix. They include STEEL-01-AGED and STEEL-02-AGED. Control specimens are designated by a CON suffix. They include STEEL-03-CON and STEEL-04-CON.

The summary of test results describing the measured bow load, bow deflection and crack width is given in Table 1. To describe the Table, several definitions are needed as follows:

- "Load @First Crack" is the load level immediately before the occurrence of the first crack
- "Deflection @First Crack" is the horizontal deflection of the structure (read by DCDT#1) at the time of occurrence of the first crack.
- "Crack Width @End of Test" is the width of the first crack

Table 1 Summary of Test Results for Unaged Specimens

	STEEL01	STEEL02	GFRP01	GFRP02
Load @First Crack, kN	24.88	21.75	20.74	24.59
Deflection @First Crack, mm	0.66	0.84	3.20	2.90
Crack Width @First Crack, mm	0.05	0.08	1.04	0.97
Load @End of Test, kN	60.10	62.35	26.16	24.19
Deflection @End of Test, mm	[3].81	3.99	10.52	7.29
Crack Width @End of Test, mm	0.33	0.25	2.13	2.49

All specimens reached cracking moment around the same load level. Once cracking load was reached, a crack appeared near the maximum moment region. The specimens reinforced with steel were loaded until a crack width of 0.25 mm (0.01 inch) or a little above this targeted value was achieved. At that crack width the maximum applied load for STEEL01 was 60.10 kN (13,512 lbf), and for STEEL02, it was 62.35 kN (14,017 lbf).

Cracking in GFRP specimens was significantly different than the cracking of steel specimens. Once cracking load was reached the one major crack that appeared, was significantly wider than that of the steel reinforced specimens; the width of this crack was 1.04 mm (0.041 inch). This first crack exceeded the design of the load application procedure. Load application for GFRP01 was continued until a second crack occurred at a load level of 22.04 kN (4,953 lbf). The width of the second crack was measured as 0.79 mm (0.031 inch). The first crack width widened to 1.60 mm (0.063 inch).

The additional crack in GFRP01 seemed to occur at or near the same bowstring force. At that point, a secondary objective was introduced that the specimens would be loaded after cracking to a minimum of the same force that was measured immediately prior to cracking. Thus, load application was continued and terminated around 26.16 kN (5,880 lbf), corresponding to a calculated 279.7 MPa (40.57 ksi) bow stress in the GFRP bar. At 26.16 kN (5,880 lbf) crack widths measured were 2.13 mm (0.084 inch) for the first crack and 1.63 mm (0.064 inch) for the second crack.

GFRP02 was loaded to 24.59 kN (5,528 lbf) with only one crack up to that load. The crack width was measured as 2.49 mm (0.098 inch) at a maximum load around 24.19 kN (5,439 lbf) with a calculated bow stress of 233.1 MPa (33.81 ksi) for the reinforcement.

Table 2 shows the results from testing of the specimens subjected to accelerated ageing. The "Max. Load" shown in the table corresponds to the bowstring force measured when the force plateau was reached. "Crack Width" is the width of the first crack at the maximum load. "Deflection" is the horizontal displacement of the free end of the specimen under the maximum load. Some values are designated as "Failure" due to specimen failure before the measurement could be made.

Table 2 Summary of test results for aged specimens

	STEEL01	STEEL02	GFRP01	GFRP02
Max. Load, kN	78.85	78.84	21.81	Failure
Deflection @ Max. Load, mm	7.24	7.11	Failure	Failure
Crack Width @ Max. Load, mm	0.81	0.69	Failure	Failure

The specimen GFRP02 failed during cyclical ageing process. After the third cycle in the ageing chamber, cracks were observed on the compression side of the specimen in the process of specimen alteration in and out of the ageing environment. Specimen GFRP01 survived the ageing process but failed catastrophically when the GFRP bar broke in tension at a bowstring force of 21.81 kN (4902 lbf) which corresponded to 235.1 MPa (34.1 ksi.).

Both steel reinforced specimens retained their structural integrity up to the expected force plateau and failed by yielding. The average bowstring force measured at the occurrence of the force plateau for the steel reinforced specimens was about 77.84 kN (17,500 lbf), which corresponded to 493.0 MPa (71.5 ksi.). The horizontal deformation was about 7.11 mm (0.28 inch) with the first crack width about 0.76 mm (0.030 inch). For comparison, two more specimens were made identical to the previous specimens. These control specimens were then used for comparison with specimens under investigation. In order to adequately provide comparison to both cases (pre-ageing and post-ageing), the control specimens had to be loaded by the same procedures and criteria that governed the loading of the investigative samples. Table 3 shows the cracking force, initial crack width and deflection as well as the maximum force, deflection and first-crack width of the steel reinforced control specimens. These values can be compared directly to the unaged properties shown in Table 1.

Table 3 Summary of initial loading test results for control specimens

	STEEL03(CON)	STEEL04(CON)
Load @First Crack, kN	20.20	20.17
Deflection @First Crack, mm	0.71	0.66
Crack Width @First Crack, mm	0.15	0.08
Load @End of Test, kN	45.97	46.12
Deflection @End of Test, mm	4.06	4.75
Crack Width @End of Test, mm	0.33	0.31

Capacity loading tests were also performed on the control specimens. These tests consisted of loading the specimens until a plateau in the force/deformation relationship was reached. Table 4 shows the capacities of the control specimens. This table can be directly compared to Table 2. Once again, the maximum load was the bowstring force at the point where the deformation increases rapidly compared to any gain in force. At this point the average width of the first crack (that one which was the first to appear on the surface of the specimen) was reported as the crack width and the corresponding horizontal displacement was measured as the deflection at maximum load.

Table 4 Summary of capacity loading test results for control specimens

	STEEL03(CON)	STEEL04(CON)
Max. Load, kN	71.06	67.26
Deflection @ Max. Load, mm	10.21	11.66
Crack Width @ Max. Load, mm	0.84	0.69

CONCLUSIONS

The comparative responses of RC culverts reinforced with steel and GFRP bars were examined. The behavior of each culvert was characterized by its response to deflection and crack width at certain level of loads. The test results clearly show that the deflections and crack widths are similar for both steel and GFRP reinforced culverts until cracking moment is

reached. After cracking, the behavior is dependent on the type of reinforcement used. Culverts reinforced with GFRP bars show much larger deflections than culverts with steel reinforcement due to the low elasticity modulus of GFRP bars. Cracking behavior also differed significantly. Specimens reinforced with steel had evenly distributed cracks with crack widths of below the maximum value of 0.25 mm (0.01 inch) at a load level of around 61.21 kN (13,760 lbf). GFRP reinforced specimens had one major crack with a crack width of eight or nine times larger than the limiting value of 0.25 mm (0.01 inch) at a load level of around 25.18 kN (5,660 lbf).

One of the GFRP reinforced specimens failed during the ageing process. The other investigative sample reinforced with GFRP bars survived the ageing process, however, failed early in the post ageing loading phase catastrophically. The failure of the GFRP reinforced specimens was presumed to be due to alkali attack on the glass fibres. The test program also showed severe effects of having sustained stresses in GFRP bars in the order of 36 % of ultimate stress on the deterioration due to the alkaline reaction with the glass fibres. This justifies the low limits placed on the stresses allowed in GFRP bars by the ACI 440.1R-01, Emerging Technology Series, "Guide for the Design and Construction of Concrete Reinforced with FRP Bars (May 2001)". It may also be noted that the degree of alkaline resistance of GFRP bars differ considerably between different manufacturers using different glass fibres and/or different matrices.

REFERENCES

1. TOUTANJI A. H., SAAFI M., Flexural Behavior of Concrete Beams Reinforced with GFRP Bars, ACI Structural Journal, Sept-Oct 2000, pp 712-718

2. GRACE N.F., SOLIMAN A.K., ABDEL-SAYED G., SALEH K.R., Behavior and Ductility of Simple and Continuous FRP Reinforced Beams, Journal of Composites for Construction 2:4, 1998, pp 186-194

3. AN W., SAADATMANESH H., EHSANI M.R., RC Beams Strengthened with FRP plates. II: Analysis and Parametric Study, Journal of Structural Engineering 2:11, 1991, pp 3434-3455

4. DESKOVIC N., TRIANTAFILLOU T.C., MEIER U., Innovative Design of FRP Combined with Concrete:Short-Term Behavior, Journal of Structural Engineering 121:7, 1995, pp 1069-1078

5. DESKOVIC N., TRIANTAFILLOU T.C., MEIER U., Innovative Design of FRP Combined with Concrete:Long-Term Behavior, Journal of Structural Engineering 121:7, 1995, pp 1079-1088

6. RAZAQPUR A.G., SVECOVA D., CHEUNG M.S., Rational Method for Calculating Deflection of FRP Reinforced Beams, ACI Structural Journal, Jan-Feb 2000, pp 175-183

7. LITHERLAND K.L., OAKLEY D.R., PROCTOR B.A., The Use of Accelerated Ageing Procedures to Predict the Long-Term Strength of GRC Composites, Cement and Concrete Research 11, 1981, pp 455-466

SPACING AND WIDTH OF CRACKS IN POLYMER MODIFIED STEEL FIBRE REINFORCED CONCRETE FLEXURAL MEMBERS

N Ganesan

Regional Engineering College

K P Shivananda

Sidda Ganga Institute of Technology

India

ABSTRACT. A method has been proposed to determine the spacing and width of cracks in polymer modified steel fibre reinforced concrete flexural members. Totally 16 beams of 125 x 200 x 2000 mm were cast and tested. The polymer considered in this study was natural rubber latex. Three different values of percentages of volume fraction of steel fibres (V_f) ie 0.5, 1.0 and 1.5 and three different percentages of dry rubber content (DRC) ie 0.5, 1.0 and 1.5% were used as variables. The computation indicated that the presence of latex and steel fibres influences strain in steel. Hence a correction factor F to that effect was introduced in the proposed method. With the corrected values of steel strains, the maximum width of cracks have been computed and compared with the experimental values obtained in this study. The proposed method for computing the spacing and maximum width of cracks was found to compare satisfactorily with the experimental results.

Keywords: Cracking, Crackwidth, Crack propagation, Bending moment, Computation, Fibre reinforced concrete, Polymer, Strains, Strength of materials.

N Ganesan is currently working as Professor of Structural Engineering at the Regional Engineering College, Calicut, India. He is a Fellow of The Institution of Engineers, India. His field of research includes reinforced concrete, ferrocement and steel fibre concrete, fracture mechanics and infilled frames. He has published more than 50 research papers in National and International Journals and Conferences.

K P Shivananda is working as Assistant Professor in the Department of Civil Engineering of S I T, Tumkur, India. His field of research includes reinforced concrete, steel fibre and polymer concrete.

INTRODUCTION

Strength and ductility are the two important factors to be considered in the design of structures subjected to large deformations. Hence many attempts have been made in the recent past to develop new materials which exhibit higher strength and ductility. Incorporation of steel fibres into cementitious materials like mortar and concrete has been found to improve the structural properties of ductility, energy absorption capacity, post crack resistance, dimensional stability etc. of the composite [1-3]. Also the recent studies on polymer modified concrete indicate that the addition of natural or synthetic polymers up to a certain percentage enhances the strength, toughness, post peak load deflection characteristics and durability of concrete [4,5]. However no attempts have been found on the combined effect of steel fibres and natural polymers on the strength and behaviour of conventional concrete. Recently the authors carried out a large scale investigation on the combined effect of steel fibres and latex (natural polymer) on the strength and ductility of reinforced concrete flexural members. As cracking is one of the important limit states in the limit state design of reinforced concrete structures, an attempt is made to predict the spacing and width of cracks in the latex modified steel fibre reinforced concrete flexural members.

PROPOSED METHOD

The method proposed in this study follows the one proposed earlier by Desayi and Ganesan [6] for reinforced concrete flexural members which is primarily based on the bond-slip hypothesis. In order to account for the effect of steel fibres and latex, suitable modifications are introduced.

Desayi and Ganesan [6] considered a concrete member with a reinforcing bar under tension and explained the formation of new crack at section XX (Figure 1) which is at a distance l_1 from an already formed crack. A new crack could form at this section when the bond force developed by the bar causes a maximum stress equal to the tensile strength of concrete at this section. Based on the statistical analysis of a number of test results, they obtained the following equations for spacing and maximum width of cracks in reinforced concrete flexural members.

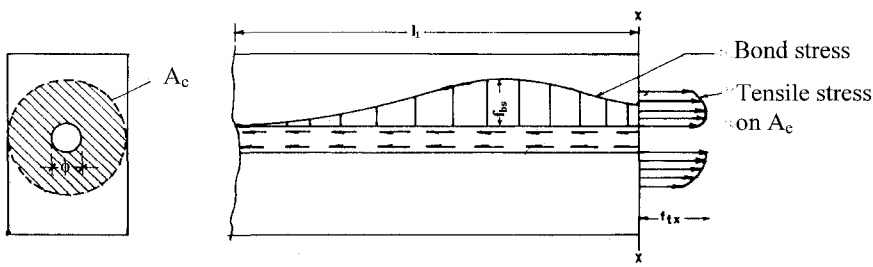

Figure 1 Bond and tensile stress distribution in concrete at a section distance l_1 from a crack formed in a reinforced concrete member

Average crack spacing, $$a_c = \frac{k_t f_{ct} A_e}{K_b f_{bu} \left[\frac{M}{M_u}\right]^{\gamma} \sum \pi\phi} \quad (1)$$

Maximum crack spacing, $$a_m = \frac{k_t f_{ct} A_e}{K_b f_{bu} \left[\frac{M_{cr}}{M_u}\right]^{\gamma} \sum \pi\phi} \quad (2)$$

Maximum crackwidth at the soffit,

$$W_{bt} = a_m \epsilon_s \frac{(h-x)}{(d-x)} \quad (3)$$

MODIFICATIONS PROPOSED IN THIS STUDY

It may be noted from Equation 3 that, for a given beam, all the parameters of Equation 3 are constant except the strain in steel ϵ_s which depends on the external load. This was obtained based on elastic cracked section theory. Since the steel strain is an important parameter for estimating the width of cracks in the case of reinforced concrete members, an attempt is made to compare the values of strain computed based on the cracked section theory with that of experimental values.

The stress in steel (f_s) at any moment, M, after cracking is [6],

$$f_s = m\frac{M}{I_{cr}}(d-x) \quad (4)$$

The strain in steel ϵ_s corresponding to the stress f_s is

$$\epsilon_s = \frac{f_s}{E_s} \quad (5)$$

where $$m = \frac{E_s}{E_c} \quad (6)$$

The computed values of ϵ_s from Equations 4 and 5 are compared with the experimental values obtained from the test results.

TEST RESULTS

The experimental programme consisted of casting and testing of 16 latex modified reinforced concrete beams of 125 x 200 x 2000 mm size under third point loading. The main variables considered in this study are:

(i) Three different values of percentage of volume fraction (V_f) of steel fibres (0.5, 1.0 and 1.5%)

(ii) Three different values of volume fraction of dry rubber content (DRC) of latex (0.5, 1.0 and 1.5%)

The aspect ratio of steel fibres used in this investigation was kept constant for all the specimens and is 50. The reinforcement used were high yield strength deformed bars of three numbers of 12 mm diameter in the tension zone and two 8 mm diameter in the compression zone. The shear reinforcement consists of 2 legged 6 mm diameter stirrups at 75 mm centres in the shear span and 150 mm centres in the flexure span. Ordinary Portland cement of 43 grade conforming to IS:8112-1989 was used. River sand passing through 4.75 mm IS sieves conforming to grading zone III and crushed stone with a nominal maximum size of 20 mm and having a fineness modulus of 6.8 were used as aggregates. A concrete mix proportion of 1:2:4 by weight with a water cement ratio of 0.45 by weight was used. The polymer used in this investigation was natural rubber latex having a dry rubber content of 41% by weight. To prevent early coagulation of latex and to disperse the latex molecules uniformly in concrete, a water reducing super plasticizer was used while mixing the natural rubber latex with concrete. The details of casting and testing were presented elsewhere [5].

Figure 2 shows the plot relating to the experimental values of strain at the level of steel with the computed values of strain ϵ_s. From the plot, it may be noted that, the equation for computing the values of strain (Equations 4 and 5) over estimate the strains. This may be due to the following reasons. In the case of latex modified steel fibre reinforced concrete members, the steel fibres and latex in the tension zone increase the elastic deformation of the material surrounding the main reinforcement. Also the stiffening effect of latex modified steel fibre concrete between cracks at initial stages is high when compared to that of plain concrete. This results in significant reduction of strain in steel. The conventional method of computing strain in steel, based on cracked section theory overestimates the values of strain in the case of latex modified steel fibre concrete members as the stiffening effect in between cracks is not taken into account.

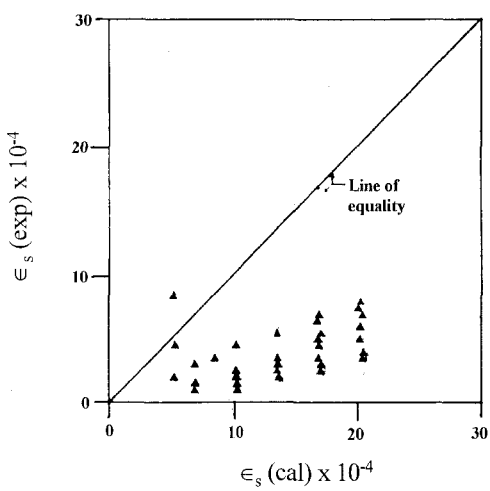

Figure 2 Comparison of experimental strain with calculated strain

As several variables such as effective area of concrete in the tension zone, volume fraction and aspect ratio of steel fibres, addition of latex and tensile force in steel influence the stiffening effect of concrete, an attempt is made to obtain a parameter which gives the combined effect of all these variables. A parameter known Latex – Fibre index (F) was introduced after trying several combinations of these variables to evaluate the strain in steel in the case of latex modified steel fibre concrete. The factor F takes into account geometrical and mechanical properties which were thought to affect cracking behaviour of the member. The factor F is given by,

$$F = \frac{b(h-x) f_{ct} A_f V_f L_e}{A_s f_s 10^6} \quad (7)$$

In the above equation the contribution of matrix is incorporated in the form of b (h-x) f_{ct} which represents the tensile force in the matrix. The amount of steel fibres which increases the elastic deformation of the matrix, surrounding the tensile reinforcement, is an important parameter and is represented by the combination of volume fraction and aspect ratio of fibres, V_f and A_f respectively. The presence of latex is represented by L_e. As the tensile force in steel is also another important parameter, it is incorporated in the equation by the term $A_s f_s$.

The values of $\epsilon_{s\,(cal)} - \epsilon_{s\,(exp)}$ are plotted against the correction factor F and is shown in Figure 3. The regression equation for the plot is obtained and is

$$\epsilon_{s\,(cal)} - \epsilon_{s\,(exp)} = 1400\,F^2 - 5.0F + 5.5E\text{-}4 \quad (8)$$

As the experimental strain should be equal to the corrected strain, $\epsilon_{s\,(exp)}$ is replaced on the LHS by $\epsilon_{s\,(cor)}$ and thus,

$$\epsilon_{s\,(cor)} = \epsilon_{s\,(cal)} - (1400\,F^2 - 5.0F + 5.5E\text{-}4) \quad (9)$$

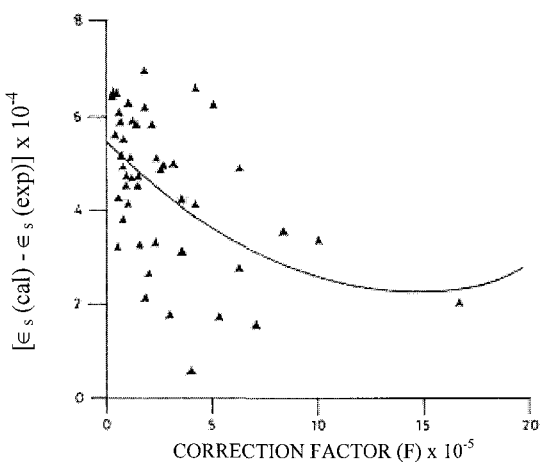

Figure 3 Plot [ϵ_s(cal) - ϵ_s (exp)] versus correction factor (F)

Figure 4 shows the variation of corrected strain $\epsilon_{s\,(cor)}$ with the experimental strain. From the figure it can be seen that the Equation 9 satisfactorily predicts the strain in steel in the case of latex modified steel fibre reinforced concrete members. The Equation 3 for determining the maximum crackwidth at the soffit is modified by replacing ϵ_s by $\epsilon_{s\,(cor)}$ and is given as follows:

$$W_{bt} = a_m \epsilon_{s\,(cor)} \frac{(h-x)}{(d-x)} \qquad (10)$$

Equation 10 is used to obtain the maximum crackwidth at the soffit and these values are compared with the measured width of cracks.

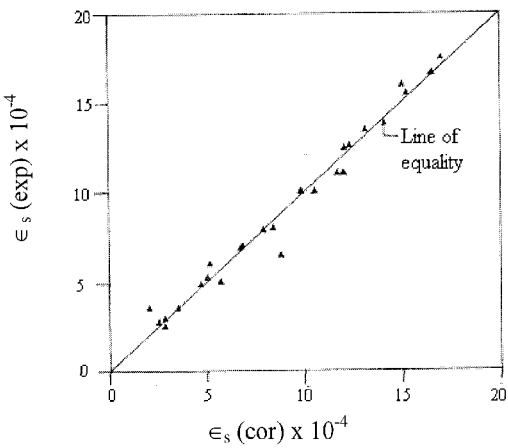

Figure 4 Comparison of experimental strain with calculated strain after modification

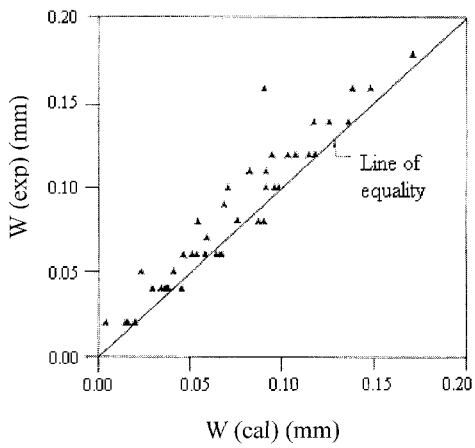

Figure 5 Comparison of W (exp) with W (cal) after modification

Figure 5 shows the plot relating the values of W_{cal} with W_{exp} and most of the points are close to the line of equality. Table 1 gives the average values of $W_{(cal)}/W_{(exp)}$ and coefficient of variation. It may be noted that the proposed method underestimates the values of crackwidth by 10% with a coefficient of variation of 19.2%. As cracking in reinforced concrete members is a random phenomenon and subjected to a large degree of scatter, the comparison may be considered to be satisfactory.

SPACING OF CRACKS

The earlier studies on spacing of cracks in the case of steel fibre reinforced concrete indicate that the addition of steel fibres have negligible effect on the crack initiation [5]. The fibres play a vital role only after the cracking of matrix in extreme tensile zone by bridging across the faces of cracks which in turn causes reduction in the widening of cracks and delay the propagation of cracks. Also the addition of latex improves the strength, ductility, energy absorption capacity of conventional concrete.

In view of the above, the existing equation for spacing of cracks in the case of plain reinforced cement concrete (without steel fibres and latex) has been used to compute the crack spacing. The computed values of spacing of cracks using Equation 1 have been compared with the experimental values. Table 2 gives the average value of the ratio of computed spacing of cracks to the experimental values and the coefficient of variation. It may be noted that the proposed equation under estimates the values of spacing of crack by 6% with a coefficient of variation of 29.25%. Figure 6 shows the plot of computed and experimental values of average spacing of cracks. From the figure it may be noted that most of the points lie around the line of equality and this indicate that the Equation 1 predicate the average spacing of cracks in latex modified steel fibre reinforced concrete flexural members satisfactorily.

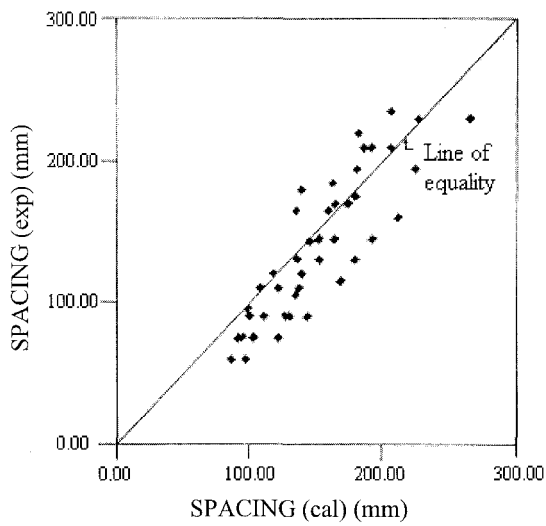

Figure 6 Comparison of computed crack spacing with experimental crack spacing

Table 1 Comparison of maximum crackwidth computed using the proposed method with the test results

EQUATION	NO OF OBSERVATIONS	W_{cal}/W_{exp}	
		Average	Coefficient of variation, %
Proposed method	47	0.9	19.2

Table 2 Comparison of spacing of cracks computed with the test results

EQUATION	NO OF OBSERVATIONS	SPACING (CAL)/SPACING (EXP)	
		Average	Coefficient of variation, %
Proposed method	47	0.94	29.25

CONCLUSIONS

A method has been proposed for predicting the spacing and maximum width of cracks in latex modified steel fibre reinforced concrete flexural members. The values of spacing and width of cracks computed using the proposed method compare satisfactorily with the test results.

NOTATION

A_e - Effective area of concrete in tension
A_f - Aspect ratio of fibres
A_s - Area of main reinforcement
a_c - Average crack spacing
a_m - Average spacing of cracks when they have just formed
b - Width of section
d - Effective depth
E_c - Modulus of elasticity of concrete
E_s - Modulus of elasticity of steel
F - Latex – fibre index
f_s - Stress in steel
f_{ct} - Tensile strength of concrete
h - Overall depth of section
K_b - Factor giving average bond stress
K_t - Factor giving average tensile stress
M - Bending moment
M_{cr} - Moment at cracking
M_u - Ultimate moment

m	-	Modular ratio
V_f	-	Volume fraction of fibres
W_{bt}	-	Maximum crack width at soffit
x	-	Neutral axis depth of cracked section
ϵ_s	-	Strain in steel
γ	-	a constant
ϕ	-	diameter of bar

ACKNOWLEDGMENTS

The authors would like to acknowledge the financial support provided for the research project by the Indian National Committee on Construction Materials and Structures (INCCMS), Ministry of Water Resources, Government of India and the Principal, Regional Engineering College, Calicut, India.

REFERENCES

1. RAMAKRISHNAN,V, Materials and properties of fibre reinforced concrete, Proc of ISFRC, Vol, Dec , 16-19, 1987, Madras, India, pp 2.3-2.24.
2. SHAH, S P, VIJAYARANGAN, B, Fibre reinforced concrete properties, ACI Journal, Vol 1, Feb 1971, pp 126-135.
3. KUMAR, V et al, Rotational capacity of SFRC beams with equal reinforcement on tension and compression faces, Journal of Structural Engineering, Vol 22, No 3, Oct 1995, pp 129-134.
4. NAGARAJ, T S, IYENGAR, K T S, AMESWARA R A O, B, Super plasticized natural rubber latex modified concrete, International Journal of Cement and Concrete Research, No 1, Jan 1988, pp 138-144.
5. GANESAN, N, SHIVANANDA K P, Strength and ductility of latex modified steel fibre reinforced concrete flexural members, Journal of Structural Engineering, Vol 27, No 2, July 2000, pp 111-116.
6. DESAYI, P, GANESAN, N, An investigation on spacing of cracks and maximum crackwidth in reinforced concrete flexural members, Materials and Structures, RILEM, Vol 18, March-April, 1985, pp 123-133.

INTERACTION OF ELASTIC WAVES WITH FIBRE REINFORCED CONCRETE

M J Katwan
Mustansarya University
S S Abdulnoor **Y K Al-Ani**
University of Technology Baghdad University
Iraq

ABSTRACT. An elastic wave would interact with the medium it propagates through, and this interactive process may result in an energy exchange, the amount of which depends on the nature of the propagating wave and that of the medium. In this work two series of fibre reinforced concrete composites were prepared containing steel and polypropylene fibres separately at various volume fractions. The measured pulse velocity was found to vary directly with the curing age, and inversely with fibre volume fractions. While the attenuation coefficient was found to vary directly with fibre volume fraction and inversely with curing age. Moreover, the attenuation coefficient was found to vary directly with the frequency of the propagating wave which might be due to the associated reduction of the wave length. The overall behaviours was found to depend on the degree of rigidity of the medium, the type of reinforcing fibres, and on how the wave length of the propagating ultrasonic wave is correlated to the geometry of the constituents of the composite medium.

Keywords: Elastic waves, Polypropylene fibre, Steel fibre, Fibre reinforced concrete, Pulse velocity, Attenuation coefficient

Dr Moufaq J Katwan is the Assistance Professor, Collage of Engineering, Al-Mustansarya University, Baghdad, Iraq. He obtained his Ph.D. degree in Civil Engineering from the University of Glasgow, UK, 1988. His research interests are Corrosion Fatigue of Reinforced Concrete and Durability of Concrete Structures. He is the editor of two books and the author of one book and more than 65 technical papers and reports.

Dr Sabah S Abdulnoor obtained his Ph.D. in materials from Salford University 1973. Worked in the industrial sector as a chief researcher until 1997. Presently he is an assisstant Professor in material sciences at the department of Applied sciences-University of Technology in Baghdad- Iraq.

Dr Yaser K Al-Ani obtained his M.Sc. in material sciences in 1994 from Baghdad University, after several years working in material research in the industrial sector, he obtained his Ph.D. in the same line from Baghdad University. Presently working in research in the Iraqi industrial sector.

INTRODUCTION

Ultrasonic waves are forms of vibration which have high frequency beyond the range of human hearing (> 16000 Hz). In this range of frequency the sound waves behave, in many aspects, as light waves except that they can not travel in the space [1,2]. These waves are generated by exciting a piezo electric crystal with a high voltage pulse. The wave is then transmitted through the test material which is in contact with a second crystal sensor, a piezoelectric crystal which produces an emf. output when subjected to mechanical pressure [1, 2].

Depending on the cut of the crystals and the coupling used, the waves transmitted as a propagating set of compressional or shear stresses through the material. Accordingly these two types of waves are referred to as pressure waves and shear waves. In the concrete industry, compression waves have been used for most ultrasonic testing [3]. The use of ultrasonic pulse velocities to monitor the quality of concrete has been increasingly accepted in recent years and a British Standard on the subject has existed since 1974 [4].

Attenuation or damping is the conversion of some fraction of elastic energy into heat, as a result of the anelasticity of a medium. Damping may also be defined as that property of the material which causes its vibration energy to decrease even when the specimen is isolated from all external disspative forces [5]. Hence, as the wave propagates through a material it will lose energy, which may be measured as a loss of signal amplitude. The mechanism for the energy loss may be explained in terms of absorption processes in addition to scattering processes [6]. Absorption processes may be initiated by dislocations within the medium or by thermoelastic interaction within the solid. On the other hand, scattering can occur from features such as grain boundaries, voids, inclusions, and micro and macro cracks [6]. Attenuation may be explained by

$$\alpha(f) = \alpha_a (f) + \alpha_s (f) \tag{1}$$

where:

α_a (f) : Absorption contribution

α_s (f) : Scattering contribution; to the total attenuation

f : Frequency.

The above coefficients are frequency dependent.

In non-metals the losses appear to arise from two main sources: the first is a set of mechanisms responsible for the static hysteresis loss which occurs when a specimen is subjected to a complete stress cycle. In concrete this loss is thought to provide the major contribution to the damping process. It is associated with the presence of voids, cracks and imperfections at the bond between aggregate and cement paste. The second source is attributed to viscous losses arising from velocity gradients during vibration. This effect is likely to be relatively small in concrete [7].

Ultrasonic pulses travelling through a concrete bulk are always subject to considerable scattering. Because concrete is essentially a multiphase material and ultrasonic pulses would partially be reflected at every interface between matrix and aggregate [8]. The factors affecting the damping nature of concrete are: stress level, the presence of micro cracks, curing conditions of concrete, loading frequency, and mix proportions [9].

Wimal Suaris et al [10], using ultrasonic pulse attenuation as a tool for assessing the extent of crack growth during cyclic loading of concrete, observed that the amplitude attenuation of wave form was much more sensitive to crack growth than the widely used pulse velocity technique. Mark [11], used the latter technique to measure two important features of fracture in notched concrete beams. The authors [12, 13] have also utilized the ultrasonic pulse technique to determine the dynamic mechanical parameters of various concrete composites. They found that the amplitude of a propagating ultrasonic wave have declined with increasing presence of reinforcing fibres, suggesting an increased dissipation of the incoming wave energy within the bulk.

RESEARCH SIGNIFICANCE

Compositing of concrete with various fibres has been reported to initiate energy absorption of an incoming vibration, but the mechanism of this process is not properly understand. It is not clear if what is applicable to vibration would also apply to ultrasonic waves. Moreover, the process of reinforcing a brittle concrete matrix with ductile steel or polypropylene fibres, would result in a matrix of different mechanical properties. It is not known, however, how much would the new bulk follow the well known rule of mixtures, and what are the factors affecting the degree of it's applicability.

The present work aims at studying the interaction of the elastic compressional waves with the bulk of various concrete composites, and to investigate the effect of fibre type and volume fractions on the velocity of an ultrasonic wave propagating through the composite

EXPERIMENTAL PROGRAM

The laboratory tests were conducted on (100x100x400 mm) composite specimens. The materials used were Type I Portland cement, natural sand and crushed gravel. The mix proportion was 1:1.6:1.8 respectively with w/c ratio of 0.45. Maximum size of coarse aggregate was 12.5 mm. The size selection was aimed at optimizing workability and to ensure uniform fibre dispersion [14]. Two types of fibres (fibrillated polypropylene and crimped steel fibres) were examined. Mixing of concrete ingredients was conducted in a pan mixer and the compaction was carried out using a vibrating table. Plain and fibre reinforced concrete were cast in steel molds and kept under room temperature conditions for 24 hours. The moulds were then stripped and the specimens were cured in water. Tests were performed after (3, 7 and 28) days to obtain the dissipation energy of the elastic waves travelling through concrete composites. Each data point in this paper represents the average of the test results obtained from three identical specimens. The scatter of the results, however, has been very limited. The ultrasonic system used was as shown in Figure 1. The time interval required for a compression pulse to pass through a specimen, of known length "L" is used, to calculate the compresional elastic wave velocities using the formula.

$$V = \frac{L}{t} \tag{2}$$

Where:

V: Pulse velocity (m/sec).

t : distance travel time (sec).

In this study, the device OYO-SONIC VIEWER, Model 5217A, was utilized to measure the velocity of compression waves, using various ultrasonic frequencies. P-wave crystals with frequencies (37, 54, 66, and 150 kHz) were used for the axial direction.

In concrete industry, the compression waves have been used exclusively for ultrasonic testing and this was attributed to the difficulties associated with coupling shear transducer and also to the higher attenuation characteristics of shear waves.

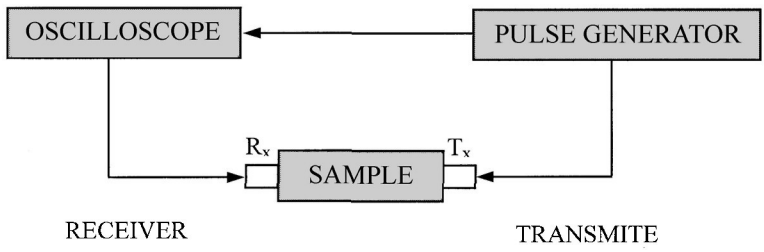

Figure 1 Ultrasonic pulse measurement system

In most attenuation measurements the data are commonly used to determine the attenuation coefficient, which is the exponential decay of amplitude of a plane wave travelling through the media.

$$\alpha d = 20 \log \left(\frac{A1}{A2}\right) \quad \text{decibel (dB)} \qquad (3)$$

where:

α : Attenuation coefficient.
d : distance.
(A1, A2): The amplitude of the compression wave at the beginning and the end respectively.

RESULTS AND DISCUSSION

The present work involves a non-destructive investigation of fibre-reinforced concrete composites using ultrasonic waves travelling through the bulk of these composites. The expected data covers the attenuation behaviour of these composited media and the mechanisms of absorbing energies associated with these mechanical waves.

Attempt was made to correlate a number of dynamic mechanical parameters to the ultrasonic wave interaction with the medium it is travelling through. It has been demonstrated [13] that the amplitude of the compressional waves have generally varied inversely with increasing content of fibre volume fraction.

Attenuation Coefficient

The correlation between the curing time of the concrete matrix and the attenuation coefficient (α) is shown in Figure 2. It is clear that longer curing periods would lead to a reduced value of (α). Moreover, the set of curves presented in Figure 2 also indicates that higher fibre volume fraction leads to greater attenuation coefficients. Both types of reinforcing fibres

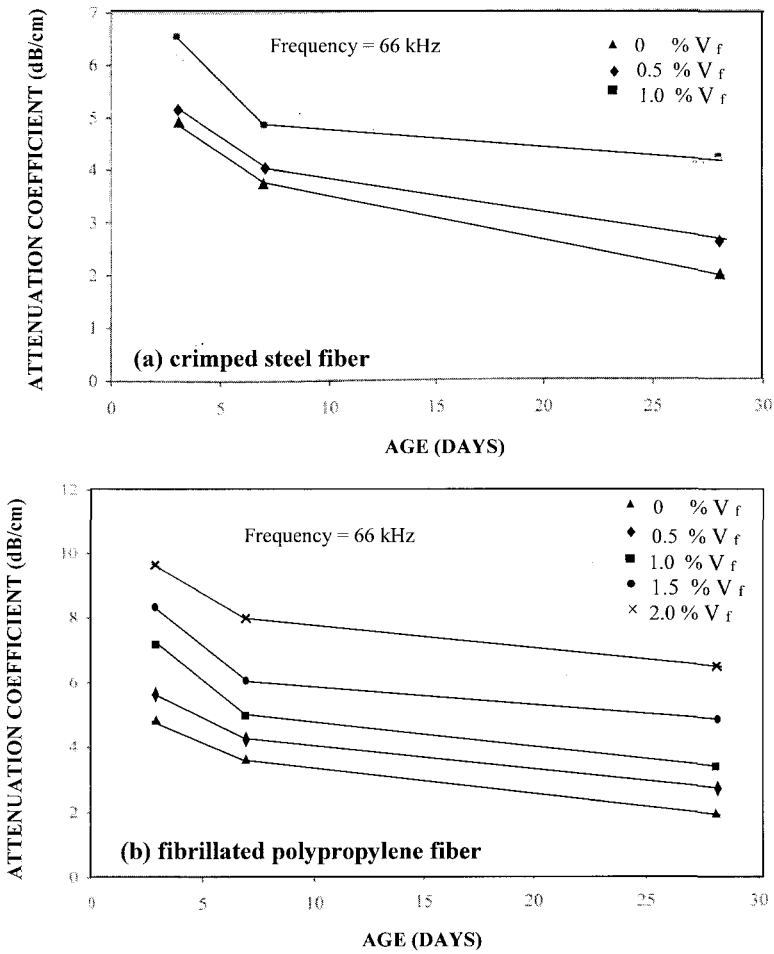

Figure 2 Attenuation coefficient of concrete composite containing various volume fraction of fibres compared to plain concrete

This behaviour is readily explainable in terms of continued hydration process which progressively changes the internal structure of the cement paste to a more dense medium, hence supports the mobility of the travailing mechanical wave. Accordingly less energy is lost during the particles movement in the direction of oscillation. Moreover, bonding between the matrix and the fibres has added to the role played by the fibre in bearing the compressive

stresses applied to the medium. It has been concluded [15] that polypropylene fibres would not sustain the compressive stresses as good as steel fibres do. This would suggest that the presence of polypropylene fibres through the matrix would in many ways resemble the state of ordinary pores. Thus, allowing the particles of the bulk to oscillate more freely than in the case of steel fibre reinforcement, leading to higher energy absorption.

The frequency of the travelling ultrasonic compressional elastic waves may also be correlated to their state of attenuation. It was found that for each composite geometry there was a certain range of frequencies which were considered suitable for experimentation. In our case the frequency of (66) kHz was found to be the most suitable for this investigation, beyond which the results tended to be distorted. In Figure 3 the attenuation coefficient is shown as a function of the frequency of the travelling ultrasonic waves.

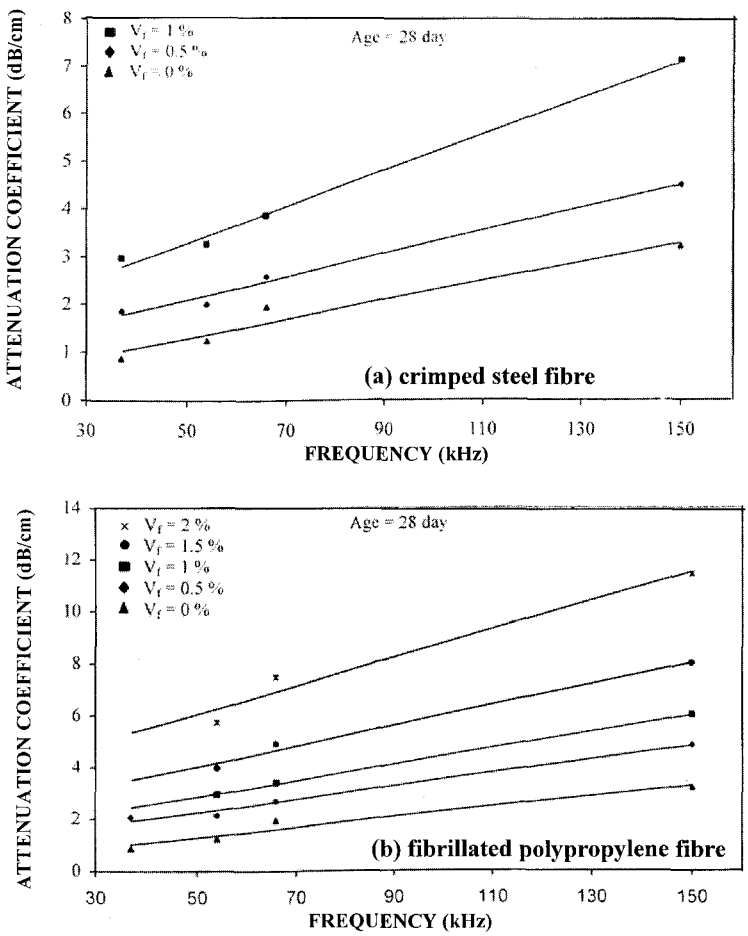

Figure 3 Relationship between attenuation coefficient of various concrete composites and frequency

The general behaviour is a direct relationship, where higher frequencies seem to result in higher coefficients. This may be due to two factors, the first is that higher frequencies would result in a larger number of compression and expansion regions within the bulk of the medium. Generally, in these compression regions the particles of the bulk are compressed, thus the temperature of that region is raised by the energy absorbed from the mechanical wave. However, when these particles interchange regions and reside in an expansion region, this heat will be lost to the bulk of the composite. The second point is that higher frequencies are normally associated with shorter wavelengths of the travelling ultrasonic waves. Therefore as the wavelength gets shoter, it will approach the sizes of constituents of the bulk such as voids interfaces and fibres. Thus, the travelling wave will resonate or make these constituents oscillate and the energy will transfer to the medium.

Moreover, it is also noticeable that higher fibre volume fractions have resulted in higher values of attenuation coefficients, but this increase is more pronounced in the case of polypropylene fibres. In general, fibres act in a way which enhances the scattering of the travelling ultrasonic wave. In fact the nature of the fibre could play an important role in this process. For steel fibres whose density is much higher than that of the matrix, the waves will travel through the faster route, and the fibres will act as shorter cuts. But the randomness of their directions will cause the wave to scatter of their paths. The polypropylene fibres have a much lower density than the matrix and thus would act as a void, since polypropylene is not expected to share matrix in bearing any external stress. This would result in a much more effective wave scattering process.

Pulse Velocity

To further correlate the properties of the travelling waves and those of the media, the pulse velocity is plotted in Figure 4 as a function of the degree of curing (aging time) of the concrete matrix.

The results clearly demonstrate that longer curing period i.e. greater hydration process would facilitate quicker wave travelling through concrete. However, the pulse velocity and the fibre volume fraction seem to vary in an inverse manner. Generally, the ultrasonic waves tend to travel in as straight paths as possible, in the absence of any impedance. However, when the travelling medium contains some inhomogeneieties then the resulting scattering will prolong the path and the time taken by the wave to cross the medium. This is more pronounced in the case of polypropylene fibre as discussed earlier.

Dynamical Properties

The measured pulse velocities were used to determine the dynamic elastic modulus of the various composites [12] and their correlation is plotted in Figure 5. The curves indicate, as expected, that higher values of the dynamic young moduli will be found in more rigid bodies. Thus higher pulse velocities would be associated with more rigid media.

Consequently, the attenuation coefficients are found to vary inversely with dynamic young modulus as shown in Figure 6. This may be viewed in terms of the densification of the travelling medium, where those with lower young moduli would be expected to absorb more energy of the travelling wave.

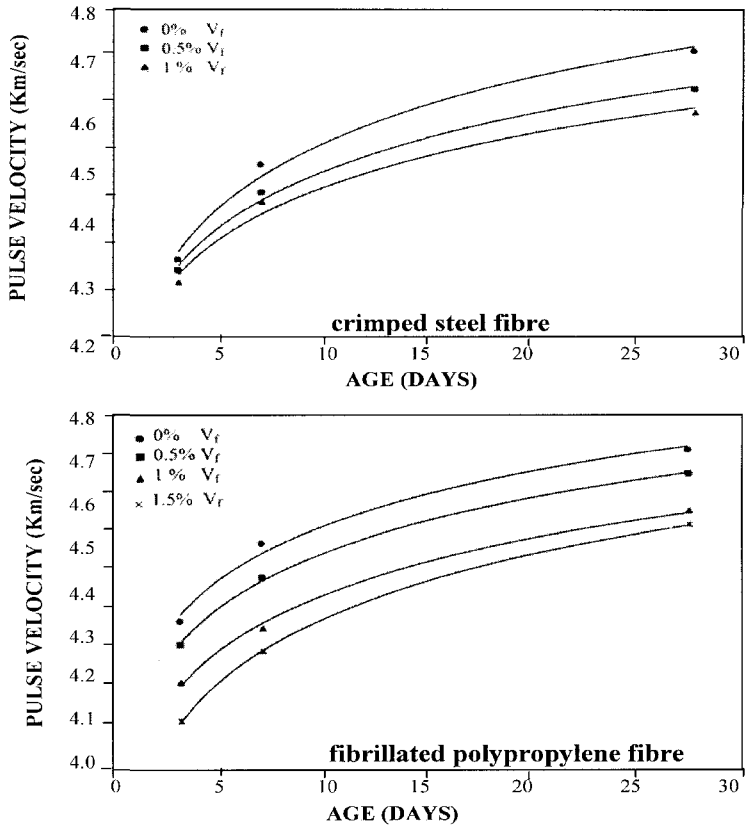

Figure 4 Pulse velocity of concrete composites containing various volume fractions of fibres compared to plain concrete.

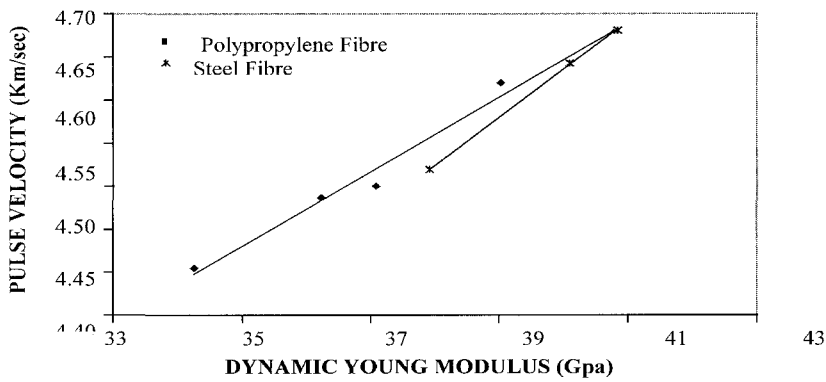

Figure 5 Relationship between dynamic modulus of elasticity and pulse velocity for two concrete composites

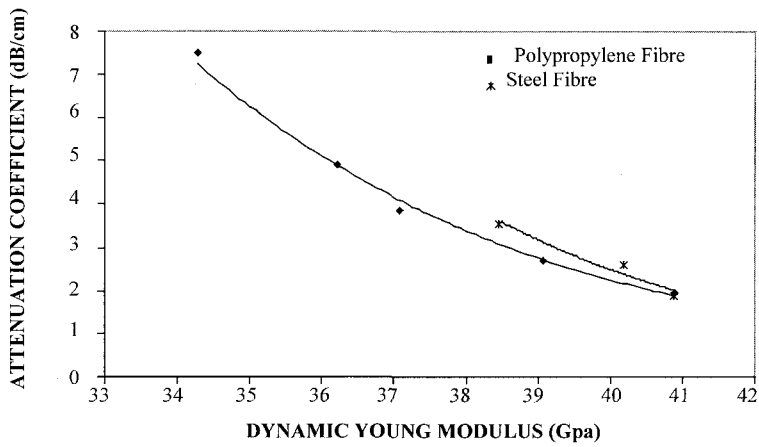

Figure 6 Relationship between attenuation coefficient and dynamic young modulus of fibre reinforced concrete

CONCLUSIONS

1- The interactive process depends totally upon the nature of the medium and the characteristics of the propagating wave.

2- The reinforcing fibres act as an energy absorber and also as a wave scatterer.

3- The amount of energy exchange depends on dimensional order of the elastic wave length and that of the micro structure.

REFERENCES

1. WELLS P.N.T. "Physical Principles of Ultrasonic Diagnosis" Academic press London, New York. (1969)

2. KRAUTKRAMER J., KRAUTKRAMER. H "Ultrasonic Testing of Material" George Allen and Unwin ltd London. (1969)

3. WIMAL SUARIS and VIRAJ FERNANDO " Detection of crack growth in concrete from ultrasonic intensity measurements" Materials and structures Vol. 20, 1987 PP. 214-220.

4. REYNOLDS W.N., S.J. WILLCINSON and D.C SPOONER "Ultrasonic wave velocities in concrete" Magazine of Concrete Research Vol. 30 No. 104, September 1978.

5. RAOUF, Z.A., "Dynamic Mechanical Properties of Fibre Reinforced Cement Composition" Ph.D. Thesis, the Victoria University of Manchester, UMIST, May. 1975.

6. SMITH, R.L. "Ultrasonic Materials characterization" NDT. Int. Feb. 1987.

7. DHIEA ABID "Properties of Polypropylene Fibres Reinforced Concrete" M.Sc., Thesis, University of Baghdad, Jan. 1984.

8. BRITISH STANDARD INSTITUTION BS 1881 part 203: 1986 "Recommendation for Measurement of Velocity of Ultrasonic Pulses in Concrete".

9. JORDAN R.W. "The Effect of Stress Frequency, Mix & Age upon the Damping of Concrete" Magazine of Concrete Research Vol. 32, No. 113, Des. 1980 PP. 195-205.

10. WIMAL SUARIS and VIRAG FERNANDO "Ultrasonic pulse Attenuation as a Measure of Damage Growth during Cyclic Loading of Concrete" ACI Material Journal / May. June 1987 PP. 185-193.

11. ALEXANDER, M.G "Use of Ultrasonic Pulse Velocity for Fracture Testing of Cemented Materials" Cement, Concrete, and Aggregate. Vol. 10, No. 1 1988, PP. 9-14.

12. KATWAN, M. J., ABDULNOOR, S. S. and AL-ANI, Y. K., "Dynamical Mechanics of Concrete Composites" Al-Muhandis Journal of The Scientific Society Vol. 142, No. 2, Jun 2000, PP. 106-113.

13. ABDULNOOR, S. S., KATWAN, M. J., and AL-ANI, Y. K., "Ultrasonic Waves Atenuation in Various Concrete Composites" Proceeding of the Jordan second Civil Engineering Conference, Material Engineering. Amman-Jordan. 16-17 Nov. 1999, PP. 73-80.

14. HANNANT, D. J. (1978). "Fibre cements and Fibre Concretes". John wily and Sons, Inc., New York, N.Y.

15. ABDULNOOR, S. S., KATWAN, M. J., and AL-ANI, Y. K., "Static Characteristics of Fibre Reinforced Concrete" to be published.

EFFICIENCY OF PERMEABLE CAISSON SEAWALL REINFORCED WITH FIBRE REINFORCED POLYMERS

M Balah

S Abdel-Mawla

University of Suez Canal

Egypt

ABSTRACT. Despite the high wave-absorbing capacity of vertical slotted-wall breakwaters, they may slide or overturn due to waves. It was suggested to use inclined front wall to enhance wave energy dissipation. The hydrodynamic performance of 45° inclined slotted-wall breakwater was experimentally studied. It gives 10% more dissipated wave energy than that of vertical wall at high wave steepness. In addition, the breakwater stability was improved. Furthermore, less wave reflection gives less toe protection seaward the structure. In this paper, the application of this system as a seawall is discussed. A complete hydraulic and structural design is prepared for El-Gamil shoreline at Port Said as a case study. The proposed permeable caisson seawall could be prepared as prefabricated units with a good quality control. These units can be constructed from plain or reinforced concrete. Plain concrete means large volumes and weights, that leads to difficulties in transportation and positioning of the seawall. On the other hand, the steel reinforcements of the reinforced concrete seawalls are subjected to corrosion in the harsh conditions of the seawater. Fiber Reinforced Polymers (FRP) is non-corrosive material of very high strength to weight ratio. Their use in civil engineering applications attracts nowadays more interest than at anytime before. Excellent resistance to creep and fatigue are some advantages of FRP. A comparative study between the different types of FRP was conducted to select the most appropriate type for seawalls. In addition, a feasibility study of reinforcing inclined slotted seawall with conventional steel or FRP reinforcements is addressed in this paper.

Keywords: Permeable, Caisson, Seawall, FRP, Reinforcement.

M Balah, is a Prof in Harbour Engineering in Civil Engineering Department at Faculty of Engineering at the University of Suez Canal. He supervises and manages studies on Harbour structures.

S Abdel-Mawla, is a Lecturer in the Civil Engineering Department at Faculty of Engineering at the University of Suez Canal. His research focuses mainly on the efficiency of permeable breakwaters.

INTRODUCTION

The obliquity of waves to seawall is generally greater as they are angled about 45° to the shoreline. Some obliquity must be accepted, because there would be no littoral drift and no erosion problem without obliquity. This is true in both cases of storm waves and swell. Figure 1, shows a typical wall constructed along a portion of coast [1]. It is shown that waves refracting shoreward are still angled to the face on arrival and hence will be reflected at an equal angle. The limiting orthogonals of these reflected waves are shown, which approach each other offshore as refraction seawards also occur. They may even cross, as illustrated, and so produce a wave caustic, implying an infinite concentration of energy. This results in wave breaking, not only for the reflected waves, but also for the incident waves in that area. Material is quickly removed downcoast beyond the limit of the seawall. This results in recession of the shoreline. Such erosion downcoast of seawalls is ubiquitous. On the upcoast end of the wall, the diffraction of reflected waves can create a net movement upcoast that could result in a slight accretion.

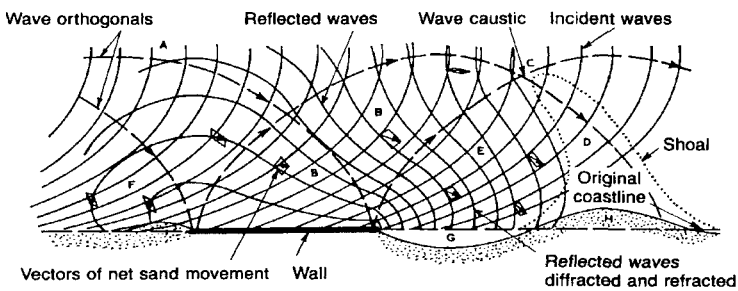

Figure 1 Influence of oblique wave reflection from a seawall

Behaviour of Slotted Wall Breakwater

Jarlan proposed a perforated wall breakwater that consists of a perforated front wall and a wave chamber located just behind it [2]. It has been investigated intensively with porosity performed by perforations or vertical slots. Sawaragi [4], and Chwang and Dong [5] found that reflection is reduced to its minimum if the distance between the front and back porous walls is equal to a quarter-wave length or an odd multiple of this distance. Sawaragi suggested a porosity ratio of 30% to have minimum reflection and transmission coefficients. The slotted breakwater behaves as a resonant system with dissipation. The energy dissipation mechanism is explained in details in [3]. Yip and Chwang [6] studied a perforated wall breakwater with an internal horizontal plate to enhance the stability of the structure and reduce the size of the wave chamber. Abdel-Mawla and Balah [3] studied the inclination of the outer walls. They compared vertical walls to those inclined at an angle 45° to water level. Generally, the hydrodynamic performance of a breakwater is similar with or without inclination at low wave steepness. When wave steepness increases, the inclination improves the wave absorbing capacity by about 10%. This highly effective wave-absorber has been used world wide for construction of seawalls and breakwaters for its good features; cost effective, less impact on bed erosion, and capable of delivering the desired degree of wave attenuation [3].

One is constructed at the front of the reclaimed land on the north coast of Kashima port in Japan as shown in Figure 2. This wall showed an excellent performance regarding absorbing wave energy and exhibition low reflection [7].

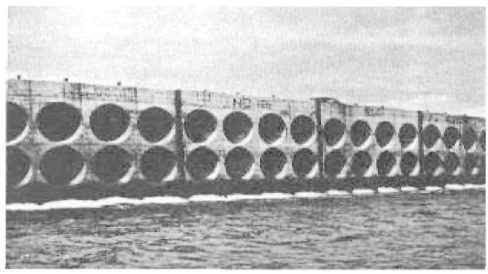

Figure 2 Perforated seawall at Kashima Harbor, Japan

HYDRAULIC DESIGN

The proposed seawall consists of pre-fabricated units as shown in Figure 3. Each unit composes of a vertical solid backwall and an inclined permeable front wall. The water wave is a phenomenon of the free surface, and the peak wave load may cause the front wall to slide or overturn. To avoid the sliding, the wave chamber has a bottom slab and an intermediate web.

The relevant geometrical parameters are:

- Width of the wave chamber at water mid-depth; X,
- Permeability of the front wall, expressed as a percentage or as D/C (D is the gab width while C is rib width),
- Inclination angle; θ and Freeboard; h.

Experiments and Results

The experiments were carried out using a flume of clear width 0.3 m, and wall height 0.5 m. The wave generator is capable of producing regular waves. The used wave period ranged from 0.81 to 1.19 sec. while the wave height ranged from 1.0 to 9.0 cm. The models were made of PVC sheets. Their height and width were 50 and 30 cm respectively. Rib width (C) and rib thickness (t) were set to 3 and 0.6 cm respectively. The entire distance at mid-depth (x) and the water depth (d) were kept constant and equaled to 135 and 30 cm respectively. A 8-mm video camera with a negative picture effect was used to record waves. For each measuring point, the zoom of the camera was exactly perpendicular to the scaled glass (flume side). The videotape was used to measure the crest and trough elevations for each wave. More details about the flume and measuring technique can be found in [3].

In order to determine incident and reflected wave heights, two measuring points were used at distances L/4 and L/2 seaward the model face. This was based on the assumption that these two points met maximum and minimum of a standing wave envelope. Reflection coefficient; K_r can expressed as:

$$K_r = H_r/H_i = (H_{max}-H_{min})/(H_{max}+H_{min})$$

Where: H_r: Reflected wave height [L]
H_i: Incident wave height [L]
H_{max}: Maximum water level [L]
H_{min}: Minimum water level [L]

Reflection coefficient was studied against wave steepness (Hi/gT^2) as shown in Figure 4-a. Figure 4-b shows a frozen shot from the recorded videotape when wave encounter on the front wall.

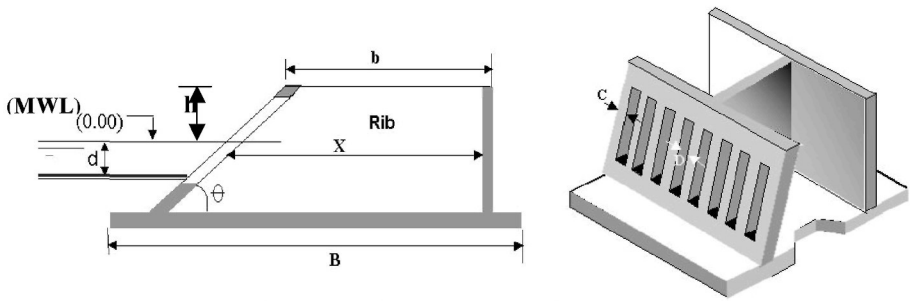

Figure 3 Relevant geometrical parameters

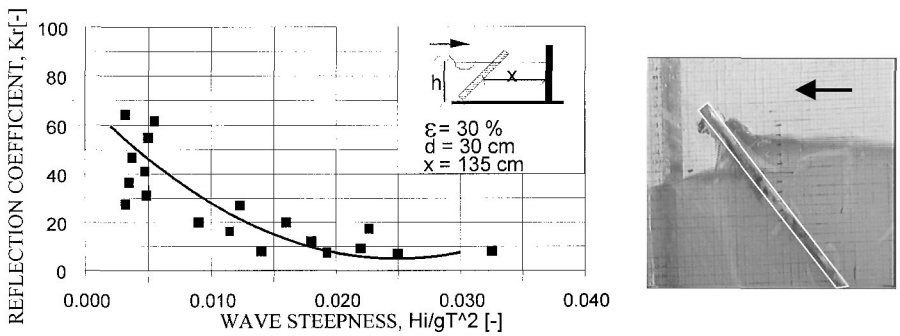

a - Reflection coefficient against wave steepness b - Inward wave attack the front wall

Figure 4 Results of the experimental work

Description of Field

Coastal erosion has been occurring at several locations along the northern coast of Egypt. Ashtoom El-Gameel to the west of Port-Said, Figure 5, is one of these locations. To protect the beach from future erosion, a detached breakwater was constructed in 1997. The detached breakwater consists of six breakwater segments covering about 1700 m. Because of sand trapping by the system; erosion occurred downstream the project as shown in Figure 5. A dike of gravel is executed along the eroded reach as a temporarily protection for the highway between Port Said and Damiatta. A permanent seawall is required, due to the vitality of this highway.

From Tetra Tech. [8]; the predominant wave direction is from the North-West, whereas, wave heights exceed one meter about 50% of the time. Abo-Elazm divided the wave climate to stormy condition and dominant condition [9]. The stormy period is 15 days per year with 3.5-meter significant wave height and 7.0 seconds wave period. The dominant period is 350 day per year with 1.5-meter significant wave height and 5.0 second period. In turn, the typical wave steepness (H_i/gT^2) = 0.003 which is within the tested values.

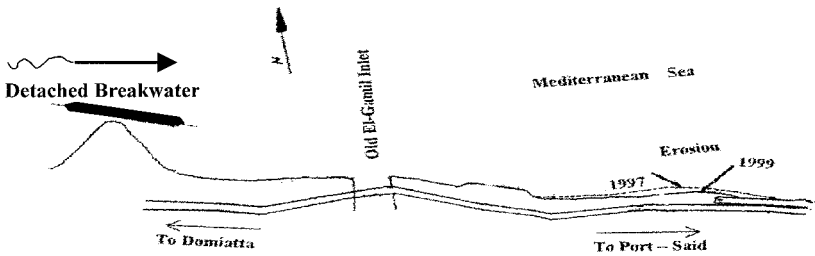

Figure 5 Down drift the detached breakwater with the resulted erosion

Hydraulic Calculations of Seawall

The expected water depth in front of the seawall is about 1.0 m. Assuming that the tested model is non distorted; the horizontal scale will be taken as the vertical scale and equal to 3.3. Then the prototype entire distance (x) = 4.50 m, (D) = 0.185 m, and (C) = 0.4 m.

The computations of wave loads are based on the incident waves directly before the seawall. It can be assumed that the foreland of the seawall is a nearly horizontal plane with a constant water depth determined by the still water level at the location during a storm. The waves from the open sea are mostly transformed by diffraction (island etc), by refraction (due to underwater morphology), by shoaling effects, and by breaking processes in the offshore and nearshore areas. It is generally difficult to compute reliably the incident wave parameters from the deepwater values. Therefore, it will be necessary to have measured values or to estimate the wave parameters for the worst conditions. To calculate the impact wave force,

$$P_m = 101w\frac{H_b}{L_D}\frac{d}{D}(D+d)$$

Minikin's formula is used for two wave conditions [10]; the prevailing and stormy conditions. The maximum pressure assumed to act at the SWL is given by:

Where:	Pm: maximum dynamic pressure	[M/LT^2]
	H_b: Incident wave height	[L]
	d : Depth at the toe of the wall	[L]
	D: Depth at one wavelength in front of the wall	[L]
	L_D: Wave length in water depth D	[L]

Figure 6-a shows the parameters of the calculated pressure. Waves force is calculated by two methods. The first was assuming that the sloped face was impervious and subjected to the whole force. Secondly, distributing the wave force between the front and back wall according to the dissipated and the remaining energy (from the experimental work) and assuming that the maximum forces will be at the same phase. Figures 6 and 7 show these two cases for both the prevailing and stormy conditions. Minikin proposed this formula based on speculations on the mechanism of impulsive breaking wave pressures. Although the formula has been cited in many references, few breakwaters have been designed with Minikin's formula. This formula overestimates the pressure giving excessively large intensity leading to uneconomic design. Goda demonstrated this tendency of overestimation in a case study at high wave [11].

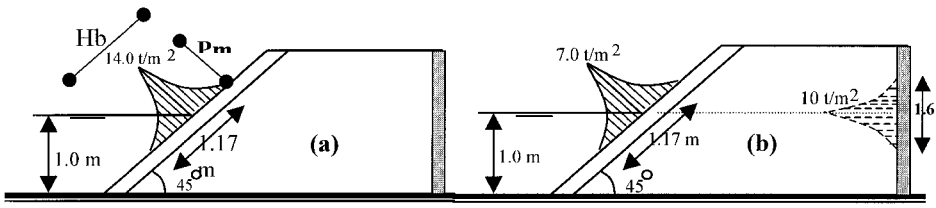

Figure 6 Impact dynamic pressure for prevailing conditions

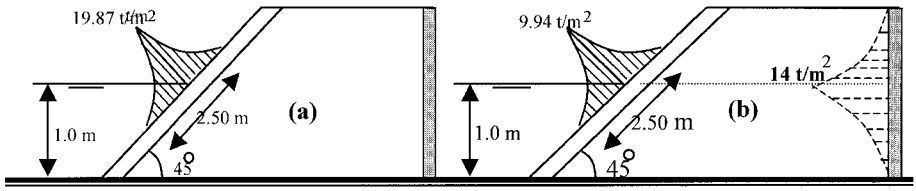

Figure 7 Impact dynamic pressure for stormy conditions

STRUCTURAL DESIGN

The proposed permeable caisson seawall can be prepared as prefabricated units with a good quality control. These units may be constructed from plain or reinforced concrete. Plain concrete means large volumes and weights, which leads to transition and positioning difficulties. This type of seawalls is not suitable as of the technical problems of constructing, transportation, and usage. On the other hand, the steel reinforcements of the reinforced concrete are corroded in the harsh conditions of the seawater.

Many people in the construction industry believe that concrete would last for generations without any maintenance, no matter what environment it is exposed to. However, the current condition of many reinforced concrete structures exposed to the marine environment makes one wonder if this belief is still true. The authors are not proposing that concrete is not durable. In fact, it is still the most durable man-made material known to mankind. The point is that there are certain environments that can compromise the durability of concrete and reduce its service life.

The high pH environment of concrete, above 12, normally protects the reinforcing steel from corrosion. Passive film forms on the steel surface in the presence of water and oxygen in the alkaline environment produced by cement hydration. Corrosion won't occur as long as there are no breaks in the passive layer over steel. The layer may be broken by two mechanisms; one involves carbonation, the other, chloride ions. Most corrosion problems are related to chlorides in marine areas. Controversy exists about the role chlorides play. A commonly cited theory says the formation of an iron chloride complex ion frees the iron to begin the corrosion process [12].

In marine environments, concrete structures can be divided into two categories of exposure; direct and indirect. The direct exposure category includes structures that are partially or fully submerged; and the indirect category includes structures along the coastline, which do not come into direct contact with seawater. Seawalls, wharves, bridge substructure elements and retaining walls are examples of structures in the direct exposure category, whereas other buildings along the coast are examples of structures in the indirect exposure category. Marine structures, especially, the areas located within the splash zone or tidal zone, are subjected to an environment conducive to deterioration of the concrete and corrosion of the reinforcing steel.

The problem of carbonation can be dealt with by use of good quality concrete and adequate cover to the steel. The problem of chloride ingress is less easily dealt with. To find a solution, research has been conducting throughout the last few decades. As a result of this continuous research work, several methods were introduced such as galvanization, cathodic protection, usage of stainless steel bars, epoxy-coating steel bars, usage of concrete additions like corrosion inhibitors...etc. However, none of these methods provided an answer to the problem that is still existing, rather they are intended to delay the onset of corrosion beyond the nominal design life of the structure. In addition, it is implicit with some of these solutions that the owner will have to accept an additional maintenance burden.

As the Fiber Reinforced Polymers (FRP) are of high resistance to corrosion, strength to weight ratio and fatigue resistance, they may be considered as an alternative solution for this problem. In the last few years, significant progress has been achieved in the field of using FRP in civil engineering applications. Using these new materials in marine structures may be considered as one of the choices in the near future [13].

What Are FRP?

When two or more distinct materials are combined on a macroscopic scale to form a useful material, the resulting product is called *composite material.* Usually these composite materials show superior properties compared to the individual constituents. FRP composites are obtained by inserting fibers of relatively high strength in light matrices. Carbon, Glass and Aramid fibers (CFRP, GFRP and AFRP) are commonly used. While matrices can be organic, metallic or ceramic material; resinous materials such as polymers are the most common. The fibers are supported and protected by the resin matrices. Epoxies and polyesters are often used as the composite matrix. Polyester resins are not very resistant to alkalis and are typically avoided for uses in concrete. Vinyl-ester resins are resistant to a wide range of acids (sulfuric, hydrochloric, hydrofluoric, phosphoric, nitric) as well as to chloride salts and chlorine making them ideal for marine environments. Chemical additions may be added to improve certain material or mechanical characteristics [14].

Choice Of FRP Bars To Be Used In Permeable Caisson Seawall

AFRP bars (such as Kevlar) are resistant to many solvents and chemicals, but are affected by strong acids and bases [15]. AFRP will show strength decay when in contact with concrete. Higher-moduli AFRP bars exhibit better alkali resistance and may be used in such applications. Glass fibers are chemically vulnerable to many acids and bases and will deteriorate if in direct contact with concrete. Glass fiber composites can exhibit "spontaneous loss over time of much of the flexural and tensile strengths of the composite to little more than that of the matrix" in case of exposure to wet conditions in an alkaline environment. The resins used in the composite must provide a twofold protection in a concrete environment; the matrix toughness must be high enough to prevent the development of matrix micro cracks, and diffusion through the matrix must be minimal. In summary, CFRP have the potential to withstand direct interaction with concrete for long periods and will be used in reinforcing permeable caisson seawall.

Behaviour Of FRP Reinforcements

The stress-strain relationships for all FRP materials (bars or laminates) are linear up to failure. This is true; no matter what kind of fiber it is (GFRP, AFRP or CFRP). There is no yield at any stage of loading. Figure 8 shows a typical stress-strain relationship for a CFRP bar. It is shown that the strength is much higher than the reinforcing steel, and even higher than that of the high strength tendons. This relationship is linear with no ductility. The ultimate strain of the FRP is less than that of steel. Both steel and the CFRP bars show alike values at service loads. It should be emphasized that the behaviour of the FRP is constant and independent on the load level, unlike steel that goes through different stages. The strength of the FRP reinforcements depends on many factors; the type of the fiber, the type of epoxy, manufacturing and curing process, and ratio of fiber in the matrix. In the Canadian Code [16], the use of AFRP and CFRP was restricted as follows:

- Stresses in AFRP tendons at transfer are limited to *35%* of short-term ultimate
- Stresses in CFRP tendons at transfer are limited to 60% of short-term ultimate
- High modulus AFRP reinforcements are better suited for exposure to concrete.
- The use of pH-neutral concrete is strongly recommended to prevent alkali attack

The safety factors were assigned according to the Japanese recommendations for design and construction of concrete structures using continuous fiber reinforcing materials [17]. Table 1 shows the safety factor values, which agrees with those proposed in the ACI state-of-the-art [18].

DESIGN RESULTS

Before performing the structural analysis, the overall stability of the seawall was addressed, including sliding, overturning and bearing stresses checks. The analysis of the permeable caisson seawall was performed using the well-known commercial SAP 2000. The straining actions of moment, shear and normal forces were calculated and the design was performed according to the Japanese guideline [17]. The dimensions and reinforcements details are shown in Figure 9.

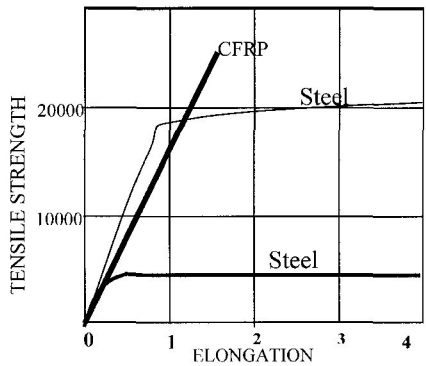

Figure 8 Typical stress-strain relationship of FRP compared to steel

Table 1 Safety factors used in the design of the permeable caisson seawall

	MATERIAL			MEMBER	STRUCTURAL	LOAD	STRUCTURAL
	CONCRETE	FRP	STEEL	FACTOR	ANALYSIS FACTOR	FACTOR	FACTOR
Ultimate Limit State	1.3[(1)] or 1.5	1.15[(2)] to 1.3	1.0 or 1.05	1.15 to 1.3	1.0	1.0 to 1.2	1.0 to 1.2
Serviceability Limit State	1.0	1.0	1.0	1.0	1.0	1.0	1.0
Fatigue Limit State	1.3[(1)] or 1.5	1.15[(2)] to 1.3	1.05	1.0 to 1.1	1.0	1.0	0 to 1.1

[(1)] 1.3 where characteristic value of concrete compressive strength is less then 50 N/mm^2
[(2)] 1.15 for CFRP or AFRP

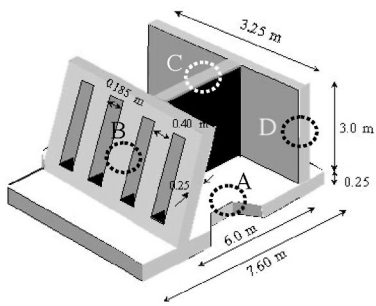

Figure 9 Dimensions and reinforcements of FRP and steel reinforced seawalls

Table 2 Reinforcements of permeable caisson Seawall

SEC	STEEL REINFORCEMENT	CFRP REINFORCEMENT	REMARKS
A	5 ϕ 16 /m`	7 # 3 /m`	
B	8 ϕ 18 /m`	9 # 3.5 /m`	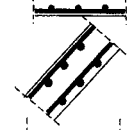
C	8 ϕ 18 /m`	9 # 3.5 /m`	
D	7 ϕ 16 /m`	7 # 3 /m`	

CONCLUSIONS

Using the permeable caisson seawall enhances the energy dissipation and the stability of the breakwater against sliding and overturning. As non-corroded materials, the Fiber Reinforced Polymers (FRP) can be used in reinforcing these seawalls. Carbon FRP (CFRP) showed superior properties that it may be recommended to be used as main reinforcement in the permeable caisson seawalls. Although, the high initial cost of constructing FRP reinforced permeable caisson seawalls, their maintenance free extended life makes their usage an economical solution.

REFERENCES

1. SILVESTER, R., Design of Seawall and Groins, Handbook of coastal and ocean engineering, Vol 1, 1990, Ch 23.

2. JARLAN, G. E., A Perforated Vertical Breakwater, The Dock and Harbour Authority, 41(488), 1961.

3. ABDEL-MAWLA, S., and BALAH, M., Wave Energy Absorption by an Inclined Slotted-Wall Breakwater, Journal of Scientific Research, Faculty of Engineering, Suez Canal University, Port-Said, Sep 2001.

4. SAWARGI, I., On Wave Deformation Due to Permeable Structures, Coastal Engineering in Japan, Vol 16, 1973.

5. CHWANG A.T., Dong Z., Wave-Trapping Due to a Porous Plate, Procedure Of the 15th Symposium on Naval Hydrodynamics, Hamburg, West Germany, 1984, pp 407-417.

6. YIP T., CHWANG A., Perforated Wall Breakwater with Internal Horizontal Plate, Journal of Engineering Mechanics, Vol 126, No 5, 2000.

7. SATO S., TANAKA N., HORIGUCHI T., FUSE S., Beach Erosions and a Permeable Offshore Breakwater, Procedure of the 25th Congress on Inland & Maritime waterways & Ports, Edinburgh, Vol 5, Section II, 1981.

8. TETRA, T., Shoreline Master Plan for the Nile Delta Coast, Prog Report 1, 1984.

9. ABO-ELAZM, A., Economical Length of Breakwaters for the Protection of Approach Navigable Channels, M.Sc. thesis, Cairo University, 1983.

10. Shore Protection Manual, Vol. I, Waterways Experiment Station, Corps of Engineers, COASTAL ENGINEERING RESEARCH CENTER, Washington, USA, 1984.

11. GODA, Y., A New Method of Wave Pressure Calculation for the Design of Composite Breakwater, Procedure of the 14th International Conference of Coastal Engineering, Copenhagen, 1973.

12. SALEH K., Grace N.F., SOLIMAN A.K., ABDEL-SAYED G., Strengthening Reinforced Concrete Beams Using FRP Laminates, ACI Structural Journal, Vol 96, No 5, 1999, pp 865-874.

13. SALEH K., GRACE N.F., SOLIMAN A.K., ABDEL-SAYED G., Strengthening of Continuous Beams using FRP Laminates, Procedure of 4th International Symposium on FRP Reinforcement for RC Structures, Baltimore, USA, Nov, 1999, pp 647-657.

14. SALEH K., GRACE N.F., SOLIMAN A.K., ABDEL-SAYED G., Choice of FRP is Important, What About the Epoxy Adhesive? Procedure of the 2nd Middle East Symposium on Structural Composites for Infrastructure Applications, Hurghada, Egypt, April 1999 pp 22-32.

15. SALEH K., GRACE N.F., SOLIMAN A.K., ABDEL-SAYED G., Behaviour and Ductility of Simple and Continuous FRP Reinforced Beams, ASCE Journal of Composites for Construction, Vol 2, No 4, Nov. 1998, pp186-194.

16. Design Provisions for Fibre Reinforced Structures in the Canadian Highway Bridge Design Code, Advanced Composite Materials in Bridges and Structures, 2nd conference, Montreal, 1996, pp391-406.

17. Recommendations for Design and Construction of Concrete Structures Using Continuous Fiber Reinforcing Materials, Research Committee on CFRM, Japanese Society of Civil Engineers, Tokyo, Japan, 1997.

18. Guidelines for Selection, Design, and Installation of FRP Systems for Externally Strengthening Concrete Structures, ACI Committee 440, Detroit, Michigan, 1996.

EVALUATION OF CFRP COMPOSITES FOR SEISMIC RETROFIT OF BEAM-COLUMN JOINTS

M A Issa

M El-Metwally

G Monroy

University of Illinois

United States of America

ABSTRACT. This paper presents a study on beam-column joints for concrete structures located in high seismic zones, which do not have the ductility and strength required for modern construction in high and medium seismic zones. At present, most of these structures have not yet deteriorated, but are structurally inadequate. Solutions for the upgrade of these structures using economical and reliable techniques are of great interest. This paper presents the structural behaviour of beam-column joints confined externally by means of carbon fibre reinforced polymer (CFRP) wrapping using actual column-beam joints. Eight beam-column joints were cast. Four of the eight beam-column joints were unwrapped and the other four were wrapped with one layer of CFRP sheet of 1.93 mm (0.076 in.) thickness. The specimens had four different details of confinement reinforcement. All specimens were subjected to cyclic loading simulating seismic conditions. The parameters in this study were wrapped versus unwrapped specimens, spacing of confinement reinforcement, and the thickness of CFRP.

Keywords: Seismic, Beam-column joints, Carbon fibre reinforced polymers, Concrete structures, Wrapped, Confinement reinforcement, Ductility, Strength.

M A Issa is a Professor of Civil and Materials Engineering in the Department of Civil and Materials Engineering at the University of Illinois at Chicago. His research focuses mainly on concrete structures, durability of high performance concrete, advanced composites, surface characterization in fracture of cementitious materials, and bridge rehabilitation.

M El-Metwally is a Visiting Associate Professor in the Department of Civil and Materials Engineering at the University of Illinois at Chicago. His research focuses mainly on repair and maintenance of concrete structures.

G Monroy is an Undergraduate Research Assistant in the Department of Civil and Materials Engineering at the University of Illinois at Chicago.

INTRODUCTION

Concrete structures such as bridges and buildings are constantly deteriorating and are in need of major maintenance or total rehabilitation. Recent earthquakes caused extensive damage to many structures built in the 1950's and 1960's, which were designed prior to the year 1971 codes. As a result, these structures do not have enough ductility and strength required by the modern construction codes for seismic zones. Because of this, many authorities demand the retrofit of existing concrete structures to meet code requirements and provide enough strength and ductility to resist the seismic forces encountered during earthquakes. At this time, many of these concrete structures are still serving their purpose, but are not structurally sound. Solutions to solving this problem in an economical and reliable way are in great demand.

In the past two decades, the use of epoxy bonded steel plates on concrete members was widely used as a repair technique worldwide to retrofit damaged structures. This technique never gained great acceptance because of the many problems encountered with it, such as poor bonding, corrosion, and difficulty of placement. Due of this, many designers and engineers turned to new technologies that would provide them with more efficient materials. Some of those materials are fibre reinforced polymers (FRP) which are lighter, have higher tensile strength and modulus, and are less susceptible to corrosion and fatigue. At first, FRP's were used in the form of high strength plates bonded to inadequate concrete members.

However, the development of thin FRP fabric sheets that easily clung to the structural members and confined them well provided an easier and more efficient way of rehabilitating concrete structures. FRP sheets are superior to the steel plates in a way that they provide less weight, higher resistance to corrosion and fatigue, light weight, good workability, shorter construction time, and are easier to handle and form to any shape. Rehabilitation of concrete structures is geared toward the prevention of loss of life, and the destruction of the structure itself during earthquakes.

In order for the application of CFRP to become a promising seismic retrofitting technology, it is very important to understand the existing problems. The main objective of this research is to investigate the effects of varied applications of CFRP sheets on the structural performance, ductility, and modes of failure of reinforced concrete beam-column joints. There are many uses for CFRP; such as to increase the bending and shear strength of concrete beams, slabs, and walls, improve the capacity of concrete pipes, and tunnels, replace reinforcing steel lost to corrosion, replace damaged post-tensioning tendons, provide confinement to concrete repairs, and to substitute for missing reinforcing steel.

RESEARCH SIGNIFICANCE

Designers are increasingly confronted with the task of assessing the seismic risk of existing reinforced concrete structures. The main focus goes to structures that were constructed before the 1970's, when very little attention was given to seismic activity. The greatest uncertainty when assessing the seismic performance of reinforced concrete frames is the likely behavior of beam-column joints with limited transverse reinforcement in the joint core. Most frames built before the 1970's did not include any transverse reinforcement in joint core. Shear failure of beam-column joint cores without transverse reinforcement is due to extensive diagonal tension cracking that may eventually lead to diagonal compression failure in the joint core.

LITERATURE REVIEW

In the United States more than 30% of the nation's bridges are classified as deficient, i.e., deteriorated, under strength and/or geometrically obsolete for the demands of today's traffic volumes and load [1]. The nation's economy in the new millennium relies heavily on the timely transport of goods and people. Yet, these deficient bridges and the intrusive repair work necessary to improve them represent a significant impediment to the nation's mobility and have a negative impact on productivity. Similarly, in the office-building industry, there are a significant number of buildings that were designed and built in previous decades when important analytical design ideas had not reached a widespread consensus. By today's standards and building codes, these buildings are deficient and/or deteriorated as a result of a lack of adherence to stricter analytical design methods [2]. The Transportation Equity Act for the 21st Century (TEA-21), legislation enacted in June of 1998 authorizes the $20.4 billion to rehabilitate or replace bridges. Even though local and federal funds such as these have been set aside to alleviate the problem, the nation's economic and population growth and the rate at which buildings are decaying is greater than that at which the nation's infrastructure and buildings may be rehabilitated. In a recent tests provided by Hakuto, Park, and Tanaka, it was concluded that the seismic performance of typical interior beam-column joints of pre-1970's designed reinforced concrete frames was very poor and would not withstand a severe earthquake.

Widely accepted methods of retrofitting and rehabilitating structural members have some serious disadvantages in that they are costly, cumbersome and difficult to install, reduce the space/area surrounding the member, decay or corrode easily, and increase the dead load significantly. But more importantly, traditional methods of rehabilitating concrete structures were obsolete or inapplicable to the most critical segment of a structure, the joints.

In recent years there seemed to be no pressing need to seek alternative means of remedying the situation. The major influence of beam-column connections on the structural integrity and seismic performance of reinforced concrete structures has become more evident after the following earthquakes: 1989 Loma Prieta, the 1994 Northridge, the Kobe earthquake of Japan, and the 2001 Seattle earthquake [3]. Post earthquake reports of the Loma Prieta, indicated that one of the main reasons behind the collapse of the Cypress Viaduct bridge, the damage of the China Basin bridge, and the I-80 Nemit Freeway was the failure of connections (beam-column and column-base connections).

Carbon Fibre Reinforced Polymers (CFRPs) have been analyzed with promising results. Their use in the concrete rehabilitation industry needs extensive research in order to disseminate and record conclusively what has been now proven to be fact. Since 1997, in the UK, the Highways Agency embarked on research to investigate the feasibility of using FRPs to strengthen substandard bridge connections and supports [4]. Various government and industry sponsored research projects have been conducted by academia to provide voluminous data and results supporting the advantages of CFRPs over traditional materials [5]. In particular, studies of wrapped joints have demonstrated both analytically and experimentally that the seismic response of reinforced concrete joints repaired and retrofitted with composite laminates was more ductile and capable of withstanding increased shear loads [6]. Mosallam's study and results indicated that the use of CFRP/epoxy composite laminates not only succeed in restoring the ultimate capacity of decayed/damaged specimens but also resulted in a strength gain of more than 34%. In addition, an upgrade of almost 60% in the connection initial stiffness was achieved.

However, and unlike the control specimen, both stiffness and strength degradation were observed for the repaired specimen. This could be attributed to the fact that the steel reinforcement of the repaired connection yielded before the test was even conducted. The same study also reported an increase of initial stiffness up to 167%, as compared to the average stiffness of the control specimen. In addition, a 75% increase in the initial joint strength was achieved.

Shmoldas et al. [7] investigated the retrofit of a rectangular column using carbon fibre for the Arroyo Seco Bridge in Pasadena, California. A full-scale test was performed to assess the effectiveness of confinement in the column in strong and weak axis bending. The column had a high, 3 to 1, aspect ratio. The results of the test showed no increase in ductility for weak axis bending, but a doubling of ductility for the strong axis as compared to the built in place. Zhang et al. [8] examined the seismic performance of existing RC columns retrofitted with carbon fibre sheets. Quantity, retrofitting types of continuous fibre sheets were adopted as the experimental variables. The failure mode of the columns changed from shear to flexural failure. However, if the ply of continuous fibre sheet is not enough, columns collapse due to crushing of concrete just after yielding of longitudinal reinforcement steel.

Application of CFRP improved the flexural and shear capacities of structural members. A normal column that was shear-strengthened by carbon fibre sheet changed the failure mode from shear failure to flexural failure with improved ductility, as the amount of shear reinforcement was increased [9]. Pantelides et al. [10] found that the CFRP composite strengthened the beam-column joints effectively. The bent retrofitted with CFRP composite reached a system displacement ductility of 6.3 as compared to the bent in the as-is condition, which reached a ductility of 2.8. The peak lateral load capacity was increased by 16%.

Overwhelmingly, all studies researched echoed the conclusions reported by Issa et al. [11] study of an extensive ongoing research project:

1. The shearing strength of beam-column joint wrapped with one thin layer of CFRP, 0.66 mm (0.026 in.), was 13% higher than that of the unwrapped joint.
2. Wrapped joints resisted more loading cycles than unwrapped joints. The observed ductility of the specimen wrapped with one thin layer of CFRP was 4.3, while for the unwrapped specimen the ductility was 3.

The failure mode of the wrapped specimens of this ongoing study resulted in the diagonal rupture of the CFRP sheets on both faces of the joints as shown in Figure 1. The thickness of the CFRP sheets used was 0.66 mm (0.026 in). The ductility shown in Figures 2 and 3 would be higher if more than one layer or thicker layer of CFRP sheets was used. As a result of this observation, it was decided to use thicker CFRP sheets of 1.8 mm (0.071 in).

MATERIALS, SPECIMEN CONFIGURATION, AND PREPARATION

For the purpose of this study, eight beam-column joints were cast. Only one specific mix-proportion was designed to achieve HPC, which would have 28-day compressive strength of at least 41.37 N/mm^2 (6000 psi). The detailed mix proportions are provided in Table 1. The arrangement of longitudinal and transverse reinforcement was designed after some preliminary research of sources relating to the actual reinforcement, which is used in actual structures. Grade A60 steel was used as main reinforcement.

Table 1 Mixture proportions of concrete

INGREDIENTS	MIX PROPORTIONS, per m^3
Cement, kg	273.06 (602 lb)
Silica fume, kg	13.60 (30 lb)
Fly ash, kg	54.43 (120 lb)
Water, kg	122.90 (271 lb)
Coarse aggregate, kg	784.26 (1729 lb)
Fine aggregate, kg	493.51 (1088 lb)
RB 1000 superplasticizer, ml	2661.62 (90 fl oz)
MB-VR Air-Entraining, ml	443.6 (15 fl oz)

Each specimen consisted of a 127 mm x 196.9 mm (5" x 7.75") beam and a 127 mm x 203 mm (5" x 8") column, with 304.8 mm (12") beam overhang and 762 mm (30") columns length on each side of the joint. The column was reinforced with 4 #10 (4 #3) bars with rectangular closed ties of 4.76 mm ($^3/_{16}$") in diameter, with different spacing for each of the four different specimens.

The spacing of confined reinforcement in the joint core was made with four different configurations. One set was made with no reinforcement in the joint core, the second set with 127 mm (5 in.) spacing, the third set with 63.5 mm (2.5 in.) spacing, and the fourth set with 31.75 mm (1.25 in.) spacing. The beam was reinforced with 4 #10 (4 #3) bars with two on top and two on bottom, used as longitudinal reinforcement. As the transverse reinforcement used for confinement, closed ties of 4.76 mm ($^3/_{16}$") diameter and spacing of 50.8 mm (2") were used as shear reinforcement.

Four specimens were wrapped with a thick layer of bi-directional CFRP sheets of 1.8 mm (0.071 in.) thickness at an angle of 45° and the remaining four were left unwrapped. The specimens were wrapped in a specific way using the two parts epoxy and CFRP. The properties of the CFRP materials are presented in Table 2. After 28 days, the specimens were prepared for wrapping by smoothening sharp edges of rectangular members, followed by sandblasting of all of the surfaces until the coarse aggregate was slightly exposed.

Table 2 Properties of carbon fibre sheet

PROPERTIES	THORNEL T-300 12K	FORTAFIL AKZO 50K
Tensile strength	3.65 KN/mm^2 (530 ksi)	3.79 KN/mm^2 (550 ksi)
Tensile modulus	231 KN/mm^2 (33.5 x 10^6 psi)	227.5 KN/mm^2 (33 x 10^6 psi)
Elongation at break	1.4%	1.7%
Filaments/strand	12,000	50,000
Sheet thickness	0.66 mm (0.026 in)	1.8 mm (0.071 in)

The dust and the remaining sandblasting materials were removed from the concrete surface using an air pressured device. The base of the epoxy reign was mixed with the curing agent using an electric mixer. After mixing, the epoxy was applied to the concrete surface and CFRP sheet simultaneously. The carbon fibre sheets were placed directly onto the clean surface of each sides of the specimen allowing 76.2 mm (3 in.) overlapping and extending 304.8 mm (12 in.) from the edge of the joint on each of the side of beam and column members. Applying pressure to the surface of CFRP using a small hand roller eliminated any entrapped air. After wrapping the epoxy was allowed to cure at laboratory conditions for at least seven days before testing.

TESTING PROCEDURE

Strain gauges were mounted at critical locations to measure the strain. The strain gauges used to monitor the strain on the outside faces of the column were placed in the same location on the unwrapped and wrapped specimens. For the wrapped specimens, they were placed on the carbon fibre. LVDT's were installed to measure the vertical displacement of the specimen tested. To simulate seismic action, the beam-column joint specimens were loaded using computer controlled machine. A cyclic loading pattern with alternating displacement reversals was applied to each specimen to simulate earthquake like conditions.

The beam ends of the joint were connected to an actuator and were subjected to push and pull motion, while the column was simultaneously subjected to a constant axial load of 222.4 KN (50 kips), which is about 20% of the ultimate compressive load of the column. The test setup for a typical beam-column joint is shown in Figure 4. Load, deflection, and strain readings were recorded via data acquisition system and the development of cracks and modes of failure were monitored throughout the testing of all specimens.

Figure 1 Failure mode of wrapped beam-column joint

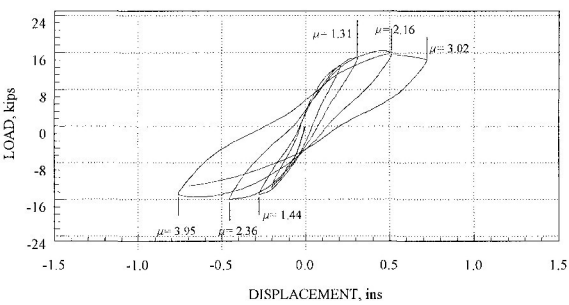

Figure 2 Load vs. displacement of unwrapped beam-column joint

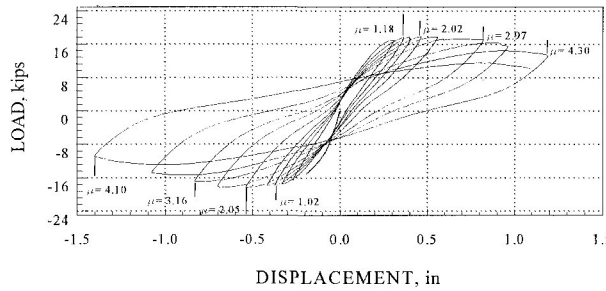

Figure 3 Load vs. displacement of CFRP wrapped beam-column joint

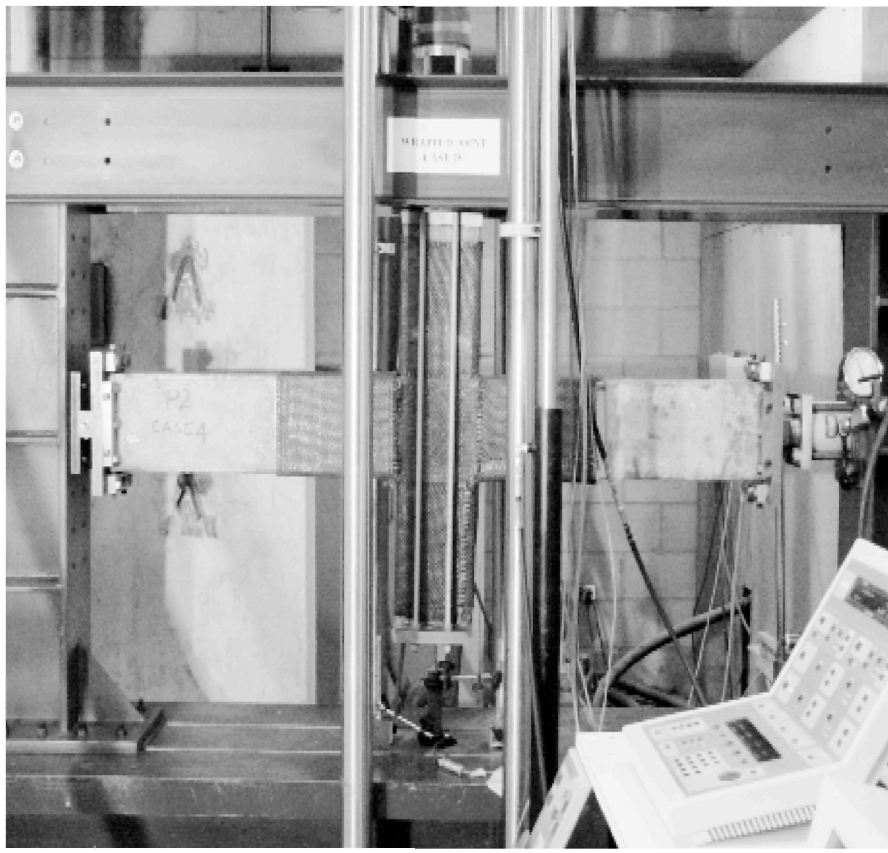

Figure 4 Test setup for beam-column joint

RESULTS AND DISCUSSION

Joints Wrapped with Thin Layer of CFRP Sheets

One set of four 4 beam–column joints wrapped with one thin layer of CFRP sheets of 0.66 mm (0.026 in.) thickness from this ongoing research project was tested. The observed results were analyzed and compared. The load-displacement hysteresis curves for unwrapped and wrapped beam-column joints are shown in Figures 2 and 3, respectively. The shearing strength of the wrapped joint was 13% higher than that of the unwrapped joint although a very thin layer of CFRP was used. The ultimate failure in the unwrapped joint specimen was due to shearing of the column, while in the case of the wrapped joint, the ultimate failure was within the joint at an angle of 45° as shown in Figure 1. It was observed that wrapped specimens could resist more loading cycles than unwrapped specimens. It was also noticed that the wrapped specimen could undergo 86% more displacement than the unwrapped specimen as depicted in Figures 2 and 3.

Joints Wrapped with Thick Layer of CFRP Sheets

A set of eight beam-column joints were tested, four unwrapped and four wrapped with thick layer of CFRP sheets of 1.8 mm (0.071 in.) thickness. The typical load-displacement hysteresis curves for unwrapped and wrapped beam-column joints for cases I and IV are shown in Figures 5-8. The shearing strength of the wrapped joint for Case I and Case IV was 38% and 12% higher than that of the unwrapped joint corresponding to the same case. The ductility of the wrapped joint for Case I and Case IV was 70% and 17% than that of the unwrapped joint, respectively. It was also noticed that wrapped specimens could resist more loading cycles than unwrapped specimens. The observed displacement was also higher in the case of the wrapped joints, for both Case I and Case IV by approximately 140% and 90%, respectively. These differences in ductility, strength and displacement can be observed on the plots depicted in Figures 5-8. The contribution of the CFRP sheets in terms of ductility and strength of the joints was greatest for Case I specimen. This difference can be attributed to the fact that the steel reinforcement of Case I was not confined with ties inside the joint area compared to case IV that was confined with ties of 31.75 mm (1.25 in) spacing.

Table 3 Test results

SPECIMEN DESIGNAT.	CONFINEMENT REINF. SPAC, in	LOAD, kips		DEFLECTION, in	
		(+)	(-)	(+)	(-)
UC1	0	16.03	16.13	0.82	0.61
WC1	0	20.89	23.57	1.75	1.39
UC2	5.0	13.50	14.00	0.77	0.65
WC2	5.0	19.50	21.50	2.05	1.92
UC3	2.5	17.00	17.00	0.95	0.80
WC3	2.5	22.00	22.00	1.67	1.63
UC4	1.25	18.31	18.31	1.03	0.88
WC4	1.25	21.72	21.72	1.83	1.85

1 Kip = 4.448 KN, 1 inch = 25.4 mm,
UC1 - Unwrapped specimen for Case 1, WC1 - Wrapped specimen for Case 1

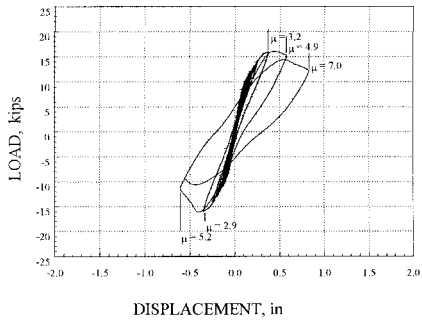

Figure 5 Load vs. displacement of Case I unwrapped beam-column joint

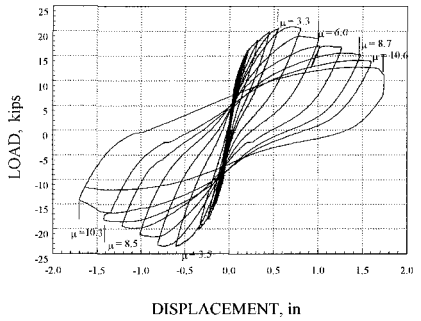

Figure 6 Load vs. displacement of Case I CFRP wrapped beam-column joint

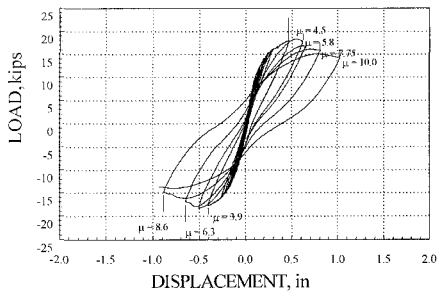

Figure 7 Load vs. displacement of Case IV unwrapped beam-column joint

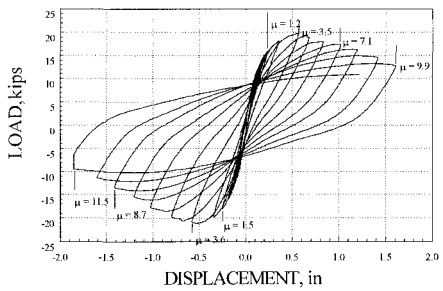

Figure 8 Load vs. displacement of CFRP wrapped beam-column joint

CONCLUSIONS

The test results provided sound and strong evidence that retrofit using CFRP composites is a viable and feasible option for improving the seismic performance of reinforced concrete structures. An extensive experimental program is underway to investigate the durability and structural behavior of beams, columns, and slabs wrapped with CFRP sheets and strips and subjected to severe environment, and sustained loading. Based on the results of the ongoing project, the following conclusions can be drawn:

1. Strength and ductility of the beam-column joints were increased as a result of increasing the thickness of CFRP sheets. Observed ductility of the specimen wrapped with one thin layer of CFRP was 4.3 compared to a ductility of 10.3 for specimens wrapped with one thick layer of CFRP sheets.

2. Typical strengths of Case I and Case IV joints wrapped with one thick layer of CFRP were 38% and 12% higher than those of unwrapped joints

3. Displacements of wrapped joints in Case I and Case IV experienced 140% and 90% more than those of unwrapped joints

4. Ductility of Case I and Case IV joints wrapped with one thick layer of CFRP was 70% and 17% higher than those of unwrapped joints

5. The contribution of CFRP sheets in terms of strength and ductility was the most for Case I specimen. This is attributed to the fact that the joints of Case I specimens were not confined by ties in the joint core.

6. The wrapped joints resisted more loading cycles than unwrapped joints.

REFERENCES

1. MEIER, U 1997. "Post Strengthening by Continuous Fiber laminates in Europe, Non-Metalic (FRP) reinforcement for Concrete Structures," Proceedings of the Third International Symposium, 1:42-56.

2. NANNI, A, Ed. 1993. "Fiber-Reinforced Plastic Reinforcement for Concrete Structures: Properties and Application," Developments in Civil Engineering, Elsevier, 42:450.

3. MARUYAMA, K, UEDA, T, HOSHIJIMA, T, UEMURA, M 1999. "Japan Society of Civil Engineers Activity on Continuous Fiber Sheet for Retrofit of Concrete Structures," Proceedings of the Fourth International Symposium on Fiber Reinforced Polymer Reinforcement for Reinforced Concrete Structures, Eds. Charles et. al., ACI International, pp. 151-157.

4. CATBAS, K H. 1997. "Performance of Beams Externally Reinforced with Carbon Fiber Reinforced Plastic Laminates," Masters Thesis, Department of Civil and Environmental Engineering, University of Cincinnati, pp. 92.

5. GRACE, N F, SOLIMAN, A K, ABDEL-SAYED, G, SALEH, K R. 1999. "Strengthening of Continuous Beams Using Fiber Reinforced Polymer Laminates," Proceedings of the Fourth International Symposium on Fiber Reinforced Polymer Reinforcement for Reinforced Concrete Structures, Eds. Charles et. al., ACI International, SP 188-57, pp. 647-657.

6. TALY, N, GANGARAO, H V S. 1999. "Guidelines for Design of Concrete Structures Reinforced with FRP Materials," 44th International SAMPE Symposium, May 23-27, 1999, pp. 1689-1696.

7. SHMOLDAS, A, SCHLEIFER, G, SEIBLE, F, INNAMORATO, D 1997. "Carbon Fiber Retrofit of the Arroyo Seco Spandrel Column," Report No. SSRP-97/13, Division of Structural Engineering, University of California, San Diego.

8. ZHANG, A, YAMAKAWA, T, ZHONG, P, OKA, T 1999. "Experimental Study on Seismic Performance of Reinforced Concrete Columns Retrofitted with Composite-Materials Jackets," Proceedings of the Fourth International Symposium on Fiber Reinforced Polymer Reinforcement for Reinforced Concrete Structures, Eds. Charles et. al., ACI International, SP 188-24, pp. 269-278.

9. MATSUZAKI, Y, NAKANO, K, FUJII, S, FUKUYAMA, H 1999. "Japanese State of the Art on Seismic Retrofit by Fiber Wrapping for Building Structures: Research," Proceedings of the Fourth International Symposium on Fiber Reinforced Polymer Reinforcement for Reinforced Concrete Structures, Eds. Charles et. al., ACI International, SP 188-75, pp. 879-893.

10. PANTELIDES, C P, GERGELY, J, REAVELEY, L D, VOLNYY, V A 1999. "Retrofit of Reinforced Concrete Bridges with Carbon Fiber Reinforced Polymer Composites," Proceedings of the Fourth International Symposium on Fiber Reinforced Polymer Reinforcement for Reinforced Concrete Structures, Eds. Charles et. al., ACI International, SP 188-40, pp. 441-453.

11. ISSA, M A, ISLAM, M D S, LESLIE, M, ABDALLA, H, DO VALLE, C. "Seismic Retrofit of Reinforced Concrete Members with CFRP Composites," Innovative Systems for Seismic Repair and Rehabilitation of Structures – Design and Applications, Proceedings of the Second Conference on Seismic Repair and Rehabilitation of Structures (SRRS2), March 2000, Fullerton, CA, pp. 37-49.

SHEAR CAPACITY OF RC BEAMS STRENGTHENED WITH FRP LAMINATES

F Micelli **L De Lorenzis** **A La Tegola**

University of Lecce

Italy

A Nanni

University of Missouri Rolla

United States of America

ABSTRACT. Shear strengthening of RC beams using fibre-reinforced polymer (FRP) composites has recently proved successful. Several experimental data mostly related to shallow beams have been collected, and design Equations have been proposed for the computation of the shear capacity of a strengthened RC beam taking into account the FRP contribution. As part of an experimental study conducted in a real building, RC joists were strengthened with FRP laminates to increase their flexural capacity. The joists were also strengthened in shear and loaded until failure close to the support with a low shear span-to-depth ratio. The experimental results showed that FRP contribution to the shear capacity was less than predicted by the current analytical methods because of premature debonding of FRP sheets. In this paper a model is developed to predict the shear capacity of the tested RC beams strengthened in shear with FRP composites, using a strut-and-tie approach. A comparison with experimental results is shown as practical application of the proposed analytical procedure.

Keywords: FRP, Composites, Shear strengthening, Reinforced concrete.

Francesco Micelli is a Ph.D Candidate at University of Lecce, he is an ACI and SAMPE Member.

Laura De Lorenzis is an Assistant Professor at University of Lecce, MSc at University of Missouri Rolla, she is a Ph.D Candidate at University of Lecce, ACI Member.

Antonio La Tegola is Full Professor at University of Lecce, Honorary Professor at University of Santiago in Guayaquil, (Ecuador). He is an ACI, ASCE, RILEM, and IABSE Member.

Antonio Nanni is Vernon and Maralee Jones Professor of civil Engineering at the University of Missouri Rolla, he is director of CIES at UMR, ACI Fellow, Member of ACI 440, 530, 544, and 549 Committees, Chair of 437, ASCE Member.

INTRODUCTION

Reinforced concrete (RC) beams with a low span-to-depth ratio have found wide application in offshore structures and civil engineering buildings. The study of the shear behaviour of such members cannot be based on the classical one-dimensional beam theory.

In the last decade different analytical and experimental studies have focused on the mechanical behaviour of RC beams with a short shear span, that have an increased shear capacity relative to shallow flexural members. This can be explained taking into account a stress redistribution due to cracking of the concrete generated by tensile stress that plays a significant role, therefore design Equations used for shallow beams significantly underestimate the shear capacity of deep beams, since it is common practice in design to neglect the arching effect. The strut and tie approach is the common starting point in order to develop rational design models for such RC members, and in the last years FEA (finite element analysis) and fracture mechanics models also helped to understand the real mechanisms that control the failure of non flexural RC beams [1-5].

Scientific efforts were also conducted to investigate the contribution to shear capacity furnished by FRP composites bonded to RC shallow beams [6, 7], that resulted in accurate analytical models [8, 9] and design guidelines [10].

It was found that the effectiveness of the FRP wrapping is assured when a good anchor system is provided and when the stiffness of the FRP reinforcement is lower than critical values. In most cases delamination of FRP sheets was observed before fibre rupture, that means a low exploitation of FRP capacity.

All experimental cases were conducted in a laboratory environment with a long shear span load scheme, therefore it should be investigated if these results could be used also for beams with a lower shear span.

In this paper a theoretical analysis is presented in order to predict experimental results observed from shear controlled RC beams tested in a real building, since it was found that theoretical models used to calculate shear capacity enhanced by FRP furnish unsatisfactory predictions.

All mechanisms that contribute to the overall shear strength of RC beams are computed, considering the effects of shear cracking. The presence of FRP sheets is also considered for strengthened members taking into account the occurrence of premature peeling that avoids to reach the ultimate stress-strain values of the fibres.

THEORETICAL ANALYSIS

The analysis of the shear mechanisms that should be considered to calculate the ultimate capacity of RC beams without web internal reinforcement or FRP external wrapping, are the arching effect, the dowel action and mechanical interlock by concrete aggregates.

All these strength mechanisms have a different behaviour in correspondence of the collapse, mainly due to the fact that concrete has a brittle behaviour in tension and compression, while steel reinforcement can be considered as a ductile material with unlimited elongation.

The presence of longitudinal steel in both sides of the cross section generates the arching effect and the dowel action. Since the load scheme of the tested beams led to a ratio of 2.4 between the shear span a and the height H of the cross section, the arching action can be computed using a strut and tie approach as showed in Figure 1. A concrete strut starts from the point in correspondence of load application until the point in correspondence of the far end support of the beam, while the longitudinal steel reinforcement of the upper part of the cross section is the tie of the arch.

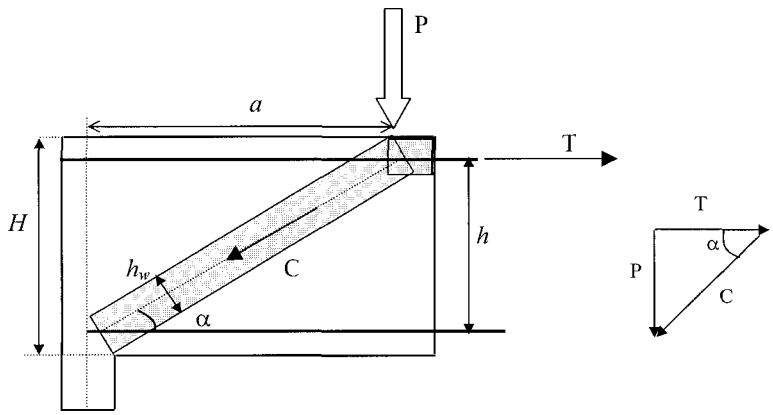

Figure 1 Strut and tie scheme for arching effect

From the geometry of the proposed scheme and from equilibrium Equations the following Equations can be considered:

$$\frac{h}{a} = tg\alpha \tag{1}$$

where:
h = internal lever arm [mm]
a = shear span [mm]
α = angle between concrete diagonal strut and steel tie

$$\frac{T}{P} = tg\alpha \tag{2}$$

where:
T = tension force [N]
C = compressive force [N]

The maximum tensile and compressive strengths can be expressed as a function of material properties:

$$T_{max} = A_{ss} \cdot f_y \tag{3}$$

$$C_{\max} = A_{strut} \cdot f_c^{'} \tag{4}$$

where:

A_{ss} = area of superior longitudinal steel [mm^2]
A_{strut} = area of concrete strut [mm^2]
f_y = yielding tension of steel [N/mm^2]
f'_c = compressive strength of concrete [N/mm^2]

The equilibrium between the vertical forces in correspondence of the failure can be written as follows:

$$P_{ut} = A_{ss} \cdot f_y \cdot \tan\alpha \tag{5}$$

$$P_{uc} = b_w \cdot h_w \cdot f_c^{'} \cdot \sin\alpha \tag{6}$$

where:

P_{ut} = ultimate tensile force furnished by steel tie in the vertical direction [N]
P_{uc} = ultimate compressive force furnished by concrete strut in the vertical direction [N]
b_w = width of the cross section [mm]
h_w = width of the concrete diagonal strut [mm]

If the steel is yielded when the crushing of the concrete will occur, thus the tension in the steel tie is equal to f_y. Therefore the following Equation can be written at failure, assuming that $P_{uc} = P_{ut}$:

$$h_w = \frac{A_{ss} \cdot f_y \cdot \cos\alpha}{f_c^{'} \cdot b_w} \tag{7}$$

At the same time, from the geometry in Figure 1 the internal lever arm can be expressed as:

$$h = H - d_c - \frac{h_w}{2} \tag{8}$$

where:

H = total height of the cross section [mm]
d_c = concrete cover related to the lower longitudinal steel [mm]

The values of h_w and α can be easily computed from Equations (7) and (8), and then the values of V_{arch} can be calculated from Equation (5) or (6).

For the computation of the dowel action, it can be assumed that at failure the steel is yielded, since the beams are under reinforced. According to failure criterion by Mises, when the steel results yielded by tension forces, then it is not able to carry any other transversal tension and vice versa. The longitudinal steel A_{si} in the lower part of the cross section can be considered yielded with a tangential tension $\tau_y = \frac{f_y}{\sqrt{3}}$, and the contribution to the shear capacity can be

considered equal to $A_{si} \cdot \tau_y$. As it regards the longitudinal steel in the upper side of the cross section, it can be yielded or can work in the elastic field. In the first case the contribution to the dowel action is null, while the steel work as a tie mechanism in the arch configuration of the cracked beam. If the second hypothesis is true, it means that the ultimate strength mechanism will be furnished by the dowel action of the superior steel more than the splitting of the compression strut of the arch scheme. This can be easily understood by considering the brittle behaviour of the concrete. In this case the shear contribution furnished by the longitudinal steel in the upper side is $A_{ss} \cdot \tau_y$.

For the RC beams unstrengthened with FRP it can be considered that the width of the diagonal crack is not so large to avoid a contribution by mechanical interlock of the aggregates.

It is difficult to compute this contribution to the shear capacity, especially in the cases in which the characteristics of concrete are not well known. In general, the shear carried by mechanical interlock should be computed as a tension τ_{int} that is related to the type and size of aggregates multiplied by the area of interlocking. According to Figure 1 this area is computed as:

$$A_{\text{int}} = \frac{a}{\cos\alpha} \cdot b_w \tag{9}$$

in which the term $\frac{a}{\cos\alpha}$ is the crack length.

The value of τ_{int} can be considered equal to a maximum tangential interfacial stress. The computation of this stress is not easy and different values could be used. A first attempt adopted in this work was to consider τ_{int} equal to the tensile strength of concrete according to Eurocode: $0.27 \cdot \sqrt[3]{f_c'^2}$ in which f'_c is the compressive strength of concrete in N/mm^2. Therefore the contribution of the aggregates interlock to shear capacity can be written as:

$$P_{\text{int}} = \frac{a}{\cos\alpha} \cdot b_w \cdot 0.27 \cdot \sqrt[3]{f_c'^2} \tag{10}$$

This value is closer to reality when the crack width is smaller than the aggregate dimensions, otherwise the mechanical contact should be neglected.

Therefore the contributions to the ultimate shear capacity of a RC beam will be the dowel action furnished by the steel in the lower side, the concrete splitting due to the arch effect, and mechanical interlock when the shear crack will be sufficiently narrow, when the steel in the upper side is yielded. Otherwise the dowel action furnished by the upper steel will be present after the concrete splitting caused by the arch effect, thus the yielding of the upper steel will correspond to the ultimate failure.

When the beam is strengthened with unidirectional FRP sheets, another brittle mechanism will furnish a contribution to the ultimate shear capacity. The additional mechanism may correspond to the ultimate strength of the fibres when the tensile fibre rupture will occur, but this means that the concrete/resin interface should transfer the high stress to the fibres. This could be possible when the beam is fully wrapped, or a perfect FRP anchorage is provided. In all other cases a premature peeling of FRP sheets will control the structural collapse.

To understand the FRP contribution it should be noted that after shear crack will form the FRP will be stressed in order to carry the shear forces. The FRP sheets will be bonded to the concrete until a sufficient anchorage length will be available, when the cracking will develop, then the anchorage length will reduce in the upper side of the crack as shown in figure 2 for a T-beam with FRP-wrapped web with 90° fibres respect of the beam axis.

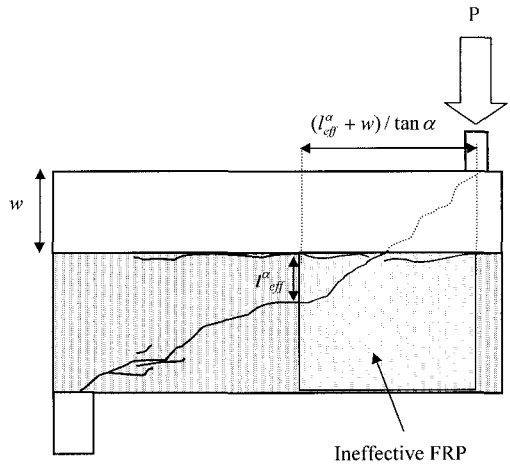

Figure 2 Effects of cracking on FRP shear carrying capacity in RC T-beams

Therefore the FRP close to the upper side of the cross section will not be able to carry the stress. The collapse will occur when the ultimate bond stress will be developed; in this stage the ultimate mechanisms that contribute to the shear capacity will be the dowel action, the arch effect, and FRP contribute, while the mechanical interlock should be disregarded since the crack opening will be much more than the unstrengthened beams.

The computation of FRP shear carrying capacity can be computed using the experimental values found by Miller et al. [11]. The values were found by testing concrete beams bonded with different amounts of unidirectional Carbon FRP (CFRP), the suggested effective bond length l_{eff} was found to be 80 mm while the tangential stress value τ_{peel} that causes debonding of FRP is calculated by:

$$\tau_{peel} = 0.0184 \cdot \sqrt{t \cdot E} \tag{11}$$

where:

τ_{peel} = maximum bond stress	[N/mm^2]
t = thickness of FRP reinforcement	[mm]
E = Young modulus of FRP reinforcement	[N/mm^2]

According to these values the FRP contribution was computed taking into account the slope of the crack and the ineffective region in which the anchorage length is less then the effective length. Therefore the effective length in the fibre direction was computed as $l_{eff}^{\alpha} = l_{eff} \cdot \cos\alpha$ that is $l_{eff}^{\alpha} = 80 \cdot \cos\alpha$ [mm], therefore the effective force carried by the FRP is:

$$P_{FRP} = 2 \cdot l_{eff}^{\alpha} \cdot \left[a - \left(\frac{w + l_{eff}^{\alpha}}{\tan\alpha} \right) \right] \cdot 0.0184 \cdot \sqrt{t \cdot E} \qquad (12)$$

where:

l_{eff}^{α} = effective bond length in the direction of the fibres [mm]
w = height of the flange [mm]

The term $a - \left(\frac{l_{eff}^{\alpha} + w}{\tan\alpha} \right)$ is related to the fact that the FRP is not able to carry shear forces for a length of $\left(\frac{l_{eff}^{\alpha} + w}{\tan\alpha} \right)$ in which the anchorage length is not sufficient or the FRP sheets will not resist to shear forces in correspondence of the flange. Therefore the ultimate shear capacity of the FRP strengthened beams can be computed assuming the contributions of the arch effect, the dowel action, the shear carried by the FRP until the debonding will start. If anchorage devices may be provided it means that the length of the ineffective region will be less than $\left(l_{eff}^{\alpha} / \tan\alpha \right)$, since the FRP sheets are locally fixed to the RC beam. The estimation of the V_{FRP} could not be easy in these cases, and it will depend mostly on the type of anchorage, but theoretically it should be more than the value computed by (12).

Taking into account the hypothesis mentioned above, shear capacity of the tested beams was computed taking into account the contributions of the arch effect, dowel action, and mechanical interlock, for unstrengthened specimens, while for strengthened specimens FRP contribution was also included and mechanical interlock was disregarded.

EXPERIMENTAL PROGRAMME

The experimental tests were conducted in a decommissioned building, where twelve RC T-joists were tested. The joists were isolated by saw cutting from the rest of the floor to avoid load redistribution effects. Concrete cylinders with a diameter of 80 mm and height of 150 mm were extracted from the building.

A compressive strength f'_c of 20.68 MPa was found after mechanical tests, these value confirmed the assumptions from the original design. The average yield strength of steel was assumed to be 345 MPa with elastic modulus of 200,000 MPa.

Two strengthening FRP systems were used, CFRP and Aramid FRP (AFRP). The material properties are presented in Table 1 with reference to fiber content only.

Table 1 FRP sheets properties

MATERIALS	DIMENSIONS t_f (mm)	TENSILE STRENGTH f_{fu} (MPa)	ELASTIC MODULUS E_f (MPa)
CFRP	0.165	3790	228,000
AFRP	0.300	1517	117,000

The cross-section of the joists is shown in Figure 3. The test specimens were 2743 mm long. Longitudinal steel reinforcement was provided by 2-13-mm and 2-19-mm diameter steel rebars. No transverse reinforcement for shear was provided. Five different shear strengthening schemes were considered for evaluation. The different schemes are presented in Table 2.

The end anchoring of FRP sheets adopted for JS3 and JS5 specimens was carried out by inserting 13-mm glass FRP rods into grooves made at the intersection of the joist web and the flange. The grooves were 1.5 times the diameter of the glass FRP rods, and were filled with a high viscosity epoxy paste.

Linear variable displacement transducers (LVDT) all along the span length were used to measure deflection, and inclinometers were used to read the rotation of the end-sections; this helped in ascertaining the fixity of the end supports of the member. For each strengthened member, four strain gauges were attached directly to the FRP on the sides of the strengthened joists, these strain gauges were oriented in the vertical direction (parallel to the fibers). The strain gauges were located at the most likely position of occurrence of a shear crack. A strain gauge was placed on the concrete, at the location of the load, to measure the compressive strain.

Extensometers were also used for measuring strain in the sheets. The loading was applied using one or more hydraulic jacks reacting against the floor above, and recorded with a load cell and an automatic data acquisition system was used to collect data.

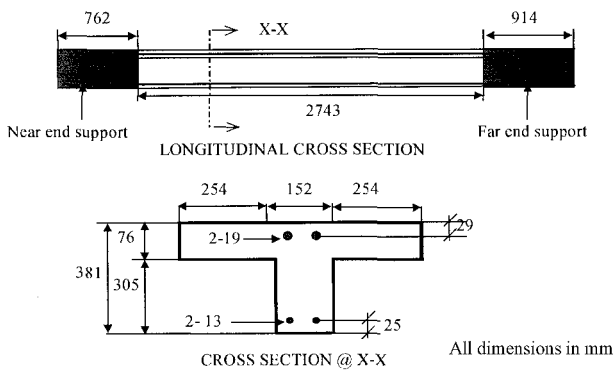

Figure 3 Cross section of tested RC T-joists

Table 2 Experimental program and FRP strengthening schemes

MEMBER	EXTERNAL STRENGTHENING				
	FRP type	Schemes			
		Shear		Positive flexure (102-mm wide ply)	Negative flexure (508-mm wide ply)
		Plies	Anchor		
JS1 A and B	--	0	No	--	--
JS2 A and B	Carbon	1	No	1	1
JS3 A and B	Carbon	1	Yes	1	1
JS4 A and B	Carbon	2	No	3	2
JS5 A and B	Carbon	2	Yes	3	2
JS6 A and B	Aramid	2	Yes	3	2

EXPERIMENTAL RESULTS

The experimental values measured after testing are reported in Table 3. JS(i) A and JS(i) B, represent two repetitions of the same specimen type. The first column shows the maximum applied load, the second column shows the ultimate shear force. Since the end supports showed differential settlements recorded by LVDTs and inclinometers the values of $V_{u_{exp}}$ were computed taking into account moment redistribution. In the last column the ultimate shear values computed without the moment redistribution are illustrated.

Specimen JS1A, one of the two control specimens showed a diagonal shear failure. The initial shear cracks appeared close to the near-end support at a loading of 133 kN. The diagonal cracks, once formed, spread towards and partially into the compression zone becoming flat in the region close to the flange-web intersection. The widening of one of the shear cracks in the web region, and its propagation at its ends led to eventual failure of the specimen in the left shear span at a load of 315kN. The joist JS1B showed a similar failure mode, with an ultimate load of 320 kN.

The specimens JS2 A and B were strengthened with a single U-wrap of CFRP (90^{o}), placed perpendicular to the longitudinal axis of the member. The positive flexure strengthening was carried out with a single CFRP ply applied to the soffit of the joist. The negative flexure strengthening was carried out by applying a single CFRP sheet on the flange of the joist. The specimens JS4 A and B were U-wrapped with two CFRP sheets. The positive flexure strengthening was carried out by applying three plies of CFRP sheets and the negative strengthening was carried out by applying two plies of CFRP sheets. The failure as observed in both the cases was due to premature peeling of CFRP sheets.

Specimens JS2 A and B failed at an ultimate load of 355 kN and 351 kN respectively, whereas the specimens JS4 A and B failed at an ultimate load of 364 and 311 kN, respectively. In all cases, shear failure of the member lead to severe delamination of the CFRP sheets in the near end corner. Fiber rupture was observed also in the lower web corner due to stress concentration.

Table 3 Experimental results

SPECIMEN	P_{max} (kN)	V_{uexp} (kN)	V_{cexp} (kN)	V_{fexp} (kN)	V^*_{uexp} **(kN)**
JS1A	315	209	209	-	233
JS1B	320	212	212	-	237
JS2A	355	236	-	25	263
JS2B	351	233	-	22	260
JS3A	440	298	-	87	326
JS3B	414	277	-	66	307
JS4A	364	256	-	45	270
JS4B	311	208	-	0	230
JS5A	418	298	-	87	310
JS5B	400	285	-	74	296
JS6A	404	245	-	34	299
JS6B	360	218	-	9	266

V^*u_{exp} was computed disregarding the settlement at the supports, without considering a moment redistribution.
V_{cexp} is the shear capacity of the unstrengthened specimens
V_{fexp} is the increase in shear capacity due to the presence of FRP

Specimens JS4 A and B failed at a higher load then the single wrapped JS2 members. The failure mode JS4 was similar to that of JS2. The high shear developed at the near end lead to severe delamination, which in turn resulted in fibre rupture at the bottom of the member.

The specimens JS3 A and B were strengthened with a single U-wrap of CFRP sheet, with end anchors, while the specimens JS5 A and B were strengthened with two anchored plies. The function of the end-anchors was to prevent the premature peeling of the CFRP sheets.

Specimens JS3 A and B failed at an ultimate load of 440 kN and 414 kN, whereas the specimens JS5 A and B failed at an ultimate load of 418 kN and 400 kN. The joists JS6 A and B were strengthened with two plies of aramid fibres. Specimens of JS6 A and B failed at an ultimate load of 404 kN. The failure of the members JS3, JS5 and JS6 was due to end-anchor pulling out as shown in Figure 4.

DISCUSSION

After the shear crack opened in the unstrengthened members a further shear capacity was furnished, since the ultimate load was more than two times the cracking load. This highlighted the presence of the arching effect that was significant. The contribution of arch action and FRP sheets computed the proposed simple model was also compared with a computation of the shear capacity by ACI.

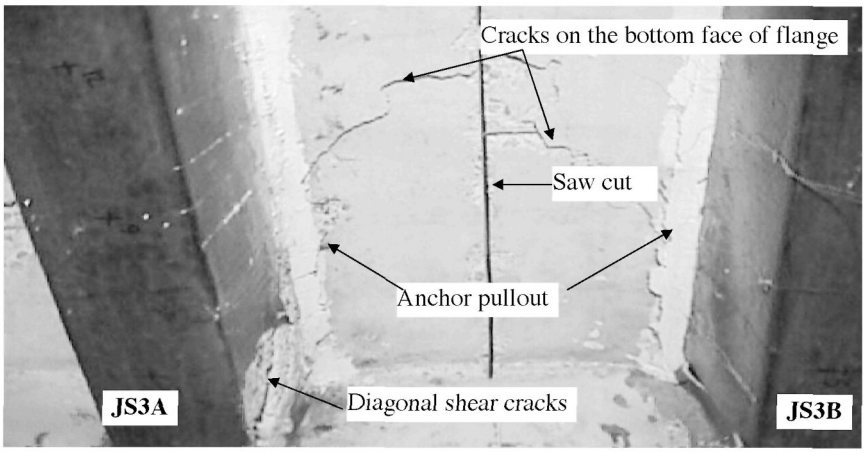

Figure 4 Peeling failure of members JS3-A and JS3-B

Shear capacity of unstrengthened beams was computed by ACI Code 11.8, and was found to be 101 kN. A simplified computation according to ACI code 11.3.1 used for a shallow beam, would give a value of V_c equal to 45 kN. The contribution of FRP was calculated using ACI 440F and results are compared in Table 4 in which the analytical values of shear capacity of the tested specimens are illustrated and compared with the experimental values reported in Table 3. Shear capacity computed by ACI seemed to be more conservative than the analytical results of this study even if the contribution of FRP was computed without considering the safety factors proposed in ACI 440.

The theoretical FRP shear contribution was computed using Equation (12) without taking into account the presence of the anchorage systems, since it is not easy to quantify the effects of the anchors on the effective bond length.

The experimental results highlighted that the presence of the anchorages was less effective than what expected, since the flat crack in the web-flange corner led to anchors pull-out.

A double amount of FRP reinforcement did not show to be an effective solution since the rupture was controlled by debonding of FRP sheets caused by cracking development that dramatically affected the effective bond length, in fact there are not significant difference between JS2 and JS4 specimens, while there is a small reduction of the ultimate load in JS5 when compared with JS3 beams.

A good accordance between theoretical and experimental values was found for FRP wrapped specimens, the analytical shear capacity underestimated by about 20% the real values found in the field for unstrengthened specimens while the theoretical FRP contribution over estimated the experimental values for JS4 members.

CONCLUSIONS

A theoretical approach was presented in order to predict the shear capacity of unstrengthened and FRP strengthened RC T-joists that were loaded in a short shear span scheme.

Table 4 Analytical values of shear capacity

SPECIMEN	V_{utheor} (kN)	V_{utheor}/V_{uexp}	V_{ACI} (kN)
JS1A	162	0.78	101
JS1B		0.76	
JS2A	282	1.19	165
JS2B		1.21	
JS3A	282	0.94	185
JS3B		1.01	
JS4A	361	1.41	195
JS4B		1.73	
JS5A	361	1.21	227
JS5B		1.26	
JS6A	274	1.11	187
JS6B		1.25	

The analytical model was based on a simple strut and tie approach to take into account the arch contribution that is always neglected in design procedures. The presence of the other shear mechanisms was discussed with or without the presence of the FRP reinforcement, since the shear cracking is influenced by the external FRP sheets.

Twelve RC T-joists were tested until failure with different FRP amount, providing different anchorage systems to enhance the effectiveness of the FRP action. All the tested specimens failed in shear, and all strengthened beams showed FRP debonding caused by high bond stress and insufficient FRP effective bond length that was affected by the crack opening. Anchored sheets peeled off the web since the anchorage devices were pulled out by the flat crack at the web-flange interface

Experimental results were compared with analytical values and a good accordance was found between them, except for members that were strengthened with two unanchored carbon FRP sheets that showed a premature debonding.

Further investigations are needed to see how the shear span can affect the effectiveness of FRP external reinforcement and how a good anchorage device can be provided to avoid a premature peeling failure.

ACKNOWLEDGMENTS

This research was supported by The "Repair of Buildings and Bridges with Composites (RB2C)"of the CIES at the University of Missouri Rolla (USA), and the Innovation Engineering Dept. of the University of Lecce (Italy).

REFERENCES

1. AVERBUCH, D., DE BUHAN, P., "Shear design of reinforced concrete deep beams: a numerical approach", Journal of Structural Engineering, ASCE, 125 (3), March 1999, pp. 309-318.

2. FOSTER, S.J., "Design of non-flexural members for shear", Cement and Concrete Composites, (20) 1998, pp.465-475.

3. LIN, Z., RAOOF, M., "Application of non linear finite strip technique to concrete deep beams", *Engineering Structures,* 17 (10), 1995, pp. 725-736.

4. KIM, D., KIM, W., WHITE, R.N., "Arch Action in Reinforced Concrete Beams – A rational Prediction of Shear Strength ", ACI Structural Journal, 96(4), 1999, pp.586-593.

5. OH, J.K., SHIN, S.W., "Shear strength of reinforced high strength concrete deep beams", ACI Structural Journal, 98 (2), 2001, pp.164-173.

6. CHALLAL, O., NOLLET, M.J., PERRATON, D.,"Shear Strengthening of RC Beams by Externally Bonded Side CFRP Strips", Journal of Advanced Composites, (Vol. II) 1998, pp. 111-113.

7. GENDRON, G., PICARD, A., GUERIN, M.C., "A Theoretical Study on Shear of Reinforced Concrete Beams Using Composite Plates", Composite Structures, Vol.45, No.4, 1999, pp.303-309.

8. KHALIFA, A., GOLD, W., NANNI, A., ABDEL -AZIZ M. I., "Contribution of Externally Bonded FRP to the Shear Capacity of RC Flexural Members", Journal of Composites for Construction, ASCE, Vol. 2, No. 4, 1998, pp.195-202.

9. TRIANTAFILLOU, T.C. , "Design of Concrete Flexural Members Strengthened in Shear with FRP", Journal of Composites for Construction, ASCE, 4(4), 2000, pp.198-205.

10. ACI 440 DRAFT, "Guide for the Design and Construction of Externally Bonded FRP Systems for Strengthening Concrete Structures", ACI 440 Committee, Externally Bonded FRP Systems for Strengthening Concrete Structures, 2000, pp.54-58.

11. MILLER, B., NANNI, A., AND BAKIS, C. E., "Analytical Model for CFRP Sheets Bonded to Concrete," Proc. 8th Int. Structural Faults and Repair Conf., M.C. Forde, Ed., Engineering Technics Press, Edinburgh, Scotland, 1999, 10 pp.

EVALUATION OF DIFFERENT FIBRE ADDITIONS IN CONCRETE AND THEIR EFFECT ON MECHANICAL PROPERTIES AND CORROSION OF STEEL IN CONCRETE EXPOSED TO CHLORIDE IONS

Ch Dehghanian
A R Baratifard
University of Technology in Isfahan
Iran

ABSTRACT. In this work, Polypropylene and glass fibres as an additive material were used in concrete. Fibres with different volume percent were added into concrete. These concretes were exposed to 3.5% salt solutions. Corrosion behavior of steel in these concrete was determined using the electrochemical methods. Compressive and tensile strength of these concretes were also measured. Addition of Fibre showed an increase of 49% in tensile strength of concrete compared to the control concrete. In addition, use of fibre in concrete increased the resistance of steel against pitting corrosion and uniform corrosion. The compressive strength of polypropylene fibre increased with age, while the compressive strength of glass fibre decreased with age. Resistance of steel against pitting and uniform corrosion in the concrete containing glass fibre was better than that in the concrete with polypropylene.

Keywords: Fibre, Concrete, Corrosion, Steel, Polypropylene, Glass, Compressive Strength, and cyclic polarization

Ch Dehghanian, is an associate professor in the Department of Chemical Engineering at the University of Technology in Isfahan. He conducts research in various phases of corrosion of steel in concrete including effect of additives in strength and corrosion behavior of steel in concrete. He also conducts research on coatings, inhibitors and cathodic protection.

A R Baratifard is a graduate student in Department of Chemical Engineering at the University of Technology in Isfahan. He conducts research in corrosion of steel in concrete containing fibre.

INTRODUCTION

Recently, concrete with fibres has received considerable interest due to its high toughness and increased tensile and flexural strength. Steel fibres [1-3], polymer fibres [4,5] and carbon fibres [6,7] are the main fibres, which are frequently used. Control of crack and corrosion of steel in concrete has been given special attention in design of concrete structures. Thus there is an interest in developing means to stifle corrosion of steel in concrete.

Use of fibres in concrete is one of the methods in increasing the strength and lowering the corrosion of steel in concrete. Low-volume polypropylene in the plastic stage has shown to be effective in reducing the crack tendency [8,9]. Testing of properly cured and uncracked low volume polypropylene concrete has shown a marginal improvement in mechanical properties [10] and corrosion of steel in concrete [11].

The main impetus of this research is to use different volume percent of polypropylene and glass fibres in concrete to investigate their effect on mechanical properties and corrosion behavior of steel in concrete exposed to 3.5 % NaCl solution. Electrochemical methods such as cyclic, linear and Tafel polarization was used in this study.

EXPERIMENTAL PROCEDURE

A number of concrete blocks with the dimensions of 70x70x70 mm were cast. These samples had steel rebar in it (see Figure 1). These samples were used for electrochemical testing. Some other concrete samples similar to Figure 1 also were made but without steel rebar. These samples were used for compressive strength tests. All samples were made with different volume percent of polypropylene and some with glass fibres. The fibre volume percent ranged from 0 to 0.5 percent. Mix design for the concrete samples were based on ACI-211 and the sizes of sand aggregates were in the range determined by ASTM-C33. Portland cement Type I with the composition shown in Table 1 was used. Water-cement ratio was controlled with superplasticizer to be 0.45.

The properties of fibres used are shown in Table 2. The concrete samples were cured in distilled water for 28 days. After 28 days of curing, the concrete samples were stored in 3.5% NaCl solution. Electrochemical tests such as cyclic polarization, Tafel and linear polarization were carried out on the concrete samples after 72 days of exposure to solution.

Mechanical and Electrochemical Tests

Compressive and tensile strengths of the concrete samples were measured at 28 and 90 days. Electrochemical tests for steel in concrete were conducted after 72 days of exposure to solution. In cyclic polarization, steel potential was polarized from –400 mv with respect to saturated calomel electrode (SCE) until 900 mv Vs SCE, then the potential was reversed to– 400 mv. The scan rate of 2 mv/sec was selected. In Tafel polarization, the steel potential was started from –250 mv until +250 mv with respect to open circuit potential. The scan rate of 0.5 mv/sec was used in these tests. Finally, the linear polarization was carried out from –20 mv to +20 mv Vs SCE with the scan rate of 0.1 mv/sec. From the resulting polarization curves, corrosion potential, corrosion rate, pitting potential of steel were obtained.

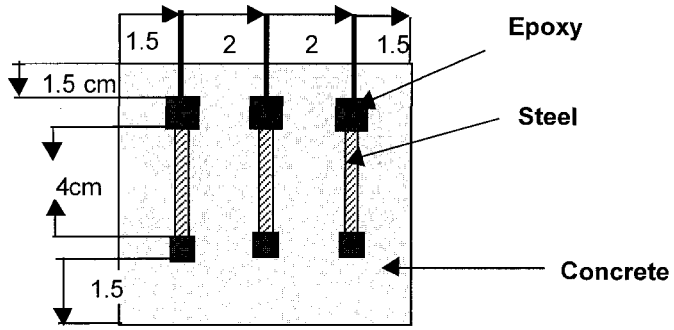

Figure 1 Schematic of concrete sample with steel rebar configuration

Table 1 Portland cement Type I composition

PERCENT	OXIDE
65.03	CaO
21.02	SiO_2
5.71	Al_2O_3
2.96	Fe_2O_3
1.55	MgO
1.42	SO_3
0.45	K_2O
0.35	Na_2O
1.27	L.O.I
0.21	Insoluble
0.06	Others

Table 2 Properties of fibres

TYPE OF FIBRES	LENGTH (mm)	DENSITY (g/cm^3)	% ELONGATION	TENSILE STRENGTH (MPa)
Polypropylene	12	0.96	7	425
Glass	12	2.4	55	1173

RESULTS AND DISCUSSION

Figure 2 is a typical cyclic polarization curves for steel in concrete. This figure shows the pitting potential (E_n) and repassivating potential (E_p) which was used in the results. Figures 3 and 4 are compressive strengths of concrete containing polypropylene and glass fibres respectively. The compressive strengths in the concrete with polypropylene fibre for 28 and 90 days showed an improvement in comparison to the concrete with no fibres. However, the compressive strength of concrete at 28 days increased with an increase from 0.1 to 0.5

volume percent of fibre. The compressive strengths of concrete after 90 days were reduced at 0.3 and 0.5 volume percent fibre in comparison to 0.1 volume percent. However, the compressive strengths of concrete with 0.1, 0.3 and 0.5 volume percent at 90 days were increased in comparison to that of 28 days of concrete age.

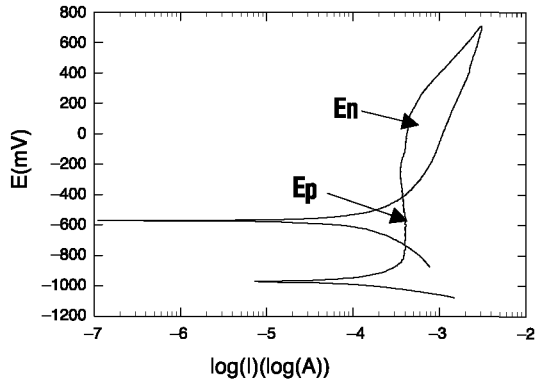

Figure 2 A typical cyclic polarization curve for steel in concrete

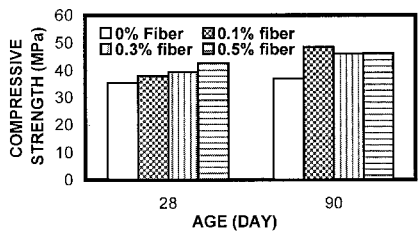

Figure 3 Compressive strength with respect to time as a volume percent of polyproperlene fiber added to concrete

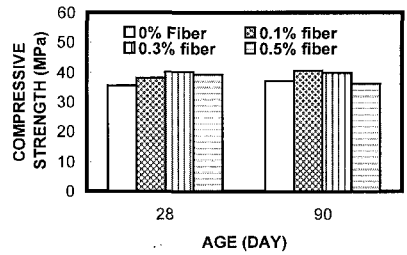

Figure 4 Compressive strength with respect to time as a volume percent of glass fiber added to concrete

The compressive strengths of concrete with glass fibre was higher than concrete with no fibre at 28 days of age. However, at 0.3 volume percent of fibre the compressive strength was higher than 0.1 and 0.5 volume percent. At 90 days of age, the compressive strength decreased with increasing fibre volume percent and even for 0.5 volume percent the strength was lower than the concrete with no fibre.

Figures 5 and 6 indicate the tensile strengths of concrete containing polypropylene and glass fibre respectively. The tensile strength of concrete with polypropylene fibre increased with increasing the volume percent of fibre at 28 days of age. This increase was slower at 90 days of age. Tensile strengths of the concrete with glass fibre increased significantly in comparison to the concrete with no fibre at 28 days of age. However, an increase in volume percent of fibre increased the strength of concrete slowly. At 90 days of age, even though the concretes with fibre showed higher strength than the concrete with no fibre, but the strength for concretes with glass fibre decreased with respect to the concretes with 28 days of age.

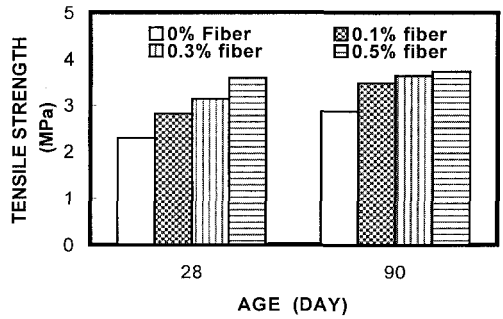

Figure 5 Tensile strength with respect to time as a function of volume percent of polypropylene added to concrete

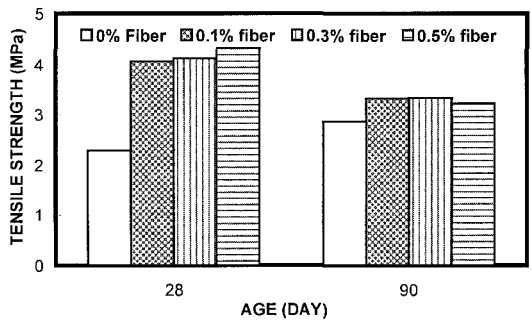

Figure 6 Tensile strength with respect to time as a function of volume percent of glass fiber added to concrete

Figure 7 is a comparison between the compressive strengths of the concretes with 0.3 volume percent of polypropylene and glass fibres in concrete. At 28 days of age, compressive strength for both fibres was almost the same. However, at 90 days of age, the concrete with polypropylene fibre gained more strength than the concrete with glass fibre.

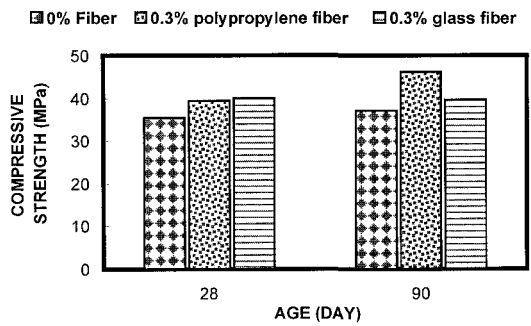

Figure 7 A comparison between different fiber concretes as a function of time

Figure 8 is a comparison between tensile strength for the concretes with 0.1 volume percent of polypropylene and glass fibres. At 28 days of age, the concrete with glass fibre gained higher strength in comparison to polypropylene fibre. However, at 90 days of age, the concrete with polypropylene fibre gained more strength than the concrete with glass fibre. As a matter of fact the strength for the concrete with glass fibre was reduced at 90 days of age in comparison to the same concrete at 28 days of age.

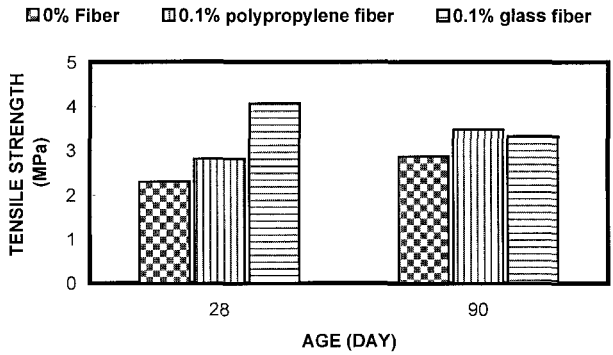

Figure 8 A comparison between tensile strength of concrete with different fibers

Figure 9 is a plot of corrosion potential for steel in the concrete containing different volume percent of polypropylene fibre. The corrosion potential of steel for all percentages of fibre was more positive than that in the concrete with no fibre. The potential of steel in the concrete with fibre remained almost uniform with time while the potential shifted towards more negative values with time for the steel in concrete with no fibre.

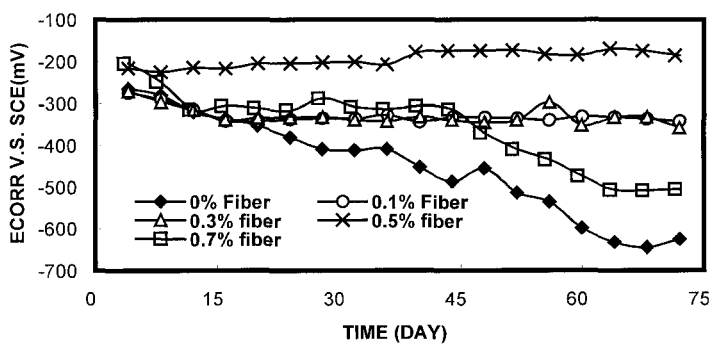

Figure 9 Corrosion potential of steel as a function of volume percent of polypropylene fiber in concrete. Samples were in 5% NaCl solution

Similar results were obtained for the steel in the concrete containing different volume percent of glass fibre (see Figure 10).

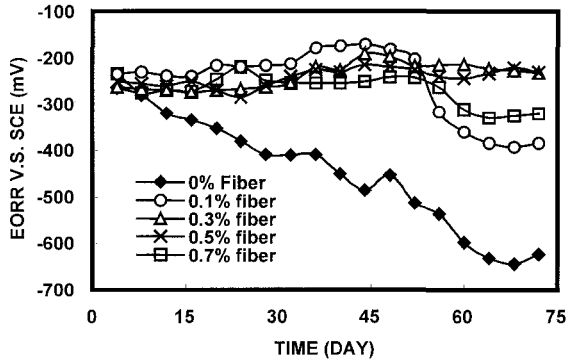

Figure 10 Corrosion potential of steel in concrete containing different volume percent of glass fiber

Figure 11 is a plot of pitting potentials of steel in concretes with different volume percent of polypropylene and glass fibres. Steel in the concretes with polypropylene fibres showed more resistance to pitting corrosion in comparison to the concrete with no fibre. However, at 0.1 volume percent fibre, the steel resistance to pitting corrosion was the highest, but with an increase in volume percent of fibre the resistance to pitting corrosion was reduced. Steel resistance to pitting corrosion in the concrete with glass fibre increased with an increase in volume percent of fibre. However, steel resistance to pitting corrosion in the concretes with 0.1 and 0.3 volume percent of polypropylene fibre was much higher than that with glass fibre.

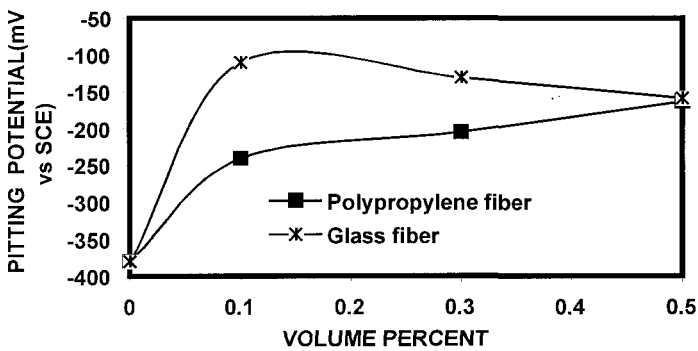

Figure 11 Pitting potential of steel in concrete containing fiber. Samples were in 3.5% NaCl solution for 72 days

Figure 12 is a plot of difference in pitting and repassivating potential of steel in the concretes with different volume percent of polypropylene and glass fibres. This difference was decreased with an increase in volume percent of fibre in concrete. However, this decrease for the concretes with 0.1 and 0.3 volume percent of glass fibre was much higher than the concretes with equal volume percent of polypropylene fibre.

This difference at 0.5 volume percent for both fibres was almost the same. A decrease in difference between pitting and repassivating potential of steel is an indicative of how easily the steel will repassivate and repair the broken film. Therefore, steel in the concretes with glass fibre especially, at 0.1 volume percent of fibre can repassivate better than in the concretes with polypropylene fibre.

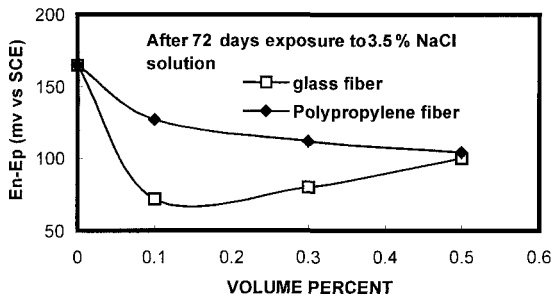

Figure 12 Difference in pitting and passivating potential of steel in concrete containing fiber

Figure 13 is a plot of corrosion rate of steel in the concretes with different volume percent of polypropylene and glass fibres. The uniform corrosion rate for steel in the concretes with 0.1 and 0.3 volume percent of polypropylene fibre decreased in comparison to the concrete with no fibre. This decrease was highest at 0.3 volume percent of fibre. However, the corrosion rate of steel increased in the concretes with 0.5 volume percent fibre. The corrosion rate of steel in the concretes with 0.1 volume percent glass fibre increased in comparison to the concrete with no fibre. However, the corrosion rates for steel decreased in the concretes with 0.3 and 0.5 volume percent of glass fibre. The corrosion rate of steel in the concretes with 0.3 and 0.5 volume percent of glass fibre was much lower than the concretes with the same amount of polypropylene fibre.

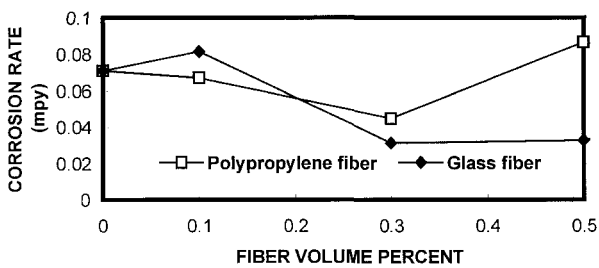

Figure 13 Corrosion rate of steel in concrete containing different fibers. Samples were exposed to 3.5% NaCl solution for 72 days

Based on the results presented here, polypropylene fibre in comparison to glass fibre seems to behave differently. The mechanical properties of concrete improve with polypropylene fibre much better than glass fibre especially at 90 days of age. However, the resistance of steel to uniform corrosion and initiation to pitting corrosion in the concretes with 0.3 volume percent

of glass fibre is better than that in the concretes with the same amount of polypropylene fibre. The results presented here are for the short term (maximum of 90 days). However, to get a better picture for performance of these fibres in concrete, long-term results has to be obtained. This work is in progress to evaluate the performance of these fibres in concrete for longer period of time.

CONCLUSION

1. Addition of polypropylene and glass fibres to concrete increases the compressive strength with respect to concrete with no fibre. This increase for concrete with polypropylene fibre is higher than that with glass fibre, especially at 90 days of age.

2. Addition of polypropylene and glass fibres in concrete increases the tensile strength of concrete with respect to the concrete with no fibre. The tensile strength of concrete with glass fibre decreases with concrete age. This did not occur for the concretes with polypropylene fibre.

3. Resistance of steel to initiation of pitting corrosion in the concretes with polypropylene and glass fibres is better than that of concretes with no fibres. This improvement for concretes with glass fibre is higher than that with polypropylene fibre.

4. Resistance of steel to uniform corrosion in the concretes with 0.3 and 0.5-volume percent glass fibre is higher than that in the concretes with the same amount of polypropylene fibre.

5. 0.3 volume percent fibre is an optimum fibre content to resist corrosion of steel in concrete.

REFERENCES

1. SHAABAN, A. M., AND GESUND, H., "Splitting Tensile Strength of Steel Fiber Reinforced

2. Concrete Cylinders Consolidated by Rodding or Vibrating," ACI Materials Journal, 1993, Vol. 90, No. 4, pp.366-369.

3. BAUN, M.D., "Steel Fiber Reinforced Concrete Bridge Deck Overlays," Transportation Research Record No. 1392. Transportation Research Board, National Research Council, National Academy Press, Washington, D.C., 1993, pp.73-78.

4. HACKMAN, L. E., "Steel Fiber Reinforcement in Structural Application," Proceedings, Structural Engineering in Natural Hazards Mitigation, 1993, pp.1415-1420.

5. SOROUSHIAN, P., KHAN, A., AND HSU, J., "Mechanical Properties of Concrete Materials Reinforced with Polypropylene or Polyethylene Fibers," ACI Materials Journal, Vol. 89, No. 6, 1992, pp.535-540.

6. SOROUSHIAN, P., TLILI, A., ALHOZAIMY, A., AND KHAN, A., "Development and Characterization of Hybrid Polyethylene Fiber Reinforced Cement Composites," ACI Materials Journal, 1996, Vol. 27B, pp. 11-20.

7. CHEN, P., AND CHUNG, D.D.L., "Concrete Reinforced with up to 0.2 Volume percent of Short carbon Fibers," Composites, 1993, Vol. 24, No.1, pp. 33-52.

8. CHEN, P., AND CHUNG, D.D.L., " Carbon Fibers Reinforced Concrete for Smart Structures Capable of Nondestructive Flaw Detection," Smart Materials Structures, 1993, Vol. 2, pp.22-30.

9. STRONG, H., MOBASHAR, B., AND SHAH, S. P., "Quantitative Damage Characterization in Polypropylene Fiber Reinforced Concrete," Cement and Concrete Research, 1990, Vol. 20, pp. 540-558.

10. KOVLER, K., SIKULER, J., AND BENTUR, A., "Free and Restrained Shrinkage of Fiber Reinforced Concrete with Low Polypropylene Fiber Content at Early Age," Fiber Reinforced Cement and Concrete, Proceedings, Fourth RILEM International Symposium, Sheffield, 1992, pp.91-101.

11. BENTUR, A., AND MINDESS, A., Fiber Reinforced Cementitious Composites, Elsevier Applied Science, England, 1990.

12. AL-TAYYID, A.H. J., AND AL-ZAHRANI, M.M., "Corrosion of Steel Reinforcement in Polypropylene Fiber Reinforced Concrete Structures," ACI Materials Journal, 1990, Vol. 87, No. 2, pp. 108-113.

BEHAVIOUR INVESTIGATION OF FRP BARS IN MORTAR SPECIMENS EXPOSED TO EXTREME CONDITIONS

G Batis
National Technical University
A Routoulas
Technological Educational Institute of Piraeus
M S Konsta-Gdoutos
Democritus University of Thrace
Greece

ABSTRACT. In the present work, pultruded glass and carbon fibre reinforced composite bars were subjected to UV radiation and exposure to fire conditions, to study the behaviour of FRP bars as reinforcement in concrete, through the Strain Gauges technique. To determine the conditions that most likely attack FRP bars, and to relate these to the environmental conditions found in natural concrete exposure, mortar cubes were reinforced with treated and untreated bars as reference, and were exposed to corrosive environment of 3.5% wt. NaCl solution for 3 months. Swelling stresses, caused by FRP degradation, were monitored using strain gauges. Before casting the FRP reinforcements were subjected to the following treatments: The first group was tested without any treatment, as reference. The second and the third group were heated at 200 and 300°C respectively for 2 hours, in order to simulate fire conditions and finally the forth group was exposed to irradiation with Xenon lamp in order to simulate sunlight exposure. Considerable differences were observed between the CFRP and GFRP behaviour in the case of simulated sunlight exposure. In addition, both CFRP and GFRP reinforcing bars, exposed to simulated sunlight and thermal process, exhibit a different behavior than the reference one. Results obtained confirm the important role of the properties of the matrix in the degradation mechanisms of FRPs, as well as the importance of performance in severe operating environments, fire resistance, and maintainability.

Keywords: CFRP reinforcement, GFRP reinforcement, Durability, Strain gauges.

Dr George Batis Chem Eng Assoc Professor, National Technical University, Chemical Engineering Department, Materials Science & Engineering Section, Athens, Greece.

Dr Ath Routoulas Chem Eng Professor Technological Educational Institute of Piraeus, Physics, Chemistry & Materials Technology Department, Egaleo, Athens, Greece.

Dr M Konsta-Gdoutos Civil Eng Assistant Professor, Democritus University of Thrace, Department of Civil Engineering.

INTRODUCTION

Corrosion of steel reinforcement is considered as major factor of deterioration in concrete infrastructures such as bridges, marine constructions, buildings and chemical plants. Therefore, the development and use of alternative materials to steel reinforcement in the construction industry is urgent and necessary [1].

Fibre-reinforced polymer-matrix composite materials (also called fiber-reinforced plastics, FRP) have received much attention worldwide in the last 10 years, as it is known to offer excellent corrosion resistance to environmental agents. They also have the advantage of high stiffness-to-weight and strength-to-weight ratios when compared to conventional construction materials [2]. Other advantages of FRP include low thermal expansion, good fatigue performance and electromagnetic neutrality. All these advantages could lead to competitive with conventional materials life cycle cost of concrete structures.

Common reinforcements for FRPs are glass, aramid and carbon fibres. Their composites are referred to as GFRP, AFRP and CFRP hereafter. Carbon and aramid fibres are quite resistant to alkaline environment, such as in concrete, however, they are expensive, especially carbon fiber in comparison to glass fibers. Therefore GFRP has a higher potential to be cost-effective. Although extensive research has been conducted on the areas of creep, stress corrosion, fatigue, chemical and physical aging and natural weathering of FRPs, most of these are not aimed at applications for construction industry. The expected service life of a structure is the major factor and the acceptance of FRPs will ultimately depend on its durability. The investigation of FRPs durability in the alkaline environment of concrete, exposed to corrosive environment of a 3.5 % wt. NaCl solution is therefore important [3].

Taking into consideration that FRP reinforcements could stay for a period before casting under sunlight irradiation conditions, the study of FRP durability into concrete environment is useful. There is also very important to consider the FRP durability after thermal distress at temperatures involved in cases of fire condition.

The Strain Gauge (SG) technique, already used for a fast monitoring of steel reinforcements corrosion, is based on the appearance of swelling stresses on the area of steel rebars into the concrete. The cause of the appearance of swelling tension is the formation of corrosion products (Fe_3O_4, Fe_2O_3, FeO(OH)), which have higher specific volume than iron (Fe) or the measurement of the swelling tension mentioned above, special SG sensors were embedded into the mortars specimens during casting [4].

The effect of the alkaline fluid of mortar mass through diffusion into FRPs and the relevant swelling of plastic matrix is investigated by Strain Gauge (SG) technique.

MATERIALS AND METHODS

Materials

The materials used for the construction of the mortar specimens were Ordinary Portland Cement (PC), English sand BS4550P6 and drinking water from Athens water supply network.

The composite reinforcing bars used were made of polyester matrix, carbon or glass fibres with a cross section of 10x10 mm and a 100mm length.

In particular, reinforcement material was a fibre composite produced by the pultrusion process, its main matrix and fibre characteristics are given in Table 1.

Table 1 Characteristics of pultruted materials

PROPERTIES	POLYESTER	CARBON FIBRES	GLASS FIBRES E
Elastic Modulus (Mpa)	3310	250000	72450
Tensile strength (mpa)	77	3850	3450
Elongation at break (%)	4.2	1.8	4.8
Density (Kg/m^3)	1130	1720	2540

Methods

GFRP and CFRP rebars were used in this study. Before mortar specimens casting, the reinforcing bars weighed and prepared according to the following procedure. The first one of each type heated into a furnace for 2 hours at 200°C and mass-loss determination followed. The second one of each type heated into a furnace for 2 hours at 300°C and mass-loss determination followed. The third one of each type exposed to irradiation with XENON 2000 W lamp for 2 hours longitudinal one acme, equivalent to three month sunlight exposure and mass-loss determination followed. The last rebar of each type without any preparation used as reference.

Specimens

The mortar test specimens were in the form of 80 mm x 80 mm x 100 mm prisms with one FRP reinforcement. The shape and dimensions of specimens are shown in Figure 1.

The characteristics of the SG sensor used were KM-30-120 type KYOWA. Distances and directions between the SGs are shown in Figure 1.

In each specimen embedded two SG sensors. The first of them was measured the swelling of the specimen due to cumulative effect of reinforcement expansion and other parameters, which change he specimen's volume. This sensor was placed near the reinforcement. The second one was compensating the parameters of specimen volume variation except reinforcement expansion and it was placed far from the reinforcement [5].

Mortar specimens were stored in the curing room for seven days and were immersed to the corrosive environment 3.5% wt NaCl solution.

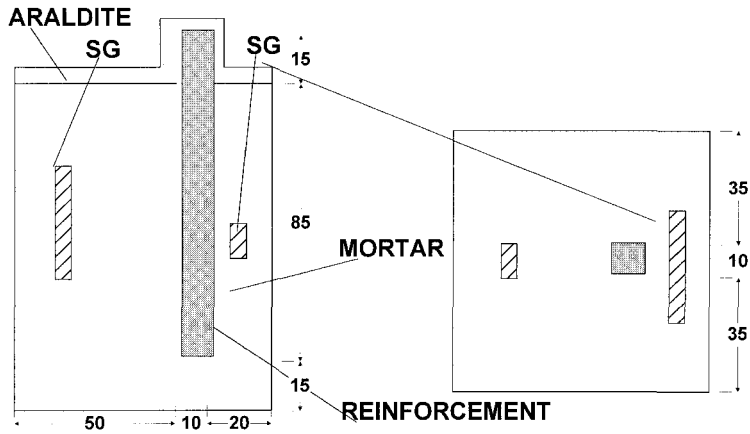

Figure 1 Shape and Dimensions of specimens

Eight (8) categories of the specimens were cast. The proportion of materials used and their code names are shown in Table 2.

Table 2 Categories of Specimens- Composition Proportions (Wt)

CODE NAME	OPC	SAND	WATER	REMARKS
GF	1.0	3	0.5	Reference GFRP Reinforcement
GF200	1.0	3	0.5	GFRP Reinforcement Heated at 200 ^{0}C
GF300	1.0	3	0.5	GFRP Reinforcement Heated at 300 ^{0}C
GFL	1.0	3	0.5	GFRP Reinforcement Exposed to Irradiation with Xenon Lamp
CF	1.0	3	0.5	Reference CFRP Reinforcement
CF200	1.0	3	0.5	CFRP Reinforcement Heated at 200 ^{0}C
CF300	1.0	3	0.5	CFRP Reinforcement Heated at 300 ^{0}C
CFL	1.0	3	0.5	CFRP Reinforcement Exposed to Irradiation with Xenon Lamp

The test set-up, including SG bridge - amplifier circuit and the multimeter for SG elongation measurement, is shown in Figure 2.

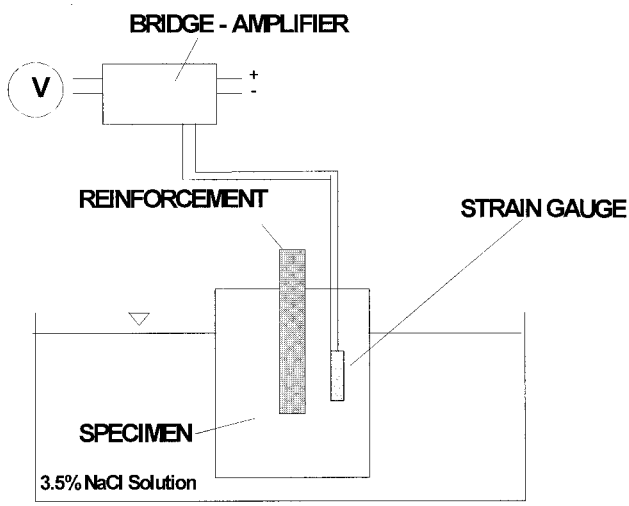

Figure 2 Schematic diagram of reinforcement expansion measurement set-up

RESULTS AND DISCUSSION

The test results obtained for the GFRP categories of specimens by the SG technique are illustrated in Figure 3 as a function of time.

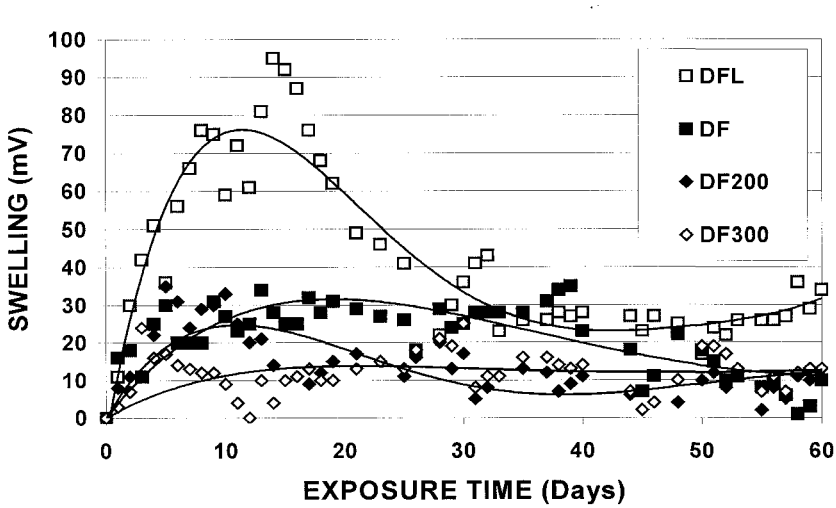

Figure 3 Swelling values versus exposure time for different GFRP specimens

During the first few days after specimens casting, a relatively high rate of reinforcement swelling is observed which turn out in lower values. This swelling development could be explained by the liquid ingress and absorption behavior of the rebars polymer matrix. At the beginning, the absorption rate was high and then decreased with time, as water concentration gradient between the surface and the inner part of reinforcement decreased. It is observed that the GFL reinforcement shows a higher swelling compared to that of the specimens GF, GF200 and GF300.

It is known that the diffusibility of glass fibre composites depends on the type of plastic matrix and the fibers content. High fiber content with a good protection should lead to low diffusibility. Glass fibers are considered to have negligible water permeability. The quality of the rebar outer surface also affects diffusibility [6]. The higher water absorption and reinforcement swelling observed in GFL specimen could be attributed to the surface micro cracking caused by solar radiation. Among reinforcements exposed to heating process GF200 and GF300, the relatively higher swelling of GF200 could be explained by the lower mass loss after heating. The lower polymer mass loss, leads to the lower fiber content, and consequently to the higher diffusibility.

Regarding the test results obtained for the CFRP categories of specimens by the SG technique, shown in Figure 4, we could point out the following:

The swelling curves show that all specimens have a fluid sorption of pseudo-Fickian tendency. The fluid saturation level is higher compared to that of GFRP reinforcements. The CFL specimen shows lower water absorption and diffusibility than GFL.

The swelling correlation of reinforcements exposed to extreme conditions referred to reference specimens is illustrated in Figures 5 and 6.

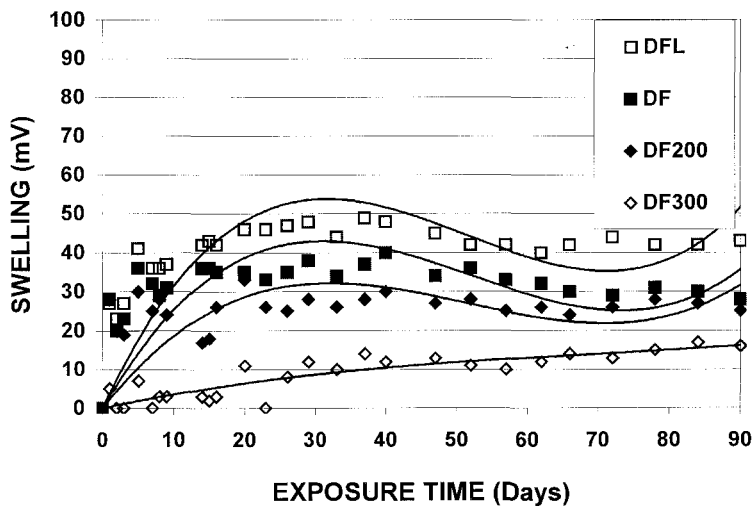

Figure 4 Swelling values versus exposure time for different CFRP specimens

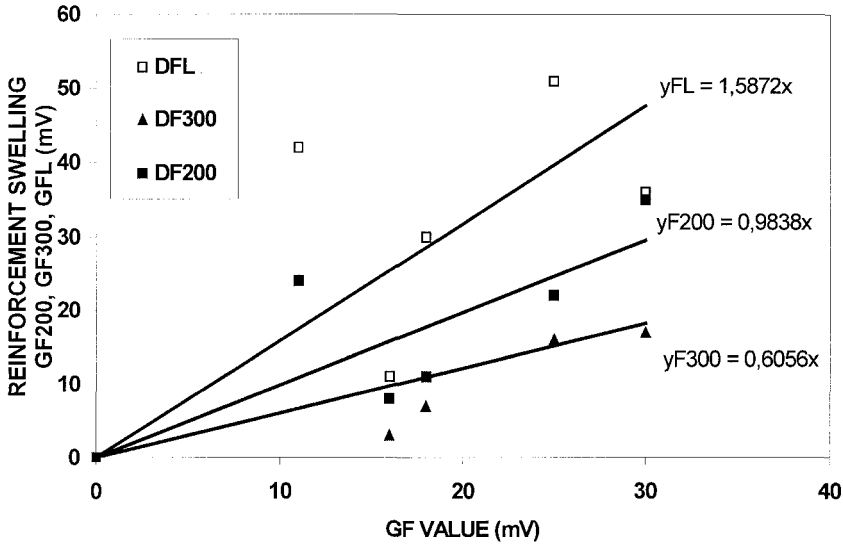

Figure 5 Swelling Correlation of GFRP reinforcements exposed in various conditions

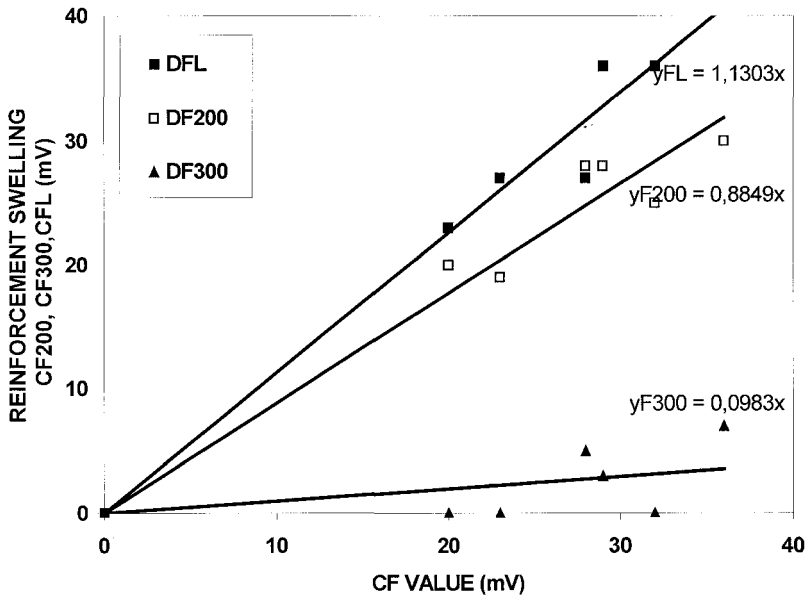

Figure 6 Swelling Correlation of CFRP reinforcements exposed in various conditions

The higher relative rate of swelling was observed in GFL specimen (1.587), the lower (0.606) was shown in GF300 and the GF200 specimen had similar swelling rate with reference one (0.984).

A similar rating is achieved for specimens CFRP, (Figure 6) but the CF300 shows much lower swelling rate than the reference.

Table 3 shows the mass loss comparison of reinforcements after heating or irradiation. It is clear that the mass loss of heated specimens is higher than light exposed ones. All heated GFRP and CFRP reinforcements gave less swelling than the reference.

Table 3 Correlations Between Reinforcements Swelling and Mass-Loss

SPECIMEN CODE	MASS LOSS (mg)	FINAL SWELLING SG (mV)	RELATIVE SWELLING RATE
GF	-	12	1.000
GF200	187	12	0.984
GF300	456	12	0.606
GFL	24	30	1.587
CF	-	30	1.000
CF200	85	30	0.885
CF300	345	15	0.098
CFL	18	40	1.130

After 90 days of exposure at 3.5%w.t NaCl solution mortar specimens were broken in order to reveal reinforcements. The revealing of GF reinforcement was impossible because of a very strong cohesion between mortar and reinforcement. This resulted in reinforcement damage as it is shown in Figure 7. However the CF revealing was normal (Figure 8).

The GF and CF reinforcements cross-section illustrated in Figures 9 and 10 are characterized by homogeneity without crackings. Some fibre disorders were observed in the surface terminals.

The GF200 reinforcement cross-section (Figure 11) shows large crackings and material degradation caused by reinforcement heating.

The GF300 reinforcement cross-section (Figure 13) shows less crackings than GF200 and color changes of the polymer matrix.

The CF200 and CF300 reinforcements cross-section illustrated in Figures 12 and 14 are characterized by homogeneity without crackings.

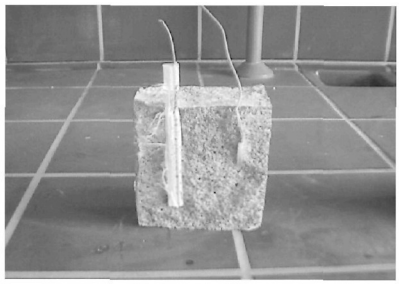

Figure 7 GFRP reinforcement

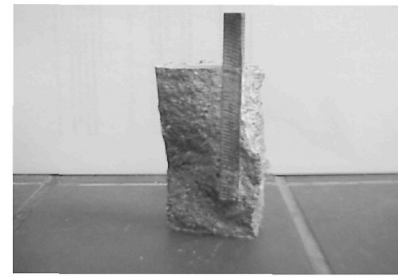

Figure 8 CFRP reinforcement

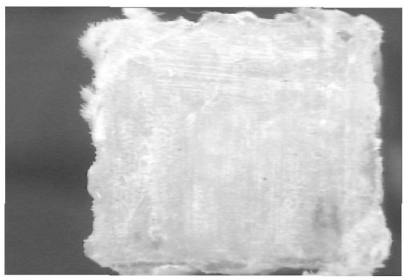

Figure 9 Reinforcement GF cross-section

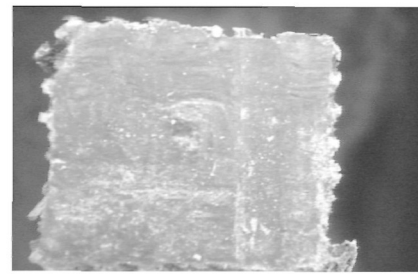

Figure 10 Reinforcement CF cross-section

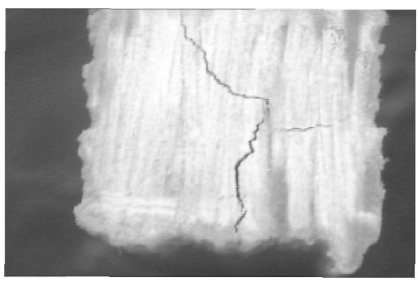

Figure 11 Reinforcement GF200 cross-section

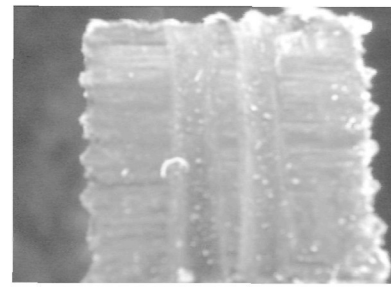

Figure 12 Reinforcement GF200 cross-section

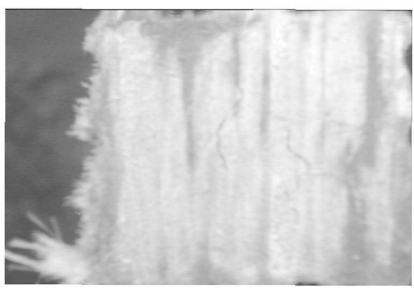

Figure 13 Reinforcement GF300 cross-section

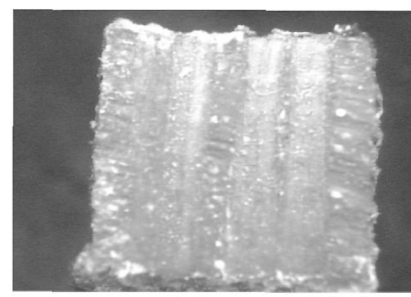

Figure 14 Reinforcement CF300 cross-section

CONCLUSIONS

Based on the measurements of the FRPs swelling with strain gauge technique the following conclusions can be drawn:

1. Mortar specimens reinforced with FRP exposed to conditions of sunlight irradiation show sensitively higher reinforcement swelling compared to that of reference ones.

2. Mortar specimens reinforced with FRP exposed to heating conditions show lower reinforcement swelling compared to that of reference ones. Especially, the FRP exposed to 200 °C heating had similar behavior to the reference.

REFERENCES

1. TASSIOS, TH P, ALIGIZAKI, K, Durability of Reinforced Concrete, Fivos Publ, Athens, 1993.

2. M.KONSTA-GDOUTOS AND CH KARAYIANNIS, "Flexural behavior of Concrete Beams Reinforced with FRP Bars," Advanced Composite Letters,1998, 7(5) pp 33-137.

3. TON-THAT, T.M., BENMOKRANE, B., RAHMAN, H., ROBERT, J-F "Durability Test of GFRP Rod in Alkaline Environment". Proceedings of International Conference at University of Sheffield, 1999 pp. 553-566.

4. ROUTOULAS, A., BATIS, G. "Performance Evaluation of Steel Rebars Corrosion Inhibitors with Strain Gauges ", Anti - Corrosion Methods and Materials, 46, 1999 No 4, pp 276-283.

5. COLOMBO, G. Automazione Industriale. Vol 4 Dott. Giorgio, Torino, 1986.

6. PANTUSO, A, SPADEA, G, SWAMY, R N "Study of the Shear and Elastic Characteristics of FRP Bars Subject to Moisture and Alkaline Environment". Proceedings of International Conference at University of Sheffield, 1999, pp 567-579.

OPTIMISATION AND GLASS FIBRE REINFORCEMENT OF MORTARS WITH VERY FINE FILLERS

A H H Waellisch **H Moertel**

University Erlangen-Nuernberg

V Rudert

Wilhelm Dyckerhoff Institute for Building Materials

Germany

ABSTRACT. The durability of different glass fibre composites in dense cement microstructures was studied. With the mix-program of Dinger and Funk can be calculated the optimum dosages of very fine reactive fillers to OPC to achieve a dense binder packing. E- and AR-Glass-fiber composites made of these optimised binders show low porosities, but have a unsufficient durability of the flexure properties, when accelerated aged in 60° C hot water. Good durability can be achieved with AR-glass-fibre composites which contain a high amount of metakaolin in combination with silicafume.

Keywords: Glassfibre, Glassfibre reinforced concrete (GRC), Filler, Durability, Porosity, Composite.

A H H Waellisch graduated from University Erlangen-Nuernberg in 1998 in advanced mineralogy and hydraulic binder systems. Since 1998 he has been a co-worker of Dr Moertel in the working group "raw materials, silicate ceramics and building materials" and writing his thesis on optimised and fibre reinforced cement systems. He is now dealing also with projects of classical ceramics.

Dr H Moertel graduated from University Erlangen-Nuernberg 1969 in mineralogy and material sciences. 1970-1972 research on zeolites and chromite ores. Since then coworker of Prof Dr H J Oel, Institute of Glass and Ceramics at the Technical Faculty of University Erlangen-Nuernberg. He became senior scientist and head of the working group "raw materials, silicate ceramics and building materials". Fields of interest are characterisation of raw materials, batch formulation and processing, especially of fast firing ceramics, porcelain in particular, recycling of secondary raw materials, waste, steam cured materials as sand lime bricks and aerated concrete, and ultra fine ground slag based cements, testing and characterisation of products in these fields.

Dr V Rudert is a graduated mineralogist and is the director of the Wilhelm Dyckerhoff Institute for building materials, Wiesbaden, Germany.

INTRODUCTION

In general it is well-known that glass is not resistant in a medium with pH higher than nine. Fibres made of glass are cheap and have a high E-modulus and it would be expected they can reinforce mortar or concrete properly. For a certain period this is true, but aged composites with cheap E- or C- glass fibres never show a good long-time performance. The development of so-called alkali resistent (AR) glass fibres led to glass fibre concrete (GRC) in which fly ash the pozzolanic material reacted with the Ca (OH_2) in concrete. In more recent publications one can find compositions including silica fume and metakaolin.

In this study it was proved to be able to improve the filler effect of a ultrafine latent hydraulic or pozzolanic material like ultrafine grounded granulated blast furnace slag, silica fume and metakaolin by means of calculating the appropriate dosage to a binder system.

Mathematical models and computer implementations of J E Funk and D R Dinger [1] are very efficient tools for exploring the optimal amount of a very fine or ultrafine reactive filler to achieve a dense cement paste packing [2].

RAW MATERIALS

For the samples was used an OPC and mixed with three fine binders (reactive fillers). The first was Mikrodur® RU, a very fine blast furnace slag based cement, i.e. a blend of ultrafine ground blast furnace slag and ordinary cement. A full description of chemical, mineralogical, and granulometric properties are given in [2] and [3]. Second a micro-silica of a blue-gray type with >96% SiO2. The third was metakaolin, a pure calcinated kaolin, which is described with the formula 2 SiO_2 ▪ Al_2O_3. As a fine aggregate was used a standard sand 0/2 according to standard EN 196.

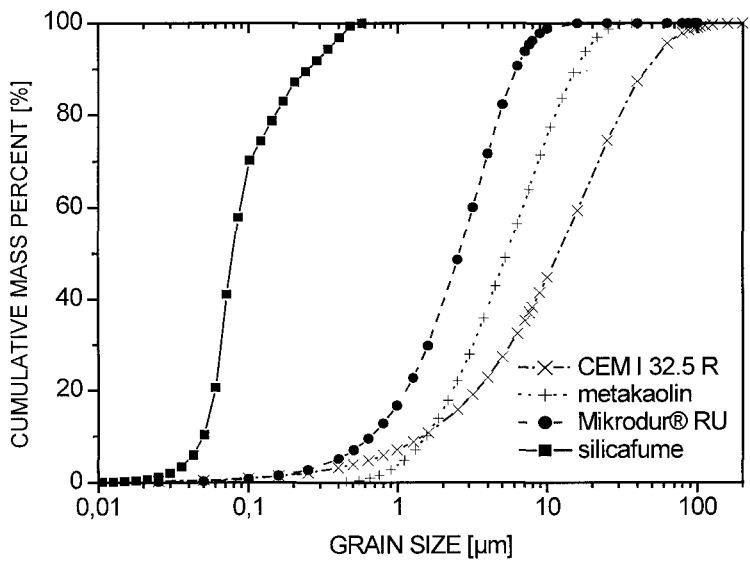

Figure 1 Particle size distribution of the raw materials

In Figure 1 the grain size distributions of the used ordinary portland cement in comparision with the reactive fillers are represented as well as the density of the binders in Table 1.

Table 1 Density of the binders

RAW MATERIALS	DENSITY, g/cm^3
CEM I 32.5 R	3.13
Mikrodur® RU	2.95
Metakaolin	2.55
Silicafume	2.21

The glass fibres, which were mixed in the composites were E-glass-fibres and alkali-resistent (AR) glass fibres with a filament diameter of 13 µm and a length of the chopped strands of 12 mm.

CALCULATIONS AND PREPARATION OF SAMPLES

From the particle size distribution function of the very fine fillers was calculated the optimum volumen increment to achieve a dense grain packing with the "mix"-program of Dinger and Funk. It is based on the implementation of the following formula [1]:

$$\frac{CPFT}{100\%} = \frac{D^n - D_s^n}{D_L^n - D_s^n}$$

The results of the calculations are listed in the Table 2. The theoretical porosity of an optimized binder with Mikrodur® is lower that one of a pure OPC, but a better result is achievable with a mix of OPC with Mikrodur® and silicafume.

Table 2 Calculations

FINE FILLER(S)	OPTIMUM DOSAGE, MASS-%	THEORETICAL POROSITY, VOL-%
Mikrodur® RU	9.7	9.0
Mikrodur® RU + silicafume	10.0 + 3.8	7.3
	FOR COMPARISON:	
pure OPC		10.3

Glass-fibre-concrete (GRC) plates were fabricated with the calculated optimum dosages of filler and OPC. Additional a composite with a binder containing 20 mass-% metakaolin and 13 mass-% silicafume was prepared. The high amount of these components not exceeding 33 mass-% [2] was taken because they will react with Ca $(OH)_2$, especially the metakaolin.

The water-cement-ration and the cement-aggregate-ratio were varied slightly to achieve a good workabilty. The plates were after sawing them in specimens with dimension of approx. 225 mm x 50 mm x 10 mm aged in a hot water bath of 60° C for at least 28 days. Supposing a mean annual temperature of 8° C in Germany 28 days of 60° C in water are equivalent to more than 30 years exposition in german weather [4].

Table 3 Test programme

SAMPLE NAME	BINDER SYSTEM	WATER-CEMENT-RATIO	CEMENT-AGGREGATE-RATIO	GLASS-FIBRES, VOL-%/TYPE
OPC	100% OPC	0.32	1.25	0
Mik-E	9.7 % Mikrodur®	0.35	1.25	2 E
Mik-AR	9.7 % Mikrodur®	0.35	1.25	2 AR
Sili-E	10 % Mikrodur® + 3.8 % silicafume	0.3	1.125	3 E
Sili-AR	10 % Mikrodur® + 3.8 % silicafume	0.3	1.25	3 AR
Meta-E	20 % metakaoline + 13 % silicafume	0.35	1	3.5 E
Meta-AR	20 % metakaoline + 13 % silicafume	0.35	1	3.5 AR

RESULTS AND DISCUSSION

Porosity

The open porosity of the samples was measured with mercury intrusion porosimetry from 0,008 µm to 100 µm. In Figure 2 one can see before aging all values of the samples with fillers are significant lower than the sample of OPC. As expected from theoretical porosity the lowest porosity have the sili-series over the whole aging process. All curves are parallel more or less and the value of porosity is lower after 28 days at 60° C, because the pores accrete.

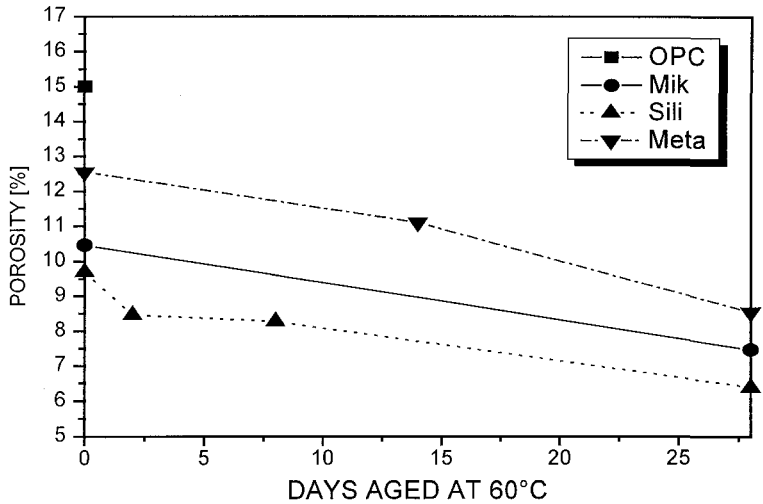

Figure 2 Open porosity measured with mercury intrusion porosimetry

Flexural tests

The four-point-flexural test was performed according to EN 1171-6. The load point as well as the mid-point deflections were measured. From load-deflection-curves were calculated the stress-strain-curves.

Examples of the stress-strain-curves are listed in the following Figures 3 - in which are presented the aging effects on the stress-strain behaviour of the composites. In Figure 3 (serie Mik 9,7 mass-% Mikrodur®) it can be seen that 2 vol-% fibres are not enough to reinforce the composites. According to [5] it should be theoretically sufficient. One reason why not, may be the short length (12 mm) of the fibres. Modulus of Rupture (MOR) is at the same level as the limit of proportionality (LOP). But the long subcritical curve is very short after 28 days of aging of the E- and AR-glass reinforced samples, so it can be concluded the fibres are not stable in this matrix.

The Sili-composites in Figure 4 (with 3 vol-% E-glass-fibres) and 5 (with 3 vol-% AR-glass-fibres) show a better post-peak performance and a higher post-peak stress, but the E-glass-composites have a very short part of a super-critical behaviour. The E-glass-fibres are worse in reinforcing, because they disintegrate during mixing more in their single filaments, which posses no reinforcing effect. Already after 2 days in 60° C hot water the effect of the E-glass fibres in the matrix with 10% Mikrodur® and 4% microsilica is near zero. The AR-glass fibres behave better, but the stress-strain curve is after 2 days aging subcritical too.

The best post-peak performance exhibit the Meta-AR-composites (Figure 7). Even after 28 days accelerated aging the composites perform very well. The MOR is even higher than this of the unaged samples. For the E-glass in the Meta-composites are the conditions not appropriate to protect them from dissolving. The stress-strain curves of the Meta E-glass samples after 14 and 28 at 60° C in water are noticeable subcritical.

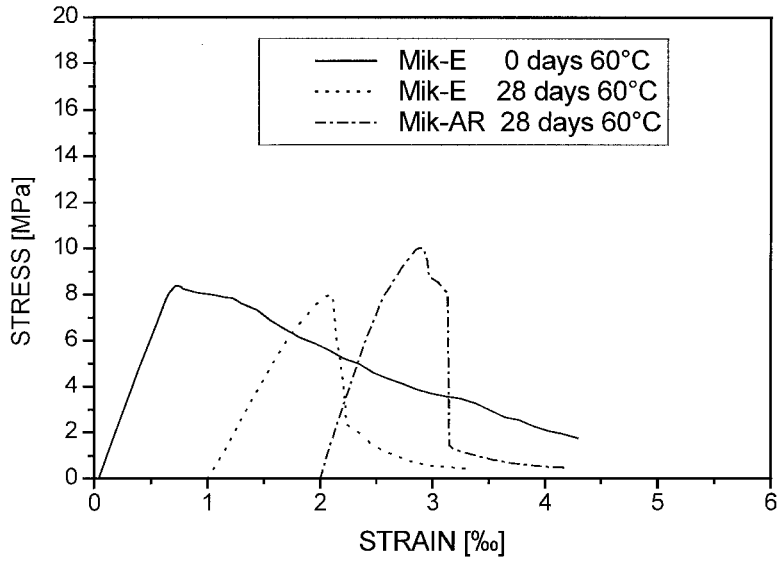

Figure 3 Stress-strain curve of mortar Mik-E and Mik-AR

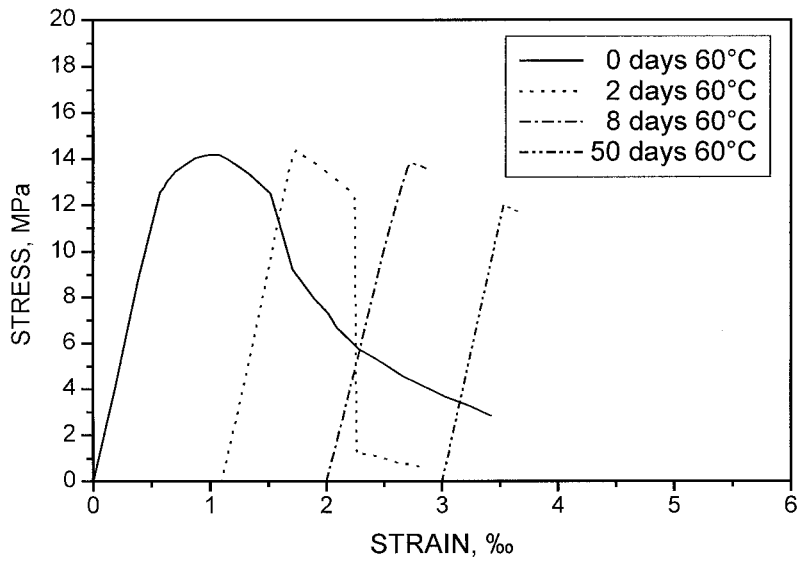

Figure 4 Stress-strain curve of mortar Sili-E

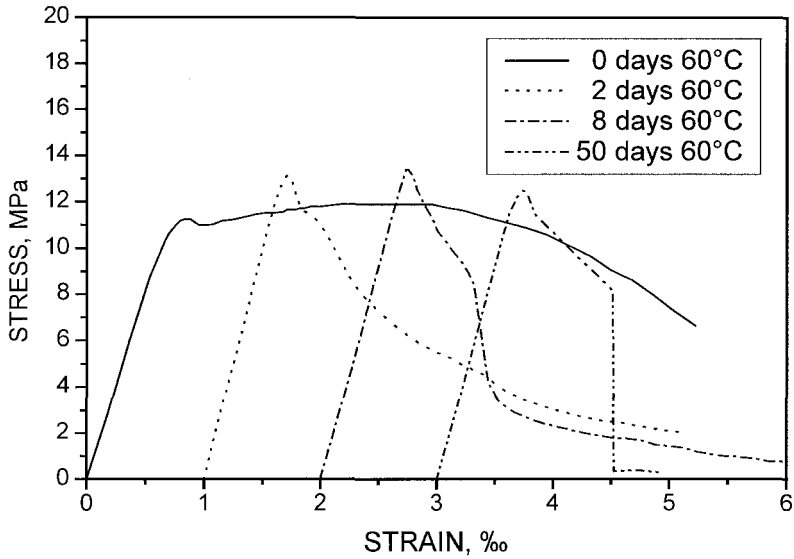

Figure 5 Stress-strain curve of mortar Sili-AR

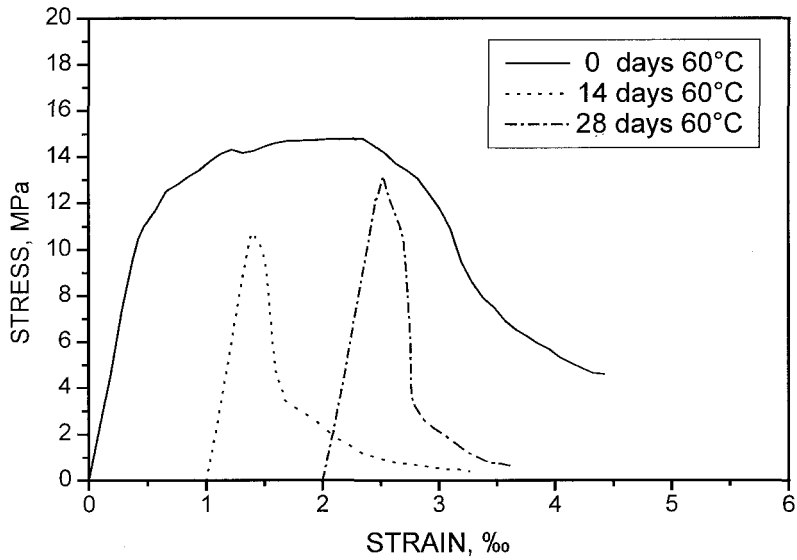

Figure 6 Stress-strain curve of mortar Meta-E

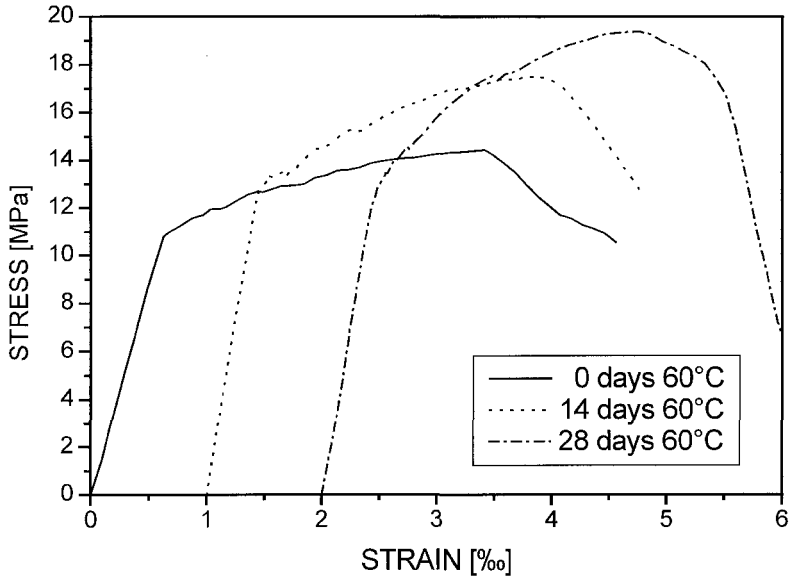

Figure 7 Stress-strain curve of mortar Meta-AR

SUMMARY

E- and AR-glass fibre composites were produced with a calculated optimum dosage of very fine reactive fillers to OPC. The fillers were Mikrodur®, a very fine GGBS and a combination of Mikrodur® and silicafume. Especially the composites with the combination of the two fillers had a open porosity of only 9,7 vol-% of the unaged samples compared with 15 vol-% of a OPC sample. The flexure behaviour of unaged and in 60° C hot water up to at least 28 days aged glass-fibre reinforced composites was measured and the performance of the matrices and the E- and AR- fibres was compared. In all cases the AR-glass fibres show better results. The best result was achieved with a matrix containing a high amount of metakaolin in combination with silicafume. The matrix was optimised to achieve a minimum of free lime. AR-glass fibre reinforced composites made of this matrix retain their properties and show an excellent durability.

REFERENCES

1. FUNK J. E., DINGER D. R. Predictive Process Control of Crowded Particulate Suspensions Kluwer Academic Publishers, Boston/Dortrecht London, 1994.

2. LANGE F. Gefügeuntersuchungen und Eigenschaften von Hüttensand enthaltenden Zementen, Exploration of microstructure and properties of blast furnace slag containing cements. PhD Thesis, University Erlangen-Nuernberg, Institute of Materials Science, Glass and Ceramics, Erlangen, Germany, 1996.

3. LANGE F., MÖRTEL H., RUDERT V. Dense Packing of Cement Pastes and Resulting Consequences on Mortar properties. Cem and Concr Res 27, H10, 1997, 1481-1488.

4. PROCTOR B. A., OAKLEY D.R., LITHERLAND K.L. Developments in the assessment and performance of GRC over 10 years. Composites, April 1997, 173-179.

5. GLASFASERBETON, Fachvereinigung Faserbeton, Beton-Verlag, Düsseldorf, 1994.

6. WEISER W. New matrix improves GRC durability. Construction and building materials Vol 4 , No 1, march 1990, 25-28.

7. BENTUR, A. Silica fume treatments as means for improving durability of glass fiber reinforced cements, Journals of Materials in Civil Engineering, Vol 1, No 3, 1989.

8. FERRY, R. Glassfibre reinforced cement, Concrete Engineering International, En-No. 29, 1998, 60-63.

9. MARICUNTE S., ALDEA C.M., SHAH S.P. Matrix modification to improve the durability of glass fiber reinforced cement composites. Brittle Matrix Compos. 5, Proc Int Symp 5th, 1997, 90-102.

10. NEVILLE, A. (Ed) Fibre reinforced cement and concrete, RILEM Symp, 1975.

11. MASTHOFF SiC-Untersuchungen und H-Tests an Fasern aus alkaliresistentem Glas sowie E- und C-Glas, Studie, Institut für Faserbaustoffe Berlin, 1998.

12. BAUER, H. Verhalten von Glasfasern in Zementsuspensionen, PhD Thesis, University Erlangen-Nuernberg, Institute of Materials Science, Glass and Ceramics, Erlangen, Germany 1979.

DISTINCTIVE FEATURES OF THE CORROSION OF BASALT FIBRES IN ALKALI MEDIA AT ELEVATED TEMPERATURES

Y I Tsybulya

T A Selyanina

BEIM

O O Medvedyev

Ukrainian Academy of Building & Architecture

Ukraine

ABSTRACT. This paper describes the distinctive features of mineral (basalt) continuous fibre corrosion in concentrated alkaline solutions at high temperature. Precipitates with different chemical composition and form were discovered on the surface of basalt fibre after etching in boiling NaOH solutions. Based on X-ray microanalysis data it is possible to assume that mentioned precipitates were formed during fibre formation from the melt. Precipitates probably have an influence upon mechanical and thermal resistance of basalt continuous fibres. Detailed investigation of "soda paradox" for basalt fibres shows the concentration dependence of mentioned phenomenon. Probably this phenomenon is inherent in basalt as mineral raw material, and the mechanism of basalt fibres destruction under the influence of alkalis differs essentially from the mechanisms taken place for silicate glasses. Such difference opens additional opportunities to improve alkaline resistance of basalt continuous fibres.

Keywords: Alkaline corrosion, Basalt continuous Fibre, Precipitate, "Soda Paradox" phenomenon.

Y L Tsybulya is a Chartered Chemical Engineer and the Director of small venture "BEIM". His researches focused mainly on investigation of technology of mineral continuous fibres and performance characteristics of basalt fibres.

O O Medvedyev is an academician of Ukrainian Academy of Building and Architecture and the director of JSC "Belichi Factory "Teplozvukoisoliatsya". His researches focused mainly on technology of mineral fibres, insulation and construction composite materials.

T A Selyanina is a Chartered Chemical Engineer involved in researches concerning chemical resistance of basalt continuous fibres in alkali and acid media. She is R & D engineer in small venture "BEIM".

INTRODUCTION

The problem of corrosion resistance of basalt fibres in alkali media has been studied in detail [1,2], as it is of great importance for fibre reinforced concrete. It was determined that basalt continuous fibres (BCF) are close to well-known special-purpose fibres CemFil™ as to their alkali resistance.

However after the development of new types of inorganic binders, e.g. geocements [3], and design of manufacturing technology of composites based on such binders using hot-pressing [4], the problem to investigate the chemical resistance of basalt fibres in concentrated alkali solutions at elevated temperatures was stated.

INVESTIGATION OF BCF SURFACE AFTER TREATMENT IN CONCENTRATED BOILING HYDRATE OF SODIUM

The fullest description of the changes of the basalt fibre surface structure and its strength after treatment with alkali solutions of 0.1N to 0.5N within temperature range between 20 and 90^0C was given in [1,2]. However the effect of treatments with more concentrated alkali solutions on the surface of BCF remained beyond the researchers' field of interest.

The investigation of the state of the surface of basalt fibres after boiling in 2N NaOH is of special interest because it allows to estimate the character of disturbances after a treatment for rather long time – up to 6 hours. The pictures of the surface of basalt fibres after treatment with boiling NaOH for 0.5 hours made by X-ray microanalyser REMMA-101A in a regime of electronic microscope are given in Figure 1.

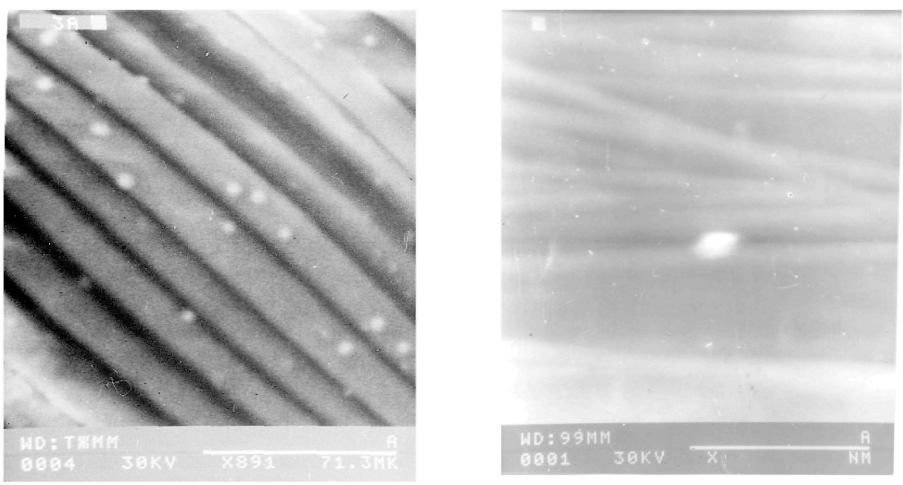

(a) (b)

Figure 1 Precipitates on the surface of BCF after 0.5 hour boiling in 2N NaOH: (a) small cupola-shaped precipitates; (b) large precipitate with clear boundaries

The distinguishing feature of the texture of their surface is the presence of precipitates of various shape and dimensions. In particular, the photo of large precipitate having rather clear boundaries is given in Figure 1b. During more severe destruction after treatment for 6 hours the deep etch figures appear on the surface mainly perpendicular to the axis of the fibre (See Figure 2) what points to the anisotropy of the etching of basalt by alkalis.

Figure 2 BCF surface after 6 hour treatment in boiling 2N NaOH

Because the precipitates on the surface of basalt fibre after treatment with NaOH were not observed earlier [1,2] the study of their structure and composition by means of X-ray microwave analysis with REMMA-101A device was of interest. Quantitative results for the different areas of precipitates are given in Table 1.

Table 1 Chemical composition of precipitates on the surface of BCF

LOCATION OF THE RESEARCHED AREA	ANALYSIS, ATOMIC %*				
	Si	Ca	Al	Mg	The rest
Precipitate of Figure1a	38	17	13	Traces	41.5
Area adjacent to the top of the precipitate of Figure 1b	38	15	3.8	Traces	43.2
Area adjacent to the base of the precipitate of Figure 1b	38.8	2	18	Traces	41.2

* Atomic % - the number of atoms of the element in 100 atoms of the lattice

As it is seen from the data given in Table 1, there are not calcium and magnesium hydroxides in cupola-shaped precipitates (Figure 1a). It is unexpected result because there are 9-11 % of CaO and 6-8 % of MgO by weight in basalt. Besides that, the presence of calcium silicates with CaO to SiO_2 ratio ≥ 1 is practically impossible. Calcium silicates having the composition CaO 2...3 SiO_2 may present in the precipitates. Al_2O_3 both in a free crystalline state and in the form of aluminium silicates $Al_2O_3 : nSiO_2$ of crystalline or amorphous structure also presents there. The forming of aluminium silicates is possible thanks to silicon oxide exceeding the stoichiometric quantities.

For the compounds given in Table 1, the possibility of forming of calcium aluminates is very small because of higher reactivity of silicon oxide and small quantity of calcium in the precipitate.

Another unusual result is the distribution of elements' concentration in the precipitate presented in Figure 1b. Concentrations of Ca and Al vary significantly along the surface of the precipitate. The varying analysis of the precipitate and also its shape allows to conclude that it is a crystalline inclusion in the amorphous body of basalt fibre.

The presence of crystalline Al_2O_3 and aluminium silicates as a part of formations on the surface of basalt fibres after treatment in concentrated solution of NaOH is of interest for understanding of peculiarities of basalt fibre forming from molten rock. Mentioned crystalline formations could not be formed during the treatment with NaOH, but only during fibre forming.

The discovery of precipitates of various shape and composition as a result of non-isotropic etching of basalt fibres is of great practical importance for further study of properties of basalt fibrous materials. It was presumed earlier [5, 6], that basalt fibre is an amorphous body where crystallisation processes could run only during heating up to temperatures more than 600^0C. The presence of precipitates with admittedly crystalline structure included into amorphous body of basalt fibre could stimulate re-crystallisation processes at lower temperatures of 400-500^0C. This fact can explain the strength loss of basalt fibrous materials during heat treatment at mentioned temperatures. Besides that, the precipitates could have an influence on mechanical strength of basalt fibres being reinforcing elements of glassy body of fibres, and govern the range of other properties. The nature of precipitates and their contribution to performance characteristics of basalt fibres should be a matter of additional study.

PHENOMENON OF "SODA PARADOX" OF BCF

The "Soda paradox" is considered to be one of the most interesting phenomenon during an interaction between glasses and alkali solutions. It is difficult to explain it based on existing theory of etching of silicates with alkali [7]. "Soda paradoxes" clearly show the variety of chemical and physical processes taken place during destruction of silicate glasses by alkalis.

Sometimes the stronger effect of carbonates than that of hydroxides of the same metals is observed during the solution of silicate glasses in alkali media. Such cases for solutions of sodium compounds may be called as "Soda paradoxes" because the destructive effect of alkali solution should, it might seem, depend on an activity of hydroxyl ions most of all, and this activity should be less in carbonate solution (even highly hydrolysed) than that in equivalent solution of hydroxide.

It is accepted to distinguish two phenomena in works of Grebenshchikov school [7]:

1. "Soda paradox of the first type" is stronger destruction of glasses in carbonate solutions than that in hydroxide solutions of the same metal at the same concentration;

2. "Soda paradox of the second type" is stronger effect of the mixture of NaOH and Na_2CO_3 in comparison with the effect of solutions of the same compounds taken separately.

The data of weight losses after boiling the basalt staple fibres in 1N Na_2CO_3 for 3 hours are given in [8]. However the data concerned the etching in the equivalent solution of NaOH are not given. The comparison of weight losses during the etching in 1N Na_2CO_3 and 0.5N NaOH allows to make a conclusion that "The Soda paradox of the first type" is not typical for basalt fibres.

The investigation of etching rate of basalt yarn with the weight of 0.3 g and linear density 330 ± 30 tex was carried out. The samples were boiled for 0.5 hour in NaOH and Na_2CO_3 solutions having concentrations from 0.5N to 5N. To prepare the mixture of NaOH and Na_2CO_3 solutions, the equal volumes of respective separate solutions of mentioned components were taken. The weight of solution for treatment was not less than 30 g. The results are shown in Figure 3.

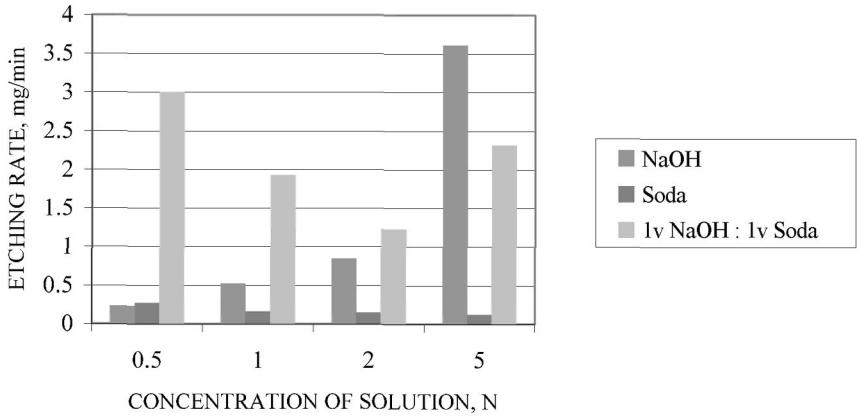

Figure 3 Etching rates of BCF in alkaline and carbonate-alkaline media

An analysis of obtained data shows that feebly marked "Soda paradox of the first type" and strongly pronounced "Soda paradox of the second type" are typical for basalt fibre at NaOH concentration of 0.5N. At the same time, "Soda paradox of the first type" was not observed at concentrations of 1N and 2N, while "Soda paradox of the second type" was revealed though the rate of destruction of the fibre in the mixture of NaOH and Na_2CO_3 reduced notably. At concentrations of 5N neither "Soda paradox of the first type" nor "Soda paradox of the second type" were observed.

A somewhat different picture than that for glasses was seen during an interaction between basalt fibres and water solutions of sodium ortho-phosphate and their mixtures with NaOH. It is known [7] that Na_3PO_4 has extremely high destructive effect on silicate glasses characterised by strongly pronounced "Soda paradox of the first type", eg, Na_3PO_4 destroys glass No 31 (SiO_2 55·K_2O 13·SrO 32) 30 times higher than NaOH; for the glass No 9 (SiO_2 55·Na_2O 13·CaO 32) the difference is more than ten times.

The weight losses after boiling of basalt yarns in solutions of Na_3PO_4 and Na_3PO_4 : NaOH for 0.5 hours are shown in Figure 4.

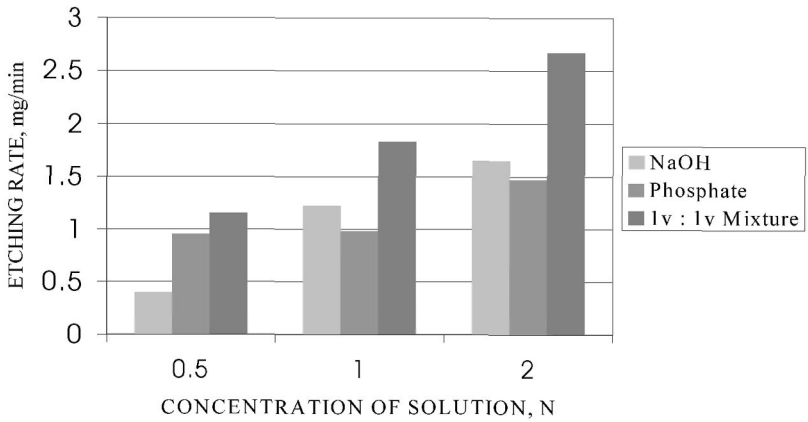

Figure 4 Etching rates of BCF in alkaline and phosphate-alkaline media

As it follows from given data, the rate of destruction of basalt with 0.5N solution of Na_3PO_4 is 2 to 3 times higher than that of NaOH, ie "Soda paradox of the first type" is observed for above concentration. However as the concentration increases this difference reduces, and it is possible to say about 2N solution that "Soda paradox of the second type" is not already observed. At the same time, for the Na_3PO_4 : NaOH mixture "Soda paradox of the second type" takes place within the whole interval of concentrations.

Concentration dependence of "Soda paradoxes" revealed for the treatment of basalt fibres with alkali solutions is not described in the scientific literature concerning silicate glasses. Probably this phenomenon is inherent in basalt as mineral raw material, and the mechanism of basalt fibres destruction under the influence of alkalis differs essentially from the mechanisms taken place for silicate glasses.

The stability of silicate glasses in alkali media is governed mainly by their chemical composition while this factor is not the only one for basalt fibres. Mineralogical composition and conditions of fibre forming presumably also could have an effect on alkali resistance of basalt fibrous materials.

CONCLUSIONS

Detailed investigation of basalt fibre corrosion in alkali media at elevated temperatures revealed the presence of precipitates in the body of basalt continuous fibres. Taking into account the composition of mentioned precipitates, it is possible to assume that they have great influence on mechanical properties and thermal resistance of BCF and relative structures.

Moreover, precipitates which were etched on basalt fibre surface during corrosion in cement matrix could be additional reinforcement elements of fibrous composite cement structure. Concentration dependence of "soda paradox" phenomenon confirmed specific mechanism of alkaline corrosion for BCF compare to glass fibres. In such case it seems possible to improve alkaline resistance of basalt and other basaltic mineral fibres by using of distinctive features of mineral raw material – mineralogical composition and great influence of fibre forming conditions to the performance characteristics of fibres.

REFERENCES

1. PASCHENKO A A, SERBIN V P, PASLAVSKAYA A P, GLUKHOVSKIY V V, BYRUKOVICH Y L, SOLODOVNIK A B, Reinforcement of inorganic binding materials by mineral fibres, Moscow: Stroyisdat, 1988.

2. RAMACHANDRAN B E, VELPARI V, BALASUBRAMANIAN N, Chemical durability studies on basalt fibers, J Material Science, 16, 1981, pp 3393-3397.

3. KRIVENKO P V, Alkaline Cements: Terminology, Classification, Aspects of Durability, In: Proceedings of the 10-th Intern Congress on Chemistry of Cement, 2-6 June 1997, Gothenburg, Sweden – Göteborg: Inform Trycket AB, Vol 4, 1997, 4iv046-6pp.

4. MOKHORT M A, Numerical modelling of manufacturing process of composite fibrous materials based on geocements. In: Proceedings Of the 2-d International Conference "Alkaline Cements and Concerts", Kyiv, 18-20 May, 1999, Kyiv:Oranta Ltd, 1999, pp 248-268.

5. PELEKH B L, MAKHOVA M F, DZIGIRIS D D, Methods of investigation of basalt fibres and physics-chemical properties of basalt fibres, In: Basalt composite materials and constructions, Kyiv, Naukova Dumka, 1980, pp 81-112.

6. MAKHOVA M F, About crystallisation of basalt fibres, Steklo i Keramica, 11, 1968, pp 22-23.

7. MOLCHANOV V S, PRIKHIDKO N E, Corrosion of silicate glasses in alkali solutions. Statement 1. Destruction of quartz, quartz glass and other apparatus glasses in caustic soda and soda, Izvestia AN USSR, Department of Chemical Science, 6, 1959, pp 975-980.

8. DUBROVSKAYA T S, KOSMINA N E, Chemical durability of staple basalt fibres, In: Structure, composition, properties and forming of glass fibres, part 1, Moscow, VNIISPV, 1968, pp 140-147.

THE USE OF ADVANCED COMPOSITE MATERIALS IN RETROFITTING OF CIVIL ENGINEERING INFRASTRUCTURE

G Horrigmoe
NORUT Technology
Norway

ABSTRACT. A growing number of reinforced concrete structures is reaching a stage where deterioration is affecting serviceability, load-carrying capacity and safety. Together with the introduction of fibre reinforced polymers (FRP) for strengthening and rehabilitation, this has exposed the need for reliable methods for estimating stiffness and strength of deteriorating and retrofitted concrete structures. The present paper describes a procedure for solving this problem based on nonlinear finite element analysis. Key ingredients in the proposed method are accurate constitutive and kinematical models together with a specially developed procedure for simulating the true loading and straining history of deteriorating and repaired concrete members. Numerical examples are presented in order to verify the accuracy of the proposed method.

Keywords: Concrete, Deterioration, Corrosion, Fibre reinforced polymers, Strengthening, Finite element analysis.

Dr G Horrigmoe, is Director of NORUT Technology in Narvik, Norway. He specializes in finite element analysis and durability and retrofitting of reinforced concrete structures. His interests also include numerical modelling and analysis of composite materials and ice mechanics.

INTRODUCTION

Widespread problems of deterioration of civil engineering infrastructure have been experienced in many countries during the last decades. The major portion of the infrastructure is built from reinforced concrete and corrosion of reinforcing steel is the principal cause of deterioration, although alkali silica reactions, freeze-thaw damage, sulphur attack, etc. also play a significant role. The registered need for rehabilitation and repair and the associated costs is a matter of great concern for those responsible for assessment and maintenance of affected structures.

At the same time, existing infrastructure is subjected to new demands brought about by societal changes. Globalisation of the economy leads to increased competition and needs for rapid adaptations in industry. Reuse of production facilities and office buildings follows as a natural consequence of this and is often accompanied by changes in design requirements. A similar situation is emerging in the public sector as new objectives have to be met by governmental agencies and municipalities. Increased safety requirements, changes in design loads or revisions of design codes may also render structural members or entire structures inadequate.

Repair of concrete structures attacked by corrosion has in many cases proved to be inefficient in preventing further corrosion. Moreover, the high costs of repair, often cause delayed or insufficient actions and thus permitting deterioration to continue. As a result, a growing number of reinforced concrete structures is reaching a stage where serviceability, load-carrying capacity and safety may be affected. In addition, increased design loads, code revisions, etc have exposed the need for safe and effective procedures for strengthening of existing structures.

It seems natural to assume that in the future, repair and strengthening of reinforced concrete structures more often will be combined and carried out in one operation. The objectives of the combined repair and strengthening operations will be to provide increased stiffness and load-carrying capacity and, simultaneously, improve durability and extend service life, thereby further increasing the demands on concrete repair technology. Thus, there is a need for significant improvements and innovations of repair techniques to meet future requirements regarding performance and costs [1]. The introduction of fibre reinforced polymer (FRP) composites as a means of retrofitting concrete structures is an example of innovative developments that may enable the concrete industry to meet some of the challenges of the 21st century with respect to maintenance and retrofitting of civil engineering infrastructure.

The present paper focuses attention on repair and strengthening of reinforced concrete structures using externally bonded FRP materials. Properties and applications of composites in concrete structures are reviewed. A critical examination is presented of unresolved questions and areas of particular concern with respect to practical use of fibre reinforced composites for external strengthening of concrete structures.

Special attention is given to the role of numerical simulation in assessment of deteriorating concrete structures as well as in analysis and design of FRP strengthened members. Brittle failure caused by debonding of the composite material represents a particular challenge in achieving safe designs. Results from nonlinear finite element simulations of delamination failure of strengthened beams are presented. The numerical computations are shown to be in very good agreement with data from laboratory tests.

CURRENT PRACTICES FOR REHABILITATION AND RETROFITTING OF CONCRETE STRUCTURES

Concrete repair is being conducted by various methods, some of these are relatively new techniques developed during the last decade, or so. Repairs are sometimes classified as either structural (ie, load-carrying) or non-structural. Although this distinction may represent an adequate description of the main purpose of the repair, it may also be confusing since durability and performance are generally related. Lack of durability will eventually affect mechanical behaviour or structural properties such as stiffness and ultimate load capacity. Thus, it seems more appropriate to classify the various techniques applied to prevent deterioration or remedy damage of concrete structures in accordance with their actual effect, that is, what is really being accomplished. Accordingly, current methods may be grouped into three main categories:

- Protection systems
- Repair systems
- Strengthening systems

Protection methods seek to maintain the existing condition by limiting the intrusion of moisture, chlorides, carbon dioxide, etc. This is accomplished by use of surface treatments, inhibitors or electrochemical methods. To this category belongs various forms of sealers, membranes and overlays. Many of these products will delay the onset of corrosion of steel reinforcing bars. Anodic corrosion inhibitors improve the concrete's natural ability to protect embedded steel bars by forming a passivating oxide layer on the steel. Cathodic protection systems seek to control corrosion by making the embedded reinforcement cathodic. It is important to note that cathodic protection is only concerned with controlling future corrosion and does not reinstate corroded steel bars.

Repair methods seek to restore mechanical properties (ie, stiffness, strength) and durability in order to maintain design service life. This is achieved by reducing or removing the actual cause of corrosion. The most widely used repair technique continues to be that of mechanical removal of carbonated or chloride contaminated concrete, followed by sandblasting of corroded reinforcing bars and application of a cement-based mortar or concrete to replace the removed, damaged material. This procedure is commonly referred to as "mechanical repair". Unless repair work is carefully executed and all contaminated concrete is removed, mechanical repair may under certain circumstances increase future corrosion rather than prevent it. The removal of contaminated concrete is limited by structural strength and safety requirements, hence one may be forced to accept less than optimum removal of damaged material. Mechanical repair is sometimes denoted "structural repair". However, this is somewhat misleading since residual strength after completion of the repair is often neither considered nor is it documented. Concrete repair may also be conducted by electrochemical treatments. In the chloride extraction method, chloride ions are removed under the influence of an electrical field, whereas realkalization is a method that restores the high pH level in concrete. Spalled and cracked concrete must be removed and exposed reinforcement cleaned prior to application of these techniques. The major advantage of electrochemical treatments is that it deals with the actual cause of corrosion. Promising results with these methods have been reported, but unwanted side effects in the form of reduced bond strength, alkali-silica reactions and hydrogen embrittlement of high strength tendons seem to hamper their practical use.

There exist differences in opinion regarding the relative merits and actual performance of the various methods for protection and repair of concrete structures. One obvious reason for this is that systematic and objective studies of the performance of executed concrete repair are lacking and such research should be encouraged [2]. Protection methods and repair techniques are sometimes confused as alternative or competing measures of repairing deteriorating concrete structures. However, one should bear in mind that these methods have different objectives and serve different purposes. In many cases, it may be worthwhile to consider the combination of repair and protection procedures in order to achieve more efficient concrete repair by improving durability and extending service life of mechanical repair.

Procedures for strengthening of concrete structures seek to increase structural stiffness and strength. Traditionally, this has been accomplished by either increasing the concrete dimensions (including additional reinforcement) or by external post tensioning. The introduction of fibre reinforced polymer materials as a means of strengthening existing concrete structures is one of the most significant innovations in concrete technology during the last decade. Improved structural performance can be obtained by means of laminated plates or thin, flexible fabrics bonded to the concrete surface using epoxy resin. The major driving force behind this development has been the need for seismic retrofit of bridge structures in the United States and Japan. Following the immediate success of FRP strengthening of structures subjected to earthquake loading, a large number of non-seismic applications have been reported, and the practical use of this technique is gaining strong momentum.

The excellent durability of especially carbon fibres combined with high strength, low weight and low installation costs makes externally bonded carbon fibre reinforced polymers (CFRP) attractive also for repair of deteriorated concrete members. The basic idea is the protection of the concrete surface provided by the CFRP sheet together with the extra strength. Promising results have been obtained with this technique, which represents an important step forward for concrete repair technology. Since the effect of carbon fibre wrappings hinges on the bond between concrete and composite, long time effects on bond strength need verification.

USE OF FRP COMPOSITE MATERIALS IN CONCRETE STRUCTURES

A composite material can be defined as a material system consisting of one or more discontinuous phases embedded in a continuous phase on a macroscopic level. The mechanical performance and properties of a composite material are designed to be superior to those of the constituent materials acting independently. The discontinuous phase is usually stiffer and stronger than the continuous phase and is called the reinforcement, whereas the less stiff and weaker continuous phase is termed matrix (Figure 1). Sometimes, an additional phase, called interface, exists between the reinforcement and the matrix. Properties of composites are strongly influenced by the properties of their constituent materials, their distribution, and the interaction among them. For the high performance structural composites considered herein, the continuous-fibre reinforcement is the backbone of the material that determines its stiffness and strength in the direction of the fibres. The matrix provides protection for the fibres and local stress transfer from one fibre to another. The interphase, although small in size, can have a strong influence on failure mechanisms and overall stress-strain behaviour of the material. The major advantages of composite materials over monolithic materials are high stiffness and strength, low density, and adaptability to the intended function of the structure.

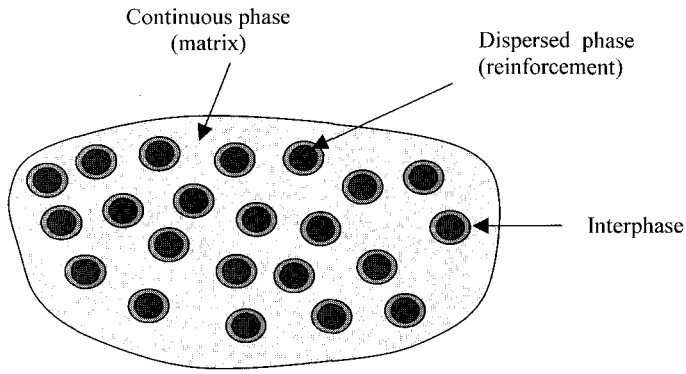

Figure 1 Phases of a composite material

The use of polymer composites in civil engineering infrastructure originated during the second world war. During the following decades, significant developments in material technology took place and the use of composite materials in the building and construction industry grew steadily. These early applications of composites were mainly roof and skeletal structures, although building blocks and building systems began to appear in the 1980's. The last decade, or so, has seen major advances of composite materials, especially in bridge engineering.

Since reinforced concrete is the most widely used engineering material, it is natural that efforts have been made to apply FRP composites in concrete structures. The need for strengthening and repair of reinforced concrete infrastructure has been the major driving force behind innovative applications of composite materials in concrete. The most significant of these developments include:

- Externally bonded plates or flexible sheets for repair and strengthening
- Reinforcing bars (standard or prestressed)
- Near surface mounted (NSM) bars
- High strength cables
- Permanent formwork
- Hybrid structures
- Bridge superstructures

In the first four of these types of application, FRP is used as a direct substitute for internal or external steel reinforcement. The use of steel or wood as protective, permanent formwork has a long tradition in concrete construction. In hybrid FRP/concrete members, the two materials are used to their best advantage. A case in point is a beam element with tee or hollow box cross section, where the vertical webs, made of high strength, pultruded FRPs, carry the tensile stresses, while the concrete flange provides compressive strength and rigidity. For concrete bridges with severe structural deterioration conventional repair is time consuming and it may be necessary to close lanes and reroute traffic for at considerable period of time. In such cases it has been demonstrated that replacement of the entire bridge superstructure with one made of FRP materials can be a viable solution for short span bridges.

Commercial systems for strengthening and rehabilitation of concrete structures basically fall into two categories: laminated plates or flexible sheets. These composites contain high-resistance unidirectional or bi-directional fibres embedded in a polymer resin matrix. Typical properties of commonly used fibres and resins are listed in Table 1 and Table 2, respectively. Laminated plates are made from unidirectional carbon fibres. Typical widths are 50 to 120 mm whereas plate thicknesses are 1.2 - 1.4 mm. Flexible sheets or fabrics are available with uni- or bi-directional glass, carbon or aramid fibres. Each layer has a thickness of approximately 0.4 - 0.6 mm and the weight varies between 200 and 300 g/m^2. The properties of FRP materials differ from one manufacturer to another and the properties reported by the manufacturers usually reflect the guaranteed values (ie, mean value minus three standard deviations). It is also possible to estimate the properties of any FRP system from the properties of the individual constituents using the rule of mixtures.

Table 1 Properties of fibres

FIBRE	ELASTIC MODULUS [GPa]	TENSILE STRENGTH [MPa]	ULTIMATE STRAIN [‰]
E-glass	72	3450	48
S-glass	87	4300	50
Carbon	160-725	1400-3100	5-14
Aramid (Kevlar)	83-186	3400-4100	20-40

Table 2 Properties of resins

RESIN	ELASTIC MODULUS [GPa]	TENSILE STRENGTH [MPa]	ULTIMATE STRAIN [‰]
Polyester	3.0	50-65	20-30
Vinylester	3.5	70-80	40-60
Epoxy	3.0	50-90	20-80

Table 3 Properties of commercial CFRP systems

PRODUCT	TYPE	ELASTIC MODULUS [GPa]	TENSILE STRENGTH [MPa]	ULTIMATE STRAIN [‰]
Flexible sheets:				
BPE Composite	S	234	4500	19
BPE Composite	M	377	4400	12
BFE Composite	H	465	3920	8
Laminates:				
SIKA Carbodur	S	165	3050	17
SIKA Carbodur	M	210	2900	12
SIKA Carbodur	H	300	1450	5

For retrofitting of concrete structures carbon fibre reinforced polymers (CFRP) have been the most widely used material. CFRP composites can be manufactured with varying strengths and elastic moduli, these systems are commonly referred to as standard (S), medium (M) and high (H). A number of commercial systems are being offered. Table 3 lists mechanical properties of typical commercial CFRP systems based on flexible sheets or laminates.

AREAS OF PARTICULAR INTEREST OR CONCERN

The first pioneering steps of using externally epoxy-bonded fibre composites for strengthening of concrete structures occurred in the 1980's. The strengthening of flexural members to enhance moment capacity [3] - [5] and shear capacity [6] – [9] is well documented. Laboratory investigations have also been conducted to study the behaviour of FRP systems for other loading situations such as torsion and fatigue. During the last decade FRP repair and strengthening methods have gained wide acceptance as effective and economic infrastructure rehabilitation technologies. It is in many ways remarkable that this material technology, which to a large extent is unfamiliar to the construction industry, has been put to practical use so rapidly. Despite the rapid growth in applications of fibre reinforced polymers for strengthening and rehabilitation of concrete structures, a number of unresolved problems remain. These questions, which can only be settled through continued research, are briefly reviewed in the following.

Long time performance

Practical applications of FRPs for rehabilitation and strengthening of concrete infrastructure cover a wide range of structural components and loading situations and have been conducted in countries with a variety of environmental conditions. Reported results from such projects are generally good, but it is important to bear in mind that the bulk of field applications are from the 1990's and that long time experience is lacking.

It should be noted that applications of FRPs in concrete infrastructure represent different loadings and environmental conditions as compared to, those encountered in, for example aerospace industry. Bridges, etc. are designed for a service life up to 100 years. The structures are subjected to mainly static loadings and externally bonded FRP composites are vulnerable to temperature variations, freezing and thawing. Moreover, use of fibre reinforced polymer materials in civil constructions faces particular challenges caused by unsystematic inspection and maintenance and the industry's traditional sharp focus on low construction and maintenance costs.

Durability

Concerns regarding durability should not be confused with the durability of the FRP material itself, which is generally excellent. The problems relate to the applications of FRPs in concrete infrastructure and the associated environmental conditions.

First of all, the integrity of externally bonded fibre reinforced polymers for strengthening and rehabilitation hinges on the composite action, ie, bond between FRP and concrete. Hence, the durability or long time performance of bond is of paramount importance. Temperature changes and high humidity can cause deformations and micro cracking in the composite which may affect bond. Exposed concrete infrastructure generally has a relatively high and

stable pore humidity (approximately 80%). The performance of FRP systems in marine environment is of particular concern since vital components of concrete infrastructure are located either in or close to sea water (eg, piers, bridges). Repeated cycles of drying and rewetting and intrusion of salts may have a negative influence on bond strength [10]. In cold climates, cycles of freezing and thawing can cause reduction of bond either directly or indirectly through degradation of the underlying concrete material. However, results from laboratory testing of specimens subjected to freeze-thaw cycles have shown only minor reductions in performance [11], [12] while other investigators [13] have reported more significant degradation.

Whereas FRP strengthening of unloaded, uncracked concrete members has been studied extensively, only a relatively minor research effort has been devoted to the repair of deteriorated concrete structures. Use of externally bonded FRP systems for repair of concrete structures where the embedded steel reinforcement is attacked by corrosion, presents special problems. The corrosion process is an expansive reaction which may cause cracking of the concrete cover and possible loss of bond between composite and concrete. It is therefore reasonable to assume that the efficiency of FRP repair will be reduced as a result of corrosion damage, and it has been advocated that one should not attempt to apply externally bonded FRPs to concrete structures with corroding reinforcement. A distinction should be made between FRP wrapping of columns [14], where the composite provides external confinement accommodating the expansive forces due to corrosion, and the use of FRP sheets for repair of flexural members [15] subjected to reinforcement corrosion.

Finally, there are some problems of durability that are directly related to FRP materials. Thermosetting polymers such as polyester and epoxy have glass transition temperatures in the range 150° C to 200° C, hence, FRP composites need special protection against fire. Moreover, polymer composites must be effectively protected against ultraviolet radiation.

Brittle failure

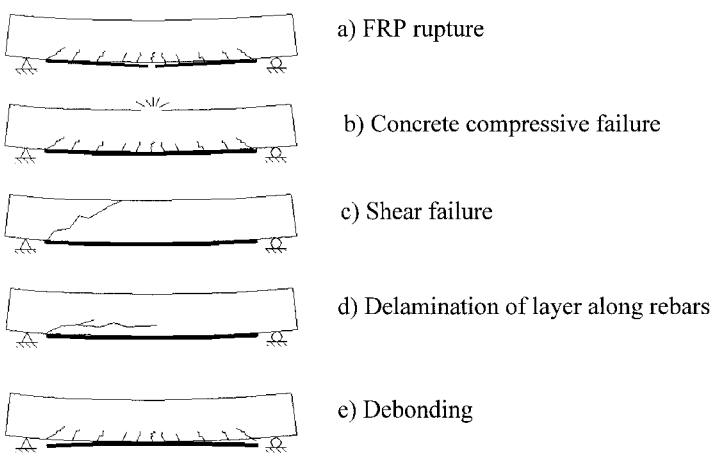

Figure 2 Possible failure modes of strengthened beam

Concrete flexural members are designed to produce ductile failure, by limiting the amount of tensile reinforcement. Strengthening by externally bonded of FRP composites poses special problems in this regard. The composite material is brittle and behaves linearly elastic until rupture. Thus, strengthening of flexural members usually implies changes in failure modes from that of ductile to brittle behaviour. Possible failure modes of a strengthened beam are illustrated in Figure 2. Delamination of a concrete layer along the reinforcing bars (Figure 2 d) and debonding between composite and concrete (Figure 2 e) are of particular concern since these failure modes lead to premature, brittle failure of the strengthened beam, hence, the full potential of FRP strengthening cannot be realized. The behaviour depicted in Figure 2 d and 2 e can be effectively prevented by providing sufficient anchorage of the composite material. However, in many practical applications this is not easily accomplished. Anchorage lengths and bond strengths of bonded FRP have therefore been studied extensively [16] - [22] and a number of analytical models for predicting interfacial stresses in strengthened beams have been proposed [23] - [28]. These procedures are based on linearly elastic behaviour and their application is limited to simple beam cases.

Design issues

A major obstacle in adopting FRPs in repair and strengthening of concrete structures has been the lack of recommendations and accepted standards for design and quality control. The guidelines and codes for design of FRP strengthening that have been developed in recent years [29] – [34] should therefore represent a major step forward in taking full advantage of this emerging technology. In principle, design of concrete members externally strengthened with FRP fabrics or plates follows the same basic principles as used for conventional reinforced concrete. However, certain aspects of design philosophy and issues related to the methodology for the design of post-strengthened concrete structures using FRP composites remain unsettled.

It is obvious that there should be a minimum required load-carrying capacity of the unstrengthened element to prevent collapse if the composite is compromised due to uncontrollable events, eg fire. Another important design philosophy issue is related to maintaining "pseudo-ductile" behaviour by limiting the allowable strength enhancement. To compensate for the lack of ductility, the margin of safety against failure should be higher than that used in design of traditional steel-reinforced concrete structures. The lack of engineering experience, testing and performance data makes the choice of appropriate safety factors difficult to justify. Moreover, FRP systems are manufactured differently; each system has distinct material and performance properties, and each system is designed in a unique way. Material safety factors should account for deviations in material properties, variations due to manufacturing procedures and installation procedures and conditions, type of loading, and environmental effects. In addition, it is necessary to consider the type of application, governing failure mode, etc. Last but not least, the condition of the concrete substrate is of vital importance for successful applications of epoxy-bonded FRP systems and criteria and verification methods need to be developed.

Inspection and testing to determine feasibility of applying FRP strengthening

In order to select an appropriate FRP strengthening strategy, a systematic assessment of the existing structure should be conducted. The objectives would be to determine the condition of the existing structure, to identify the causes of any deficiencies, to verify the structure's load-carrying capacity, and to evaluate the feasibility of applying externally bonded FRP

systems. Proper inspection and testing are significantly more important for FRP strengthening than for conventional repair methods. Thus, standard procedures for condition assessment including necessary sampling and testing should be developed.

Installation of FRP materials

As opposed to conventional engineering materials, adequate installation of FRP composites is essential to ensure proper performance. Each FRP system is unique and it is necessary to follow the specifications provided by the manufacturer regarding handling and storage, concrete surface preparation, curing, and protection.

Barriers to uptake of FRP technology for rehabilitation of concrete infrastructure

Externally bonded fibre reinforced polymers offer a viable alternative for service life extension of reinforced concrete members. During the last decade, the lack of approved design codes has hampered the practical use of FRP technology in concrete infrastructure. Although this obstacle is now being reduced by the introduction of design codes in several countries, it will take some time before important aspects of design philosophy are generally agreed. In the meantime, and until long time performance is well documented, a conservative approach is recommended. FRP systems are not standardized and it may be required that the actual performance is verified by tests conducted in the laboratory or in the field.

In the longer term, the greatest barrier against uptake of FRP technology in rehabilitation of concrete infrastructure is the general unfamiliarity with composite materials in the building and construction industry. The challenge for universities is to prepare a new generation of civil engineers to utilize the full potential of composite materials. This requires systematic education and training in the manufacture and design of fibre composites for the construction industry.

THE ROLE OF NUMERICAL SIMULATION IN ASSESSING DETERIORATING AND RETROFITTED CONCRETE STRUCTURES

The widespread problems of corrosion of embedded steel reinforcement in concrete infrastructure have exposed the need for improved understanding of the influence of corrosion damage upon structural performance [35]. In particular, there is a growing need for reliable methods for estimating stiffness and strength of deteriorating and repaired concrete structures since any attempt to optimize maintenance and repair requires the capability to predict the remaining service life of corroding structures. This is a very demanding problem since the constitutive and kinematical behaviour of deteriorating concrete structures is highly complex and path dependent. The application of FRP materials adds further complexities. Fibre reinforced composites are anisotropic and brittle failure modes such as debonding between the composite and concrete represent strongly nonlinear behaviour. Simplified analytical procedures are lacking and may be of limited value. Instead, it is attempted to seek numerical solutions to problems of this kind by means of nonlinear finite element analysis. For the numerical simulations to be accurate, it is necessary that constitutive and kinematical assumptions represent realistic approximations of concrete structures suffering from corrosion of embedded reinforcing bars. The assumptions should cover the entire path of loading, deterioration and repair [36]. The mechanical behaviour of deteriorating concrete structures is strongly path dependent, ie, the response depends on the history of loading and

straining. Therefore, it is important that a close approximation to the true path of deterioration, repair and strengthening can be simulated. A typical history of corrosion attack, repair and strengthening of concrete structures can be explained from Figure 3, in which a simply supported beam is used for illustration. In the initial stage, the discretized beam is gradually subjected to the full service load (SLS), during which cracking occurs (Figure 3 a). Simultaneously, corrosion of reinforcing steel takes place. As a result, the cross sectional area of the attacked bars and the bond between the bars and surrounding concrete are reduced. In the finite element model, the properties (ie, cross sectional area, bond characteristics) of the affected elements are changed while the external loading is maintained. Thus, the bending stiffness of the beam is reduced and increased deflections and strains result. The structure is taken out of service and the variable component of the loading is eliminated so that only the permanent load remains (Figure 3 c). At this stage, contami-nated concrete is removed and the tensile reinforcement is exposed over the entire deteriorated region of the beam (Figure 3 d). This is achieved by removing the associated finite elements from the mesh. The associated loss of composite action causes additional deflections. Attacked bars are cleaned by sandblasting and their cross section and bond strength are permanently reduced. If necessary, extra steel bars may be introduced. The removed, contaminated concrete is replaced by a suitable concrete or repair material, which is strain-free, whereas the adjacent concrete remains strained and cracked (Figure 3 e). This is accomplished by adding new finite elements to the discretized structure. External strengthening by bonded FRP sheets or plates is applied at this stage (Figure 3 f). Again, new finite elements are introduced while the structure remains under constant loading. Finally, the loading is incrementally increased until failure of the retrofitted beam occurs (Figure 3 g). The simulation of sequence of deterioration, repair and strengthening such as that depicted in Figure 3, should be accomplished in a single analysis.

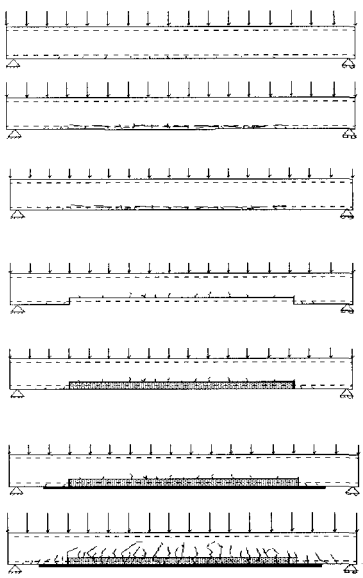

a) The undamaged beam is subjected to the full service load (SLS).

b) Corrosion of reinforcing steel.

c) Variable load component removed.

d) Removal of deteriorated concrete material, cleaning of corroded rebars.

e) Application of repair mortar (and additional reinforcement).

f) Application of externally bonded FRP sheet or plates.

g) Repaired and strengthened beam is loaded until failure.

Figure 3 Tracing a sequence of deterioration, repair and strengthening of concrete structures

NUMERICAL EXAMPLES

The first example concerns the simulation of a reinforced concrete beam which was subjected to corrosion attack and then repaired. No FRP strengthening was applied in this case. The beam was simply supported with a free span L = 8.0 m. The loading consisted of a uniformly distributed dead load of 23.8 kN/m plus a variable component of 8.0 kN/m, see Figure 4.

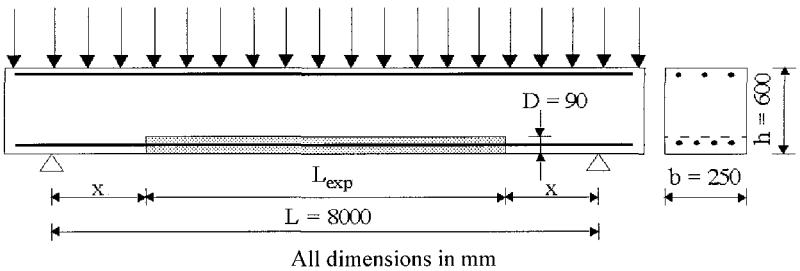

Figure 4 Beam subjected to deterioration and repair

Material constants for concrete and steel are given in [37]. The corrosion attack was defined to take place uniformly over a length L_{exp} located symmetrically about the mid section of the beam. Contaminated concrete was removed over the entire length L_{exp} and depth D. For simplicity, the properties of the repair material were taken identical to those of the original concrete and perfect bond was imposed between the two materials. In the finite element simulations, the length L_{exp} of the deteriorated zone was varied between 0.5 L and 0.7 L. Two different levels of corrosion were considered by reducing the cross section of the tensile reinforcement by 10% and 25%, respectively. Reduced bond strength of corroded reinforcement was modelled as described in [37]. Numerical simulations of a complete sequence of deterioration and repair, as illustrated in Figure 3, were carried out. Load versus central deflection curves are portrayed in Figure 5 for the highest level of corrosion (ie, 25% reduction of cross sectional area).

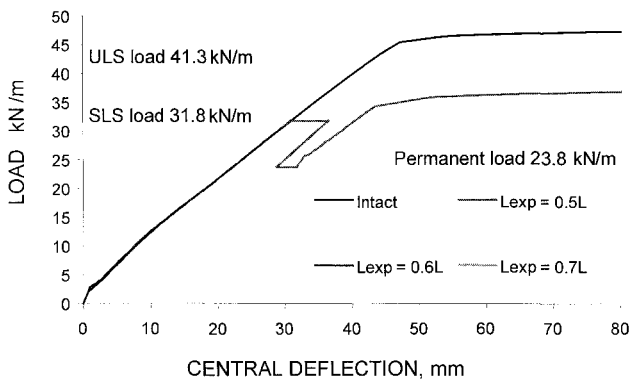

Figure 5 Load versus deflection curves for deteriorated and repaired beams where the tensile reinforcement has been reduced by 25 % due to corrosion

From this diagram it is noted that corrosion and the associated reduction in bending stiffness leads to increased deflections under constant, SLS load of 31.8 kN/m. The additional deflections become even more pronounced after unloading to the permanent load 23.8 kN/m, where contaminated concrete is removed accompanied by complete loss of composite action over the entire attacked region. It should be noted that due to the permanent reduction in cross section and bond strength of the attacked reinforcement, conventional mechanical repair was unsuccessful in restoring the initial design strength of the beam.

The second example was chosen in order to illustrate the simulation of progressive delamination failure of a beam externally strengthened by CFRP laminate. In simple cases, analytical formulas can be applied to calculate the necessary anchor lengths of the laminate. For more complex structures with two- or three-dimensional states of stress, numerical computations may be the only viable option. Test results for the simply supported beam shown in Figure 6 have been reported by Nitereka and Neale [38].

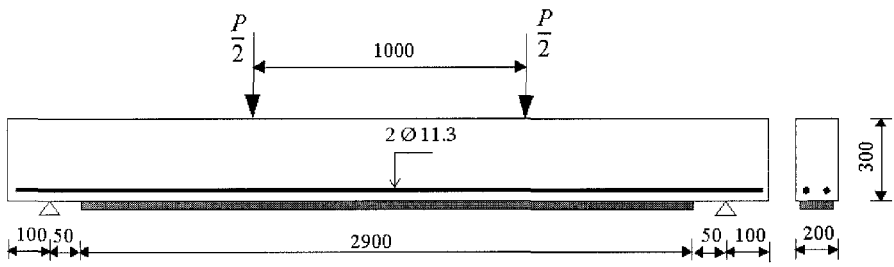

All dimensions in mm

Figure 6 Strengthened beam

The geometric dimensions of the beam and CFRP laminate are given in and material parameters for concrete steel and composite can be found in [38]. A special model for progressive delamination was developed, using interface elements. These interface elements are, in effect, spring elements with nonlinear stiffness characteristics derived from experimental data. The laboratory testing also included a reference beam without any CFRP strengthening. Load-deflection curves for both the unstrengthened reference beam and the CFRP strengthened beam are portrayed in Figure 7. Several interesting observations can be made from this diagram: First, external strengthening changes the behaviour of the beam from ductile to relatively brittle, and, second, a significant increase in load-carrying capacity is achieved by CFRP strengthening. This example was chosen to validate the proposed constitutive and kinematical model for progressive delamination. It is seen from Figure 7 that the results from finite element simulations are in excellent agreement with test data.

CONCLUDING REMARKS

Corrosion of embedded reinforcing steel due to carbonation or chloride intrusion continues to pose threats to the performance and integrity of concrete infrastructure. Conventional methods for repair of concrete structures have in many cases shown less than satisfactory performance.

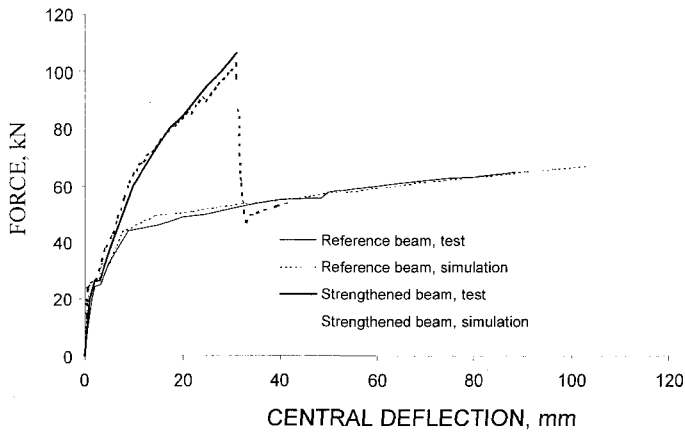

Figure 7 Load-deflection diagrams for unstrengthened and strengthened beams

Increased design loads, code revisions, reuse of existing facilities, etc. also contribute to the growing need for new innovative systems for repair and strengthening of concrete structures. Over the last ten years, or so, epoxy-bonded, fibre reinforced polymers have gained widespread acceptance as an effective method for rehabilitation of concrete infrastructure. Despite the rapid growth in applications of FRP materials for retrofitting of concrete structures, a number of unresolved issues remain. The most important of these are the lack of data for long time performance and durability in civil engineering infrastructure applications. Certain basic questions regarding design philosophy and selection of material safety factors also need careful consideration. The behaviour of deteriorating concrete structures is strongly nonlinear and path dependent. Simple, analytical methods for predicting stiffness and strength of deteriorating, repaired and strengthened concrete structures are therefore of limited value. The present paper has focused attention on the use of nonlinear finite element analysis to assess residual strength of deteriorating and retrofitted structures. A special procedure was introduced for simulation of the true loading and straining history of concrete structures subjected to reinforcement corrosion, repair and strengthening. The numerical examples presented in the paper encompassed deteriorating and repaired concrete beams as well as simulation of progressive delamination failure of beams strengthened with CFRP. In the latter case, the numerical results were compared with test data and excellent agreement was achieved.

ACKNOWLEDGEMENTS

The author would like to acknowledge the support provided by The Research Council of Norway (project no. 121363/420) and by The Norwegian Public Roads Administration.

REFERENCES

1. HORRIGMOE G., Future needs in concrete repair technology, Concrete Technology for a Sustainable Development in the 21st Century (eds. O.E. Gjørv and K. Sakai), E&FN Spon, London, 2000, pp 332-340.

2. ARNTSEN B., Durability of mechanically repaired concrete structures subjected to chloride induced corrosion, Ph.D. thesis (in preparation), NORUT Technology, Narvik, Norway.

3. SAADATMANESH, H. and EHSANI, M.R., RC beams strengthened with FRP plates I: Experimental study, ASCE Journal of Structural Engineering, Vol. 117, No 11, 1991, pp 3417-3433.

4. GANGARAO H.V.S. and VIJAY P.V., Bending behaviour of concrete beams wrapped with carbon fabric, ASCE Journal of Structural Engineering, Vol 124, No 1, 1998, pp 3-10.

5. BUYUKOZTURK O. and HEARING B., Failure behaviour of precracked concrete beams retrofitted with FRP, ASCE Journal of Composites for Construction, Vol 2, No 3, 1998, pp 138-144.

6. CHAJES M.J., JANUSKA T.F., MERTZ D.R., THOMASON T.A., and FINCH W.W., Shear strengthening of reinforced concrete beams using externally applied composite fabrics, ACI Structural Journal, Vol 92, No 3, 1995, pp 295-303.

7. TRIANTAFILLOU T.C., Shear strengthening of reinforced concrete beams using epoxy-bonded FRP composites, ACI Structural Journal, Vol 95, No 2, 1998, pp 107-115.

8. KHALIFA A., GOLD W.J., NANNI A., and AZIZ A., Contribution of externally bonded FRP to shear capacity of RC flexural members, ASCE Journal of Composites for Construction, Vol 2, No 4, 1998, pp 195-202.

9. MALEK, A.M. and SAADATMANESH, H., Ultimate shear capacity of reinforced concrete beams strengthened with web-bonded-reinforced plastic plates, ACI Structural Journal, Vol 95 No 4, 1998, pp 391-399.

10. SEN R., SHAHAWY M., MULLINS G., and SPAIN J., Durability of carbon fiber-reinforced polymer/epoxy/concrete bond in marine environment, ACI Structural Journal, Vol 96, No 6, 1999, pp 906-914.

11. HOMAN S.M., SHEIKH S.A., PERNICA G., and MUKHERJEE P.K., Durability of fibre reinforced polymers (FRP) used in concrete structures, Department of Civil Engineering, University of Toronto, Research Report No. HS-01-00, February 2000.

12. ARNTSEN B. and HORRIGMOE G., Freeze-thaw durability of concrete beams and slabs strengthened with CFRP, Concrete Under Severe Conditions (eds. N. Banthia, K. Sakai and O.E. Gjørv), University of British Columbia, Vancouver, Canada, Vol 2, 2001, pp 1730-1739.

13. TOTUTANJI, H. and BALAGURU P., Durability characteristics of concrete columns wrapped with FRP tow sheets, ASCE Journal of Materials in Civil Engineering, Vol. 10, No. 1, 1998, pp. 52-57.

14. PANTAZOPOULOU S.J., BONACCI J.F., SHEIKH S., THOMAS M.D.A., and HEARN N., Repair of corrosion-damaged columns with FRP wraps, ASCE Journal of Composites for Construction, Vol. 5, No. 1, 2001, pp. 3-11.

15. BONACCI J.F. and MAALEJ M., Externally bonded fiber-reinforced polymer for rehabilitation of corrosion damaged concrete beams, ACI Structural Journal, Vol. 97, No. 5, 2000, pp. 703-711.

16. BIZINDAVYI L. and NEAL K.W., Transfer lengths and bond strengths for composites bonded to concrete, ASCE Journal of Composites for Construction, Vol. 3, No. 4, 1999, pp. 153-160.

17. NGUYEN D.M., CHAN T.K., and CHEONG H.K., Brittle failure and bond development length of CFRP-concrete beams, ASCE Journal of Composites for Construction, Vol. 5, No. 1, 2001, pp. 12-17.

18. MUKHOPADHYAYA P. and SWAMY N., Interface shear stress: A new design criterion for plate debonding, ASCE Journal of Composites for Construction, Vol. 5, No. 1, 2001, pp. 35-43.

19. DE LORENSIS L., MILLER B., and NANNI A., Bond of fiber-reinforced polymer laminates to concrete, ACI Materials Journal, Vol. 98, No. 3, 2001, pp. 256-264.

20. EL-MIHILMY M.T. and TEDESCO J.W., Prediction of anchorage failure for reinforced concrete beams strengthened with fiber-reinforced polymer plates, ACI Structural Journal, Vol. 98, No. 3, 2001, pp. 301-314.

21. CHEN J.F. and TENG J.G., Anchorage strength models for FRP and steel plates bonded to concrete, ASCE Journal of Structural Engineering, Vol. 127, No. 7, 2001, pp. 784-791.

22. SEBASTIAN W.M., Significance of midspan debonding failure in FRP-plated concrete beams, ASCE Journal of Structural Engineering, Vol. 127, No. 7, 2001, pp. 792-798.

23. TÄLJSTEN B., Plate bonding, Doctoral thesis, Division of Structural Engineering, Luleå University of Technology, Report No. 1994: 152 D, Luleå, Sweden, 1994.

24. ARDUINI M. and NANNI A., Parametric study of beams with externally bonded FRP reinforcement, ACI Structural Journal, Vol. 94, No. 5, 1997, pp. 493-501.

25. MALEK A.M., SAADATMANESH H., and ESHANI M.R., Prediction of failure load of R/C beams strengthened with FRP plate due to stress concentration at the plate end, ACI Structural Journal, Vol. 95, No. 4, 1998, pp. 142-152.

26. SHEN H.-S., TENG J.G., and YANG J., Interfacial stresses in beams and slabs bonded with thin plate, ASCE Journal of Engineering Mechanics, Vol. 127, No. 4, 2001, pp. 399-406.

27. LEUNG C.K.Y., Delamination failure in concrete beams retrofitted with a bonded plate, ASCE Journal of Materials in Civil Engineering, Vol. 13, No. 2, 2001, pp. 106-113.

28. SMITH S.T. and TENG J.G., Interfacial stresses in plated beams, Engineering Structures, Vol. 23, 2001, pp. 857-871.

29. SAADATMANESH H. and MALEK A.M., Design guidelines for flexural strengthening of RC beams with FRP plates, ASCE Journal of Composites for Construction, Vol. 2, No. 4, 1998, pp. 158-164.

30. EL-MIHILMY M.T. and TEDESCO, J.W., Analysis of reinforced concrete beams strengthened with FRP laminates, ASCE Journal of Structural Engineering, Vol. 126, No. 6, 2000, pp. 684-691.

31. TÄLJSTEN B., Strengthening of concrete structures by carbon fibre reinforced fabrics and laminates: Design, materials and installation (in Swedish), Division of Structural Engineering, Luleå University of Technology, Sweden, Report No. 2000: 16, Luleå, Sweden, 2000.

32. ISIS CANADA, Strengthening reinforced concrete structures with externally-bonded fibre reinforced polymers (Draft), Report No. ISIS-M05-00-06, June 2000.

33. ACI COMMITTEE 440, Guide for the design and construction of externally bonded FRP systems for strengthening concrete structures (Draft), American Concrete Institute, Michigan, U.S.A., September 2001.

34. FIB, Design and use of externally bonded FRP reinforcement (FRP EBR) for reinforced concrete structures Progress Report of fib Task Group 9.3, EBR Group, International Federation for Structural Concrete, Lausanne, Switzerland.

35. CAIRNS J., Assessment of effects of reinforcement corrosion on residual strength of deteriorating concrete structures, Proceedings of the First International Conference on Behaviour of Damaged Structures, Rio de Janeiro, Brasil, 1998.

36. HORRIGMOE G., Structural assessment of deterioration and repair of concrete structures by means of nonlinear finite element simulations, Concrete Under Severe Conditions (eds. N. Banthia, K. Sakai and O.E. Gjørv, University of British Columbia, Vancouver, Canada, Vol. 2, 2001, pp. 1882-1891.

37. SAND B., "Nonlinear finite element analysis of deteriorated and repaired RC beams", NORUT Technology, Report No. NTAS F2001-19, Narvik, Norway, 2001.

38. NITEREKA C. and NEALE K.W., Analysis of reinforced concrete beams strengthened in flexure with composite laminate, Canadian Journal of Civil Engineering, Vol. 26, No. 5, 1999, pp. 646-654.

CONCRETE: VADE MECUM

P C Hewlett
British Board of Agrément
United Kingdom

ABSTRACT. In putting together this Congress review from the many papers submitted, I have been looking for significant trends that can give direction to the way forward. Both the Seminars and Conferences have been taken into account but it has been written in advance. As a consequence the views expressed and conclusions drawn may well change as a result of the Congress itself and the exchanges that will occur during the event. There will be opportunity to cover such developments during the Closing Address Ceremony.

A number of ongoing challenges for concrete have been identified that suggest a way forward. The intent to change is serious but the consequences of not changing are even more so. Quo Vardis?

Keywords: Cement, Environment, Durability, Composite materials, Toughness, Pathology, Sustainability, Aesthetics, Waste, Deconstruction.

P C Hewlett is a chartered chemist and Chief Executive of the British Board of Agrément. He is visiting Industrial Professor in the Department of Civil Engineering at the University of Dundee and an active member of the Concrete Technology Unit. He is Chairman of the Technical Executive Committee of the UK Concrete Society and Chairman of the Editorial Board of the Magazine of Concrete Research.

Particular research interests cover durability, surface and bulk characteristics of concrete modified using chemical additions.

INTRODUCTION

A Congress is defined as a formal meeting of delegates with the purpose of discussing between those present issues such as special studies. In this regard, a Congress about concrete is both timely and needed and since concrete is a global material an International Congress seems very appropriate. This is now the 5th event held in Dundee on a triennial basis, the others being:

'Protection of Concrete' 1990
'Concrete 2000' 1993
'Concrete in the Service of Mankind' 1996
'Creating with Concrete' 1999

For those not involved with concrete it may seem strange after so many years of use, thousands of published papers and many books on the subject, all that could be known about concrete was known. So why does the debate and development continue?

Firstly, concrete is the most widely used construction material globally, it has become established in technically advanced countries and it has been estimated that some 1,200-2,400 kg per head of population are made per year [1]

Secondly, because of its adaptability it can be used for almost all construction situations, both structural and non-structural.

Thirdly, it is capable of being developed further in response to environmental concerns, energy considerations and new functional demands extending the material's performance in answer to engineering needs.

In other words, concrete and concreting are dynamic and will never reach a static position, unless of course our imaginations stagnate and we run out of ideas. For all of these reasons concrete is a material of opportunity and the debate will continue.

The theme of the present Congress is 'Challenges of Concrete Construction' embracing the weather, fire, seismic and marine situations and all that interlinks them. However, concrete faces other challenges from alternative materials such as steel, wood, glass, plastics and natural masonry. Alternatives do not readily have their justification in being straight material's replacements so much as finding their own niche in the design and functional requirements of buildings.

Other challenges covered at this Congress are,

1. Exploitation of the planet – Awakening of conscience in our own self interest
   – Environmental concerns/auditing/marking

2. Adoption of cleaner technologies

3. Sustainability – Design aspects
   – Brownfield development
   – Role of taxing and charging (landfill and aggregate tax)
   – Standardisation of components to assist reuse.

4. Elimination of waste
5. Whole life costing – life and death
6. Design for deconstruction
7. Alternatives to Portland cement
8. Wide/mandated use of cement replacement materials
9. High volume use of by-products
10. Energy conservation
11. Education for such involvements

Notwithstanding such challenges, concrete remains the most widely used construction material globally and that situation is likely to continue.

There is a constant probing for new developments reflecting drivers for change both direct and indirect and some suggested drivers are noted below.

- functional
- decorative
- competitiveness
- opportunity
- serviceability
- environmental issues
- safety
- fashion

These matters are dealt with in the Congress that comprises three Seminars and three Conferences.

CONGRESS REVIEW

Seminar 1 is concerned with 'Composite Materials used Internally and Externally', both organic and in-organic. These new materials offer better durability, lower weight and higher strength, ease of transportation, low thermal conductivity and reduced energy to make. For all of these reasons, adoption of composite materials technology should be welcomed but as with so many innovations in our industry, exploitation is guarded. It is clear that questions are being raised over slowness to adopt new ideas and innovations within concrete construction.

Conceptually fibre reinforced composites are not new and the ground rules for design and selecting them are established [2]. However, reinforced concrete is still conceptually large steel fibres (rebar) as reinforcement in an inorganic matrix rather than organic.

Proven performance based on unequivocal data are key to acceptance by specifiers and users alike to give confidence in the adoption of such new technologies.

Ironically, reinforced concrete itself was originally not backed up by a great deal of pre-use data as are fibre reinforced composites today and yet it was adopted with commitment. Why was this? Perhaps we are both set in our ways as well as worried about litigation. In this respect the composite beam example of Van Elp, Cattel and Heldt [3] is a good one that contradicts the apparent trend. The logical and prospective replacement of the established convention by optimum use of new materials resulting in a hybrid beam that outperforms the traditional reinforced concrete beam. The new types of beam have high load capacity, excellent fatigue resistance, outstanding durability, although detailed reaction to fire and comparable costs need to be addressed.

Are such radical developments welcomed and do we express the functional benefits well enough to persuade clients and specifiers and designers to adopt the new options? When considering new possibilities there is also the issue of appropriate technology. It is sometimes tacitly assumed that technologies rooted in advanced industrialised countries, may be used with equal effect in less developed countries where materials and skills may be different. Since concrete in one form or another is global, it should be possible to evolve appropriate applications for different locations. We talk readily of buildability but in the area of new ideas we should also consider adoptability.

There is merit in simplicity, both in concept, manufacture and use and a shift in Europe to prefabrication, giving better control over the process and a reduction in the need for established site skills.

Composite materials should respond in a ductile manner, eg be tough rather than simply strong. The issue of toughness is repeated throughout the Congress papers. The same trend applies to the development of lightweight structural materials, probably based on waste products, reflecting the emergence of conscience as well as functional and cost requirements. The phrase 'priorities for change' appears in Lowe's keynote paper [4].

It is suggested that value should replace cost in selecting options. This is compatible with the concept of whole life costing, another strand repeated throughout the Congress.

Do regulations and standardisation stimulate or impede innovation? Regulation can stimulate by demanding new and more exacting performance levels. The means of showing compliance with the regulation, eg conforming to a standard or established technical specification may not assist change. Performance based not on prescriptive specifications are an answer but to implement such an approach requires a will to adopt and change.

Mention is made to high temperature and fire effects on organic binders and one paper by Ballaguru [5] introduced an inorganic adhesive for bonding carbon fibre sheets to concrete beams. The water-based adhesive is composed of an alumna-silicate and is stable up to 1000°C. Despite a very complicated application procedure it is indicative of what can be achieved.

One stimulant to development of fibre-reinforced plastics has been seismic performance. Typical fibres are carbon, glass and aramids maintaining cohesion beyond the point of failure.

The pursuit of lightweight and toughness is highly desirable and whilst carbon fibres have a role to play in achieving this objective it needs to be remembered that carbon can act as a noble metal in the galvanic series and whilst it will not corrode it may cause less noble metals relative to it to do so. The carbon itself is conductive and given the right combination of conditions may exacerbate the process.

Seminar 2 is concerned with 'Floors and Slabs' with an emphasis on flooring that seems to represent a typical case of 'we seem to know what to do but do not always do it'. Self imposed inadequacy!

Flooring is undoubtedly a substantial activity in the distribution depot and monolithic construction sectors that use some $1.5m^3$ of concrete a year of concrete in the UK alone.

However, what in principle could be simpler than a slab? What could be simpler than a slab made of concrete? The physical principles of which are known – or are they? When you take regard of the conditions under which concrete for flooring is laid that assumption might be questioned.

There would appear to be too many homespun practices observes Harvey [7] but the problems with floors are global and commonplace. Notwithstanding all of this there would appear to be no substitute for concrete.

There is still much emphasis on Concrete Society Report TR34 [8]

Seidler [9] challenged that notwithstanding progress in concrete generally over the last 150-200 years, concrete flooring has not advanced significantly.

Incipient cheapness whilst a determining factor in this apparent lack of progress at some 27 Euros per square metre (approximately £17.50 per square metre) the equivalent of a medium quality fitted carpet! I cannot image the average fitted carpet functioning like an industrial floor. The requirements of industrial floors are clearly stated, namely,

- non shrink concrete
- monolithic construction
- non dusting
- adequate strength and surface resistance
- complex serviceability requirements

Chemical modifications can help overcome the known problems but the addition of polymers increases the cost substantially.

An industrial floor is a good example of a multi faceted performance requirement from something that is basically very simple. Why has this topic received so little attention? Value, longevity and robust performance rather than cost might be a better approach. In this sector cost seems to dominate.

Fast track construction leading to long strip and large bays are a trend to be acknowledged, together with joint-free slabs with speciality surface finishing and finishes. These are added demands to what superficially is a simple functional element.

Floor quality appears to have reached a plateau in terms of economically obtained quality. Again a plea for whole life costing.

The paper by Watanabe et al [10], suggests a form of flooring categorisation in the range 1-7, linked to the use to which the floor may be put and the development of a so-called U-scale as a measure of anti-static performance.

Seminar 3 deals with 'Repair, Rejuvenation and Enhancement of Concrete'.

Concrete repair and rehabilitation still dominate the concrete scene and yet concrete's failures are a relatively small proportion of concrete's use. Failure is also small, relative to new applications of concrete, eg, self compacting and ultra-high strength concrete and in relation to major projects such as the second Severn Crossing. However, in money and nuisance value terms, the profile of rehabilitation and repair is high and in that sense it attracts attention. It is the longer term inadequacies such as poor appearance, sulphate and chloride attack, sulphation and carbonation, that need to be addressed. Have these problems resulted from pursuing cost containment, lower cement contents, reduced cover rather than long term value?

The entire topic of concrete's pathology and degradation processes is worthy of our attention, how do we extend with confidence, the lifespan of concrete structures?

I refer to the paper of Tuutti [11] that quotes some telling figures relating capital values of buildings and structures to the value of all stocks as they apply to Sweden but may well reflect global trends in industrialised countries. Much of this stock has to be repaired and/or replaced on a 50 year cycle and that represents vast sums of money. If that is so, do we simply use concrete and design buildings, towns and cities as we have always done? Is such an approach sustainable?

Exploitation of new materials options that will have a longer service life and perhaps even be 'smart' will become the norm. Autogenous healing of cracked concrete is an example of a 'smart' material. It is difficult to predict where the initiative for change will come from. Will it be radical design, reflecting efficient function or will it be ad hoc picking up on personal preferences and available options? Will the drive be regulation or market opportunism? Did the development of self-compacting concrete start with an engineering need or more the availability of such a material's option, driven in turn by dispersant technology applied to cementitious suspensions rather than sound market research? In a capitalist economy the ultimate drive is financial well-being and planning and opportunism will live close together resulting in a somewhat volatile cocktail. So will concrete's future development be ad hoc and random or will sustainability, efficiency and environmental concerns dominate? Will such concerns only be responded to by wealthy economies with the less endowed creating their own appropriate technologies?

The existence of historical structures built from concrete is tangible evidence of the material's good latent durability. However, what remains is the best and a great deal has not lasted and for many reasons. Therefore the historical legacy has lessons to teach us and they are worthy of study.

In determining the effect of challenges to concrete, the diagnosis stage is very important. A comparison with forensic science is justified and the diagnostician has many techniques at his disposal. I am of course referring to the paper by Sims [12].

Threats, such as thaumasite sulphate attack (TSA), alkali-silica reaction (ASR), alkali-carbonate reaction (ACR) and delayed ettringite formation (DEF), all challenge concrete but we have to keep the potential problems in context. Notwithstanding this the avoidance of alkali-silica and alkali-carbonate reaction by selecting suitable aggregates remains a global issue.

Physico-chemical techniques have resulted in preventative and remedial measures such as cathodic protection, electro chemical realkalisation and chloride removal. All have a place and the last two may well have moved on from being something of a curiosity to full-scale practical application [13].

The themes developed in the Seminars enlarge and extend into the three Conferences. Conference 1 is concerned with 'Innovations and Developments in Concrete Materials and Construction' and Shah [14] sees the following targets for concrete in the 21st Century,

- more durable
- more constructable
- more predictable
- greener

I would add, more sustainable and more competitive.

By judicious use of investigative and monitoring techniques, all these objectives are attainable. However, since concrete is a global material, a case could be made for such developments to be globally supported with the results available to all. At the present time research cultures are very national and even regional, resulting in considerable duplication of effort on the one hand but also inventive variety on the other. The basic principle of such issues as rheology, hydration, corrosion and loading characteristics could be conducted in one or two locations whereas much effort is dispersed at numerous locations around the world, competing for funds and technical recognition. It is only when we draw people together in a Congress such as this that we identify the common features. It depends upon whether a global material such as concrete requires global development in a global economy with appropriate planning and prioritising or whether the more parochial approach is more beneficial if somewhat wasteful.

For instance, the use of electronic speckle pattern interferometry (ESPI) to study cracking in fibre reinforced concrete [14] compared with the K and F functions to describe fibre distributions resulting in stress intensity factors that govern crack propagation, assists in defining the capability limits of such reinforcements. Do such studies need to be duplicated? Is the study itself not definitive?

Shah et al's work[14] has shown that extrusion can improve fibre distribution and result in a stronger and tougher composite. Prefabricated components might well lend themselves to such techniques.

In the area of self compacting concrete, rheological studies assisted the optimisation of concrete mixes. A balance has to be struck between high flow and no segregation with yield values permitting deformability of the concrete to accommodate awkward shapes. The absolute rheological terms of yield value and viscosity do not relate directly to deformability, placeability and segregation that describe what the material has to do in practice. However, such an approach permits judgements and selection to be made.

Rossi [15] has developed ultra high strength performance fibre reinforced concrete (UHPFRC) to the point that concrete without conventional reinforcement might be a prospect. This concept is represented by the MSCC (multi scale concept concrete) that consists of short fibres (6mm) and long fibres (13mm) mixed together at 7% of the cement content.

Perhaps we have too many options e.g.

- MDF (macro defect free) concrete
- DSP (densified small particle concrete)
- CRC (compact reinforced composites) and its BPR variant (similar to CRC but with longer fibres)
- RPC (reactive powder concrete)
- MSCC (multi-scale cement composite)
- SIFCON (slurry infiltrated fibre concrete)
- ECC (engineered cementitous composite)

to mention but a few.

Having developed new materials, techniques of placing and finishing them have to be considered. These are not concretes as we know them. With approximately 1000 kg/m^3 of cement and cement:aggregate ratios of 4:1 and tensile strengths of 40-50 MPa being attainable!

Costs of these developments, at this stage, are not given but clearly it is cost effectiveness and value that matters – they are not like for like replacements of normal concretes. The importance of such extreme developments as this is that it shows what can be done and, like radical fashions, they set a pattern within which there is general advancement.

It is encouraging to note in a paper by Garshol and Constantiner [16] that at long last the concept of incorporating chemicals to control and modify the plastic and harden states of concretes and mortars has consolidated into normal practice. Indeed without certain admixtures and reactive additives these new concepts would remain only a wish.

Admixtures are now being tailored to the known chemistry of cements and the required physical and chemical characteristics of resulting mortars and concretes. Science is replacing intuitive flair and materials engineering replacing a 'try and see' approach. Integrating disciplines in this way will bring construction in line with other process engineered activities, eg, aircraft construction. Such trends are predicted in the Egan Report – 'Rethinking Construction' [17].

Having made and placed the concrete its maintained appearance does not receive the status it deserves. The visual impact of concrete is not popular with the community at large and Kronlof [18] is concerned with the aesthetics of concrete, as we all should be. The phrase 'concrete is beautiful when it makes the designer and user happy' can hardly be argued with.

Concrete's form and appearance should be predictable – no unpleasant surprises. Natural ageing should be taken into account and neatness should be a prime aim for concrete development but again a low cost outlook does not aid aesthetic development.

General expectations of society and designers may differ from those of the industry and users. Kukko [19] considers that designers and society may be concerned with image and public benefit, but industry is more concerned with economic and technical profits. Is this division true? If it is how can it ever be reconciled?

Production of high quality surfaces, edges and joints is a priority with high quality materials being required, resulting in ready for finishing details, eg, painting and wallpapering.

There are opportunities for higher strengths and toughness – thinner and slender structures, shells, lattices, profiled beams and columns, all are attainable. Kukko identifies some aims, namely,

- environmental friendliness
- improving the quality of life
- competitiveness
- improved employment prospects
- improved working conditions, in particular, safety

Concrete is 'a material for all reasons' and, if its permanency could be assured, we might invest more in some of these value added options.

Conference 2 deals with 'Sustainable Concrete Construction' and Nixon's paper [20] is both forthright, to the point and very relevant. He makes some telling criticisms of man's exploitation of the planet. He contends we should be concerned with,

- adaptable buildings
- minimum waste
- design for deconstruction
- low energy cements
- reduced energy in use by using concrete intelligently

In attaining these aims concrete is the premier construction material.

Firstly, some disturbing facts.

In the UK about 25% of the energy used in industry is accounted for by the manufacture and transportation of building materials.

- It is estimated that 8% of global CO_2 emissions result from concrete production.
- One ton of CO_2 is produced per ton of Portland cement.
- Cement production is growing, particularly in developing countries and what we gain by going in one direction to save the environment may be offset by trends in the opposite direction.
- In summary we need an alternative to Portland cement – such options are coming into play already.

Cements that require reduced energy for production (less by 16%) and in turn produce less carbon dioxide (less by 10%) are seemingly attainable. Cements based upon belite with properties comparable to Portland cements and with some evidence to indicate that durability of resulting concretes might even be improved have been produced on a commercial scale in China. There is also the recent TecEco development based on magnesium oxide.[21] What is the future for these alternatives?

Nixon also makes the point that we should use concrete innovatively, taking regard of its high thermal mass resulting in substantial economies in the running of buildings.

Jensen and Glavind [22] remind us that to make $1m^3$ of office space requires something in the region of 500 MJ whereas for the same office space it requires 15,000 MJ to heat and light. How can concrete assist in the use and running of buildings is an issue that needs to be addressed.

Jensen and Glavind continue a similar theme noting that 2-6% of worldwide CO_2 stems from cement production and cement manufacture is increasing at 5% per year, equivalent to an increase of 10 million tons of CO_2 per year.

Perhaps we will only take the environmental issues seriously when failure to achieve set aims is legislated for. The Eco Management and Audit Scheme (EMAS) coupled with a statutory instrument against which a company can be registered might be a way forward. Various tools are available to engendering an environmental culture but what creates the will to do so? The principles of life cycle assessment (LCA) and life cycle inventory (LCI) can have aims and set targets such as,

- CO_2 reduction by at least 30%
- 20% of all concrete should use residual products as aggregates
- use concrete industry's own residual products
- CO_2 neutral waste derived fuel being used at a rate of at least 10% of all fuel used in cement production

In the USA some 5 billion tons of non hazardous by-product materials are produced annually (NAIK [23]). Major inputs from agriculture (2.1 billion tons) and mineral sources (1.8 billion tons).The UK construction industry produces 20% of all UK waste [24].

The use of fly ash and bottom ash and clean coal ash in cement production with new energy generating technologies yielding different coal derived ashes assists the quest for energy containment. There are many new end uses for waste materials, for instance, sewage sludge for lightweight aggregates and for making clay bricks.

The task of carrying the environmental banner often falls to the lot of the manufacturer but contractors have a role to play as well (Goring [25]). Greater integration and co-operation emphasising quality and safety and less so cost, as has been the habit to date. These principles are set out in Egan's 'Rethinking Construction' [25]. How do these attitudes impinge upon concreting activities? Firstly, starting with design concepts – concrete can play a role by way of its thermal mass in providing better air quality and natural ventilation. To effect radical change we need an integrated approach involving concrete design and function and increasing the overlap between environmental concerns and how we build.

Torring and Lauritzen [26] estimate a potential of 400 million tons of reusable concrete, stone and brick from industrialised countries. We have to consider the means of deconstruction and reclaiming the materials used. – Joined up construction underwritten by a joined up sense of public conscience.

Pocklington and Glass [24] believe that the energy performance of buildings are a key to sustainability in which case there is good reason for using concrete. Phrases such as 'burn and bury', 'dilute and disperse' and 'end of pipe' are no longer acceptable. The term anthropogenic was used – greenhouse gas emissions caused by man. We need some form of fiscal encouragement to create a culture of change. We also need to plan for longer life and adaptability of buildings.

Further telling statistics supplied by Glavind and Munch-Petersen [27]. Some 5 km^3 of concrete are used per year globally and whilst some would contend that CO_2 produced per ton of cement is small in itself, it becomes large due to the amount of concrete produced. The prospect of quantified benchmarking of attainable objectives for CO_2 reduction say by 30% and recycled concrete used as aggregate, making an energy reduction of 20% is tantalising. The authors also consider that waste derived fuels should replace 10% of fossil fuels and their paper results in a specification for 'green' concrete types – some 14 in number. The authors were very conscious of solving one problem but creating a second order unwelcome legacy, eg, kiln dust containing zinc, vanadium, lead and copper as well as phosphorus pentoxide. We have to maintain a sense of proportion and perspective. The various phases of materials production and construction activity cannot be dealt with in isolation, one from the other.

Conference 3 deals with 'Concrete for Extreme Conditions' and the paper by De Vries [28] endeavours to put the problems of durability into perspective. On balance the performance of concrete is not as bad as many would contend. However, there are problems of poor workmanship and with new materials. Codes and specifications are not particular enough and matters of maintenance and repair not covered sufficiently well. De Vries would like to see performance and reliability based service life design and makes reference to the European Brite/Euram research project – 'Duracrete'. A plea is made to involve the client and give contractors a number of options.

Durability design should get as much attention as structural design. The Eastern Schedlt barrier has a service life-span of some 200 years! However, a period of 85 years was settled for the concrete when it was accepted that the cover will have to be replaced. An example of integrating maintenance with design life. We have to quantify the anticipated functional life-span. To do this a knowledge of the durability of materials is required and the effect of workmanship on achieving these properties needs to be addressed.

De Vries is also concerned with the interaction of structure and the environment and uses a probabilistic technique to determine the likelihood of failure and target service life. There are problems of defining the limit state requirements eg the onset of corrosion. Models exist for defining degradation conditions and the design can be modified to offset adverse predictions of service life based on such models – a preemptive approach.

Slater [29] concentrates on marine structures and these represent a severe exposure condition but relates the data so that it is relevant to all types of construction. The emphasis is on buildability and durability. Buildability covering such issues as safety and economy and durability fixed by design and exposure (environment). Reassuring to see a preference for

low w:c ratios and a useful quoted rule of thumb 'a reduction in w:c ratio of .05 is the equivalent of an increase in a cover of 5mm'. Slater concludes with an excellent series of pragmatic recommendations.

Over recent times there has been much discussion on the existence of threshold chloride levels below which passivation is maintained and above which active corrosion commences. The paper by Paramasivam et al [30] is a good example of data obtained on an actual structure, in this case a 32 year old wharf from which 6 marine piles (driven) were recovered and analysed for chloride content and penetration. Comparisons were made of the actual with predicted ingress levels of chloride and the relationship between such levels and loss in mass of reinforcing bars. Reference is made to threshold chloride levels (Reference 2 of [30])again and the establishment of critical chloride levels in the range .03 - .1% weight/weight concrete, covering in the first instance the splash zone and the latter submerged (Reference 6 [30]). Alternatively, Browne (Reference 7 of [3]) again showed such values to be in the range .2 - .49% w/w cement. Therefore values of .034 - .068% w/w concrete were considered appropriate.

These figures are to be doubted where a plentiful supply of oxygen is available. There was broad agreement between predicted and actual values confirming the various models used. As an extension to the problems caused by chloride ingress and contamination, Masuda [31] considered salt damage to reinforced concrete buildings resulting from both seawater and airborne salt. Some 4,363 buildings were investigated, covering everything from domestic to industrial, schools, offices, hospitals, etc resulting in 60% or so being perfectly satisfactory in the age range 7-46 years old. The distance from the coast was a significant factor in determining the residual chloride levels. Insufficient cover was the cause of deterioration in most cases but the examination was primarily visual. The threshold levels in this study were broadly corroborated.

CONCLUSIONS

This Congress has brought together a great deal of data and experience that within itself has trends that indicate the way ahead and help to establish attitudes and create priorities. Some noted trends are given below.

1. Concrete is capable of considerable further performance-based development and should not posture as a low technology stereotype .

2. Sustainability will remain a motivator for regulators, designers and concrete material providers. Is there a sustainable alternative to Portland cement?

3. Adopted technology should be in proportion to prevailing local conditions.

4. Creating a concrete culture at operative level with recognition of skill status will help to exploit new developments and make the aim of best practice a reality.

5. Laboratory-based data must reconcile with what happens in practice — transfer of micro mechanisms to macro fact. Methods of diagnosis should be accurate and unambiguous, performed by those qualified to do so and interpretation should be subject to severe scrutiny.

6. The role of water needs more committed study. It is necessary for cement to transform into masonry but is also responsible for much of concrete's degradation.

7. Development of tough concrete rather than high strength but brittle concretes.

8. The visual appearance of concrete with time is of concern. Concrete should remain pristine and not take on a patina of industrial downgrading.

9. Coating and sealing may not be sufficient. We have to understand how concrete behaves to fluctuations in its surroundings at a micro mechanistic level.

10. Does a true threshold chloride level exist before steel corrosion occurs?

11. Can we consider structures that do not contain normal reinforcement but rely solely on metal fibres and a reconstituted matrix?

12. The use of recycled and waste materials should be encouraged using legislation and tax incentives for those that comply – a stick and carrot approach.

ACKNOWLEDGEMENTS

I am indebted to all the authors of those Congress papers to which I have made reference and indeed those that I have not, I also thank colleagues with whom I have endless discussions about concrete, without which opinions and viewpoints could not be formed and conclusions drawn.

REFERENCES

With the exception of References 1, 8, 17 and 21, all are drawn from papers given at the Dundee Congress 'Challenges of Concrete Construction' 5-11 September 2002. To simplify the listing only the relevant Seminar or Conference is identified.

1. GLASSER F. P., Private Communication

2. All Authors, Composite Materials in Concrete Construction, Seminar 1.

3. VAN ERP G., CATTEL C., HELDT T., Fibre Composites in Civil Engineering: An Opportunity for a Novel Approach to Traditional Reinforced Concrete Concepts. Proceedings of International Congress: Challenges of Concrete Construction, Seminar 1 – Composite Materials in Concrete Construction, Dundee, Scotland, 5-6 September, 2002, pp 1-16

4. LOWE P., Composite Materials in Concrete Construction, Proceedings of International Congress: Challenges of Concrete Construction, Seminar 1 – Composite Materials in Concrete Construction, Dundee, Scotland, 5-6 September, 2002, pp 17-30

5. BALAGURU P.N., Inorganic Polymer Composites in Concrete Construction: Properties, Opportunities and Challenges, Proceedings of International Congress: Challenges of Concrete Construction, Seminar 1 – Composite Materials in Concrete Construction, Dundee, Scotland, 5-6 September, 2002, pp 109-126

6. VAN GEMERT D., BROSENS K., Non-Metallic Reinforcements for Concrete Construction, Proceedings of International Congress: Challenges of Concrete Construction, Seminar 1 – Composite Materials in Concrete Construction, Dundee, Scotland, 5-6 September, 2002, pp 225-236

7. HARVEY D.J.J., Developing a Greater Understanding of the Nature and Usability of Concrete in Industrial Floor Applications, Proceedings of International Congress: Challenges of Concrete Construction, Seminar 2 – Concrete Floors and Slabs, Dundee, Scotland, 5-6 September, 2002, pp 183-194

8. CONCRETE SOCIETY, Concrete Industrial Ground Floors – A Guide to their Design and Construction, Technical Report No 34, 1994, pp 170.

9. SEIDLER P., How Polymers Improve Floors – Possibilities Today and Prospects for the Future, Proceedings of International Congress: Challenges of Concrete Construction, Seminar 2 – Concrete Floors and Slabs, Dundee, Scotland, 5-6 September, 2002, pp 1-14

10. WATANABE H., ONO H., KAIZU H., Performance Evaluation of Floors for Static Charge on Human Body – Proposal of a New Method, Proceedings of International Congress: Challenges of Concrete Construction, Seminar 2 –Concrete Floors and Slabs, Dundee, Scotland, 5-6 September, 2002, pp 233-244

11. TUUTTI K., Repair, Rejuvenation and Enhancement of Concrete – A Fast Growing Market, Proceedings of International Congress: Challenges of Concrete Construction, Seminar 3 – Repair, Rejuvenation and Enhancement of Concrete, Dundee, Scotland, 5-6 September, 2002, pp 1-10

12. SIMS I., Diagnosing and Avoiding the Causes of Concrete Degradation, Proceedings of International Congress: Challenges of Concrete Construction, Seminar 3 – Repair, Rejuvenation and Enhancement of Concrete, Dundee, Scotland, 5-6 September, 2002, pp 11-24

13. VENNESLAND O., Documentation of Electrochemical Maintenance Methods, Proceedings of International Congress: Challenges of Concrete Construction, Seminar 3 – Repair, Rejuvenation and Enhancement of Concrete, Dundee, Scotland, 5-6 September, 2002, pp 191-198

14. SHAH S.P., AKKAYA Y., BUI V.K., Innovations in Microstructure, Processing and Properties, Proceedings of International Congress: Challenges of Concrete Construction, Conference 1 - Innovations and Developments in Concrete Materials and Construction, Dundee, Scotland, 9-11 September, 2002, pp 1-16

15. ROSSI P., Developments of New Cement Composite Materials for Construction, Proceedings of International Congress: Challenges of Concrete Construction, Conference 1 - Innovations and Developments in Concrete Materials and Construction, Dundee, Scotland, 9-11 September, 2002, pp 17-30

16. GARSHOL K.F., CONSTANTINER D., Super-Concrete Examples: Complete Rheology Control and Passive Fire Protection, Proceedings of International Congress: Challenges of Concrete Construction, Conference 1 - Innovations and Developments in Concrete Materials and Construction, Dundee, Scotland, 9-11 September, 2002, pp 411-422

17. EGAN J., Rethinking Construction, July 1998, pp 39.

18. KRONLÖF A., Concrete Aesthetics: Flexible or Stiff – Humble or Arrogant, Proceedings of International Congress: Challenges of Concrete Construction, Conference 1 - Innovations and Developments in Concrete Materials and Construction, Dundee, Scotland, 9-11 September, 2002, pp 751-762

19. KUKKO H., Requirements for Advanced Concrete Materials, Proceedings of International Congress: Challenges of Concrete Construction, Conference 1 - Innovations and Developments in Concrete Materials and Construction, Dundee, Scotland, 9-11 September, 2002, pp 949-956

20. NIXON P.J., More Sustainable Construction: The Role of Concrete, Proceedings of International Congress: Challenges of Concrete Construction, Conference 2 – Sustainable Concrete Construction, Dundee, Scotland, 9-11 September, 2002, pp 1-12

21. GLASSER F.P., TecEco: Cements Based on Magnesium Oxide, A Private Communication, 2001, pp 9.

22. JENSEN B.L., GLAVIND M., Consider the Environment – Why and How, Proceedings of International Congress: Challenges of Concrete Construction, Conference 2 – Sustainable Concrete Construction, Dundee, Scotland, 9-11 September, 2002, pp 13-22

23. NAIK T.R., The Role of Combustion By-Products in Sustainable Construction Materials, Proceedings of International Congress: Challenges of Concrete Construction, Conference 2 – Sustainable Concrete Construction, Dundee, Scotland, 9-11 September, 2002, pp 117-130

24. POCKLINGTON D., GLASS J., Economics, Sustainability and Concrete, Proceedings of International Congress: Challenges of Concrete Construction, Conference 2 – Sustainable Concrete Construction, Dundee, Scotland, 9-11 September, 2002, pp 683-694

25. GORING P.G., Rethinking Sustainable Concrete Construction, Proceedings of International Congress: Challenges of Concrete Construction, Conference 2 – Sustainable Concrete Construction, Dundee, Scotland, 9-11 September, 2002, pp 439-456

26. TORRING M., LAURITZEN E., Total Recycling Opportunities – Tasting the Topics for the Conference Session, Proceedings of International Congress: Challenges of Concrete Construction, Conference 2 – Sustainable Concrete Construction, Dundee, Scotland, 9-11 September, 2002, pp 501-510

27. GLAVIND M., MUNCH-PETERSEN C., Green Concrete – A Life Cycle Approach, Proceedings of International Congress: Challenges of Concrete Construction, Conference 2 – Sustainable Concrete Construction, Dundee, Scotland, 9-11 September, 2002, pp 771-786

28. DE VRIES H., Durability of Concrete : A Major Concern to Owners of Reinforced Concrete Structures, Proceedings of International Congress: Challenges of Concrete Construction, Conference 3 – Concrete for Extreme Conditions, Dundee, Scotland, 9-11 September, 2002, pp 1-16

29. SLATER D., Marine and Underwater Concrete – Buildability and Durability, Proceedings of International Congress: Challenges of Concrete Construction, Conference 3 – Concrete for Extreme Conditions, Dundee, Scotland, 9-11 September, 2002, pp 189-204

30. PARAMASIVAM P., LIM C.T.E., ONG K.C.G., Performance of Reinforced Concrete Piles Exposed to Marine Environment, Proceedings of International Congress: Challenges of Concrete Construction, Conference 3 – Concrete for Extreme Conditions, Dundee, Scotland, 9-11 September, 2002, pp 525-536

31. MASUDA M.Y., Condition Survey of Salt Damage to Reinforced Concrete Buildings in Japan. Proceedings of International Congress: Challenges of Concrete Construction, Conference 3 – Concrete for Extreme Conditions, Dundee, Scotland, 9-11 September, 2002, pp 823-836

INDEX OF AUTHORS

SUBJECT INDEX

This index has been compiled from the keywords assigned to the papers, edited and extended as appropriate. The page references are to the first page of the relevant paper.